/
Article / Book Information

(　　)	
Title(English)	Finite element analysis of an anisotropic soil model with non-smooth yield surface using implicit integration algorithms
(　　)	
Author(English)	Thirapong Pipatpongsa
(　　)	：　(　　), ： ：　　5054　, ：2002　3　26　, ： ：
Citation(English)	Degree:Doctor (Engineering), Conferring organization: Tokyo Institute of Technology, Report number:　　5054　, Conferred date:2002/3/26, Degree Type:Course doctor, Examiner:Hideki Ohta
(　　)	
Type(English)	Doctoral Thesis

Finite element analysis of an anisotropic soil model with non-smooth yield surface using implicit integration algorithms

PIPATPONGSA   Thirapong

Finite element analysis of an anisotropic soil model with non-smooth yield surface using implicit integration algorithms

A dissertation submitted to
the department of International Development Engineering
and the committee on graduate studies of Tokyo Institute of Technology
in partial fulfillment of the requirements for the degree of

Doctor of Engineering

by

Mr. Thirapong PIPATPONGSA

Academic Advisor: Prof. Dr. Hideki Ohta

Geotechnical Engineering Group
Tokyo Institute of Technology, Japan

February 2002

ABSTRACT

Since Sekiguchi and Ohta (1977) proposed a soil constitutive model to account for stress-induced anisotropy and time-dependency, numerous of theoretical works have been geared toward numerical implementations for engineering practice. The performance of model has been proven to produce predicted ground responses that are consistent with observed field measurements. However, there are some theoretical contradictions in which the model and its numerical implementations still cannot cover, commented as the following.

The singularity found at the corner of the SO (Sekiguci-Ohta) yield surface rules out the normality postulate. The SO model cannot show a particular relation between K_o and ϕ'. The consistency condition is always violated after stress update, that is, yield function $f(\sigma', \sigma'_o) > 0$, e.g. in computer code applicable to the model (DACSAR, 1985-1997). A reference of the model set to initial yield stress σ'_o at t=0 breaks the principle of objectivity (frame indifferent) at all times. Relative responses mapping between isotropy due to elasticity and anisotropy due to plasticity are unclearly quantified. In short, there are missing links among stress-induced anisotropy (K_o), failure property (ϕ'), associative plastic flow, consistency requirement, objectivity and non-coaxiality.

Based on the recent theoretical principles regarding to the seamlessly-linked mechanics and mathematic framework rigorously established by Simo et al. (1985-1997), all of these scattered concepts were satisfactorily corrected and mutually connected within the new generalized concept in this study by the following suggestions,

Koiter's associated flow rule (1953) is applied to the singular corner intersected by upper and lower yield loci that is selected as candidates of conceivable yield loci passing the discontinuous slope in stress space. Concepts of mobilized and immobilized K_o conditions are employed to a typical normality of individual yield surface in triaxial stress plane. Implicit time integration algorithm based on return-mapping method is implemented to enforce plastic consistency for the model, making a methodology accurate, unconditionally stable and converged to the solution quadratically. The hardening variable of the SO model is modified from volumetric plastic strain and initial yield stress σ'_o to the current stress hardening σ'_c. Therefore, the model is adapted to $f(\sigma', \sigma'_c)$ without losing the generality and satisfies the objectivity requirement by the form-invariance principle. According to the principle of material invariance (Baker & Desai, 1984), the joint invariants retained in constitutive model can characterize the relative orientation of the stress and plastic strain tensors in space. Therefore, a linear mapping quantity between Cartesian and reciprocal basics is associated in order to clearly characterize non-coaxial response between stress and strain in Euclidean vector space.

In addition to its in-depth examination in fundamental concepts to practical computer implementations, major theoretical developments contributed by the study include the stiffness matrix considering plastic flow at the corner of the SO model, K_o-value in regard to the SO model, the consistent tangential moduli in regard to anisotropic models and finally the inversion techniques of forth-order tensors based on reciprocal tensor basics.

As a consequence, an integrated viewpoint is settled for the SO model while providing a comprehensive background and a short-cut technique in calculation for further advanced development. The study may share the potential descriptions of implicit finite element method for non-smooth anisotropic models to researchers working in similar fields and modern soil mechanics.

ACKNOWLEDGMENT

COMMITTEE

1. Prof. Hideki OHTA
   Department of International Development Engineering

2. Prof. Nobuaki OTSUKI
   Department of International Development Engineering

3. Prof. Osamu KUSAKABE
   Department of Civil Engineering

4. Assoc. Prof. Jiro KUWANO
   Department of Civil Engineering

5. Dr. Masa-aki TERASHI
   Principal of Nikken Sekkei Nakase Geotechnical Institute)

6. Prof. Mark Zarco
   University of the Philippines

RECORD

Finite Element Analysis of an Anisotropic Soil Model with Non-smooth Yield Surface using Implicit Integration Algorithms

Name	Mr. Thirapong PIPATPONGSA (99D18093)
Nationality	Thai
Date of birth	July 17, 1974
Academic advisor	Prof. Hideki OHTA (International Development Engineering)

Education record

1991-1994	Bachelor of Engineering (Civil Engineering)
	Chulalongkorn University, Bangkok, Thailand
1997-1999	Master of Engineering (Geotechnical Engineering)
	Kanazawa University, Kanazawa, Japan
1999-present	Graduate student, Department of International Development Engineering
	Tokyo Institute of Technology, Tokyo, Japan

Professional experience

1993-1993	Internship civil engineer
	Thai-Bauer Co., Ltd., Bangkok, Thailand
1994-1995	Structural engineer
	Metropolitan Engineering Consultant Co., Ltd., Bangkok

Academic awards

a) Outstanding Award in Computer-Mathematics-Electronics remarked by Engineering Institute of Thailand (1991)

b) Youth Candidate for Computer Olympic selected by the office of Ministry of Science and Technology, Kingdom of Thailand (1990)

c) Excellent Certificate in Mathematics approved by the Education Information Center, Thailand (1988)

Publications

Domestic journal papers

1. Pipatpongsa, T., Iizuka, A., Kobayashi, I. Ohta, H. & Suzuki, Y., Nonlinear analysis for stress-strain-strength of clays using return-mapping algorithms, *Journal of Applied Mechanics Vol.4,* JSCE, pp.295-306, 2001

2. Pipatpongsa, T., Iizuka, A., Kobayashi, I. & Ohta, H., FEM formulation for analysis of soil constitutive model with a corner in the yield surface, *Journal of Structural Engineering Vol.48A*, JSCE, pp.185-194, 2002

International conference proceedings

3. Pipatpongsa, T., Ohta, H., Iizuka, A. and Hashimoto, M., Effects of some parameters on braced-excavation of soft clay by numerical studies, *Proceedings of the International Symposium-IS-YOKOHAMA 2000,* Yokohama, Japan, pp.351-356, 2000

National conference proceedings

4. Pipatpongsa, T., Ohta, H., Iizuka, A., Yamakami, T. & Hashimoto, M., Application of F.E.M. to excavation of soft clay, *Proc. of 34th Japanese Nat. Conf. on Geotech. Engrg,* pp.1629-1630, 1999

5. Pipatpongsa, T. and Ohta, H., Application of F.E.M. to excavation of soft clay, *1st Inter. Summer Sym.,* JSCE, pp.205-208, 1999

6. Pipatpongsa, T. and Ohta, H., Return-mapping algorithm for Sekiguchi-Ohta model, *2nd Inter. Summer Sym.,* JSCE, pp.229-232, 2000

7. Pipatpongsa, T., Ohta, H., Kobayashi, I. and Iizuka, A., Associated plastic flow at the intersection corner of plastic potential functions in soil mechanics, *Proc. of 36th Japanese Nat. Conf. on Geotech. Engrg.*, pp.935-936, 2001

8. Pipatpongsa, T., Ohta, H., Kobayashi, I. and Iizuka, A., Dependence of K_o-value on effective internal friction angle in regard to the Sekiguchi-Ohta model, *Proc. of 36th Japanese Nat. Conf. on Geotech. Engrg,* pp.937-938, 2001

9. Pipatpongsa, T., Ohta, H., Kobayashi, I. and Iizuka, A., Integration algorithms for soil constitutive

equations with a singular hardening vertex, 3rd *Inter. Summer Sym.,* JSCE, 201-204, 2001

10. Pipatpongsa, T., Kobayashi, I., Ohta, H., and Iizuka, A., The vertex singularity in the Sekiguchi-Ohta model, *56th JSCE Annual Meeting,* CD III-B341, 2001

11. Pipatpongsa, T., Kobayashi, I., Iizuka, A., and Ohta, H., Implicit finite element implementation of an anisotropic soil model, *Proc. of 51th Jap. Nat. Conf. on Theo. Appl. Mech,*: 211-212, 2002

12. Pipatpongsa, T., Yuttapongtada, Y., Iizuka, A., Kobayashi, I. & Ohta, H., Interpretation of Koiter's associated flow rule to the corner of the Sekiguchi-Ohta model, *Proc. of 37th Japanese Nat. Conf. on Geotech. Engrg,* 351-352, 2002

13. Pipatpongsa, T., Osakabe, K., Iizuka, A., Kobayashi, I. & Ohta, H., Stress update algorithm for rate-independent Sekiguchi-Ohta model, *Proc. of 37th Japanese Nat. Conf. on Geotech. Engrg,* 331-332, 2002

14. Pipatpongsa, T., Osakabe, K., Iizuka, A., Kobayashi, I. & Ohta, H., Consistent tangential moduli for rate-independent Sekiguchi-Ohta model, *Proc. of 37th Japanese Nat. Conf. on Geotech. Engrg,* 329-330, 2002

15. Pipatpongsa, T., Iizuka, A., Kobayashi, I. & Ohta, H., Consistent tangential tensor in regard to rate-independent Sekiguchi-Ohta model, *Proc. of 38th Japanese Nat. Conf. on Geotech. Engrg,* on submission, 2003

CONTENT

Chapter 1: Introduction

Chapter 2: Theoretical Background

Chapter 3: Convex Analysis

Chapter 4: Soil Initial Anisotropy

Chapter 5: Singular Hardening Vertex

Chapter 6: Stress Update Algorithm

Chapter 7: Closest Point Projection Method

Chapter 8: Consistent Tangential Stiffness Tensor

Chapter 9: Tensorial Inversion Technique

Chapter 10: Implicit Finite Element Method

Chapter 11: Numerical Analysis

Chapter 12: Summary and Discussion

FIGURE

TABLE

BOX

APPENDIX

CHAPTER 1

Introduction

1-1 Purposes

The objectives of this thesis can be itemized as followed,

1. To break the limitation confined by normality when involving non-smooth yield surfaces (plastic potentials) in Geomechanics
2. To describe the vertex singularity in the model proposed by Sekiguchi and Ohta (1977) [1] as the unique point of material memory on yield surface in stress space
3. To implement the mathematical treatment to deal with the singular vertex based on Koiter's associative flow rule (1953) [2]
4. To evaluate the relation between K_o and M in regard to the SO model
5. To extend the FEM code by considering the singular vertex in the SO model
6. To generalize a form of the SO model to satisfy a principle of objectivity
7. To develop the implicit stress update algorithms based on CPPM (Closest Point Projection Method)
8. To provide basis descriptions of implicit FEM procedures of an anisotropic soil model based on return-mapping methods
9. To express the non-coaxiality between stress and plastic strain increment found in the SO model by a reciprocal basis
10. To advance a technique in numerical computation with high efficiency and accuracy

Briefly, the overall purposes of this study is to connect missing links existed in the numerical implementation of the SO plasticity as outlined in Figure 1.1.
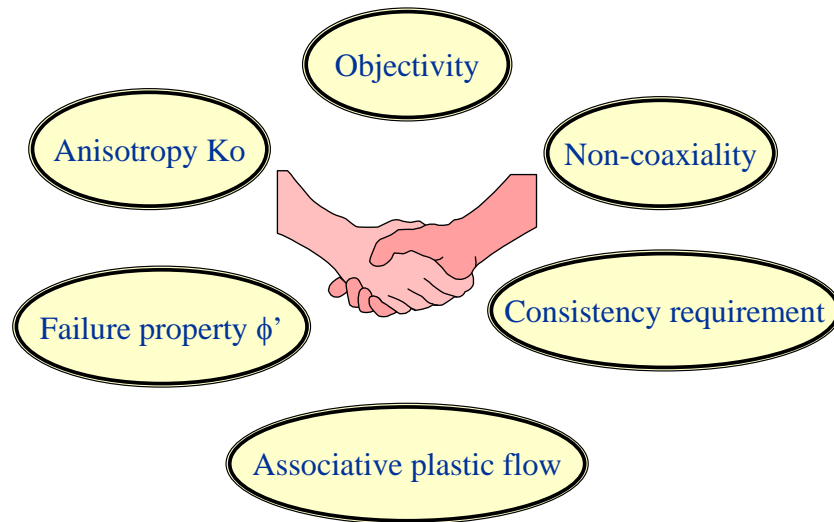
Figure 1.1 Missing links in SO plasticity numerical implementation

1-2 Methodology

1-2-1 Methodology for handling the corner in the SO model

It is our first step to show that a geometric representation of the SO has a corner in stress space. We found that this corner in the yield surface moves along the anisotropic K_o consolidation line during a hardening process. Therefore, we looked into a relation between the virgin K_o consolidated and the corner. Then, we found that the corner keeps this virgin K_o consolidated stress as a stress hardening parameter of the model. We named this corner as a singular hardening vertex due to its property. It is known that associated flow rule cannot apply to non-smooth yield surface. In order to evaluate a plastic flow at the singular hardening vertex, we extended the concept of associated flow rule by referring to Koiter's associated flow rule, which can handle a non-smooth yield surface. It is a Koiter's condition to specify all discontinuous yield surfaces at the point or edge of intersection of yield surfaces. Since, there are many individual yield surfaces passing the conical vertex and it is impossible to include all of these countless yield loci. Only two of yield loci, which are mutually conjugate of each other, were chosen as our candidates. One is referred to triaxial K_o compression and another one is K_o extension loci. The reason why we used these candidates is because we found that the hardening vertex can be found only in axisymmetric triaxial stress plane or Rendulic's stress plane. And a section of the SO yield surface with this plane resulted in two individual yield loci, namely, upper and lower yield loci. The corner is the intersection point of both yield loci.

We evaluated the plastic flow at the corner by a sum of two plastic flows, which are normal to upper yield and lower yield loci respectively. A consistency requirement is enforced on both yield loci and we obtained two consistency parameters in corresponding to upper and lower yield loci. Information of these consistency

parameters can give a magnitude of plastic flow at corner and tell us whether the subsequent stress would be placed at or escape from the corner. Moreover, we examined conditions for loading/unloading using upper and lower yield loci's loading parameters. We also considered the conditions to check whether a current stress is located at the corner or not. If a current stress is located out of corner, then the regular method for smooth yield surface is employed, if not, our particular method developed have to be employed. So, under K_o-condition, we can obtain calculation results that are consistent with e-log(p') curves during loading/unloading.

1-2-2 Methodology for evaluating the theoretical K_o in regard to the SO model

Next step, we tried to explore the initial anisotropy or K_o value governed by the SO model. We can evaluate the incremental stress under K_o-condition where plastic flow is evaluated at the corner. According to the result, K_o is depended on Poisson's ratio similar to a relation found in elastic behavior, which contradicts to the fact that K_o is related internal friction angle or Critical state parameter. We employed a more flexible condition by allowing some variation of stress along K_o-line. Then, we named this condition as mobilized K_o while a state kept strictly at the corner, which is named as immobilized K_o we had determined its value already as Poisson's ratio function. We expected that in real experiments for finding K_o on triaxial apparatus, we start from K_o compression/extension test and reverse back by extension/compression test in order to correct lateral strain to zero repeatedly. That is, a mobilized K_o state is gradually approached immobilized K_o state. We can evaluate a mobilized K_o value from individual plastic flow of upper and lower yield loci (in implicit form) while a immobilized K_o value is evaluated from a coupled plastic flow of upper and lower yield loci. The K_o value obtained by each method gave different functions. By the assumption that the mobilized K_o would eventually approach to immobilized K_o condition, we equated these two K_o values and found that the relation can be reduced to an expression for K_o depended solely on critical state parameter M. Then we compared the relation obtained with famous empirical relations to convince our theoretical K_o.

1-2-3 Methodology for formulating FEM considering the corner in the SO model

After we knew the plastic strain rate evaluated at the corner for a given strain increment, a corresponding elastic strain increment can be obtained as well as incremental stress. A ratio of incremental stress to incremental strain gives a tangential elasto-plastic stiffness tensor. At first, this forth-order tensor was complicated due to the coupled effect of upper and lower yield loci, but after the condition of stress at the corner was employed. Many of terms can be vanished because of mutual conjugates in the expression. Then we determined a compacted form of tangential stiffness forth-order tensor and formulated it with standard FEM procedure. In FEM code we had modified from a standard one, we made a switch to let program consider whether a stress is on hardening vertex or not. If so, a standard tangential stiffness tensor and its loading/unloading judgment are activated. If not, our special tangential stiffness and its loading/unloading judgment are activated instead. Finally, we verified the program with simple K_o consolidation problems and discussed calculation results.

1-2-4 Methodology for adapting the SO model to satisfy the principle of objectivity

In the original version of the SO model, a strain-hardening parameter is employed but we changed to use a stress-hardening parameter and changed generalized stress ratio to generalized relative stress ratio instead. As a result, we can remove a reference to initial yield stress at t=0 in the model. After doing stress invariance study, we can show that first and second invariance of stress tensor, first and second invariance of stress-hardening tensor and joint invariance between first invariance of both stress tensor and stress-hardening tensor, totally 5 individual invariants, are included in the SO model. We found that the model can characterize anisotropy due to its joint invariance. As a consequence, we can propose the new form of the SO model that satisfies the principle of objectivity. Not only isotropic hardening stress is considered but also deviatoric hardening stress is included in generalized relative stress ratio of the model. Providing that a rotational hardening is frozen, the resulted response can be reduced to the original version of the SO model without losing the generality in infinitesimal problem.

1-2-5 Methodology for enforcing a consistency requirement to the SO model

In previous numerical implementation of the SO model, we update a stress forwardly. A consistency requirement is satisfied providing that a very small incrementation is imposed. So the solution is said to be stable conditionally. If we update a stress backwardly and consider the consistency requirement simultaneously, a solution is said to be stable unconditionally. This technique has been well developed and it is called return-mapping algorithm. There are many types of stress update algorithm under return-mapping algorithm but we selected to develop one that is called Closest Point Projection Method (CPPM) because it is the most general and rigorous algorithm. Actually, the return-mapping method needs hyperelastic rule (path-independent) in its formulation. However, elasticity in soil mechanics usually refers to hypoelastic rule (path-independent) in which bulk and shear moduli are depended on isotropic pressure, $[K(p'),G(p')]$. A class of lenient hyperelasticity is also considered in which bulk modulus is depended on isotropic pressure while shear modulus is depended on a virgin consolidated stress, $[K(p'), G(p'_c)]$. Inside yield surface, hyperelasticity is satisfied but if the yield surface

is expanded its size, a response of stress on the yield surface will become hypoelasticity. A damage effect of strain-energy is considered during expanding/contracting of yield surface. Both classes of elastic rule were employed in this study. There is no problem to use hypoelasticity in monotonic loading problem but hyperelasticity is suited for repeated loading problem because energy can be conserved within a loop of stress-path. However, we will focus on hypoelasticity more than hyperelasticity in our study because many of past researches in SO model have referred to this class of elastic model, therefore, it is convenient to compare one another.

1-2-6 Methodology for formulating stress update algorithm for the SO model

A set of rate constitutive equations is composed of six governing equations. There are decomposition of elastic-plastic strain rate, nonlinear elastic stiffness, stress-strain relationship, associated flow rule, evolution law of hardening stress and yield function. Loading/unloading criteria are governed by Kuhn-Tucker complementarity condition. We obtained incremental forms of these six equations using backward-Euler differential scheme. In order to solve such a non-linear equation system, we employed a Newton method to search for solution iteratively. To start the iteration, we determined the feasible value of stress for the first step by mapping incremental strain to stress using purely elastic stiffness tensor. The relaxation of plastic strain is iteratively determined in Newton loop until the convergence of solution is reached. A Jacobian matrix of Newton method would be large if we consider all six equations in the system; therefore, we reduced the number of equations by substituted one other and obtained two equations. These are a tensorial expression for strain and a scalar equation for consistency parameter. A corresponding Jacobian matrix was obtained by tensorial manipulation. As a result, updated form of elastic strain and consistency parameter can be determined. Other state variables like those of incremental stress and hardening stress will be substituted later. Finally, all of updated processes will be stopped if the criteria for convergence are met by a specific tolerance.

1-2-7 Methodology for forming consistent tangential stiffness tensor

According to the incremental form of governing equations obtained in previous section, we differentiated these equations to obtain the variational forms. By tensorial manipulation of high order tensor, we reduced six variational equations into one variational form of stress strain relation.

A consistent tangential stiffness tensor is different from a continuum tangential stiffness tensor. A consistent tangential stiffness tensor is a gradient of updated stress tensor to updated strain tensor based on backward-Euler. There is a consistency parameter contained in the expression to enforce consistency requirement. A continuum tangential stiffness tensor is a gradient of updated stress tensor to updated strain tensor based on forward-Euler. There is no consistency parameter contained in the expression. Evaluation of consistent tangent modulus is far complicated than that of continuum tangent modulus. Consequently, a higher degree of non-linearity can be obtained in consistent tangent modulus. According to Simo and Taylor (1985) [3], it is able to show that asymptotic rate of convergence reaches a solution quadratically in a way that is faster than that of continuum tangential modulus can do.

However, we accepted that it is quite difficult to obtain the exactly backward-Euler-based consistent tangential tensor because a rank of tensor as high as sixth order is required when we differentiate an elastic stiffness tensor, which is depended on stress tensor, in respect to stress tensor. To soften the difficulty of high-order tensor, the semi-backward Euler is practiced instead. We ignored this sixth-degree order of stiffness terms in order to simplify the formulation. We simplified it by using forward Euler for elastic stiffness tensor referred to previously iterated stress point. A determination of consistent tangential tensor for anisotropic models is more difficult and complex than that of isotropic model (Borja et al. 1990, 1991 [4, 5]). Expression of elastoplastic tangential tensor is expected to expand more and more due to non-coaxiality if a complicated form of consistent elastic tensor is used. Therefore, we primarily froze the determination up to forth-order degree in this study and wish to develop for higher degree in further step of algorithm development.

Our consistent tangential tensor is numerically obtained rather than algebraically. The exactly backward-Euler-based consistent tangential tensor would be achieved when state variables converge to a solution. An error due to a disregard of sixth-order degree can be lenient when a solution is nearly approached. The same accuracy can be obtained at the end of iteration but the rate of convergence and stability may not be as good as the performance gained by that of exact backward-Euler. However, we can get the simpler form of consistent stiffness tensor by semi-backward Euler.

1-2-8 Methodology for finding an inverse of forth-order unsymmetrical tensor

We had applied the reciprocal basis to characterize stress and stress increment from previous section. We showed that in stress space, 3 individual tensor bases, which are isotropic, anisotropic and deviatoric second-order tensor bases could represent a state of stress. Later, we proved that the same 3 individual tensor bases could indicate a state of strain in strain space as well. Therefore, a forth-order tensor mapping a particular stress in stress space to the corresponding strain in strain space is existed. The spectral composition of this forth-order tensor is the summation of mapping forth-order tensor among reciprocal basis. As a result, there are 9

combinations of mapping reciprocal basis plus one deviatoric forth-order tensor. These 10 tensor bases are obviously served to map incremental stress-strain and strain-stress relations, which are stiffness tensor and compliance tensor respectively. Therefore, both stiffness and compliance tensors share the same tensor bases in their representation. The difference is the corresponding coefficients derived from the constitutive equations. We named them as constitutive coefficients.

If we refer to the consistent stiffness tensor derived in previous section. We found that it is inevitable to obtain the consistent stiffness tensor in implicit form, that is, in terms of its own inversion. We obtain the exact form of consistent compliance tensor from the constitutive equations. In order to exactly obtain the consistent stiffness tensor, we need to inverse the consistent compliance tensor. From the knowledge we had known that both tensor share the same tensor bases, we can write the spectral representation of the consistent stiffness tensor in terms of reciprocal tensor bases and their own respective unknown constitutive coefficient. The identity forth-order tensor is preserved on both space no matter Cartesian basis or reciprocal basis are applied. As a consequence, the double product of consistent stiffness tensor with compliance tensor would result in the identity tensor, which has its representation given by isotropic and deviatoric forth-order tensors. We performed the double product, which resulted in 10 by 10 multiple pairs of double product of each basis, and represented in terms of reciprocal basis of forth-order tensor. Then, we equated the double product to identity forth-order tensor. By comparison of the coefficients of each forth-order tensor bases, we obtain a linear system of 10 unknown variables. After solving these 10 unknown variables, we obtained the constitutive coefficients for the consistent tangential stiffness tensor. To ensure our solution, we verified the solution with a closed-form obtained by isotropic consistent stiffness tensor by reducing its anisotropic property.

1-2-9 Methodology for formulating implicit FEM based on the SO model

In fact, our algorithm can be applied to other anisotropic models but herein, we focused on the SO model. According to the return-mapping algorithm, there are two levels of Newton's method. First is global level for internal force update on whole nodes and second is local level for stress update on each element. A notion of elastic-split-plastic-corrector scheme based on CPPM was applied in local Newton's loop. The consistent tangential tensor was employed in global Newton's loop by casting into global stiffness matrix of FEM. A local Newton's loop is called to correct a trial stress determined by nodal displacement in global Newton's loop. An updated stress and other state parameters will be employed to compute internal forces and check whether the unbalanced force and unbalanced energy norm meet convergent criteria. If not, the updated stress and other state parameters will be used to determine the updated tangential stiffness tensor of each element and subsequently form the updated global stiffness matrix. Later, nodal displacement is recomputed repeatedly until a solution reaches convergence criteria.

4-noded rectangular with 4 Gauss points was used for spatial integration. A higher non-linearity with pore pressure node 9u-1p is subjected to develop in the future. CPPM applicable to the SO model was checked by simple problems such as drained/undrained compression tests, K_o-consolidation test, drained/undrained simple shear tests. In global level, an example of IBVP (initial-boundary-value-problem) using 4 elements uni-axial compression simulation was investigated. A more complicated soil/water coupling IBVP is subjected to test when full implementation of the method is coded to computer program.

1-3 Structure of the dissertation

Chapter 1:Introduction
State of purposes and introductory outline are noted. The notations, definitions and symbols used all over a thesis are defined. Finally, a flow of study and guideline for reader are presented.

Chapter 2: Theoretical background
This section provides the mathematical foundation used throughout the study. The theoretical backgrounds include mathematical preliminary, tensor theory ranging from first, second, third, forth and high order tensor, tensor analyses, theory of stress and strain, constitutive models, numerical methods, Newton method and Central limit theorem.

Chapter 3: Convex Analysis
The fundamental implementation to deal with multiple non-smooth yield criteria is developed based on the associated flow rule extended by Koiter (1953, 1960). The condition of discontinuity in the SO model is explored. Numerical implementation of plastic flow at the corner is developed.

Chapter 4: Soil Initial Anisotropy
The derivations of Ko-value based on constitutive models are carried out. According to Koiter's associated flow rule and a concept of immobilized/mobilized plastic flow at the corner, relation between Ko-value, Poisson's ratio and internal friction angle is found. The same relation can be obtained from Central limit theorem by

interpreting Koiter's condition by a view that a plastic flow at the corner lies within a fan of equal possibility. Comparisons with empirical relations are performed to ensure the applicability of Koiter's associated flow rule to the hardening vertex of the SO model.

Chapter 5: Singular Hardening Vertex
A format of the SO model is modified in consistent with the modern theory of plasticity and current development in computational mechanics. Useful information about numerical implementation of this kind of particular constitutive model is contributed. A geometric representation of the model points out that there is only one point of singularity located in a virgin K_o-consolidation stress in axisymmetric triaxial plane of stress. This particular stress is also referred to the material memory of the model. A state of reference connected to the initial yield stress in the model is changed to the current yield stress in order to satisfy the principle of objectivity. The non-coaxiality between stress and strain can be clearly characterized by relative mapping quantity based on a reciprocal basis defined in replace of Cartesian tensor.

Chapter 6: Stress Update Algorithm
For primary study, a simple return-mapping method based on two stress invariants is applied to the SO model in triaxial stress plane. In order to evaluate the rate of convergence and solution accuracy generated by the algorithm, numerical simulations are carried out by unconsolidated undrained test and K_o-consolidation test.

Chapter 7: Closest Point Projection Method
A rigorous framework for nonlinear analysis for stress-strain-strength of clays by return-mapping algorithm based on CPPM is arranged in line with hyperelasticity considering damage process. An elastic model of pressure-dependent bulk modulus and virgin-consolidated stress-dependent shear modulus is examined. The complete stress-update algorithm for the SO in generalized space is provided.

Chapter 8: Consistent Tangential Stiffness Tensor
Generalized concept of implicit integration algorithm formulated for anisotropic soil models is developed. Semi-backward Euler for pressure-dependent hypoelasticity is employed to simplify the complexity of elastoplastic responses. Algorithmic moduli are derived from the nonlinear backward-Euler incremental system of governing equations. The consistent tangential moduli in regard to the anisotropic models and the SO model in particular are derived.

Chapter 9: Tensorial Inversion Technique
In order to raise the performance of algorithms, the mathematical technique for forth-order tensor inversion is introduced. Instead of computing the consistent tangential moduli implicitly, the exactly closed form can be obtained, giving a by-passed step in computations.

Chapter 10: Implicit Finite Element Method
The global and local solution schemes are processed by Newton method. Iteration in local Newton loop updates the stress by enforcing to yield surface while global Newton loop searches for a solution to lessen the residuals of unbalanced force and energy norms. Implicit FEM procedures are developed using 4 Gauss-point iso-parametric 2D-elelement. A program is applied to initial-boundary-value-problem to test a performance. Consolidated drained test under plane strain condition is calculated using convergence criteria by specific tolerance. An asymptotic quadratic rate of convergence is obtained for both force and energy norms of residual. It is found that the algorithm is independent of sub-incrementation. A high accuracy of a method can be obtained even a single step.

Chapter 11: Numerical Analysis
This section is devoted to the illustrations and examples generated by numerical methodology. Step-by-step procedures and detailed calculations are provided. The accuracy assessment of the stress update algorithms is evaluated by isoerror maps. The verification of semi-consistent tangential stiffness tensor is achieved via numerical differentiation.

Chapter 12: Discussion and Summary
Discussions and summaries drawn from all of chapter are collected. Prospect research plans are left for further development. The study is believed to pave a way for large-scale computation platform in the future.

Appendix A: Tensor analysis
Manipulation of tensorial expressions and proofs are assembled.

Appendix B: Sekiguchi-Ohta plasticity
A complete reference for equation manipulations concerned with the Sekiguchi-Ohta plasticity is contributed.

Appendix C: Ohta-Hata plasticity
Coupled equations of upper and lower yield loci in the notion of Ohta-Hata plasticity are handled.

Appendix D: Ko-value
Ko-values obtained by constitutive equations are derived in details and compare one another with that of original-Cam clay and modified-Cam clay.

Appendix E: Soil elasticity
Elastic tangential moduli of soil models based on linear, non-linear and secant moduli for both hypoelasticity and hyperelasticity are derived.

Appendix F: Linearization
A systematic nonlinear equations and its solution pertaining to implicit integration algorithms is compiled for comprehensive reference.

Appendix G: Form-invariance principle
A pool of invariant form of stress retained in constitutive equations is devoted. A proof for objectivity of constitutive model is supplemented.

1-4 Interdependence of chapters

It may be worthwhile to pursue the reading paths, which indicate the interdependence of the chapters shown in Figure 1.3. According to Figure 1.2, a basic guidance is required to prepare the theoretical comprehension and motivation to the concepts. An advanced guidance is suited for those who have a sufficient background; therefore, the suggested reading paths may be bypassed. For those who are interested only return-mapping methods, the sections involved corner treatment can be exempted. In the opposite way, the sections involved return-mapping algorithm can be ignored for those who are mainly focused in the corner treatment in yield surface.

Basic reader for return-mapping method
Ch.1: Introduction
Ch.2: Theoretical Background
Ch.6: Stress Update Algorithm

Basic reader for corner treatment
Ch.1: Introduction
Ch.2: Theoretical Background
Ch.3: Convex Analysis
Ch.4: Soil Initial Anisotropy

Advanced reader for return-mapping method
Ch.7: Closest Point Projection Method
Ch.8: Consistent Tangential Stiffness Tensor
Ch.9: Tensorial Inversion Technique
Ch.10: Implicit Finite Element Method
Ch.11: Numerical Analysis

Advanced reader for corner treatment
Ch.3: Convex Analysis
Ch.5: Singular Hardening Vertex

Figure 1.2 Suggestions for basis and advanced reader
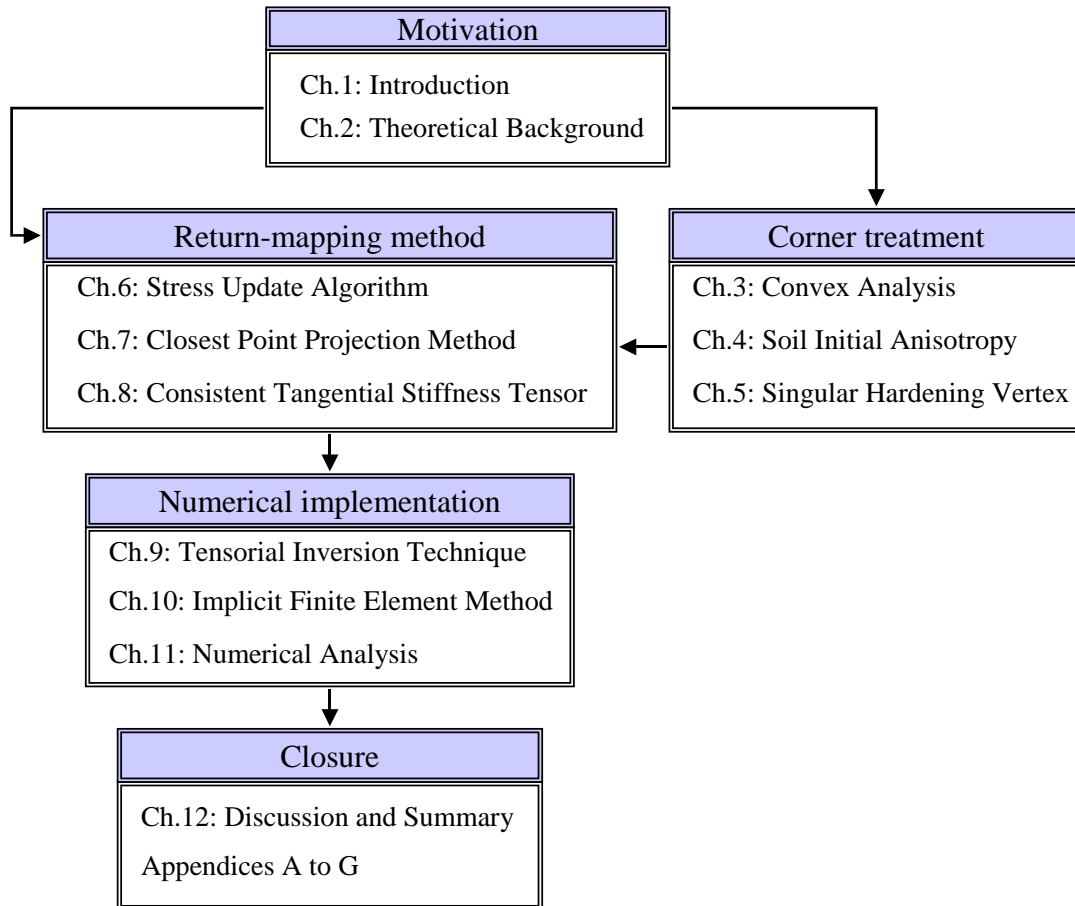
Figure 1.3 Reading paths

1-5 Notational conventions

A unified style and notation are used as much as possible throughout this thesis. Principal notations are summarized in a brief glossary.

Stresses

$\boldsymbol{\sigma}$	=	Cauchy stress tensor
$\boldsymbol{\sigma}'$	=	effective Cauchy stress tensor
$\boldsymbol{\sigma}'_o$	=	effective initial consolidated stress tensor
$\boldsymbol{\sigma}'_c$	=	effective virgin consolidated stress tensor
$\boldsymbol{\sigma}'^{tr}$	=	trial effective stress
$\boldsymbol{\sigma}'_n$	=	$\boldsymbol{\sigma}'$ at step n
$\mathbf{s}$	=	stress deviator
$\mathbf{s}_o$	=	initial K_o-consolidated stress deviator
$\mathbf{s}_c$	=	virgin K_o-consolidated stress deviator
$\overline{\mathbf{s}}$	=	relative stress deviator
σ'_{vo}	=	preconsolidation overburden pressure
σ'_{vi}	=	overburden pressure
σ_{xy}	=	stress on plane x in direction of y-axis
σ_a	=	axial stress
σ_r	=	radial stress
γ	=	shear stress

σ'_a	=	axial effective stress
σ'_r	=	radial effective stress
σ'_v	=	vertical effective stress
σ'_h	=	horizontal effective stress
σ'_1	=	major principal stress
σ'_2	=	intermediate principal stress
σ'_3	=	minor principal stress
I_1	=	first invariant of stress
I_2	=	second invariant of stress
I_3	=	third invariant of stress
J_2	=	second invariant of stress deviator
J_{c2}	=	second invariant of stress hardening
$\bar{J}_2$	=	second anisotropic invariant of relative stress deviator
p'	=	mean effective stress
p'_i	=	mean effective initial stress
p'_o	=	mean effective stress right after the completion of consolidation
p'_c	=	mean effective virgin consolidated stress
p^{tr}	=	trial mean effective stress
q	=	deviatoric stress
q^{tr}	=	trial deviatoric stress
η	=	stress ratio; q/p'
η_o	=	stress ratio at K_o-condition; q_o/p'_o
η_i	=	stress ratio at initial-condition; q_i/p'_i
η^*	=	generalized stress ratio; $\sqrt{\frac{3}{2}\left(\frac{s_{ij}}{p'} - \frac{s_{oij}}{p'_o}\right)\left(\frac{s_{ij}}{p'} - \frac{s_{oij}}{p'_o}\right)}$
$\bar{\eta}$	=	generalized relative stress ratio; $\sqrt{\frac{3}{2}\left(\frac{s_{ij}}{p'} - \frac{s_{cij}}{p'_c}\right)\left(\frac{s_{ij}}{p'} - \frac{s_{cij}}{p'_c}\right)}$
$\boldsymbol{\eta}$	=	normalized stress deviator by mean effective stress
$\boldsymbol{\eta}_o$	=	normalized stress deviator by mean effective stress (initial yielding)
$\boldsymbol{\eta}_c$	=	normalized stress deviator by mean effective stress (current yielding)
$\mathbf{n}$	=	unit normal of stress deviator

Strains

$\boldsymbol{\varepsilon}$	=	infinitesimal strain tensor (compression positive)
$\boldsymbol{\varepsilon}^e$	=	elastic strain tensor
$\boldsymbol{\varepsilon}^p$	=	plastic strain tensor
$\boldsymbol{\varepsilon}^{tr}$	=	trial strain tensor
ε_v	=	volumetric strain
ε_v^e	=	volumetric elastic strain
ε_v^p	=	volumetric plastic strain
$\boldsymbol{\varepsilon}_d$	=	distortional strain

ε_d^e	=	elastic distortional strain
ε_d^p	=	plastic distortional strain
ε_s	=	deviatoric strain
ε_s^e	=	deviatoric elastic strain
ε_s^p	=	deviatoric plastic strain
ε_a	=	axial strain
ε_r	=	radial strain
ε_a^e	=	axial elastic strain
ε_a^e	=	radial elastic strain
ε_a^p	=	axial plastic strain
ε_a^p	=	radial plastic strain

Stress-strain relations

$\mathbf{c}^e$	=	elastic stiffness forth-order tensor
$\mathbf{d}^e$	=	elastic compliance forth-order tensor
$\mathbf{c}^{ep}$	=	elastoplastic stiffness forth-order tensor
$\mathbf{d}^{ep}$	=	elastoplastic compliance forth-order tensor
$\mathbf{c}^{ep*}$	=	elastoplastic stiffness forth-order tensor for the corner
$\mathbf{C}$	=	stiffness 2x2 matrix
$\mathbf{E}$	=	compliance of stiffness 2x2 matrix
$\mathbf{\Xi}$	=	algorithmic tensor
$\mathbf{c}_s^e$	=	secant elastic stiffness forth-order tensor
$\mathbf{c}_{n+1}^e$	=	consistent elastic stiffness forth-order tensor
$\mathbf{c}_{n+1}^{ep}$	=	consistent elastoplastic stiffness forth-order tensor

Material parameters

K	=	bulk modulus of soil skeleton
G	=	shear modulus of soil skeleton
G_s	=	secant shear modulus of soil skeleton
M	=	critical state parameter
D	=	coefficient of dilatancy
K_o	=	coefficient of lateral earth pressure at rest (virgin)
K_i	=	coefficient of earth pressure at rest (in-situ)
ν'	=	Poisson's ratio of soil skeleton
μ'	=	a constant ratio of shear modulus to bulk modulus; G/K
ϕ'	=	effective internal friction angle
Λ	=	irreversibility ratio
λ	=	virgin compression index (ln-scale)
κ	=	swelling index (ln-scale)
$\overline{\lambda}$	=	compressibility index (ln-scale)
$\overline{\kappa}$	=	recompressibility index (ln-scale)
C_c	=	compression index ($\log_{10}$-scale)
C_s	=	swelling index ($\log_{10}$-scale)
e	=	void ratio
e_o	=	void ratio at σ'_{vo}

PI, I_p	=	plasticity index

Plastic symbols

D^p, D	=	plastic dissipation energy
$f()$	=	yield function
$f_U()$	=	upper yield function/locus
$f_L()$	=	lower yield function/locus
$\mathsf{H}(\alpha)$	=	hardening potential
α	=	strain hardening parameter
h	=	selective isotropic hardening parameter
γ	=	rate consistency parameter
$\Delta\gamma$	=	consistency parameter; $\gamma\Delta t$
H_e	=	scalar elastic modulus
H_p	=	scalar plastic modulus
γ_U	=	rate consistency parameter for upper yield surface
γ_L	=	rate consistency parameter for lower yield surface
$\mathbf{q}$	=	set of hardening parameters
$\mathbf{L}$	=	vector of loading parameters (upper-lower yield surfaces)
L_U	=	loading parameter in corresponding to upper yield surface
L_L	=	loading parameter in corresponding to lower yield surface
$\bar{\mathbf{X}}, \mathbf{X}$	=	matrix of coupled-hardening plasticity (upper-lower yield surfaces)
$\tilde{\mathbf{X}}$	=	matrix of decoupled-hardening plasticity (upper-lower yield surfaces)
χ	=	inversion of $\mathbf{X}$
β	=	angle of dilation
θ	=	angle of third invariant in deviatoric plane

Tensors

(x_1, x_2, x_3)	=	spatial coordinates
x,y,z	=	x/y/z-axis of Cartesian coordinates
i,j,k,l	=	spatial indices
δ_{ij}	=	Kronecker delta
$\mathbf{e}_i$	=	orthonormal basis
$\mathbf{Q}$	=	proper orthogonal second-order tensor
$\mathbf{1}$	=	second-order identity tensor
$\mathbf{n}$	=	second-order unit normal of stress deviator
$\bar{\mathbf{n}}$	=	second-order unit normal of relative stress deviator
$\mathbf{1} \otimes \mathbf{1}$	=	forth -order isotropic tensor
$\mathbf{A}$	=	forth-order deviatoric tensor
$\bar{\mathbf{A}}$	=	forth-order anisotropic tensor

Operators

$\dot{x}$	=	rate of x
Δx	=	x increment, delta x
δx	=	variation of x
$x^{<k>}$	=	x at iteration number k
x_n	=	x at step n

$\dfrac{\partial F}{\partial x}$ = the derivative of F with respect to x

$\dfrac{\partial^2 F}{\partial x^2}$ = the second derivative of F with respect to x

$\dfrac{\partial F}{\partial t}, \dfrac{dF}{dt}$ = time derivative of F

$\dfrac{\partial F}{\partial x_i}, \dfrac{\partial F}{\partial \mathbf{x}}, \partial_{\mathbf{x}} F$ = divergence of F

$\langle x \rangle$ = ramp function; $\dfrac{x + |x|}{2}$

$\|\mathbf{x}\|$ = norm of tensor $\mathbf{x}$

FEM

$\mathbf{B}$	=	strain-displacment matrix, kinematic matrix
$\mathbf{d}$	=	nodal displacement
$\mathbf{k}$	=	element tangent stiffness matrix
$\mathbf{K}$	=	global stiffness matrix
$\mathbf{N}$	=	interpolation function
$\mathbf{N}'$	=	derivative of interpolation function
$\mathbf{F}^{ext}$	=	external force vector
$\mathbf{F}^{int}$	=	internal force vector
Γ	=	problem boundary
Ω	=	problem domain

Sets

$\in$	=	"is a member of"
$\subset$	=	"is a subset of
$\mathbb{R}$	=	real numbers
$\mathbb{S}$	=	vector space of symmetric second-order tensor

Constants

k_c	=	controlled-step of convergence
TOL	=	tolerance

1-6 Reference

1 Sekiguchi, H. & Ohta, H., Induced anisotropy and time dependency in clays, Proc. ICSMFE 9th, Tokyo: 229-238, 1977

2 Koiter, W.T., Stress-strain relations, uniqueness and variational theorems for elastic-plastic materials with a singular yield surface, Quart. Appl. Math. (11):350-354, 1953

3 Simo, J.C. & Tayor, R.L., Consistent tangent operators for rate-independent elastoplasticity, Comput. Methods Appl. Mech. Engrg., 48:101-118, 1985

4 Borja, R.I. & Seung, R.L., Cam-Clay plasticity, part I: implicit integration of elasto-plastic constitutive relations, Comput. Methods Appl. Mech. Engrg., 78:49-72, 1990

5 Borja, R.I., Cam-Clay plasticity, Part II, Implicit integration of constitutive equation based on a nonlinear elastic stress predictor, Comput. Methods Appl. Mech. Engrg. 88:225-240, 1991

CHAPTER 2

Theoretical Background

2-1 Tensors

Due to the heavily mathematical subject matter, the basic preliminary is necessary to include in the beginning of this thesis. Other eminent text books (Bird, R.B. et al, 1960 [1], Ogden, R.W., 1984 [2], Bonet, J. et al, 1997 [3]) are suggested for additional references. The main concepts to cover are vector and tensor algebra, directional derivative, linearization of nonlinear quantities and Newton method.

2-1-1 First-order tensors

The basic concepts that will be used throughout the thesis are introduced and summarized. Boldface symbols denote tensors. Italic symbols denote scalar components. Three unit vectors in rectangular Cartesian coordinate systems are denoted by e_1, e_2 and e_3. Any given vector v can be expressed as a linear combination of these orthonormal vectors as,

$$\mathbf{v} = \sum_{i=1}^{3} v_i \mathbf{e}_i \tag{2.1}$$

Components of $\mathbf{v}$ can be presented by,

$$v_i = \mathbf{v} \cdot \mathbf{e}_i \tag{2.2}$$

The unit base vector $\{\mathbf{e}_i\}$ in the direction of three coordinate axes are expressed by

$$\mathbf{e}_1 = \begin{Bmatrix} 1 \\ 0 \\ 0 \end{Bmatrix}; \mathbf{e}_2 = \begin{Bmatrix} 0 \\ 1 \\ 0 \end{Bmatrix}; \mathbf{e}_3 = \begin{Bmatrix} 0 \\ 0 \\ 1 \end{Bmatrix} \tag{2.3}$$

The scalar or dot product of these two vectors can be given by,

$$\mathbf{e}_i \cdot \mathbf{e}_j = \delta_{ij} \tag{2.4}$$

Actually, scalar can be regarded as zero-order tensor, vectors as first-order tensor.

Where $\delta_{ij} = \begin{cases} 1 & if \quad i = j \\ 0 & if \quad i \neq j \end{cases}$ is Kronecker delta

Scalar product (simple product) of two vectors is defined as,

$$\mathbf{u} \cdot \mathbf{v} = u_i v_i \tag{2.5}$$

Norm of vector $\mathbf{v}$ is,

$$\|\mathbf{v}\| = (\mathbf{v} \cdot \mathbf{v})^{\frac{1}{2}} \tag{2.6}$$

Unit vector in direction of $\mathbf{v}$ is marked by,

$$\hat{\mathbf{v}} = \frac{\mathbf{v}}{\|\mathbf{v}\|} \tag{2.7}$$

A tensor product is defined by operator $\otimes$ in such a way that,

$$\mathbf{u} \otimes \mathbf{v} = u_i v_j \mathbf{e}_i \otimes \mathbf{e}_j \quad \text{or} \quad (\mathbf{u} \otimes \mathbf{v})_{ij} = u_i v_j \tag{2.8}$$

The product becomes a second-order tensor. Consequently,

$$(\mathbf{u} \otimes \mathbf{v})^T = \mathbf{v} \otimes \mathbf{u} \tag{2.9}$$

The result in above equations can be viewed simply as,

$$\mathbf{u} \otimes \mathbf{v} = \mathbf{u} \cdot \mathbf{v}^T \tag{2.10}$$

The distribution property can be observed,

$$\mathbf{u} \otimes (\mathbf{v} + \mathbf{w}) = \mathbf{u} \otimes \mathbf{v} + \mathbf{u} \otimes \mathbf{w} \tag{2.11}$$

A mapping from vector $\mathbf{w}$ to $\mathbf{u}$ can be presented by,

$$(\mathbf{u} \otimes \mathbf{v}) \cdot \mathbf{w} = (\mathbf{w} \cdot \mathbf{v})\mathbf{u} \tag{2.12}$$

A mapping from tensor $\mathbf{x} \otimes \mathbf{y}$ to $\mathbf{u} \otimes \mathbf{v}$ can be presented by,

$$(\mathbf{u} \otimes \mathbf{v}) \cdot (\mathbf{x} \otimes \mathbf{y}) = (\mathbf{v} \cdot \mathbf{x})\mathbf{u} \otimes \mathbf{y} \quad \text{or} \quad ((\mathbf{u} \otimes \mathbf{v}) \cdot (\mathbf{x} \otimes \mathbf{y}))_{ij} = u_i v_k x_k y_j \tag{2.13}$$

The multiplication signs may be interpreted as,

Multiplication signs	Product	Order of result
$\otimes$	tensor product	Σ
$\times$	vector product	Σ-1
$\cdot$	dot product	Σ-2
$:$	double dot product	Σ-4

where Σ represents the sum of the orders of the quantities being multiplied.

2-1-2 Second-order tensors

A second-order tensor $\mathbf{T}$ on Euclidean space $\mathbb{E}$ in respect to an orthonormal basis $\{\mathbf{e}_i\}$ are shown by,

$$\mathbf{T} = T_{ij}\mathbf{e}_i \otimes \mathbf{e}_j \tag{2.14}$$

Several kinds of multiplication are possible for vectors and tensors. Single dot is used to indicate simple product defined as following,

$$\begin{aligned}
\mathbf{T} \cdot \mathbf{v} &= T_{ij}v_k \left(\mathbf{e}_i \otimes \mathbf{e}_j\right) \cdot \mathbf{e}_k \\
&= T_{ij}v_k \mathbf{e}_i \left(\mathbf{e}_j \cdot \mathbf{e}_k\right) \\
&= T_{ik}v_k \mathbf{e}_i
\end{aligned} \tag{2.15}$$

A second-order tensor $\mathbf{T}$ is a linear mapping that associates a given vector $\mathbf{u}$ with a second vector $\mathbf{v}$ as,

$$\mathbf{v} = \mathbf{T} \cdot \mathbf{u} \tag{2.16}$$

A resulting linear transformation can be shown in such that

$$\left(\alpha\mathbf{T} + \beta\mathbf{S}\right) \cdot \mathbf{u} = \alpha\mathbf{T} \cdot \mathbf{u} + \beta\mathbf{S} \cdot \mathbf{u} \tag{2.17}$$

$$\mathbf{T} \cdot \left(\alpha\mathbf{u} + \beta\mathbf{v}\right) = \alpha\mathbf{T} \cdot \mathbf{u} + \beta\mathbf{T} \cdot \mathbf{v} \tag{2.18}$$

The zero second-order tensor maps every vector to zero vector.

$$\mathbf{0} \cdot \mathbf{u} = \mathbf{0} \tag{2.19}$$

A second-order tensor that maps any given vector onto itself is the identity tensor

$$\mathbf{1} \cdot \mathbf{u} = \mathbf{u} \tag{2.20}$$

The identity second-order tensor is shown by,

$$\mathbf{1} = \begin{bmatrix} 1 & 0 & 0 \\ 0 & 1 & 0 \\ 0 & 0 & 1 \end{bmatrix} = \sum_{i,j=1}^{3} \delta_{ij}\mathbf{e}_i \otimes \mathbf{e}_j = \sum_{i=1}^{3} \mathbf{e}_i \otimes \mathbf{e}_i \tag{2.21}$$

Components of second-order tensor $\mathbf{T}$ can be identified by,

$$T_{ij} = \mathbf{e}_i \cdot \mathbf{T} \cdot \mathbf{e}_j \tag{2.22}$$

A single product of second-order tensor $\mathbf{T}$ and tensor $\mathbf{S}$ is expressed by,

$$\begin{aligned}
\mathbf{T} \cdot \mathbf{S} &= T_{ij}S_{kl} \left(\mathbf{e}_i \otimes \mathbf{e}_j\right) \cdot \left(\mathbf{e}_k \otimes \mathbf{e}_l\right) \\
&= T_{ij}S_{kl} \left(\mathbf{e}_i \otimes \mathbf{e}_l\right)\left(\mathbf{e}_j \cdot \mathbf{e}_k\right) \\
&= T_{ik}S_{kl} \left(\mathbf{e}_i \otimes \mathbf{e}_l\right)
\end{aligned} \tag{2.23}$$

The result shown in Eq.(2.23) is a second-order tensor where components can be expressed as,

$$\left(\mathbf{T} \cdot \mathbf{S}\right)_{ij} = \mathbf{T}_{ik}\mathbf{S}_{kj} \tag{2.24}$$

$$\left(\mathbf{T} \cdot \mathbf{S}\right) \cdot \mathbf{u} = \mathbf{T} \cdot \left(\mathbf{S} \cdot \mathbf{u}\right) \tag{2.25}$$

A transpose of $\mathbf{T}$ can be defined by,

$$\mathbf{u} \cdot \mathbf{T}^T \cdot \mathbf{v} = \mathbf{T} \cdot \mathbf{u} \cdot \mathbf{v} \tag{2.26}$$

A transpose of a second-order tensor $\mathbf{T}$ can be shown by,

$$\mathbf{T}^T = T_{ij}\mathbf{e}_j \otimes \mathbf{e}_i = T_{ji}\mathbf{e}_i \otimes \mathbf{e}_j \tag{2.27}$$

Corollary,

$$\left(\mathbf{T}^T\right)^T = \mathbf{T} \tag{2.28}$$

$$\left(\alpha\mathbf{T} + \beta\mathbf{S}\right)^T = \alpha\mathbf{T}^T + \beta\mathbf{S}^T \tag{2.29}$$

$$\left(\mathbf{T} \cdot \mathbf{S} \cdot \mathbf{R}\right)^T = \mathbf{R}^T \cdot \mathbf{S}^T \cdot \mathbf{T}^T \tag{2.30}$$

$$\left(\mathbf{T}^{-1}\right)^T = \left(\mathbf{T}^T\right)^{-1} \equiv \mathbf{T}^{-T} \tag{2.31}$$

$$\mathbf{S} \cdot \left(\mathbf{u} \otimes \mathbf{v}\right) = \mathbf{S} \cdot \mathbf{u} \otimes \mathbf{v} \tag{2.32}$$

$$\left(\mathbf{u} \otimes \mathbf{v}\right) \cdot \mathbf{S} = \mathbf{u} \otimes \mathbf{S}^T \cdot \mathbf{v} \tag{2.33}$$

If $\mathbf{T}^T = \mathbf{T}$, then $\mathbf{T}$ is symmetric tensor. If $\mathbf{T}^T = -\mathbf{T}$, then $\mathbf{T}$ is skew-symmetric tensor.
An arbitrary tensor can be expressed uniquely as the sum of symmetric and skew-symmetric parts as shown,

$$\mathbf{T} = \underbrace{\frac{1}{2}(\mathbf{T} + \mathbf{T}^T)}_{(symmetric)} + \underbrace{\frac{1}{2}(\mathbf{T} - \mathbf{T}^T)}_{(skew-symmetric)} \tag{2.34}$$

Double dot are used to indicate double product (contraction) defined as following,

$$\mathbf{T}:\mathbf{S} = T_{ij}S_{kl}\left(\mathbf{e}_i \otimes \mathbf{e}_j\right):\left(\mathbf{e}_k \otimes \mathbf{e}_l\right)$$
$$= T_{ij}S_{kl}\left(\mathbf{e}_i \cdot \mathbf{e}_k\right)\left(\mathbf{e}_j \cdot \mathbf{e}_l\right) \qquad (2.35)$$
$$= T_{ij}S_{ij}$$

The result shown in Eq.(2.35) is scalar. Magnitude of a second-order tensor $\mathbf{T}$ can be defined by,

$$\|\mathbf{T}\| = \left(\mathbf{T}:\mathbf{T}\right)^{\frac{1}{2}} \qquad (2.36)$$

According to Eq.(2.35), for $\mathbf{S}=\mathbf{1}$, a double product is a trace of second-order tensor which can be shown by,

$$\mathbf{T}:\mathbf{1} = T_{ij}\delta_{ij} = T_{ii} = tr\left(\mathbf{T}\right) \qquad (2.37)$$

Corollary,

$$tr\left(\mathbf{u} \otimes \mathbf{v}\right) = \mathbf{u} \cdot \mathbf{v} \qquad (2.38)$$

$$tr\left(\mathbf{T}^T\right) = tr\left(\mathbf{T}\right) \qquad (2.39)$$

$$tr\left(\alpha\mathbf{T} + \beta\mathbf{S}\right) = \alpha tr\mathbf{T} + \beta tr\mathbf{S} \qquad (2.40)$$

$$tr\left(\mathbf{T} \cdot \mathbf{S}\right) = tr\left(\mathbf{S} \cdot \mathbf{T}\right) \qquad (2.41)$$

$$tr\left(\mathbf{T} \cdot \mathbf{S} \cdot \mathbf{R}\right) = tr\left(\mathbf{R} \cdot \mathbf{T} \cdot \mathbf{S}\right) = tr(\mathbf{S} \cdot \mathbf{R} \cdot \mathbf{T}) \qquad (2.42)$$

The relation between double dot product and trace can be presented by,

$$\mathbf{S}:\mathbf{T} = tr\left(\mathbf{S}^T \cdot \mathbf{T}\right) = tr\left(\mathbf{T} \cdot \mathbf{S}^T\right) = tr\left(\mathbf{S} \cdot \mathbf{T}^T\right) = tr\left(\mathbf{T}^T \cdot \mathbf{S}\right) = S_{ij}T_{ij} \qquad (2.43)$$

For $\mathbf{S}=\mathbf{T}$, a double product is a trace of second-order tensor which can be shown by,

$$\mathbf{T}:\mathbf{T} = tr\left(\mathbf{T}^T \cdot \mathbf{T}\right) = T_{ij}T_{ij} \qquad (2.44)$$

Further useful properties of the double product are,

$$\mathbf{T}:(\mathbf{u} \otimes \mathbf{v}) = T_{ij}u_i v_j = u_i T_{ij} v_j = \left(\mathbf{T} \cdot \mathbf{v}\right) \cdot \mathbf{u} \qquad (2.45)$$

$$\left(\mathbf{u} \otimes \mathbf{v}\right):\left(\mathbf{x} \otimes \mathbf{y}\right) = u_i v_j x_i y_j = u_i x_i v_j y_j = \left(\mathbf{u} \cdot \mathbf{x}\right)\left(\mathbf{v} \cdot \mathbf{y}\right) \qquad (2.46)$$

A product of a given second-order tensor $\mathbf{T}$ and its inverse $\mathbf{T}^{-1}$ results in the identity tensor.

$$\mathbf{T} \cdot \mathbf{T}^{-1} = \mathbf{T}^{-1} \cdot \mathbf{T} = \mathbf{1} \qquad (2.47)$$

Then $\mathbf{T}$ is called an invertible tensor or non-singular tensor defined in a way that

$$\det\left(\mathbf{T}\right) \neq 0 \qquad (2.48)$$

Determinant of $\mathbf{T}$ is defined as the determinant of the matrix T with respect to an orthonormal basis. Det($\mathbf{T}$) is scalar invariant of $\mathbf{T}$.

$$\det\left(\mathbf{T}\right) = \varepsilon_{ijk}T_{i1}T_{j2}T_{k3} \qquad (2.49)$$

where ε_{ijk}, which is called the alternating symbol, is defined by,

$$\varepsilon_{ijk} = \begin{cases} 1 & (ijk) \quad is \quad a \quad cyclic \quad permutation \quad of \quad (123) \\ -1 & (ijk) \quad is \quad an \quad anticyclic \quad permutation \quad of \quad (123) \\ 0 & otherwise \end{cases} \qquad (2.50)$$

For $\det\left(\mathbf{S}\right) \neq 0$,

$$\left(\mathbf{S} \cdot \mathbf{T}\right)^{-1} = \mathbf{T}^{-1} \cdot \mathbf{S}^{-1} \qquad (2.51)$$

Since $\mathbf{u} \otimes \mathbf{v}$ is rank 1 tensor, the determinant is zero,

$$\det\left(\mathbf{u} \otimes \mathbf{v}\right) = 0 \qquad (2.52)$$

Some properties of the determinant for second-order tensors are summarized as following,

$$\det\left(\mathbf{1}\right) = 1 \qquad (2.53)$$

$$\det\left(\mathbf{T}^T\right) = \det\left(\mathbf{T}\right) \qquad (2.54)$$

$$\det\left(\alpha\mathbf{T}\right) = \alpha^3 \det\left(\mathbf{T}\right) \qquad (2.55)$$

$$\det\left(\mathbf{T} \cdot \mathbf{S}\right) = \det\left(\mathbf{T}\right)\det\left(\mathbf{S}\right) \qquad (2.56)$$

$$\det\left(\mathbf{T}^{-1}\right) = \det\left(\mathbf{T}\right)^{-1} \qquad (2.57)$$

The relationship between determinant and trace is expressed by,

$$\det\left(\mathbf{S}\right) = \frac{1}{3}tr(\mathbf{S} \cdot \mathbf{S} \cdot \mathbf{S}) = \frac{1}{3}\mathbf{S}^T :\left(\mathbf{S} \cdot \mathbf{S}\right) \qquad (2.58)$$

2-1-3 Eigenvalues and Eigenvectors

For an arbitrary second-order tensor $\mathbf{T}$, a mapping to vector $\mathbf{v}$ can be existed to itself in such a way that,

$$\mathbf{T} \cdot \mathbf{v} = \lambda \mathbf{v} \tag{2.59}$$

Alternatively,

$$(\mathbf{T} - \lambda \mathbf{1}) \cdot \mathbf{v} = \mathbf{0} \tag{2.60}$$

λ is called the eigenvalue or proper number of T corresponding to the eigenvector $\mathbf{v}$.

For non-trivial solution for $\mathbf{v}$, that is $\mathbf{v} \neq \mathbf{0}$, if and only if, the characteristic equation for $\mathbf{T}$ is satisfied by

$$\det(\mathbf{T} - \lambda \mathbf{1}) = 0 \tag{2.61}$$

In according to Eq.(2.49), the determinant term can be expanded to,

$$\lambda^3 - I_1 \lambda^2 + I_2 \lambda - I_3 = 0 \tag{2.62}$$

where

$$I_1 = tr(\mathbf{T}) \tag{2.63}$$

$$I_2 = \frac{1}{2}\left\{ tr(\mathbf{T})^2 - tr(\mathbf{T}^2) \right\} \tag{2.64}$$

$$I_3 = \det(\mathbf{T}) = \frac{1}{6}\left\{ tr(\mathbf{T})^3 - 3tr(\mathbf{T})tr(\mathbf{T}^2) + 2tr(\mathbf{T}^3) \right\} \tag{2.65}$$

Referring to Eq.(2.59), repeated application of $\mathbf{T}$ can be obtained for any positive integer n.

$$\mathbf{T}^n \cdot \mathbf{v} = \lambda^n \mathbf{v} \tag{2.66}$$

Multiply Eq.(2.62) with $\mathbf{v}$ and consider Eq.(2.66), Cayley-Hamilton theorem can be proved,

$$\mathbf{T}^3 - I_1 \mathbf{T}^2 + I_2 \mathbf{T} - I_3 \mathbf{1} = \mathbf{0} \tag{2.67}$$

Furthermore, it is proven that $\mathbf{T}^n$ is expressible in terms of $\mathbf{1}$, $\mathbf{T}$ and $\mathbf{T}^2$ for any positive or negative integer n.

2-1-4 Symmetric tensors

For a symmetry tensor $\mathbf{T} = \mathbf{T}^T$, the eigenvectors of T are mutually orthogonal and the eigenvalues are real. The spectral representation of symmetric tensor T with respect to the basis $\{\mathbf{v}_i\}$ is identified by,

$$\mathbf{T} = \sum_{i=1}^{3} \lambda_i \mathbf{v}_i \otimes \mathbf{v}_i \tag{2.68}$$

where $\mathbf{v}_i$ (i=1,2,3) are orthonormal sets of proper vectors

λ_i (i=1,2,3) are associated proper numbers

For positive semi-definite, that is $\mathbf{v} \cdot \mathbf{T} \cdot \mathbf{v} \geq 0$ where $\forall \mathbf{v} \in \mathbb{R}^1, \mathbf{v} \neq \mathbf{0}, \lambda_i \geq 0$

$$\mathbf{T}^{\frac{1}{2}} = \sum_{i=1}^{3} \lambda_i^{\frac{1}{2}} \mathbf{v}_i \otimes \mathbf{v}_i \tag{2.69}$$

For positive definite, that is $\mathbf{v} \cdot \mathbf{T} \cdot \mathbf{v} > 0$ where $\forall \mathbf{v} \in \mathbb{R}^1, \mathbf{v} \neq \mathbf{0}, \lambda_i > 0$

$$\mathbf{T}^{-1} = \sum_{i=1}^{3} \lambda_i^{-1} \mathbf{v}_i \otimes \mathbf{v}_i \tag{2.70}$$

The properties shown in (2.69) and (2.70) can be employed to find out square root and inverse of second-order tensors.

2-1-5 Orthogonal tensors

Since a vector is a independent quantity of any coordinate system, vector can be represented by any particular system in different components which can be expressed as a linear mapping from basis $\{\mathbf{e}_i\}$ to $\{\mathbf{e}_i'\}$,

$$\mathbf{v} = v_i \mathbf{e}_i = v_i' \mathbf{e}_i' \tag{2.71}$$

Components of $\mathbf{v}$ transform under changes of orthonormal basis, where

$$v_i' = Q_{ij} v_j \tag{2.72}$$

$$\mathbf{e}_i' = Q_{ij} \mathbf{e}_j \tag{2.73}$$

$\mathbf{Q}$ are the direction cosines of the vectors $\{\mathbf{e}_i'\}$ relative to $\{\mathbf{e}_i\}$,

$$Q_{ij} = \mathbf{e}_i' \cdot \mathbf{e}_j \tag{2.74}$$

Transformation tensor can $\mathbf{Q}$ be expressed obviously as,

$$\mathbf{Q} = \begin{bmatrix} \mathbf{e}_1' \cdot \mathbf{e}_1 & \mathbf{e}_1' \cdot \mathbf{e}_2 & \mathbf{e}_1' \cdot \mathbf{e}_3 \\ \mathbf{e}_2' \cdot \mathbf{e}_1 & \mathbf{e}_2' \cdot \mathbf{e}_2 & \mathbf{e}_2' \cdot \mathbf{e}_3 \\ \mathbf{e}_3' \cdot \mathbf{e}_1 & \mathbf{e}_3' \cdot \mathbf{e}_2 & \mathbf{e}_3' \cdot \mathbf{e}_3 \end{bmatrix} \tag{2.75}$$

Transformation rules for changing vector under rotation of axes,
$$\mathbf{v}' = \mathbf{Q} \cdot \mathbf{v} \tag{2.76}$$
According to orthonormality,
$$\delta_{ij} = \mathbf{e}_i{}' \cdot \mathbf{e}_j{}' = Q_{ik}\mathbf{e}_k \cdot \mathbf{e}_j{}' = Q_{ik}Q_{jk} \tag{2.77}$$
As a result of Eq.(2.77),
$$\mathbf{Q} \cdot \mathbf{Q}^T = \mathbf{Q}^T \cdot \mathbf{Q} = \mathbf{1} \tag{2.78}$$
$$\mathbf{Q}^{-1} = \mathbf{Q}^T \tag{2.79}$$
For proper orthogonal tensor, corresponds to maintenance of right-handedness of the basis vector,
$$\det(\mathbf{Q}) = +1 \tag{2.80}$$
For improper orthogonal tensor,
$$\det(\mathbf{Q}) = -1 \tag{2.81}$$
A tensor exists independent of any coordinate system in such a way that,
$$\mathbf{T} = T_{ij}\mathbf{e}_i \otimes \mathbf{e}_j = T_{ij}{}'\mathbf{e}_i{}' \otimes \mathbf{e}_j{}' \tag{2.82}$$
Transformation rules for changing second-order tensor under rotation of axes,
$$\mathbf{T}' = \mathbf{Q} \cdot \mathbf{T} \cdot \mathbf{Q}^T \tag{2.83}$$
The components is expressed by,
$$T_{ij}{}' = Q_{ip}Q_{jq}T_{pq} \tag{2.84}$$
As a result, it is found that $tr(\mathbf{T})$, $tr(\mathbf{T}^2)$ and $tr(\mathbf{T}^3)=3\det(\mathbf{T})$ are scalar invariants of $\mathbf{T}$ which are shown below,
$$tr(\mathbf{T}') = tr(\mathbf{Q} \cdot \mathbf{T} \cdot \mathbf{Q}^T) = tr(\mathbf{Q}^T \cdot \mathbf{Q} \cdot \mathbf{T}) = tr(\mathbf{T}) \tag{2.85}$$
$$tr(\mathbf{T}'^2) = tr(\mathbf{Q} \cdot \mathbf{T} \cdot \mathbf{Q}^T \cdot \mathbf{Q} \cdot \mathbf{T} \cdot \mathbf{Q}^T) = tr(\mathbf{T}^2) \tag{2.86}$$
$$\det(\mathbf{T}') = \det(\mathbf{Q} \cdot \mathbf{T} \cdot \mathbf{Q}^T) = \det(\mathbf{Q})\det(\mathbf{T})\det(\mathbf{Q}^T) = \det(\mathbf{T}) \tag{2.87}$$

2-1-6 Third-order tensors

A third-order tensor is defined as a linear map from an arbitrary vector $\mathbf{v}$ to a second-order tensor $\mathbf{T}$ in such a way,
$$\mathbf{W} \cdot \mathbf{v} = \mathbf{T} \tag{2.88}$$
where $\mathbf{W}$ can be recognized by tensor products among three vectors,
$$\mathbf{W} = \mathbf{u} \otimes \mathbf{v} \otimes \mathbf{w} \tag{2.89}$$
Actually, a third-order tensor $\mathbf{W}$ is represented by
$$\mathbf{W} = \sum_{i,j,k=1}^{3} W_{ijk}\mathbf{e}_i \otimes \mathbf{e}_j \otimes \mathbf{e}_k \tag{2.90}$$
Components of third-order tensor $\mathbf{W}$ can be extracted by
$$W_{ijk} = (\mathbf{e}_i \otimes \mathbf{e}_j) : \mathbf{W} \cdot \mathbf{e}_k \tag{2.91}$$
A well-known third-order tensor is the alternating tensor $\boldsymbol{\varepsilon}$, which is defined in such a way,
$$\begin{aligned}\boldsymbol{\varepsilon} = \mathbf{e}_1 \otimes \mathbf{e}_2 \otimes \mathbf{e}_3 + \mathbf{e}_3 \otimes \mathbf{e}_1 \otimes \mathbf{e}_2 + \mathbf{e}_2 \otimes \mathbf{e}_3 \otimes \mathbf{e}_1 \\ -\mathbf{e}_3 \otimes \mathbf{e}_2 \otimes \mathbf{e}_1 - \mathbf{e}_1 \otimes \mathbf{e}_3 \otimes \mathbf{e}_2 - \mathbf{e}_2 \otimes \mathbf{e}_1 \otimes \mathbf{e}_3\end{aligned} \tag{2.92}$$
As a result of Eq.(2.92), components of $\boldsymbol{\varepsilon}$ are shown by,
$$\varepsilon_{ijk} = (\mathbf{e}_i \otimes \mathbf{e}_j) : \boldsymbol{\varepsilon} \cdot \mathbf{e}_k = \mathbf{e}_i \cdot (\mathbf{e}_j \times \mathbf{e}_k) \tag{2.93}$$
Actually, $(\boldsymbol{\varepsilon} \cdot \mathbf{v})$ is seen as skew tensor of $\mathbf{v}$ in such a way,
$$\boldsymbol{\varepsilon} : (\mathbf{u} \otimes \mathbf{v}) = (\boldsymbol{\varepsilon} \cdot \mathbf{v}) \cdot \mathbf{u} = \mathbf{u} \times \mathbf{v} \tag{2.94}$$
Additional properties of double contraction are given below,
$$(\mathbf{u} \otimes \mathbf{v} \otimes \mathbf{w}) : (\mathbf{x} \otimes \mathbf{y}) = (\mathbf{v} \otimes \mathbf{w}) : (\mathbf{x} \otimes \mathbf{y})\mathbf{u} = (\mathbf{v} \cdot \mathbf{x})(\mathbf{w} \cdot \mathbf{y})\mathbf{u} \tag{2.95}$$
$$(\mathbf{u} \otimes \mathbf{S}) : \mathbf{T} = (\mathbf{S} : \mathbf{T})\mathbf{u} \tag{2.96}$$
$$(\mathbf{S} \otimes \mathbf{u}) : \mathbf{T} = \mathbf{S} \cdot \mathbf{T} \cdot \mathbf{u} \tag{2.97}$$
$$\mathbf{W} : (\mathbf{u} \otimes \mathbf{v}) = (\mathbf{W} \cdot \mathbf{v}) \cdot \mathbf{u} \tag{2.98}$$
$$(\mathbf{W} \otimes \mathbf{u}) \cdot \mathbf{v} = (\mathbf{u} \cdot \mathbf{v})\mathbf{W} \tag{2.99}$$
$$(\mathbf{u} \otimes \mathbf{W}) \cdot \mathbf{v} = \mathbf{u} \otimes \mathbf{W} \cdot \mathbf{v} \tag{2.100}$$

2-1-7 Forth-order tensors

Forth-order tensors are obtained by extending the combinations of tensor products as

$$\mathbf{C} = \mathbf{a} \otimes \mathbf{b} \otimes \mathbf{c} \otimes \mathbf{d} \tag{2.101}$$

Essesential, the constituents of a forth-order tensor C can be represented by,

$$\mathbf{C} = \sum_{i,j,k,l=1}^{3} C_{ijk} \mathbf{e}_i \otimes \mathbf{e}_j \otimes \mathbf{e}_k \otimes \mathbf{e}_l \tag{2.102}$$

A double product of forth-order tensor and second-order tensor is expressed by,

$$\begin{aligned}
\mathbf{C} : \mathbf{D} &= C_{ijkl} \mathbf{e}_i \otimes \mathbf{e}_j \otimes \mathbf{e}_k \otimes \mathbf{e}_l : D_{mn} \mathbf{e}_m \otimes \mathbf{e}_n \\
&= C_{ijkl} \mathbf{e}_i \otimes \mathbf{e}_j (\mathbf{e}_k \cdot \mathbf{e}_m)(\mathbf{e}_l \cdot \mathbf{e}_n) D_{mn} \\
&= C_{ijkl} D_{kl} \mathbf{e}_i \otimes \mathbf{e}_j
\end{aligned} \tag{2.103}$$

The component of double product can be expressed as,

$$(\mathbf{C} : \mathbf{D})_{ij} = C_{ijkl} D_{kl} = D_{kl} C_{ijkl} \tag{2.104}$$

A component of double product of forth-order tensor and forth-order tensor is expressed by,

$$\begin{aligned}
\mathbf{C} : \mathbf{E} &= C_{ijmn} \mathbf{e}_i \otimes \mathbf{e}_j \otimes \mathbf{e}_m \otimes \mathbf{e}_n : E_{stkl} \mathbf{e}_s \otimes \mathbf{e}_t \otimes \mathbf{e}_k \otimes \mathbf{e}_l \\
&= C_{ijmn} E_{stkl} \mathbf{e}_i \otimes \mathbf{e}_j \otimes (\mathbf{e}_m \cdot \mathbf{e}_s)(\mathbf{e}_n \cdot \mathbf{e}_t) \mathbf{e}_k \otimes \mathbf{e}_l \\
&= C_{ijmn} E_{stkl} \delta_{ms} \delta_{nt} \mathbf{e}_i \otimes \mathbf{e}_j \otimes \mathbf{e}_k \otimes \mathbf{e}_l \\
&= C_{ijmn} E_{mnkl} \mathbf{e}_i \otimes \mathbf{e}_j \otimes \mathbf{e}_k \otimes \mathbf{e}_l
\end{aligned} \tag{2.105}$$

The component of double product can be expressed as,

$$(\mathbf{C} : \mathbf{E})_{ijkl} = C_{ijmn} E_{mnkl} \tag{2.106}$$

Components of forth-order tensor $\mathbf{C}$ can be given by,

$$C_{ijkl} = (\mathbf{e}_i \otimes \mathbf{e}_j) : \mathbf{C} : (\mathbf{e}_k \otimes \mathbf{e}_l) \tag{2.107}$$

A double product of forth-order tensor $\mathbf{C}$ and its inversion gives an identity forth-order tensor shown by,

$$\mathbf{C}^{-1} : \mathbf{C} = \mathbf{C} : \mathbf{C}^{-1} = \mathbf{I} \tag{2.108}$$

Identity forth-order tensor can be expressed by,

$$\mathbf{I} = \frac{1}{2} \left[\delta_{ik} \delta_{jl} + \delta_{il} \delta_{jk} \right] \mathbf{e}_i \otimes \mathbf{e}_j \otimes \mathbf{e}_k \otimes \mathbf{e}_l \tag{2.109}$$

A double product of identity forth-order tensor $\mathbf{I}$ and second-order tensor results in a symmetric projection of that second-order tensor as,

$$\begin{aligned}
\mathbf{I} : \mathbf{T} &= \frac{1}{2} \left[\delta_{ik} \delta_{jl} + \delta_{il} \delta_{jk} \right] \mathbf{e}_i \otimes \mathbf{e}_j \otimes \mathbf{e}_k \otimes \mathbf{e}_l : T_{mn} \mathbf{e}_m \otimes \mathbf{e}_n \\
&= T_{mn} \frac{1}{2} \left[\delta_{ik} \delta_{jl} + \delta_{il} \delta_{jk} \right] \mathbf{e}_i \otimes \mathbf{e}_j (\mathbf{e}_k \cdot \mathbf{e}_m)(\mathbf{e}_l \cdot \mathbf{e}_n) \\
&= T_{mn} \frac{1}{2} \left[\delta_{ik} \delta_{jl} + \delta_{il} \delta_{jk} \right] \mathbf{e}_i \otimes \mathbf{e}_j \delta_{km} \delta_{ln} \\
&= T_{kl} \frac{1}{2} \left[\delta_{ik} \delta_{jl} + \delta_{il} \delta_{jk} \right] \mathbf{e}_i \otimes \mathbf{e}_j \\
&= \frac{1}{2} \left[T_{ij} + T_{ji} \right] \mathbf{e}_i \otimes \mathbf{e}_j
\end{aligned} \tag{2.110}$$

The components of identity forth-order tensor can be viewed as 3x3 matrix in 3x3 matrix shown by,

$$\left[[\mathbf{I}]_{3\times3} \right]_{3\times3} = \begin{bmatrix}
\begin{bmatrix} 1 & 0 & 0 \\ 0 & 0 & 0 \\ 0 & 0 & 0 \end{bmatrix} & \begin{bmatrix} 0 & 0.5 & 0 \\ 0.5 & 0 & 0 \\ 0 & 0 & 0 \end{bmatrix} & \begin{bmatrix} 0 & 0 & 0.5 \\ 0 & 0 & 0 \\ 0.5 & 0 & 0 \end{bmatrix} \\
\begin{bmatrix} 0 & 0.5 & 0 \\ 0.5 & 0 & 0 \\ 0 & 0 & 0 \end{bmatrix} & \begin{bmatrix} 0 & 0 & 0 \\ 0 & 1 & 0 \\ 0 & 0 & 0 \end{bmatrix} & \begin{bmatrix} 0 & 0 & 0 \\ 0 & 0 & 0.5 \\ 0 & 0.5 & 0 \end{bmatrix} \\
\begin{bmatrix} 0 & 0 & 0.5 \\ 0 & 0 & 0 \\ 0.5 & 0 & 0 \end{bmatrix} & \begin{bmatrix} 0 & 0 & 0 \\ 0 & 0 & 0.5 \\ 0 & 0.5 & 0 \end{bmatrix} & \begin{bmatrix} 0 & 0 & 0 \\ 0 & 0 & 0 \\ 0 & 0 & 1 \end{bmatrix}
\end{bmatrix} \tag{2.111}$$

In compare with tensor product of unity second-order tensor, the difference can be recognized,

$$\left[\left[\mathbf{1}\otimes\mathbf{1}\right]_{3\times3}\right]_{3\times3} = \begin{bmatrix} \begin{bmatrix} 1 & 0 & 0 \\ 0 & 1 & 0 \\ 0 & 0 & 1 \end{bmatrix} & \begin{bmatrix} 0 & 0 & 0 \\ 0 & 0 & 0 \\ 0 & 0 & 0 \end{bmatrix} & \begin{bmatrix} 0 & 0 & 0 \\ 0 & 0 & 0 \\ 0 & 0 & 0 \end{bmatrix} \\ \begin{bmatrix} 0 & 0 & 0 \\ 0 & 0 & 0 \\ 0 & 0 & 0 \end{bmatrix} & \begin{bmatrix} 1 & 0 & 0 \\ 0 & 1 & 0 \\ 0 & 0 & 1 \end{bmatrix} & \begin{bmatrix} 0 & 0 & 0 \\ 0 & 0 & 0 \\ 0 & 0 & 0 \end{bmatrix} \\ \begin{bmatrix} 0 & 0 & 0 \\ 0 & 0 & 0 \\ 0 & 0 & 0 \end{bmatrix} & \begin{bmatrix} 0 & 0 & 0 \\ 0 & 0 & 0 \\ 0 & 0 & 0 \end{bmatrix} & \begin{bmatrix} 1 & 0 & 0 \\ 0 & 1 & 0 \\ 0 & 0 & 1 \end{bmatrix} \end{bmatrix} \tag{2.112}$$

Some properties of forth-order tensor are obtained as,

$$(\mathbf{u}_1 \otimes \mathbf{u}_2 \otimes \mathbf{u}_3 \otimes \mathbf{u}_4):(\mathbf{x}\otimes\mathbf{y}) = (\mathbf{u}_3 \cdot \mathbf{x})(\mathbf{u}_4 \cdot \mathbf{y})\mathbf{u}_1 \otimes \mathbf{u}_2 \tag{2.113}$$

$$(\mathbf{S}_1 \otimes \mathbf{S}_2):\mathbf{T} = (\mathbf{S}_2 : \mathbf{T})\mathbf{S}_1 \tag{2.114}$$

$$(\mathbf{u}\otimes\mathbf{W}):\mathbf{T} = \mathbf{u}\otimes(\mathbf{W}:\mathbf{T}) \tag{2.115}$$

$$(\mathbf{W}\otimes\mathbf{u}):\mathbf{T} = \mathbf{u}\otimes(\mathbf{W}:\mathbf{T}) \tag{2.116}$$

$$(\mathbf{T}\otimes\mathbf{S})\cdot\mathbf{v} = \mathbf{T}\otimes(\mathbf{S}\cdot\mathbf{v}) \tag{2.117}$$

2-2 Tensor analyses

2-2-1 Derivatives
Time derivative of a scalar function

$$\frac{\partial f}{\partial t} = \dot{f} \tag{2.118}$$

Partial derivative of function with respect to a point x in a region

$$\frac{\partial f(x,y,z)}{\partial x} = \partial_x f(x,y,z) \tag{2.119}$$

Second derivative of function with respect to y and x

$$\frac{\partial}{\partial x}\left(\frac{\partial f}{\partial y}\right) = \frac{\partial^2 f}{\partial x \partial y} = \partial^2_{yx} f \tag{2.120}$$

First derivative of a scalar function with respect to a second-order tensor

$$\frac{\partial f(\boldsymbol{\sigma}')}{\partial \boldsymbol{\sigma}'} = \partial_{\boldsymbol{\sigma}'} f \tag{2.121}$$

Second derivative of a scalar function with respect to second-order tensors

$$\frac{\partial}{\partial \boldsymbol{\sigma}'}\left(\frac{\partial f}{\partial \mathbf{q}}\right) = \frac{\partial^2 f}{\partial \boldsymbol{\sigma}' \partial \mathbf{q}} = \partial^2_{\mathbf{q}\boldsymbol{\sigma}'} f \tag{2.122}$$

2-2-2 Directional derivatives
Differentiation of scalar field

$$\nabla f = \frac{\partial f}{\partial \mathbf{x}} = \frac{\partial f}{\partial x_i}\mathbf{e}_i = f_{,i}\mathbf{e}_i \tag{2.123}$$

Differentiation of vector field

$$\nabla \mathbf{v} = \frac{\partial \mathbf{v}}{\partial \mathbf{x}} = \frac{\partial v_i}{\partial x_j}\mathbf{e}_i \otimes \mathbf{e}_j = v_{i,j}\mathbf{e}_i \otimes \mathbf{e}_j \tag{2.124}$$

$$div(\mathbf{v}) = tr(\nabla\mathbf{v}) = \frac{\partial v_i}{\partial x_i} = v_{i,i} \tag{2.125}$$

Differentiation of tensor field

$$\nabla\mathbf{S} = \frac{\partial \mathbf{S}}{\partial \mathbf{x}} = \frac{\partial S_{ij}}{\partial x_k}\mathbf{e}_i \otimes \mathbf{e}_j \otimes \mathbf{e}_k = S_{ij,k}\mathbf{e}_i \otimes \mathbf{e}_j \otimes \mathbf{e}_k \tag{2.126}$$

$$div(\mathbf{S}) = \nabla\mathbf{S}:\mathbf{1} = \sum_{i,j=1}^{3}\frac{\partial S_{ij}}{\partial x_j}\mathbf{e}_i = \sum_{i,j=1}^{3} S_{ij,j}\mathbf{e}_i \tag{2.127}$$

The following properties of the gradient and divergence are a result of the product rule,

$$\nabla(f\mathbf{v}) = f\nabla\mathbf{v} + \mathbf{v}\otimes\nabla f \tag{2.128}$$

$$\nabla(f\mathbf{S}) = f\nabla\mathbf{S} + \mathbf{S} \otimes \nabla f \tag{2.129}$$

$$\nabla(\mathbf{v} \cdot \mathbf{w}) = (\nabla\mathbf{v})^T \cdot \mathbf{w} + (\nabla\mathbf{w})^T \cdot \mathbf{v} \tag{2.130}$$

$$div(f\mathbf{v}) = f\,div(\mathbf{v}) + \mathbf{v} \cdot \nabla f \tag{2.131}$$

$$div(f\mathbf{S}) = f\,div(\mathbf{S}) + \mathbf{S}\nabla f \tag{2.132}$$

$$div(\mathbf{v} \otimes \mathbf{w}) = \mathbf{v}\,div(\mathbf{w}) + \nabla\mathbf{v} \cdot \mathbf{w} \tag{2.133}$$

$$div(\mathbf{S}^T \cdot \mathbf{v}) = \mathbf{S} : \nabla\mathbf{v} + \mathbf{v} \cdot div\mathbf{S} \tag{2.134}$$

2-2-3 Tensorial derivatives

Some properties of tensorial derivatives can be given by

$$\frac{\partial \alpha}{\partial \mathbf{T}} = \frac{\partial \alpha}{\partial T_{ij}} \mathbf{e}_i \otimes \mathbf{e}_j \tag{2.135}$$

$$\frac{\partial \mathbf{S}}{\partial \mathbf{T}} = \frac{\partial S_{ij}}{\partial T_{kl}} \mathbf{e}_i \otimes \mathbf{e}_j \otimes \mathbf{e}_k \otimes \mathbf{e}_l \tag{2.136}$$

$$\frac{\partial \mathbf{T}}{\partial \mathbf{T}} = \mathbf{I} \tag{2.137}$$

$$\frac{\partial (\mathbf{R} : \mathbf{S})}{\partial \mathbf{T}} = \left[\frac{\partial \mathbf{S}}{\partial \mathbf{T}}\right]^T : \mathbf{R} + \left[\frac{\partial \mathbf{R}}{\partial \mathbf{T}}\right]^T : \mathbf{S} \tag{2.138}$$

$$\frac{\partial (\mathbf{1} : \mathbf{T})}{\partial \mathbf{T}} = \mathbf{I} : \mathbf{1} = \mathbf{1} \tag{2.139}$$

$$\frac{\partial (\mathbf{T} : \mathbf{T})}{\partial \mathbf{T}} = \mathbf{I} : \mathbf{T} + \mathbf{I} : \mathbf{T} = 2\mathbf{T} \tag{2.140}$$

2-2-4 Integrations

For the vector field $\mathbf{u}$ has continuous first-order partial derivatives at all points in a regular region $\mathbb{R}$, $\mathbf{n}$ is the outward unit vector normal to the boundary $\partial\mathbb{R}$. dV and dS are elements of volume and surface area respectively, then,

$$\iiint\limits_{\mathbb{R}} div(\mathbf{u})dV = \iint\limits_{\partial\mathbb{R}} \mathbf{u} \cdot \mathbf{n}dS \tag{2.141}$$

In terms of components,

$$\iiint\limits_{\mathbb{R}} u_{i,i}dV = \iint\limits_{\partial\mathbb{R}} u_i n_i dS \tag{2.142}$$

The divergence theorem can also be applied to second-order tensors, such as,

$$\iiint\limits_{\mathbb{R}} T_{ij,i}dV = \iint\limits_{\partial\mathbb{R}} T_{ij} n_i dS \tag{2.143}$$

2-3 Stress tensors

Definition of stress can be seen in many standard textbooks; [4, 5, 6, 7, 8]. The basic introduction is summarized in this topic. Generally, Chauchy's stress in term of Cartesian components is expressed by a second-order tensor of nine components shown by,

$$\boldsymbol{\sigma} = \begin{bmatrix} \sigma_{11} & \sigma_{12} & \sigma_{13} \\ \sigma_{21} & \sigma_{22} & \sigma_{23} \\ \sigma_{31} & \sigma_{32} & \sigma_{33} \end{bmatrix} \tag{2.144}$$

The stress tensor components are displayed with reference to the coordinate planes. The components perpendicular to the planes which are (σ_{11}, σ_{22}, σ_{33}) are called normal stresses while others acting in tangent planes are called shear stresses. The balance laws of angular momentum implies that the stress tensor is symmetric, therefore,

$$\boldsymbol{\sigma} = \boldsymbol{\sigma}^T \quad \text{or} \quad \sigma_{ij} = \sigma_{ji} \tag{2.145}$$

2-3-1 Principal stresses

According to Cayley-Hamilton theorem shown in Eq. (2.67), the following equations can be given,

$$\boldsymbol{\sigma}^3 - I_1\boldsymbol{\sigma}^2 + I_2\boldsymbol{\sigma} - I_3\mathbf{1} = \mathbf{0} \tag{2.146}$$

where the invariants of $\boldsymbol{\sigma}$ are given below,

$$I_1 = \mathbf{1} : \boldsymbol{\sigma} = tr(\boldsymbol{\sigma}) \tag{2.147}$$

$$I_2 = \frac{1}{2}\left\{tr(\boldsymbol{\sigma})^2 - tr(\boldsymbol{\sigma}^2)\right\} \tag{2.148}$$

$$I_3 = \det(\boldsymbol{\sigma}) \tag{2.149}$$

According to characteristic equations shown in Eq.(2.62), the following equations can be given,

$$\sigma^3 - I_1\sigma^2 + I_2\sigma - I_3 = 0 \tag{2.150}$$

The solutions of above cubic equation are the eigenvalues of $\boldsymbol{\sigma}$ which are referred to the principal stresses.
In principal stress space, only diagonal terms are existed. Therefore, a stress tensor can be shown in short as,

$$\boldsymbol{\sigma} = diag\begin{bmatrix} \sigma_1 & \sigma_2 & \sigma_3 \end{bmatrix} \tag{2.151}$$

For real roots [9], (compression as positive)

$$Q = -\frac{I_1^2 - 3I_2}{9}, \qquad R = \frac{2I_1^3 - 9I_1I_2 + 27I_3}{54}, \qquad \theta = \cos^{-1}\left(\frac{R}{\sqrt{-Q^3}}\right) \tag{2.152}$$

$$\sigma_1 = 2\sqrt{-Q}\cos(\frac{\theta}{3}) + \frac{I_1}{3} \tag{2.153}$$

$$\sigma_2 = 2\sqrt{-Q}\cos(\frac{\theta}{3} - \frac{2}{3}\pi) + \frac{I_1}{3} \tag{2.154}$$

$$\sigma_2 = 2\sqrt{-Q}\cos(\frac{\theta}{3} + \frac{2}{3}\pi) + \frac{I_1}{3} \tag{2.155}$$

Properties of three roots are,

$$\sigma_1 + \sigma_2 + \sigma_3 = I_1 \tag{2.156}$$

$$\sigma_1\sigma_2 + \sigma_2\sigma_3 + \sigma_3\sigma_1 = I_2 \tag{2.157}$$

$$\sigma_1\sigma_2\sigma_3 = I_3 \tag{2.158}$$

2-3-2 Stress deviator tensor

A given stress can be separated into isotropic pressure and stress deviator as follows,

$$\boldsymbol{\sigma} = p\mathbf{1} + \mathbf{s} \tag{2.159}$$

where

$$p = \frac{1}{3}\mathbf{1} : \boldsymbol{\sigma} = \frac{1}{3}tr(\boldsymbol{\sigma}) = \frac{1}{3}I_1 \tag{2.160}$$

$$\mathbf{s} = \boldsymbol{\sigma} - \frac{1}{3}(\mathbf{1} : \boldsymbol{\sigma})\mathbf{1} = \boldsymbol{\sigma} - p\mathbf{1} \tag{2.161}$$

A forth-order tensor mapping stress and stress deviator is defined herein as deviatoric forth-order tensor $\mathbf{A}$. The derivation is shown below, (See more about deviatoric forth-order tensor $\mathbf{A}$ in Appendix A)

$$\mathbf{s} = \boldsymbol{\sigma} - \frac{1}{3}(\mathbf{1} : \boldsymbol{\sigma})\mathbf{1} = \left[\mathbf{I} - \frac{1}{3}\mathbf{1}\otimes\mathbf{1}\right] : \boldsymbol{\sigma} = \mathbf{A} : \boldsymbol{\sigma} \tag{2.162}$$

$\mathbf{s}$ and $\boldsymbol{\sigma}$ share the same principal axes. Invariants of the deviatoric stress tensor can be defined by the corresponding characteristic equations,

$$s^3 - J_1 s^2 - J_2 s - J_3 = 0 \tag{2.163}$$

where

$$J_1 = tr(\mathbf{s}) = \mathbf{1} : \mathbf{s} = 0 \tag{2.164}$$

$$J_2 = \frac{1}{2}tr(\mathbf{s}^2) = \frac{1}{2}\mathbf{s} : \mathbf{s} \tag{2.165}$$

$$J_3 = \frac{1}{3}tr(\mathbf{s}^3) = \frac{1}{3}\mathbf{s}^2 : \mathbf{s} = \det(\mathbf{s}) \tag{2.166}$$

It can be shown that the invariants J_1, J_2 and J_3 are related to the invariants I_1, I_2 and I_3 of the stress tensor s through the following relations, [10]

$$J_2 = \frac{1}{3}(I_1^2 - 3I_2) \tag{2.167}$$

$$J_3 = \frac{1}{27}(2I_1^3 - 9I_1I_2 + 27I_3) \tag{2.168}$$

Eq.(2.152)-(2.155) can be reinstated by,

$$\theta = \frac{1}{3}\sin^{-1}\left(-\frac{3\sqrt{3}}{2}\frac{J_3}{\sqrt{J_2^3}}\right) \tag{2.169}$$

$$\sigma_1 = 2\sqrt{\frac{J_2}{3}}\sin(\theta + \frac{2}{3}\pi) + \frac{I_1}{3} \tag{2.170}$$

$$\sigma_2 = 2\sqrt{\frac{J_2}{3}}\sin(\theta) + \frac{I_1}{3} \tag{2.171}$$

$$\sigma_3 = 2\sqrt{\frac{J_2}{3}}\sin(\theta - \frac{2}{3}\pi) + \frac{I_1}{3} \tag{2.172}$$

where $\sigma_1 \geq \sigma_2 \geq \sigma_3$ are major, intermediate and minor principal stresses. $-\frac{\pi}{6} < \theta < \frac{\pi}{6}$ is regarded as Lode angle.

2-3-3 Triaxial stress condition

Under reduced stress form of triaxial stress condition, the mean normal stress p' and deviatoric stress q can be expressed by the major and minor principal effective stress σ_1, σ_2 and σ_3 (in which $\sigma_2 = \sigma_3$) by

$$p' = \frac{\sigma_1 + 2\sigma_3}{3} \tag{2.173}$$

$$q = \sqrt{3J_2} = \sqrt{\frac{3}{2}\mathbf{s}:\mathbf{s}} = \sigma_1 - \sigma_3 \tag{2.174}$$

The rate of volumetric and deviatoric strains can be defined by,

$$\dot{\varepsilon}_v = \dot{\varepsilon}_1 + 2\dot{\varepsilon}_3 \tag{2.175}$$

$$\dot{\varepsilon}_s = \frac{2}{3}\left(\dot{\varepsilon}_1 - \dot{\varepsilon}_3\right) \tag{2.176}$$

2-4 Incremental stress-strain relations

2-4-1 Generalized Hooke's law

Many classical textbooks on elasticity can be taken as references for Hooke's law [11, 12, 13, 14, 15]. In summary, the rate of stress is related to the rate of elastic by,

$$\dot{\boldsymbol{\sigma}} = \mathbf{C} : \dot{\boldsymbol{\varepsilon}}^e \tag{2.177}$$

The forth-order elasticity tensor $\mathbf{C}$ for isotropic material can be expressed by,

$$\mathbf{C} = K\left(\mathbf{1} \otimes \mathbf{1}\right) + 2G\mathbf{A} \tag{2.178}$$

where K is bulk modulus and G is shear modulus of material. The symmetry of $\mathbf{C}$ can be found by

$$C_{ijkl} = C_{ijlk} = C_{klij} \tag{2.179}$$

2-4-2 Flow rule

Many textbooks on plasticity can be taken as references [16, 17, 18, 19, 20, 21] for associative flow. In summary, the rate of plastic strain can be described by,

$$\dot{\boldsymbol{\varepsilon}}^p = \lambda \frac{\partial f}{\partial \boldsymbol{\sigma}} \tag{2.180}$$

$$\frac{\partial f(\boldsymbol{\sigma})}{\partial \boldsymbol{\sigma}} = \frac{\partial f(I_1, J_2, J_3)}{\partial \boldsymbol{\sigma}} = \frac{\partial f}{\partial I_1}\frac{\partial I_1}{\partial \boldsymbol{\sigma}} + \frac{\partial f}{\partial J_2}\frac{\partial J_2}{\partial \boldsymbol{\sigma}} + \frac{\partial f}{\partial J_3}\frac{\partial J_3}{\partial \boldsymbol{\sigma}} \tag{2.181}$$

Since,

$$\frac{\partial I_1}{\partial \boldsymbol{\sigma}} = \mathbf{1} \tag{2.182}$$

$$\frac{\partial J_2}{\partial \boldsymbol{\sigma}} = \mathbf{s} \tag{2.183}$$

$$\frac{\partial J_3}{\partial \boldsymbol{\sigma}} = \mathbf{t} = \mathbf{s} \cdot \mathbf{s} - \frac{2}{3}J_2\mathbf{1} \tag{2.184}$$

2-5 Optimization theory

Optimization is a systematic approach to problem involving an optimal solution within certain constraints. Details of optimization theory can be reviewed in many texts [22, 23].

2-5-1 Optimization of functions of several variables

In the topic of optimization of functions of several variables, several keywords will be described as followed,

Stationary point

The stationary point in f($\mathbf{X}$) can be defined as,

"$\mathbf{X}_o$ is a stationary point for a function f($\mathbf{X}$) if all partial derivatives of f are zero at $\mathbf{X}_o$." $\quad \nabla f(\mathbf{X}_o) = \mathbf{0}$

(2.185)

Hessian matrix

The Hessian matrix is the (nxn) matrix of second order partial derivatives of f. The ith row of $\mathbf{H}$ holds the partial derivatives of the ith component of the gradient vector.

Quadratic form

If A is a symmetric (nxn) matrix then the function $q(\mathbf{X}) = \mathbf{X} \cdot \mathbf{A} \cdot \mathbf{X}^T$ is called a quadratic form Definiteness

A is	positive definite	if $\mathbf{X} \cdot \mathbf{A} \cdot \mathbf{X}^T > 0$	for all nonzero $\mathbf{X}$
	potive semidefinite	if $\mathbf{X} \cdot \mathbf{A} \cdot \mathbf{X}^T \geq 0$	
	negative definite	if $\mathbf{X} \cdot \mathbf{A} \cdot \mathbf{X}^T < 0$	
	negative semidefinite	if $\mathbf{X} \cdot \mathbf{A} \cdot \mathbf{X}^T \leq 0$	

otherwise, A is indefinite

Optimal point A function f($\mathbf{X}$) has a relative minimum (maximum) at a stationary point $\mathbf{X}_O$ if $\mathbf{H}(\mathbf{X}_O)$ is positive (negative) definite.

2-5-2 Convex and concave functions
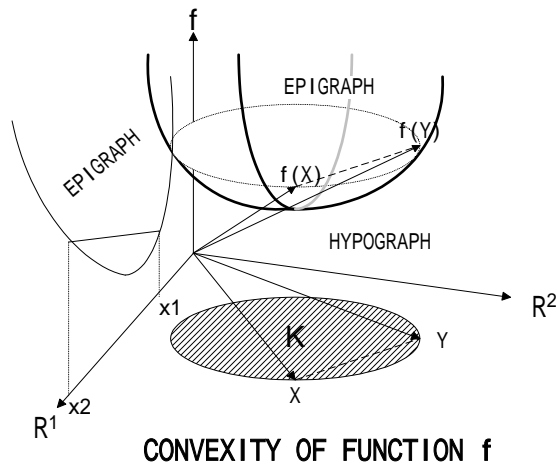
Figure 2.1 Convexity and a convex set

In all these definitions, assume that K is a convex set in R^n, X, Y are in K, $0 \leq \xi \leq 1$, and f:K $\to$ R.

Convex function

f is convex if $f(\xi X + (1-\xi)Y) \leq \xi f(X) + (1-\xi)f(Y)$.

Convex function has a relative minimum Strictly convex function

f is strictly convex if $f(\xi X + (1-\xi)Y) < \xi f(X) + (1-\xi)f(Y)$.

Concave function

f is concave if $f(\xi X + (1-\xi)Y) \geq \xi f(X) + (1-\xi)f(Y)$.

Strictly concave function

f is strictly concave if $f(\xi X + (1-\xi)Y) > \xi f(X) + (1-\xi)f(Y)$.

Affine function

f is affined if $f(\xi X + (1-\xi)Y) = \xi f(X) + (1-\xi)f(Y)$.

Epigraph

The Epigraph of a function f, denoted epi(f), is the set $\{(X, Y) \mid Y \geq f(X)\}$. Note that the epigraph is the region above the graph of f.

Hypograph

The Hypograph of a function f, denoted hyp(f), is the set $\{(X, Y) \mid Y \leq f(X)\}$. Note that the hypograph is the region below the graph of f.

2-5-3 Constrained optimization

For an objective function: f(x)
- Equality constraints: $\quad\quad\quad\quad\quad\quad\quad\quad$ $h_1(x)=0$, $h_2(x)=0$
- Inequality constraints: $\quad\quad\quad\quad\quad\quad\quad\quad$ $g_1(x) \leq 0$, $g_2(x) \geq 0$
- Equality/Inequality constraints: $\quad\quad\quad$ $h_1(x)=0$, $g_1(x) \leq 0$

Solution for Optimum
- Objective function $\quad\quad\quad\quad\quad$ $\rightarrow$ $\quad\quad\quad$ Convex analysis for minimum
- Equality constraint $\quad\quad\quad\quad\quad$ $\rightarrow$ $\quad\quad\quad$ Lagrangian functions
- Inequality constraints $\quad\quad\quad\quad$ $\rightarrow$ $\quad\quad\quad$ Kuhn-Tucker conditions
- Equality/inequality constraints $\quad\quad$ $\rightarrow$ $\quad\quad\quad$ Karush-Kuhn-Tucker conditions

Lagrangian functions The Lagrangian Function: $L(\mathbf{X}, \lambda) = f(\mathbf{X}) + \lambda.h(\mathbf{X})$

A necessary condition for f to have a stationary point at X_o subject to the constraint $h(\mathbf{X}) = 0$ is that grad($L(\mathbf{X}_o)$) = 0.

Theorem: Let f and h be twice continuously differentiable defined on a neighborhood of a point $\mathbf{X}_o$ for which $h(\mathbf{X}_o) = 0$ and suppose there exists a number λ such that $f(\mathbf{X}_o) + \lambda.\nabla h(\mathbf{X}_o) = 0$ and the matrix $H(\mathbf{X}_o) = F(\mathbf{X}_o) + \lambda.K(\mathbf{X}_o)$ is positive definite where F is the Hessian for f and K is the Hessian for h. Then $\mathbf{X}_o$ is a relative minimum for f subject to $h(\mathbf{X}) = 0$.

Equality/Inequality Constraints The following conditions are necessary for a point Xo to solve the problem: minimize f(X) subject to inequalities $g_k(X) <= 0$ for k = 1,2,...,K and equalities $h_j(\mathbf{X}) = 0$ for j = 1,2,...,J. Let the Lagrangian function $L(\mathbf{X},\mu,\lambda) = f(\mathbf{X}) + \mu_k g_k(\mathbf{X}) + \lambda_j h_j(\mathbf{X})$ where μ and λ are Lagrange multipliers. Karush-Kuhn-Tucker Conditions First-order KKT (Karush-Kunh-Tucker) condition

$\nabla f(\mathbf{X}_o) + \Sigma\, \mu_k \nabla g_k(\mathbf{X}_o) + \Sigma\, \lambda_j \nabla h_j(\mathbf{X}_o) = 0$ $\quad$ stationary condition

$h_j(\mathbf{X}_o) = 0$ for j = 1,2,...,J $\quad\quad\quad\quad\quad\quad\quad$ equalities constraints

$g_k(\mathbf{X}_o) \leq 0$ for k = 1,2,...,K $\quad\quad\quad\quad\quad\quad$ inequalities constraints

$\mu_k \geq 0$ for k = 1,2,...,K $\quad\quad\quad\quad\quad\quad\quad\quad$ constraint qualification

$\mu_k g_k(\mathbf{X}_o) = 0$ for k = 1,2,...,K $\quad\quad\quad\quad\quad$ complementary condition

Second-order KKT condition

Theorem: Let f be convex, the equality constraints all linear, and the inequality constraints all convex. If a point $(\mathbf{X}_o, \mu o, \lambda o)$ satisfies the KKT conditions for this problem, then $\mathbf{X}_o$ is the optimal solution to the problem.

2-6 Newton methods

2-6-1 Newton-Raphson methods

In non-linear problem [24], the general problem is therefore always formulated (in terms of th e discretization parameter $\mathbf{a}$) as the solution of,

$$\psi(\mathbf{a}) = p(\mathbf{a}) - f \equiv 0 \tag{2.186}$$

By Taylor's expansion formula, the residual $\psi(\mathbf{a}_{i+1})$ is expanded around $\mathbf{a}_i$ to the first order of accuracy plus second-order terms $O(\mathbf{a}_{i+1}, \mathbf{a}_i)^2$.

$$\psi(\mathbf{a}_{i+1}) = \psi(\mathbf{a}_i + \Delta\mathbf{a}) = \psi(\mathbf{a}_i) + \Delta\mathbf{a}\,\psi\,'(\mathbf{a}_i) + O(\mathbf{a}_{i+1}, \mathbf{a}_i)^2 \tag{2.187}$$

$\mathbf{a}_i$ is a starting value for searching $\mathbf{a}$, $\Delta\mathbf{a}$ is an increment, in which

$$\Delta\mathbf{a} = \mathbf{a}_{i+1} - \mathbf{a}_i \tag{2.188}$$

When $\mathbf{a}_{i+1}$ approaches to solution satisfied by Eq.(2.186), $\psi(\mathbf{a}_{i+1}) = 0$. According to Eq.(2.187) and Eq.(2.188), $\mathbf{a}_{i+1}$ is determined by,

$$\mathbf{a}_{i+1} = \mathbf{a}_i - \frac{\psi(\mathbf{a}_i) + O(\mathbf{a}_{i+1}, \mathbf{a}_i)^2}{\psi\,'(\mathbf{a}_i)} \tag{2.189}$$

To minimize $O(\mathbf{a}_{i+1}, \mathbf{a}_i)$, replace $\mathbf{a}_i$ in Eq.(2.189) by $\mathbf{a}_i \leftarrow \mathbf{a}_{i+1}$

$$\mathbf{a}_{i+1} = \mathbf{a}_i - \frac{\psi(\mathbf{a}_i)}{\psi\,'(\mathbf{a}_i)} \tag{2.190}$$

As a result, the residual $O(a, a_o)^2$ is always reduced by the quadratic rate during iteration. The way the iteration converges to the solution is depicted in Figure 2.2. This technique is sometimes called linearization because a solution of non-linear problem is solved by a series of linear problem.
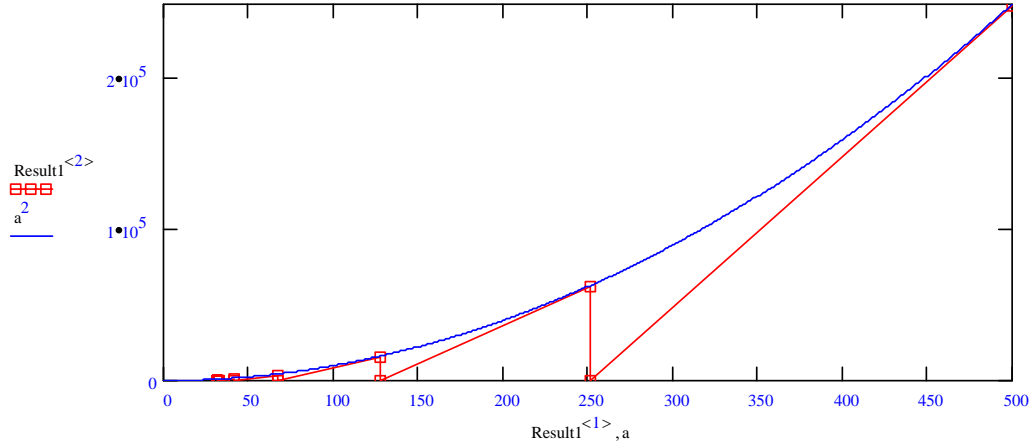
Figure 2.2 Generalized solution obtained by Newton method

That gives immediately the iterative correction as,

$$\mathbf{a}_{i+1} - \mathbf{a}_i = -\mathbf{K}_t^{-1}\psi(\mathbf{a}_i) \tag{2.191}$$

where Jacobian matrix corresponding to the tangent direction.

$$\mathbf{K}_t = \psi'(\mathbf{a}_i) = \left.\frac{\partial \psi}{\partial \mathbf{a}}\right|_i \tag{2.192}$$

Using Eq.(2.192), Eq.(2.191) can manipulate to reach,

$$\delta\mathbf{a}_{i+1} = -\mathbf{K}_t^{-1}\psi(\mathbf{a}_i) \tag{2.193}$$

A series of successive approximation gives,

$$\mathbf{a}_{i+1} = \mathbf{a}_i + \delta\mathbf{a}_{i+1} = \mathbf{a}_o + \Delta\mathbf{a}_{i+1} \tag{2.194}$$

$$\text{where} \qquad \Delta\mathbf{a}_{i+1} = \sum_{k=1}^{i+1}\delta\mathbf{a}_{i+1} \tag{2.195}$$

2-6-2 Modified Newton-Raphson methods

Just replace the variable jacobian stiffness by a constant approximation:

$$\mathbf{K}_i = \mathbf{K}_t \tag{2.196}$$

In replacing Eq.(2.193), giving,

$$\delta\mathbf{a}_{i+1} = -\mathbf{K}_i^{-1}\psi(\mathbf{a}_i) \tag{2.197}$$

can be chosen as the matrix corresponding to the first iteration $\mathbf{K_i}$, or may even one corresponding to some previous step of load incrementation $\mathbf{K_o}$. Obviously, the procedure will converge generally at a slower but simpler. Many variants of this process are used in practice and symmetric solvers can generally be used providing a symmetric form of $\mathbf{K_t}$ is chosen.

2-6-3 Quasi-Newton methods

Once, the first iteration has been established giving,

$$\delta\mathbf{a}_1 = -\mathbf{K}_i^{-1}\psi(\mathbf{a}_1) \tag{2.198}$$

A secant slope can be found such as,

$$\delta\mathbf{a}_1 = -\mathbf{K}_s^{-1}\left(\psi(\mathbf{a}_1) - \psi(\mathbf{a}_2)\right) \tag{2.199}$$

This slope can now be used to establish $\delta\mathbf{a}_2$ by expression of the form of Eq.(13), giving,

$$\delta\mathbf{a}_2 = -\mathbf{K}_s^{-1}\psi(\mathbf{a}_2) \tag{2.200}$$

Now dropping subscripts for i>1

$$\delta\mathbf{a}_i = -\mathbf{K}_s^{-1}\psi(\mathbf{a}_i) \tag{2.201}$$

and $\mathbf{K}_s^{-1}$ is determined so that

$$\mathbf{K}_s^{-1} = -\frac{\mathbf{a}_{i-1} - \mathbf{a}_i}{\psi(\mathbf{a}_{i-1}) - \psi(\mathbf{a}_i)} \tag{2.202}$$

The determination of $\mathbf{K}_s$ is trivial and the convergence is almost as rapid as with the Newton-Raphson process.

2-6-4 Direct (or Picard) iteration

To totally avoid the stability difficulties and reduce the storage and number of operations needed, the direct or Picard iteration is particularly useful in the solution of non-linear problems which can be written as,

$$\psi(\mathbf{a}) = \mathbf{K}(\mathbf{a}) \cdot \mathbf{a} - f \equiv 0 \tag{2.203}$$

In such case $\psi(\mathbf{a}_{i+1}) = 0$ is taken and the iteration proceeds without increments, writing

$$\mathbf{a}_{i+1} = \mathbf{K}(\mathbf{a}_i)^{-1} \cdot f \tag{2.204}$$

The comparisons between (i) Newton-Raphson, (ii) initial tangent, (iii) previous tangent, (iv) quasi-Newton and (v) Picard iteration have been made in Figure 2.3. It was found that Newton-Raphson method gives the fastest convergence by quadratic rate. Though, Quasi-Newton gives a slower rate than Newton-Raphson does, quadratic rate of convergence is still observed. Picard iteration gives a stable solution but lose a quadratic rate feature. The initial and previous tangent method are straightforward in methodology but show awkward feature by a linear rate of convergence.
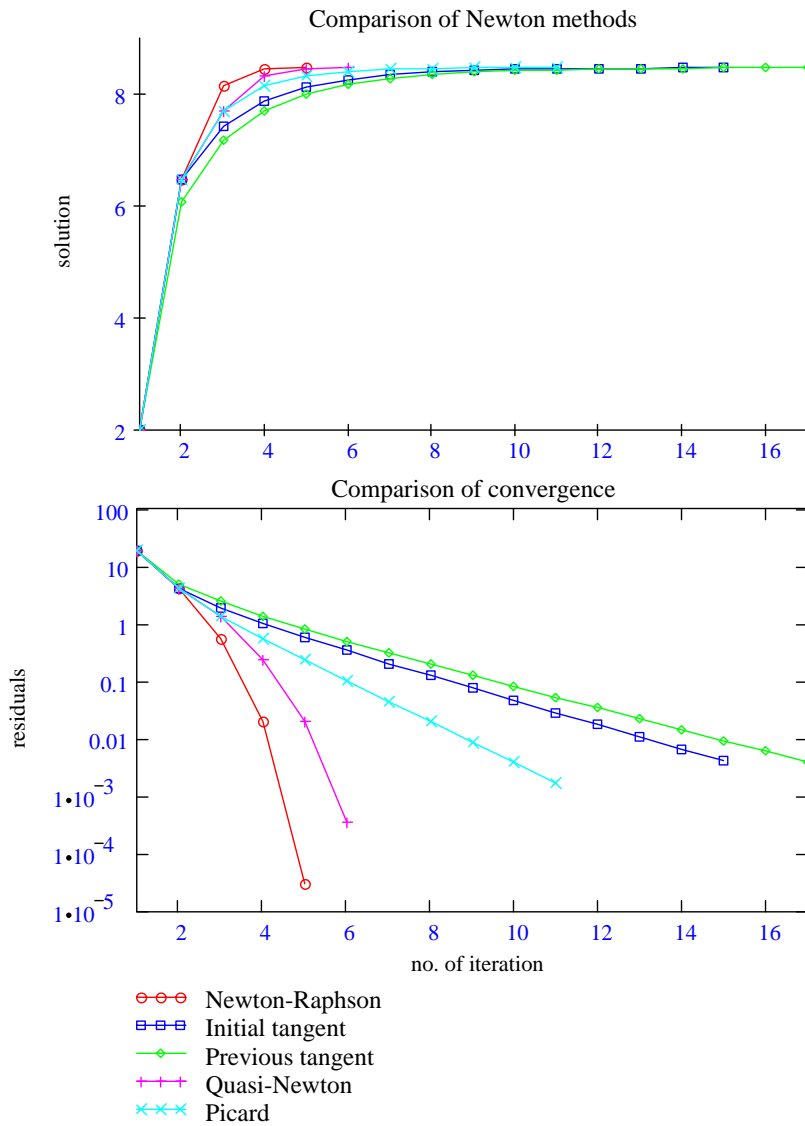
Figure 2.3 Comparison among Newton methods

2-7 Central Limit Theorem

The statement of the central limit theorem is as follows. The sampling distribution of the sample mean from a population, which has an unknown probability distribution, will still be approximately normal if the sample size n is sufficiently large. If x_1, x_2,.. x_n are random samples of sizes n taken from a population (either finite or infinite) with mean μ and finite variance σ^2 and if $\overline{x}$ is the sample mean then,

$$\lim_{n\to\infty} P\left(\frac{\overline{x}-\mu}{\sigma/\sqrt{n}} \le z\right) = \Phi(z) = \frac{1}{2\pi}\int_{-\infty}^{z}\exp(-0.5u^2)du \qquad (2.205)$$

Central limit theorem, named by G. Polya in 1920 [25], is the most remarkable of all probability theory. Under very general conditions, the distribution of the sum of number a random variables converges to, or approaches, the normal distribution as the number of variables in the num becomes large. The specific example by tolling dices can be imaged in Figure 2.4.
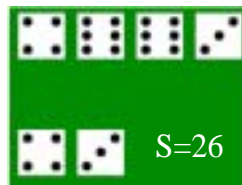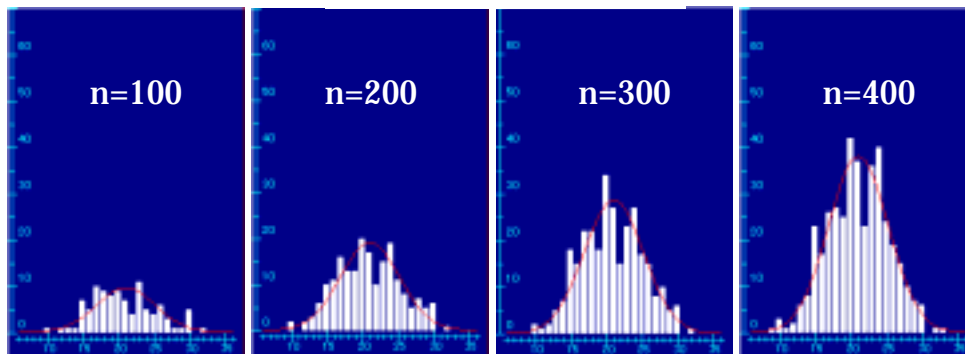
Figure 2.4 Illustration of Central limit theorem [26]

2-8 Reference

1 Bird, R. B., E. S. Warren , N. L. Edwin, Transport phenomena, John Wiley, 1960

2 Ogden, R.W., Non-linear elastic deformations, Ellis Horwood Limited, 1984

3 Bonet, Javier & Wood, Richard, D., Nonlinear continuum mechanics for finite element analysis, Cambridge University Press, 1997

4 Mal, A.K. & Singh, S.J., Deformation of Elasitc Solids, Prentice-Hall, 1991

5 Mase, G.E., Theory and Problems of Continuum Mechanics, McGraw-Hill, 1970

6 Fung, Y.C., A First Course in Continuum Mechanics, Prentice-Hall, 1977

7 Chadwick, P., Continuum Mechanics: Concise Theory and Problems, George Allen & Unwin Ltd., 1976

8 Chen, W.F. & Mizuno, E., Nonlinear Analysis in Soil Mechanics, Elsevier, 1990

9 Spiegel, M.R., Mathematical Handbook of formulas and tables, Schaum's Outlines Series, 1990

10 Chen, W.F. & Saleeb, A.F., Constitutive Equations for Engineering Materials, Vol 1: Elasticity and Modeling, John Wiley & Sons, 1982

11 Timoshenko, S.P. & Goodier, J.N., Theory of Elasticity, McGraw-Hill, 1970

12 Green, A.E. & Zerna, W., Theoretical Elasticity, Oxford University Press, 1968

13 Marsden, J.E. & Hughes, T.J.R., Mathematical Foundations of Elasticity, Prentice-Hall, 1983

14 Novozhilov, V.V., Foundations of the Nonlinear Theory of Elasticity, Graylock Press, 1953

15 Washizu, K., Variational Methods in Elasticity & Plasticity, Pergamon Press, 1982

16 Salençon, J., Application of the Theory of Plasticity in Soil Mechanics, John Willey & Sons, 1977

17 Khan, A.S & Huang, S., Continuum Theory of Plasticity, John Wiley & Sons, 1995

18 Chen, W.F., Limit Analysis and Soil Plasticity, Elsevier, 1975

19 Chen, W.F. & Baladi, G.Y., Soil Plasticity: Theory and Implementation, Elsevier, 1985

20 Chen, W.F. & Liu, X.L., Limit Analysis in Soil Mechanics, Elsevier, 1990

21 Chakrabarty, J., Theory of Plasticity, McGraw-Hill, 1998

22 Bazaraa, M.S., Sherali, H.D. & Shetty, C.M., Nonlinear programming: theory and algorithms, John Wiley & Sons, Ltd., 1993

23 Wismer, D.A. & Chattergy, R., Introduction to Nonlinear Optimization, Elsevier, 1978

24 Zienkiewicz, O.C., The finite element method: Vol. 2. Solid and fluid mechanics, Dynamics and non-linearity –4th, McGraw-Hill, 1991

25 Harr, M.E., Reliability Based Design in Civil Engineering, Dover, 1987

26 http://www.math.csusb.edu/faculty/stanton/probstat/clt.html

CHAPTER 3
Convex Analysis

3-1 Associated plastic flow at the intersection corner of plastic potential functions in soil mechanics

3-1-1 Introduction

A hypothesis of associated flow rule has been generally applied to elasto-plastic models in order to determine irreversible plastic flow emerged in an outward normal direction to the yield loci. It has been found that the expressions in the original Cam-Clay [1] (Roscoe, Schofield & Thurairajah, 1963) and the Sekiguchi-Ohta models [2] (Sekiguchi & Ohta, 1977) cause the discontinuity in stress space by accommodating the intersection corner of two continuously differentiable convex yield surfaces.

The discontinuous yield/plastic potential function can cause computational difficulties in numerical analyses; careful study of the relevant subroutines in the finite element program CRISP described by Britto , A.M. & Gunn, M.J. (1987) [3] shows that, for practical use in numerical calculations, the point of the original Cam clay plastic potential has to be rounded off and the discontinuity eliminated.

Gens, A. & Potts, D.M. (1988) [4] pointed out that the discontinuity of the yield surface of the original Cam-clay model at zero stress ratio implies difficulties both theoretical and practical. As the flow rule is associated, isotropic stress changes at that point will cause non-zero shear strains. Also, the model may have problems in yielding a reasonable stress response for some applied increment strain ratios. The modified Cam-clay model overcomes those drawbacks by adopting ellipse as yield locus in replacing logarithmic spiral in original Cam clay.

The arisen singularity at the corner rules out the normality postulate, therefore, plastic strain increment is indeterminate thus it should be marked as a limitation of the models which none of algorithm has yet to set forth. The aim of this study is to provide the mathematical treatment for evaluating the irregular plastic flow on the intersection corner of the yield functions of the original Cam-Clay and the Sekiguchi-Ohta models by broader foundation. Results of this study may suggest a solution to the problem concerned and serve as the basis for further research and development on the models and related fields.

3-1-2 Governing equations

The fundamental implementation to deal with the problem encountered is based on the associated flow rule for multiple non-smooth yield criteria extended by Koiter (1953, 1960) [5,6] (See Figure 3.1 and Figure 3.2). The governing equations are formed in Box 3.1 following the general approach advocated in Simo, Kennedy and Govindjee (1988) [7]. The classical Kuhn-Tucker complementarily conditions of convex mathematical programming are capable to appropriately characterize loading/unloading constraints using two active independent Lagrangian multipliers. The scope to concern is narrow to rate-independent infinitesimal plasticity. For convenience, all equations corresponding to both models are considered at a time by specifying η_o of the Sekiguchi-Ohta model to zero for those of the original Cam-Clay model.
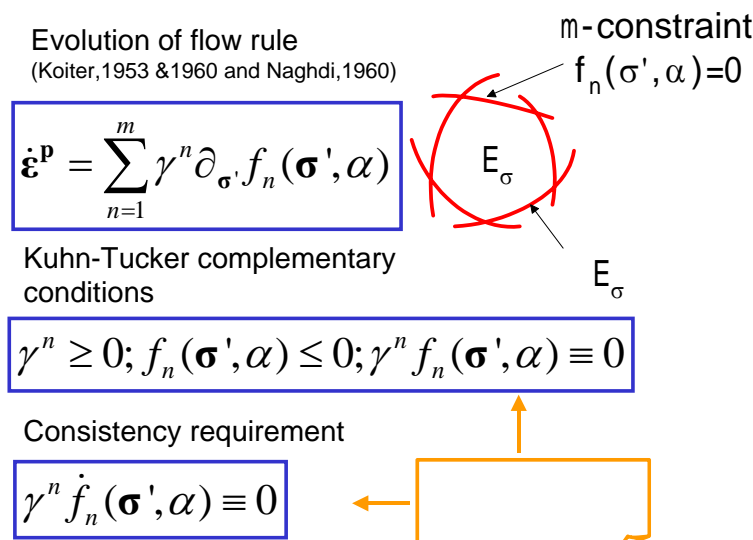
Figure 3.1 Koiter's associated flow rule for nonsmooth yield surface

3-1-3 Loading/Unloading & Consistency conditions

Figure 3.3 shows admissible stresses on the state of boundary surface of the original Cam-clay. In strain space, the region of M⁻ defines the bunch of unloading boundaries while the normal cone of M⁺ borders the associated plastic flow from the corner. The direction of plastic flow can be expressed by the angle of dilation (β). Loading/unloading criteria are listed in Box 3.2.

γ = flow speed $\partial_{\sigma'} f$ = flow direction   Koiter, W.T. (1953)

$$\dot{\boldsymbol{\varepsilon}}_{\mathbf{p}} = \gamma_1 \partial_{\boldsymbol{\sigma'}} f_1 \qquad \dot{\boldsymbol{\varepsilon}}_{\mathbf{p}} = \gamma_1 \partial_{\boldsymbol{\sigma'}} f_1 + \gamma_2 \partial_{\boldsymbol{\sigma'}} f_2 \qquad \dot{\boldsymbol{\varepsilon}}_{\mathbf{p}} = \sum_{i=1}^{4} \gamma_i \partial_{\boldsymbol{\sigma'}} f_i$$

$$\dot{f}_1 = 0 \qquad\qquad \dot{f}_1 = 0 \quad \dot{f}_2 = 0 \qquad\qquad \dot{f}_i = 0 \quad {}_{i=1..4}$$
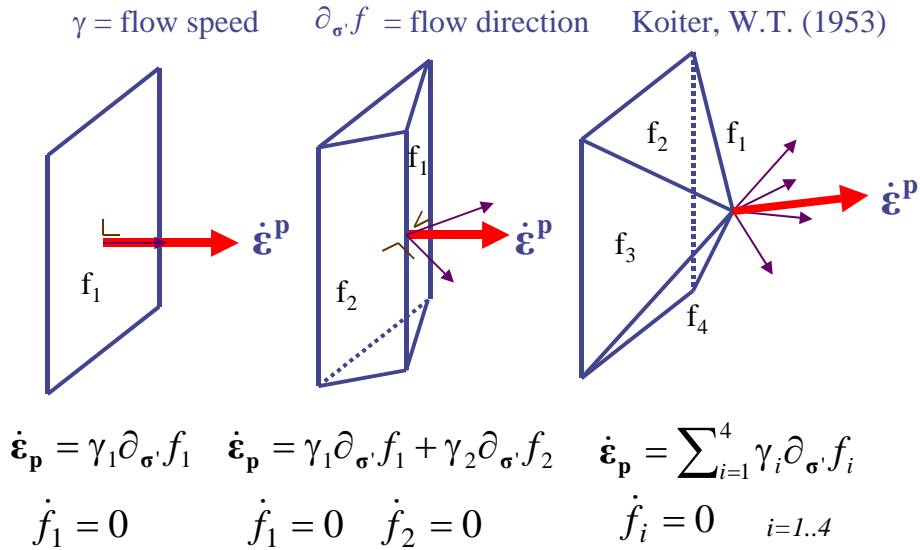
Figure 3.2 Associated plastic flow for multi-yield surfaces
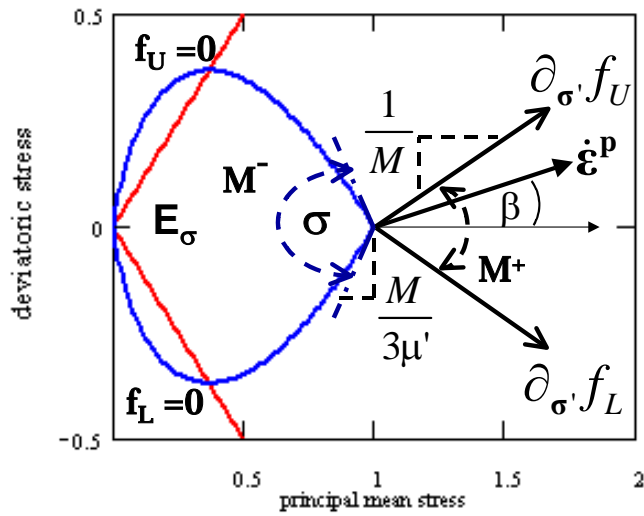
Figure 3.3 Plastic flow regulated by the original Cam-clay model

3-1-4 Evaluation of plastic flow at the corner

Box 3.3 contains the basic equations to evaluate plastic flow for case 2.1.1 in Box 3.2, as the classical flow rule is applied to other cases. It is required that matrix **X** must be positive definite 2x2 matrix. (See Box 3.3)

Box 3.1 Governing equations

Yield function: Sekiguchi-Ohta model (1977)

$$\mathrm{f}(\boldsymbol{\sigma}',\alpha) = f(p',\eta^*,\alpha) \equiv MD\ln\left(\frac{p'}{p'_o}\right) + D\eta^* - \alpha = 0$$

In triaxial stress condition $\left(\sigma'_2 \equiv \sigma'_3, \sigma'_{12} = \sigma'_{23} = \sigma'_{31} \equiv 0\right)$

$$\mathrm{f}(\boldsymbol{\sigma}',\alpha) = MD\ln\left(\frac{p'}{p'_o}\right) + D\left|\frac{q}{p'} - \eta_o\right| - \alpha = 0$$

where $\alpha \equiv \varepsilon_v^p = \int \dot{\varepsilon}_v^p dt$; $p' \equiv \frac{1}{3}tr(\boldsymbol{\sigma}')$; $p'_o \equiv \frac{1}{3}tr(\boldsymbol{\sigma}'_o)$; $\mathbf{s} \equiv \boldsymbol{\sigma}' - p'\mathbf{1}$; $\mathbf{s}_o \equiv \boldsymbol{\sigma}'_o - p'_o\mathbf{1}$;

$\boldsymbol{\eta} \equiv \dfrac{\mathbf{s}}{p'}$; $\boldsymbol{\eta}_o \equiv \dfrac{\mathbf{s}_o}{p'_o}$; $\eta^* \equiv \sqrt{\dfrac{3}{2}}\|\boldsymbol{\eta} - \boldsymbol{\eta}_o\|$; $q \equiv \sqrt{\dfrac{3}{2}}\|\mathbf{s}\|$; $\eta_o = \dfrac{3(1-K_o)}{1+2K_o}$; $\mathbf{n} \equiv \dfrac{\mathbf{s}}{\|\mathbf{s}\|}$

Heterogeneity of yield function (compression & extension boundary)

i) Upper yield locus: $\mathrm{f}_U(\boldsymbol{\sigma}',\alpha) \equiv MD\ln\left(\frac{p'}{p'_o}\right) + D\left(\frac{q}{p'} - \eta_o\right) - \alpha = 0$

ii) Lower yield locus: $\mathrm{f}_L(\boldsymbol{\sigma}',\alpha) \equiv MD\ln\left(\frac{p'}{p'_o}\right) - D\left(\frac{q}{p'} - \eta_o\right) - \alpha = 0$

Associated flow rule: Koiter (1953, 1960)

$$\dot{\boldsymbol{\varepsilon}}^p \equiv \gamma_U \partial_{\boldsymbol{\sigma}'} f_U(\boldsymbol{\sigma}',\alpha) + \gamma_L \partial_{\boldsymbol{\sigma}'} f_L(\boldsymbol{\sigma}',\alpha)$$

Hardening law (isotropic strain-hardening)

$$\dot{\alpha} = \dot{\varepsilon}_v^p \equiv \gamma_U \partial_{p'} f_U + \gamma_L \partial_{p'} f_U$$

Kuhn-Tucker complementary conditions

$\gamma_U \geq 0; f_U(\boldsymbol{\sigma}',\alpha) \leq 0; \gamma_U f_U(\boldsymbol{\sigma}',\alpha) \equiv 0$ (compression side) and

$\gamma_L \geq 0; f_L(\boldsymbol{\sigma}',\alpha) \leq 0; \gamma_L f_L(\boldsymbol{\sigma}',\alpha) \equiv 0$ (extension side)

Consistency requirement

$\gamma_U \dot{f}_U(\boldsymbol{\sigma}',\alpha) \equiv 0$ and $\gamma_L \dot{f}_L(\boldsymbol{\sigma}',\alpha) \equiv 0$

where $\dot{f}_U = \partial_{\boldsymbol{\sigma}'} f_U : \dot{\boldsymbol{\sigma}}' + \partial_\alpha f_U \dot{\alpha}$; $\dot{f}_L = \partial_{\boldsymbol{\sigma}'} f_L : \dot{\boldsymbol{\sigma}}' + \partial_\alpha f_L \dot{\alpha}$; $\partial_\alpha f_U = \partial_\alpha f_L = -1$;

$\partial_{\boldsymbol{\sigma}'} f_U = \dfrac{1}{3}\partial_{p'} f_U \mathbf{1} + \sqrt{\dfrac{3}{2}}\partial_q f_U \mathbf{n}$; $\partial_{\boldsymbol{\sigma}'} f_L = \dfrac{1}{3}\partial_{p'} f_L \mathbf{1} + \sqrt{\dfrac{3}{2}}\partial_q f_L \mathbf{n}$

Hookean relation for isotropic hypo-elasticity

$$\dot{\boldsymbol{\sigma}}' \equiv \mathbf{c}^e : \left(\dot{\boldsymbol{\varepsilon}} - \dot{\boldsymbol{\varepsilon}}^p\right)$$

where $\mathbf{c}^e \equiv K\mathbf{1}\otimes\mathbf{1} + 2G\left[\mathbf{I} - \dfrac{1}{3}\mathbf{1}\otimes\mathbf{1}\right]$

$\mathbf{I} \equiv \dfrac{1}{2}\left[\delta_{ik}\delta_{jl} + \delta_{il}\delta_{jk}\right]\mathbf{e_i}\otimes\mathbf{e_j}\otimes\mathbf{e_k}\otimes\mathbf{e_l}$; $\mathbf{1} \equiv \delta_{ij}\mathbf{e_i}\otimes\mathbf{e_j}$;

$\Lambda = 1 - \dfrac{\kappa}{\lambda}$; $\mu' = \dfrac{3}{2}\left(\dfrac{1-2\nu'}{1+\nu'}\right)$; $K = K(p') = \dfrac{\Lambda}{MD(1-\Lambda)}p'$; $G = G(p') = \mu' K(p')$

Box 3.3 demonstrates the assessment of plastic flow in regard to the original Cam-clay model under isotropic strain rate. The resulting slopes of e-ln(p') curves provide the verification of the method. Angle of dilation corresponding to associated flow rule applied on both smooth surface and at corner are given in Figure 3.5.

3-1-5 Closure

Though the discontinuity still exists, the arguable plastic flow can be theoretically settled using the scheme developed. States of stresses at the corner lie in the margin among many conceivable plastic flow directions depended on the strain rate applied. Heterogeneous soil deformation is characterized by the coupled contribution of intersecting yield loci at the corner.

Box 3.2 Yield, consistency and loading/unloading criteria

Covariant components of $\dot{\boldsymbol{\varepsilon}}$ relative to $\{\partial_{\boldsymbol{\sigma}'}f_U, \partial_{\boldsymbol{\sigma}'}f_L\}$

$L_U = \partial_{\boldsymbol{\sigma}'}f_U : \mathbf{c}^e : \dot{\boldsymbol{\varepsilon}}$; $L_L = \partial_{\boldsymbol{\sigma}'}f_L : \mathbf{c}^e : \dot{\boldsymbol{\varepsilon}}$

For any $(\boldsymbol{\sigma}', \alpha) \in E_{\boldsymbol{\sigma}'}$

1) Inside elastic region:

$f_U(\boldsymbol{\sigma}', \alpha) < 0$ and $f_L(\boldsymbol{\sigma}', \alpha) < 0 \rightarrow \gamma_U = 0; \gamma_L = 0$

2) At the corner: $f_U(\boldsymbol{\sigma}', \alpha) = 0$ and $f_L(\boldsymbol{\sigma}', \alpha) = 0$

  2.1) Plastic loading: $L_U > 0$ or $L_L > 0$

    2.1.1) To the normal cone of the intersection corner:

      $\dot{f}_U(\boldsymbol{\sigma}', \alpha) = 0$ and $\dot{f}_L(\boldsymbol{\sigma}', \alpha) = 0 \rightarrow \gamma_U > 0; \gamma_L > 0$

    2.1.2) To the region of upper yield locus:

      $\dot{f}_U(\boldsymbol{\sigma}', \alpha) = 0$ and $\dot{f}_L(\boldsymbol{\sigma}', \alpha) < 0 \rightarrow \gamma_U > 0; \gamma_L = 0$

    2.1.3) To the region of lower yield locus:

      $\dot{f}_U(\boldsymbol{\sigma}', \alpha) < 0$ and $\dot{f}_L(\boldsymbol{\sigma}', \alpha) = 0 \rightarrow \gamma_U = 0; \gamma_L > 0$

  2.2) Elastic unloading:

    $L_U < 0$ and $L_L < 0 \rightarrow \gamma_U = 0; \gamma_L = 0$

3) On upper yield locus:

$f_U(\boldsymbol{\sigma}', \alpha) = 0$ and $f_L(\boldsymbol{\sigma}', \alpha) < 0 \rightarrow \gamma_L = 0$

  3.1) Plastic loading:

$L_U > 0$ and $\dot{f}_U(\boldsymbol{\sigma}', \alpha) = 0 \rightarrow \gamma_U > 0$

  3.2) Elastic unloading:

$L_U < 0$ or $\dot{f}_U(\boldsymbol{\sigma}', \alpha) < 0 \rightarrow \gamma_U = 0$

4) On lower yield locus: $f_U(\boldsymbol{\sigma}', \alpha) < 0$ and $f_L(\boldsymbol{\sigma}', \alpha) = 0$

  {The same manner in parallel with item 3}

Box 3.3 Plastic strain increment vector at the corner

Admissible stress constrained at the corner

$f_U(\boldsymbol{\sigma}', \alpha) = 0$ and $f_L(\boldsymbol{\sigma}', \alpha) = 0$

Plastic strain increment   Consistency parameters

$$\begin{pmatrix} \dot{\varepsilon}_v^p \\ \dot{\varepsilon}_s^p \end{pmatrix} = \begin{pmatrix} \partial_{p'}f_U & \partial_{p'}f_L \\ \partial_q f_U & \partial_q f_L \end{pmatrix} \cdot \begin{pmatrix} \gamma_U \\ \gamma_L \end{pmatrix} \qquad \begin{pmatrix} \gamma_U \\ \gamma_L \end{pmatrix} = \mathbf{X}^{-1}_{(2 \times 2)} \cdot \langle \mathbf{L} \rangle_{(2 \times 1)}$$

$$\text{where } \begin{pmatrix} \partial_{p'}f_U & \partial_{p'}f_L \\ \partial_q f_U & \partial_q f_L \end{pmatrix} = \begin{pmatrix} \dfrac{D}{p'}(M - \dfrac{q}{p'}) & \dfrac{D}{p'}(M + \dfrac{q}{p'}) \\ \dfrac{D}{p'} & -\dfrac{D}{p'} \end{pmatrix}$$

$$\mathbf{L} = \begin{bmatrix} K\partial_{p'}f_U & 3G\partial_q f_U \\ K\partial_{p'}f_L & 3G\partial_q f_U \end{bmatrix} \begin{pmatrix} \dot{\varepsilon}_v \\ \dot{\varepsilon}_s \end{pmatrix} \quad \text{where} \quad \langle \mathbf{L} \rangle_i \equiv \dfrac{\mathbf{L}_i + |\mathbf{L}_i|}{2}$$

Coupled-hardening matrix

$$\mathbf{X} = \begin{bmatrix} K\left(\partial_{p'}f_U\right)^2 + 3G\left(\partial_q f_U\right)^2 + \partial_{p'}f_U & K\left(\partial_{p'}f_U.\partial_{p'}f_L\right) + 3G\left(\partial_q f_U.\partial_q f_L\right) + \partial_{p'}f_L \\ K\left(\partial_{p'}f_U.\partial_{p'}f_L\right) + 3G\left(\partial_q f_U.\partial_q f_L\right) + \partial_{p'}f_U & K\left(\partial_{p'}f_L\right)^2 + 3G\left(\partial_q f_L\right)^2 + \partial_{p'}f_L \end{bmatrix}$$

$$\dot{\sigma}' \equiv \mathbf{c}^e : \left(\dot{\varepsilon} - \dot{\varepsilon}^p\right)$$

$$\dot{f}_U = \partial_{\sigma'} f_U : \dot{\sigma}' + \partial_\alpha f_U \dot{\alpha} \equiv 0$$

$$\mathbf{c}^e \equiv K\mathbf{1} \otimes \mathbf{1} + 2G\left(\mathbf{I} - \frac{1}{3}\mathbf{1} \otimes \mathbf{1}\right)$$

$$\dot{f}_L = \partial_{\sigma'} f_L : \dot{\sigma}' + \partial_\alpha f_L \dot{\alpha} \equiv 0$$

$$\dot{\varepsilon}^p = \gamma_U \partial_{\sigma'} f_U + \gamma_L \partial_{\sigma'} f_L$$

$$\partial_{\sigma'} f_U = \frac{1}{3}\partial_p f_U \mathbf{1} + \sqrt{\frac{3}{2}}\partial_q f_U \mathbf{n}$$

$$\sqrt{} \qquad ? \qquad \sqrt{}$$

$$\partial_{\sigma'} f_L = \frac{1}{3}\partial_p f_L \mathbf{1} + \sqrt{\frac{3}{2}}\partial_q f_L \mathbf{n}$$

$$\mathbf{X}_{(2 \times 2)} \cdot \begin{pmatrix} \gamma_U \\ \gamma_L \end{pmatrix} = \mathbf{L}_{(2 \times 1)}$$

$$\partial_\alpha f_U = \partial_\alpha f_L = -1 \qquad \dot{\alpha} = \dot{\varepsilon}_v^p$$

X must be positive-definite
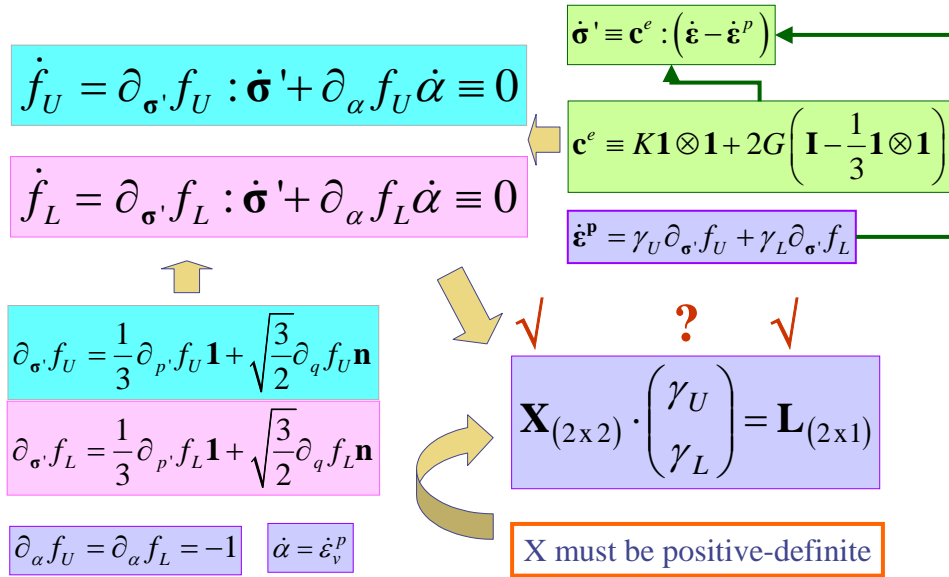
Figure 3.4 Evaluation of consistency parameters at the corner

Box 3.4 Plastic flow for isotropic volumetric compression

Rate of strain during isotropic volumetric compression

$$\dot{\varepsilon} = \frac{1}{3}\dot{\varepsilon}_v \mathbf{1} + \sqrt{\frac{3}{2}}\dot{\varepsilon}_s \mathbf{n}; \quad \dot{\varepsilon}_v = -\frac{\dot{e}}{1+e_o}; \quad \dot{\varepsilon}_s = 0$$

Covariance of strain rate   Consistency parameters

$$\begin{pmatrix} L_U \\ L_L \end{pmatrix} = \frac{KMD}{p'}\begin{pmatrix} \dot{\varepsilon}_v \\ \dot{\varepsilon}_v \end{pmatrix} \qquad \begin{pmatrix} \gamma_U \\ \gamma_L \end{pmatrix} = \frac{Kp'}{2(p'+KMD)}\begin{pmatrix} \dot{\varepsilon}_v \\ \dot{\varepsilon}_v \end{pmatrix}$$

Plastic strain increment   Stress increment

$$\begin{pmatrix} \dot{\varepsilon}_v^p \\ \dot{\varepsilon}_s^p \end{pmatrix} = \frac{KMD}{p'+KMD}\cdot\begin{pmatrix} \dot{\varepsilon}_v \\ 0 \end{pmatrix} \qquad \begin{pmatrix} \dot{p}' \\ \dot{q} \end{pmatrix} = \frac{p'\Lambda}{MD}\begin{pmatrix} \dot{\varepsilon}_v \\ 0 \end{pmatrix}$$

where $\quad D = \dfrac{\lambda \Lambda}{(1+e_o)M} \quad$: coefficient of dilatancy

e-ln(p') curves;   loading: $\dot{e} = -\lambda\dfrac{\dot{p}'}{p'}$,   unloading: $\dot{e} = -\kappa\dfrac{\dot{p}'}{p'}$

Angle of dilation   **On continuous surface**

if $\dfrac{q}{p'} > 0$

$$\tan \beta = \frac{1}{M - \dfrac{q}{p'}}$$

At the corner

if $\quad \dfrac{q}{p'} = 0$

$$\tan \beta = \frac{1}{\Lambda}\frac{\dot{\varepsilon}_s}{\dot{\varepsilon}_v}$$

if $\dfrac{q}{p'} < 0$

$$\tan \beta = \frac{-1}{M + \dfrac{q}{p'}}$$
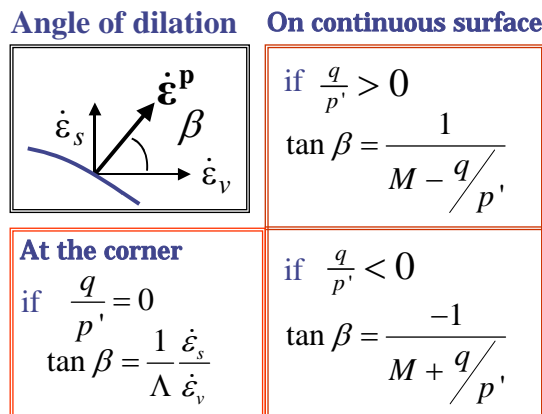
Figure 3.5 Angle of dilation corresponding to the original Cam-clay flow rule

3-2 The vertex singularity in the Sekiguchi-Ohta model

3-2-1 Introduction

The Critical state theory incorporated with normality criterion has released many numerical implementations in soil mechanics. Sekiguchi and Ohta (1977) [2] proposed the constitutive model to address the stress anisotropy induced during the natural clay deposition in addition to those of Cambridge models by introducing the non-negative normalized shear stress η^* taking principal stresses reorientation into account. The expression causes the inevitable discontinuity by accommodating the singular vertex in stress space. In recent days, Pipatpongsa et al. (2001a,b) [8, 9] developed the mathematical treatment for the intersecting corner of two continuously differentiable convex yield loci; namely, upper and lower yield loci, and evaluated theoretical K_o-value and Poisson's ratio in corresponding to the Sekiguchi-Ohta model. However, it is not clear the implementation, which is based on the triaxial condition, is valid for general conditions. The study discusses the scope of method by considering the existence of the vertex in principal stress space and plane strain condition. This study may lead to a better understanding of the vertex singularity in the model and its implementation.

3-2-2 Deviatoric view of yield surface

In addition to three stress invariants, the stress-induced anisotropic yield function for an inherent isotropic media must depend on the state of stress at the completion of consolidation. Herein, the invicid form of yield function proposed by Sekiguchi and Ohta (1977) is shown by Eq.(3.1).

$$\mathrm{f}(\boldsymbol{\sigma'}, \boldsymbol{\sigma'_o}, \alpha) = f(p', \eta^*, \alpha) \equiv MD \ln\left(\frac{p'}{p'_o}\right) + D\eta^* - \alpha = 0 \tag{3.1}$$

where $\alpha \equiv \varepsilon_v^p = \int \dot{\varepsilon}_v^p dt$; $\boldsymbol{\eta} \equiv \dfrac{\mathbf{s}}{p'}$; $\boldsymbol{\eta_o} \equiv \dfrac{\mathbf{s_o}}{p'_o}$; $\eta^* \equiv \sqrt{\dfrac{3}{2}} \|\boldsymbol{\eta} - \boldsymbol{\eta}_o\|$

The set of intersection of the yield surface with π-plane is yield curve, which is conveniently given by the expression transformed to polar coordinates where θ is angle measured anti-clockwise on π-plane. The substitution of θ=const. gives the meridional section relating $\|\mathbf{s}\|$ and p'.

$$s(p', \theta) = \sqrt{\frac{2}{3}} p' \left[\cos(\theta)\eta_o + \sqrt{M^2 \ln(\frac{p'}{p'_o})^2 - \sin(\theta)^2 \eta_o^2} \right] \tag{3.2}$$

Deviatoric plane
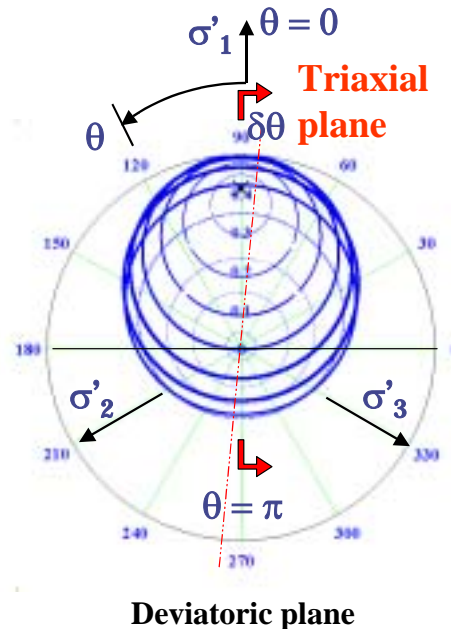
Figure 3.6 Circular yield curves formed by intersection of yield surface with planes of constant mean stress

The major principal stress axis at θ=0 locally coincides with the major principal direction of stress-induced initial anisotropy, in general, the vertical stress direction. Figure 3.6 shows the plot of Eq.(3.2). The physical meanings of the angle θ are given as following.

$\pi/3 \geq \theta \geq 0$ for $\sigma'_z \geq \sigma'_y \geq \sigma'_x$, compression test: θ=0

$$2\pi/3 \ge \theta \ge \pi/3 \quad \text{for} \quad \sigma'_y \ge \sigma'_z \ge \sigma'_x$$

$$\pi \ge \theta \ge 2\pi/3 \quad \text{for} \quad \sigma'_y \ge \sigma'_x \ge \sigma'_z, \text{ extension test: } \theta = \pi$$

Taking $\theta=0$ and π will cut the Sekiguchi-Ohta yield surface by a triaxial plane relating to customary p'-q plane where upper and lower yield loci with intersecting corner can be observed in Figure 3.7. It is clearly seen this particular state of stress totally passes the singular vertex ($\eta^*=0$) where the serious numerical convergence occurs. The corner is rounded off for a small rotation $\delta\theta$, indicating the special treatment is only required for state of stress under axis-symmetry in which the Sekiguchi-Ohta model is reduced to the Ohta-Hata model (1971) [10]. In the case of plane-strain, the intermediate effective stress is determined by Eq.(3.3), thus diverting the stress condition from the vertex. However, K_o-condition can be deduced from plane-strain under condition by Eq.(3.4).

$$\sigma'_{22} = \sigma'_{yy} = v'(\sigma'_{xx} + \sigma'_{zz}) = \frac{K_o}{1+K_o}(\sigma'_{xx} + \sigma'_{zz}) \tag{3.3}$$

$$\tau_{zx} = 0, \quad \sigma'_{xx} = K_o \sigma'_{zz} \tag{3.4}$$
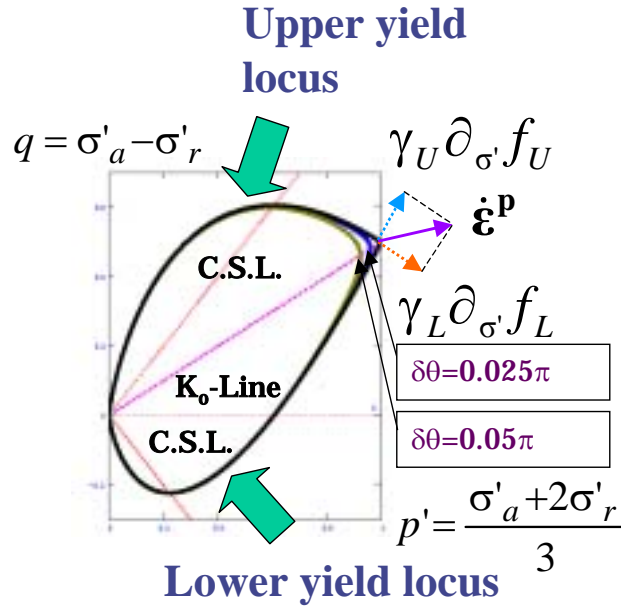
Figure 3.7 p'-q plane relating to meridional section at $\theta=0$ and π

3-2-3 Implementation at the vertex singularity

Singular yield surfaces with edges or corners may be described by a finite number of yield functions based on Koiter's suggestion [5]. Concerning with the Sekiguchi-Ohta model, the discontinuity is observed on triaxial plane where upper and lower yield locus expressed by Eq.(3.5) and (3.6) intersecting each other to form the corner. At the singular stress $\boldsymbol{\sigma}'$ in which $f_U(\boldsymbol{\sigma}',\alpha) = f_L(\boldsymbol{\sigma}',\alpha) = 0$, a consistency requirement guarantees the actual values of $\gamma_U \ge 0$ and $\gamma_L \ge 0$ can be determined, then $\boldsymbol{\sigma}'$ must keep on the hardening vertex so that $\dot{f}_U(\boldsymbol{\sigma}',\alpha) = \dot{f}_L(\boldsymbol{\sigma}',\alpha) = 0$. For a certain imposed strain rate in which either $\gamma_U = 0$ or $\gamma_L = 0$ is evaluated, this particular method will reduce to the ordinary method applicable to the Sekiguchi-Ohta model and the stress point $\boldsymbol{\sigma}'$ will move out of the singularity. The basic equations in tensor notation are available below.

$$f_U(p',q,\alpha) \equiv MD\ln\left(\frac{p'}{p'_o}\right) + D\left(\frac{q}{p'} - \eta_o\right) - \alpha = 0 \tag{3.5}$$

$$f_L(p',q,\alpha) \equiv MD\ln\left(\frac{p'}{p'_o}\right) - D\left(\frac{q}{p'} - \eta_o\right) - \alpha = 0 \tag{3.6}$$

Incremental elastic stress-strain relations:

$$\dot{\boldsymbol{\sigma}}' \equiv \mathbf{c}^e : \left(\dot{\boldsymbol{\varepsilon}} - \dot{\boldsymbol{\varepsilon}}^p\right) \tag{3.7}$$

Evolution of associated flow rule: Koiter (1953)

$$\dot{\boldsymbol{\varepsilon}}^p \equiv \gamma_U \partial_{\boldsymbol{\sigma}'} f_U(\boldsymbol{\sigma}',\alpha) + \gamma_L \partial_{\boldsymbol{\sigma}'} f_L(\boldsymbol{\sigma}',\alpha) \tag{3.8}$$

Consistency requirement at the corner:

$$\dot{f}_U = \partial_{\boldsymbol{\sigma}'} f_U : \dot{\boldsymbol{\sigma}}' + \partial_\alpha f_U \dot{\alpha} \equiv 0 \tag{3.9}$$

$$\dot{f}_L = \partial_{\boldsymbol{\sigma}'} f_L : \dot{\boldsymbol{\sigma}}' + \partial_\alpha f_L \dot{\alpha} \equiv 0 \tag{3.10}$$

From Eq.(3.5)-(3.10), the manipulation for unknowns is shown by

$$\begin{bmatrix} \mathbf{c}^{e^{-1}} & \{\partial_{\boldsymbol{\sigma}'} f_U\} & \{\partial_{\boldsymbol{\sigma}'} f_L\} \\ \{\partial_{\boldsymbol{\sigma}'} f_U\}^T & \partial_\alpha f_U . \partial_{p'} f_U & \partial_\alpha f_U . \partial_{p'} f_L \\ \{\partial_{\boldsymbol{\sigma}'} f_L\}^T & \partial_\alpha f_L . \partial_{p'} f_U & \partial_\alpha f_L . \partial_{p'} f_L \end{bmatrix} \cdot \begin{pmatrix} \dot{\boldsymbol{\sigma}}' \\ \gamma_U \\ \gamma_L \end{pmatrix} = \begin{pmatrix} \dot{\boldsymbol{\varepsilon}} \\ 0 \\ 0 \end{pmatrix} \tag{3.11}$$

To solve Eq.(3.11), $\mathbf{X}_{(2\times2)}$, $\mathbf{L}_{(2\times1)}$ and consistency parameters must be primarily obtained by calculating Eq. (3.12)-(3.14).

Coupled hardening matrix:

$$\mathbf{X} = \begin{bmatrix} \partial_{\boldsymbol{\sigma}'} f_U : \mathbf{c}^e : \partial_{\boldsymbol{\sigma}'} f_U - \partial_\alpha f_U . \partial_{p'} f_U & \partial_{\boldsymbol{\sigma}'} f_U : \mathbf{c}^e : \partial_{\boldsymbol{\sigma}'} f_L - \partial_\alpha f_U . \partial_{p'} f_L \\ \partial_{\boldsymbol{\sigma}'} f_L : \mathbf{c}^e : \partial_{\boldsymbol{\sigma}'} f_U - \partial_\alpha f_L . \partial_{p'} f_U & \partial_{\boldsymbol{\sigma}'} f_L : \mathbf{c}^e : \partial_{\boldsymbol{\sigma}'} f_L - \partial_\alpha f_L . \partial_{p'} f_L \end{bmatrix} \tag{3.12}$$

Loading parameters:

$$\mathbf{L} = \begin{pmatrix} \partial_{\boldsymbol{\sigma}'} f_U : \mathbf{c}^e : \dot{\boldsymbol{\varepsilon}} \\ \partial_{\boldsymbol{\sigma}'} f_L : \mathbf{c}^e : \dot{\boldsymbol{\varepsilon}} \end{pmatrix} \tag{3.13}$$

Consistency parameters:

$$\begin{pmatrix} \gamma_U \\ \gamma_L \end{pmatrix} = \mathbf{X}^{-1} \cdot \mathbf{L} \tag{3.14}$$

Incremental stress-strain relations:

$$\dot{\boldsymbol{\sigma}}' \equiv \mathbf{c}^{ep} : \dot{\boldsymbol{\varepsilon}} \tag{3.15}$$

Tangential elastoplastic moduli:

$$\mathbf{c}^{ep} = \mathbf{c}^e - \sum_{\alpha,\beta \in \{1,2\}} \left[\mathbf{X}^{-1} \right]_{\alpha,\beta} \{ \mathbf{g}_\alpha \otimes \mathbf{g}_\beta \} \tag{3.16}$$

where $\mathbf{g} = \begin{bmatrix} \mathbf{c}^e : \partial_{\boldsymbol{\sigma}'} f_U \\ \mathbf{c}^e : \partial_{\boldsymbol{\sigma}'} f_L \end{bmatrix}$

The details of proof are shown in Appendix C.

3-2-4 Conclusion

A generalized concept to the Sekiguchi-Ohta yield surface possessing the singular point where the gradients of yield surface (or potential) to stress space are indeterminate is implemented. Though Koiter's method does not apply to the Sekiguchi-Ohta model in stress space, it is particularly applied to the intersecting corner of two yield loci characterized by the Sekiguchi-Ohta model on Rendulic's stress plane or triaxial plane, where the plane of induced anisotropy is coincided, resulting in simple formulation.

3-3 References

1 Roscoe, K.H., Schofield, A.N. & Thurairajah, A, "Yielding of clays in states wetter than critical", Geotechnique 13(3), 211-240 (1963)

2 Sekiguchi, H. & Ohta, H., "Induced anisotropy and time dependency in clays", Proc. ICSMFE 9th, Tokyo: 229-238 (1977)

3 Britto, A.M. & Gunn, M.J., "Critical state soil mechanics via finite elements", Chichester: Ellis Horwood LTD. (1987)

4 Gens, A. & Potts, D.M., "Critical state models in computational geomechanics", Eng. Comput., 5: 178-197 (1988)

5 Koiter, W.T., "Stress-strain relations, uniqueness and variational theorems for elastic-plastic materials with a singular yield surface", Quart. Appl. Math. (11): 350-354 (1953)

6 Koiter, W.T., "General theorems for elastic-plastic solids", Prog. Solid Mechanics 6, eds., Amsterdam: 167-221 (1960)

7 Simo, J.C., Kennedy, J.G. & Govindjee, S., "Non-smooth multisurface plasticity and viscoplasticity loading/unloading conditions and numerical algorithms", IJNME (26): 2161-2185 (1988)

8 Pipatpongsa, T., Ohta, H., Kobayashi, I. & Iizuka, A, "Associated plastic flow at the intersection corner of plastic potential functions in soil mechanics", Proc. of 36th Japanese Nat. Conf. on Geotech. Engrg.: 935-936 (2001)

9 Pipatpongsa, T., Ohta, H., Kobayashi, I. & Iizuka, A., "Dependence of K_o-value on effective internal friction angle in regard to the Sekiguchi-Ohta model", Proc. of 36th Japanese Nat. Conf. on Geotech. Engrg.: 936-937 (2001)

10 Ohta, H. & Hata, S., A theoretical study of the stress-strain relations for clays, Soils and Foundations 11(3): 765-89 (1971)

CHAPTER 4
Soil Initial Anisotropy

4-1 Coefficient of lateral earth pressure at rest, K_o-value

The sedimentary processes over a long period engage in a creation of all natural clays which is laid down under a condition of zero lateral strain. This initial condition is the starting state of stress in every kind of practical engineering problem. The definitions of geostatic coefficient of lateral earth pressure are shown in Table 4.1.

Table 4.1 Definition of coefficient of earth pressure at rest, K_o

Definition	Interpretation
K_O is a ratio of horizontal to vertical effective stresses for one-dimensionally compressed soil. [1]	$K_o = \dfrac{\sigma'_h}{\sigma'_v}$ 1-D compression
During monotonic one-dimensional normal compression, the value of K_o is found to be a constant. [1]	$\dot{K}_o = 0$, $\left. K_o = \dfrac{d\sigma'_h}{d\sigma'_v}\right|_{K_o}$
A soil mass at a particular level stabilizes into a steady state where the vertical and lateral stresses become principal stress action on principal planes; this effective stress state is termed as at-rest or K_O condition. [2]	Vertical direction is the major principal direction $K_o \leq 1$
K_O is the lateral stress ratio in a special case where there has been no lateral strain within the ground. [3]	$\varepsilon_r = 0$
After a mass of soil has been deposited by either a natural or an artificial process, $K_a < K_O < K_p$. [4]	$K_a < K_O < K_p$
K_O must depend on the amount of friction resistance mobilized at contact points between particles. [3]	$K_o = K_o(\phi')$

It is a common physical behavior describing that lateral movement in soil media can be prevented itself due to internal friction angle; therefore, K_o would has a relation with internal friction angle. Jâky (1944) [10] managed to arrive the expression for K_o by thinking of conditions at the center of the base of a heap of granular material,

$$K_o = \left(1 + \frac{2}{3}\sin\phi'\right)\left(\frac{1 - \sin\phi'}{1 + \sin\phi'}\right) \tag{4.1}$$

Simplified form was suggested for values of ϕ' between 20°-45°,

$$K_o = 1 - \sin\phi' \tag{4.2}$$

Massarsch (1979) [5]

$$K_o = 0.44 + 0.42\frac{I_p}{100} \tag{4.3}$$

Kenney (1959) [6]

$$\sin\phi' = 0.81 - 0.233\log I_p \tag{4.4}$$

Usually, K_o is defined in terms of principal stress ratio between horizontal to vertical stress. Since K_o condition is defined in axisymmetric condition where horizontal stress is equal in radial direction, the stress parameter p' and q can be used to define K_o value by referring the relations given below,
The stress ratio in p'-q diagram on K_o-line is given by,

$$\eta_o = \left(\frac{q}{p'}\right)_{Ko} = \frac{q_o}{p'_o} \tag{4.5}$$

Under axisymmetric or triaxial stress condition at initial state, which is referred to σ'_{1o}, $\sigma'_{2o} = \sigma'_{3o}$, a stress ratio is shown by,

$$\frac{q_o}{p'_o} = \frac{\sigma'_{1o} - \sigma'_{3o}}{\frac{1}{3}(\sigma'_{1o} + 2\sigma'_{3o})}, \qquad \sigma'_{3o} = K_o\sigma'_{1o} \tag{4.6, 4.7}$$

According to Eqs.(4.6), (4.7), the stress ratio in Eq.(4.5) is related to K_o value by

$$\eta_o = \frac{3(1 - K_o)}{1 + 2K_o} \quad \text{and} \quad K_o = \frac{3 - \eta_o}{2\eta_o + 3} \tag{4.8, 4.9}$$

Under zero lateral strain, volumetric and deviatoric strains are

$$\dot{\varepsilon}_v = \dot{\varepsilon}_1 \,, \quad \dot{\varepsilon}_s = \frac{2}{3}\dot{\varepsilon}_1 \qquad\qquad\qquad\qquad (4.10),\ (4.11)$$

Eqs.(4.10), (4.11) suggest the following property during 1-D consolidation,

$$\frac{\dot{\varepsilon}_s}{\dot{\varepsilon}_v} = \frac{2}{3} \qquad\qquad\qquad\qquad (4.12)$$

The study of Alpan (1967) [7] found that K_o given by swelling loading is larger than K_o given by consolidation loading. The empirical correlation with OCR was then proposed,

$$K_i = K_o OCR^{0.54\exp(-\frac{PI}{122})} \qquad\qquad\qquad\qquad (4.13)$$

where PI is plasticity index.

Stress paths in p-q plane under triaxial condition given by K_o-loading and K_o-swelling loading plotted with the Sekiguchi-Ohta yield surface can be presented in Figure 4-1.

4-2 K_o obtained from smooth constitutive equations

Theoretical K_o expressions derived from Original Cam-clay and Modified Cam-clay models can be summarized below. It is discussed that the value of K_o is over-predicted by the modified theory. See proof in Appendix D.

Original Cam-clay [8]

$$K_o = \frac{9 - 2M}{4M} \qquad\qquad \text{(neglect all elastic components)} \qquad\qquad (4.14)$$

$$K_o = \frac{6 - 2M + 3\Lambda}{6 + 4M - 6\Lambda} \qquad\qquad \text{(neglect elastic shear components)} \qquad\qquad (4.15)$$

Modified Cam-clay [1, 9]

$$K_o = \frac{9 - \sqrt{9 + 4M^2}}{2\sqrt{9 + 4M^2}} \qquad\qquad \text{(neglect all elastic components)} \qquad\qquad (4.16)$$

$$K_o = \frac{6 - \sqrt{9\Lambda^2 + 4M^2} + 3\Lambda}{6 + 2\sqrt{9\Lambda^2 + 4M^2} - 6\Lambda} \qquad\qquad \text{(neglect elastic shear components)} \qquad\qquad (4.17)$$
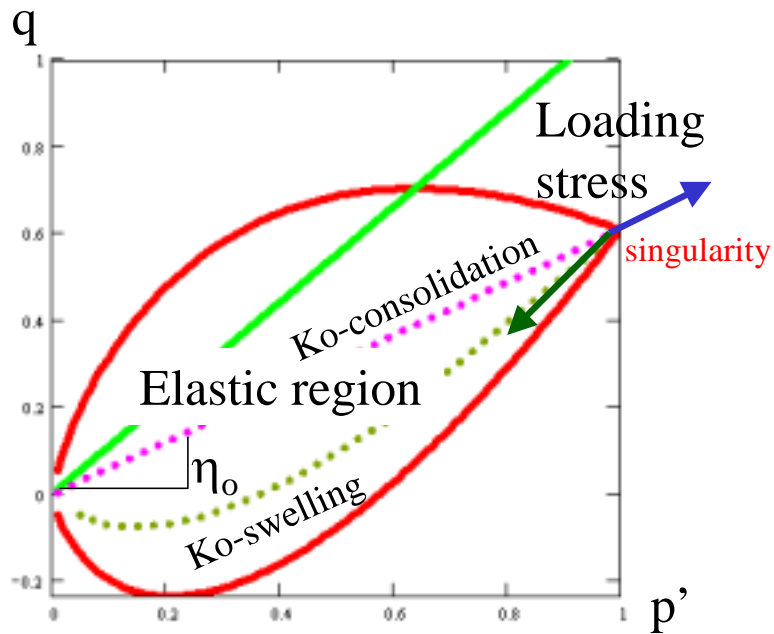
Figure 4-1 K_o-consolidation and K_o-swelling

4-3 Plastic flow adjacent to the corner

Oedometer test is designed to model the uniaxial compression corresponding to K_o -consolidation in natural stratum by subjecting a monotonic compressive loading to a specimen. However, a K_o -consolidation performed in triaxial apparatus can be achieved by lateral strain control keeping at zero during applying a compressive loading. Repetitive adjustments between cell pressure and vertical pressure bring about the varied loading steps subjecting to a specimen rather than monotonic loading steps. As shown in Figure 4-2, it is found that in triaxial test, soils are repetitively adjusted to nearly K_o-state from compression or extension tests, namely mobilized K_o condition, while in oedometer test, soils are thoroughly set to K_o-state under monotonic loading, namely, immobilized K_o condition. These different kinds of loading concepts would result in different modeling. From the previous section, it is known that a plastic flow at the corner can be evaluated by Koiter's flow rule by considering active yield at current stress point. By immobilized K_o condition, it is secured that stress point is placed at the corner; therefore, both upper and lower yield surfaces are active throughout loading steps. But under mobilized K_o condition, only a single yield surface either upper or lower yield surface, is active at a particular time during repetitive loading steps, therefore, the coupling effect between both surfaces is diminished in plastic flow.
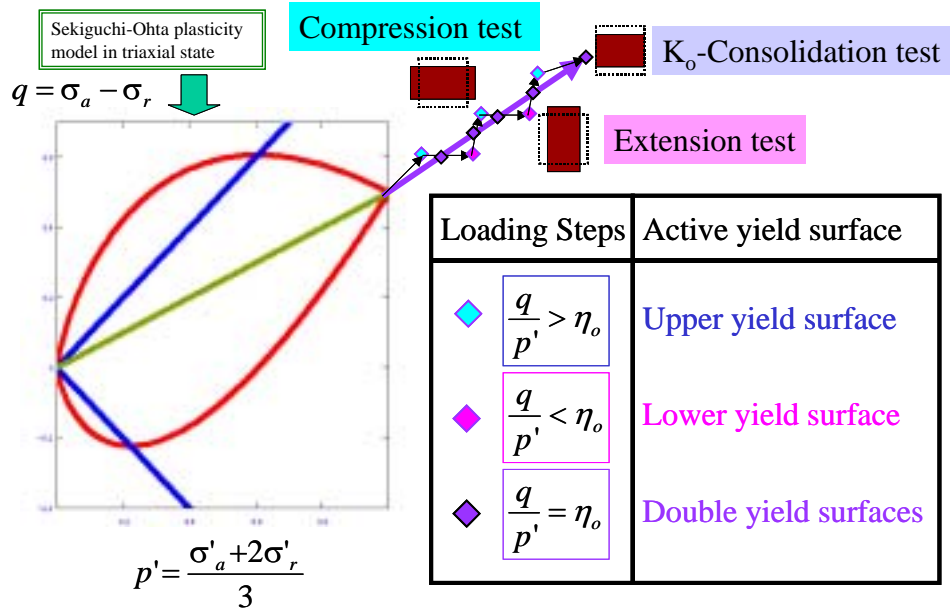
Figure 4-2 Monotonic & Varied Loading Steps

The governing equations under mobilized K_o condition is different from immobilized K_o condition set in previous section. The plastic flow is a sum of individual plastic flow on upper and lower yield surface and then accumulated by a strain history parameter. The consistency parameter is also determined individually without coupling effect. The guideline of the governing equations is shown in Figure 4-3.

Consistency parameters of upper and lower yield surface are determined individually from consistency condition of each surface. Stress increment is determined individually but only plastic volumetric strain is a sum of both plastic flows, thus, only a coupled parameter of both yield surfaces in governing equations. The procedures to determined plastic flow (See Figure 4-4) is similar to the immobilized K_o condition. Firstly, the positive-definite hardening matrix **X** is determined; consequently, consistency parameters can be evaluated using loading vector **L** and hardening matrix **X**. Under this scheme, the coupling parts between upper/lower yield surface in **X** matrix is vanished. **X** is evidently positive-definite by determining its determinant, which always gives a positive number greater than zero as shown in Eq.(4.19).

$$\mathbf{X} = \begin{bmatrix} K\left(\dfrac{\partial f_U}{\partial p'}\right)^2 + 3G\left(\dfrac{\partial f_U}{\partial q}\right)^2 + \dfrac{\partial f_U}{\partial p'} & 0 \\ 0 & K\left(\dfrac{\partial f_L}{\partial p'}\right)^2 + 3G\left(\dfrac{\partial f_L}{\partial q}\right)^2 + \dfrac{\partial f_L}{\partial p'} \end{bmatrix} \qquad (4.18)$$

$$\dot{\boldsymbol{\varepsilon}}^{\mathbf{p}} \equiv \dot{\boldsymbol{\varepsilon}}^{\mathbf{p}}_{\mathbf{U}} + \dot{\boldsymbol{\varepsilon}}^{\mathbf{p}}_{\mathbf{L}}$$

Upper yield function

$$\dot{\boldsymbol{\varepsilon}}^{\mathbf{p}}_{\mathbf{U}} \equiv \gamma_U \partial_{\boldsymbol{\sigma}'} f_U(\boldsymbol{\sigma}', \alpha)$$

$$\alpha \equiv \varepsilon_v^p = \int \dot{\varepsilon}_v^p \, dt$$

$$\gamma_L \geq 0; \; f_L(\boldsymbol{\sigma}', \alpha) \leq 0; \; \gamma_L f_L(\boldsymbol{\sigma}', \alpha) \equiv 0$$

$$\gamma_U \dot{f}_U(\boldsymbol{\sigma}', \alpha) \equiv 0$$

Flow rules

Hardening functions

Kuhn-Tucker conditions

Consistency conditions

Lower yield function

$$\dot{\boldsymbol{\varepsilon}}^{\mathbf{p}}_{\mathbf{L}} \equiv \gamma_L \partial_{\boldsymbol{\sigma}'} f_L(\boldsymbol{\sigma}', \alpha)$$

$$\alpha \equiv \varepsilon_v^p = \int \dot{\varepsilon}_v^p \, dt$$

$$\gamma_U \geq 0; \; f_U(\boldsymbol{\sigma}', \alpha) \leq 0; \; \gamma_U f_U(\boldsymbol{\sigma}', \alpha) \equiv 0$$

$$\gamma_L \dot{f}_L(\boldsymbol{\sigma}', \alpha) \equiv 0$$

Individual formulation
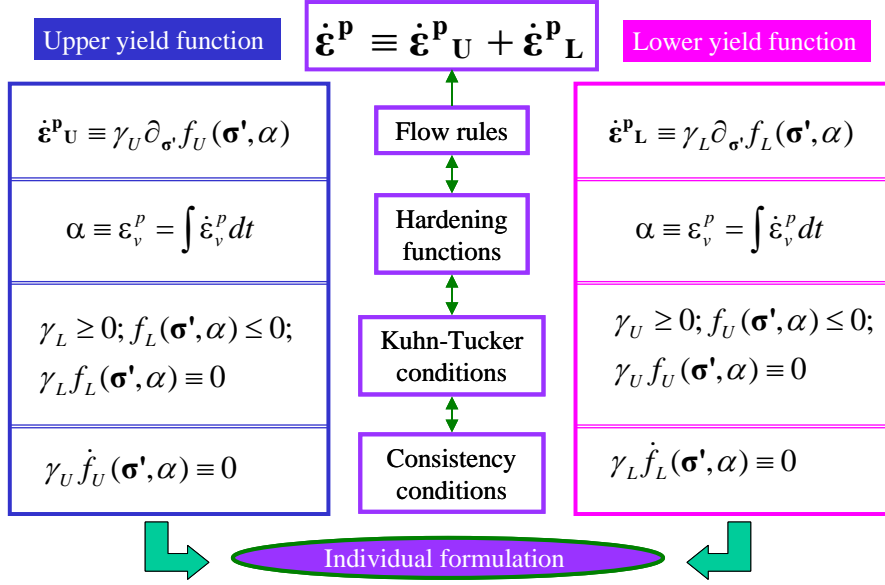
Figure 4-3 Governing equation for plastic flow adjacent to the corner

$$\dot{f}_U = \partial_{\boldsymbol{\sigma}'} f_U \cdot \dot{\boldsymbol{\sigma}}' + \frac{\partial f_U}{\partial \alpha} \dot{\alpha} \equiv 0$$

$$\dot{f}_L = \partial_{\boldsymbol{\sigma}'} f_L \cdot \dot{\boldsymbol{\sigma}}' + \frac{\partial f_L}{\partial \alpha} \dot{\alpha} \equiv 0$$

$$\dot{\boldsymbol{\sigma}}' \equiv \mathbf{c}^e : (\dot{\boldsymbol{\varepsilon}} - \dot{\boldsymbol{\varepsilon}}^p_U)$$

$$\dot{\boldsymbol{\varepsilon}}^p_U \equiv \gamma_U \partial_{\boldsymbol{\sigma}'} f_U(\boldsymbol{\sigma}', \alpha)$$

$$\dot{\boldsymbol{\sigma}}' \equiv \mathbf{c}^e : (\dot{\boldsymbol{\varepsilon}} - \dot{\boldsymbol{\varepsilon}}^p_L)$$

$$\dot{\boldsymbol{\varepsilon}}^p_L \equiv \gamma_L \partial_{\boldsymbol{\sigma}'} f_L(\boldsymbol{\sigma}', \alpha)$$

$$\mathbf{c}^e \equiv K \mathbf{1} \otimes \mathbf{1} + 2G \left(\mathbf{I} - \frac{1}{3} \mathbf{1} \otimes \mathbf{1} \right)$$

$$\partial_{\boldsymbol{\sigma}'} f_U = \frac{1}{3} \mathbf{1} \frac{\partial f_U}{\partial p'} + \sqrt{\frac{3}{2}} \mathbf{n} \frac{\partial f_U}{\partial q}$$

$$\partial_{\boldsymbol{\sigma}'} f_L = \frac{1}{3} \mathbf{1} \frac{\partial f_L}{\partial p'} + \sqrt{\frac{3}{2}} \mathbf{n} \frac{\partial f_L}{\partial q}$$

$$\frac{\partial f_U}{\partial \alpha} = \frac{\partial f_L}{\partial \alpha} = -1 \qquad \dot{\alpha} = \dot{\varepsilon}_v^p$$

$$\mathbf{X}_{(2 \times 2)} \cdot \begin{pmatrix} \gamma_U \\ \gamma_L \end{pmatrix} = \mathbf{L}_{(2 \times 1)}$$

X must be positive-definite
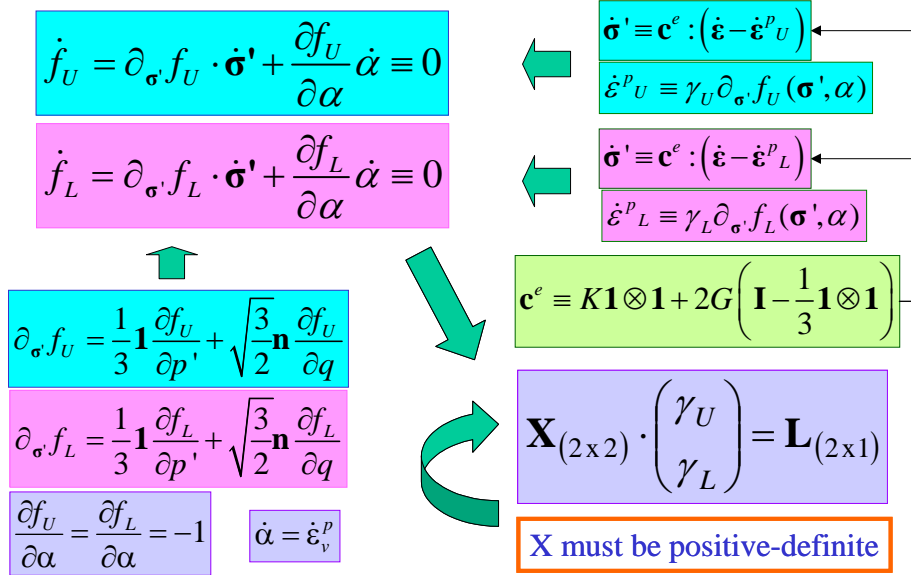
Figure 4-4 Evaluation of consistency parameters adjacent to the corner

$$\left(K \left(\frac{\partial f_U}{\partial p'} \right)^2 + 3G \left(\frac{\partial f_U}{\partial q} \right)^2 + \frac{\partial f_U}{\partial p'} \right) \left(K \left(\frac{\partial f_L}{\partial p'} \right)^2 + 3G \left(\frac{\partial f_L}{\partial q} \right)^2 + \frac{\partial f_L}{\partial p'} \right) > 0 \tag{4.19}$$

In order to distinguish $\mathbf{X}$ by concepts of immobilized and mobilized K_o condition, coupled-hardening matrix $\bar{\mathbf{X}}$ and decoupled-hardening matrix $\tilde{\mathbf{X}}$ are referred respectively from now on. The derivatives of upper and lower yield surface are common each other. If one compare $\bar{\mathbf{X}}$ and $\tilde{\mathbf{X}}$, it would be found that the different between them is that the coupling parts of upper/lower yield surface in $\bar{\mathbf{X}}$ is removed in $\tilde{\mathbf{X}}$ as shown in Figure 4-5. That is, $\bar{\mathbf{X}}$ matrix is decoupled between the connection of upper and lower yield surfaces and reduced to $\tilde{\mathbf{X}}$. Criteria for loading/unloading conditions are also common for both Ko conditions. The discrete form of strain rate imposed during triaxial Ko consolidation can be shown in Figure 4-6. Even though rate of radial strain is not zero during variedly repetitive loading $\dot{\varepsilon}_r \neq 0$, the incremental form under a small period of time is expected as zero, $\Delta \varepsilon_r = 0$, due to zero lateral strain corrections.

Immobilized loading step ~ Coupled Hardening Matrix

$$\overline{\mathbf{X}} = \begin{bmatrix} K\left(\dfrac{\partial f_U}{\partial p'}\right)^2 + 3G\left(\dfrac{\partial f_U}{\partial q}\right)^2 + \dfrac{\partial f_U}{\partial p'} & K\dfrac{\partial f_U}{\partial p'}\dfrac{\partial f_L}{\partial p'} + 3G\dfrac{\partial f_U}{\partial q}\dfrac{\partial f_L}{\partial q} + \dfrac{\partial f_L}{\partial p'} \\[4mm] K\dfrac{\partial f_U}{\partial p'}\dfrac{\partial f_L}{\partial p'} + 3G\dfrac{\partial f_U}{\partial q}\dfrac{\partial f_L}{\partial q} + \dfrac{\partial f_U}{\partial p'} & K\left(\dfrac{\partial f_L}{\partial p'}\right)^2 + 3G\left(\dfrac{\partial f_L}{\partial q}\right)^2 + \dfrac{\partial f_L}{\partial p'} \end{bmatrix}$$

Mobilized loading step ~ Decoupled Hardening Matrix

$$\tilde{\mathbf{X}} = \begin{bmatrix} K\left(\dfrac{\partial f_U}{\partial p'}\right)^2 + 3G\left(\dfrac{\partial f_U}{\partial q}\right)^2 + \dfrac{\partial f_U}{\partial p'} \quad \text{Coupling part} & 0 \\[4mm] 0 & K\left(\dfrac{\partial f_L}{\partial p'}\right)^2 + 3G\left(\dfrac{\partial f_L}{\partial q}\right)^2 + \dfrac{\partial f_L}{\partial p'} \end{bmatrix}$$

Figure 4-5 Coupling/decoupling hardening matrices

$$\Delta\varepsilon = \Delta\varepsilon_e + \Delta\varepsilon_p$$

$$\Delta\boldsymbol{\varepsilon} = \begin{bmatrix} 0 & 0 & 0 \\ 0 & \Delta\varepsilon_a & 0 \\ 0 & 0 & 0 \end{bmatrix}$$

$$\Delta\varepsilon_v = \Delta\varepsilon_a \qquad \Delta\varepsilon_s = \frac{2}{3}\Delta\varepsilon_a$$

$$\mathbf{1} = \begin{bmatrix} 1 & 0 & 0 \\ 0 & 1 & 0 \\ 0 & 0 & 1 \end{bmatrix} \qquad \mathbf{n} = \begin{bmatrix} -\frac{1}{\sqrt{6}} & 0 & 0 \\ 0 & \sqrt{\frac{2}{3}} & 0 \\ 0 & 0 & -\frac{1}{\sqrt{6}} \end{bmatrix}$$

$$\Delta\boldsymbol{\varepsilon} = \frac{1}{3}\Delta\varepsilon_v \mathbf{1} + \sqrt{\frac{3}{2}}\Delta\varepsilon_s \mathbf{n}$$
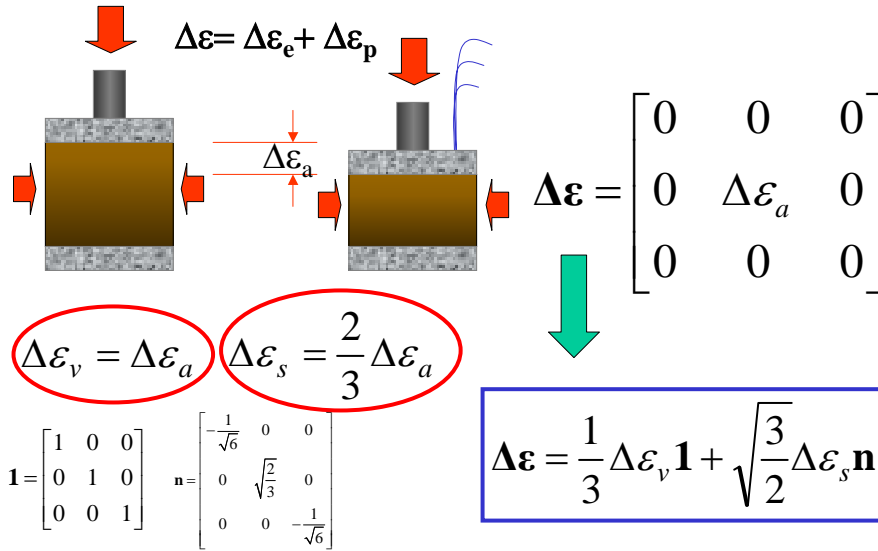
Figure 4-6 Strain increment under triaxial Ko consolidation

The discrete consistency parameters corresponding to the mobilized Ko condition can be determined by,

$$\begin{pmatrix} \Delta\gamma_U \\ \Delta\gamma_L \end{pmatrix} = \tilde{\mathbf{X}}^{-1} \cdot \mathbf{L} \tag{4.20}$$

where

$$\mathbf{L} = \begin{Bmatrix} L_U \\ L_L \end{Bmatrix} = \begin{bmatrix} K\dfrac{\partial f_U}{\partial p'} & 3G\dfrac{\partial f_U}{\partial q} \\[3mm] K\dfrac{\partial f_L}{\partial p'} & 3G\dfrac{\partial f_L}{\partial q} \end{bmatrix} \cdot \begin{Bmatrix} \Delta\varepsilon_v \\ \Delta\varepsilon_s \end{Bmatrix} = \begin{bmatrix} K(Mp'-q) & 3Gp' \\ K(Mp'+q) & -3Gp' \end{bmatrix} \cdot \begin{Bmatrix} \Delta\varepsilon_a \\ \frac{2}{3}\Delta\varepsilon_a \end{Bmatrix} \tag{4.21}$$

$$\tilde{\mathbf{X}}_{1,1} = KD\frac{q^2}{p'^2} - (2KDM + p')\frac{q}{p'} + KDM^2 + 3GD + Mp' \tag{4.22}$$

$$\tilde{\mathbf{X}}_{1,2} = \tilde{\mathbf{X}}_{2,1} = 0 \tag{4.23), (4.24}$$

$$\tilde{\mathbf{X}}_{2,2} = KD\frac{q^2}{p'^2} + (2KDM + p')\frac{q}{p'} + KDM^2 + 3GD + Mp' \tag{4.25}$$

According to Eqs.(4.21)-(4.25) together with a state of stress at (p'=p'$_o$, q=q$_o$), the consistency parameters (4.20) is determined as,

$$\begin{pmatrix} \Delta\gamma_U \\ \Delta\gamma_L \end{pmatrix} = \Delta\varepsilon_a p'_o \left\{ \begin{array}{c} \dfrac{KM - K\eta_o + 2G}{KDM^2 - 2KDM\eta_o + KD\eta_o^2 + 3GD + Mp'_o - \eta_o p'_o} \\[2ex] \dfrac{KM + K\eta_o - 2G}{KDM^2 + 2KDM\eta_o + KD\eta_o^2 + 3GD + Mp'_o + \eta_o p'_o} \end{array} \right\} \tag{4.26}$$

Consequently, the plastic flow adjacent to the corner is eventually determined by,

$$\begin{pmatrix} \Delta\varepsilon_v^p \\ \Delta\varepsilon_s^p \end{pmatrix} = \begin{pmatrix} \dfrac{\partial f_U}{\partial p'} & \dfrac{\partial f_L}{\partial p'} \\[2ex] \dfrac{\partial f_U}{\partial q} & \dfrac{\partial f_L}{\partial q} \end{pmatrix} \cdot \begin{pmatrix} \Delta\gamma_U \\ \Delta\gamma_L \end{pmatrix} = \begin{bmatrix} \dfrac{D}{p'}(M - \dfrac{q}{p'}) & \dfrac{D}{p'}(M + \dfrac{q}{p'}) \\[2ex] \dfrac{D}{p'} & -\dfrac{D}{p'} \end{bmatrix} \cdot \begin{pmatrix} \Delta\gamma_U \\ \Delta\gamma_L \end{pmatrix} \Bigg|_{p'=p'_o, q=\eta_o p'_o}$$

$$= 2D\Delta\varepsilon_a \frac{\left(\begin{array}{c} 2K^2M^2D\eta_o^2 + 3KM^2GD - MK\eta_o^2 p'_o + 2M^2GKD\eta_o + 3\eta_o^2GKD - 2\eta_o^3GKD + K^2M^4D + M^3Kp'_o \\ +K^2\eta_o^4D - 6\eta_oG^2D + 2GMp'_o + 6G^2D - 3K\eta_oGD - K^2\eta_o^3D + K^2M^2D\eta_o + 2KM^2GD + 2K\eta_o^2GD \end{array} \right)}{(KDM^2 - 2KDM\eta_o + KD\eta_o^2 + 3GD + Mp'_o - \eta_o p'_o)(KDM^2 + 2KDM\eta_o + KD\eta_o^2 + 3GD + Mp'_o + \eta_o p'_o)} \tag{4.27}$$

According to Figure 4-7, the incremental strain ratio between deviatoric strain to volumetric strain is not equal to 2/3 as obtained under immobilized K_o condition. This fact signifies the clue that this condition can be imposed to the expression to obtain relation for K_o-value in next section.
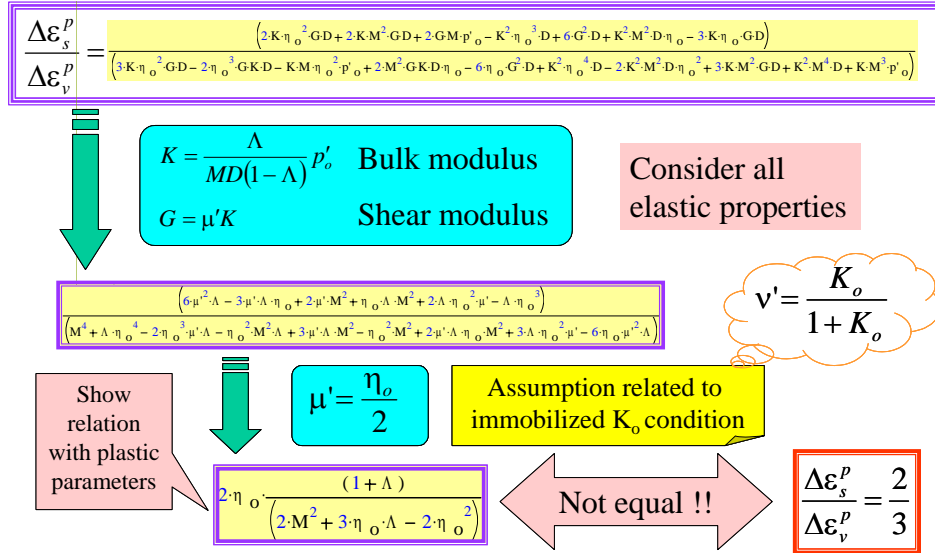
Figure 4-7 Incremental plastic strain ratio

Stress increment under Ko-consolidation can be computed by,

$$\begin{pmatrix} \Delta p' \\ \Delta q \end{pmatrix} = \begin{bmatrix} K & 0 \\ 0 & 3G \end{bmatrix} \cdot \begin{pmatrix} \Delta\varepsilon_v - \Delta\varepsilon_v^p \\ \Delta\varepsilon_s - \Delta\varepsilon_s^p \end{pmatrix} = \tag{4.28}$$

$$= \frac{\left(\begin{array}{c} -K\Delta\varepsilon_a\left(K^2D^2\eta_o^4 + K^2D^2M^4 + \eta_o^2 p'^2_o - M^2 p'^2_o - 9G^2D^2 - 6GDMp'_o - 2K^2D^2M^2\eta_o^2 + 4M^2GKD^2\eta_o - 4\eta_o^3GKD^2 - 12\eta_oG^2D^2\right) \\ +2G\Delta\varepsilon_a(K^2D^2\eta_o^4 + K^2D^2M^4 - \eta_o^2 p'^2_o + M^2 p'^2_o - 9G^2D^2 - 2KDM\eta_o^2 p'_o + 2KDM^3 p'_o - 2K^2D^2M^2\eta_o^2 + 9GKD^2\eta_o - 3K^2M^2D^2\eta_o + 3K^2\eta_o^3D^2) \end{array} \right)}{(KDM^2 - 2KDM\eta_o + KD\eta_o^2 + 3GD + Mp'_o - \eta_o p'_o)(KDM^2 + 2KDM\eta_o + KD\eta_o^2 + 3GD + Mp'_o + \eta_o p'_o)}$$

Substitution of $G = \mu'K$, $K = \dfrac{\Lambda}{MD(1-\Lambda)}p'_o$ into Eq.(4.28) gives the ratio of deviatoric stress to mean stress as shown by,

$$\eta_o = \frac{\Delta q}{\Delta p'} \bigg|_{K_o} \tag{4.29}$$

$$= -2\mu' \frac{(-\Lambda^2\eta_o^4 + \eta_o^2M^2 + \Lambda^2\eta_o^2M^2 - M^4 + 9\mu'^2\Lambda^2 - 9\mu'\Lambda^2\eta_o + 3\Lambda^2\eta_oM^2 - 3\Lambda^2\eta_o^3)}{-\Lambda^2\eta_o^4 - \eta_o^2M^2 + 2\Lambda\eta_o^2M^2 + \Lambda^2\eta_o^2M^2 + M^4 - 2M^4\Lambda + 9\mu'^2\Lambda^2 + 6\Lambda\mu'M^2 - 6\mu'\Lambda^2M^2 - 4\mu'\Lambda^2\eta_oM^2 + 4\eta_o^3\mu'\Lambda^2 + 12\eta_o\mu'\Lambda^2}$$

Manipulation of Eq.(4.29) for solving an unknown η_o results in a implicit form of fifth-degree polynomial expressed by,

$$\begin{Bmatrix} 2\mu'M^4 - 18\mu'^3\Lambda^2 \\ 9\mu'^2\Lambda^2 + 2M^4\Lambda - M^4 - 6\mu'\Lambda M^2 \\ 2\mu'\Lambda^2 M^2 - 12\mu'^2\Lambda^2 - 2\mu'M^2 \\ M^2 - 2\Lambda M^2 - \Lambda^2 M^2 + 6\mu'\Lambda^2 \\ -2\mu'\Lambda^2 \\ \Lambda^2 \end{Bmatrix} \cdot \begin{Bmatrix} 1 \\ \eta_o \\ \eta_o^2 \\ \eta_o^3 \\ \eta_o^4 \\ \eta_o^5 \end{Bmatrix} = 0 \tag{4.30}$$

The solution of η_o in Eq.(4.30) is possibly solved numerically for a given set of basic material parameters M, Λ and μ'. However, by an additional assumption using relation between μ'(or v') and η_o, the solution of η_o can be simply obtained algebraically in the next section.

4-4 Dependence of K_o-value on effective internal friction angle in regard to the Sekiguchi-Ohta model

4-4-1 Introduction

By the process of soil deposition, which has the history of one-dimensional deformation, a coefficient of earth pressure at rest K_o is generally found to be constant and depended on the friction resistance. K_o condition can be retained over the virgin loading (normal compression) restricted to the special condition of zero lateral strain. Many studies have shown some particular relations between K_o and angle of internal friction [10,11,12,13]. Values of K_o predicted by the original Cam-clay model are much higher than those measured in practice [8]. Roscoe and Burland (1968) [9] derived K_o expression from modified Cam-clay model but it tends to over-estimate the empirical relationship. This study aims to establish the alternative relationship derived from the Sekiguchi-Ohta model (1977) [14] employing the extension of normality to the intersection corner of yield surfaces. The findings may provide the theoretical relationships among basic parameters reciprocally describing the physical nature of soil grains.

4-4-2 Theoretical background

Since the conventional flow rule limits the determination of plastic flow to the smooth convex yield surface, the singular point where the Sekiguchi-Ohta model has a corner, produces uncertain plastic flow. Consequently, the stress ratio during K_o consolidation is undetermined but the difficulty met can be overcome by employing the extended flow rule to upper and lower yield surfaces (Pipatpongsa et al., 2001) [15].

4-4-3 Determination of K_o value

The effective stress state during soil deposition can be reproduced in a conventional triaxial apparatus, which subjects to repetitive corrections by compression/extension tests to maintain zero lateral strain. The admissible plastic strain increment vector is the summation of associated plastic flows on each upper and lower yield loci depicted in Figure 4-8. In Box 4.1, the matrix $\mathbf{X}$ is determined whether consistency conditions are simultaneously or consecutively active, resulting in the coupled and decoupled hardening plasticity matrix $\overline{\mathbf{X}}$ and $\tilde{\mathbf{X}}$, which is formulated by removing coupling parts of $\overline{\mathbf{X}}$. During the mobilization of shearing resistance along series of the random kicks and shoves of soil particles on the correction paths approaching to K_o-condition given by uniformly distributed regions of extension/compression tests, the consistency parameters can be evaluated by taking matrix $\tilde{\mathbf{X}}$ into account.

The loading vector of mobilized Ko condition can be considered similar to that of immobilized Ko condition by the following assumptions,

A) Both regions are uniformly distributed and balanced each other
B) Both regions are kept considerably small
C) Stress & strain paths are kept close to K_o-condition
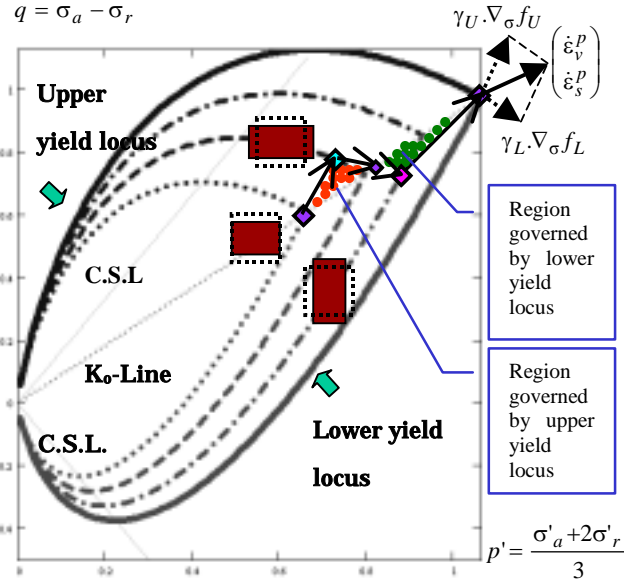
Figure 4-8 Incremental plastic strain under K_o-condition

In Box 4.2, contribution of elastic moduli manages to arrive K_o expression, namely, mobilized K_o in an implicit polynomial form having coefficients related to Critical state parameter, Poisson's ratio and irreversibility ratio as noted in Eq.(4.31). Once the repetitive loadings gradually approach to monotonic one-dimensional normal compression, the consistency conditions are satisfied with those of coupled heterogeneous plasticity thus concerning with $\overline{\overline{\mathbf{X}}}$, giving K_o as a function of Poisson's ratio, namely, immobilized K_o shown in Eq.(4.33). The transition of K_o value stabilized between both states can be obtained by combining Eq. (4.31) and Eq. (4.32) expressed by Eq.(4.33) (See details in Appendix D). Regarding to Eq(4.31)-(4.34), the plots in Figure 4-9, Figure 4-10 and Figure 4-11 show an acceptable agreement with many experiment results and widely-used correlations, confirming the relations among K_o, ϕ' and v' in according to the Sekiguchi-Ohta model.

$$K_o(M, v', \Lambda) = 0 \tag{4.31}$$

$$K_o = \frac{v'}{1 - v'} \tag{4.32}$$

$$K_o = \frac{15 - \sqrt{9 + 16M^2}}{6 + 2\sqrt{9 + 16M^2}} \tag{4.33}$$

$$M = \frac{6\sin\phi'}{3 - \sin\phi'} \tag{4.34}$$

4-4-4 Closure

Apart from the theoretical relations obtained, the study may suggest a solution to break the limitation of the Sekiguchi-Ohta and related models in evaluating incremental plastic strain at the intersection corner. There are many K_o values (mobilized) found before the steady K_o value (immobilized) is approached.

Box 4.1 Rate of plastic strain at the corner

Rate of strain under triaxial K_O-condition

$$\dot{\boldsymbol{\varepsilon}} = \begin{bmatrix} 0 & 0 & 0 \\ 0 & \dot{\varepsilon}_a & 0 \\ 0 & 0 & 0 \end{bmatrix} \quad \text{implies} \quad \dot{\boldsymbol{\varepsilon}} = \frac{1}{3}\dot{\varepsilon}_v \mathbf{1} + \sqrt{\frac{3}{2}}\dot{\varepsilon}_s \mathbf{n}$$

where $\dot{\varepsilon}_v = \dot{\varepsilon}_a$, $\dot{\varepsilon}_s = \frac{2}{3}\dot{\varepsilon}_a$

$$\mathbf{n} = \begin{bmatrix} -\dfrac{1}{\sqrt{6}} & 0 & 0 \\ 0 & \sqrt{\dfrac{2}{3}} & 0 \\ 0 & 0 & -\dfrac{1}{\sqrt{6}} \end{bmatrix} \qquad \mathbf{1} = \begin{bmatrix} 1 & 0 & 0 \\ 0 & 1 & 0 \\ 0 & 0 & 1 \end{bmatrix}$$
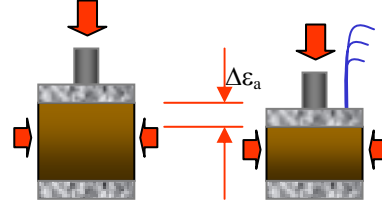
Rate of plastic strain

$$\begin{pmatrix} \dot{\varepsilon}_v^p \\ \dot{\varepsilon}_s^p \end{pmatrix} = \begin{pmatrix} \partial_{p'} f_U & \partial_{p'} f_L \\ \partial_q f_U & \partial_q f_L \end{pmatrix} \cdot \begin{pmatrix} \gamma_U \\ \gamma_L \end{pmatrix}$$

Consistency parameters

$$\begin{pmatrix} \gamma_U \\ \gamma_L \end{pmatrix} = \mathbf{X}^{-1}{}_{(2\times 2)} \cdot \mathbf{L}_{(2\times 1)}$$

Loading parameters (covariance of $\dot{\boldsymbol{\varepsilon}}$): $\quad \mathbf{L} = \begin{bmatrix} K\partial_{p'} f_U & 3G\partial_q f_U \\ K\partial_{p'} f_L & 3G\partial_q f_L \end{bmatrix}\begin{pmatrix} \dot{\varepsilon}_v \\ \dot{\varepsilon}_s \end{pmatrix}$

$\mathbf{X} \in \{\bar{\mathbf{X}}, \tilde{\mathbf{X}}\}$ must be positive definite as defined below

Matrix of coupled hardening plasticity

$$\bar{\mathbf{X}} = \begin{bmatrix} K\left(\partial_{p'} f_U\right)^2 + 3G\left(\partial_q f_U\right)^2 + \partial_{p'} f_U & K\partial_{p'} f_U.\partial_{p'} f_L + 3G\partial_q f_U.\partial_q f_L + \partial_{p'} f_L \\ K\partial_{p'} f_U.\partial_{p'} f_L + 3G\partial_q f_U.\partial_q f_L + \partial_{p'} f_U & K\left(\partial_{p'} f_L\right)^2 + 3G\left(\partial_q f_L\right)^2 + \partial_{p'} f_L \end{bmatrix}$$

Matrix of decoupled hardening plasticity

$$\tilde{\mathbf{X}} = \begin{bmatrix} K\left(\partial_{p'} f_U\right)^2 + 3G\left(\partial_q f_U\right)^2 + \partial_{p'} f_U & 0 \\ 0 & K\left(\partial_{p'} f_L\right)^2 + 3G\left(\partial_q f_L\right)^2 + \partial_{p'} f_L \end{bmatrix}$$

Box 4.2 Determination of immobilized and mobilized K_o

Incremental stress-strain relation

$$\begin{pmatrix} \dot{p}' \\ \dot{q} \end{pmatrix} = \begin{bmatrix} K & 0 \\ 0 & 3G \end{bmatrix} \left[\begin{pmatrix} \dot{\varepsilon}_v \\ \dot{\varepsilon}_s \end{pmatrix} - \begin{pmatrix} \dot{\varepsilon}_v^p \\ \dot{\varepsilon}_s^p \end{pmatrix} \right] \quad \text{and} \quad \eta_o = \left. \frac{\dot{q}}{\dot{p}'} \right|_{K_o}$$

for decoupled heterogeneous plasticity, η_o is obtained by solving the polynomial:

$$\begin{bmatrix} 2\mu'M^4 - 18\mu'^3\Lambda^2 \\ 9\mu'\Lambda^2 + 2M^4\Lambda - M^4 - 6\mu'\Lambda M^2 \\ 2\mu'\Lambda^2 M^2 - 12\mu'^2\Lambda^2 - 2\mu'M^2 \\ M^2 - 2\Lambda M^2 - \Lambda^2 M^2 + 6\mu'\Lambda^2 \\ -2\mu'\Lambda^2 \\ \Lambda^2 \end{bmatrix} \cdot \begin{bmatrix} 1 \\ \eta_o \\ \eta_o^2 \\ \eta_o^3 \\ \eta_o^4 \\ \eta_o^5 \end{bmatrix} = 0 \qquad \text{(mobilized } K_o\text{)}$$

Plastic strain rate for coupled heterogeneous plasticity

$$\begin{pmatrix} \dot{\varepsilon}_v^p \\ \dot{\varepsilon}_s^p \end{pmatrix} = \frac{\dot{\varepsilon}_a}{\dfrac{p'_o}{MDK} + 1} \left(\dfrac{1}{\dfrac{2}{3} + \dfrac{(2G - K\eta_o)p'_o}{3MDKG}} \right) \qquad \text{(immobilized } K_o\text{)}$$

By the assumption of isotropic material under K_o-condition

$$\frac{\dot{\varepsilon}_a^p}{\dot{\varepsilon}_a} = \frac{\dot{\varepsilon}_v^p}{\dot{\varepsilon}_v} = \Lambda \quad \text{yield} \quad \eta_o = 2\frac{G}{K} \quad \text{or} \quad K_o = \frac{v'}{1 - v'}$$
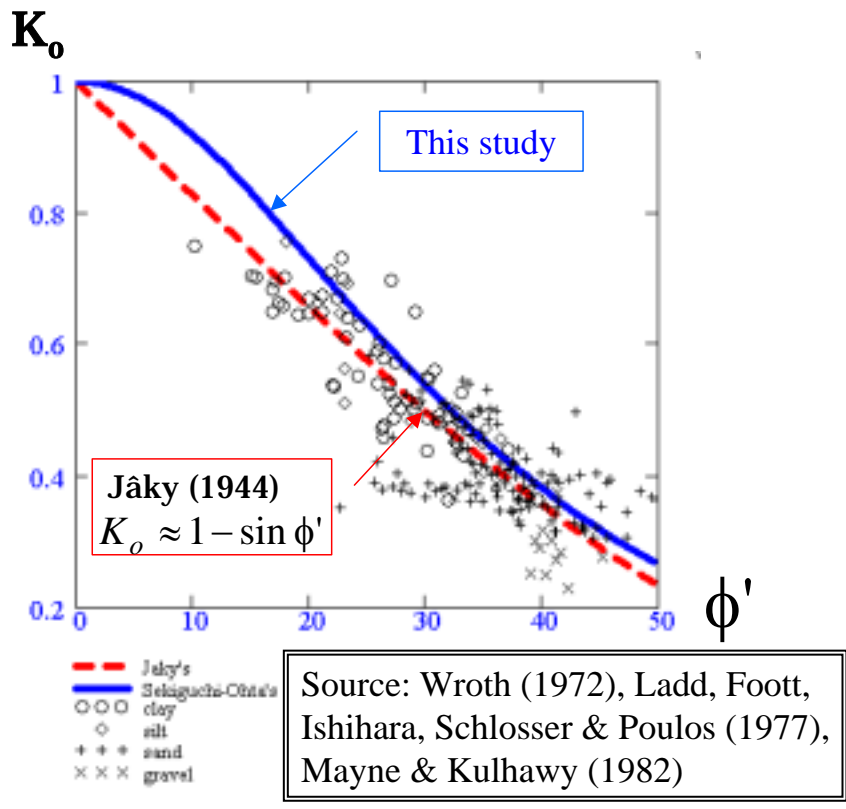
Figure 4-9 Relation between K_o and ϕ' [16]
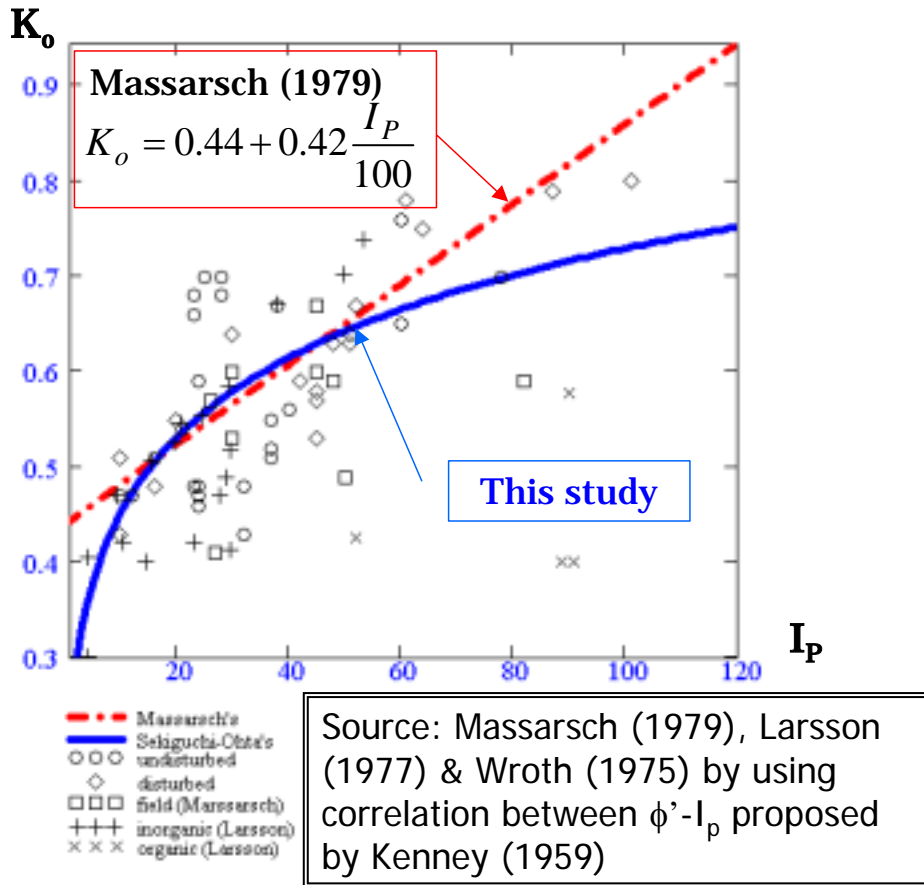
Figure 4-10 Relations between K_o and PI   [17]
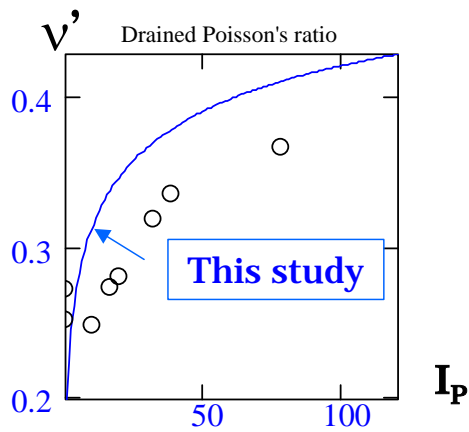
Figure 4-11 Relations between ν' and I_p for several LOC soils (Wroth, 1975) [16]

4-5 Determination of K_o-value by Central limit theorem

4-5-1 Introduction

According to Koiter's associated flow rule (1953) [18], the plastic flow at the corner of the Sekiguchi-Ohta model can be determined by yield surfaces' curvatures enclosing the corner and the strain rate imposed. Provided that the stress point is continuously kept along the corner, the arbitrary strain rate is varied within the certain limit, resulting in upper and lower limits of uniform possibility of plastic flow as depicted in Figure 4-12. The consolidation process is obtained by successive summation of random plastic flow, leading to the normal distribution of total plastic strain accounted by the Central limit theorem. As a consequence, the theoretical K_o-value was formulated. This study may suggest the new concept of K_o-consolidation.

4-5-2 The rate-independent Sekiguchi-Ohta model

The inviscid form of the soil constitutive model proposed by Sekiguchi and Ohta (1977) [14] can be expressed in terms of invariants as shown in Eq.(4.35).

$$f(\boldsymbol{\sigma}', \boldsymbol{\sigma}'_c) = f(I_1, \overline{J}_2, I_{c1}) = MD\ln\left(\frac{I_1}{I_{c1}}\right) + D\frac{3\sqrt{3\overline{J}_2}}{I_1} \tag{4.35}$$

where the stress parameters are listed as following,

$$I_1 = tr(\boldsymbol{\sigma}'), \ I_{c1} = tr(\boldsymbol{\sigma}'_c), \ \mathbf{s} = dev(\boldsymbol{\sigma}'), \ \mathbf{s}_c = dev(\boldsymbol{\sigma}'_c), \ \boldsymbol{\eta}_c = \frac{\mathbf{s}_c}{p'_c}, \ \overline{\mathbf{s}} = \mathbf{s} - \frac{1}{3}I_1\boldsymbol{\eta_c}, \ \overline{J}_2 = \frac{1}{2}tr(\overline{\mathbf{s}}^2), \ J_2 = \frac{1}{2}tr(\mathbf{s}^2),$$

$$\mathbf{1} = diag\begin{bmatrix}1 & 1 & 1\end{bmatrix}, dev(\bullet) = \bullet - \frac{1}{3}(\bullet:\mathbf{1})\mathbf{1}, \ n(\bullet) = \frac{\bullet}{\|\bullet\|}, \ \eta_o = \frac{3(1-K_o)}{1+2K_o}$$

Geometric boundary of K_o-consolidation is restricted to an axisymmetric condition. Therefore, among the discretized yield surfaces enclosing the corner, only yield surfaces in K_o-compression and K_o-extension, as shown in Eqs.(4.36)-(4.37), are active and activated during plastic loading. The criteria of yielding at the corner during K_o-consolidation is satisfied by,

$$f_U(\boldsymbol{\sigma}', \boldsymbol{\sigma}'_c) = f_U(I_1, J_2, I_{c1}) = MD\ln\left(\frac{I_1}{I_{c1}}\right) + D\left(\frac{3\sqrt{3J_2}}{I_1} - \eta_o\right) = 0 \tag{4.36}$$

$$f_L(\boldsymbol{\sigma}', \boldsymbol{\sigma}'_c) = f_L(I_1, J_2, I_{c1}) = MD\ln\left(\frac{I_1}{I_{c1}}\right) - D\left(\frac{3\sqrt{3J_2}}{I_1} - \eta_o\right) = 0 \tag{4.37}$$
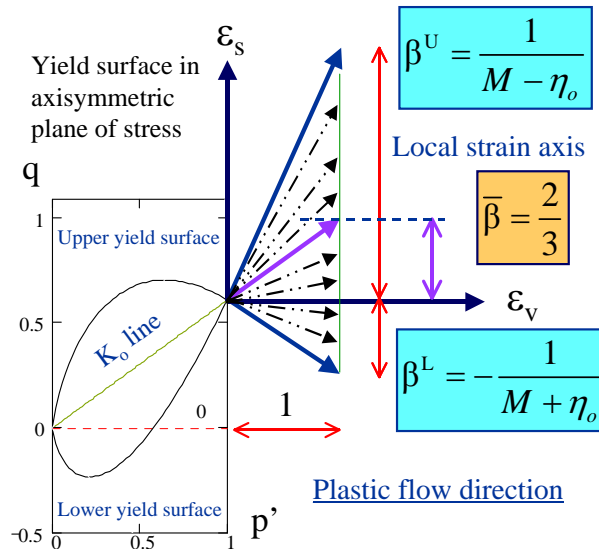
Figure 4-12 Arbitrary plastic flow at the corner

4-5-3 Koiter's associated flow rule

In Eq.(4.38), plastic flow at the corner is computed by assigning $\boldsymbol{\sigma}' = \boldsymbol{\sigma}'_c$ to the sum of associated plastic flow on each upper and lower yield surfaces in according to Koiter's associated flow rule.

$$\dot{\boldsymbol{\varepsilon}}^p = \left\{ \gamma_U \frac{\partial f_U}{\partial \boldsymbol{\sigma}'} + \gamma_L \frac{\partial f_L}{\partial \boldsymbol{\sigma}'} \right\} \Bigg|_{\boldsymbol{\sigma}'=\boldsymbol{\sigma}'_c} \tag{4.38}$$

$$\frac{\partial f_U}{\partial \boldsymbol{\sigma}'}\Bigg|_{\boldsymbol{\sigma}'=\boldsymbol{\sigma}'_c} = \frac{D}{I_{c1}}(M - \eta_o)\mathbf{1} + \sqrt{\frac{3}{2}}\frac{3D}{I_{c1}}\mathbf{n}_c \tag{4.39}$$

$$\frac{\partial f_L}{\partial \boldsymbol{\sigma}'}\Bigg|_{\boldsymbol{\sigma}'=\boldsymbol{\sigma}'_c} = \frac{D}{I_{c1}}(M + \eta_o)\mathbf{1} - \sqrt{\frac{3}{2}}\frac{3D}{I_{c1}}\mathbf{n}_c \tag{4.40}$$

$$\mathbf{n}_c = n(\mathbf{s}_c) = diag\left[-\frac{\sqrt{6}}{6} \quad \frac{\sqrt{6}}{3} \quad -\frac{\sqrt{6}}{6} \right] \tag{4.41}$$

$$\dot{\boldsymbol{\varepsilon}}^p = \frac{1}{3}\left((\gamma_U + \gamma_L)M - (\gamma_U - \gamma_L)\eta_o\right)\frac{3D}{I_{c1}}\mathbf{1} + \sqrt{\frac{3}{2}}(\gamma_U - \gamma_L)\frac{3D}{I_{c1}}\mathbf{n}_c = \frac{1}{3}\dot{\varepsilon}_v^p\mathbf{1} + \sqrt{\frac{3}{2}}\dot{\varepsilon}_s^p\mathbf{n}_c \tag{4.42}$$

According to Eq.(4.38)-(4.41), the plastic flow can be expressed by Eq.(4.42) as components of volumetric and deviatoric parts in an axisymmetric plane governed by tensor basis $\mathbf{1}$ and $\mathbf{n}_c$. The consistency requirement enforcing a continuously yielding stress implies the subsequent yielding stress by three cases,

  a) To the normal fan of the intersection corner: $\gamma_U > 0; \gamma_L > 0$

  b) To the region of upper yield surface: $\gamma_U > 0; \gamma_L = 0$

  c) To the region of lower yield surface: $\gamma_U = 0; \gamma_L > 0$
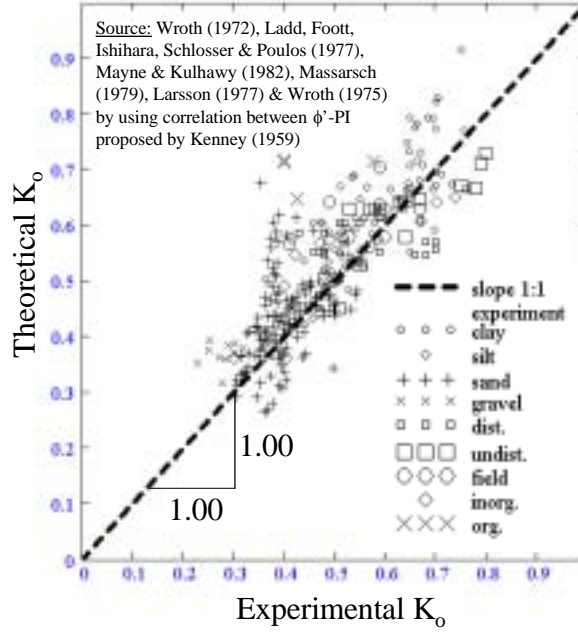
Figure 4-13 Theoretical and Experimental values of K_o

Consistency parameters γ_U and γ_L have a linear mapping relation with imposed strain rate. Hence, for an arbitrary strain rate applied to state of stress at the corner, the corresponding plastic flow is randomly varied between upper and lower limit given by Eqs.(4.43)-(4.44). The random, upper, lower and mean ratios of deviatoric to volumetric plastic strain rate are given by Eqs.(4.45)-(4.48). The mean ratio of an arbitrarily distributed plastic flow is the average of both limits.

$$\dot{\boldsymbol{\varepsilon}}_U^p = \frac{1}{3}\dot{\varepsilon}_{vU}^p\mathbf{1} + \sqrt{\frac{3}{2}}\dot{\varepsilon}_{sU}^p\mathbf{n}_c \tag{4.43}$$

$$\dot{\boldsymbol{\varepsilon}}_L^p = \frac{1}{3}\dot{\varepsilon}_{vL}^p\mathbf{1} + \sqrt{\frac{3}{2}}\dot{\varepsilon}_{sL}^p\mathbf{n}_c \tag{4.44}$$

$$\beta = \frac{\dot{\varepsilon}_s^p}{\dot{\varepsilon}_v^p} = \frac{\gamma_U - \gamma_L}{(\gamma_U + \gamma_L)M - (\gamma_U - \gamma_L)\eta_o} \tag{4.45}$$

$$\beta^U = \beta|_{\gamma_L=0} = \frac{1}{M - \eta_o} \tag{4.46}$$

$$\beta^L = \beta\big|_{\gamma_U=0} = -\frac{1}{M+\eta_o} \tag{4.47}$$

$$\overline{\beta} = \frac{\beta^U + \beta^L}{2} = \frac{\eta_o}{M^2 - \eta_o{}^2} \tag{4.48}$$

100 steps 100 trials
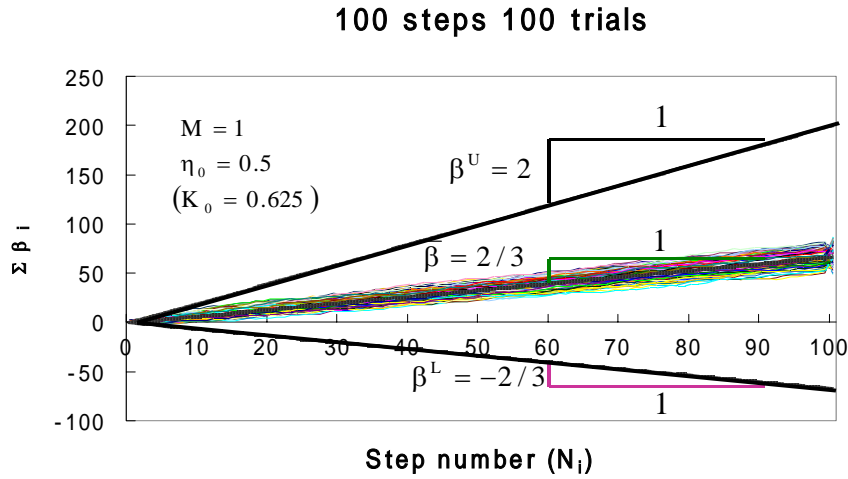
Figure 4-14 Accumulated plastic flow at the corner

4-5-4 Determination of theoretical K_o

If the irreversible response (Eqs.(4.49)-(4.51)) of plastic strain ratio obtained from one-dimensional consolidation or oedometer test result is considered as population mean shown by Eq.(4.52), the sample means are considered by the mean of plastic strain ratios of several loading steps taken from many trials. According to the central limit theorem, when a sufficiently large size of loading steps is employed, the sample mean will be approached to mean of normal distribution $\overline{\beta}$ of Eq.(4.48), which is equivalent to 2/3 as given in Eq.(4.52). Then, K_o expression can be solved as shown in Eq.(4.53) and plotted with experimental results in Figure 4-13. Theoretical K_o confirms an agreement with past experiments.
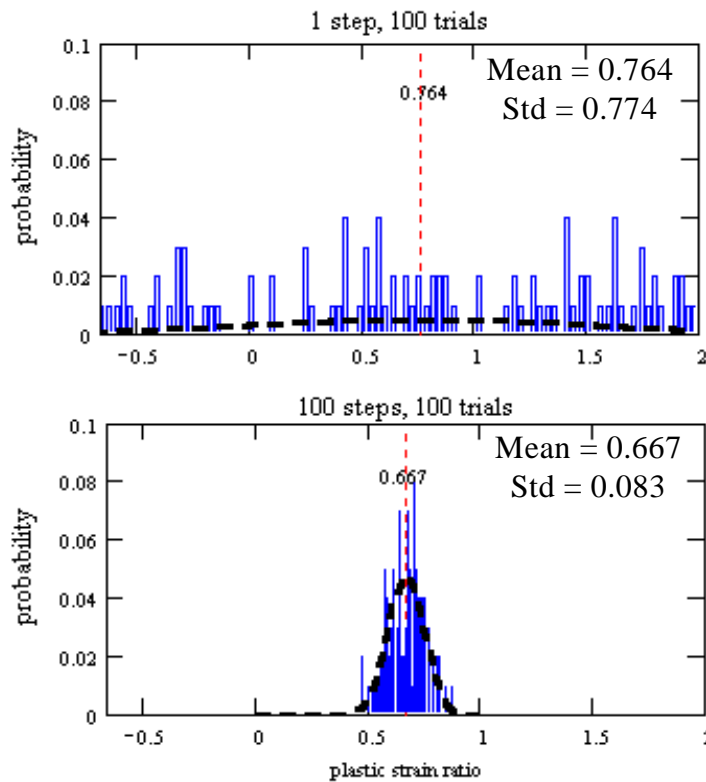
Figure 4-15 Distribution of plastic strain ratio at each step

$$\boldsymbol{\Delta\varepsilon}^p = diag[0 \quad \Delta\varepsilon_a^p \quad 0] \tag{4.49}$$

$$\Delta\varepsilon_s^p = \sqrt{\frac{2}{3}} \left\| dev(\boldsymbol{\Delta\varepsilon}^p) \right\| = \frac{2}{3}\Delta\varepsilon_a^p \tag{4.50}$$

$$\Delta\varepsilon_v^p = tr(\boldsymbol{\Delta\varepsilon}^p) = \Delta\varepsilon_a^p \tag{4.51}$$

$$\frac{\Delta\varepsilon_s^p}{\Delta\varepsilon_v^p} = \frac{2}{3} \tag{4.52}$$

$$K_o = \frac{15 - \sqrt{9 + 16M^2}}{6 + 2\sqrt{9 + 16M^2}} \tag{4.53}$$

4-5-5 Numerical illustration Numerical illustration

The plastic flow is uniformly generated as described in Figure 4-16 by 100 trials for 100 steps with M=1. The generated results are shown in Figure 4-14 where the distribution of plastic strain ratio at step 1 and step 100 are shown in Figure 4-15. For 100 steps, total plastic strains are approached to normal distribution with an expected value 2/3, which is consistent with value obtained by rigorous implementation of Koiter's flow rule to the corner of SO model. Plastic flow during K_o-consolidation process may be interpreted as uniformly distributed plastic flow along the vertical direction in a ground.
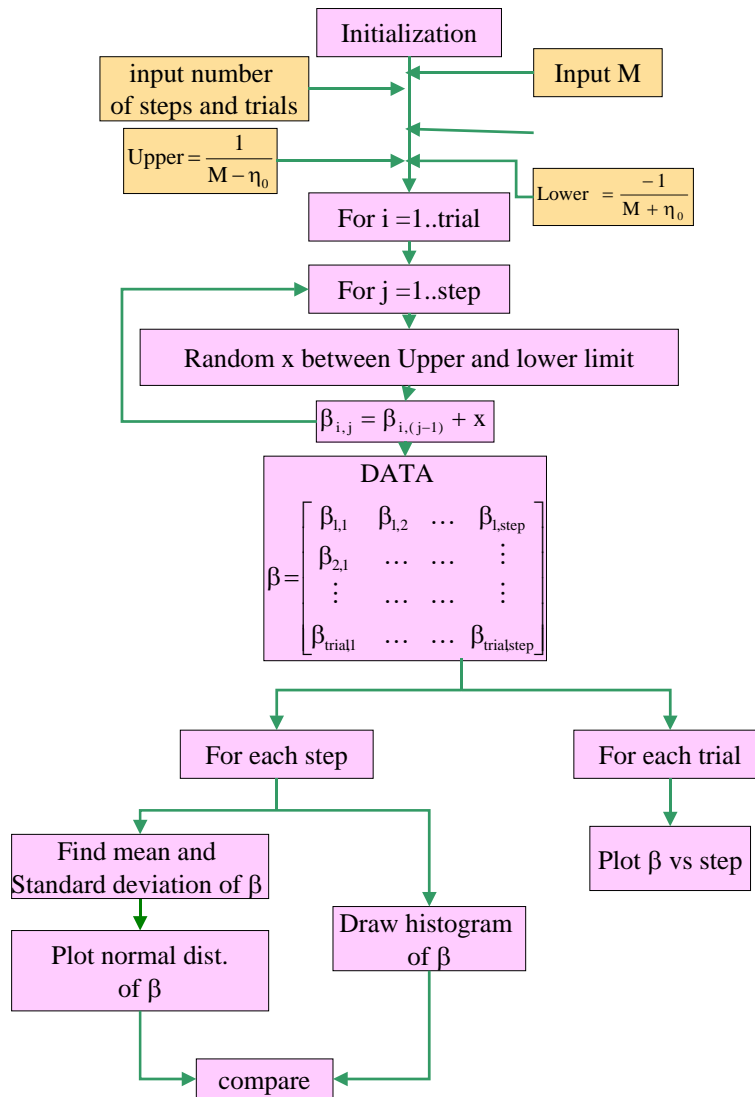
Figure 4-16 Approach by the central limit theorem

4-6 References

1 Wood, D.M. (1990), Soil behavior and Critical state soil mechanics, Cambridge University Press

2 Bowles, J.E. (1988). Foundation analysis and design, McGraw-Hill International editions

3 Lambe, T.William & Whitman, Robert V. (1979). Soil Mechanics, John Wiley & Sons

4 Terzaghi, Karl & Peck, Ralph B. (1967). Soil Mechanics in Engineering Practice, John Wiley & Sons

5 Massarsch, K.R. (1979). Lateral earth pressure in normally consolidated clay, Design parameters in Geotechnical engineering, Proc. 7th ECSMFE, vol. 2: 245-49.

6 Kenney, T.C. (1959): Discussion, Proc. ASCE, vol.85, No. SM3, pp: 67-79.

7 Alpan, I. (1967), The empirical evaluation of the coefficient K_o, K_{or}, Soils & Foundations, vol 7(1): 31-40

8 Schofield, A. & Wroth, P. (1968). Critical State Soil Mechanics, McGRAW-HILL

9 Roscoe, K.H. & Burland, J.B., On the Generalised Stress-Strain Behavior of Wet Clay, Engineering Plasticity, Cambridge University Press, 1968

10 Jâky, J. (1944). The coefficients of earth pressure at rest, J.Hung. Arch. Engrs. Soc., Budapest: 355-8.

11 Wroth, C.P. (1972). General theories of earth pressure and deformation, Proc. 5th ECSMFE, Madrid, vol. 2: 33-52.

12 Ladd, C.C., Foott, R., Ishihara, K., Schlosser, F., & Poulos, H.G. (1977). Stress-deformation and strength characteristics, Proc. 9th ICSMFE, Tokyo, vol. 2: 421-94.

13 Mayne, P.W. & Kulhawy, F.H. (1982). Ko-OCR relationships in soil, JGE Division, ASCE, vol 108, No. GT6: 851-72.

14 Sekiguchi, H. & Ohta, H. (1977). Induced anisotropy and time dependency in clays, Proc. ICSMFE 9th, Tokyo: 229-38.

15 Pipatpongsa, T., Ohta, H., Kobayashi, I. & Iizuka, A. (2001), Dependence of Ko-value on effective internal friction angle in regard to the Sekiguchi-Ohta model, Proc. of 36th Japanese Nat. Conf. on Geotech. Engrg: 936-937.

16 Wroth, C.P. (1975). In-situ measurement of initial stresses and deformation characteristics, in Proc. Specialty Conf. On In-Situ Measurement of Soil Properties, Raleigh, North Carolina (New York: ASCE), vol. 2: 181-230.

17 Larsson, R. (1977): Basic behaviour of Scandinavian soft clays, Swedish Geotechnical Institute, Linkoping, Report 4.

18 Koiter, W.T. (1953), "Stress-strain relations, uniqueness and variational theorems for elastic-plastic materials with a singular yield surface", *Quart. Appl. Math. (11)*: 350-354

CHAPTER 5
Singular Hardening Vertex

5-1 Introduction

Formulation and numerical implementation of soil constitutive models with a smooth/single yield surface have already been well developed and become a standard code for finite element method. Among many of engineering software and package, general FEM codes based on the soil constitutive model proposed by Sekiguchi and Ohta (1977) [1] have been extensively recognized in Japan and still being improved continuously. However, it has been found that a plastic flow at the point of preconsolidated stress, which is related to a material memory of the model, is unable to correctly evaluate plastic strain increments due to a problem of mathematical singularity on yield surface at which the gradient is not uniquely defined. A geometrical representation of the yield surface in stress space shows this point representing a ridge corner of asymmetrical logarithmic spiral. As a consequence, the discontinuous slope at the corner rules out the normality postulate; the similar difficulty in numerical implementation is also found by Britto & Gunn (1987) and Gens & Potts (1988) [2, 3] in original Cam-clay model (Roscoe, Schofield & Thurairajah, 1963) [4].

Unsurprisingly, the same difficulty is found in the original Cam-clay model in which the mathematical prescription produces uncertainties due to the presence of distortion when predicting volumetric strain under imposed isotropic compression boundary conditions. This is an example of a difficulty met in the theory of plasticity when a yield curve has a corner. For the reason of metastable (yield under any increment of p' of effective spherical pressure), the volumetric strains under this condition are directly presented by virgin compressed curve of normally consolidated clays without any association with Cam-clay flow rule. Moreover, any attempt to choose a particular plastic flow normal to yield curve at or near the corner would produce a much higher value of K_o than those measured in practice [5].

The discontinuity is suggested to eliminate either by rounding off using smooth approximating functions (Zienkiewicz & Pande, 1977) [6] or adopting an ellipsoidal yield surface (Roscoe & Burland, 1968). [7] Actually, there is no theoretical objection to non-smooth yield surface (Koiter, 1953, Rudnicki & Rice, 1975, Christoffersen & Hutchinson, 1979) [8, 9, 10]. Moreover, evaluation of plastic flow at the point of singularity can be achieved theoretically without any modification of a yield surface's curvature.

One of the theoretical extensions to cover constitutive models with the point of discontinuity, where elastic domain is defined by non-smooth convex boundaries, is developed by Simo, Kennedy & Govindjee (1988) [11], showing that the standard Kuhn-Tucker optimality conditions of convex mathematical programming are essentially equivalent to the multisurface counterpart of the conditions in Koiter (1953). By the abovementioned approach, Pipatpongsa et al. (2001a, b) [12, 13] described an additional procedure to handle a difficulty when a particular stress point is placed at the corner of yield surface in stress space. Under this concept, K_o consolidation process is regulated by two activated yield loci referred to upper and lower yield surfaces intersecting each other in axisymmetric triaxial plane to form the hardening vertex, in which plastic flow at the point of discontinuity lie within the fan of possible directions.

The approach of adjoining the singular corner by only two conceivable yield functions can reduce bulky equations required by Koiter's condition for non-smooth multisurface plasticity. The typically reasonable values of coefficient of earth pressure at rest governed by the SO (Sekiguchi-Ohta) model can be obtained by connecting a typical normality of individual yield surface to Koiter's associated flow rule (Pipatpongsa et al., 2001c) [14]. The application of compatible Kuhn-Tucker optimality conditions and Koiter's flow rule to corner of the model is illustrated by stress update algorithm (Pipatpongsa et al., 2001d) [15].

In a view of practice, most of natural soil formation possesses a certain degree of over-consolidated ratio; therefore, an initial stress is placed inside a yield surface rather than at the corner. To avoid the same problem in normal consolidated young clay, an initial stress placed at the corner is put inside yield surface intentionally by factoring it with a number that is slightly less than one. Besides, a calculation of one-dimensional consolidation is obtained by assuming soil media as an elastic material. By means of those reasons, error due to the singularity is not exaggerated in finite element program applicable to the SO model, for example DACSAR (Iizuka & Ohta, 1987) [16]. However, in rigorous aspect, this fact cannot be overlooked and violated any longer.

In this paper, a standard FEM procedures based on smooth yield surface was corrected by adding a corner mode to assess plastic flow when stress is defined at the corner in particular. Detailed procedures with theoretical background are provided. A continuum tangential stiffness tensor corresponding to the singular corner of the SO model was formulated. The comparisons between methods with/without a consideration corner mode under K_o-condition were illustrated under plane strain and axisymmetric conditions. The effects of element assemblage and size of sub-incrementation were discussed. The study may provide a source of numerical implementation to fill in the overlooked procedure in previous development of FEM applicable to the SO or similar models.

5-2 Soil Constitutive Equations

The SO model has been proven to produce predicted behaviors which are consistent with observed field responses for anisotropically consolidated soils. The model is based on critical state theory considering dilatancy,

reorientation of principal stresses, anisotropy and time dependency. The SO model is reduced to be the original Cam-clay model in case of initially isotropic stress condition.

5-2-1 Forms of the Sekiguchi-Ohta Model

The two-invariant, rate-independent elastoplastic associative soil constitutive model proposed by Sekiguchi and Ohta (1977) is originally expressed by a convex yield (plastic potential) function:

$$f(\mathbf{\sigma'}, h) \equiv f(p', \eta^*, \varepsilon_v^p) = MD \ln\left(\frac{p'}{p_o'}\right) + D\eta^* - \varepsilon_v^p = 0 \tag{5.1}$$

where
$\mathbf{\sigma'}$ = effective stress tensor;
h = selective isotropic hardening parameter;
p' = effective mean stress;
$\eta*$ = generalized stress ratio;
ε_v^p = volumetric plastic strain;
p'_o = effective mean stress at the end of completion of anisotropic consolidation (typically, K_o consolidation);
M = slope of critical state line in a p'-q plane;
D = coefficient of dilatancy

Internal variable h controls a size of a yield surface and can be selected either as stress-like or strain-like variable. A form in Eq.(5.1) serves as strain-like type, which physically means that a hardening/softening characteristics of material is induced by a plastic volumetric strain. On the other hand, a stress-like type can be formulated from Eq.(5.1) using relation given in Eq.(5.2) and expression of coefficient of dilatancy in Eq.(5.3) (Ohta & Hata, 1971) [17].

$$p'_c = p'_o \exp\left(\frac{\varepsilon_v^p}{(\lambda - \kappa)/(1 + e_o)}\right) \tag{5.2}$$

$$D = \frac{\lambda - \kappa}{M(1 + e_o)} \tag{5.3}$$

Without loss of originality, an alternative form of the Sekiguchi-Ohta model with stress hardening as parameter can be expressed by Eq.(5.4). Figure 5.1 shows the outline of two corresponding forms of the Sekiguchi-Ohta model.

$$f(\mathbf{\sigma'}, h) \equiv f(p', \eta^*, p_c') = MD \ln\left(\frac{p'}{p_c'}\right) + D\eta^* = 0 \tag{5.4}$$

where p'_c = stress hardening parameter

Strain-Hardening Form

$$f(\mathbf{\sigma}, h) \equiv f(p', \eta^*, \varepsilon_v^p) = MD \ln\left(\frac{p'}{p_o'}\right) + D\eta^* - \varepsilon_v^p = 0$$

$$p'_c = p'_o \exp\left(\frac{\varepsilon_v^p}{(\lambda - \kappa)/(1 + e_o)}\right) \qquad D = \frac{\lambda - \kappa}{M(1 + e_o)}$$

Stress-Hardening Form

$$f(\mathbf{\sigma}, h) \equiv f(p', \eta^*, p_c') = MD \ln\left(\frac{p'}{p_c'}\right) + D\eta^* = 0$$
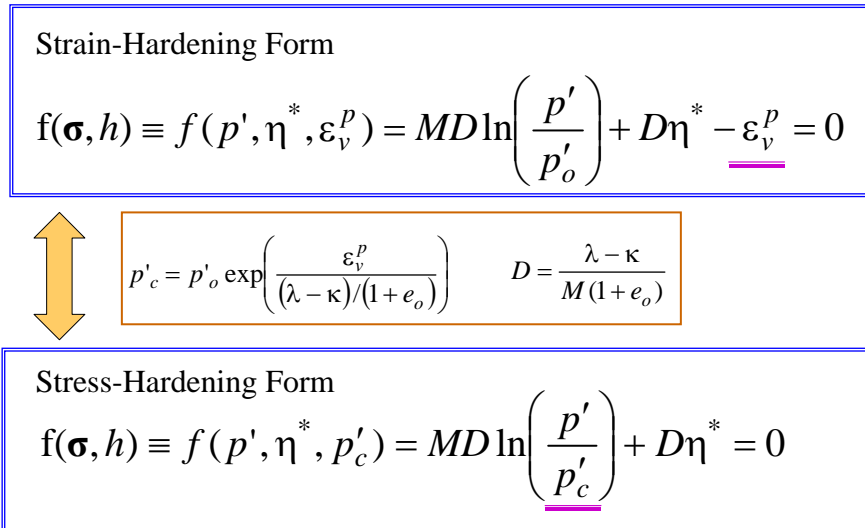
Figure 5.1 Forms of the Sekiguchi-Ohta model

5-2-2 Geometrical Representation

The SO yield surface in three principal stresses space can be conveniently presented by referring to new Cartesian coordinate system (X_1, X_2, X_3) on the deviatoric plane (π-plane) as shown in Figure 5.2. The parametric form of yield surface on (p', ω) is formulated by coordinate transformation system (see Appendix A).

Figure 5.3 shows a distorted bullet shape of elastic domain in principal stress space and in different views on plane A, B and C which refer to deviatoric plane, meridional plane at ω=0 and π, and top view (σ'_2- σ'_3) plane respectively. The existence of a singular corner on K_o-line reveals that the SO yield surface is not smooth at the particular stress point where material memory of consolidation history is kept as hardening parameter, therefore, this point is identified as the hardening vertex of the model.

$$\boxed{\boldsymbol{\sigma}' = \mathbf{Q}^T \cdot \mathbf{x}}$$

$$\mathbf{Q} = \begin{bmatrix} 0 & \frac{-1}{\sqrt{2}} & \frac{1}{\sqrt{2}} \\ \sqrt{\frac{2}{3}} & \frac{-1}{\sqrt{6}} & \frac{-1}{\sqrt{6}} \\ \frac{1}{\sqrt{3}} & \frac{1}{\sqrt{3}} & \frac{1}{\sqrt{3}} \end{bmatrix} \quad \boldsymbol{\sigma}' = \begin{pmatrix} \sigma'_1 \\ \sigma'_2 \\ \sigma'_3 \end{pmatrix} \quad \mathbf{x} = \begin{pmatrix} x_1 \\ x_2 \\ x_3 \end{pmatrix}$$

$$x_1^2 + \left(x_2 - \frac{2}{\sqrt{6}} \eta_o p' \right)^2 = \left(\frac{2M}{\sqrt{6}} \ln\left(\frac{p'}{p'_c} \right) p' \right)^2$$

$$R = \frac{2M}{\sqrt{6}} \ln\left(\frac{p'}{p'_c} \right) p'$$

$$X = R\sin\omega \qquad Y = R\cos\omega + \frac{2}{\sqrt{6}} \eta_o p'$$

$$p' \in (0, p'_c] \qquad \omega \in [0, 2\pi]$$
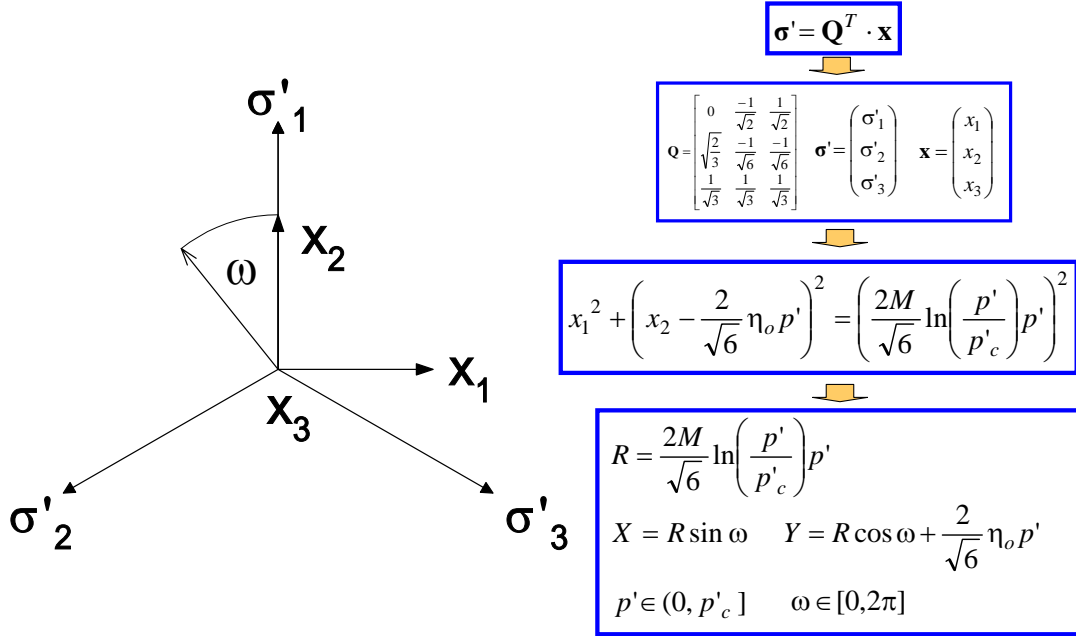
Figure 5.2 Deviatoric plane in principal stress space

5-2-3 Generalized Convex Format

The initially stress-induced anisotropic consolidation history is recorded at the corner of Sekiguchi-Ohta yield surface given by **σ'$_c$**. Under the stage of natural deposition, the state of stress at the corner, which its vertical direction (also the major principal axis) is coincided with the direction of gravity force, can be given in terms of Cartesian components as,

$$\boldsymbol{\sigma}'_c = \begin{bmatrix} \sigma'_{c11(xx)} & \sigma'_{c12(xy)} & \sigma'_{c13(xz)} \\ \sigma'_{c21(yx)} & \sigma'_{c22(yy)} & \sigma'_{c23(yz)} \\ \sigma'_{c31(zx)} & \sigma'_{c32(zy)} & \sigma'_{c33(zz)} \end{bmatrix} = \begin{bmatrix} K_o \sigma'_{vc} & 0 & 0 \\ 0 & \sigma'_{vc} & 0 \\ 0 & 0 & K_o \sigma'_{vc} \end{bmatrix} \tag{5.5}$$

σ'$_c$ is referred to the currently stress-induced anisotropic consolidation history at a current time of interest (subsequent stage). **σ'$_o$** is distinguished from **σ'$_c$** by the fact **σ'$_o$** is referred to **σ'$_c$** right after at the completion of natural K_o-consolidation and serves as the initially stress-induced anisotropic consolidation stress history at the starting time of interest (initial stage, t=0). A reference state of the SO model is set to initial yield stress **σ'$_o$** at t=0, therefore, this sort of format breaks the principle of objectivity (frame indifferent) at all times. It is suggested to have the model changed its reference state to current yield stress **σ'$_c$** in order to satisfy principle of objectivity.

Baker and Desai (1984) [18] showed that it is necessary to include joint invariants of stress in a constitutive equation in order to completely describe the anisotropic behaviour of soils. The joint invariants characterize the relative orientation of the stress and plastic strain tensors in space. In order to characterize this anisotropy, a mapping rule is adopted with respect to the anisotropic consolidation axis (K_o-line) into stress deviators. i.e., **s** is the current stress deviator, $\overline{\mathbf{s}}$ is the relative stress deviator using mapping quantity defined in Eq.(5.14)) [18,19,20,21].

For later reference throughout the paper, it is more convenient and general to rewrite the yield function of Eq.(5.4) in terms of stress invariants and joint invariants between stress tensor **σ'** and stress hardening tensor **σ'$_c$** which is kept along paths of corner as,

$$\mathrm{f}(\boldsymbol{\sigma}', \boldsymbol{\sigma}'_c) = f(I_1, \overline{J}_2, I_{c1}) = MD\ln\left(\frac{I_1}{I_{c1}} \right) + D\frac{3\sqrt{3\overline{J}_2}}{I_1} = 0 \tag{5.6}$$
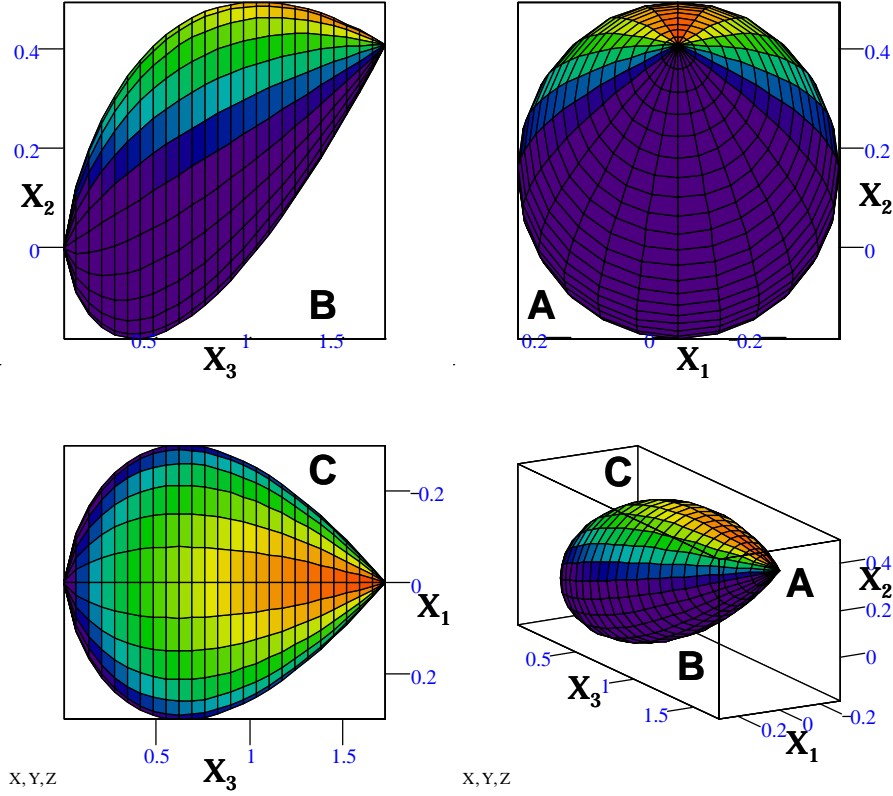
Figure 5.3 Various views of the Sekiguchi-Ohta yield surface in principal stress space

where

$$p' = \frac{1}{3}I_1 = \frac{1}{3}tr(\boldsymbol{\sigma}') = \frac{1}{3}\mathbf{1}:\boldsymbol{\sigma}' \qquad \text{;mean effective stress} \qquad (5.7)$$

$$p'_c = \frac{1}{3}I_{c1} = \frac{1}{3}tr(\boldsymbol{\sigma}'_c) = \frac{1}{3}\mathbf{1}:\boldsymbol{\sigma}'_c \qquad \text{;mean effective virgin consolidated stress} \qquad (5.8)$$

$$\mathbf{s} = \boldsymbol{\sigma}' - \frac{1}{3}I_1\mathbf{1} = \mathbf{A}:\boldsymbol{\sigma}' \qquad \text{;stress deviator} \qquad (5.9)$$

$$\mathbf{s}_c = \boldsymbol{\sigma}'_c - \frac{1}{3}I_{c1}\mathbf{1} = \mathbf{A}:\boldsymbol{\sigma}'_c \qquad \text{;virgin } K_o\text{-consolidated stress deviator} \qquad (5.10)$$

$$J_2 = \frac{1}{2}tr(\mathbf{s}^2) = \frac{1}{2}\mathbf{s}:\mathbf{s} \qquad \text{;the second invariant of stress deviator} \qquad (5.11)$$

$$J_{c2} = \frac{1}{2}tr(\mathbf{s}_c^2) = \frac{1}{2}\mathbf{s}_c:\mathbf{s}_c \qquad \text{;the second invariant of stress hardening} \qquad (5.12)$$

$$\boldsymbol{\eta}_c = \frac{\mathbf{s}_c}{p'_c} \qquad \text{;orientation of yield surface in second order tensor quantity} \qquad (5.13)$$

$$\bar{\mathbf{s}} = \mathbf{s} - \frac{1}{3}I_1\boldsymbol{\eta}_c = \left(\mathbf{A} - \frac{1}{3}\boldsymbol{\eta}_c \otimes \mathbf{1}\right):\boldsymbol{\sigma}' \qquad \text{;relative stress deviator} \qquad (5.14)$$

$$\bar{J}_2 = \frac{1}{2}tr(\bar{\mathbf{s}}^2) = \frac{1}{2}\bar{\mathbf{s}}:\bar{\mathbf{s}} \qquad \text{;the second anisotropic invariant} \qquad (5.15)$$

The outline of relation between $\hat{\eta}$ (not η^*) and $\bar{J}_2$ is shown in Figure 5.4.
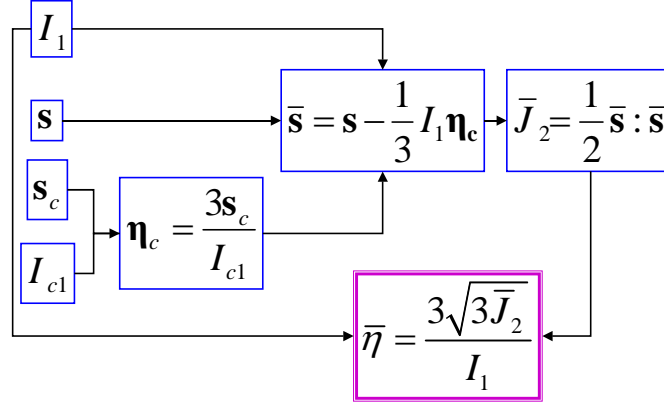
Figure 5.4 Relation between joint invariant and generalized stress ratio

The second-order identity tensor is defined by

$$\mathbf{1} \equiv \delta_{ij} \mathbf{e}_i \otimes \mathbf{e}_j \qquad (5.16)$$

The forth-order identity tensor is defined by

$$\mathbf{I} \equiv \frac{1}{2} \left[\delta_{ik} \delta_{jl} + \delta_{il} \delta_{jk} \right] \mathbf{e_i} \otimes \mathbf{e_j} \otimes \mathbf{e_k} \otimes \mathbf{e_l} \qquad (5.17)$$

The forth-order deviatoric tensor (forth-order tensor mapping stress and stress deviator) is defined by [22] (See more in Appendix A)

$$\mathbf{A} \equiv \mathbf{I} - \frac{1}{3} (\mathbf{1} \otimes \mathbf{1}) \qquad (5.18)$$

5-2-4 Reciprocal basic

Apart from the tensor basis $\mathbf{e}_i \otimes \mathbf{e}_j$, which is independent of any preferred choice of basic for E, there is an additional linear mapping $\mathbf{\eta_c}$ set in space to characterize material anisotropy in particular. A resulting reciprocal basic considering a relative relation between Cartesian and anisotropic mapping quantity is schematized in Figure 5.5 and also written in expressions given below,
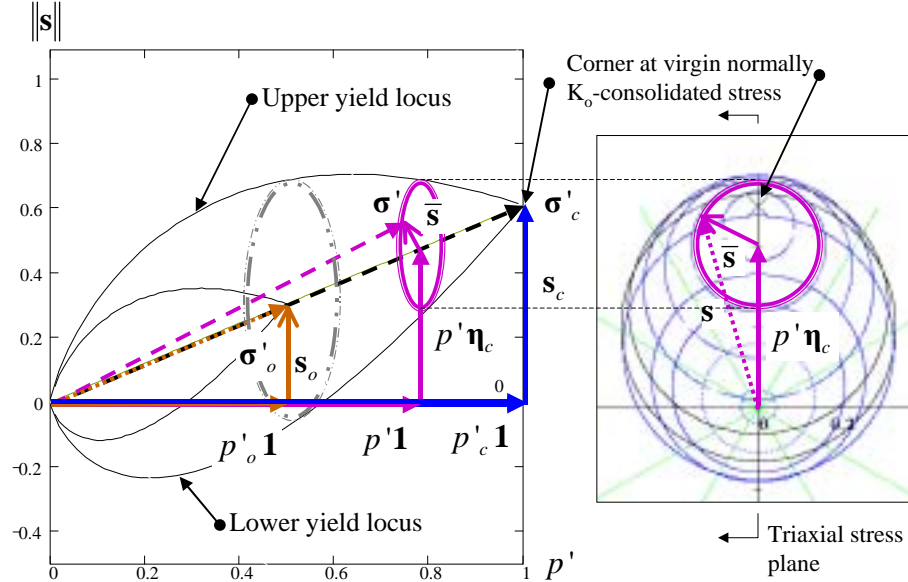
Figure 5.5 Schematization of reciprocal basics employed in mapping quantity

$$\boldsymbol{\sigma}' = p' \mathbf{1} + p' \mathbf{\eta}_c + \overline{\mathbf{s}} \qquad (5.19)$$

$$\boldsymbol{\sigma}'_c = p'_c \mathbf{1} + p'_c \mathbf{\eta}_c \qquad (5.20)$$

Relative stress deviator $\overline{\mathbf{s}}$ in Eq.(5.21) is coaxial with deviatoric plastic flow; thus, it is more suitable than

stress deviator $\mathbf{s}$ in the manipulation of anisotropic constitutive equations.

$$\overline{\mathbf{s}} = \mathbf{s} - p'\boldsymbol{\eta}_c = \sqrt{2\overline{J}_2}\,\overline{\mathbf{n}} \tag{5.21}$$

As a result, a stress tensor can be efficiently represented in terms of reciprocal tensor basis $\{\mathbf{1}, \boldsymbol{\eta}_c, \overline{\mathbf{n}}\}$.

5-2-5 Form-Invariance Principle
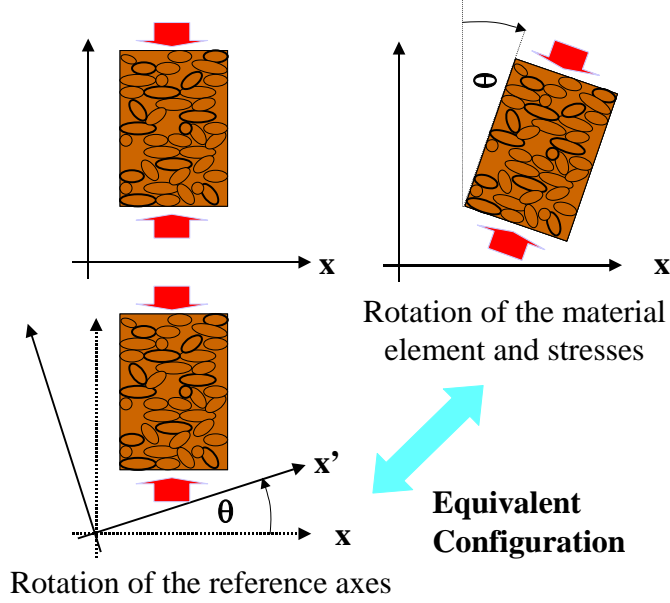
Figure 5.6 Schematic representation of form-invariance principle (Baker & Desai, 1984)

The material response described by the constitutive equations should be satisfied the objectivity requirement as depicted in Figure 5.6 (Baker & Desai, 1984) [18] where a rotation of both reference axes and material elements result in equivalent configurations. A transformation tensor $\mathbf{Q}$ is a proper orthogonal second-order tensor, in which,

$$\mathbf{Q}\cdot\mathbf{Q}^T = \mathbf{Q}^T\cdot\mathbf{Q} = \mathbf{1}, \quad \det(\mathbf{Q}) = 1 \tag{5.22}, (5.23)$$

The stress and stress hardening variable after rotation can be expressed as,

$$\boldsymbol{\sigma'}^* = \mathbf{Q}\cdot\boldsymbol{\sigma'}\cdot\mathbf{Q}^T, \quad \boldsymbol{\sigma'_c}^* = \mathbf{Q}\cdot\boldsymbol{\sigma'_c}\cdot\mathbf{Q}^T \tag{5.24}, (5.25)$$

The stress invariants under the new reference can be calculated by transformation rule shown in Appendix G. It is found that,

$$I_1^* = I_1, \quad \overline{J}_2^* = \overline{J}_2, \quad I_{c1}^* = I_{c1} \tag{5.26}, (5.27), (5.28)$$

The previous equations simply mean the property of yield function satisfies the principle of objectivity.

$$f(I_1^*, \overline{J}_2^*, I_{c1}^*) = f(I_1, \overline{J}_2, I_{c1}) \tag{5.29}$$

Then, the objectivity of the constitutive equation is proven by

$$f(\boldsymbol{\sigma'}^*, \boldsymbol{\sigma'_c}^*) = f(\mathbf{Q}\cdot\boldsymbol{\sigma'}\cdot\mathbf{Q}^T, \mathbf{Q}\cdot\boldsymbol{\sigma'_c}\cdot\mathbf{Q}^T) = f(\boldsymbol{\sigma'}, \boldsymbol{\sigma'_c}) \tag{5.30}$$

It is noted that the original concept of the SO model has an expression referred to the initial yield stress. As a result, the objectivity is not satisfied in the way that,

$$\boldsymbol{\sigma'_o}^* = \boldsymbol{\sigma'_o} \neq \mathbf{Q}\cdot\boldsymbol{\sigma'_o}\cdot\mathbf{Q}^T \tag{5.31}$$

5-2-6 Stress-induced anisotropy

Under the assumption of homogeneous and isotropic material, anisotropy response is generated if either yield or potential functions depends on the joint invariants between stress and hardening variables. Difference in sampling in anisotropic media give difference in stress-strain response as depicted in Figure 5.7 (Baker & Desai, 1984) [18]. According to the SO model, $\eta^* = \eta^*(\boldsymbol{\sigma'}, \boldsymbol{\sigma'_o})$ in the expression is referred to the joint invariant. Therefore, the model can characterize the anisotropy response. However, $\eta^* = \eta^*(\boldsymbol{\sigma'}, \boldsymbol{\sigma'_o})$ is also referred to the initially stress-induced anisotropy, which is no longer satisfied with the principle of objectivity. In the study, the generalized convex format referring to a current stress-hardening variable is suggested. Under this concept, $\overline{\eta} = \overline{\eta}(\boldsymbol{\sigma'}, \boldsymbol{\sigma'_c})$ is employed instead, which is referred to the stress-induced anisotropy providing that there is no rotational-hardening response.
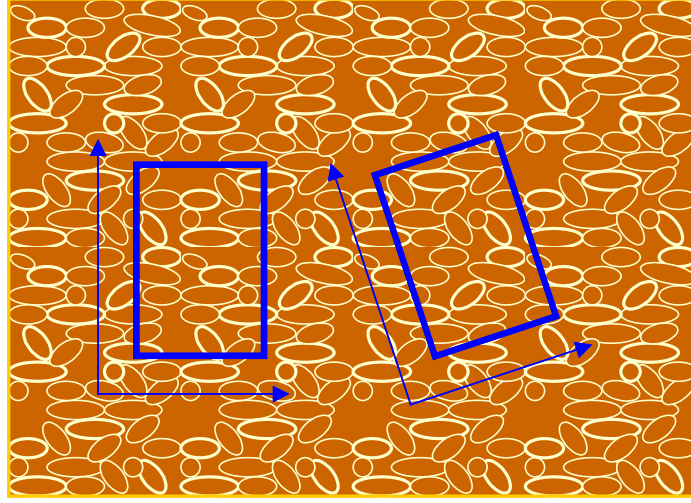
Figure 5.7 Effect of rotation on the joint invariants (Baker & Desai, 1984)

In order to have the SO model satisfied the principle of objectivity, the generalized stress ratio η^* is replaced by generalized relative stress ratio $\bar{\eta}$ presented by,

$$\bar{\eta} = \bar{\eta}(\boldsymbol{\sigma}', \boldsymbol{\sigma}'_c) = \frac{3\sqrt{3\bar{J}_2}}{I_1} = \sqrt{\frac{3}{2}\left\{\frac{\mathbf{s}_{ij}}{p'} - \frac{\mathbf{s}_{cij}}{p'_c}\right\}\left\{\frac{\mathbf{s}_{ij}}{p'} - \frac{\mathbf{s}_{cij}}{p'_c}\right\}} \tag{5.32}$$

where $\dfrac{\mathbf{s}_{cij}}{p'_c} = \boldsymbol{\eta}_c = \sqrt{\dfrac{2}{3}}\eta_o diag\left[-\dfrac{\sqrt{6}}{6} \quad \dfrac{\sqrt{6}}{3} \quad -\dfrac{\sqrt{6}}{6}\right]$ providing that $\dot{\boldsymbol{\eta}}_c = \mathbf{0}$ (5.33)

5-3 Incremental Stress-Strain Relation

It is generally assumed that strain increment can be decomposed into elastic and plastic parts, denoted by

$$\dot{\boldsymbol{\varepsilon}} = \dot{\boldsymbol{\varepsilon}}^e + \dot{\boldsymbol{\varepsilon}}^p \tag{5.34}$$

Associated flow rule is applied to the SO model to determine irreversible plastic flow emerged in an outward normal direction to the plastic potential coincided with yield surface.

$$\dot{\boldsymbol{\varepsilon}}^p = \gamma \frac{\partial f}{\partial \boldsymbol{\sigma}'} = \gamma \partial_{\boldsymbol{\sigma}'} f \tag{5.35}$$

where γ is a proportional factor or consistency parameter.
Consequence of the consistency relation gives

$$\gamma = \frac{\partial_{\boldsymbol{\sigma}'} f : \mathbf{c}^e : \dot{\boldsymbol{\varepsilon}}}{H_e + H_p} \tag{5.36}$$

Tensorial moduli $\mathbf{c}^e$, scalar moduli H_e and H_p are defined by

$$\mathbf{c}^e = K\mathbf{1} \otimes \mathbf{1} + 2G\mathbf{A} \tag{5.37}$$

$$H_e = \partial_{\boldsymbol{\sigma}'} f : \mathbf{c}^e : \partial_{\boldsymbol{\sigma}'} f \tag{5.38}$$

$$H_p = -\frac{1+e_o}{\lambda - \kappa} tr\left(\partial_{\boldsymbol{\sigma}'} f\right) p'_c \partial_{p'_c} f = tr\left(\partial_{\boldsymbol{\sigma}'} f\right) \tag{5.39}$$

e_o is a reference void ratio at a state of σ'_o. λ (=0.434C_c) and κ (=0.434C_s) are compression and swelling indices obtained from triaxial tests. Failure condition is defined when the plastic modulus H_p approaches zero. According to Eqs.(5.34)-(5.39), the incremental stress-strain relation can be formulated by

$$\dot{\boldsymbol{\sigma}}' = \mathbf{c}^e : (\dot{\boldsymbol{\varepsilon}} - \gamma\partial_{\boldsymbol{\sigma}'} f) = \left\{\mathbf{c}^e - \frac{\mathbf{c}^e : \partial_{\boldsymbol{\sigma}'} f \otimes \partial_{\boldsymbol{\sigma}'} f : \mathbf{c}^e}{H_e + H_p}\right\} : \dot{\boldsymbol{\varepsilon}} \tag{5.40}$$

K and G are referred to bulk and shear moduli respectively. ν' is Poisson's ratio of soil skeleton. Dependence of K and G on p' suggests a hypo-elastic model is employed in a formulation.

$$K = \frac{p'}{\kappa}\left(1 + e_o\right) \tag{5.41}$$

$$G = \frac{3(1-2v')}{2(1+v')}K \tag{5.42}$$

The first derivative of the SO model respective to stress tensor is shown in Appendix B. Substitution of these terms to Eq.(5.40), obtains a term,

$$\frac{\mathbf{c}^e : \partial_\sigma f \otimes \partial_\sigma f : \mathbf{c}^e}{H_e + H_p} = \frac{\left(K\beta\mathbf{1} + \sqrt{6G}\overline{\mathbf{n}}\right) \otimes \left(K\beta\mathbf{1} + \sqrt{6G}\overline{\mathbf{n}}\right)}{K\beta^2 + 3G + \dfrac{I_1}{3D}\beta} \tag{5.43}$$

where

$$\mathbf{c}^e : \partial_{\sigma'} f = 3\frac{D}{I_1}\left(K\beta\mathbf{1} + 2G\sqrt{\frac{3}{2}}\overline{\mathbf{n}}\right) \tag{5.44}$$

$$H_e + H_p = \left(3\frac{D}{I_1}\right)^2\left(K\beta^2 + 3G\right) + 3\frac{D}{I_1}\beta \tag{5.45}$$

$$\beta = M - 3\frac{\sqrt{3\overline{J}_2}}{I_1} - \sqrt{\frac{3}{2}}\left(\mathbf{\eta}_c : \overline{\mathbf{n}}\right) \tag{5.46}$$

Under K_o condition

$$\eta_o = \frac{3(1-K_o)}{1+2K_o} \tag{5.47}$$

$$\mathbf{\eta}_c = \sqrt{\frac{2}{3}}\eta_o diag\left[-\frac{\sqrt{6}}{6} \quad \frac{\sqrt{6}}{3} \quad -\frac{\sqrt{6}}{6}\right] \qquad \text{(See Appendix B)} \tag{5.48}$$

$\mathbf{\eta}_c$ is an aligned direction along hardening vertex in stress space. $(\mathbf{\eta}_c)_{ij}$ is a component of $\mathbf{\eta}_c$ in stress space in which a direction of $(\mathbf{\eta}_c)_{22}$ is corresponding to a component of $\mathbf{\eta}_c$ in parallel with a major principle axis of preconsolidation stress.

5-4 Treatment of the Singular Corner

Since the state of stress at the singular corner is referred the stress at triaxial condition [13], Figure 5.8 shows the yield loci and intersecting corner in the meridional plane associated to the triaxial stress plane (Rendulic's stress plane). The upper and lower yield loci are expressed by Eq.(4.1, 4.2) shown as,

$$f_U(I_1, J_2, I_{c1}) = MD\ln\left(\frac{I_1}{I_{c1}}\right) + D\left(\frac{3\sqrt{3J_2}}{I_1} - \frac{3\sqrt{3J_{c2}}}{I_{c1}}\right) = 0 \tag{5.49}$$

$$f_L(I_1, J_2, I_{c1}) = MD\ln\left(\frac{I_1}{I_{c1}}\right) - D\left(\frac{3\sqrt{3J_2}}{I_1} - \frac{3\sqrt{3J_{c2}}}{I_{c1}}\right) = 0 \tag{5.50}$$

Eq.(5.49) and its conjugate Eq.(5.50) are selected as candidates among conceivable yield functions passing the corner needed by Koiter's condition. This approach refrains from dealing with bulky equations may arise from using many slopes of discontinuous yield functions since bulky equations are generated in corresponding to the number of non-smooth yield functions in concern. Therefore, this approach gives the smallest forms needed by Koiter's condition.

Concerning with Koiter's associated flow rule, plastic flow at the corner is interpreted as a resulting vector of plastic flow of upper and lower yield loci and expressed by,

$$\dot{\mathbf{\varepsilon}}^p = \gamma_U \partial_{\sigma'} f_U + \gamma_L \partial_{\sigma'} f_L \tag{5.51}$$

Incremental stress-strain relation is expressed by

$$\dot{\mathbf{\sigma}}' = \mathbf{c}^e : (\dot{\mathbf{\varepsilon}} - \dot{\mathbf{\varepsilon}}^p) \tag{5.52}$$

According to App. C-3, substitute values of consistency parameters into Eq.(5.51), obtain

$$\dot{\mathbf{\varepsilon}}^p = \begin{pmatrix}\gamma_U \\ \gamma_L\end{pmatrix} \cdot \begin{pmatrix}\partial_{\sigma'} f_U \\ \partial_{\sigma'} f_L\end{pmatrix} = \mathbf{X}^{-1} \cdot \begin{pmatrix}\partial_{\sigma'} f_U : \mathbf{c}^e : \dot{\mathbf{\varepsilon}} \\ \partial_{\sigma'} f_L : \mathbf{c}^e : \dot{\mathbf{\varepsilon}}\end{pmatrix} \cdot \begin{pmatrix}\partial_{\sigma'} f_U \\ \partial_{\sigma'} f_L\end{pmatrix} \tag{5.53}$$

Substitute Eq.(5.53) into Eq.(5.52) to obtain stress increment

$$\dot{\mathbf{\sigma}}' = \left(\mathbf{c}^e - \begin{pmatrix}\chi_{UU}\mathbf{g}_U \otimes \mathbf{g}_U + \chi_{UL}\mathbf{g}_U \otimes \mathbf{g}_L \\ +\chi_{LU}\mathbf{g}_L \otimes \mathbf{g}_U + \chi_{LL}\mathbf{g}_L \otimes \mathbf{g}_L\end{pmatrix}\right) : \dot{\mathbf{\varepsilon}} \tag{5.54}$$

$$q = \sigma'_a - \sigma'_r$$

$$\gamma_U \partial_{\sigma'} f_U$$

$$\dot{\boldsymbol{\varepsilon}}^{\mathbf{p}}$$

$$\gamma_L \partial_{\sigma'} f_L$$

Upper yield locus

$$f_U(I_1, J_2, I_{c1}) = MD\ln\left(\frac{I_1}{I_{c1}}\right) + D\left(\frac{3\sqrt{3J_2}}{I_1} - \frac{3\sqrt{3J_{2c}}}{I_{c1}}\right) = 0$$

Lower yield locus

$$f_L(I_1, J_2, I_{c1}) = MD\ln\left(\frac{I_1}{I_{c1}}\right) - D\left(\frac{3\sqrt{3J_2}}{I_1} - \frac{3\sqrt{3J_{2c}}}{I_{c1}}\right) = 0$$

Koiter's associated flow rule

$$\dot{\boldsymbol{\varepsilon}}^p = \gamma_U \partial_{\sigma'} f_U + \gamma_L \partial_{\sigma'} f_L$$

Consistency conditions

$$\dot{f}_U = 0 \qquad \dot{f}_L = 0$$

$$p' = \frac{\sigma'_a + 2\sigma'_r}{3}$$
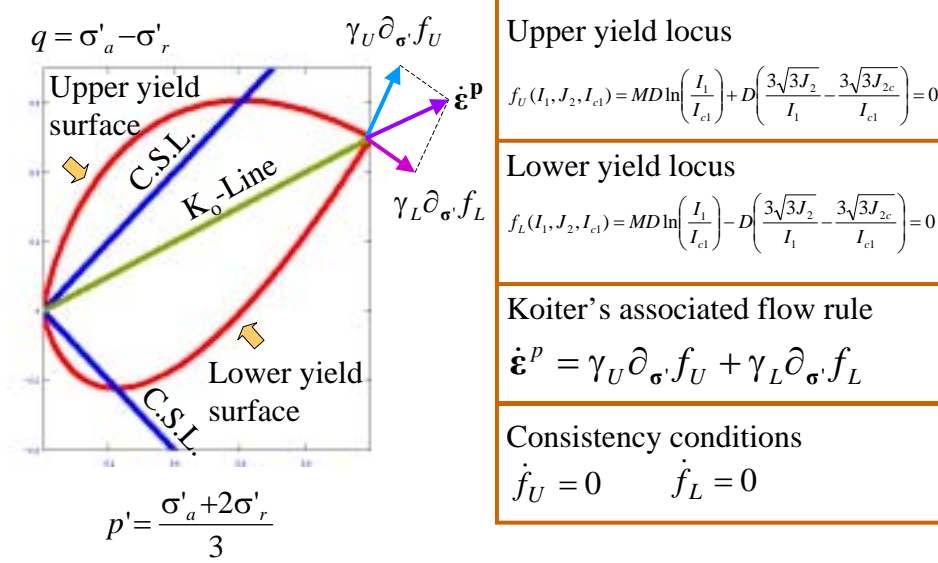
Figure 5.8 p'-q plane relating to the meridional section associated to the triaxial stress plane where the corner is placed

where

$$\mathbf{g}_U = \mathbf{c}^e : \partial_{\sigma'} f_U = \frac{3D}{I_1}\left(K\left(M - 3\frac{\sqrt{3J_2}}{I_1}\right)\mathbf{1} + 2G\sqrt{\frac{3}{2}}\mathbf{n}\right) \tag{5.55}$$

$$\mathbf{g}_L = \mathbf{c}^e : \partial_{\sigma'} f_L = \frac{3D}{I_1}\left(K\left(M + 3\frac{\sqrt{3J_2}}{I_1}\right)\mathbf{1} - 2G\sqrt{\frac{3}{2}}\mathbf{n}\right) \tag{5.56}$$

$\chi = \mathbf{X}^{-1}$ is defined in a way that $\chi_{UU} = \chi_{1,1}$; $\chi_{UL} = \chi_{1,2}$; $\chi_{LU} = \chi_{2,1}$; $\chi_{LL} = \chi_{2,2}$ (5.57)

According to Appendix C-4, coupled hardening matrix is expressed by,

$$\mathbf{X} = \left(3\frac{D}{I_1}\right)^2 \begin{bmatrix} K\beta_U^2 + 3G + \frac{I_1}{3D}\beta_U & K\beta_U\beta_L - 3G + \frac{I_1}{3D}\beta_L \\ K\beta_L\beta_U - 3G + \frac{I_1}{3D}\beta_U & K\beta_L^2 + 3G + \frac{I_1}{3D}\beta_L \end{bmatrix} \tag{5.58}$$

Eq.(5.54)-(5.58) reveals a tangential elastoplastic moduli considering corner mode is expressed by Eq.(5.59) as,

$$\mathbf{c}^{ep*} = \mathbf{c}^e - \sum_{\alpha,\beta \in \{U,L\}} \chi_{\alpha,\beta}\left(\mathbf{g}_\alpha \otimes \mathbf{g}_\beta\right) \tag{5.59}$$

A more compacted form is derived in Appendix C-7 as shown by,

$$\mathbf{c}^{ep*} = (1-\Lambda)K\mathbf{1}\otimes\mathbf{1} + \sqrt{\frac{2}{3}}(1-\Lambda)\eta_o K\mathbf{n}_c \otimes \mathbf{1} + 2G\left[\mathbf{A} - \mathbf{n}_c \otimes \mathbf{n}_c\right] \tag{5.60}$$

5-5 FEM Formulation

Four-node displacement-based element with 2x2 Gauss integration is formulated by standard FEM methodology for both plane strain and axisymmetric conditions. A procedure for corner mode is added to normal mode by employing tangential elastoplastic moduli defined in (5.60). A corner mode is judged to activate by extra condition given in Eq.(5.61). If the condition is invalid then a computation is handled by a general mode, which simply means stress is located out of the corner. (See Figure 5.9) A condition for elastic unloading is defined in Eq.

$$f_U \geq ZERO \quad \text{and} \quad f_L \geq ZERO \tag{5.61}$$

$$L_U < ZERO \quad \text{and} \quad L_L < ZERO \tag{5.62}$$

where ZERO is a zero truncation allowed in computation, usually set to a very small positive number, e.g. 10^{-12}

FEM simulations of K_o-condition can be performed by considering one-quarter of specimen enclosed by stiff lateral boundary depicted by Figure 5.10. Type A model refers to a true K_o condition controlled by zero lateral strain while type B refers to a reversed K_o condition controlled by a lateral pressure generated by K_o value. Geometric boundary conditions are shown in Figure 5.11 showing both single and four-element assemblage denoted by numerator 1 and 2 respectively. Material parameters with initial conditions for a class of inviscid SO

model are listed in   Table 5.1. Code names of all cases are tabulated in Table 5.2. Symbols + and - notify a calculation performed with or without corner mode. Applied vertical load of σ'_{vo} (100 kN/m^2) is further subdivided into 100 sub-steps for all cases except two latest cases where 1000 and 5000 sub-steps are applied to observe sizes of sub-steps affected in computation.
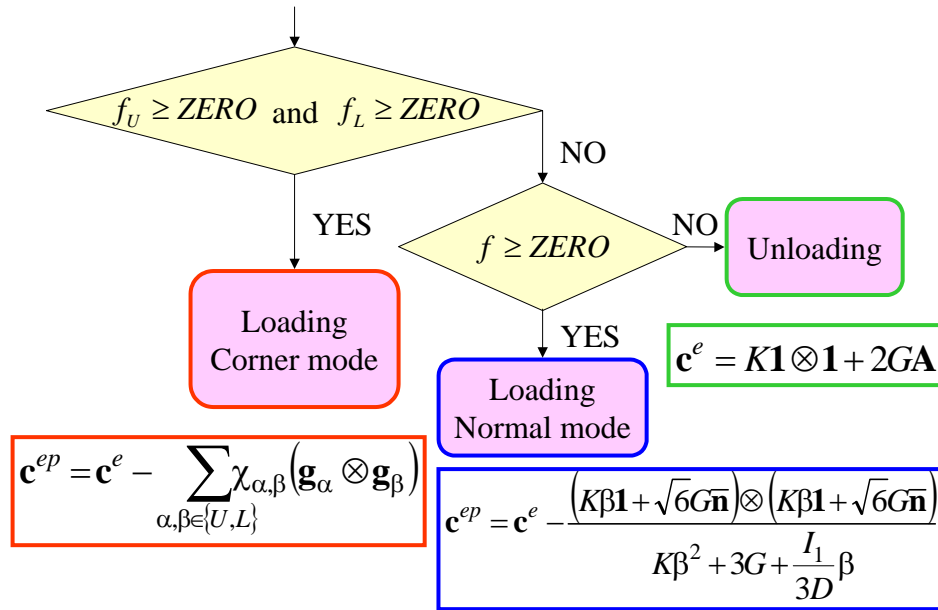
Figure 5.9 Mode judgment

Table 5.1 Soil parameters

Parameter	Description	Value
D	Coefficient of dilatancy	0.101
Λ	Irreversibility ratio	0.825
M	Critical state parameter	1.120
ν'	Effective Poisson's ratio	0.364
K_o	Coefficient of earth pressure (NC)	0.572
K_i	Coefficient of earth pressure (in-situ)	0.572
λ	Compression index	0.342
e_o	Void ratio at σ'_{vo}	1.500
σ'_{vo}	Eff. preconsolidation pressure (kN/m^2)	100
σ'_{vi}	Eff. overburden pressure (kN/m^2)	100

5-6 Calculation Results

Results of effective stresses, shear stress and ratio of horizontal stress to vertical stress were listed in Table 5.3. Strains and ratio of deviatoric strain to volumetric strain were shown in Table 5.4. Isotropic hardening stress, volumetric and deviatoric plastic strain, ratio of deviatoric to volumetric plastic strain and ratio of volumetric plastic strain to volumetric strain were shown in Table 5.5. Results in Table 5.3-Table 5.5 indicated that under K_o-condition, FEM procedures with/without corner mode give a substantially different results. The exact solutions given in Eqs.(5.63)-(5.70) are obtained from a basic 1-D consolidation problem. Therefore, cases of A1a+, A1p+, B1p+, A2a+, A2p+ and B2p+ were equivalent one another and provided the reasonable results. Calculations without corner mode failed to give reasonable results.
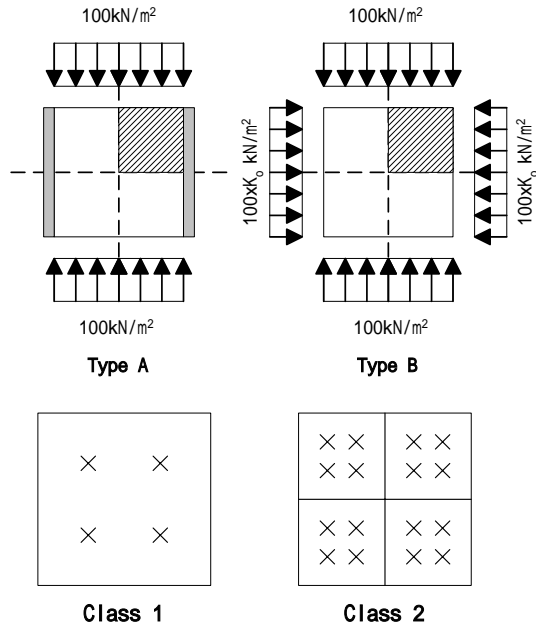
Figure 5.10 K_o condition (type A) and reversed K_o condition (type B), single element (class 1) and four elements (class 2)
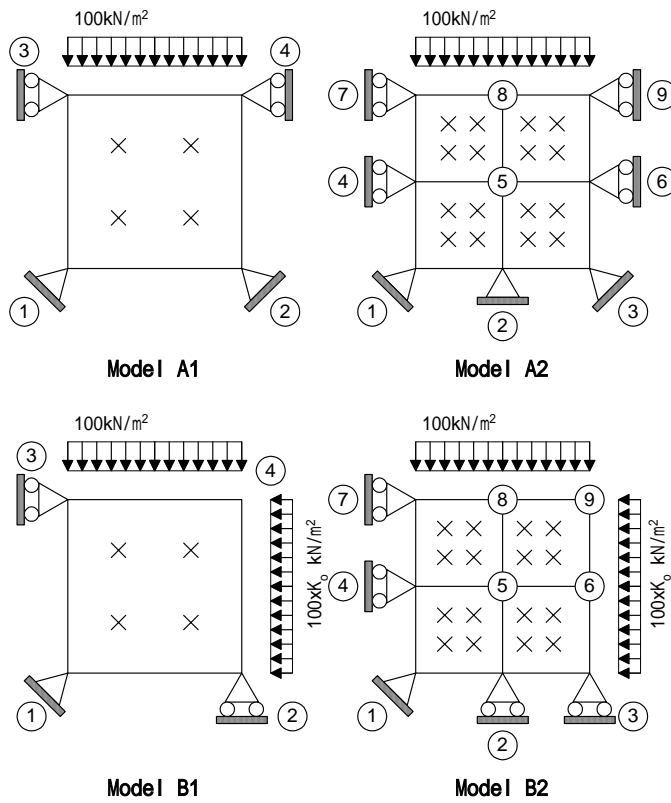
Figure 5.11 Schematic description of single element and four-element assemblage

$$\sigma'_{y(z)} = \sigma'_{oy(z)} + \Delta\sigma'_{y(z)}, \quad \sigma'_{x(r)} = \sigma'_{z(\theta)} = K_o\sigma'_{y(z)} \qquad (5.63),(5.64)$$

$$\tau_{xy(rz)} = 0 , \quad p'_c = \frac{1}{3}\sigma'_{y(z)}(1+2K_o)$$

(5.65),(5.66)

$$\varepsilon_{y(z)} = \frac{\lambda}{1+e_o}\ln\left(\frac{\sigma'_{y(z)}}{\sigma'_{oy(z)}}\right) , \quad \varepsilon_{x(r)} = \varepsilon_{z(\theta)} = 0$$

(5.67),(5.68)

$$\frac{\varepsilon_s}{\varepsilon_v} = \frac{\varepsilon_s^p}{\varepsilon_v^p} = \frac{2}{3} , \quad \frac{\varepsilon_v^p}{\varepsilon_v} = \Lambda$$

(5.69),(5.70)

It was found that results obtained by single element (for A1a+, A1p+, B1p+) and four-element (for A2a+, A2p+, B2p+) generated almost same responses due to a class of homogeneous deformation. There is no effect of subdivision of spatial domain in the calculation, but there is an effect of subdivision of time domain (sub-incrementation of loading) as illustrated by results obtained from case A1a+* and A1a+**, that is, a more exact result can be taken for a finer sub-step. Herein, 5000 sub-steps are required to yield an exact solution. Type B model gave correct responses only for plane strain condition. Therefore, a restraint in plane strain condition is satisfied for a reversed or stress-controlled K_o-condition where stress path is kept along the corner. A comparison between A1a+ and A1a- alone were shown in Figure 5.12-Figure 5.15. It is clearly found that without corner mode, stress paths were mobilized along K_o-line, resulting in fluctuated paths in Figure 5.12. Volumetric contraction given by cases without corner mode is less than a solution (see Figure 5.13 and Figure 5.14). Moreover, the slope of e-log(σ'_v) curve (see Figure 5.15) is not equal to swelling index (in $\log_{10}$-scale) C_c while a procedure with corner mode can produce responses associated to the solution.

5-7 Conclusion

FEM procedures including a corner mode are formulated using Koiter's associated flow rule to evaluate the plastic flow at the intersecting corner of the Sekiguchi-Ohta yield surface in meridional plane under K_o-condition. The extra implementation is added without any modification to the whole procedures of a normal mode and general FEM codes. Ignorance of special treatment for the corner would produce unacceptable results. It was clearly seen a corner mode is considerably needed especially for a particular type of problems such as analysis of K_o consolidation, self-weight consolidation, K_o creep and ageing as well as site responses when a level of water table is changed.

Table 5.2 Case study classification (100 sub-steps)

Code	Geometry/Elements	Corner effect
A1a+	axisymmetric/A1	considered
A1a-	axisymmetric/A1	ignored
A1p+	plane strain/A1	considered
A1p-	plane strain/A1	ignored
B1a+	axisymmetric/B1	considered
B1a-	axisymmetric/B1	ignored
B1p+	plane strain/B1	considered
B1p-	plane strain/B1	ignored
A2a+	plane strain/A2	considered
B2a+	axisymmetric/B2	considered
B2p+	plane strain/B2	considered
A1a+*	A1a+ by 1000 sub-steps	
A1a+**	A1a+ by 5000 sub-steps	

Table 5.3 Calculation results: effective stress (kN/m^2)

Case	$\sigma'_{x(r)}$	$\sigma'_{y(z)}$	$\tau_{xy(rz)}$	$\sigma'_{z(\theta)}$	$\sigma'_{x(r)}/\sigma'_{y(z)}$
A1a+	114.50	200	0	114.50	0.572
A1a-	114.98	200	0	114.98	0.575
A1p+	114.50	200	0	114.50	0.572
A1p-	114.98	200	0	114.98	0.575
B1a+	113.75	198.13	-9.08E-5	113.75	0.572
B1a-	114.50	200	0	114.50	0.572
B1p+	114.50	200	0	114.50	0.572
B1p-	114.50	200	0	114.35	0.572
A2a+	114.50	200	0	114.50	0.572
A2p+	114.50	200	0	114.50	0.572
B2a+	113.80	199.50	0.03	113.55	0.570
B2p+	114.50	200	0	114.50	0.572
A1a+*	114.50	200	0	114.50	0.572
A1a+**	114.50	200	0	114.50	0.572
Exact	114.50	200	0	114.50	0.572

Table 5.4 Calculation results: strain

Case	$\varepsilon_{x(r)}$	$\varepsilon_{y(z)}$	$\gamma_{xy(rz)}$	$\varepsilon_{z(\theta)}$	$\varepsilon_s/\varepsilon_v$
A1a+	0	0.094	0	0	0.667
A1a-	0	0.030	0	0	0.667
A1p+	0	0.094	0	0	0.667
A1p-	0	0.030	0	0	0.667
B1a+	0.025	0.043	1.21E-3	0.025	0.137
B1a-	5.89E-3	0.022	0	5.89E-3	0.323
B1p+	0	0.094	0	0	0.667
B1p-	7.28E-3	0.025	0	0	0.462
A2a+	0	0.094	0	0	0.667
A2p+	0	0.094	0	0	0.667
B2a+	0.020	0.046	9.27E-4	0.019	0.208
B2p+	0	0.094	0	0	0.667
A1a+*	0	0.095	0	0	0.667
A1a+**	0	0.095	0	0	0.667
Exact	0	0.095	0	0	0.667

Table 5.5 Calculation results: plastic variables

Case	p'_c	ε_v^p	ε_s^p	$\varepsilon_s^p/\varepsilon_v^p$	$\varepsilon_v^p/\varepsilon_v$
A1a+	142.28	0.077	0.052	0.667	0.823
A1a-	143.84	0.014	9.24E-3	0.683	0.448
A1p+	142.28	0.077	0.052	0.667	0.823
A1p-	143.84	0.014	9.24E-3	0.683	0.448
B1a+	141.57	0.076	2.13E-3	0.028	0.823
B1a-	142.28	0.018	0.000	0.000	0.515
B1p+	142.28	0.077	0.052	0.667	0.823
B1p-	142.69	0.016	5.42E-3	0.339	0.491
A2a+	142.28	0.077	0.052	0.667	0.823
A2p+	142.28	0.077	0.052	0.667	0.823
B2a+	142.45	0.069	6.67E-3	0.097	0.807
B2p+	142.28	0.077	0.052	0.667	0.823
A1a+*	142.93	0.078	0.052	0.667	0.825
A1a+**	142.98	0.078	0.052	0.667	0.825
Exact	143.00	0.078	0.052	0.667	0.825
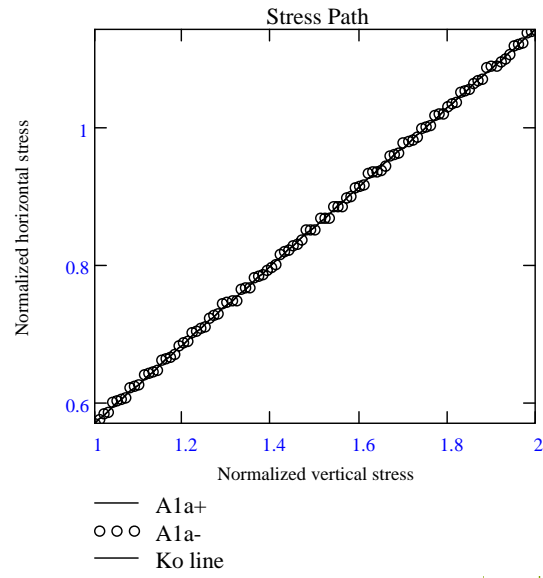
Figure 5.12 Normalized stress paths of vertical and horizontal stresses

Figure 5.13 Normalized vertical stress-vertical strain curves
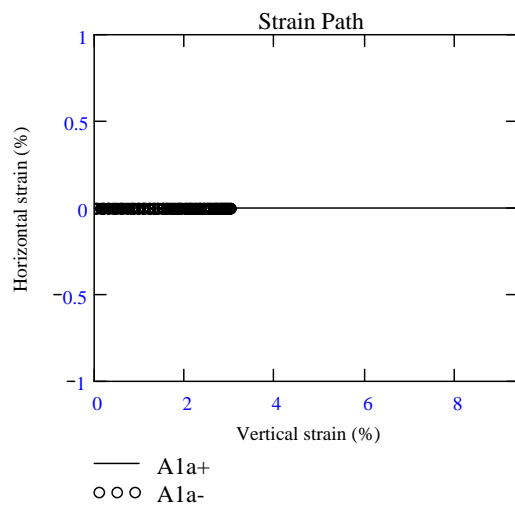
Figure 5.14 Strain paths of vertical and horizontal strains
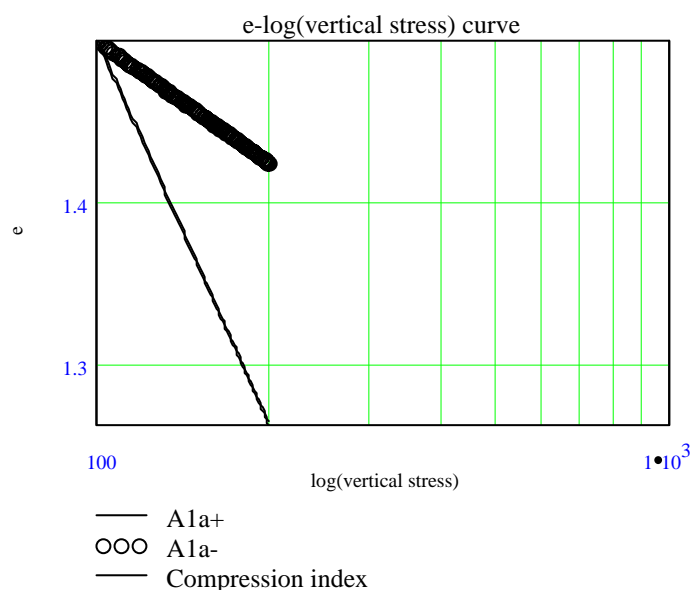
Figure 5.15 e-log(σ'$_v$) curve under compression loading

5-8 References

1 Sekiguchi, H. & Ohta, H., "Induced anisotropy and time dependency in clays", *9th ICSMFE*, Tokyo, Constitutive equations of Soils: 229-238 (1977)

2 Britto, A.M. & Gunn, M.J., "Critical state soil mechanics via finite elements", Chichester: Ellis Horwood LTD. (1987)

3 Gens, A. & Potts, D.M., "Critical state models in computational geomechanics", *Eng. Comput. 5*, pp.178-197 (1988)

4 Roscoe, K.H., Schofield, A.N. & Thurairajah, A., "Yielding of clays in states wetter than critical", *Géotechnique 13(3)*: 211-240, 1963

5 Schofield, A. & Wroth, P., "Critical State Soil Mechanics, Chapter 6", McGRAW-HILL: 135-166 (1968)

6 Zienkiewics, O.C. & Pande, G.N., "Some useful forms of isotropic yield surfaces for soil and rock mechanics", in Finite elements in Geomechanics (ed. G. Gudehus), Wiley, Chichester: 171-190 (1977)

7 Rosco, K.H. & Burland, J.B., "On the generalized stress-strain behavior of 'wet' clay, in J.Heymand & F.A. Leckie (eds.), *Engineering plasticity*, Cambridge University Press: 535-609 (1968)

8 Koiter, W.T., "Stress-strain relations, uniqueness and variational theorems for elastic-plastic materials with a singular yield surface", *Quart. Appl. Math. (11)*: 350-354 (1953)

9 Rudnicki, J.W. & Rice, J.R., "Conditions for the localization of deformation in pressure-sensitive dilatant materials", *J. Mech. Phys. Solids 23*: 371-394 (1975)

10 Christoffersen, J. & Hutchinson, J.W., "A class of phenomenological corner theories", *J. Mech. Phys. Solids 27* : 465-487 (1979)

11 Simo, J.C., Kennedy, J.G. & Govindjee, S., "Non-smooth multisurface plasticity and viscoplasticity. Loading/unloading conditions and numerical algorithms", *Int. J. Numer. Methods Engrg.*, 26: 2161-2185 (1988)

12 Pipatpongsa, T., Ohta, H., Kobayashi, I. & Iizuka, A., "Associated plastic flow at the intersection corner of plastic potential functions in soil mechanics", *Proc. of 36th Japanese Nat. Conf. on Geotech. Engrg.*: 935-936 (2001)

13 Pipatpongsa, T., Kobayashi, I., Ohta, H., & Iizuka, A., "The vertex singularity in the Sekiguchi-Ohta model", *56th JSCE Annual Meeting,* III-B341 (2001)

14 Pipatpongsa, T., Ohta, H., Kobayashi, I. & Iizuka, A., "Dependence of K$_o$-value on effective internal friction angle in regard to the Sekiguchi-Ohta model", *Proc. of 36th Japanese Nat. Conf. on Geotech. Engrg*: 936-937 (2001)

15 Pipatpongsa, T., Ohta, H., Kobayashi, I. & Iizuka, A., "Integration algorithms for soil constitutive equations with a singular hardening vertex", *3rd Inter. Summer Sym.,* JSCE,: 201-204 (2001)

16 Iizuka, A. & Ohta, H., "A determination procedure of input parameters in elasto-viscoplastic finite element analysis", *SOILS and FOUNDATIONS 27(3)*: 71-87 (1987)

17 Ohta, H. and Hata, S., A theoretical study of the stress-strain relations for clays, *Soils and Foundations* 11(3): 65-89 (1971)

18 Baker, R. & Desai, C.S.: "Induced anisotropy during plastic straining", *Int. J. Numer. Anal. Meth. Geomech.*, 8: 167-185 (1984)

19 Hashiguchi, K., "Constitutive equations of granular media with an anisotropic hardening", *Proc. 3rd Inter. Conf. on Numer. Meth. Geomech*, Aachen: 435-439 (1979)

20 Banerjee, P.K. & Yousif, N.B., "A plasticity model for the mechanical behaviour of anisotropically consolidated clay", *Int. J. Numer. Anal. Meth. Geomech.*, 10: 521-541 (1984)

21 Whittle, A.J., "Evaluation of a constitutive model for overconsolidated clays", *Géotechnique*, 43(2): 289-313 (1993)

22 Simo, J.C. & Hughes, T.J.R., "Computational inelasticity", *SPRINGER*, Chapter 2: 71-110 (1994)

CHAPTER 6

Stress Update Algorithm

6-1 Integration schemes

Integration of the constitutive model by computing the stress and strain changes corresponding to the total change of the displacement is important in FEM procedure. As shown in Figure 6.1, the stresses have to be integrated in terms of the elastoplastic stiffness matrix $\mathbf{C^{ep}}$ that is dependent on the state of current stress, strain and a linear increase of strain. The integration procedure adopted in elastoplastic computation can be classified into sub-incrementation and iteration methods, simply referring to explicit and implicit categories [1].

$$\boxed{\mathbf{d\sigma} = \mathbf{C^{ep}}(\mathbf{\sigma}, \mathbf{\varepsilon}, \mathbf{d\varepsilon}).\mathbf{d\varepsilon}}$$

Generalized elasto-plastic incremental relationship

$$(\mathbf{\sigma_0}, \mathbf{\varepsilon_0}) \Downarrow \ \mathbf{\Delta\varepsilon}$$

Total strain change subjects to initial conditions

$$\boxed{\mathbf{\Delta\sigma} = \int_{\mathbf{\varepsilon_o}}^{\mathbf{\varepsilon_o}+\mathbf{\Delta\varepsilon}} \mathbf{C^{ep}}(\mathbf{\sigma}, \mathbf{\varepsilon}, \mathbf{d\varepsilon}).\mathbf{d\varepsilon}}$$

Integral form incorporating into the dependence on state variables
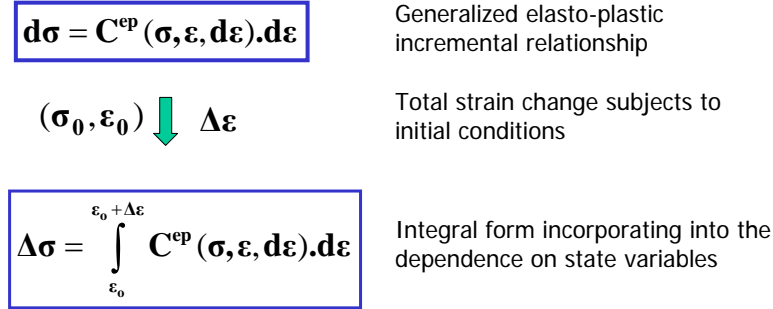
Figure 6.1 Integral form of elastoplastic stress-strain relation

6-1-1 Explicit method

The early days of computational rate-independent plasticity used this technique. The direct summation of small increments is adopted. The prescribed strain $\mathbf{\Delta\varepsilon}$ is given and the integral from shown in Figure 6.1 can be replaced by,

$$\mathbf{\Delta\sigma}_{n+1} = \mathbf{C^{ep}}(\mathbf{\sigma}_n, \mathbf{\varepsilon}_n, \mathbf{\Delta\varepsilon}) : \mathbf{\Delta\varepsilon} \tag{6.1}$$

Most of the FEM employs the sub-incremental method to handle numerical integration of the constitutive models. The accuracy of computation is entirely depended on the size of stress/displacement sub-increments. Consequently, to attain a high accuracy degree, computational time is substantially required. The stress change will generally depart from the yield surface by some margin. These updated state parameters do not satisfy the yield condition at the next step, that is, $f_{n+1} = f(\mathbf{\sigma}_{n+1}, \mathbf{q}_{n+1}) \neq 0$ and the solution drifts from the yield surface. A single-step computation may lead to considerable errors and inaccurate solutions. The more precise explicit procedure can be provided by use of some form of the Runge-Kutta process for second-order accuracy.

Due to inaccuracies of the method, it is no longer favored. Therefore, the dissertation will focus on the iteration method to solve the disadvantage.

6-1-2 Implicit method

Stress increment during iteration is evaluated by using tangential matrix referred to the state at the end of the increment denoted by,

$$\mathbf{\Delta\sigma}_{n+1} = \mathbf{C^{ep}}(\mathbf{\sigma}_{n+1}, \mathbf{\varepsilon}_{n+1}, \mathbf{\Delta\varepsilon}) : \mathbf{\Delta\varepsilon} \tag{6.2}$$

The derivation in Eq.(6.2) can be seen as Backward Euler difference while Eq.(6.1) is seen as Forward Euler difference. Formulation for $\mathbf{C^{ep}}$ is complex and depends crucially on the particular constitutive model chosen. In some case, a serious error is committed in the approximation form of $\mathbf{C^{ep}}$. The set of equations is iteratively solved by Newton-Rapson process. This type of algorithm usually starts in the first iteration with a purely elastic increment and iteratively reduces the stress to the yield surface if plastic deformation occurs. For this reason, it is called a return-mapping algorithm.

The merits of the scheme over explicit method are described by less computer time and storage for the same level of accuracy, less unwanted information and suitable for finite deformation analysis. It has been proven that wide range of model's features can be applied, for example, nonlinear hardening laws/Kinematics & Isotropic, associative/non-associative plastic flow, complex/nonsmooth multisurface yield criteria, time independent/dependent features [2].

6-2 Return-mapping algorithms

6-2-1 Overview

Return-mapping algorithms are the numerical algorithms for integrating the rate constitutive equations. The overview for the function of return-mapping algorithm is shown in Figure 6.2. The stress is updated by a prescribed strain increment. The operator splitting theory is referred as the break of updated state by 2 parts. First part is called elastic predictor, which is related to the guessed value of the solution. The second part is

called plastic corrector, which is related to the iteratively corrected value of the solution.

State-variables update algorithm

Strain increment

$$\sigma'_n, \varepsilon_n, \varepsilon_n^p \quad \Rightarrow \quad \text{RETURN-MAPPING ALGORITHM} \quad \Rightarrow \quad \sigma'_{n+1}, \varepsilon_{n+1}, \varepsilon_{n+1}^p$$

Elastic predictor ⟷ Plastic corrector

Operator-splitting theory
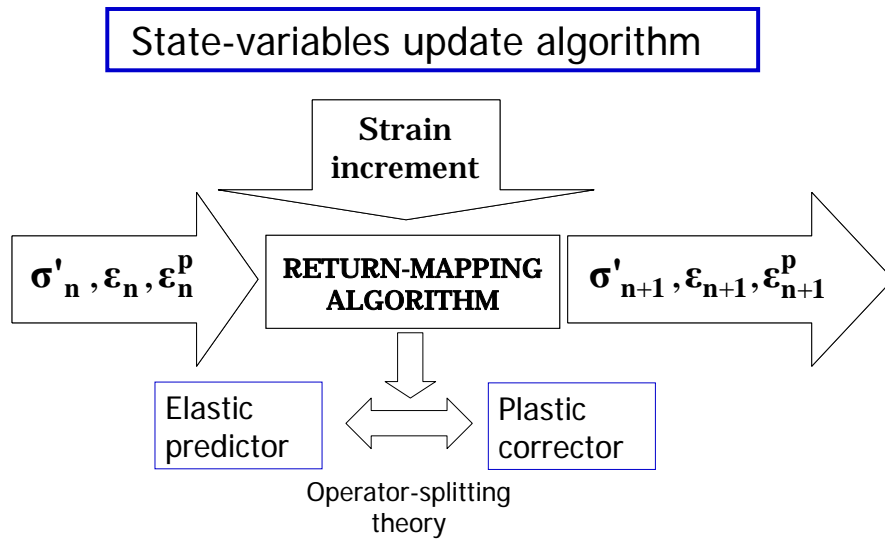
Figure 6.2 The role of return-mapping algorithm for integrating the constitutive model

The algorithm was generalized by Simo et al. [2] as the frame work set by the optimization theory to the principle of maximum plastic dissipation (See Figure 6.3). Dissipation energy is considered as the objective function while yield functions are considered as constraints. A set of equations is governed by Lagrangian function, Lagrange multipliers and Kuhn-Tucker optimality condition. By these principles, the stationary state, associativity of plastic flow as well as hardening laws and loading/unloading conditions can be recognized.

Principle of Maximum Plastic Dissipation

Optimization Theory

Dissipation energy

Yield functions

Objective function

Constraints

Stationary State

Associativity of Plastic Flow & Hardening Laws

Loading/Unloading conditions
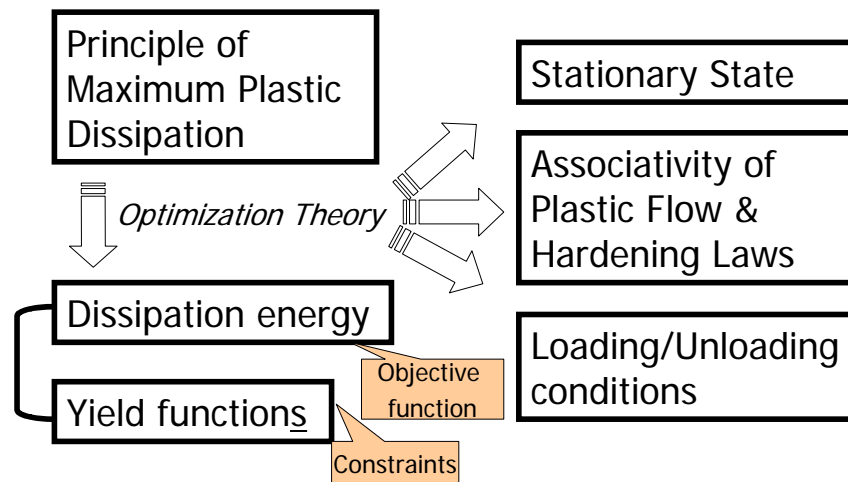
Figure 6.3 Frame work set by the optimization theory

The more interesting interpretation of the algorithm can be viewed as ski analogy as shown in Figure 6.4. Elastic predictor is interpreted as a shift to higher potential energy. Contour levels are interpreted as yield surfaces. The intersection of contours is interpreted as non-smooth multi-surfaces yield criteria. The fastest direction is usually normal outward to contour level. This normal direction is referred to associative plastic flow. Energy is dissipated along the way. According to loading/unloading forced by skier, the successive flow path or plastic corrector will lead to the stable position or solution of the problem.

For an associative flow rule, σ_{n+1} is interpreted as the closest point projection onto the yield surface of the trial elastic stress $\sigma_{n+1}^{\text{trial}}$ in the energy norm induced by elastic and plastic moduli. The geometric interpretation in stress space is represented in Figure 6.5. The plastic correctors in normal direction to yield surfaces are iteratively determined until the convergence is met.

The integration of the nonlinear constitutive equations over a finite-step was pioneered by the contribution of Wilkins [3] on the radial return algorithm. The extension to the case of kinematic hardening laws was presented by Krieg and Key [4]. The radial return method has been generalized to several plasticity models

in [5, 6, 7, 8]. The accuracy and stability of the algorithms have been investigated in [9, 10, 11, 12].

Return-mapping algorithms substantially impact on overall computation accuracy and rate of convergence in two levels. First level is corresponding to the stress update for local stability, which will be extended to comprehensive details in this chapter. Second level is corresponding to the consistent tangent modulus for global equilibrium, which will be explained in the next chapter.
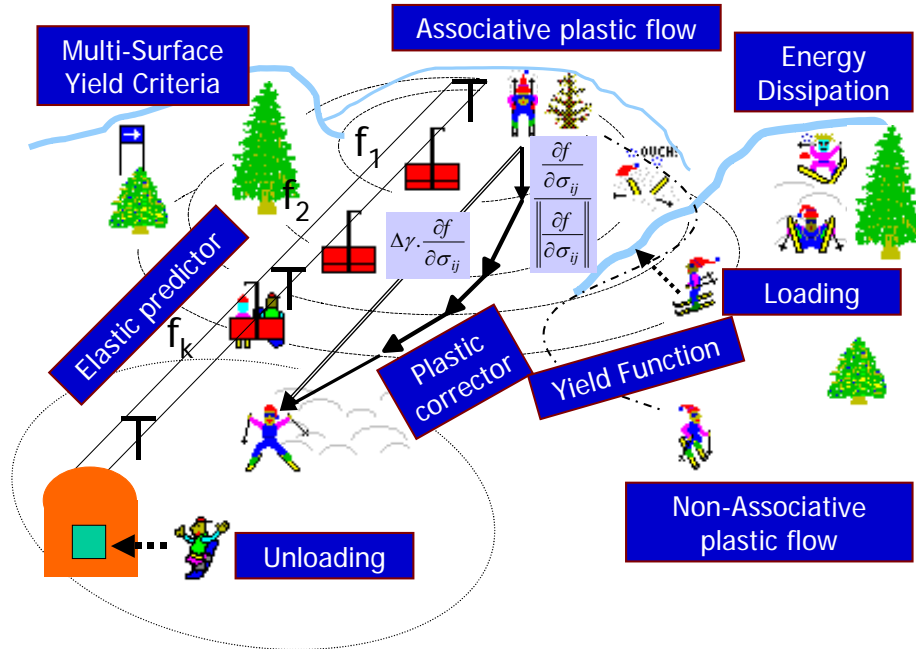
Figure 6.4 Ski analogy sorting all important keywords in the study
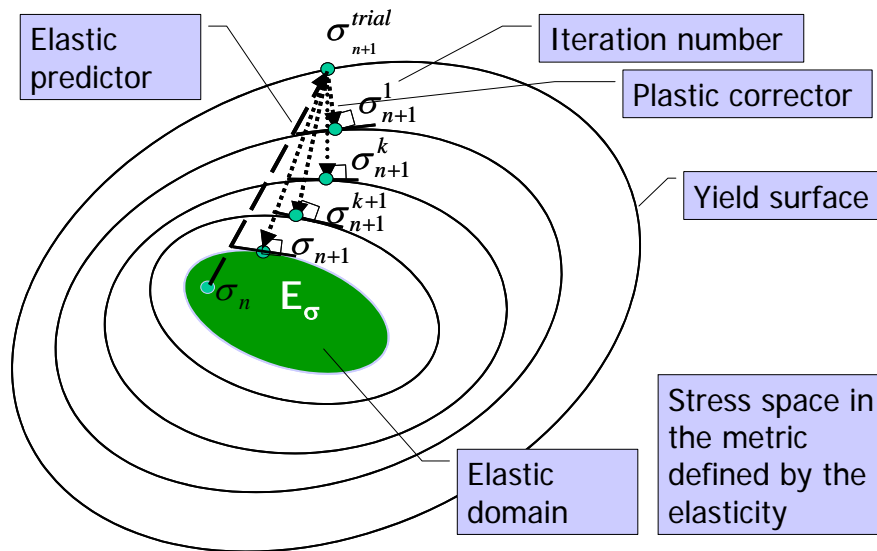
Figure 6.5 Geometric interpretation of return-mapping algorithms

6-2-2 Rate-independent plasticity

The typical constitutive model $f(\boldsymbol{\sigma}, \mathbf{q}) = 0$ is considered whose parameters are the current state of stress and hardening variables. The formulation of rate-independent plasticity is [13]

(a) Additive decomposition of rate of strain into elastic and plastic parts

$$\dot{\boldsymbol{\varepsilon}} = \dot{\boldsymbol{\varepsilon}}^e + \dot{\boldsymbol{\varepsilon}}^p \tag{6.3}$$

(b) Relation between stress rate and elastic strain rate

$$\dot{\boldsymbol{\sigma}} = \mathbf{c}^e : \dot{\boldsymbol{\varepsilon}}^e = \mathbf{c}^e : \left(\dot{\boldsymbol{\varepsilon}} - \dot{\boldsymbol{\varepsilon}}^p \right) \tag{6.4}$$

(c) Plastic flow rule and evolution of hardening variables

$$\dot{\boldsymbol{\varepsilon}}^p = \gamma \mathbf{r}(\boldsymbol{\sigma}, \mathbf{q}) \tag{6.5}$$

$$\dot{\mathbf{q}} = \gamma \mathbf{h}(\boldsymbol{\sigma}, \mathbf{q}) \tag{6.6}$$

(d) Yield condition

$$f(\boldsymbol{\sigma}, \mathbf{q}) = 0 \tag{6.7}$$

(e) Loading/unloading condition

$$\gamma \geq 0; f \leq 0; \gamma f = 0 \tag{6.8}$$

(f) Consistency parameter

$$\gamma = \frac{\partial_{\boldsymbol{\sigma}} f : \mathbf{c}^e : \dot{\boldsymbol{\varepsilon}}}{\partial_{\boldsymbol{\sigma}} f : \mathbf{c}^e : \mathbf{r} - \partial_{\mathbf{q}} f : \mathbf{h}} \tag{6.9}$$

(g) Stress rate and strain rate relation

$$\dot{\boldsymbol{\sigma}} = \mathbf{c}^{ep} : \dot{\boldsymbol{\varepsilon}} \tag{6.10}$$

(h) Continuum elasto-plastic tangent modulus

$$\mathbf{c}^{ep} = \mathbf{c}^e - \frac{\mathbf{c}^e : \mathbf{r} \otimes \partial_{\boldsymbol{\sigma}} f : \mathbf{c}^e}{\partial_{\boldsymbol{\sigma}} f : \mathbf{c}^e : \mathbf{r} - \partial_{\mathbf{q}} f : \mathbf{h}} \tag{6.11}$$

which is symmetric if plastic flow is associative $\mathbf{r}(\boldsymbol{\sigma}, \mathbf{q}) = \partial_{\boldsymbol{\sigma}} f$ and $\mathbf{h}(\boldsymbol{\sigma}, \mathbf{q}) = \partial_{\mathbf{q}} f$

6-2-3 Fully-implicit backward Euler scheme

This method enforces consistency at the end of time step n+1, i.e., $f_{n+1} = 0$, to avoid drift from the yield surface. The plastic strains and hardening variables are calculated at the end of the step updated from the converged values at the end of previous time step n. The integration scheme is written as,

$$\boldsymbol{\varepsilon}_{n+1} = \boldsymbol{\varepsilon}_n + \Delta\boldsymbol{\varepsilon} \qquad \text{where} \quad \Delta\boldsymbol{\varepsilon} = \dot{\boldsymbol{\varepsilon}}\Delta t \tag{6.12}$$

$$\boldsymbol{\varepsilon}_{n+1}^p = \boldsymbol{\varepsilon}_n^p + \Delta\gamma_{n+1} \mathbf{r}_{n+1} \qquad \text{where} \quad \Delta\gamma = \gamma\Delta t \tag{6.13}$$

$$\mathbf{q}_{n+1} = \mathbf{q}_n + \Delta\gamma_{n+1} \mathbf{h}_{n+1} \tag{6.14}$$

$$\boldsymbol{\sigma}_{n+1} = \mathbf{c}^e : \left(\boldsymbol{\varepsilon}_{n+1} - \boldsymbol{\varepsilon}_{n+1}^p \right) \tag{6.15}$$

$$f_{n+1} = f\left(\boldsymbol{\sigma}_{n+1}, \mathbf{q}_{n+1} \right) = 0 \tag{6.16}$$

Substitution of Eq.(6.13), (6.12) into Eq.(6.15) gives

$$\begin{aligned}
\boldsymbol{\sigma}_{n+1} &= \mathbf{c}^e : \left(\boldsymbol{\varepsilon}_{n+1} - \boldsymbol{\varepsilon}_n^p - \Delta\gamma_{n+1} \mathbf{r}_{n+1} \right) \\
&= \mathbf{c}^e : \left(\boldsymbol{\varepsilon}_n + \Delta\boldsymbol{\varepsilon} - \boldsymbol{\varepsilon}_n^p - \Delta\gamma_{n+1} \mathbf{r}_{n+1} \right) = \mathbf{c}^e : \left(\boldsymbol{\varepsilon}_n - \boldsymbol{\varepsilon}_n^p \right) + \mathbf{c}^e : \Delta\boldsymbol{\varepsilon} - \mathbf{c}^e : \Delta\gamma_{n+1} \mathbf{r}_{n+1} \\
&= \left(\boldsymbol{\sigma}_n + \mathbf{c}^e : \Delta\boldsymbol{\varepsilon} \right) - \Delta\gamma_{n+1} \mathbf{c}^e : \mathbf{r}_{n+1} = \boldsymbol{\sigma}_{n+1}^{trial} + \boldsymbol{\sigma}_{n+1}^{return}
\end{aligned} \tag{6.17}$$

where $\boldsymbol{\sigma}_{n+1}^{trial} = \boldsymbol{\sigma}_n + \mathbf{c}^e : \Delta\boldsymbol{\varepsilon}$ is the trial stress of elastic predictor

$\boldsymbol{\sigma}_{n+1}^{return} = -\Delta\gamma_{n+1} \mathbf{c}^e : \mathbf{r}_{n+1}$ is the plastic corrector

It is found that the elastic-predictor phrase is driven by the increment in total strain while the plastic-corrector phase is driven by the increment of consistency parameter. The solution of the set of nonlinear equations (6.14), (6.16) and (6.17) is typically obtained by a Newton procedure, resulted in the concept of closest point projection [14].

To form the suitable Newton iteration, considering the following 3 equations of three unknowns $\boldsymbol{\sigma}_{n+1}$, $\mathbf{q}_{n+1}$ and $\Delta\gamma_{n+1}$. These 3 equations are formulated by Eqs.(6.17), (6.14) and (6.16) as shown below,

$$\mathbf{F}(\boldsymbol{\sigma}_{n+1}, \mathbf{q}_{n+1}, \Delta\gamma_{n+1}) = \left\{ \begin{array}{c} \bar{f}\left(\boldsymbol{\sigma}_{n+1}, \mathbf{q}_{n+1}, \Delta\gamma_{n+1} \right) \\ f\left(\boldsymbol{\sigma}_{n+1}, \mathbf{q}_{n+1} \right) \end{array} \right\} = \left\{ \begin{array}{c} \left\{ \begin{array}{c} \mathbf{0} \\ \mathbf{0} \end{array} \right\} \\ 0 \end{array} \right\} \tag{6.18}$$

where the sub-function of tensors are assigned by,

$$\bar{f}\left(\boldsymbol{\sigma}_{n+1}, \mathbf{q}_{n+1}, \Delta\gamma_{n+1} \right) = \left\{ \begin{array}{c} \mathbf{c}^{e-1} : \boldsymbol{\sigma}_{n+1} - \mathbf{c}^{e-1} : \boldsymbol{\sigma}_{n+1}^{trial} + \Delta\gamma_{n+1} \mathbf{r}_{n+1} \\ -\mathbf{q}_{n+1} + \mathbf{q}_n + \Delta\gamma_{n+1} \mathbf{h}_{n+1} \end{array} \right\} \tag{6.19}$$

It is noted that in general $\mathbf{r}_{n+1} = \mathbf{r}_{n+1}(\boldsymbol{\sigma}_{n+1}, \mathbf{q}_{n+1})$ and $\mathbf{h}_{n+1} = \mathbf{h}_{n+1}(\boldsymbol{\sigma}_{n+1}, \mathbf{q}_{n+1})$. Linearization can be retrieved by quoting to Newton method. Superscript (k) marks iteration number.

$$
\left\{ \begin{Bmatrix} \Delta\boldsymbol{\sigma}_{n+1}^{(k)} \\ \Delta\mathbf{q}_{n+1}^{(k)} \end{Bmatrix} \\ \Delta^2\gamma_{n+1}^{(k)} \right\} = -\nabla\mathbf{F}(\boldsymbol{\sigma}_{n+1}^{(k)},\mathbf{q}_{n+1}^{(k)},\Delta\gamma_{n+1}^{(k)})^{-1} \cdot \mathbf{F}(\boldsymbol{\sigma}_{n+1}^{(k)},\mathbf{q}_{n+1}^{(k)},\Delta\gamma_{n+1}^{(k)})
\tag{6.20}
$$

The left side of above equation is the difference of variables between current and previous iterations.

$$
\left\{ \begin{Bmatrix} \Delta\boldsymbol{\sigma}_{n+1}^{(k)} \\ \Delta\mathbf{q}_{n+1}^{(k)} \end{Bmatrix} \\ \Delta^2\gamma_{n+1}^{(k)} \right\} = \left\{ \begin{Bmatrix} \boldsymbol{\sigma}_{n+1}^{(k+1)} \\ \mathbf{q}_{n+1}^{(k+1)} \end{Bmatrix} \\ \Delta\gamma_{n+1}^{(k+1)} \right\} - \left\{ \begin{Bmatrix} \boldsymbol{\sigma}_{n+1}^{(k)} \\ \mathbf{q}_{n+1}^{(k)} \end{Bmatrix} \\ \Delta\gamma_{n+1}^{(k)} \right\}
\tag{6.21}
$$

The gradient of function F is determined by,

$$
\nabla\mathbf{F}(\boldsymbol{\sigma}_{n+1},\mathbf{q}_{n+1},\Delta\gamma_{n+1}) = \begin{bmatrix} \boldsymbol{\Xi}_{n+1}^{-1} & \begin{Bmatrix} \mathbf{r}_{n+1} \\ \mathbf{h}_{n+1} \end{Bmatrix} \\ \{\partial_\sigma f \quad \partial_\mathbf{q} f\} & 0 \end{bmatrix}
\tag{6.22}
$$

The algorithmic moduli are defined by,

$$
\boldsymbol{\Xi}_{n+1} = \begin{bmatrix} \mathbf{c}^{e^{-1}} + \Delta\gamma_{n+1}\partial_\sigma\mathbf{r}_{n+1} & \Delta\gamma_{n+1}\partial_\mathbf{q}\mathbf{r}_{n+1} \\ \Delta\gamma_{n+1}\partial_\sigma\mathbf{h}_{n+1} & -\mathbf{I}+\Delta\gamma_{n+1}\partial_\mathbf{q}\mathbf{h}_{n+1} \end{bmatrix}^{-1}
\tag{6.23}
$$

In Eq.(6.20), the inversion of $\nabla\mathbf{F}$ is required to accomplish. However, high-order tensorial inversion would be sluggish tasks especially for complicated yield function, the form without inversion is preferred,

$$
\nabla\mathbf{F}(\boldsymbol{\sigma}_{n+1}^{(k)},\mathbf{q}_{n+1}^{(k)},\Delta\gamma_{n+1}^{(k)}) \cdot \left\{ \begin{Bmatrix} \Delta\boldsymbol{\sigma}_{n+1}^{(k)} \\ \Delta\mathbf{q}_{n+1}^{(k)} \end{Bmatrix} \\ \Delta^2\gamma_{n+1}^{(k)} \right\} = - \left\{ \begin{matrix} \overline{f}\left(\boldsymbol{\sigma}_{n+1}^{(k)},\mathbf{q}_{n+1}^{(k)},\Delta\gamma_{n+1}^{(k)}\right) \\ f\left(\boldsymbol{\sigma}_{n+1}^{(k)},\mathbf{q}_{n+1}^{(k)}\right) \end{matrix} \right\}
\tag{6.24}
$$

Substitution of Eq.(6.22) into Eq.(6.24) yields two equations of tensor and scalar below,

$$
\begin{Bmatrix} \Delta\boldsymbol{\sigma}_{n+1}^{(k)} \\ \Delta\mathbf{q}_{n+1}^{(k)} \end{Bmatrix} + \Delta^2\gamma_{n+1}^{(k)}\boldsymbol{\Xi}_{n+1}^{(k)} \cdot \begin{Bmatrix} \mathbf{r}_{n+1}^{(k)} \\ \mathbf{h}_{n+1}^{(k)} \end{Bmatrix} = -\boldsymbol{\Xi}_{n+1}^{(k)} \cdot \overline{f}_{n+1}^{(k)}
\tag{6.25}
$$

$$
\{\partial_\sigma f_{n+1}^{(k)} \quad \partial_\mathbf{q} f_{n+1}^{(k)}\} \cdot \begin{Bmatrix} \Delta\boldsymbol{\sigma}_{n+1}^{(k)} \\ \Delta\mathbf{q}_{n+1}^{(k)} \end{Bmatrix} = -f_{n+1}^{(k)}
\tag{6.26}
$$

Multiply both sides of Eq.(6.25) by $\{\partial_\sigma f_{n+1}^{(k)} \quad \partial_\mathbf{q} f_{n+1}^{(k)}\}$, subsequently subtracted by Eq.(6.26) gives,

$$
\Delta^2\gamma_{n+1}^{(k)}\{\partial_\sigma f_{n+1}^{(k)} \quad \partial_\mathbf{q} f_{n+1}^{(k)}\} \cdot \boldsymbol{\Xi}_{n+1}^{(k)} \cdot \begin{Bmatrix} \mathbf{r}_{n+1}^{(k)} \\ \mathbf{h}_{n+1}^{(k)} \end{Bmatrix} = f_{n+1}^{(k)} - \{\partial_\sigma f_{n+1}^{(k)} \quad \partial_\mathbf{q} f_{n+1}^{(k)}\} \cdot \boldsymbol{\Xi}_{n+1}^{(k)} \cdot \overline{f}_{n+1}^{(k)}
\tag{6.27}
$$

Since Eq.(6.27) is scalar equation, the unknown $\Delta^2\gamma_{n+1}^{(k)}$ can be solved,

$$
\Delta^2\gamma_{n+1}^{(k)} = \frac{f_{n+1}^{(k)} - \{\partial_\sigma f_{n+1}^{(k)} \quad \partial_\mathbf{q} f_{n+1}^{(k)}\} : \boldsymbol{\Xi}_{n+1}^{(k)} : \overline{f}_{n+1}^{(k)}}{\{\partial_\sigma f_{n+1}^{(k)} \quad \partial_\mathbf{q} f_{n+1}^{(k)}\} : \boldsymbol{\Xi}_{n+1}^{(k)} : \begin{Bmatrix} \mathbf{r}_{n+1}^{(k)} \\ \mathbf{h}_{n+1}^{(k)} \end{Bmatrix}}
\tag{6.28}
$$

Back substitution of $\Delta^2\gamma_{n+1}^{(k)}$ given in Eq.(6.28) into Eq.(6.25) results in,

$$
\begin{Bmatrix} \Delta\boldsymbol{\sigma}_{n+1}^{(k)} \\ \Delta\mathbf{q}_{n+1}^{(k)} \end{Bmatrix} = -\boldsymbol{\Xi}_{n+1}^{(k)^{-1}} : \left\{ \overline{f}_{n+1}^{(k)} + \Delta^2\gamma_{n+1}^{(k)} \begin{Bmatrix} \mathbf{r}_{n+1}^{(k)} \\ \mathbf{h}_{n+1}^{(k)} \end{Bmatrix} \right\}
\tag{6.29}
$$

Updated unknowns are proceeded by,

$$
\begin{Bmatrix} \boldsymbol{\sigma}_{n+1}^{(k+1)} \\ \mathbf{q}_{n+1}^{(k+1)} \end{Bmatrix} = \begin{Bmatrix} \boldsymbol{\sigma}_{n+1}^{(k)} \\ \mathbf{q}_{n+1}^{(k)} \end{Bmatrix} + \begin{Bmatrix} \Delta\boldsymbol{\sigma}_{n+1}^{(k)} \\ \Delta\mathbf{q}_{n+1}^{(k)} \end{Bmatrix}, \quad \Delta\gamma_{n+1}^{(k+1)} = \Delta\gamma_{n+1}^{(k)} + \Delta^2\gamma_{n+1}^{(k)}
\tag{6.30}
$$

where the values at the initial stages for k=0 are set by,

$$
\begin{Bmatrix} \boldsymbol{\sigma}_{n+1}^{(0)} \\ \mathbf{q}_{n+1}^{(0)} \end{Bmatrix} = \begin{Bmatrix} \boldsymbol{\sigma}_{n+1}^{trial} \\ \mathbf{q}_n \end{Bmatrix}, \quad \Delta\gamma_{n+1}^{(0)} = 0
\tag{6.31}
$$

Repetitions of Eq.(6.25)-(6.30) would be terminated if no longer the significant change of unknowns is found,

$$
\begin{Bmatrix} \Delta\boldsymbol{\sigma}_{n+1}^{(k+1)} \\ \Delta\mathbf{q}_{n+1}^{(k+1)} \end{Bmatrix} \approx \begin{Bmatrix} \mathbf{0} \\ \mathbf{0} \end{Bmatrix}, \quad \Delta^2\gamma_{n+1}^{(k+1)} \approx 0
\tag{6.32}
$$

At the final iteration, updated unknowns shown in Eq.(6.30) are entirely determined.

6-2-4 Semi-implicit backward Euler scheme

By this scheme, the formulation is implicit in plasticity parameter and explicit in the plastic flow direction and plastic moduli, i.e., the increments in plasticity parameter are calculated at the end of the step but the plastic flow direction and plastic moduli are calculated at the beginning of the step, resulted in the concept of cutting plane [7].

$$\boldsymbol{\varepsilon}_{n+1} = \boldsymbol{\varepsilon}_n + \Delta\boldsymbol{\varepsilon} \tag{6.33}$$

$$\boldsymbol{\varepsilon}^p_{n+1} = \boldsymbol{\varepsilon}^p_n + \Delta\gamma_{n+1}\mathbf{r}_n \tag{6.34}$$

$$\mathbf{q}_{n+1} = \mathbf{q}_n + \Delta\gamma_{n+1}\mathbf{h}_n \tag{6.35}$$

$$\boldsymbol{\sigma}_{n+1} = \mathbf{c}^e : \left(\boldsymbol{\varepsilon}_{n+1} - \boldsymbol{\varepsilon}^p_{n+1}\right) \tag{6.36}$$

$$f_{n+1} = f\left(\boldsymbol{\sigma}_{n+1}, \mathbf{q}_{n+1}\right) = 0 \tag{6.37}$$

According to the system of Eq.(6.33)-(6.37), the substitution of Eq.(6.33)-(6.34) into Eq.(6.36), and substitution of Eq.(6.35)-(6.36) into Eq.(6.37) can reduce to one unknown in one equation by

$$f_{n+1} = f\left(\Delta\gamma_{n+1}\right) = f\left(\boldsymbol{\sigma}^{\text{trial}}_{n+1} - \Delta\gamma_{n+1}\mathbf{c}^e : \mathbf{r}_n, \mathbf{q}_n + \Delta\gamma_{n+1}\mathbf{h}_n\right) = 0 \tag{6.38}$$

Linearization can be retrieved by,

$$\partial_{\Delta\gamma} f_{n+1} = -\partial_{\boldsymbol{\sigma}} f : \mathbf{c}^e : \mathbf{r}_n + \partial_{\mathbf{q}} f : \mathbf{h}_n \tag{6.39}$$

$$\Delta^2\gamma^{(k)}_{n+1} = \frac{f\left(\Delta\gamma_{n+1}\right)}{\partial_{\boldsymbol{\sigma}} f : \mathbf{c}^e : \mathbf{r}_n - \partial_{\mathbf{q}} f : \mathbf{h}_n} \tag{6.40}$$

The update procedures are the same as Eq.(6.30)-(6.32). Due to the explicit treatment of the plastic flow direction and plastic moduli, a simple equation is obtained. By employing associative flow rule, the difference of both schemes can be described by Figure 6.6. According to their appearances, fully implicit Backward Euler scheme was coined as Closest Point Projection Method [14] while the semi-implicit Backward Euler was coined as Cutting Plane Method [7].
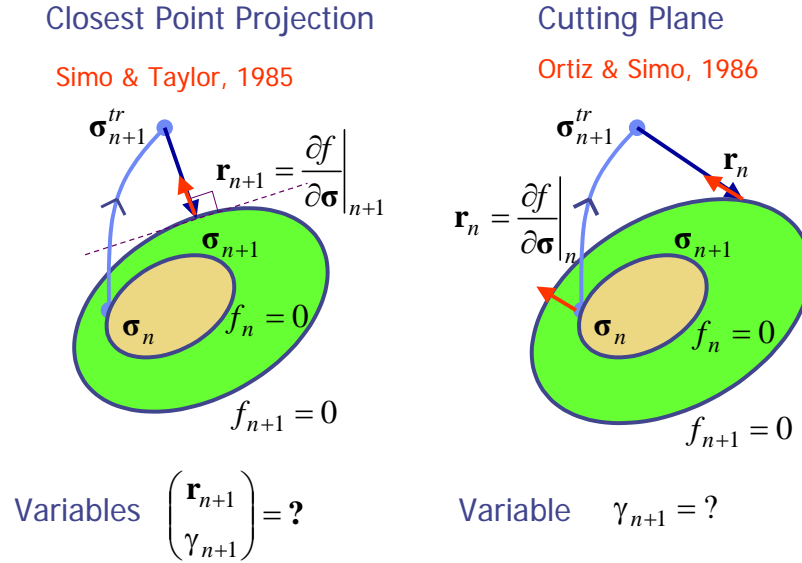
Figure 6.6 CPPM vs. CPM

6-3 Return-mapping algorithm for the Ohta-Hata model

6-3-1 Introduction

The Sekiguchi-Ohta model is one of the most widely used soil constitutive models based on critical state theory. The model characterizes nonlinear stress-strain behavior including softening/hardening and dilatancy responses, principal stress reorientation, stress-induced anisotropy and time dependency (Sekiguchi and Ohta, 1977) [15]. Applications of the model to numerical analysis for predicting soil behaviors have been proved to be consistent with many field responses (Ohta and Iizuka, 1992) [16]. Generally, the numerical solution of initial boundary-value problem is cast into FEM involving spatial and time discretization. The integration of constitutive equation over a time step is commonly accomplished by incremental solution for a given strain increment, in other words, a strain-driven process what is classified into explicit and implicit categories. The

first method simplifies the integration to the summation of sub-increments while the latter one applies the iterative scheme using Newton-Raphson method formulated in more complicated expressions.

In nonlinear problem, the size of increments substantially affect the quality of analysis, that is, a large step size will cause inaccuracy while a finer one will become a drawback in computation speed. Therefore, the alternative way to handle the problem is to apply the implicit integration method using return-mapping algorithm, the algorithm that usually starts in the first iteration with a purely elastic increment. Borja et al. (1990) [17] has developed the implementation of return-mapping algorithm applicable to the modified Cam-Clay model with a remarkable solution accuracy and quadratic rate of convergence. However, the procedures concerned show a sign of incompatibility with Sekiguchi-Ohta model because both have lost much in common since the advent of modified version.

Lagrangian function:

maximize D^p subject to $(\boldsymbol{\sigma}, \alpha) \in E_\sigma$; $f(\boldsymbol{\sigma}, \alpha) \le 0$

$$\boxed{L(\boldsymbol{\sigma}) = -D^p(\boldsymbol{\sigma}) + \gamma. f(\boldsymbol{\sigma}, \alpha)}$$

By Kuhn-Tucker condition Order 1st

$$\nabla L = -\dot{\boldsymbol{\varepsilon}}^{\mathbf{p}} + \gamma \frac{\partial f}{\partial \boldsymbol{\sigma}} = 0 \quad \Longrightarrow \quad \dot{\boldsymbol{\varepsilon}}^{\mathbf{p}} = \gamma \frac{\partial f}{\partial \boldsymbol{\sigma}} \quad \text{:Flow rule}$$

which $\boxed{\gamma \ge 0; f \le 0; \gamma. f = 0}$

Invariant forms

$$\boxed{\dot{\varepsilon}_v^p = \gamma \frac{\partial f}{\partial p'}} \quad \boxed{\dot{\varepsilon}_s^p = \gamma \frac{\partial f}{\partial q}}$$

Order 2nd $\nabla^2 L$

Must be positive-definite $\Longrightarrow$ Convexity of -D^p

Figure 6.7 Optimization for stationary state of plastic dissipation energy

Stationary state:

Possible stationary state: $\dot{\boldsymbol{\varepsilon}}^{\mathbf{p}} = \gamma \left. \frac{\partial f}{\partial \boldsymbol{\sigma}} \right|_{\left(\sigma^*, \alpha^*\right)}$

Elastic stress-strain relation

$$\boxed{\dot{\boldsymbol{\sigma}} = \mathbf{C}(\boldsymbol{\sigma}^*)\left(\dot{\boldsymbol{\varepsilon}} - \gamma \left.\frac{\partial f}{\partial \sigma}\right|_{\left(\sigma^*, \alpha^*\right)}\right)} \text{ and } \boxed{\dot{\alpha}^* = \gamma \left.\frac{\partial f}{\partial p'}\right|_{\left(\sigma^*, \alpha^*\right)}}$$

Necessary conditions: $\boxed{\gamma \ge 0; f(\boldsymbol{\sigma}^*, \alpha^*) \le 0; \gamma. f(\boldsymbol{\sigma}^*, \alpha^*) = 0}$

Initial condition: $\boxed{(\boldsymbol{\sigma}_{\mathbf{n}}, \alpha_n)}$

Figure 6.8 Solution for stationary state

In a bid to formulate the governing equations for return-mapping algorithm applicable to Sekiguchi-Ohta model, rate-independent Ohta-Hata model (1971) [18], the inactivated principal stress reorientation version, is employed to motivate the development to the theory based on a generalized framework for nonlinear isotropic hardening plasticity (Simo and Hughes, 1997) [2]. The regularization of operator splitting theory restricted to yield condition and hardening function entails an iterative determination of the consistency parameter, the

Lagrange multiplier that satisfies a constrained-optimization to the principle of maximum plastic dissipation (See Figure 6.8, Figure 6.9). Attention is also paid to Kuhn-Tucker complementarity for appropriately holding the conventional loading/unloading judgment proposed by Hill (1950) [19]. The performance of this implementation is evaluated by a number of iterative calculations to reach the solution in compare with the explicitly incremental method.

Backward difference scheme:

$$\dot{x}(t) = f(x(t))$$
$$x(0) = x_n$$

in [0,T] $\Longrightarrow$ $x_{n+1} = x_n + \Delta t . f(x_{n+1})$

Implicit expression
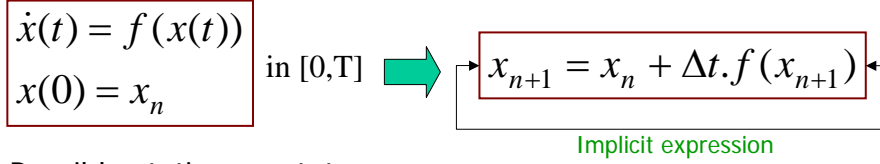
Possible stationary state:

$$\boldsymbol{\sigma}^* - \boldsymbol{\sigma}_n = \Delta\boldsymbol{\sigma} = \mathbf{C}(\boldsymbol{\sigma}^*)\left(\Delta\boldsymbol{\varepsilon} - \Delta\gamma \left.\frac{\partial f}{\partial\sigma}\right|_{(\boldsymbol{\sigma}^*,\alpha^*)} \right)$$

$$\alpha^* - \alpha_n = \Delta\alpha = \Delta\gamma \left.\frac{\partial f}{\partial p'}\right|_{(\boldsymbol{\sigma}^*,\alpha^*)} \qquad \text{where} \quad \Delta\gamma = \gamma.\Delta t$$

Figure 6.9 Time integration carried out by backward Euler difference
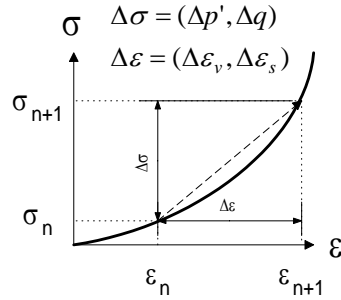
For monotonic loading

<u>Stress increment</u> (closed form)

$$\Delta p' = \left(\exp(\omega\Delta\varepsilon_v) - 1\right)p'_n$$

$$\Delta q = 3G_s(\Delta\varepsilon_v)\Delta\varepsilon_s$$

Secant shear modulus

$$G_s(\Delta\varepsilon_v) = \frac{\exp(\omega\Delta\varepsilon_v) - 1}{\omega\Delta\varepsilon_v}G(p'_n)$$

For undrained condition

$$\lim_{\Delta\varepsilon_v \to 0} G_s(\Delta\varepsilon_v) = G(p'_n)$$

Figure 6.10 Integration of soil elastic constitutive equation

6-3-2 The algorithm

The principle implementation, uniqueness and stability of the algorithm are explained and discussed in detailed by Simo and Hughes (1997). Box 6.1 contains the basic equations, yield function with derivatives and the plastic correctors with their derivatives in corresponding to associativity. The variable elastic shear modulus is derived in term of secant modulus to accord with monotonic loading (See Figure 6.10).

Sub-local Newton shown in Box 6.2 marked to refine the convergent direction with a suggested constant k for securing iteration from a divergent loophole. The relevant governing equations for computing consistency parameter and the main engine of return-mapping algorithm are summarized in Box 6.3 and Box 6.1 respectively. Schematizations of the algorithms are presented in Figure 6.11-Figure 6.13.

Box 6.1 Basic equations

Common-used functions

$dev(\mathbf{x}) \equiv \mathbf{x} - \dfrac{1}{3} tr(\mathbf{x})\mathbf{1}$, where $1_{ij} \equiv \delta_{ij}$ $\qquad\qquad sign(x) \equiv \begin{cases} \dfrac{|x|}{x} \leftarrow x \neq 0 \\ 0 \leftarrow x = 0 \end{cases}$

Elastic properties

$\omega = \dfrac{\Lambda}{MD(1-\Lambda)}$, $\quad K(p') = \omega.p'$, $\quad \mu' = \dfrac{3(1-2v')}{2(1+v')}$, $\quad G(p') = \mu' K(p')$

$G_s(\Delta\varepsilon_v, p') = \dfrac{\exp(\omega.\Delta\varepsilon_v) - 1}{\omega.\Delta\varepsilon_v} G(p')$ $\qquad$, in which $\quad \lim_{\Delta\varepsilon_v \to 0} G_s(\Delta\varepsilon_v, p') = G(p')$

Yield function: Ohta-Hata model (1971)

$f(p', q, \varepsilon_v^p) = MD\ln(\dfrac{p'}{p'_o}) + D\left|\dfrac{q}{p'} - \eta_o\right| - \varepsilon_v^p$ $\qquad$, where $\quad \eta_o = \dfrac{q_o}{p'_o}$

Derivatives of yield function

$\dfrac{\partial f}{\partial p'} = \dfrac{D}{p'}\left(M - \dfrac{q}{p'}sign(\dfrac{q}{p'} - \eta_o)\right)$, $\quad \dfrac{\partial f}{\partial q} = \dfrac{D}{p'}sign(\dfrac{q}{p'} - \eta_o)$, $\quad \dfrac{\partial f}{\partial \varepsilon_v^p} = -1$, $\quad \dfrac{\partial q}{\partial \mathbf{s}} = \dfrac{3}{2}\dfrac{\mathbf{s}}{q}$

Plastic correctors

$p' = p'(\eta, \Delta\gamma) = p^{tr} - \Delta\gamma\omega D(M - \eta \cdot sign(\eta - \eta_o))$, $\quad$ where $\qquad \eta = \dfrac{q}{p'}$

$q = q(\eta, \Delta\gamma) = q^{tr} - 3\Delta\gamma\mu'\omega D \cdot sign(\eta - \eta_o)$, $\quad \varepsilon_v^p = \varepsilon_v^p(p', q, \Delta\gamma) = \left(\varepsilon_v^p\right)_n + \Delta\gamma\dfrac{\partial f}{\partial p'}$

Derivatives of state variables on consistency parameter

$\dfrac{\partial p'}{\partial \Delta\gamma} = -\omega D(M - \eta \cdot sign(\eta - \eta_o))$, $\quad \dfrac{\partial q}{\partial \Delta\gamma} = -3\mu'\omega D \cdot sign(\eta - \eta_o)$, $\quad \dfrac{\partial \varepsilon_v^p}{\partial \Delta\gamma} = \dfrac{\partial f}{\partial p'}$

Box 6.2 Sub-local Newton method for computing stress condition

1. Input: $p', q, \Delta\gamma$ and Set: $k = \dfrac{3}{4}$ (suggested value)

2. Do Iteration: (see BOX 1 for equation descriptions)

$g = \begin{bmatrix} p'(\dfrac{q}{p'}, \Delta\gamma) - p' \\ q(\dfrac{q}{p'}, \Delta\gamma) - q \end{bmatrix}$, $\quad \partial g = \begin{bmatrix} -\Delta\gamma\omega D\dfrac{q}{p'^2}sign(\dfrac{q}{p'} - \eta_o) & \Delta\gamma\omega\dfrac{D}{p'}sign(\dfrac{q}{p'} - \eta_o) \\ 0 & -1 \end{bmatrix}$

$\begin{bmatrix} p' \\ q \end{bmatrix}_{n+1} = \begin{bmatrix} p' \\ q \end{bmatrix}_n - k\left(\partial g^{-1}\right) \cdot g$

3. Until: $\left\| \begin{bmatrix} p' \\ q \end{bmatrix}_{n+1} - \begin{bmatrix} p' \\ q \end{bmatrix}_n \right\| < TOL \left\| \begin{bmatrix} p' \\ q \end{bmatrix}_n \right\|$

4. Output: $p', q, \varepsilon_v^p = \varepsilon_v^p(p', q, \Delta\gamma)$ and Return

Box 6.3 Local Newton method for computing consistency parameter

1. Input: $p' = p'^{trial}, q = q^{trial}, \varepsilon_v^p = \left(\varepsilon_v^p\right)_n$ and set $\Delta\gamma = 0$

2. Do Iteration: (see BOX 1 for equation descriptions)

$f = f(p', q, \varepsilon_v^p)$, $\quad f' = \dfrac{\partial f}{\partial p'}\dfrac{\partial p'}{\partial \Delta\gamma} + \dfrac{\partial f}{\partial q}\dfrac{\partial q}{\partial \Delta\gamma} + \dfrac{\partial f}{\partial \varepsilon_v^p}\dfrac{\partial \varepsilon_v^p}{\partial \Delta\gamma}$, $\quad \Delta\gamma_{n+1} = \Delta\gamma_n - k\dfrac{f}{f'}$

Compute p', q, ε_v^p from BOX 2

3. Until: $|f| < TOL$

4. Output: $p', q, \varepsilon_v^p, \Delta\gamma$ and Return

Box 6.4 Return-Mapping Algorithm

1. Input: $\boldsymbol{\sigma'_n} = \boldsymbol{\sigma'_o}, \boldsymbol{\varepsilon_n} = \boldsymbol{\varepsilon_o}, \boldsymbol{\varepsilon}^p_{dn} = \boldsymbol{\varepsilon}^p_{do}, \left(\varepsilon_v^p\right)_n = \left(\varepsilon_v^p\right)_o, \Delta\boldsymbol{\varepsilon}$

2. Initialize: $p'_n = \dfrac{tr(\boldsymbol{\sigma'_n})}{3}$, $\quad \mathbf{s_n} = dev(\boldsymbol{\sigma'_n})$, $\quad q_n = \sqrt{\dfrac{3}{2}}\|\mathbf{s_n}\|$, $\quad \boldsymbol{\varepsilon_{n+1}} = \boldsymbol{\varepsilon_n} + \Delta\boldsymbol{\varepsilon}$,

$\Delta\varepsilon_v = tr(\Delta\boldsymbol{\varepsilon})$, $\quad \Delta\boldsymbol{\varepsilon}_d = dev(\Delta\boldsymbol{\varepsilon})$, $\quad \Delta\varepsilon_s = \sqrt{\dfrac{2}{3}}\|\Delta\boldsymbol{\varepsilon}\|$, $\quad \Delta\mathbf{n} = \dfrac{\Delta\boldsymbol{\varepsilon}_d^p}{\|\Delta\boldsymbol{\varepsilon}_d^p\|}$

3. Compute trial stress: $\quad p^{tr} = \exp(\omega\Delta\varepsilon_v)p'_n$, $\quad \Delta q = 3G_s(\Delta\varepsilon_v, p'_n)\Delta\varepsilon_s$

$q^{tr} = q_n + \Delta q$, $\quad \mathbf{s^{tr}} = \mathbf{s_n} + \sqrt{\dfrac{2}{3}}\Delta q\Delta\mathbf{n}$, $\quad \boldsymbol{\sigma'^{tr}} = p^{tr}\mathbf{1} + \mathbf{s^{tr}}$

4. Check yield function: $\quad f^{tr} = f(p^{tr}, q^{tr}, \left(\varepsilon_v^p\right)_n)$

If $f^{tr} \leq 0$ then Set $(\bullet)_{n+1} = (\bullet)^{tr}$ and Exit

5. Correct plastic stress and strain: $\quad \boldsymbol{\varepsilon}_{dn+1} = dev(\boldsymbol{\varepsilon}_{n+1})$, $\quad \mathbf{n}_{n+1} = \dfrac{\boldsymbol{\varepsilon}_{dn+1}}{\|\boldsymbol{\varepsilon}_{dn+1}\|}$

Compute $p', q, \varepsilon_v^p, \Delta\gamma$ from BOX 3 and Set $\left(\varepsilon_v^p\right)_{n+1} = \varepsilon_v^p$

6. Update stress and plastic strain: $\quad \boldsymbol{\sigma'_{n+1}} = p'\mathbf{1} + \sqrt{\dfrac{2}{3}}q\mathbf{n}_{n+1}$, $\quad \mathbf{s}_{n+1} = dev(\boldsymbol{\sigma'_{n+1}})$

$\Delta\boldsymbol{\varepsilon}_d^p = \Delta\gamma\dfrac{\partial f}{\partial q}\dfrac{\partial q}{\partial \mathbf{s}}$, $\quad \boldsymbol{\varepsilon}^p_{dn+1} = \boldsymbol{\varepsilon}^p_{dn} + \Delta\boldsymbol{\varepsilon}_d^p$, $\quad \boldsymbol{\varepsilon}^p_{n+1} = \dfrac{\left(\varepsilon_v^p\right)_{n+1}}{3}\mathbf{1} + \boldsymbol{\varepsilon}^p_{dn+1}$

7. Output: $\boldsymbol{\sigma'_{n+1}}, \boldsymbol{\varepsilon_{n+1}}, \boldsymbol{\varepsilon}^p_{dn+1}, \left(\varepsilon_v^p\right)_{n+1}$ and Exit

(1) Elastic predictor: for feasible region $\Delta\gamma = 0$

$$\boxed{\boldsymbol{\sigma}^{tr} - \boldsymbol{\sigma}_n = \Delta\boldsymbol{\sigma} = \mathbf{C}(\boldsymbol{\sigma}^{tr}).\Delta\boldsymbol{\varepsilon}} \qquad \boxed{\alpha^{tr} = \alpha_n}$$

(2) Check yield function: $f(\boldsymbol{\sigma}, \alpha) \leq 0$? $\xrightarrow{\text{YES}}$ Terminate

↓ NO

(3) Plastic corrector: solve for $\Delta\gamma$ (Lagrangian multiplier)

$$f(\boldsymbol{\sigma}^{tr} - \Delta\gamma.\mathbf{C}.\dfrac{\partial f}{\partial\boldsymbol{\sigma}}, \alpha^{tr} - \Delta\gamma\dfrac{\partial f}{\partial p'}) = \bar{f}(\Delta\gamma) = 0$$

variable

By Newton method: $\quad \Delta\gamma_{n+1} = \Delta\gamma_n - \dfrac{\bar{f}(\Delta\gamma_n)}{\left.\dfrac{d\bar{f}}{d\Delta\gamma}\right|_{\Delta\gamma_n}}$

(4) Repeat until obtain stationary state

Figure 6.11 Solution procedure: outline
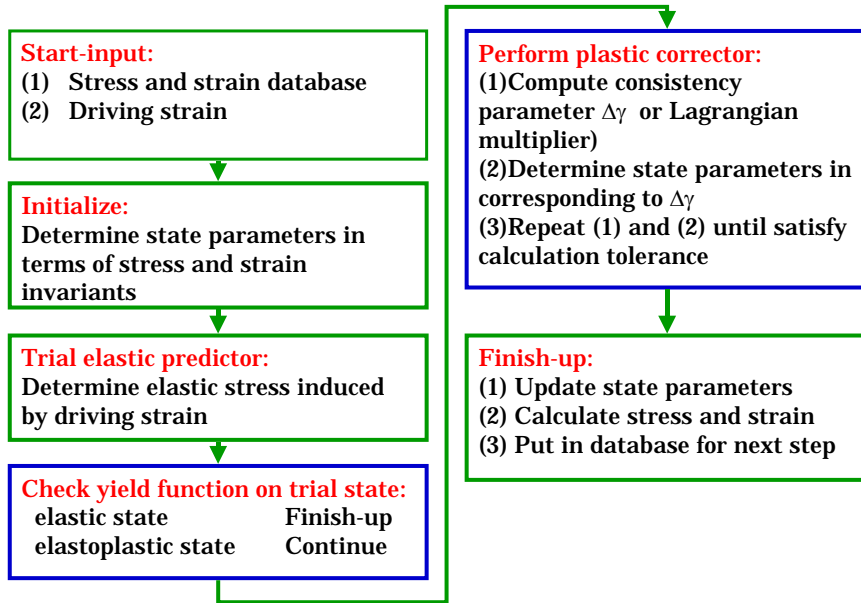
Figure 6.12 Solution procedure: step
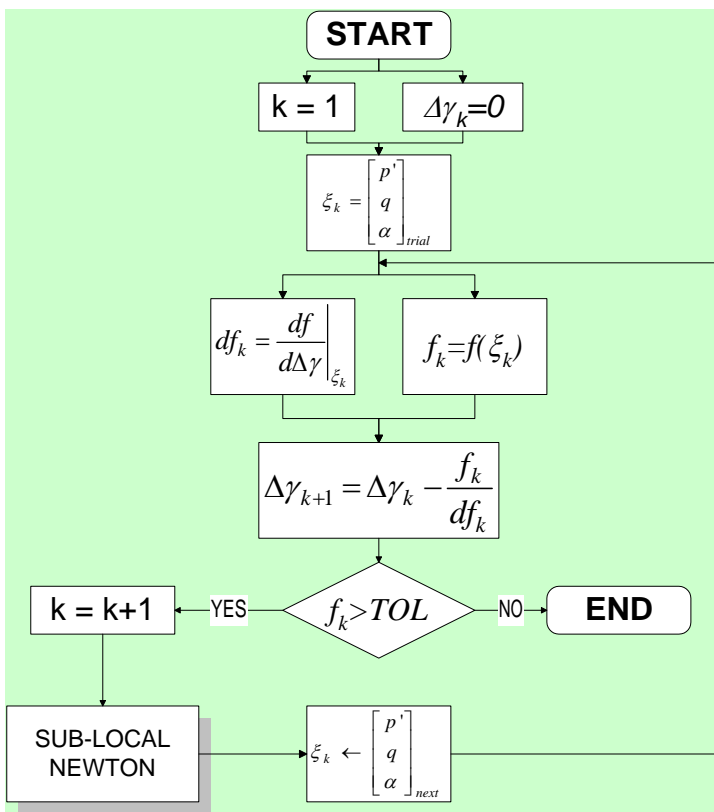
Figure 6.13 Solution local Newton procedure
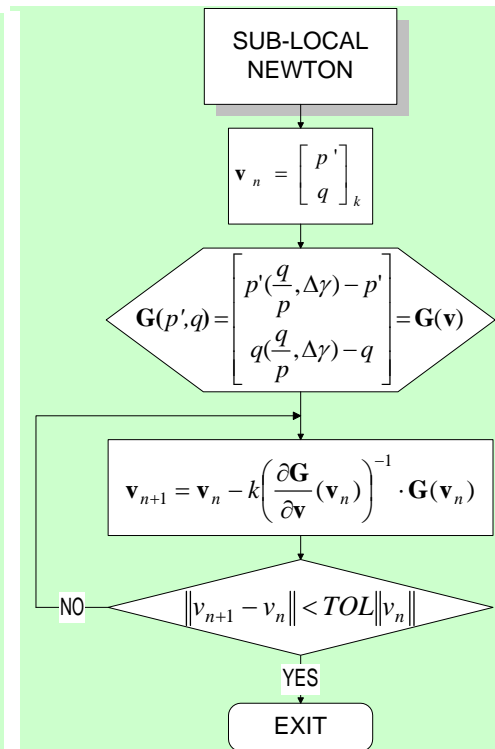
Figure 6.14 Solution local Newton procedure

6-3-3 Numerical example

The UU test predicted results (see Figure 6.15) based on soil parameters shown in Table 6.1 are plotted with results performed by return-mapping and sub-stepping methods to 7% axial strain on ideal sample (see Figure 6.16).

Table 6.1 Soil Parameters

D	0.11	Coefficient of dilatancy
Λ	0.83	Irreversibility ratio
M	1.02	Critical state parameter
v'	0.38	Effective Poisson's ratio
K_O	0.61	Coefficient of earth pressure at rest (NC)
K_i	0.70	Coefficient of earth pressure at rest (in-situ)
λ	0.38	Compression index
e_O	1.73	Void ratio at σ'_{vo}
σ'_{vo}	100	Preconsolidation pressure (kN/m^2)
σ'_{vi}	69	Overburden pressure (kN/m^2)
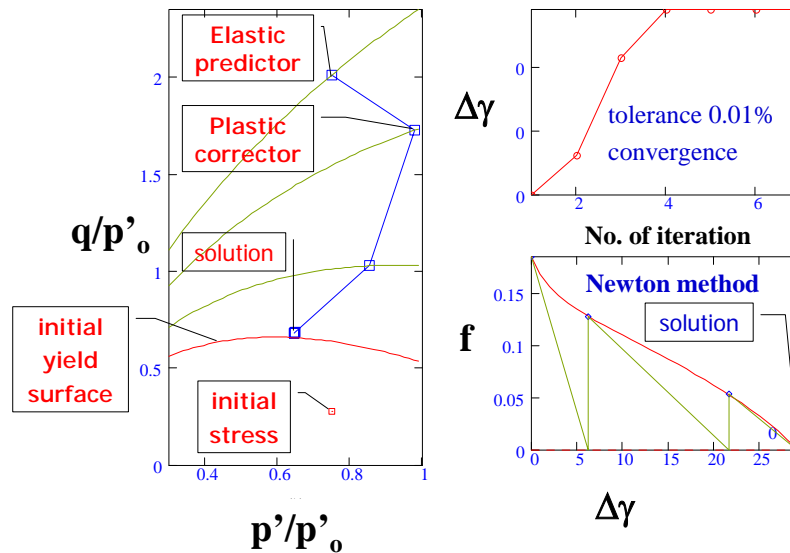
Figure 6.15 Iterative solutions
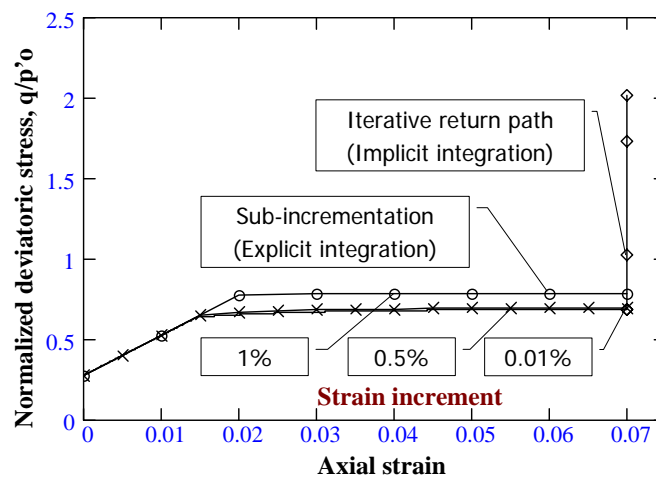
Figure 6.16 Comparative results between solutions obtained by return-mapping algorithm and sub-stepping method

6-3-4 Conclusions

The stress integration algorithm in the context of strain-driven process for Ohta-Hata model, the simplified form of Sekiguchi-Ohta soil constitutive model is developed as guidance for ongoing investigation. A comparison with the closed form and incremental method on a numerical analysis of a soil specimen under unconsolidated undrained test shows a good accuracy and a promising efficiency. Under the new implementation, input steps incurred by dividing load/displacement into small increments are replaced by employing the optimum step sizes governed by return-mapping algorithm to catch up the solutions at quadratic rate. The fundamental mathematical disciplines pave a way to the modest scheme of FEM and the emerged evolution of finite deformation analysis.

6-4 Integration Algorithms for Soil Constitutive Equation with a Singular Hardening Vertex

6-4-1 Introduction

Return-mapping methods have been extensively proved to be one of the most robust, stable and accurate integration algorithms applied in a realm of plasticity. Simo, Kennedy and Govindjee (1988) [20] raised the performance of algorithms by coping non-smooth multi-surface plasticity and viscoplasticity with the corner flow rule proposed by Koiter (1953) [21]. The evolution of flow rule substantially provides the theoretical foundation to evaluate plastic strain increment for constitutive laws with points of singularity. In this study, the return-mapping methods for rate-independent small strain plasticity (Pipatpongsa and Ohta., 2000) [22] and corner treatment theory developed by authors (Pipatpongsa et al., 2001a-c) [23,24,25] are combined together to upgrade the integration algorithms applicable to the soil constitutive laws proposed by Sekiguchi and Ohta (1977) [15].
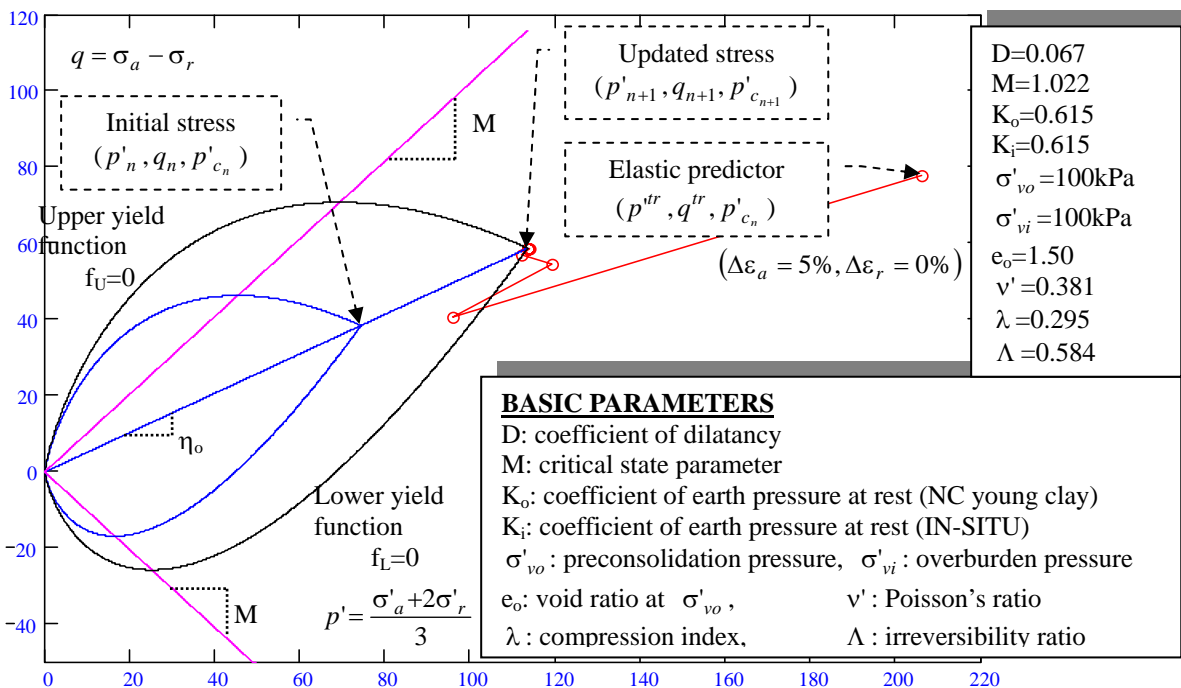
Figure 6.17 Iterative return paths in p'-q plane generated by CPPM for a single step strain increment

Attention is given to Rendulic's plane of stress or triaxial plane where the model accommodates the singular corner consisting of the intersection of differentiable upper and lower yield loci. The iterative numerical scheme driven by the Newton method is carried out for both the stress point at the corner and condition of stress passing very near or across the corner. The shape of yield surface grows in the direction of hardening vertex. The solution can reach a convergence with rapid calculation speeded by a powerful Closest Point Projection Method (CPPM). This development of theory can lead to the analytical and numerical methods for plastic flow evaluation at the corner, self-weight/K_o-consolidation, creep/ageing and rotational hardening for natural deposited clays.

6-4-2 Theoretical Descriptions

The objective of constitutive integration algorithms is to update the state variables at step n for a given strain increment $\Delta\varepsilon$. By using a sub-stepping method, though it is straight-forward, a numerical result is suffered from inaccuracy due to a drift on the yield function, i.e., $f_{n+1}=f(\sigma_{n+1},\mathbf{q}_{n+1})>0$.
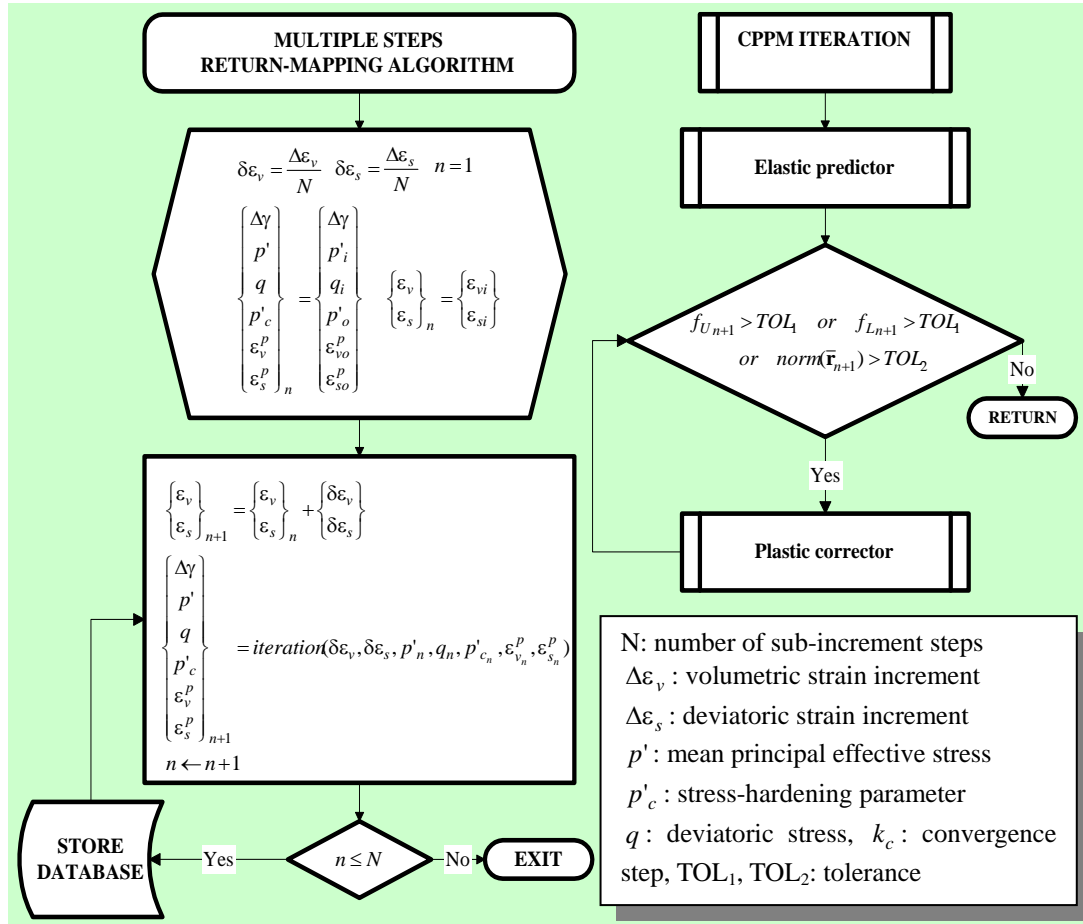
Figure 6.18 Flow chart of multiple-steps return-mapping algorithm

In CPPM, the state variables at n+1 are calculated and enforced to satisfy the yield function at the end of the step. The plastic flow emerged at the corner of the Sekiguchi-Ohta model is evaluated by the contribution of upper/lower yield surfaces considering two consistency parameters associated to each surface. Bulk modulus $K(p')$ is pressure-dependent while stress-hardening-dependent shear modulus $G(p_c')$ is employed for energy conservation during loading/unloading steps within yield surfaces. The feature of the method is shown in Figure 6.18. The outcome of multiple-steps CPPM is described in Box 6.6-Box 6.7.

Box 6.8 contains sets of equations for elastic predictor and plastic corrector steps.

6-4-3 Numerical Examples & Conclusions

The simulation of K_o-triaxial consolidation test is performed by exerting an axial strain up to 10%. The incremental strain is divided into 100 sub-increments. The ratio of deviatoric to volumetric strain increment is varied around a mean of 2/3 by a normal distribution function with standard deviation of 1. Figure 6.19-Figure 6.21. The resulting curves in Figure 6.22-Figure 6.23 show a performance of the algorithm.

Box 6.5 Common expressions

Slopes of $v - \ln(p')$ curve: compression line $\bar{\lambda} = \dfrac{\lambda}{1+e_o}$, swelling line $\bar{\kappa} = \dfrac{\kappa}{1+e_o}$

Bulk modulus: $K(p') = \dfrac{p'}{\bar{\kappa}}$, Secant shear modulus: $G_s(p'_c, p'_{co}) = \mu' \dfrac{p'_c - p'_{co}}{\bar{\kappa}\ln(\dfrac{p'_c}{p'_{co}})}$

and $\lim_{p'_c \to p'_{co}} G_s(p'_c, p'_{co}) = \mu' \dfrac{p'_c}{\bar{\kappa}}$ where $\mu' = \dfrac{3(1-2\nu')}{2(1+\nu')}$

In Rendulic's plane $\left(\sigma_{22} \equiv \sigma_{33}, \sigma_{12} = \sigma_{23} = \sigma_{31} \equiv 0\right)$

The rate-independent Sekiguchi-Ohta model reduces to

Upper: $f_U(p',q,p'_c) = MD\ln\left(\dfrac{p'}{p'_c}\right) + D\left(\dfrac{q}{p'} - \eta_o\right) = 0$;

Lower: $f_L(p',q,p'_c) = MD\ln\left(\dfrac{p'}{p'_c}\right) - D\left(\dfrac{q}{p'} - \eta_o\right) = 0$

Box 6.6 Elastic predictor

Initialization

$\begin{Bmatrix} \Delta\gamma_U \\ \Delta\gamma_L \end{Bmatrix}_{n+1} = \begin{Bmatrix} 0 \\ 0 \end{Bmatrix}$, $\begin{Bmatrix} \varepsilon_v^e \\ \varepsilon_s^e \end{Bmatrix}_n = \begin{Bmatrix} \varepsilon_v \\ \varepsilon_s \end{Bmatrix}_n - \begin{Bmatrix} \varepsilon_v^p \\ \varepsilon_s^p \end{Bmatrix}_n$, $\begin{Bmatrix} \varepsilon_v^{tr} \\ \varepsilon_s^{tr} \end{Bmatrix} = \begin{Bmatrix} \varepsilon_v^e \\ \varepsilon_s^e \end{Bmatrix}_n + \begin{Bmatrix} \delta\varepsilon_v \\ \delta\varepsilon_s \end{Bmatrix}$, $\begin{Bmatrix} \varepsilon_v^e \\ \varepsilon_s^e \end{Bmatrix}_{n+1} = \begin{Bmatrix} \varepsilon_v^{tr} \\ \varepsilon_s^{tr} \end{Bmatrix}$

$\begin{Bmatrix} \delta\varepsilon_v^p \\ \delta\varepsilon_s^p \end{Bmatrix}_{n+1} = \begin{Bmatrix} 0 \\ 0 \end{Bmatrix}$, $\begin{Bmatrix} \varepsilon_v^p \\ \varepsilon_s^p \end{Bmatrix}_{n+1} = \begin{Bmatrix} \varepsilon_v^p \\ \varepsilon_s^p \end{Bmatrix}_n + \begin{Bmatrix} \delta\varepsilon_v^p \\ \delta\varepsilon_s^p \end{Bmatrix}_{n+1}$

Elastic trial

$p'_{c_{n+1}} = p'_{c_n}\exp(\dfrac{\varepsilon_{v\,n+1}^p - \varepsilon_{v\,n}^p}{\bar{\lambda} - \bar{\kappa}})$, $\begin{Bmatrix} p'^{tr} \\ q^{tr} \end{Bmatrix} = \begin{Bmatrix} p'_n\exp(\dfrac{\varepsilon_{v\,n+1}^e - \varepsilon_{v\,n}^e}{\bar{\kappa}}) \\ q_n + 3G_s(p'_{c_{n+1}}, p'_{c_n})\left(\varepsilon_{s\,n+1}^e - \varepsilon_{s\,n}^e\right) \end{Bmatrix}$, $\begin{Bmatrix} p' \\ q \end{Bmatrix}_{n+1} = \begin{Bmatrix} p'^{tr} \\ q^{tr} \end{Bmatrix}$

Upper and lower yield values

$\begin{Bmatrix} f_U \\ f_L \end{Bmatrix} = \begin{Bmatrix} f_U\left(p'_{n+1}, q_{n+1}, p'_{c_{n+1}}\right) \\ f_L\left(p'_{n+1}, q_{n+1}, p'_{c_{n+1}}\right) \end{Bmatrix}$

First derivatives of upper and lower yield functions

$\mathbf{h}_U = \begin{Bmatrix} \dfrac{\partial f_U}{\partial p'} \\ \dfrac{\partial f_U}{\partial q} \end{Bmatrix}_{n+1} = \begin{Bmatrix} \dfrac{D}{p'}\left(M - \dfrac{q}{p'}\right) \\ \dfrac{D}{p'} \end{Bmatrix}_{n+1}$, $\mathbf{h}_L = \begin{Bmatrix} \dfrac{\partial f_L}{\partial p'} \\ \dfrac{\partial f_L}{\partial q} \end{Bmatrix}_{n+1} = \begin{Bmatrix} \dfrac{D}{p'}\left(M + \dfrac{q}{p'}\right) \\ \dfrac{-D}{p'} \end{Bmatrix}_{n+1}$

Activated signals for each yield surfaces

$\begin{Bmatrix} a_U \\ a_L \end{Bmatrix} = \begin{Bmatrix} ramp(sign(f_U)) \\ ramp(sign(f_L)) \end{Bmatrix}$

Solution residuals

$\bar{\mathbf{r}} = \begin{Bmatrix} \varepsilon_v^e \\ \varepsilon_s^e \end{Bmatrix}_{n+1} - \begin{Bmatrix} \varepsilon_v^{tr} \\ \varepsilon_s^{tr} \end{Bmatrix} + \Delta\gamma_{U\,n+1}\mathbf{h}_U a_U + \Delta\gamma_{L\,n+1}\mathbf{h}_L a_L$

Box 6.7 Plastic corrector

Second derivatives of upper and lower yield surfaces

$$\mathbf{H}_U = \begin{bmatrix} -M\dfrac{D}{p'^2} + 2D\dfrac{q}{p'^3} & \dfrac{-D}{p'^2} \\[2ex] \dfrac{-D}{p'^2} & 0 \end{bmatrix}_{n+1} \quad , \quad \mathbf{H}_L = \begin{bmatrix} -M\dfrac{D}{p'^2} - 2D\dfrac{q}{p'^3} & \dfrac{D}{p'^2} \\[2ex] \dfrac{D}{p'^2} & 0 \end{bmatrix}_{n+1}$$

Nonlinear elastic stiffness   Algorithmic moduli

$$\mathbf{C}_{n+1} = \begin{bmatrix} K(p'_{n+1}) & 0 \\ 0 & 3G_s(p'_{c_{n+1}}, p'_{c_n}) \end{bmatrix} \qquad \mathbf{\Xi}_{n+1} = \left(\mathbf{C}_{n+1}^{-1} + \Delta\gamma_{U\,n+1}\mathbf{H}_U a_U + \Delta\gamma_{L\,n+1}\mathbf{H}_L a_L\right)^{-1}$$

$$\begin{Bmatrix} v_U \\ v_L \end{Bmatrix} = k_c \begin{Bmatrix} f_U - \mathbf{h}_U \cdot (\mathbf{\Xi}_{n+1} \cdot \bar{\mathbf{r}}) \\ f_L - \mathbf{h}_L \cdot (\mathbf{\Xi}_{n+1} \cdot \bar{\mathbf{r}}) \end{Bmatrix}, \quad \mathbf{G} = \begin{bmatrix} \mathbf{h}_U \cdot (\mathbf{\Xi}_{n+1} \cdot \mathbf{h}_U) & \mathbf{h}_U \cdot (\mathbf{\Xi}_{n+1} \cdot \mathbf{h}_L) \\ \mathbf{h}_L \cdot (\mathbf{\Xi}_{n+1} \cdot \mathbf{h}_U) & \mathbf{h}_L \cdot (\mathbf{\Xi}_{n+1} \cdot \mathbf{h}_L) \end{bmatrix}$$

Iterative converged solutions

$$\begin{Bmatrix} \delta\Delta\gamma_U \\ \delta\Delta\gamma_L \end{Bmatrix}_{n+1} = \begin{cases} \begin{Bmatrix} (\mathbf{G}_{1,1})^{-1} \cdot v_U \\ 0 \end{Bmatrix} & if \quad a_L \le 0 \\[3ex] \begin{Bmatrix} 0 \\ (\mathbf{G}_{2,2})^{-1} \cdot v_L \end{Bmatrix} & if \quad a_U \le 0, \quad \delta\boldsymbol{\varepsilon}^e_{n+1} = -\mathbf{C}_{n+1}^{-1}\mathbf{\Xi}_{n+1}\left\{ k_c\bar{\mathbf{r}} + \delta\Delta\gamma_{U\,n+1}\mathbf{h}_U + \delta\Delta\gamma_{L\,n+1}\mathbf{h}_L \right\} \\[3ex] \mathbf{G}^{-1} \cdot \begin{Bmatrix} v_U \\ v_L \end{Bmatrix} & otherwise \end{cases}$$

Continue: Updated procedure

Note: $\quad ramp(x) \equiv \dfrac{x + |x|}{2}, \quad sign(x) \equiv \begin{cases} \dfrac{|x|}{x} & if \quad x \ne 0 \\ 0 & otherwise \end{cases}$

Box 6.8 Updated procedure

Updated strain   Updated consistency parameters for both yield surfaces

$$\begin{Bmatrix} \varepsilon_v^e \\ \varepsilon_s^e \end{Bmatrix}_{n+1} = \begin{Bmatrix} \varepsilon_v^e \\ \varepsilon_s^e \end{Bmatrix}_{n+1} + \delta\boldsymbol{\varepsilon}^e_{n+1} \qquad \begin{Bmatrix} \Delta\gamma_U \\ \Delta\gamma_L \end{Bmatrix}_{n+1} = \begin{Bmatrix} ramp(\Delta\gamma_{U\,n+1} + \delta\Delta\gamma_{U\,n+1}) \\ ramp(\Delta\gamma_{L\,n+1} + \delta\Delta\gamma_{L\,n+1}) \end{Bmatrix}$$

Updated activated signals of both yield surfaces

$$\begin{Bmatrix} a_U \\ a_L \end{Bmatrix} = \begin{Bmatrix} sign(\Delta\gamma_U) \\ sign(\Delta\gamma_L) \end{Bmatrix}$$

Updated plastic strain

$$\begin{Bmatrix} \delta\varepsilon_v^p \\ \delta\varepsilon_s^p \end{Bmatrix}_{n+1} = \begin{Bmatrix} \varepsilon_v^{tr} \\ \varepsilon_s^{tr} \end{Bmatrix} - \begin{Bmatrix} \varepsilon_v^e \\ \varepsilon_s^e \end{Bmatrix}_{n+1}, \quad \begin{Bmatrix} \varepsilon_v^p \\ \varepsilon_s^p \end{Bmatrix}_{n+1} = \begin{Bmatrix} \varepsilon_v^p \\ \varepsilon_s^p \end{Bmatrix}_n + \begin{Bmatrix} \delta\varepsilon_v^p \\ \delta\varepsilon_s^p \end{Bmatrix}_{n+1}$$

Updated stress

$$p'_{c_{n+1}} = p'_{c_n} \exp(\frac{\varepsilon_{v\,n+1}^p - \varepsilon_{v\,n}^p}{\bar{\lambda} - \bar{\kappa}}), \quad \begin{Bmatrix} p' \\ q \end{Bmatrix}_{n+1} = \begin{Bmatrix} p'_n \exp(\frac{\varepsilon_{v\,n+1}^e - \varepsilon_{v\,n}^e}{\bar{\kappa}}) \\ q_n + 3G_s(p'_{c_{n+1}}, p'_{c_n})\left(\varepsilon_{s\,n+1}^e - \varepsilon_{s\,n}^e\right) \end{Bmatrix}$$

Updated values of upper and lower yield functions

$$\begin{Bmatrix} f_U \\ f_L \end{Bmatrix} = \begin{Bmatrix} f_U\left(p'_{n+1}, q_{n+1}, p'_{c_{n+1}}\right) \\ f_L\left(p'_{n+1}, q_{n+1}, p'_{c_{n+1}}\right) \end{Bmatrix}$$

Updated normal to both yield surfaces   Updated solution residuals

$$\mathbf{h}_U = \begin{Bmatrix} \dfrac{D}{p'}\left(M - \dfrac{q}{p'}\right) \\[2ex] \dfrac{D}{p'} \end{Bmatrix}_{n+1} \quad , \quad \mathbf{h}_L = \begin{Bmatrix} \dfrac{D}{p'}\left(M + \dfrac{q}{p'}\right) \\[2ex] \dfrac{-D}{p'} \end{Bmatrix}_{n+1} \qquad \bar{\mathbf{r}} = \begin{Bmatrix} \varepsilon_v^e \\ \varepsilon_s^e \end{Bmatrix}_{n+1} - \begin{Bmatrix} \varepsilon_v^{tr} \\ \varepsilon_s^{tr} \end{Bmatrix} + \Delta\gamma_{U\,n+1}\mathbf{h}_U a_U + \Delta\gamma_{L\,n+1}\mathbf{h}_L a_L$$

Figure 6.19 Input strain variation $\dfrac{\delta\varepsilon_s}{\delta\varepsilon_v}$

no. of sub-increments
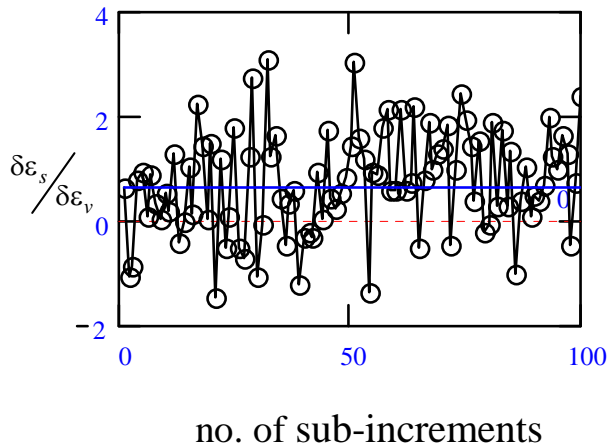
Figure 6.20 $\dfrac{\delta\varepsilon_s}{\delta\varepsilon_v}$ vs no. of sub-increments

no. of sub-increments
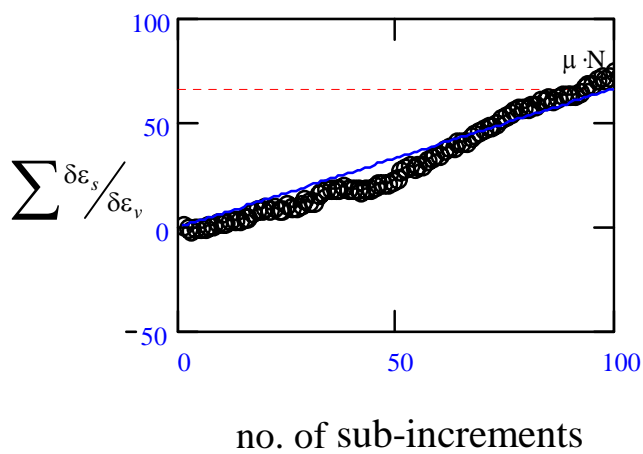
Figure 6.21 Amount of $\displaystyle\sum\dfrac{\delta\varepsilon_s}{\delta\varepsilon_v}$

$$q = \sigma_a - \sigma_r$$
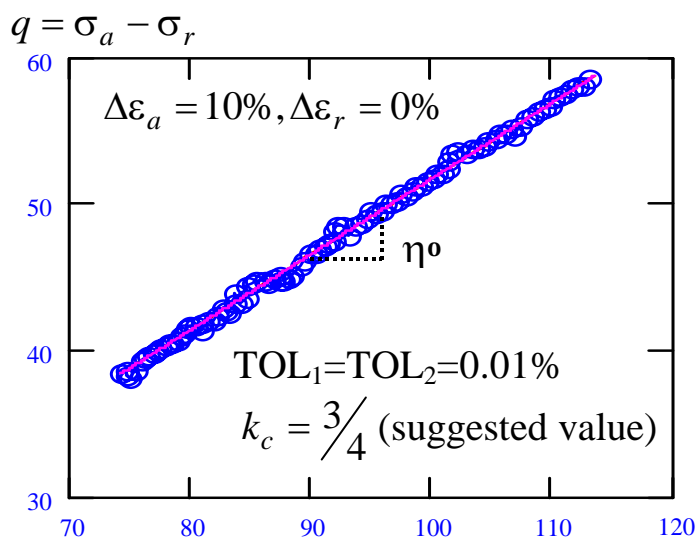
Figure 6.22 Simulated results of K_o-consolidation
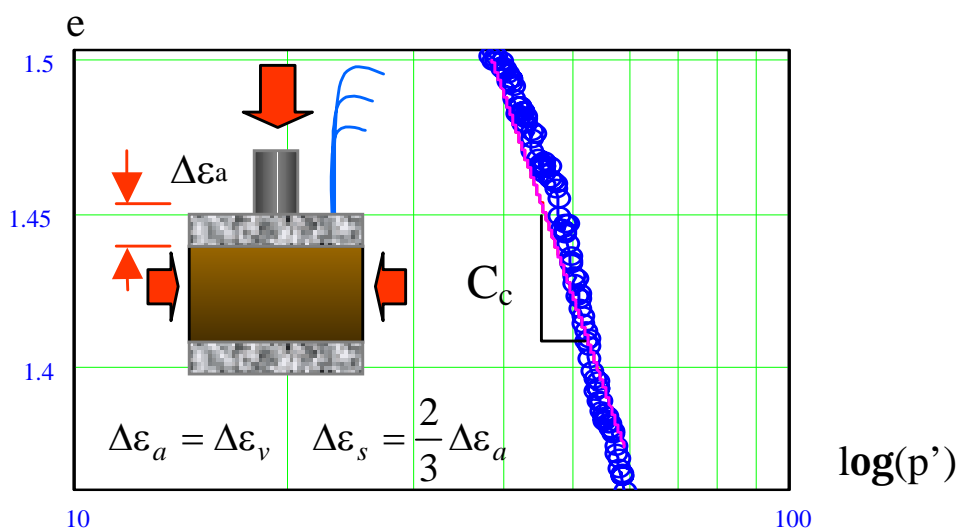
Figure 6.23 e-log(p') compression curve

6-4-4 References

1 Zienkiewicz, O.C. & Taylor, R.L., The Finite Element Method, Vol. 2, McGraw-Hill, 1991

2 Simo, J.C. & Hughes, T.J.R., Computational inelasticity, SPRINGER, 1997

3 Wilkins, ML., Calculation of elastic-plastic flow, Methods of Compuational Physics, Vol. 3 (Academic Press, New York), 1964

4 Krieg, R.D. and Key, S.W., Implementation of a time dependent plasticity theory into structural computer program, in: Constitutive Equation in Viscoplasticity: Computational and Engineering Aspects, AMD-20 (ASME, New York, 1976)

5 Hofstetter, G., Simo, J.C. & Taylor, R.L., A modified cap model: closest point projection algorithms, Comput. Struct. (46): 203-214, 1993

6 Matzenmiller, A. & Taylor, R.L., A return mapping algorithm for isotropic elastoplasticity, Int. J. Numer. Methods Engrg. (37): 813-826, 1994

7 Ortiz, M. & Simo, J.C., An analysis of a new class of integration algorithms for elastoplastic constitutive relations, Int. J. Numer. Methods Engrg. (21): 1561-1576, 1985

8 Simo, J.C., Kennedy, J. & Govindjee, S., Non-smooth multisurface plasticity and viscoplasticity. Loading/unloading conditions and numerical algorithms, Int. J. Numer. Methods Engrg. (26): 2161-2185, 1988

9 Krieg, R.D. & Krieg, D.B., Accuracies of numerical solution methods for elastic-perfectly plastic model, J.

Pressure Vessel Tech., ASME (99): 510-515, 1977

10 Schreyer, H.L., Kulak, R.F. & Kramer, M.M., Accurate numerical solutions for elastic-plastic model, J. Pressure Vessel Tech., ASME (101): 226-234, 1979

11 Ortiz, M. & Popov, E.P., Accuracy and stability of integration algorithms for elastoplastic constitutive relations, Int. J. Numer. Methods Engrg. (23): 353-366, 1986

12 Simo, J.C. & Govindjee, S., Non-linear B-stability and symmetry preserving return mapping algorithms for plasticity and viscoplasticity, Int. J. Numer. Methods Engrg. (31): 151-176, 1991

13 Belytschko, Ted, Liu, W.K. & Moran, M., Nonlinear finite elements for continua and structures, John Wiley & Sons, Ltd., 2000

14 Simo, J.C., Taylor, R.L., Consistent tangent operators for rate-independent elastoplasticity, Comput. Methods Appl. Mech. Engrg. (48): 101-118, 1985

15 Sekiguchi, H. and Ohta, H., Induced anisotropy and time dependency in clays, 9th ICSMFE, Tokyo, Constitutive equations of Soils: 229-238, 1977

16 Ohta, H. & Iizuka, A.,"Ground Response to Construction Activities", Vol. 1&2, 1992

17 Borja, R.I. & Lee, S.R., Cam-Clay plasticity, part I: Implicit integration of elasto-plastic constitutive relations, Comp. Meth. Appl. Mech. Eng., 78:49-72, 1990

18 Ohta, H. & Hata, S., A theoretical study of the stress-strain relations for clays, Soils and Foundations, 11(3): 65-89 (1971)

19 Hill, R., The mathematical theory of plasticity, Oxford University Press, Oxford, U.K., 1950

20 Simo, J.C., Kennedy, J.G. and Govindjee, S., Non-smooth multisurface plasticity and viscoplasticity. loading/unloading conditions and numerical algorithms, IJME 26,: 2161-2185, 1988

21 Koiter, W.T., "Stress-strain relations, uniqueness and variational theorems for elastic-plastic materials with a singular yield surface", Quart. Appl. Math., 11: 350-354, 1953

22 Pipatpongsa, T. and Ohta, H., Return-mapping algorithm for Sekiguchi-Ohta model, 2nd Inter. Summer Sym., JSCE,: 229-232, 2000

23 Pipatpongsa, T., Ohta, H., Kobayashi, I. and Iizuka, A., Associated plastic flow at the intersection corner of plastic potential functions in soil mechanics, Proc. of 36th Japanese Nat. Conf. on Geotech. Engrg,: 935-936, 2001

24 Pipatpongsa, T., Ohta, H., Kobayashi, I. and Iizuka, A.,Dependence of K_o-value on effective internal friction angle in regard to the Sekiguchi-Ohta model, Proc. of 36th Japanese Nat. Conf. on Geotech. Engrg,: 935-938, 2001

25 Pipatpongsa, T., Kobayashi, I., Ohta, H., & Iizuka, A., The vertex singularity in the Sekiguchi-Ohta model, 56th JSCE Annual Meeting, III-B341, 2001

CHAPTER 7

Closest Point Projection Method

7-1 Introduction

In the realm of nonlinear analysis for cohesive soils, the model proposed by Sekiguchi and Ohta (1977) [1] is one of the most widely used soil constitutive models based on Critical State theory. The model characterizes nonlinear stress-strain behavior including softening/hardening and dilatancy responses, principal stress reorientation, initial-stress-induced anisotropy and time dependency. The performance of the model has been proved to be consistent with many field responses in predicting soil behaviors (Ohta and Iizuka, 1992) [2]. The integration of constitutive equation over a discrete sequence of time step is commonly practiced by incremental solution that is classified into explicit and implicit categories. The first method simplifies the integration to the summation of sub-increments while the latter one applies the iterative scheme using Newton-Raphson method formulated in complex expressions. It has been shown that the procedure used for explicitly integrating the constitutive equations is inferior to that of implicit integration on solution stability and accuracy [3]. Moreover, in nonlinear problem, the size of increments substantially affect the quality of analysis, that is, a large step size will cause inaccuracy while a finer one will become a drawback in computation speed. According to several literatures [4,5], the effective method suggested to handle the problems is to apply the implicit integration method using return-mapping algorithm, the algorithm that usually starts in the first iteration with a purely elastic increment.

Much of foundation for the return-mapping methods for nonlinear isotropic and kinematic hardening/softening plasticity have been contributed over the passed two decade (Simo et al, 1985, 1988, 1992, 1993) [6,7,8,9] in which Closest Point Projection (CPP) and Cutting-Plane (CP) methods have been developed. Borja et al. (1990, 1991, 1998, 2001) [10,11,12,13] have developed the implementation of return-mapping algorithms applicable to the modified Cam-Clay model with a remarkable solution accuracy and quadratic rate of convergence. However, the procedures concerned show a sign of incompatibility with the Sekiguchi-Ohta model because both models have lost much in common since the advent of modified version. In addition, a number of recent studies have been proposed for the modified Cam-clay with prominent performance. Recently, Pipatpongsa and Ohta (2000) [14] developed the return-mapping algorithm applicable to an invisid form of the Sekiguchi-Ohta model as its first kind of implementation, which is fallen within the class of convex CP method coupled nonlinear hypoelastic response on two invariants stress space. The iterative return path generated by the algorithm is optimized at quadratic rate with high accuracy.

The purpose of this paper is to extend the previous work by developing an efficient CPP method applicable to the Sekiguchi-Ohta plasticity model, formulated to include a class of two-invariant stored energy function considering initial stress and damage process. The nonlinear elasticity is adopted by taking shear modulus G varied with pre-consolidation pressure while bulk modulus K is varied with mean stress. As a consequence, a conservation of energy is satisfied and path independent feature can be guaranteed in an elastic predictor step, which is rigorously required by return mapping algorithms.

An outline of the paper is as follows. In section 2, the mathematical framework is set for the algorithmic residuals and constraints. The constitutive equations and empirical hardening law are reviewed in section 3. Section 4 deals with a class of stored energy function considering initial stress. In section 5, hardening potential function appropriate with the model is defined. A procedure for damage process is accounted for changing a value of G in corresponding to a hardening parameter. A set of equations regulating the elastic constitutive law is arranged in section 6. In section 7, the implicit integrative scheme under CPP method is derived. In section 8, the nonlinear analysis for stress-strain-strength under CU and UU tests in two-invariant stress space problem were carried out to test the performance of the algorithm by comparing with sub-stepping technique and closed-form solutions. The conclusion is marked in section 9.

It is noted that in this study, attention is confined to infinitesimal deformation and rate-independent plasticity. It is out of scope in this paper to consider the existence of corner on yield surface however basic theories [7] and ongoing researches are available [15,16,17,18]. The unusual procedures can be neglected if the interested stress points lie outside and far from the corner. The further research subjected to soil/water coupling FEM for three-dimensional state of stress is being developed.

7-2 Plastic dissipation

This section illustrates the important role of the principle of maximum plastic dissipation (Hill, 1950) [19], its connection to the associated flow rule (Drucker's stability or normality postulate, 1950) [20] and basic regularization in the infinitesimal elasto-plasticity. The mathematical framework advocated by Simo (1992) [8] is rephrased but a modification is made for plastic variables in a sense to suit the hardening potential function defined in the section 5. Within a convex elastic domain of stress space defined by

$$\mathsf{E} \equiv \left\{ (\boldsymbol{\sigma}', h) \in \mathsf{S} \times R^+ \,\middle|\, f(\boldsymbol{\sigma}', h) \le 0 \right\} \qquad (7.1)$$

where S is a vector space of symmetric second-order tensors, R^+ is a real range of positive number and h is a stress-like hardening parameter of material. Based on the 2nd Law of Thermodynamics, partially a universal law

of decay, the dissipation function is defined by the difference between the stress power and the rate of change of the internal energy. The symbol ':' signifies the contraction of a tensor by 2 orders.

$$D = \boldsymbol{\sigma}' : \dot{\boldsymbol{\varepsilon}} - \dot{\Psi}(\boldsymbol{\varepsilon^e}, \alpha) \geq 0 \tag{7.2}$$

The internal energy is composed of elastic and hardening plastic components expressed by the stored energy function and hardening potential; i.e.,

$$\nabla_{\varepsilon^e} \Psi = \psi(\boldsymbol{\varepsilon^e}, \alpha), \qquad\qquad \nabla_{\alpha} \Psi = H(\alpha) \tag{7.3),(7.4}$$

The stored energy function and hardening potential function are subjected to define in section 4 and 5. The stress responses can be obtained by hyperelastic relationship. Herein, α denotes a strain-like variable conjugating to a material memory variable h.

$$\boldsymbol{\sigma}' = \frac{\partial \psi(\boldsymbol{\varepsilon^e}, \alpha)}{\partial \boldsymbol{\varepsilon^e}}, \qquad\qquad h = \frac{\partial H(\alpha)}{\partial \alpha} \tag{7.5),(7.6}$$

Using Eq.(7.3)-(7.4) and chain rule to Eq.(7.2) obtains,

$$D = [\boldsymbol{\sigma}' - \nabla_{\varepsilon^e} \psi] : \dot{\boldsymbol{\varepsilon}} + \nabla_{\varepsilon^e} \psi : \left[\dot{\boldsymbol{\varepsilon}} - \dot{\boldsymbol{\varepsilon}}^e \right] - \partial_{\alpha} H(\alpha) \dot{\alpha} \geq 0 \tag{7.7}$$

Eq.(7.5),(7.6),(7.7) imply (7.8) to hold for all admissible stress state and hence the optimum stress state for a given strain rate can be obtained by maximizing,

Objective function: $D = \boldsymbol{\sigma}' : \left[\dot{\boldsymbol{\varepsilon}} - \dot{\boldsymbol{\varepsilon}}^e \right] - h\dot{\alpha} \geq 0$ (7.8)

Optimized variable: $(\boldsymbol{\sigma}', h) \in E$

Subject to constraint: $f(\boldsymbol{\sigma}', h) \leq 0$

The corresponding Lagrangian function

$$L = -D + \gamma f(\boldsymbol{\sigma}', h) \tag{7.9}$$

By Kuhn-Tucker condition for extrema, define the residuals

$$\nabla L = \left\{ \begin{matrix} \nabla_{\sigma} L \\ \nabla_{h} L \end{matrix} \right\} = \left\{ \begin{matrix} -\left[\dot{\boldsymbol{\varepsilon}} - \dot{\boldsymbol{\varepsilon}}^e \right] + \gamma \dfrac{\partial f}{\partial \boldsymbol{\sigma}'} \\ \dot{\alpha} + \gamma \dfrac{\partial f}{\partial h} \end{matrix} \right\} = \left\{ \begin{matrix} \mathbf{0} \\ 0 \end{matrix} \right\} \tag{7.10),(7.11}$$

$$\gamma \geq 0 ; \quad f(\boldsymbol{\sigma}', h) \leq 0 ; \quad \gamma f(\boldsymbol{\sigma}', h) = 0 \tag{7.12),(7.13),(7.14}$$

Eq.(7.10),(7.11) are read as associative flow rule and associative hardening/softening law to the maximum dissipation energy principle. It is noted that Eq.(7.12),(7.13),(7.14) can judge loading/unloading condition but cannot judge for a state of hardening/softening.

$$\dot{\boldsymbol{\varepsilon}}^p = \dot{\boldsymbol{\varepsilon}} - \dot{\boldsymbol{\varepsilon}}^e = \gamma \frac{\partial f}{\partial \boldsymbol{\sigma}'}, \qquad\qquad \dot{\alpha} = -\gamma \frac{\partial f}{\partial h} \tag{7.15),(7.16}$$

Eq.(7.15) is corresponding to the postulate of associated flow rule by taking a Lagrangian multiplier γ as proportionality constant. In Critical state models, a hardening plastic variable h is chosen to p'_c and its conjugate α is referred to ε^p_v in particular. Therefore, an empirical hardening law denoted in Eq.(7.17) is commonly employed instead. Comparison of Eq.(7.16) to Eq.(7.17) implies the adopted hardening/softening law in Critical state models is non-associative sense [9,13], that is, Lagrangian function in Eq.(7.9) is not maximized because α is empirically associated to volumetric plastic strain, not theoretically associated to p'_c.

$$\dot{\alpha} = \dot{\varepsilon}^p_v = \dot{\boldsymbol{\varepsilon}}^p : \mathbf{1} = \gamma \frac{\partial f}{\partial p'} \neq -\gamma \frac{\partial f}{\partial h} \tag{7.17}$$

Eq.(7.15) is found to contain (7.17), therefore, hardening parameter updating procedure can be set aside from iteration as formulated in section 7.

7-3 Constitutive laws

Sekiguchi and Ohta (1977) proposed constitutive equations for stress-induced anisotropy in clays. The inviscid form of yield function is expressed by

$$f(\boldsymbol{\sigma}', p'_c) \equiv f(p', \eta^*, p'_c) = MD \ln \left(\frac{p'}{p'_c} \right) + D\eta^* = 0 \tag{7.18}$$

p'_c indicates an isotropic hardening stress of the subsequent yield surface which is determined by an empirical relationship based on e-$ln(p')$ curves of consolidation test (Eq.(7.19),(7.20)).

$$\varepsilon^p_v - \varepsilon^p_{vo} = \frac{\lambda - \kappa}{1 + e_o} \ln \left(\frac{p'_c}{p'_o} \right) \tag{7.19}$$

$$\varepsilon_{vc}^e - \varepsilon_{vco}^e = \frac{\kappa}{1+e_o} \ln\left(\frac{p'_c}{p'_o}\right) \tag{7.20}$$

The pre-consolidation pressure p'_o marks the isotropic pressure after the completion of K_o-consolidation. According to an infinitesimal void ratio-volumetric strain relationship denoted in Eq.(7.21), the plastic and elastic volumetric strain at p'_o equal to zero, Eq.(7.22),(7.23).

$$\dot{\varepsilon}_v = \frac{-\dot{e}}{1+e_o}, \quad \varepsilon_{vo}^p = 0, \quad \varepsilon_{vco}^e = 0 \tag{7.21),(7.22),(7.23}$$

Select the candidates of hardening variables in particular

$$h = p'_c, \qquad \alpha = \varepsilon_v^p \tag{7.24),(7.25}$$

where recompressibility and compressibility indices are

$$\bar{\kappa} = \frac{\kappa}{1+e_o}, \qquad \bar{\lambda} = \frac{\lambda}{1+e_o} \tag{7.26),(7.27}$$

A summary of constitutive laws is noted in Box 7.1.

7-4 Nonlinear elasticity

Mechanisms of strain are typically depicted by recoverable and irrecoverable parts caused by alternation in particle spacing, bending and reorientation of clay particles. Elastic stress-strain relation should cover time independent behavior, recoverable feature (monotonic & hysteretic) and small strain range. Classes of soil elasticity are among of linear, nonlinear, isotropic, anisotropic hypoelasticity and hyperelasticity. Hypoelasticity (Cauchy's elasticity) is fine for monotonic unloading/reloading but not guaranteed in energy conservation and path dependence. Hyperelasticity (Green's elasticity) is acceptable for all types of unloading/reloading, satisfying conservation of energy in any closed loop and path independence. In regardless of stiffness degradation by small strain, the typical elastic constitutive equation is related to volumetric and deviatoric stress-strain responses with stress variable stiffness as shown in Eq.(7.28).

$$\begin{Bmatrix} \dot{p}' \\ \dot{q} \end{Bmatrix} = \begin{bmatrix} K & J \\ J & 3G \end{bmatrix} \begin{Bmatrix} \dot{\varepsilon}_v^e \\ \dot{\varepsilon}_s^e \end{Bmatrix} \tag{7.28}$$

For materials that are elastic and isotropic, the coupled shear and volumetric effects are decoupled; i.e., J equals to zero [21]. Isotropic pressure-dependent bulk and shear moduli; i.e., $K=K(p')$, $G=G(p')$ are often employed but such relation does not give an energy conservative model [22,23]. Thus, the viable nonlinear elastic moduli are restricted to a sort of $K=K(p')$ and constant G [24]. Actually, an extensive study showed that G is both a function of p' and p'$_c$ [25]. For an illustrative study, G is assumed to depend only on p'$_c$ and governed by a stored energy function cast for a class of two-invariant isotropic nonlinear hyperelasticity accounted for damage effects. Energy conservation is guaranteed in the elastic domain but the material characteristics on the subsequent state boundary are path dependence and obeyed the elasto-plastic constitutive laws. The damage process is incorporated when elastic domain changes in shape due to hardening/softening process.

It is noted that a sort of $K=K(p')$ and $G=G(p'_c)$ implies a variation of apparent Poisson's ratio which may become very low or negative value for a considerably low mean stress. Thus, there is a limitation of applying $G(p'_c)$ to a certain extent of OCR values. To solve this difficulty, a light of $K=K(p',q)$ and $G=G(p')$ has come into view in recent research [25,26], though, complex expressions of non-zero coupling modulus J and elastic dilatancy response during simple shear appear questionable. By and large, soil is considered to hold initial stresses, thus, work done by initial stresses is included to the stored energy. The parameter of hardening p'_c is held constant in formulation.

7-4-1 Energy of distortion

Consider the energy as a product of deviatoric stress-strain,

$$\chi(\varepsilon_s^e, p'_c) \equiv \frac{1}{2} \mathbf{s}^T : \boldsymbol{\varepsilon}_d^e \tag{7.29}$$

where $\boldsymbol{\varepsilon}^e_d$ is the principal elastic strain deviator, $\mathbf{s}$ is the principal stress deviator.

Eq.(7.29) can be reduced to Eq.(7.30) where $G(p'_c)$ denotes the shear modulus. ε^e_s stands for deviatoric strain corresponding to $\boldsymbol{\varepsilon}^e_d$.

$$\chi(\varepsilon_s^e, p'_c) = \frac{3}{2} G(p'_c) \varepsilon_s^{e2} \tag{7.30}$$

where $\varepsilon_s^e = \sqrt{\frac{2}{3}} \|\boldsymbol{\varepsilon}_d^e\|, \quad \boldsymbol{\varepsilon}_d^e = \boldsymbol{\varepsilon}^e - \frac{1}{3} \varepsilon_v^e \mathbf{1}$

Conjugate of χ by Legendre transformation

$$\bar{\chi}(q, p'_c) = \max_{\varepsilon_s}(q\varepsilon_s^e - \chi(\varepsilon_s^e)) = \frac{1}{6}\frac{q^2}{G(p'_c)} \tag{7.31}$$

Box 7.1 Constitutive equations

Yield function proposed by Sekiguchi and Ohta (1977)

$$f(\boldsymbol{\sigma'}, p'_c) \equiv f(p', \eta^*, p'_c) = MD\ln\left(\frac{p'}{p'_c}\right) + D\eta^* = 0$$

where $p' = \frac{1}{3}tr(\boldsymbol{\sigma'})$, $p'_o = \frac{1}{3}tr(\boldsymbol{\sigma'_o})$, $\mathbf{s} = \boldsymbol{\sigma'} - p'\mathbf{1}$, $\mathbf{s}_o = \boldsymbol{\sigma'_o} - p'_o\mathbf{1}$, $\boldsymbol{\eta} = \frac{\mathbf{s}}{p'}$,

$\boldsymbol{\eta_o} = \frac{\mathbf{s_o}}{p'_o}$, $\eta^* = \sqrt{\frac{3}{2}}\|\boldsymbol{\eta} - \boldsymbol{\eta_o}\|$, $q = \sqrt{\frac{3}{2}}\|\mathbf{s}\|$, $\eta_o = \frac{3(1-K_o)}{1+2K_o}$, $D = \frac{\lambda - \kappa}{M(1+e_o)}$

In generalized convex format

$$f(\boldsymbol{\sigma'}, p'_c) \equiv f(I_1, \bar{J}_2, I_{c1}) = MD\ln\left(\frac{I_1}{I_{c1}}\right) + D\frac{3\sqrt{3\bar{J}_2}}{I_1} = 0$$

where $\bar{\mathbf{s}} = \mathbf{s} - p'\boldsymbol{\eta_o}$, $I_1 = \mathbf{1}:\boldsymbol{\sigma'}$, $\bar{J}_2 = \frac{1}{2}tr(\bar{\mathbf{s}}^2)$, $I_{c1} = 3p'_c$

$\mathbf{I} \equiv \frac{1}{2}\left[\delta_{ik}\delta_{jl} + \delta_{il}\delta_{jk}\right]\mathbf{e}_i \otimes \mathbf{e}_j \otimes \mathbf{e}_k \otimes \mathbf{e}_l$, $\mathbf{A} \equiv \mathbf{I} - \frac{1}{3}(\mathbf{1}\otimes\mathbf{1})$, $\mathbf{1} \equiv \delta_{ij}\mathbf{e}_i \otimes \mathbf{e}_j$,

$\bar{\mathbf{A}} \equiv \mathbf{A} - \frac{1}{3}\mathbf{1}\otimes\boldsymbol{\eta}_c - \frac{1}{3}\boldsymbol{\eta}_c \otimes \mathbf{1} + \frac{1}{9}\boldsymbol{\eta}_c : \boldsymbol{\eta}_c(\mathbf{1}\otimes\mathbf{1})$

First derivative of yield function

$$\frac{\partial f}{\partial \boldsymbol{\sigma'}} = \frac{\partial f}{\partial I_1}\frac{\partial I_1}{\partial \boldsymbol{\sigma'}} + \frac{\partial f}{\partial \bar{J}_2}\frac{\partial \bar{J}_2}{\partial \boldsymbol{\sigma'}}$$

where $\frac{\partial I_1}{\partial \boldsymbol{\sigma'}} = \mathbf{1}$, $\frac{\partial \bar{J}_2}{\partial \boldsymbol{\sigma'}} = \left(\mathbf{A} - \frac{1}{3}\mathbf{1}\otimes\boldsymbol{\eta_o}\right):\bar{\mathbf{s}} = \bar{\mathbf{A}}:\boldsymbol{\sigma'}$,

$\frac{\partial f}{\partial I_1} = \frac{D}{I_1}\left(M - 3\frac{\sqrt{3\bar{J}_2}}{I_1}\right)$, $\frac{\partial f}{\partial \bar{J}_2} = \frac{9D}{2I_1\sqrt{3\bar{J}_2}}$

Second derivative of yield function

$$\frac{\partial^2 f}{\partial \boldsymbol{\sigma'}\partial \boldsymbol{\sigma'}} = \frac{\partial^2 f}{\partial \boldsymbol{\sigma'}\partial I_1}\otimes\frac{\partial I_1}{\partial \boldsymbol{\sigma'}} + \frac{\partial^2 f}{\partial \boldsymbol{\sigma'}\partial \bar{J}_2}\otimes\frac{\partial \bar{J}_2}{\partial \boldsymbol{\sigma'}} + \frac{\partial f}{\partial I_1}\frac{\partial^2 I_1}{\partial \boldsymbol{\sigma'}\partial \boldsymbol{\sigma'}} + \frac{\partial f}{\partial \bar{J}_2}\frac{\partial^2 \bar{J}_2}{\partial \boldsymbol{\sigma'}\partial \boldsymbol{\sigma'}}$$

where $\frac{\partial^2 I_1}{\partial \boldsymbol{\sigma'}\partial \boldsymbol{\sigma'}} = \mathbf{0}$, $\frac{\partial^2 \bar{J}_2}{\partial \boldsymbol{\sigma'}\partial \boldsymbol{\sigma'}} = \bar{\mathbf{A}}$, $\frac{\partial^2 f}{\partial \boldsymbol{\sigma'}\partial I_1} = \frac{\partial^2 f}{\partial I_1\partial I_1}\frac{\partial I_1}{\partial \boldsymbol{\sigma'}} + \frac{\partial^2 f}{\partial \bar{J}_2\partial I_1}\frac{\partial \bar{J}_2}{\partial \boldsymbol{\sigma'}}$,

$\frac{\partial^2 f}{\partial \boldsymbol{\sigma'}\partial \bar{J}_2} = \frac{\partial^2 f}{\partial I_1\partial \bar{J}_2}\frac{\partial I_1}{\partial \boldsymbol{\sigma'}} + \frac{\partial^2 f}{\partial \bar{J}_2\partial \bar{J}_2}\frac{\partial \bar{J}_2}{\partial \boldsymbol{\sigma'}}$, $\frac{\partial^2 f}{\partial I_1\partial I_1} = -\frac{MD}{I_1^2} + \frac{6D\sqrt{3\bar{J}_2}}{I_1^3}$,

$\frac{\partial^2 f}{\partial \bar{J}_2\partial I_1} = -\frac{9D}{2I_1^2\sqrt{3\bar{J}_2}}$, $\frac{\partial^2 f}{\partial I_1\partial \bar{J}_2} = -\frac{9D}{2I_1^2\sqrt{3\bar{J}_2}}$, $\frac{\partial^2 f}{\partial \bar{J}_2\partial \bar{J}_2} = -\frac{9D}{4I_1\bar{J}_2\sqrt{3\bar{J}_2}}$

7-4-2 Energy of contraction

Based on *e-ln(p')* curve of consolidation test,

Void ratio-strain relation (elastic): $\quad \dot{\varepsilon}_v^e = \frac{-\dot{e}}{1+e_o}$ $\qquad$ (7.32)

e_o is the reference state referred to void ratio at the completion of consolidation.

Elastic swelling curve: $\qquad\qquad \dot{e} = -\frac{\kappa}{p'}\dot{p}'$ $\qquad$ (7.33)

Initial condition: $\qquad \varepsilon_v^e(p'_i) = \varepsilon_{vi}^e = 0$ $\hfill$ (7.34)

Substitute Eq.(7.33) into (7.34), integrate with initial condition

$$\varepsilon_v^e - \varepsilon_{vi}^e = \frac{\kappa}{1+e_o}\ln(\frac{p'}{p'_i}) \hfill (7.35)$$

Rewrite Eq.(7.35) to $\qquad\qquad p' = p'_i \exp(\frac{\varepsilon_v^e - \varepsilon_{vi}^e}{\bar{\kappa}}) \hfill (7.36)$

Form potential strain energy by setting: $\qquad p' = \dfrac{\partial U}{\partial \varepsilon_v^e} \hfill (7.37)$

Integrating Eq.(7.37) reveals the potential energy as follow,

$$U - U_i = \int_{\varepsilon_{vi}^e}^{\varepsilon_v^e} p'\,d\varepsilon_v^e = p'_i\,\bar{\kappa}\exp(\frac{\varepsilon_v^e - \varepsilon_{vi}^e}{\bar{\kappa}}) \hfill (7.38)$$

Potential energy is energy of state. And the state chosen to correspond to zero potential energy is arbitrary. As a consequence, the constant terms in Eq.(7.38) is omitted,

$$U = p'_i\,\bar{\kappa}\exp(\frac{\varepsilon_v^e - \varepsilon_{vi}^e}{\bar{\kappa}}) \hfill (7.39)$$

Find a conjugate of U by using Legendre transformation,

$$W = p'\bar{\kappa}\left[\ln(\frac{p'}{p'_i}) + \frac{\varepsilon_{vi}^e}{\bar{\kappa}} - 1\right] \hfill (7.40)$$

7-4-3 Stored energy function

Sum of Eq.(7.30) and (7.39) gives a stored energy function as presented by Eq.(7.41) below

$$\psi(\varepsilon_v^e, \varepsilon_s^e, p'_c) = p'_i\,\bar{\kappa}\exp(\frac{\varepsilon_v^e - \varepsilon_{vi}^e}{\bar{\kappa}}) + \frac{3}{2}G(p'_c)\varepsilon_s^{e2} \hfill (7.41)$$

Complementary stored energy function is also obtained,

$$\varpi(p', q, p'_c) = p'\bar{\kappa}\left[\ln(\frac{p'}{p'_i}) + \frac{\varepsilon_{vi}^e}{\bar{\kappa}} - 1\right] + \frac{1}{6}\frac{q^2}{G(p'_c)} \hfill (7.42)$$

Stress relation can be taken by gradient of stored energy

$$\left\{\begin{matrix} p' \\ q \end{matrix}\right\} = \nabla\psi = \left\{\begin{matrix} \dfrac{\partial\psi}{\partial\varepsilon_v^e} \\ \dfrac{\partial\psi}{\partial\varepsilon_s^e} \end{matrix}\right\} = \left\{\begin{matrix} p'_i\exp(\frac{\varepsilon_v^e - \varepsilon_{vi}^e}{\bar{\kappa}}) \\ 3G(p'_c)\varepsilon_s^e \end{matrix}\right\} \hfill (7.43)$$

By the same fashion, strain relation is,

$$\left\{\begin{matrix} \varepsilon_v^e \\ \varepsilon_s^e \end{matrix}\right\} = \nabla\varpi = \left\{\begin{matrix} \dfrac{\partial\varpi}{\partial p'} \\ \dfrac{\partial\varpi}{\partial q} \end{matrix}\right\} = \left\{\begin{matrix} \bar{\kappa}\ln(\frac{p'}{p'_i}) + \varepsilon_{vi}^e \\ \dfrac{1}{3}\dfrac{q}{G(p'_c)} \end{matrix}\right\} \hfill (7.44)$$

Stiffness matrix can be taken via stored energy function as

$$\mathbf{C} \equiv \nabla\nabla\psi = \begin{bmatrix} \dfrac{\partial^2\psi}{\partial\varepsilon_v^e\partial\varepsilon_v^e} & \dfrac{\partial^2\psi}{\partial\varepsilon_s^e\partial\varepsilon_v^e} \\ \dfrac{\partial^2\psi}{\partial\varepsilon_v^e\partial\varepsilon_s^e} & \dfrac{\partial^2\psi}{\partial\varepsilon_s^e\partial\varepsilon_s^e} \end{bmatrix} \hfill (7.45)$$

Then $\qquad \mathbf{C} = \begin{bmatrix} \dfrac{p'_i}{\bar{\kappa}}\exp(\frac{\varepsilon_v^e - \varepsilon_{vi}^e}{\bar{\kappa}}) & 0 \\ 0 & 3G(p'_c) \end{bmatrix} \hfill (7.46)$

By the same fashion, the compliance matrix is

$$\mathbf{E} = \mathbf{C}^{-1} = \nabla\nabla\varpi = \begin{bmatrix} \dfrac{\overline{\kappa}}{p'} & 0 \\ 0 & \dfrac{1}{3G(p'_c)} \end{bmatrix} \tag{7.47}$$

Compare Eq.(7.28) with (7.46) and (7.47), using Eq.(7.43) tangent bulk modulus is determined by,

$$K(\varepsilon_v^e) = \frac{p'_i}{\overline{\kappa}} \exp(\frac{\varepsilon_v^e - \varepsilon_{vi}^e}{\overline{\kappa}}) \quad \text{or} \quad K(p') = \frac{p'}{\overline{\kappa}} \tag{7.48}$$

Tangent shear modulus is set to be the function of constant Poisson's ratio v' and bulk modulus at the state of consolidation,

$$G(p'_c) = \mu' K(p'_c) = \mu' \frac{p'_c}{\overline{\kappa}} \tag{7.49}$$

where $\qquad \mu' = \dfrac{3(1-2v')}{2(1+v')}$ (7.50)

In Eq.(7.51), the parameter p'_c can be calculated from a pre-consolidation pressure p'_o and volumetric plastic strain ε_v^p or volumetric elastic strain ε_{vc}^e in loading process or consolidation on e-$ln(p')$ relation (see Eq.(7.19) -(7.23)). The rate form of p'_c will be discussed later. The change of p'_c causes a change in size of elastic domain and trigger damage process on stored energy.

$$p'_c = p'_o \exp(\frac{\varepsilon_v^p}{\overline{\lambda} - \overline{\kappa}}) = p'_o \exp(\frac{\varepsilon_{vc}^e}{\overline{\kappa}}) \tag{7.51}$$

It is concluded that, within state boundary condition, G is constant but increase exponentially with strain-hardening parameter after yielding by taking damage effect on energy conservation into account. Its explicit evaluation will be shown in the next section.
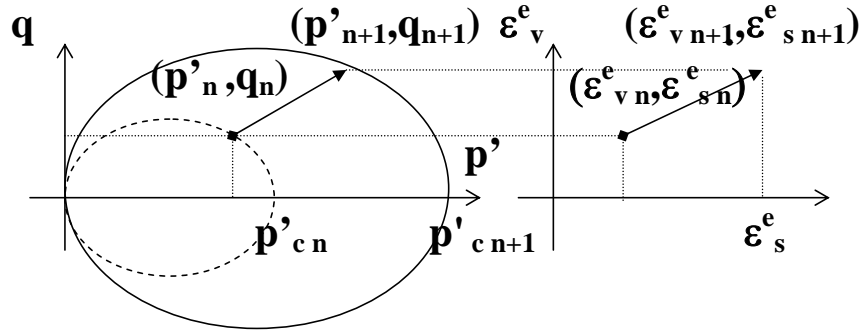
Figure 7.1 Mapping of incremental elastic strain into incremental stress

7-5 Hardening potential and inelastic damage process

Irreversible part of isotropic normal compression represents the hardening development in soil particles. A hardening potential function is defined to keep in line with a stored energy of volumetric elastic strains Eq.(7.39). Under this combining process, an internal energy and derivative can be defined straightforward by,

$$\mathsf{H}(\alpha) = p'_o \left(\overline{\lambda} - \overline{\kappa}\right) \exp(\frac{\alpha}{\overline{\lambda} - \overline{\kappa}}) \tag{7.52}$$

$$\dot{\mathsf{H}}(\alpha) = \frac{\dot{\alpha}}{\overline{\lambda} - \overline{\kappa}} \mathsf{H}(\alpha) \tag{7.53}$$

Substituting Eq.(7.52) into Eq.(7.6) obtains a stress-hardening parameter corresponds to Eq.(7.24).

$$h = p'_o \exp(\frac{\alpha}{\overline{\lambda} - \overline{\kappa}}) = p'_c \tag{7.54}$$

Nonlinear plastic modulus and rate form of p'_c are obtained by

$$H(p'_c) = \frac{p'_c}{\overline{\lambda} - \overline{\kappa}}, \qquad \dot{p}'_c = H(p'_c)\dot{\alpha} \tag{7.55},(7.56)$$

According to the stored energy in Eq.(7.41)-(7.42), the inelastic damage process affects on deviatoric stress when stress is in contact with yield surface. Refer to Eq.(7.43),(7.51) the quotient of incremental relation between q and p'_c are expressed by,

$$\frac{\delta q}{\delta p\,'_c} = \frac{3G(p\,'_c)\delta\varepsilon_s^e}{\dfrac{p\,'_o}{\overline{\kappa}}\exp(\dfrac{\varepsilon_{vc}^e}{\overline{\kappa}})\delta\varepsilon_{vc}^e} = 3\mu\,'\frac{\delta\varepsilon_s^e}{\delta\varepsilon_{vc}^e} \tag{7.57}$$

It is assumed that a material experiences a holonomic strain path; i.e., proportional increments of strain over the time interval, thus, the explicitly integrated expression can be evaluated by considering an incremental elastic strain as shown in Figure 7.1 from initial yield stress (step n) to a subsequent yield stress (step n+1).

$$\frac{q_{n+1}-q_n}{p\,'_{cn+1}-p\,'_{cn}} = 3\mu\,'\frac{\varepsilon_{s\,n+1}^e-\varepsilon_{s\,n}^e}{\varepsilon_{vc\,n+1}^e-\varepsilon_{vc\,n}^e} \tag{7.58}$$

Manipulate Eq.(7.58) and use Eq.(7.20), the nonlinear secant shear modulus including damage process due to a change in size of yield surface can be determined by,

$$\frac{q_{n+1}-q_n}{\varepsilon_{s\,n+1}^e-\varepsilon_{s\,n}^e} = 3\mu\,'\frac{p\,'_{cn+1}-p\,'_{cn}}{\varepsilon_{vcn+1}^e-\varepsilon_{vcn}^e} = 3G_s(p\,'_{cn+1},p\,'_{cn}) \tag{7.59}$$

where $$G_s(p\,'_{cn+1},p\,'_{cn}) = \mu\,'\frac{p\,'_{cn+1}-p\,'_{cn}}{\overline{\kappa}\ln(p\,'_{cn+1}/p\,'_{cn})} \tag{7.60}$$

Non-linear secant shear modulus is a result of externally integrating on the plastic hardening parameter. It is noted that the secant shear modulus is held constant inside the state boundary. In case of the initial yield surface, the secant shear modulus is the tangent shear modulus of pre-consolidated pressure.

$$\lim_{p\,'_c \to p\,'_o} G_s(p\,'_c,p\,'_o) = G(p\,'_o) = \mu\,'\frac{p\,'_o}{\overline{\kappa}} \tag{7.61}$$

By rewriting Eq.(7.59), Eq.(7.62) gives an evolution of q in Eq.(7.43) and stiffness matrix in Eq.(7.46) are thus taking damage effect into account.

$$q_{n+1} = q_n + 3G_s(p\,'_{cn+1},p\,'_{cn})\left(\varepsilon_{s\,n+1}^e-\varepsilon_{s\,n}^e\right) \tag{7.62}$$

$$\mathbf{C} = \begin{bmatrix} \dfrac{p\,'_{n+1}}{\overline{\kappa}} & 0 \\[2mm] 0 & 3G_s(p\,'_{cn+1},p\,'_{cn}) \end{bmatrix} \tag{7.63}$$

Box 7.2 Elastic parameters and moduli

| Recompressibility index: $\overline{\kappa} = \dfrac{\kappa}{1+e_o}$

 Compressibility index: $\overline{\lambda} = \dfrac{\lambda}{1+e_o}$

 Ratio of shear to bulk moduli: $\mu\,' = \dfrac{3(1-2v\,')}{2(1+v\,')}$

 Tangent bulk modulus: $K(p\,') = \dfrac{p\,'}{\overline{\kappa}}$ | Tangent shear modulus:
 $G(p\,'_c) = \mu\,'\dfrac{p\,'_c}{\overline{\kappa}}$

 Secant shear modulus:
 $G_s(p\,'_{cn+1},p\,'_{cn}) = \mu\,'\dfrac{p\,'_{cn+1}-p\,'_{cn}}{\overline{\kappa}\ln(p\,'_{cn+1}/p\,'_{cn})}$

 note: $G_s(p\,'_{cn},p\,'_{cn}) = \mu\,'\dfrac{p\,'_{cn}}{\overline{\kappa}}$ |

The relevant equations are summarized in Box 7.2.

7-6 Elastic constitutive equation

The incremental stress-strain relation can be described by,

$$\dot{\boldsymbol{\sigma}}\,' = \mathbf{c}^e : \dot{\boldsymbol{\varepsilon}}^e \tag{7.64}$$

where $$\mathbf{c}^e = \frac{\partial\boldsymbol{\sigma}\,'}{\partial\boldsymbol{\varepsilon}^e} = \mathbf{1}\otimes\frac{\partial p\,'}{\partial\boldsymbol{\varepsilon}^e} + \frac{\partial\mathbf{s}}{\partial\boldsymbol{\varepsilon}^e} \tag{7.65}$$

$$\boldsymbol{\sigma}\,' = p\,'\mathbf{1}+\mathbf{s}, \qquad \boldsymbol{\varepsilon}^e = \frac{1}{3}\varepsilon_v^e\mathbf{1}+\boldsymbol{\varepsilon}_d^e \tag{7.66),(7.67}$$

$$\frac{\partial p\,'}{\partial\boldsymbol{\varepsilon}^e} = \frac{\partial p\,'}{\partial\varepsilon_v^e}\frac{\partial\varepsilon_v^e}{\partial\boldsymbol{\varepsilon}^e} + \frac{\partial p\,'}{\partial\varepsilon_s^e}\frac{\partial\varepsilon_s^e}{\partial\boldsymbol{\varepsilon}_d^e}:\frac{\partial\boldsymbol{\varepsilon}_d^e}{\partial\boldsymbol{\varepsilon}^e} \tag{7.68}$$

$$\frac{\partial\mathbf{s}}{\partial\boldsymbol{\varepsilon}^e} = \frac{\partial\mathbf{s}}{\partial\varepsilon_v^e}\otimes\frac{\partial\varepsilon_v^e}{\partial\boldsymbol{\varepsilon}^e} + \frac{\partial\mathbf{s}}{\partial\varepsilon_s^e}\otimes\frac{\partial\varepsilon_s^e}{\partial\boldsymbol{\varepsilon}_d^e}:\frac{\partial\boldsymbol{\varepsilon}_d^e}{\partial\boldsymbol{\varepsilon}^e} \tag{7.69}$$

$\mathbf{I} \equiv \dfrac{1}{2}\left[\delta_{ik}\delta_{jl} + \delta_{il}\delta_{jk}\right]\mathbf{e}_i \otimes \mathbf{e}_j \otimes \mathbf{e}_k \otimes \mathbf{e}_l$ is the forth-order identity tensor, $\mathbf{c}^{\mathbf{e}}$ is forth-order tensor of elastic stiffness including damage effect. Elements of $\mathbf{C}$ are defined in Eq.(7.63). In this case, C_{12} and C_{21} are simply zero.

$$\mathbf{c}^e = C_{11}\mathbf{1}\otimes\mathbf{1} + \sqrt{\frac{2}{3}}C_{12}\mathbf{1}\otimes\mathbf{n} + \sqrt{\frac{2}{3}}C_{21}\mathbf{n}\otimes\mathbf{1} + \frac{2}{3}C_{22}\mathbf{A} \tag{7.70}$$

where $\qquad \mathbf{A} \equiv \mathbf{I} - \dfrac{1}{3}(\mathbf{1}\otimes\mathbf{1})$, $\mathbf{n} \equiv \dfrac{\mathbf{s}}{\|\mathbf{s}\|}$ $\hfill$ (7.71),(7.72)

7-7 Integration schemes

Solutions of elasto-plastic responses usually rely on sub-stepping technique, however, a numerical result is inaccurate due to a drift on the yield function. By fully implicit integration (Backward-Euler), the state variables at current step are calculated and enforced to satisfy the yield function at the end of the step. Iterative methods based on this scheme are more robust, stable and give a better accuracy for the same increment of driving variables; e.g., strains, displacements, forces and time periods. It is necessary to integrate the constitutive equations by assuming material is subject to a constant rate of strain over the interested time interval. Elastic-plastic operator-splitting methodology is used in the fully implicit integrative scheme, leading to the return-mapping algorithms with unconditional stability and first-order accuracy [27].

Operator splitting theory has everything to do with a decomposition of incremental elastic and plastic parts. Figure 7.2 illustrates an outline of the algorithm by referring to an elasto-perfectly-plastic one-dimensional model being pulled by force q on rough surface against friction resistance $\sigma_y=\mu p$. A slippage of box represents an irrecoverable deformation. A stretch of spring represents a recoverable deformation. The combined incremental deformation is split into two discrete steps. First is called elastic predictor step where plastic part is firmly locked and all deformation is dominated by trial elastic part. Second is called plastic corrector step where plastic part is released and elastic part is corrected. The box would stop at the stationary point where dissipation energy of a system reaches the maximum value and hence, the solution of a problem.
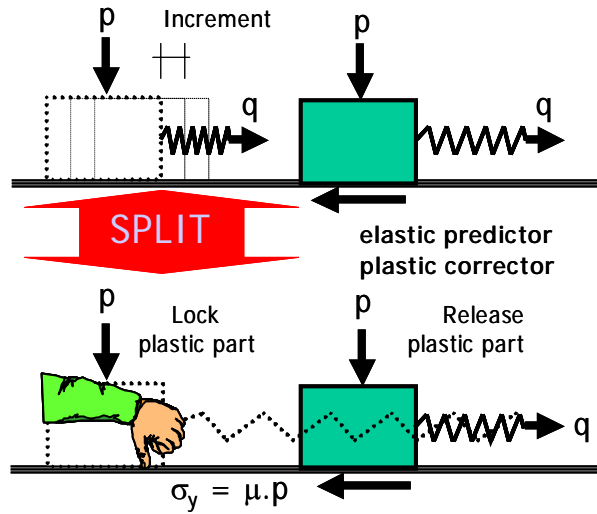
Figure 7.2 Schematization of operator-splitting theory

7-7-1 Time discretization

According to ordinary sub-incrementation technique for numerical integration, Forward-Euler difference is almost in practice giving the series of sub-increments. Though Backward-Euler difference is superior to that of explicit method by providing the iterative scheme with a quadratic rate of convergence, formulations driven by Forward-Euler are simpler than Backward-Euler, which is complex and depends crucially on the particular constitutive model chosen. Herein, the integration algorithm applicable to the Sekiguchi-Ohta model is presented. Refer to Eq.(7.15),

$$\dot{\boldsymbol{\varepsilon}}^e = \dot{\boldsymbol{\varepsilon}} - \gamma\frac{\partial f}{\partial \boldsymbol{\sigma}'} \tag{7.73}$$

The integration to Eq.(7.73) within the time interval $[t_n, t_{n+1}=t_n+\Delta t]$ can be approximated using Backward-Euler

differential scheme where plastic strain increments and hardening variable are calculated at the end of the step.

$$\mathbf{\varepsilon}_{n+1} = \mathbf{\varepsilon}_n + \Delta\mathbf{\varepsilon}, \qquad \mathbf{\varepsilon}_{n+1}^p = \mathbf{\varepsilon}_n^p + \Delta\gamma_{n+1}\left\{\frac{\partial f}{\partial\mathbf{\sigma}'}\right\}_{n+1} \tag{7.74},(7.75)$$

where $\mathbf{\varepsilon}_{n+1} = \mathbf{\varepsilon}(t_{n+1})$, $\Delta\gamma_{n+1} = \gamma_{n+1}\Delta t$, $\Delta\mathbf{\varepsilon} = \dot{\mathbf{\varepsilon}}\Delta t$

Subtraction of Eq.(7.74) by (7.75) obtains a current elastic strain tensor,

$$\mathbf{\varepsilon}_{n+1}^e = \mathbf{\varepsilon}^{tr} - \Delta\gamma_{n+1}\left\{\frac{\partial f}{\partial\mathbf{\sigma}'}\right\}_{n+1} \tag{7.76}$$

$$\mathbf{\varepsilon}^{tr} = \mathbf{\varepsilon}_n^e + \Delta\mathbf{\varepsilon} \tag{7.77}$$

$\mathbf{\varepsilon}^{tr}$ is a trial strain given by geometric update of the imposed displacement increment over the time step. $\Delta\gamma$ is taken as zero in elastic predictor step. Stresses are updated correspondingly,

$$p'_{n+1} = p'_n \exp(\frac{\varepsilon_{v\,n+1}^e - \varepsilon_{v\,n}^e}{\overline{\kappa}}) \tag{7.78}$$

$$\mathbf{s}_{n+1} = \mathbf{s}_n + 2G_s(p'_{c\,n+1}, p'_{c\,n})\left\{\mathbf{\varepsilon}_{d\,n+1}^e - \mathbf{\varepsilon}_{d\,n}^e\right\} \tag{7.79}$$

Update state variables are summarized in Box 7.3.

Box 7.3 Updated state variables

> Stress update
>
> $$p'_{n+1} = p'_n \exp(\frac{\varepsilon_{v\,n+1}^e - \varepsilon_{v\,n}^e}{\overline{\kappa}})$$
>
> $$\mathbf{s}_{n+1} = \mathbf{s}_n + 2G_s(p'_{c\,n+1}, p'_{c\,n})\left\{\mathbf{\varepsilon}_{d\,n+1}^e - \mathbf{\varepsilon}_{d\,n}^e\right\}$$
>
> Stress-hardening parameter update
>
> $$p'_{c\,n+1} = p'_{c\,n} \exp(\frac{\varepsilon_{v\,n+1}^p - \varepsilon_{v\,n}^p}{\overline{\lambda} - \overline{\kappa}})$$

7-7-2 Linearization

The goal of this section is to solve Eq.(7.76) for $\mathbf{\varepsilon}^e$ in strain space constrained by the discrete form of Kuhn-Tucker conditions given by

$$\Delta\gamma_{n+1} \geq 0 ; f_{n+1}(\mathbf{\sigma}', p'_c) \leq 0 ; \Delta\gamma_{n+1}.f_{n+1}(\mathbf{\sigma}', p'_c) = 0 \tag{7.80}$$

The solution can be achieved iteratively by Newton-Raphson method assigned on a set of equations below with p'_c fixed.

Unknown vector; $$\mathbf{x} = \left\{\begin{array}{c}\mathbf{\varepsilon}_{n+1}^e \\ \Delta\gamma_{n+1}\end{array}\right\} \tag{7.81}$$

Eq.(7.76) and yield function define a residual vector of

$$\mathbf{r} = \left\{\begin{array}{c}\overline{\mathbf{r}} \\ f_{n+1}\end{array}\right\} \qquad \text{where} \qquad \overline{\mathbf{r}} = \mathbf{\varepsilon}_{n+1}^e - \mathbf{\varepsilon}^{tr} + \Delta\gamma_{n+1}\left\{\frac{\partial f}{\partial\mathbf{\sigma}'}\right\}_{n+1} \tag{7.82}$$

Consistent Jacobian of the residuals is defined by,

$$\left\{\frac{\partial\mathbf{r}}{\partial\mathbf{x}}\right\} = \left[\begin{array}{cc}\mathbf{I} + \Delta\gamma\frac{\partial^2 f}{\partial\mathbf{\sigma}'\partial\mathbf{\sigma}'}:\mathbf{c}^e & \frac{\partial f}{\partial\mathbf{\sigma}'} \\ \frac{\partial f}{\partial\mathbf{\sigma}'}:\mathbf{c}^e & 0\end{array}\right]_{n+1} \tag{7.83}$$

Iterative scheme; $$\mathbf{x}^{(k+1)} = \mathbf{x}^{(k)} - k_c\left\{\frac{\partial\mathbf{r}}{\partial\mathbf{x}}\right\}^{-1}\cdot\mathbf{r}^{(k)} \tag{7.84}$$

Super-script k indicates an iteration number. The iteration will stop when the norm of residual vector is less than the tolerance imposed. k_c denotes a controlled step of convergence. Iterative scheme in Eq.(7.84) can be reduced to the following procedures. The algorithmic moduli Ξ replace the Hessian matrix of the Lagrangian function by reassembling

$$\mathbf{I} + \Delta\gamma_{n+1}\left\{\frac{\partial^2 f}{\partial\mathbf{\sigma}'\partial\mathbf{\sigma}'}\right\}_{n+1}:\mathbf{c}_{n+1}^e = \mathbf{\Xi}_{n+1}^{-1}:\mathbf{c}_{n+1}^e \tag{7.85}$$

Therefore, $\quad \mathbf{\Xi}_{n+1} = \left(\mathbf{c}_{n+1}^{e}{}^{-1} + \Delta\gamma_{n+1}\mathbf{H}_{n+1} \right)^{-1}$ $\qquad$ (7.86)

where $\quad \mathbf{H}_{n+1} = \left\{ \dfrac{\partial^2 f}{\partial\mathbf{\sigma}'\partial\mathbf{\sigma}'} \right\}_{n+1} \quad$ and $\quad \mathbf{h}_{n+1} = \left\{ \dfrac{\partial f}{\partial\mathbf{\sigma}'} \right\}_{n+1}$

The different of unknown vector for each iteration can be expressed by Eq.(7.87). Substitute Eq.(7.87) into Eq.(7.84) and rearrange to form Eq.(7.88),

$$\mathbf{x}^{(k+1)} - \mathbf{x}^{(k)} = \left\{ \begin{array}{c} \delta\mathbf{\varepsilon}^{e} \\ \delta\Delta\gamma \end{array} \right\} \qquad (7.87)$$

$$\begin{bmatrix} \mathbf{\Xi}^{-1}:\mathbf{c}^{e} & \mathbf{h} \\ \mathbf{h}:\mathbf{c}^{e} & 0 \end{bmatrix}_{n+1} \left\{ \begin{array}{c} \delta\mathbf{\varepsilon}^{e} \\ \delta\Delta\gamma \end{array} \right\} = -k_c \left\{ \begin{array}{c} \overline{\mathbf{r}} \\ f \end{array} \right\}_{n+1} \qquad (7.88)$$

Pre-multiply the first set of Eq.(7.88) by $\{\mathbf{h}:\mathbf{\Xi}\}_{n+1}$, then

$$\left\{ \mathbf{h}:\mathbf{c}^{e}:\delta\mathbf{\varepsilon}^{e} + \delta\Delta\gamma\,\mathbf{h}:\mathbf{\Xi}:\mathbf{h} \right\}_{n+1} = -k_c \left\{ \mathbf{h}:\mathbf{\Xi}:\overline{\mathbf{r}} \right\}_{n+1} \qquad (7.89)$$

$$\left(\mathbf{h}:\mathbf{c}^{e}:\delta\mathbf{\varepsilon}^{e} \right)_{n+1} = -k_c f_{n+1} \qquad (7.90)$$

Solve for $\delta\Delta\gamma$ by substituting R.H.S of Eq.(7.90) to Eq.(7.89). $\delta\mathbf{\varepsilon}^{e}$ can be solved by substitution of $\delta\Delta\gamma$ in Eq.(7.89) to the first set of Eq.(7.88). The difference of the increments of consistency parameter and elastic strain are as follow,

$$\delta\Delta\gamma = k_c \left(\frac{f - \mathbf{h}:\mathbf{\Xi}:\overline{\mathbf{r}}}{\mathbf{h}:\mathbf{\Xi}:\mathbf{h}} \right)_{n+1} \qquad (7.91)$$

$$\delta\mathbf{\varepsilon}^{e} = \left\{ -\mathbf{c}^{e^{-1}}:\mathbf{\Xi}:\left(k_c\overline{\mathbf{r}} + \delta\Delta\gamma\,\mathbf{h} \right) \right\}_{n+1} \qquad (7.92)$$

According to the previous research [14], a controlled-step of convergence is suggested by $k_c=3/4$ to refrain iteration from the ill convergent direction. Update the unknown variables by,

$$\Delta\gamma_{n+1}^{(k+1)} = \Delta\gamma_{n+1}^{(k)} + \delta\Delta\gamma \qquad (7.93)$$

$$\mathbf{\varepsilon}_{n+1}^{e\,(k+1)} = \mathbf{\varepsilon}_{n}^{e\,(k+1)} + \delta\mathbf{\varepsilon}^{e} \qquad (7.94)$$

$$\varepsilon_{v\,n+1}^{e\,(k+1)} = tr(\mathbf{\varepsilon}_{n+1}^{e\,(k+1)}) , \quad \mathbf{\varepsilon}_{d\,n+1}^{e\,(k+1)} = \mathbf{A}:\mathbf{\varepsilon}_{n+1}^{e\,(k+1)} \qquad (7.95),(7.96)$$

$$\varepsilon_{v\,n+1}^{p\,(k+1)} = tr\left(\mathbf{\varepsilon}_{n+1} - \mathbf{\varepsilon}_{n+1}^{e\,(k+1)} \right) \qquad (7.97)$$

$$p'_{c\,n+1}{}^{(k+1)} = p'_{c\,n} \exp(\frac{\varepsilon_{v\,n+1}^{p\,(k+1)} - \varepsilon_{v\,n}^{p}}{\overline{\lambda} - \overline{\kappa}}) \qquad (7.98)$$

$$p'_{n+1}{}^{(k+1)} = p'_{n} \exp(\frac{\varepsilon_{v\,n+1}^{e\,(k+1)} - \varepsilon_{v\,n}^{e}}{\overline{\kappa}}) \qquad (7.99)$$

$$\mathbf{s}_{n+1}^{(k+1)} = \mathbf{s}_{n} + 2G_s(p'_{c\,n+1}{}^{(k+1)}, p'_{c\,n})\left\{ \mathbf{\varepsilon}_{d\,n+1}^{e\,(k+1)} - \mathbf{\varepsilon}_{d\,n}^{e} \right\} \qquad (7.100)$$

The iterative loop of Eq.(7.84) corresponds to the Closest Point Projection (CPP) method. To bypass the need for computing the gradients in Eq.(7.83), Cutting-Plane (CP) method using an explicit procedure is developed involving quasi-Newton method [6]. CP algorithm applicable to the Sekiguchi-Ohta is available in the previous research [14]. It is obvious that CPP is superior to CP in accuracy and stability in particular for a large step increment [9]. Box 7.4 contains detailed procedures of single/multiple-step CPP method.

7-8 Numerical examples

In order to evaluate the performance of the algorithm, the numerical examples based on two-invariant stress space problem of consolidated undrained test (CU test) and unconsolidated undrained test (UU test) were performed by a strain-controlled axial compression to a maximum axial strain of 10%. Soil parameters were adopted from soil reports of the northern line of Bangkok initial subway project [28]. The systematic parameter determination suggested by Iizuka and Ohta [29] (1987) was used to determine soil parameters for calculation as listed in Table 1. The tolerances, TOL_1 and TOL_2, were set to 10^{-5}. Verification was done by comparisons with a closed-form solutions derived from the constitutive equations as well as exact results of both sub-stepping (SS) and CPP methods generated by a series of very small increments of imposed strain.

Box 7.4 Closest Point Projection iterative scheme

1. Input: $\boldsymbol{\delta\varepsilon}, \boldsymbol{\sigma'}_n, \boldsymbol{\varepsilon}_n, \boldsymbol{\varepsilon}_n^p, p'_{cn}$

2. Initialize: $k = 0$, $\Delta\gamma_{n+1}^{(k)} = 0$

$\boldsymbol{\varepsilon}_n^e = \boldsymbol{\varepsilon}_n - \boldsymbol{\varepsilon}_n^p$, $\boldsymbol{\varepsilon}_{n+1} = \boldsymbol{\varepsilon}_n + \boldsymbol{\delta\varepsilon}$, $\boldsymbol{\delta\varepsilon}_{n+1}^{p(k)} = \mathbf{0}$,

$\varepsilon_{vn+1} = tr(\boldsymbol{\varepsilon}_{n+1})$, $\varepsilon_{dn+1} = \mathbf{A} : \boldsymbol{\varepsilon}_{n+1}$,

$\varepsilon_{vn}^e = tr(\boldsymbol{\varepsilon}_n^e)$, $\varepsilon_{dn}^e = \mathbf{A} : \boldsymbol{\varepsilon}_n^e$, $\varepsilon_{vn}^p = tr(\boldsymbol{\varepsilon}_n^e)$

3. Elastic predictor:

$\boldsymbol{\varepsilon}^{tr} = \boldsymbol{\varepsilon}_n^e + \boldsymbol{\delta\varepsilon}$, $\boldsymbol{\varepsilon}_{n+1}^{e(k)} = \boldsymbol{\varepsilon}^{tr}$

$\boldsymbol{\varepsilon}_{n+1}^{p(k)} = \boldsymbol{\varepsilon}_n^p + \boldsymbol{\delta\varepsilon}_{n+1}^{p(k)}$, $\varepsilon_{vn+1}^{e(k)} = tr(\boldsymbol{\varepsilon}_{n+1}^{e(k)})$

$\boldsymbol{\varepsilon}_{dn+1}^{e(k)} = \mathbf{A} : \boldsymbol{\varepsilon}_{n+1}^{e(k)}$, $\varepsilon_{vn+1}^{p(k)} = tr(\boldsymbol{\varepsilon}_{n+1}^{p(k)})$

$\boldsymbol{\varepsilon}_{dn+1}^{p(k)} = \mathbf{A} : \boldsymbol{\varepsilon}_{n+1}^{p(k)}$

$p'^{(k)}_{cn+1} = p'_{cn} \exp(\dfrac{\varepsilon_{vn+1}^{p(k)} - \varepsilon_{vn}^p}{\bar{\lambda} - \bar{\kappa}})$

$p'^{tr} = p'^{(k)}_{n+1} = p'_n \exp(\dfrac{\varepsilon_{vn+1}^{e(k)} - \varepsilon_{vn}^e}{\bar{\kappa}})$

$\mathbf{s}^{tr} = \mathbf{s}_{n+1}^{(k)} = \mathbf{s}_n + 2G_s(p'^{(k)}_{cn+1}, p'_{cn})\{\boldsymbol{\varepsilon}_{dn+1}^{e(k)} - \boldsymbol{\varepsilon}_{dn}^e\}$

$\boldsymbol{\sigma}_{n+1}^{\prime(k)} = p'^{(k)}_{n+1}\mathbf{1} + \mathbf{s}_{n+1}^{(k)}$

4. Check yield function and residuals:

$f_{n+1} = f(\boldsymbol{\sigma}_{n+1}^{\prime(k)}, p'^{(k)}_{cn+1})$

$\mathbf{h}_{n+1} = \left\{\dfrac{\partial f}{\partial \boldsymbol{\sigma'}}\right\}_{n+1}$, $\mathbf{H}_{n+1} = \left\{\dfrac{\partial^2 f}{\partial \boldsymbol{\sigma'}\partial \boldsymbol{\sigma'}}\right\}_{n+1}$

$\bar{\mathbf{r}} = \boldsymbol{\varepsilon}_{n+1}^{e(k)} - \boldsymbol{\varepsilon}^{tr} + \Delta\gamma_{n+1}^{(k)}\mathbf{h}_{n+1}$

IF $f_{n+1} < TOL_1$ AND $\|\bar{\mathbf{r}}\| < TOL_2$

THEN Set $(\bullet)_{n+1} = (\bullet)_{n+1}^{(k)}$ and GOTO 9

5. Algorithmic moduli:

$\mathbf{c}_{n+1}^e = K(p'^{(k)}_{n+1})\mathbf{1}\otimes\mathbf{1} + 2G_s(p'^{(k)}_{cn+1}, p'_{cn})\mathbf{A}$

$\boldsymbol{\Xi}_{n+1} = \left(\mathbf{c}_{n+1}^{e^{-1}} + \Delta\gamma_{n+1}^{(k)}\mathbf{H}_{n+1}\right)^{-1}$

6. Plastic corrector:

$\delta\Delta\gamma_{n+1}^{(k)} = k_c\left(\dfrac{f - \mathbf{h}:\boldsymbol{\Xi}:\bar{\mathbf{r}}}{\mathbf{h}:\boldsymbol{\Xi}:\mathbf{h}}\right)_{n+1}^{(k)}$

$\boldsymbol{\delta\varepsilon}_{n+1}^{(k)} = \left\{-\mathbf{c}^{e^{-1}}:\boldsymbol{\Xi}:\left(k_c\bar{\mathbf{r}} + \delta\Delta\gamma\mathbf{h}\right)\right\}_{n+1}^{(k)}$

7. Update solutions:

$\boldsymbol{\varepsilon}_{n+1}^{e(k+1)} = \boldsymbol{\varepsilon}_{n+1}^{e(k)} + \boldsymbol{\delta\varepsilon}_{n+1}^{e(k)}$,

$\Delta\gamma_{n+1}^{(k+1)} = \Delta\gamma_{n+1}^{(k)} + \delta\Delta\gamma_{n+1}^{(k)}$

$\boldsymbol{\delta\varepsilon}_{n+1}^{p(k+1)} = \boldsymbol{\varepsilon}^{tr} - \boldsymbol{\varepsilon}_{n+1}^{e(k+1)}$,

$\boldsymbol{\varepsilon}_{n+1}^{p(k+1)} = \boldsymbol{\varepsilon}_n^p + \boldsymbol{\delta\varepsilon}_{n+1}^{p(k+1)}$

$\varepsilon_{vn+1}^{e(k+1)} = tr(\boldsymbol{\varepsilon}_{n+1}^{e(k+1)})$, $\boldsymbol{\varepsilon}_{dn+1}^{e(k+1)} = \mathbf{A}:\boldsymbol{\varepsilon}_{n+1}^{e(k+1)}$

$\varepsilon_{vn+1}^{p(k+1)} = tr(\boldsymbol{\varepsilon}_{n+1}^{p(k+1)})$, $\boldsymbol{\varepsilon}_{dn+1}^{p(k+1)} = \mathbf{A}:\boldsymbol{\varepsilon}_{n+1}^{p(k+1)}$

$p'^{(k+1)}_{cn+1} = p'_{cn}\exp(\dfrac{\varepsilon_{vn+1}^{p(k+1)} - \varepsilon_{vn}^p}{\bar{\lambda} - \bar{\kappa}})$

$p'^{(k+1)}_{n+1} = p'_n\exp(\dfrac{\varepsilon_{vn+1}^{e(k+1)} - \varepsilon_{vn}^e}{\bar{\kappa}})$

$\mathbf{s}_{n+1}^{(k+1)} = \mathbf{s}_n + 2G_s(p'^{(k+1)}_{cn+1}, p'_{cn})\{\boldsymbol{\varepsilon}_{dn+1}^{e(k+1)} - \boldsymbol{\varepsilon}_{dn}^e\}$

$\boldsymbol{\sigma}_{n+1}^{\prime(k+1)} = p'^{(k+1)}_{n+1}\mathbf{1} + \mathbf{s}_{n+1}^{(k+1)}$

8. Set $k = k+1$ and GOTO 4

9. Output: $\boldsymbol{\sigma'}_{n+1}, \boldsymbol{\varepsilon}_{n+1}, \boldsymbol{\varepsilon}_{n+1}^p, p'_{cn+1}$

and EXIT

Table 7.1 Soil parameters

Parameter	Description	Value
D	Coefficient of dilatancy	0.102
Λ	Irreversibility ratio	0.825
M	Critical state parameter	1.12
ν'	Effective Poisson's ratio	0.38
K_o	Coefficient of earth pressure (NC)	0.61
K_i	Coefficient of earth pressure (in-situ)	0.70
λ	Compression index	0.376
e_o	Void ratio at σ'_{vo}	1.735
σ'_{vo}	Eff. preconsolidation pressure (kN/m^2)	100
σ'_{vi}	Eff. overburden pressure (kN/m^2)	69

7-8-1 Accuracy assessment

In practice, the number of sub-increments is repeatedly applied to algorithms for improving the accuracy. To evaluate the calculation performance, a series of analyzes were performed for CU test by SS (using Forward-Euler difference) and CPP methods (using Backward-Euler difference) with a single step and incrementally multiple steps:- 5, 20, 50 and 1000 steps, in other words, with strain increments:- 2%, 0.5%, 0.2% and 0.01% respectively. The closed-form solutions relevant to the problem can be derived by directly integrating the constitutive equations over the imposed stress paths. These solutions are given for deviatoric stress and axial strain as functions of effective mean stress shown in Eq.(7.101),(7.102). The comparisons with SS and CPP methods are arranged in Figure 7.3.
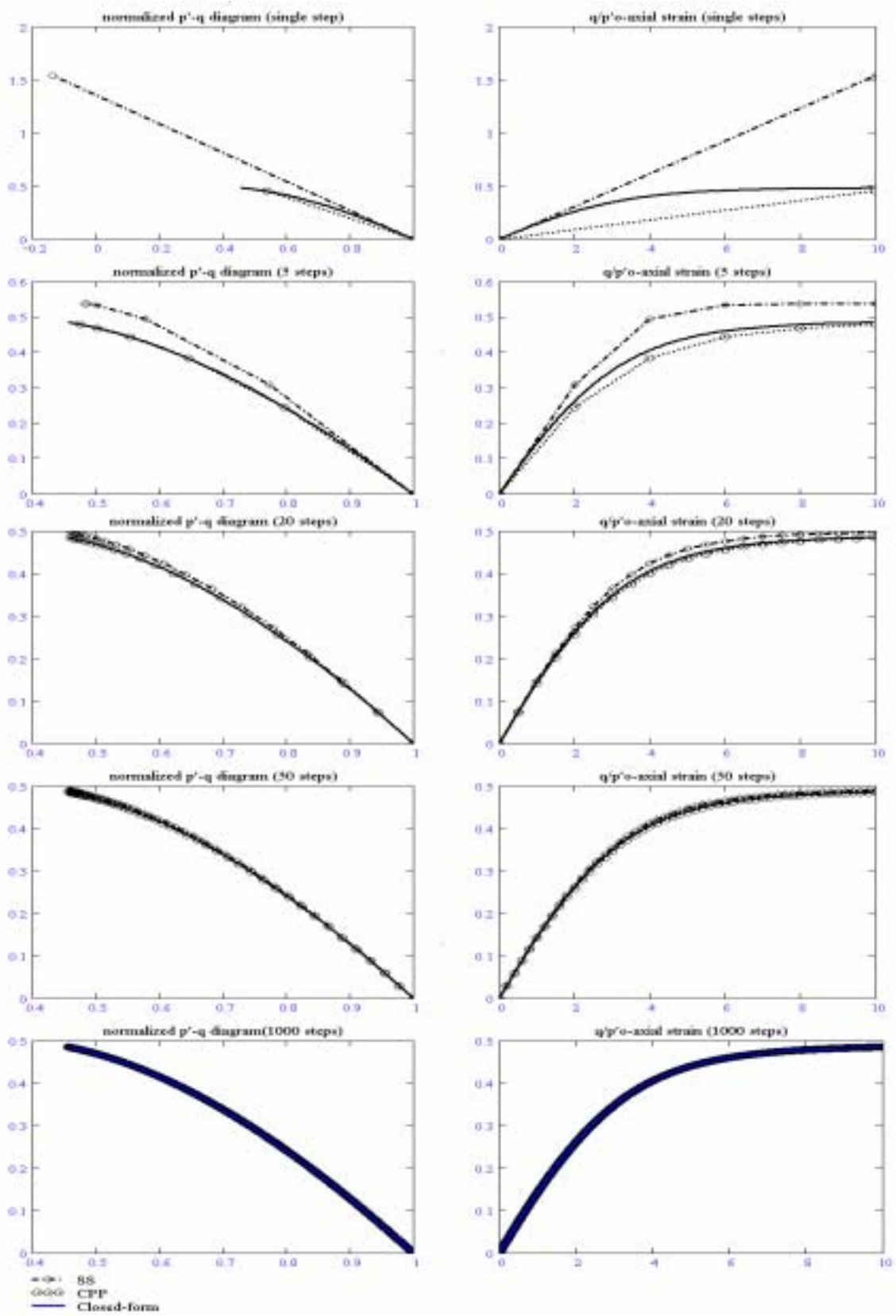
Figure 7.3 Numerical results for CU test generated by single/multiple step solutions by SS and CPP methods in compare with closed-form solution

$$q = \left(\eta_o - \frac{M}{\Lambda} \ln\left(\frac{p'}{p'_o} \right) \right) p'$$

(7.101)

$$\varepsilon_a = \left(1 - \left(\frac{p'}{p'_o} \right)^{\frac{1}{\Lambda}} \right) \cdot \left(\frac{\bar{\kappa}\Lambda}{3\mu'} \left(\frac{\bar{\kappa}}{D} - \eta_o \right) \right) + \frac{\bar{\kappa}\Lambda}{M} \ln \left(\frac{\left(\frac{p'}{p'_o} \right)^{\frac{-M^2}{3\mu'\Lambda}\left(\frac{p'}{p'_o} \right)^{\frac{1}{\Lambda}}}}{1 + \frac{M}{\Lambda(M - \eta_o)} \ln\left(\frac{p'}{p'_o} \right)} \right)$$

(7.102)

The errors of analyzes are obviously found due to the effect of increment sizes. Therefore, the emphasis is placed on selecting the size of sub-incrementation for high accuracy. According to Figure 7.3, it is clearly seen that solutions by SS are drifted from the yield surface while those of CPP are always constrained on it. That is why the accuracy performance of CPP is substantially superior to SS for coarse increments or even a single step increment however it becomes extremely laborious for a finer step using very small sub-increments. The exact solution can be obtained by repeatedly applying the increasing numbers of sub-increments to the algorithms until there is no change in results. For 0.01% strain increment (1000 steps), numerical solutions by both CPP and SS meet the closed-form solution, thus resulting in exact solution.

7-8-2 Convergence study

Figure 7.4 and Figure 7.5 show the effective stress and stress-strain responses for UU test predicted by multiple-step SS and single- step CPP methods. The convergence performance of CPP method was tested by a single increment as large as failure axial strain of 10%. The stress update iterations started from the initial stress state inside yield surface and then moved outside by elastic predictor step. The consistency condition iteratively corrected the state variables to return back to yield surface taking damage effect on stored energy into account while internal hardening variables were updated simultaneously along the return paths. The number of iterations to satisfy the tolerance was 12. Figure 7.6 shows that the consistency parameters computed at successive iterations using the consistent Jacobian can approach to the solution with a quadratic rate of convergence.

7-8-3 Evaluation of error

The undrained shear strength, S_u, is able to determine by UU tests. Expression of undrained shear strength for ideal samples is given below (Ohta et al [30] ,1989).

$$\left(\frac{S_u}{\sigma'_{vo}} \right)_{ideal} = \frac{1 + 2K_o}{6} M \exp\left(-\Lambda + \frac{\Lambda}{M} \eta_o \right) \left(OCR \frac{1 + 2K_o}{1 + 2K_i} \right)^{\Lambda - 1}$$

(7.103)

Table 7.2 shows the results of S_u, determined by SS and CPP methods with the variation of sub-increments. Errors are evaluated by comparison with Eq.(7.103). Though SS needs as much as 1000 steps for 0.20% accuracy, a single-step CPP method needs only 12 numbers of iteration for -0.77% accuracy. Therefore, CPP method is proved to give a high accuracy and stability even a single large strain near failure is imposed.

7-9 Conclusion

The implicit integration algorithm cast in form of Closest Point Projection method in the context of strain-driven process for the inviscid Sekiguchi-Ohta model was developed. The two-invariant conservative stored energy function with damage process and choice of suitable hardening potential were proposed. A class of isotropic pressure-dependent bulk modulus and stress hardening parameter-dependent shear modulus were employed as an illustrative case of hyperelastic model required by return-mapping algorithms. The developed formulations were implemented and used in numerical analyses for CU and UU tests. The numerical results showed that CPP method could provide an effective, stable and robust integration scheme to the rate constitutive equations for any variation of imposed strain increments. The exact solutions of both CPP and SS methods can be obtained by subjecting the algorithms to very small strain increments. Verification has been done by comparisons with the closed-form solutions. The errors associates with CPP method were relatively low in compare with those of SS method even at a single large strain increment near failure. It was clear that CPP method is superior to SS method in particular when a small number of steps are applied or a large size of strain increments is used. The fundamental mathematical disciplines developed in the study will pave a way to a formulation of soil/water coupled FEM and the emerged evolution of finite deformation analysis in further research stages.
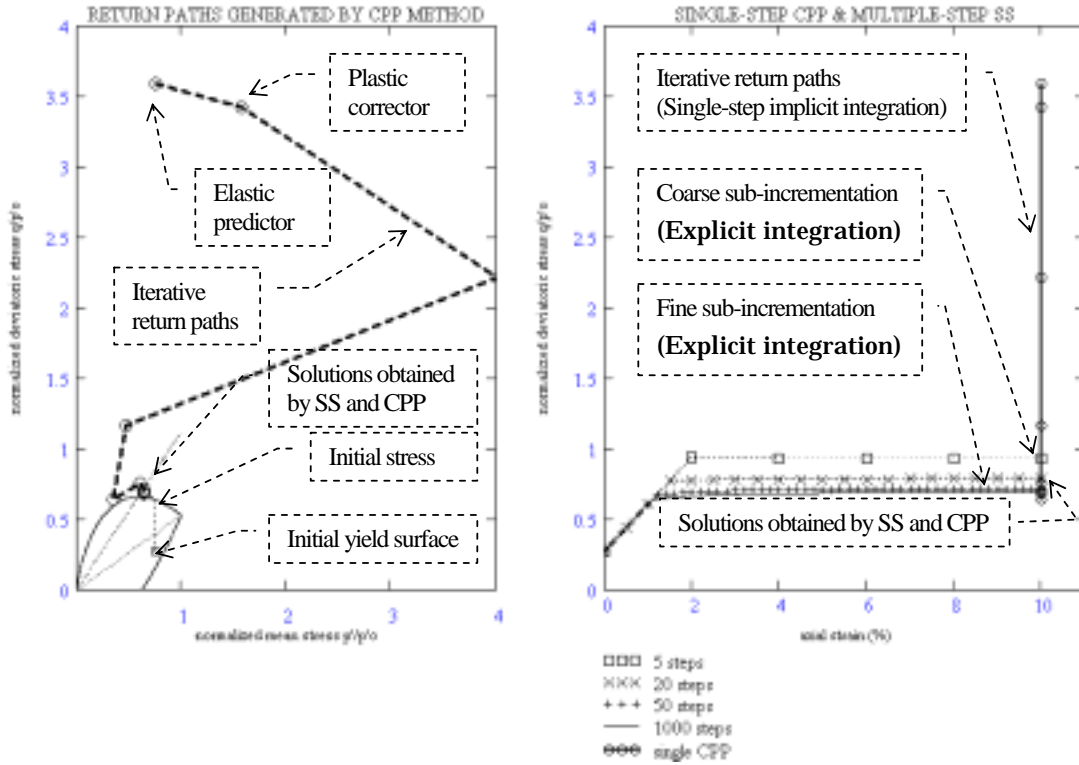
Figure 7.4 (left) Numerical results by 1000-step SS and single-step CPP methods in p'-q space for UU test at 10% axial strain
Figure 7.5 (right) Numerical results by multiple-step SS and single-step CPP methods in q-ε_a space for UU test at 10% axial strain

Table 7.2 Undrained shear strength tests (10% axial strain)

Method	Normalized strength S_u/σ'_{vo}	Error (%)
Closed-form	0.2547	0.00
SS (single step)	1.3258	420.48
SS (5 steps)	0.3443	35.16
SS (20 steps)	0.2909	14.21
SS (50 steps)	0.2639	3.60
SS (1000 steps)	0.2552	0.20
CPP (single step)	0.2528	-0.77
CPP (5 steps)	0.2543	-0.17
CPP (20 steps)	0.2545	-0.04
CPP (50 steps)	0.2546	-0.03
CPP (1000 steps)	0.2547	-0.03

SS = Sub-Stepping, CPP = Closest Point Projection
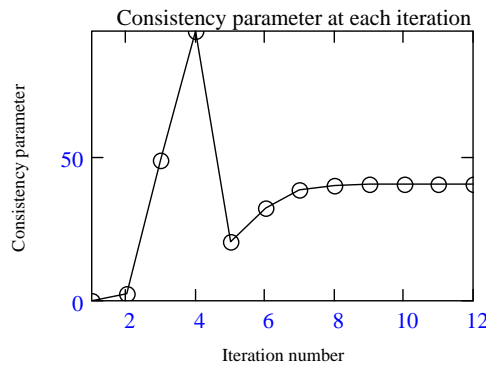
Figure 7.6 Convergence of consistency parameter approached by CPP algorithm for a single-step of 10% axial strain

7-10 References

1 Sekiguchi, H. and Ohta, H., Induced anisotropy and time dependency in clays, 9th ICSMFE, Tokyo, Constitutive equations of Soils, pp.229-238, 1977

2 Ohta, H. and Iizuka, A., Ground Response to Construction Activities, vol. 1&2, 1992

3 Nagtegaal, J.C. and De Jong, J.E., Some computational aspects of elastic-plastic large strain analysis, Int. J. Num. Meth. Engrg. 17, pp.15-41, 1981

4 Simo, J.C. and Hughes, T.J.R., Computational inelasticity, Springer, 1997

5 Suzuki, Y. and Aoyagi, R., A note on Simo's papers, private communication, 1999

6 Simo, J.C. and Ortiz, M., A unified approach to finite deformation elastoplastic analysis based on the use of hyperelasticity constitutive equations, Comput. Methods Appl. Mech. Engrg. 49, pp.221-245, 1985

7 Simo, J.C., Kennedy, J.G. and Govindjee, S., Non-smooth multisurface plasticity and viscoplasticity. Loading/unloading conditions and numerical algorithms, Int. J. Numer. Methods Engrg. 26, pp.2161-2185, 1988

8 Simo, J.C., Algorithms for static and dynamic multiplicative plasticity that preserve the classical return mapping schemes of the infinitesimal theory, Comput. Methods Appl. Mech. Engrg. 99, pp.62-112, 1992

9 Simo, J.C., Meschke, G., A new class of algorithms for classical plasticity extended to finite strains. Application to geomaterials, Comput. Mech. 11, pp.253-278, 1993

10 Borja, R.I. and Lee, S.R., Cam-Clay plasticity, Part I: Implicit integration of elasto-plastic constitutive relations, Comput. Methods Appl. Mech. Engrg. 78, pp.49-72, 1990

11 Borja, R.I., Cam-Clay plasticity, Part II: Implicit integration of constitutive equation based on a nonlinear elastic stress predictor, Comput. Methods Appl. Mech. Engrg. 88, pp.225-240, 1991

12 Borja, R.I. and Tamagnini, C., Cam-Clay plasticity, Part III: Extension of the infinitesimal model to include finite strains, Comput. Methods Appl. Mech. Engrg. 155, pp.73-95, 1998

13 Borja, R.I., Chao-Hua, L. and Francisco, J.M., Cam-Clay plasticity, Part IV: Implicit integration of anisotropic bounding surface model with nonlinear Hyperelasticity and ellipsoidal loading function, Comput. Methods Appl. Mech. Engrg. 190, pp.3293-3323, 2001

14 Pipatpongsa, T. and Ohta, H., Return-mapping algorithm for Sekiguchi-Ohta model, 2nd Inter. Summer Sym., JSCE, pp.229-232, 2000

15 Pipatpongsa, T., Ohta, H., Kobayashi, I. and Iizuka, A., Associated plastic flow at the intersection corner of plastic potential functions in soil mechanics, Proc. of 36th Japanese Nat. Conf. on Geotech. Engrg, pp.935-936, 2001

16 Pipatpongsa, T., Ohta, H., Kobayashi, I. and Iizuka, A., Dependence of K_o-value on effective internal friction angle in regard to the Sekiguchi-Ohta model, Proc. of 36th Japanese Nat. Conf. on Geotech. Engrg, pp.936-937, 2001

17 Pipatpongsa, T., Kobayashi, I., Ohta, H., and Iizuka, A., The vertex singularity in the Sekiguchi-Ohta model, 56th JSCE Annual Meeting, in press, 2001

18 Pipatpongsa, T., Ohta, H., Kobayashi, I. and Iizuka, A., Integration algorithms for soil constitutive equations with a singular hardening vertex, 3rd Inter. Summer Sym., JSCE, pp.201-204, 2001

19 Hill, R., The mathematical theory of plasticity, Oxford University Press, Oxford, U.K., 1950

20 Drucker, D.C., Some implications of work hardening and ideal plasticity, Quart. Appl. Math. 7, pp.411, 1950

21 Atkinson, J.H., An Introduction to the Mechanics of Soils and Foundations, McGRAW-HILL, London, 1993

22 Zytynski, M., Randolph, M.K., Nova, R., and Wroth, C.P., On modeling the unloading-reloading behaviour of soils, Int. J. Numer. Anal. Methods Geomech. 2, pp.87-93, 1978

23 Hueckel, T., Tutumluer, E., and Pellegrini, R., A note on non-linear elasticity of isotropic overconsolidated clays, Int. J. Numer. Anal. Methods Geomech. 16(8), pp.603-618, 1992

24 Potts, D.M. and Ganendra, D., An evaluation of substepping and implicit stress point algorithms, Comput. Methods Appl. Mech. Engrg. 119, pp.341-354, 1994

25 Houlsby, G.T., The use of variable shear modulus in elastic-plastic models for clays, Comp. And Geotech. 1, pp.3-13, 1985

26 Borja, R.I., Claudio, T. and Angelo A., Coupling plasticity and energy-conserving elasticity models for clays, Journal of Geotechnical and Geoenvironmental Engineering 123(10), pp.948-957, 1997

27 Ortiz, M. and Popov, E.P., Accuracy and stability of integration algorithms for elastoplastic constitutive relations, Int. J. Numer. Methods Engrg. 21, pp.1561-1576, 1985

28 ION Joint Venture, MRTA ISP-North Contract, Intepretative Geotechnical Report, Vol 1, Ove Arup & Partners International LTD., 1998

29 Iizuka, A. and Ohta, H., A determination procedure of input parameters in elasto-viscoplastic finite element analysis, Soils and Foundations, Vol. 27(3), pp. 71-87, 1987

30 Ohta, H., Nishihara, A, Iizuka, A., Morita, Y., Fukagawa, R. and Arai, K., Unconfined compression strength of soft clays, Proc. 12th Int. Conf. Soil Mech. & Foundation Engrg, Rio de Janeiro, Vol. 1, pp.71-74, 1989

CHAPTER 8

Consistent Tangential Stiffness Tensor

8-1 Tangent Moduli

The well-known stress-strains relation is the forth-order tensor of elastic moduli. However, in nonlinear problem, the rate relationship is rather considered and employed. As a result, the corresponding relation between rate of stress to rate of strain is called tangent moduli. In plasticity theory, many different constitutive relations can be developed to complicated elasto-plastic moduli which can include multiaxial properties, anisotropic responses, time dependent characteristics. In this section, the derivations of tangent moduli using governing equations are presented by two versions, which are continuum and discrete versions.

8-1-1 Rate form

The governing equations in rate form are reinstated. $\mathbf{r}$ is plastic flow direction which can relate to plastic flow potential or flow rule. γ is a scalar plastic flow rate or consistency parameter. $\dot{\mathbf{q}}$ is rate of hardening variables. $\mathbf{h}$ defines a type of hardening.

In general non-associative model, plastic flow is defined by

$$\dot{\boldsymbol{\varepsilon}}^p = \gamma \mathbf{r} \tag{8.1}$$

Rate of stress and elastic strains is related by elastic moduli,

$$\dot{\boldsymbol{\sigma}} = \mathbf{c}^e : (\dot{\boldsymbol{\varepsilon}} - \dot{\boldsymbol{\varepsilon}}^p) \tag{8.2}$$

The evolution of hardening or hardening law,

$$\dot{\mathbf{q}} = \gamma \mathbf{h} \tag{8.3}$$

Yield function,

$$f(\boldsymbol{\sigma}, \mathbf{q}) = 0 \tag{8.4}$$

Kuhn-Tucker loading/unloading complementarity condition

$$\gamma \geq 0 \; ; f \leq 0 \; ; \gamma f = 0 \tag{8.5}$$

8-1-2 Continuum tangent moduli

Under loading condition, Eq.(8.5) are satisfied. By a result of Kuhn-Tucker condition, consistency condition is developed by means of,

$$\dot{f}(\boldsymbol{\sigma}, \mathbf{q}) = \partial_{\boldsymbol{\sigma}} f : \dot{\boldsymbol{\sigma}} + \partial_{\mathbf{q}} f : \dot{\mathbf{q}} = 0 \tag{8.6}$$

Refer to Eq.(8.1)-(8.3), scalar Eq.(8.6) becomes

$$\partial_{\boldsymbol{\sigma}} f : \mathbf{c}^e : (\dot{\boldsymbol{\varepsilon}} - \gamma \mathbf{r}) + \partial_{\mathbf{q}} f : \gamma \mathbf{h} = 0 \tag{8.7}$$

Solve for consistency parameter,

$$\gamma = \frac{\partial_{\boldsymbol{\sigma}} f : \mathbf{c}^e : \dot{\boldsymbol{\varepsilon}}}{\partial_{\boldsymbol{\sigma}} f : \mathbf{c}^e : \mathbf{r} - \partial_{\mathbf{q}} f : \mathbf{h}} \tag{8.8}$$

Substitute to Eq.(8.2), yield

$$\dot{\boldsymbol{\sigma}} = \mathbf{c}^e : \left(\dot{\boldsymbol{\varepsilon}} - \frac{\partial_{\boldsymbol{\sigma}} f : \mathbf{c}^e : \dot{\boldsymbol{\varepsilon}}}{\partial_{\boldsymbol{\sigma}} f : \mathbf{c}^e : \mathbf{r} - \partial_{\mathbf{q}} f : \mathbf{h}} \mathbf{r} \right) = \mathbf{c}^{ep} : \dot{\boldsymbol{\varepsilon}} \tag{8.9}$$

The continuum tangent moduli are derived as,

$$\mathbf{c}^{ep} = \mathbf{c}^e - \frac{\mathbf{c}^e : \mathbf{r} \otimes \partial_{\boldsymbol{\sigma}} f : \mathbf{c}^e}{\partial_{\boldsymbol{\sigma}} f : \mathbf{c}^e : \mathbf{r} - \partial_{\mathbf{q}} f : \mathbf{h}} \tag{8.10}$$

For associative flow and evolution law, $\mathbf{r} = \partial_{\boldsymbol{\sigma}} f$, $\mathbf{h} = \partial_{\mathbf{q}} f$

$$\mathbf{c}^{ep} = \mathbf{c}^e - \frac{\mathbf{c}^e : \partial_{\boldsymbol{\sigma}} f \otimes \partial_{\boldsymbol{\sigma}} f : \mathbf{c}^e}{\partial_{\boldsymbol{\sigma}} f : \mathbf{c}^e : \partial_{\boldsymbol{\sigma}} f - \partial_{\mathbf{q}} f : \partial_{\mathbf{q}} f} \tag{8.11}$$

8-1-3 Forward Euler

By driven variable $\Delta\boldsymbol{\varepsilon} = \Delta t \dot{\boldsymbol{\varepsilon}}$ as an increment of strain, and a given set of $\left\{ \boldsymbol{\varepsilon}_n, \boldsymbol{\varepsilon}_n^p, \boldsymbol{\sigma}_n, \mathbf{q}_n \right\}$ as initial conditions, the continuum problem is transformed into a discrete problem by applying difference schemes that are explicit forward-Euler and implicit backward-Euler. The subscript n+1 refers to the current time step while n refers to the previous time step. The current strain can be given by,

$$\boldsymbol{\varepsilon}_{n+1} = \boldsymbol{\varepsilon}_n + \Delta\boldsymbol{\varepsilon} \tag{8.12}$$

By Forward-Euler scheme, continuum Eq.(8.1)-(8.3) can be discretized by,

$$\boldsymbol{\varepsilon}_{n+1}^p = \boldsymbol{\varepsilon}_n^p + \Delta\gamma_n \mathbf{r}_n \tag{8.13}$$

$$\boldsymbol{\sigma}_{n+1} = \mathbf{c}^e : (\boldsymbol{\varepsilon}_{n+1} - \boldsymbol{\varepsilon}_{n+1}^p) \tag{8.14}$$

$$\mathbf{q}_{n+1} = \mathbf{q}_n + \Delta\gamma_n \mathbf{h}_n \tag{8.15}$$

Using a result of Eq.(8.8), consistency parameter at previous step is computed by

$$\Delta\gamma_n = \frac{\partial_{\boldsymbol{\sigma}} f : \mathbf{c}^e : \Delta\boldsymbol{\varepsilon}}{\partial_{\boldsymbol{\sigma}} f : \mathbf{c}^e : \mathbf{r} - \partial_{\mathbf{q}} f : \mathbf{h}}\Bigg|_{\boldsymbol{\sigma}=\boldsymbol{\sigma}_n, \mathbf{q}=\mathbf{q}_n} \tag{8.16}$$

Using a result of Eq.(8.10), the current stress can be computed by,

$$\boldsymbol{\sigma}_{n+1} = \boldsymbol{\sigma}_n + \mathbf{c}^{ep} : \Delta\boldsymbol{\varepsilon} \tag{8.17}$$

$$\mathbf{c}^{ep} = \mathbf{c}^e - \frac{\mathbf{c}^e : \mathbf{r} \otimes \partial_{\boldsymbol{\sigma}} f : \mathbf{c}^e}{\partial_{\boldsymbol{\sigma}} f : \mathbf{c}^e : \mathbf{r} - \partial_{\mathbf{q}} f : \mathbf{h}}\Bigg|_{\boldsymbol{\sigma}=\boldsymbol{\sigma}_n, \mathbf{q}=\mathbf{q}_n} \tag{8.18}$$

Since Eq.(8.4) is not employed by this determination, as a result it is found that,

$$f(\boldsymbol{\sigma}_{n+1}, \mathbf{q}_{n+1}) \neq 0 \tag{8.19. The form}$$

of continuum tangent moduli shown in Eq.(8.18) is usually applied in incremental FEM. However the solution would meet inaccuracy if large steps of loading are involved.

8-1-4 Backward Euler

By Backward-Euler scheme, a driven variable shown in Eq.(8.12) together with initial conditions $\left\{\boldsymbol{\varepsilon}_n, \boldsymbol{\varepsilon}_n^p, \boldsymbol{\sigma}_n, \mathbf{q}_n\right\}$, a set of continuum Eq.(8.1)-(8.5) can be discretized by,

$$\boldsymbol{\sigma}_{n+1} - \boldsymbol{\sigma}_n = \mathbf{c}^e : (\Delta\boldsymbol{\varepsilon} - \Delta\boldsymbol{\varepsilon}^p) \tag{8.20}$$

Increment of plastic strain and hardening variable are given in corresponding to the state at current time step,

$$\boldsymbol{\varepsilon}_{n+1}^p - \boldsymbol{\varepsilon}_n^p = \Delta\gamma_{n+1} \mathbf{r}_{n+1} \tag{8.21}$$

$$\mathbf{q}_{n+1} - \mathbf{q}_n = \Delta\gamma_{n+1} \mathbf{h}_{n+1} \tag{8.22}$$

The value of yield function and Kuhn-Tucker conditions are marked at the state at current time step,

$$f_{n+1} = f(\boldsymbol{\sigma}_{n+1}, \mathbf{q}_{n+1}) \tag{8.23}$$

$$\Delta\gamma_{n+1} \geq 0 \; ; \; f_{n+1} \leq 0 \; ; \; \Delta\gamma_{n+1} f_{n+1} = 0 \tag{8.24}$$

Since a set of above equations or algorithms usually forms in non-linear system. A linearization of return-mapping algorithm carried out on Eq. (8.20)-(8.24), which are those of previous formulations done in Chapter 6, results in the determination of $\Delta\gamma_{n+1}$ by Newton method. The implementation of all variables satisfied with all governing equations at the current states will be used to determine the consistent tangent moduli.

8-1-5 Consistent tangent moduli

By a second exact linearization of return-mapping algorithm, the consistent elastoplastic tangent moduli are developed. These moduli relate incremental strains and incremental stresses and play a crucial role in the overall solution strategy of a boundar-value problem. The use of consistent tangent moduli are essential to preserve the quadratic rate of asymptotic convergence that characterizes Newton's method.

In case of plastic loading, the condition in Eq.(8.24); $\Delta\gamma_{n+1} \geq 0 \; ; \; f_{n+1} \leq 0 \; ; \; \Delta\gamma_{n+1} f_{n+1} = 0$ are satisfied.

By differentiating the algorithms shown in Eq.(8.20)-(8.23), one obtains

$$d\boldsymbol{\sigma}_{n+1} = \mathbf{c}^e : \left(d\boldsymbol{\varepsilon}_{n+1} - d\boldsymbol{\varepsilon}_{n+1}^p\right) \tag{8.25}$$

$$d\boldsymbol{\varepsilon}_{n+1}^p = d\Delta\gamma_{n+1} \mathbf{r}_{n+1} + \Delta\gamma_{n+1} d\mathbf{r}_{n+1} \tag{8.26}$$

$$d\mathbf{q}_{n+1} = d\Delta\gamma_{n+1} \mathbf{h}_{n+1} + \Delta\gamma_{n+1} d\mathbf{h}_{n+1} \tag{8.27}$$

$$df_{n+1} = \partial_{\boldsymbol{\sigma}} f : d\boldsymbol{\sigma}_{n+1} + \partial_{\mathbf{q}} f : d\mathbf{q}_{n+1} = 0 \tag{8.28}$$

In short, Eq.(8.28), which is equivalent to consistency condition, can be written by,

$$\begin{pmatrix} \partial_{\boldsymbol{\sigma}} f \\ \partial_{\mathbf{q}} f \end{pmatrix} : \begin{pmatrix} d\boldsymbol{\sigma}_{n+1} \\ d\mathbf{q}_{n+1} \end{pmatrix} = 0 \tag{8.29}$$

Variational forms given in Eq.(8.25)-(8.29) are kept on unknown $d\boldsymbol{\sigma}_{n+1}, d\boldsymbol{\varepsilon}_{n+1}^p, d\mathbf{q}_{n+1}, d\Delta\gamma_{n+1}$.

Substitution of Eq.(8.26) into Eq.(8.25) together with manipulation of Eq.(8.25) and Eq.(8.27) lead to,

$$\mathbf{c}^{e^{-1}} : d\boldsymbol{\sigma}_{n+1} = d\boldsymbol{\varepsilon}_{n+1} - d\Delta\gamma_{n+1} \mathbf{r}_{n+1} - \Delta\gamma_{n+1} d\mathbf{r}_{n+1} \tag{8.30}$$

$$-d\mathbf{q}_{n+1} = -d\Delta\gamma_{n+1} \mathbf{h}_{n+1} - \Delta\gamma_{n+1} d\mathbf{h}_{n+1} \tag{8.31}$$

Grouping Eq.(8.30)-(8.31), yields

$$\begin{bmatrix} \mathbf{c}^{e^{-1}} & 0 \\ 0 & -\mathbf{I} \end{bmatrix} : \begin{pmatrix} d\boldsymbol{\sigma}_{n+1} \\ d\mathbf{q}_{n+1} \end{pmatrix} = \begin{pmatrix} d\boldsymbol{\varepsilon}_{n+1} \\ 0 \end{pmatrix} - d\Delta\gamma_{n+1} \begin{pmatrix} \mathbf{r}_{n+1} \\ \mathbf{h}_{n+1} \end{pmatrix} - \Delta\gamma_{n+1} \begin{pmatrix} d\mathbf{r}_{n+1} \\ d\mathbf{h}_{n+1} \end{pmatrix} \tag{8.32}$$

Because $\mathbf{r} = \mathbf{r}(\boldsymbol{\sigma}, \mathbf{q})$ and $\mathbf{h} = \mathbf{h}(\boldsymbol{\sigma}, \mathbf{q})$. By Chain rule, the components on Eq.(8.32) can be expanded to,

$$\begin{pmatrix} d\mathbf{r}_{n+1} \\ d\mathbf{h}_{n+1} \end{pmatrix} = \begin{bmatrix} \partial_{\boldsymbol{\sigma}}\mathbf{r} & \partial_{\mathbf{q}}\mathbf{r} \\ \partial_{\boldsymbol{\sigma}}\mathbf{h} & \partial_{\mathbf{q}}\mathbf{h} \end{bmatrix} \begin{pmatrix} d\boldsymbol{\sigma}_{n+1} \\ d\mathbf{q}_{n+1} \end{pmatrix} \tag{8.33}$$

Substitution of Eq.(8.33) into Eq.(8.32), with some equation manipulation, the resulting equation becomes,

$$\begin{bmatrix} \mathbf{c}^{e-1} + \Delta\gamma_{n+1}\mathbf{r}_{\boldsymbol{\sigma}} & \Delta\gamma_{n+1}\mathbf{r}_{\mathbf{q}} \\ \Delta\gamma_{n+1}\mathbf{h}_{\boldsymbol{\sigma}} & -\mathbf{I} + \Delta\gamma_{n+1}\mathbf{h}_{\mathbf{q}} \end{bmatrix} : \begin{pmatrix} d\boldsymbol{\sigma}_{n+1} \\ d\mathbf{q}_{n+1} \end{pmatrix} = \begin{pmatrix} d\boldsymbol{\varepsilon}_{n+1} \\ 0 \end{pmatrix} - d\Delta\gamma_{n+1} \begin{pmatrix} \mathbf{r}_{n+1} \\ \mathbf{h}_{n+1} \end{pmatrix} \tag{8.34}$$

To reduce the terms of equation, define the following matrices as,

$$\boldsymbol{\Xi} \equiv \left[\mathbf{c}^{e-1} + \Delta\gamma_{n+1}\partial_{\boldsymbol{\sigma}}\mathbf{r} \right]^{-1} \tag{8.35}$$

$$\mathbf{Y} \equiv \left(-\mathbf{I} + \Delta\gamma_{n+1}\partial_{\mathbf{q}}\mathbf{h} \right)^{-1} \tag{8.36}$$

$$\mathbf{M} \equiv \begin{bmatrix} \mathbf{M}_{\boldsymbol{\sigma}\boldsymbol{\sigma}} & \mathbf{M}_{\boldsymbol{\sigma}\mathbf{q}} \\ \mathbf{M}_{\mathbf{q}\boldsymbol{\sigma}} & \mathbf{M}_{\mathbf{q}\mathbf{q}} \end{bmatrix} \equiv \begin{bmatrix} \boldsymbol{\Xi}^{-1} & \Delta\gamma\partial_{\mathbf{q}}\mathbf{r} \\ \Delta\gamma\partial_{\boldsymbol{\sigma}}\mathbf{h} & \mathbf{Y}^{-1} \end{bmatrix}^{-1} \tag{8.37}$$

Using new defitions shown in Eq.(8.35)-(8.37), Eq.(8.34) can be manipulated to be,

$$\begin{pmatrix} d\boldsymbol{\sigma}_{n+1} \\ d\mathbf{q}_{n+1} \end{pmatrix} = \mathbf{M} : \left\{ \begin{pmatrix} d\boldsymbol{\varepsilon}_{n+1} \\ 0 \end{pmatrix} - d\Delta\gamma_{n+1} \begin{pmatrix} \mathbf{r}_{n+1} \\ \mathbf{h}_{n+1} \end{pmatrix} \right\} \tag{8.38}$$

Substitution of Eq.(8.34) into scalar Eq.(8.29) gives,

$$\begin{pmatrix} \partial_{\boldsymbol{\sigma}}f \\ \partial_{\mathbf{q}}f \end{pmatrix} : \mathbf{M} : \left(\begin{pmatrix} d\boldsymbol{\varepsilon}_{n+1} \\ 0 \end{pmatrix} - d\Delta\gamma_{n+1} \begin{pmatrix} \mathbf{r}_{n+1} \\ \mathbf{h}_{n+1} \end{pmatrix} \right) = 0 \tag{8.39}$$

Since Eq.(8.39) is scalar equation, therefore, the scalar unknown can be solved,

$$d\Delta\gamma_{n+1} = \frac{\begin{pmatrix} \partial_{\boldsymbol{\sigma}}f \\ \partial_{\mathbf{q}}f \end{pmatrix} : \mathbf{M} : \begin{pmatrix} d\boldsymbol{\varepsilon}_{n+1} \\ 0 \end{pmatrix}}{\begin{pmatrix} \partial_{\boldsymbol{\sigma}}f \\ \partial_{\mathbf{q}}f \end{pmatrix} : \mathbf{M} : \begin{pmatrix} \mathbf{r}_{n+1} \\ \mathbf{h}_{n+1} \end{pmatrix}} \tag{8.40}$$

As a result, Eq.(8.38) can be determined by the substitution of Eq.(8.40) back to Eq.(8.38),

$$\begin{pmatrix} d\boldsymbol{\sigma}_{n+1} \\ d\mathbf{q}_{n+1} \end{pmatrix} = \mathbf{M} : \begin{pmatrix} d\boldsymbol{\varepsilon}_{n+1} \\ 0 \end{pmatrix} - \frac{\begin{pmatrix} \partial_{\boldsymbol{\sigma}}f \\ \partial_{\mathbf{q}}f \end{pmatrix} : \mathbf{M} : \begin{pmatrix} d\boldsymbol{\varepsilon}_{n+1} \\ 0 \end{pmatrix}}{\begin{pmatrix} \partial_{\boldsymbol{\sigma}}f \\ \partial_{\mathbf{q}}f \end{pmatrix} : \mathbf{M} : \begin{pmatrix} \mathbf{r}_{n+1} \\ \mathbf{h}_{n+1} \end{pmatrix}} \mathbf{M} : \begin{pmatrix} \mathbf{r}_{n+1} \\ \mathbf{h}_{n+1} \end{pmatrix} = \left[\mathbf{M} - \frac{\mathbf{M} : \begin{pmatrix} \mathbf{r}_{n+1} \\ \mathbf{h}_{n+1} \end{pmatrix} \otimes \begin{pmatrix} \partial_{\boldsymbol{\sigma}}f \\ \partial_{\mathbf{q}}f \end{pmatrix} : \mathbf{M}}{\begin{pmatrix} \partial_{\boldsymbol{\sigma}}f \\ \partial_{\mathbf{q}}f \end{pmatrix} : \mathbf{M} : \begin{pmatrix} \mathbf{r}_{n+1} \\ \mathbf{h}_{n+1} \end{pmatrix}} \right] : \begin{pmatrix} d\boldsymbol{\varepsilon}_{n+1} \\ 0 \end{pmatrix} \tag{8.41}$$

For associative flow rule, the direction of plastic flow and plastic variables are associative to,

$$\begin{pmatrix} \mathbf{r}_{n+1} \\ \mathbf{h}_{n+1} \end{pmatrix} = \begin{pmatrix} \partial_{\boldsymbol{\sigma}}f \\ \partial_{\mathbf{q}}f \end{pmatrix} \Bigg|_{n+1} \tag{8.42}$$

Substitution of Eq.(8.42) into Eq.(8.41) turns to,

$$\begin{pmatrix} d\boldsymbol{\sigma}_{n+1} \\ d\mathbf{q}_{n+1} \end{pmatrix} = \left[\mathbf{M} - \frac{\mathbf{M} : \begin{pmatrix} \partial_{\boldsymbol{\sigma}}f \\ \partial_{\mathbf{q}}f \end{pmatrix} \otimes \begin{pmatrix} \partial_{\boldsymbol{\sigma}}f \\ \partial_{\mathbf{q}}f \end{pmatrix} : \mathbf{M}}{\begin{pmatrix} \partial_{\boldsymbol{\sigma}}f \\ \partial_{\mathbf{q}}f \end{pmatrix} : \mathbf{M} : \begin{pmatrix} \partial_{\boldsymbol{\sigma}}f \\ \partial_{\mathbf{q}}f \end{pmatrix}} \right] : \begin{pmatrix} d\boldsymbol{\varepsilon}_{n+1} \\ 0 \end{pmatrix} \tag{8.43}$$

Each expansion can be performed as following,

$$\begin{bmatrix} \mathbf{M}_{\boldsymbol{\sigma}\boldsymbol{\sigma}} & \mathbf{M}_{\boldsymbol{\sigma}\mathbf{q}} \\ \mathbf{M}_{\mathbf{q}\boldsymbol{\sigma}} & \mathbf{M}_{\mathbf{q}\mathbf{q}} \end{bmatrix} : \begin{pmatrix} \partial_{\boldsymbol{\sigma}}f \\ \partial_{\mathbf{q}}f \end{pmatrix} = \begin{pmatrix} \mathbf{M}_{\boldsymbol{\sigma}\boldsymbol{\sigma}} : \partial_{\boldsymbol{\sigma}}f + \mathbf{M}_{\boldsymbol{\sigma}\mathbf{q}} : \partial_{\mathbf{q}}f \\ \mathbf{M}_{\mathbf{q}\boldsymbol{\sigma}} : \partial_{\boldsymbol{\sigma}}f + \mathbf{M}_{\mathbf{q}\mathbf{q}} : \partial_{\mathbf{q}}f \end{pmatrix} \tag{8.44}$$

$$\begin{pmatrix} \partial_{\boldsymbol{\sigma}}f \\ \partial_{\mathbf{q}}f \end{pmatrix} : \mathbf{M} : \begin{pmatrix} \partial_{\boldsymbol{\sigma}}f \\ \partial_{\mathbf{q}}f \end{pmatrix} = \begin{pmatrix} \partial_{\boldsymbol{\sigma}}f \\ \partial_{\mathbf{q}}f \end{pmatrix} : \begin{pmatrix} \mathbf{M}_{\boldsymbol{\sigma}\boldsymbol{\sigma}} : \partial_{\boldsymbol{\sigma}}f + \mathbf{M}_{\boldsymbol{\sigma}\mathbf{q}} : \partial_{\mathbf{q}}f \\ \mathbf{M}_{\mathbf{q}\boldsymbol{\sigma}} : \partial_{\boldsymbol{\sigma}}f + \mathbf{M}_{\mathbf{q}\mathbf{q}} : \partial_{\mathbf{q}}f \end{pmatrix} \tag{8.45}$$

$$= \partial_{\boldsymbol{\sigma}}f : \mathbf{M}_{\boldsymbol{\sigma}\boldsymbol{\sigma}} : \partial_{\boldsymbol{\sigma}}f + \partial_{\boldsymbol{\sigma}}f : \mathbf{M}_{\boldsymbol{\sigma}\mathbf{q}} : \partial_{\mathbf{q}}f + \partial_{\mathbf{q}}f : \mathbf{M}_{\mathbf{q}\boldsymbol{\sigma}} : \partial_{\boldsymbol{\sigma}}f + \partial_{\mathbf{q}}f : \mathbf{M}_{\mathbf{q}\mathbf{q}} : \partial_{\mathbf{q}}f$$

$$\begin{bmatrix} \mathbf{M}_{\boldsymbol{\sigma}\boldsymbol{\sigma}} & \mathbf{M}_{\boldsymbol{\sigma}\mathbf{q}} \\ \mathbf{M}_{\mathbf{q}\boldsymbol{\sigma}} & \mathbf{M}_{\mathbf{q}\mathbf{q}} \end{bmatrix} : \begin{pmatrix} d\boldsymbol{\varepsilon}_{n+1} \\ 0 \end{pmatrix} = \begin{pmatrix} \mathbf{M}_{\boldsymbol{\sigma}\boldsymbol{\sigma}} : d\boldsymbol{\varepsilon}_{n+1} \\ \mathbf{M}_{\mathbf{q}\boldsymbol{\sigma}} : d\boldsymbol{\varepsilon}_{n+1} \end{pmatrix} \tag{8.46}$$

The full expansion of Eq.(8.43) can be presented in accordance with Eq.(8.44)-(8.46) by,

$$\frac{d\boldsymbol{\sigma}_{n+1}}{d\boldsymbol{\varepsilon}_{n+1}} = \mathsf{M}_{\boldsymbol{\sigma}\boldsymbol{\sigma}} - \frac{\left\{\begin{array}{l}\mathsf{M}_{\boldsymbol{\sigma}\boldsymbol{\sigma}}:\partial_{\boldsymbol{\sigma}}f\otimes\partial_{\boldsymbol{\sigma}}f:\mathsf{M}_{\boldsymbol{\sigma}\boldsymbol{\sigma}}+\mathsf{M}_{\boldsymbol{\sigma}\mathbf{q}}:\partial_{\mathbf{q}}f\otimes\partial_{\boldsymbol{\sigma}}f:\mathsf{M}_{\boldsymbol{\sigma}\boldsymbol{\sigma}}\\+\mathsf{M}_{\boldsymbol{\sigma}\boldsymbol{\sigma}}:\partial_{\boldsymbol{\sigma}}f\otimes\partial_{\mathbf{q}}f:\mathsf{M}_{\mathbf{q}\boldsymbol{\sigma}}+\mathsf{M}_{\boldsymbol{\sigma}\mathbf{q}}:\partial_{\mathbf{q}}f\otimes\partial_{\mathbf{q}}f:\mathsf{M}_{\mathbf{q}\boldsymbol{\sigma}}\end{array}\right\}}{\partial_{\boldsymbol{\sigma}}f:\mathsf{M}_{\boldsymbol{\sigma}\boldsymbol{\sigma}}:\partial_{\boldsymbol{\sigma}}f+\partial_{\boldsymbol{\sigma}}f:\mathsf{M}_{\boldsymbol{\sigma}\mathbf{q}}:\partial_{\mathbf{q}}f+\partial_{\mathbf{q}}f:\mathsf{M}_{\mathbf{q}\boldsymbol{\sigma}}:\partial_{\boldsymbol{\sigma}}f+\partial_{\mathbf{q}}f:\mathsf{M}_{\mathbf{q}\mathbf{q}}:\partial_{\mathbf{q}}f} \tag{8.47}$$

For non-coupling hardening model $\partial_{\mathbf{q}}\mathbf{r}=\mathbf{0}$, $\partial_{\boldsymbol{\sigma}}\mathbf{h}=\mathbf{0}$, in other words, $\mathbf{r}=\mathbf{r}(\boldsymbol{\sigma})$, $\mathbf{h}=\mathbf{h}(\mathbf{q})$. Eq.(8.37) can be reduced particularly,

$$\mathsf{M}=\begin{bmatrix}\boldsymbol{\Xi}^{-1} & \mathbf{0}\\ \mathbf{0} & \mathbf{Y}^{-1}\end{bmatrix}^{-1}=\begin{bmatrix}\boldsymbol{\Xi} & \mathbf{0}\\ \mathbf{0} & \mathbf{Y}\end{bmatrix} \tag{8.48}$$

As a result, Eq.(8.41) can be viewed as,

$$\begin{pmatrix}d\boldsymbol{\sigma}_{n+1}\\ d\mathbf{q}_{n+1}\end{pmatrix}=\begin{pmatrix}\boldsymbol{\Xi}:d\boldsymbol{\varepsilon}_{n+1}\\ 0\end{pmatrix}-\frac{\partial_{\boldsymbol{\sigma}}f:\boldsymbol{\Xi}:d\boldsymbol{\varepsilon}_{n+1}}{\partial_{\boldsymbol{\sigma}}f:\boldsymbol{\Xi}:\mathbf{r}_{n+1}+\partial_{\mathbf{q}}f:\mathbf{Y}:\mathbf{h}_{n+1}}\begin{pmatrix}\boldsymbol{\Xi}:\mathbf{r}_{n+1}\\ \mathbf{Y}:\mathbf{h}_{n+1}\end{pmatrix} \tag{8.49}$$

Eq.(8.49) can be individually spitted into incremental equations of stress and plastic variable tensors by,

$$d\boldsymbol{\sigma}_{n+1}=\left[\boldsymbol{\Xi}-\frac{\boldsymbol{\Xi}:\mathbf{r}_{n+1}\otimes\partial_{\boldsymbol{\sigma}}f:\boldsymbol{\Xi}}{\partial_{\boldsymbol{\sigma}}f:\boldsymbol{\Xi}:\mathbf{r}_{n+1}+\partial_{\mathbf{q}}f:\mathbf{Y}:\mathbf{h}_{n+1}}\right]:d\boldsymbol{\varepsilon}_{n+1} \tag{8.50}$$

$$d\mathbf{q}_{n+1}=-\frac{\mathbf{Y}:\mathbf{h}_{n+1}\otimes\partial_{\boldsymbol{\sigma}}f:\boldsymbol{\Xi}}{\partial_{\boldsymbol{\sigma}}f:\boldsymbol{\Xi}:\mathbf{r}_{n+1}+\partial_{\mathbf{q}}f:\mathbf{Y}:\mathbf{h}_{n+1}}:d\boldsymbol{\varepsilon}_{n+1} \tag{8.51}$$

From Eq.(8.50), consistent tangent moduli can be simply given by,

$$\mathbf{c}_{n+1}^{ep}=\frac{d\boldsymbol{\sigma}_{n+1}}{d\boldsymbol{\varepsilon}_{n+1}}=\boldsymbol{\Xi}-\frac{\boldsymbol{\Xi}:\mathbf{r}_{n+1}\otimes\partial_{\boldsymbol{\sigma}}f:\boldsymbol{\Xi}}{\partial_{\boldsymbol{\sigma}}f:\boldsymbol{\Xi}:\mathbf{r}_{n+1}+\partial_{\mathbf{q}}f:\mathbf{Y}:\mathbf{h}_{n+1}} \tag{8.52}$$

In case of associative flow rule, Eq.(8.52) is reduced to,

$$\mathbf{c}_{n+1}^{ep}=\frac{d\boldsymbol{\sigma}_{n+1}}{d\boldsymbol{\varepsilon}_{n+1}}=\boldsymbol{\Xi}-\frac{\boldsymbol{\Xi}:\partial_{\boldsymbol{\sigma}}f\otimes\partial_{\boldsymbol{\sigma}}f:\boldsymbol{\Xi}}{\partial_{\boldsymbol{\sigma}}f:\boldsymbol{\Xi}:\partial_{\boldsymbol{\sigma}}f+\partial_{\mathbf{q}}f:\mathbf{Y}:\partial_{\mathbf{q}}f} \tag{8.53}$$

where algorithmic moduli are also reduced to terms with second derivatives revealed below,

$$\boldsymbol{\Xi}=\left[\mathbf{c}^{e^{-1}}+\Delta\gamma_{n+1}\partial_{\boldsymbol{\sigma}\boldsymbol{\sigma}}f\right]^{-1}, \quad \mathbf{Y}=\left(-\mathbf{I}+\Delta\gamma_{n+1}\partial_{\mathbf{q}\mathbf{q}}f\right)^{-1} \tag{8.54}$$

It is noted here that the determination of $\Delta\gamma_{n+1}$ has already stated in Chapter 6.

In case of semi-implicit scheme, Eq.(8.52) is reduced to,

$$\mathbf{c}_{n+1}^{ep}=\frac{d\boldsymbol{\sigma}_{n+1}}{d\boldsymbol{\varepsilon}_{n+1}}=\boldsymbol{\Xi}-\frac{\boldsymbol{\Xi}:\mathbf{r}_{n}\otimes\partial_{\boldsymbol{\sigma}}f:\boldsymbol{\Xi}}{\partial_{\boldsymbol{\sigma}}f:\boldsymbol{\Xi}:\mathbf{r}_{n}+\partial_{\mathbf{q}}f:\mathbf{Y}:\mathbf{h}_{n}} \tag{8.55}$$

In this expression, all quantities except for plastic flow and hardening type are evaluated at time n+1. This moduli is in general not symmetric even plastic flow is associative [4].

8-2 Return Mapping Algorithm for Anisotropic models

8-2-1 Introduction

Implicit numerical algorithm using return-mapping method [1] has been proven to provide an excellent performance when integrating a nonlinear isotropic elastoplasticity (See for major past researches [2,3,4,5,6,7,8,9,10]); i.e., a pressure-dependent model, in particular, where only a few scalar equations are required to formulate whole governing equations (Aravas, 1987 [3]). The simplicity lies in the fact that return directions to yield surface are coaxial with updated stresses in principle stress space. (See Figure 8.1, Figure 8.2) Accordingly, a closed form of a consistent tangent operator in regard to a modified Cam-clay was derived by Borja et al. (1990) [11], giving by-passed steps needed for evaluating a costly inversion of material stiffness tensor. However, the similar procedure is not conveniently applicable to an anisotropic model mainly because return directions to anisotropic yield surface are not coaxial with updated state of stresses. (See Figure 8.3)

Luccioni et al. (2000) [8] employed a return-mapping technique to an anisotropic Bear-Clay model and concluded that the formulation of governing equations under a return-mapping scheme is complicated and relatively cumbersome due to the complexity of anisotropy; therefore, the method loses a performance and appears impractical to initial boundary value problems.

- *Simo & Taylor (1985), U. Berkeley*
- *Ortiz & Simo (1986)*
- *Aravas (1987), U. Pennsylvania*
- *Ortiz & Martin (1989), U. Brown*
- *Simo (1992), U. Stanford*
- *Alawaji et al. (1992), U. King Saud*
- *Borja et al. (1998), U. Stanford*
- *Luccioni et al. (2000), U. Berkeley*
- *Borja et al. (2001), U. Stanford*
- *Majid et al. (2001), U. George Washington*

- *J_2 plasticity (von Mises)*
- *Isotropic model (Modified Cam-clay)*
- *Pressure-dependent (Gurson's model)*
- *Algorithmic moduli*
- *Finite deformation theory*
- *Soil-water coupling (Modified Cam-clay*
- *Finite deformation (Modified Cam-clay)*
- *Anisotropic model (Bear-clay)*
- *Bounding surface (Modified Cam-clay)*
- *Cyclic plasticity*

Isotropic plasticity models have been successful in high performance

Anisotropic plasticity models have been suffered complex formulation and impractical

Figure 8.1 Past Research on Return-Mapping Algorithms
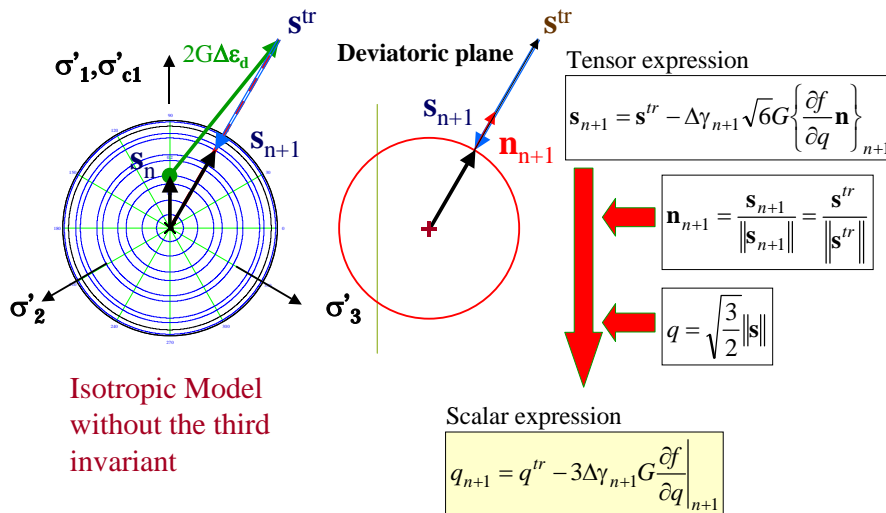
Figure 8.2 Co-axial Return Path

In this study, a return-mapping regularization applicable to anisotropic models was developed following a typical procedure [12] but a newly developed process corresponding to invariant-based tensor basis was applied to solve a concerned limitation. An implementation of implicit finite element method and numerical illustration were presented to demonstrate a computational performance under the proposed procedure. The mathematical technique may suggest a solution or extend a performance to other similar anisotropic plasticity models.

8-2-2 Anisotropic plasticity

The anisotropic soil plasticity proposed by Sekiguchi and Ohta (1977) is adopted in the study. A stress-strain-strength response of model behaves anisotropically due to the existence of the joint invariant between current stresses and stress history induced by the initial yield stress. The yield function expressed in terms of stress invariants, hardening stress parameter and their related tensorial notations are summarized in Box 1.
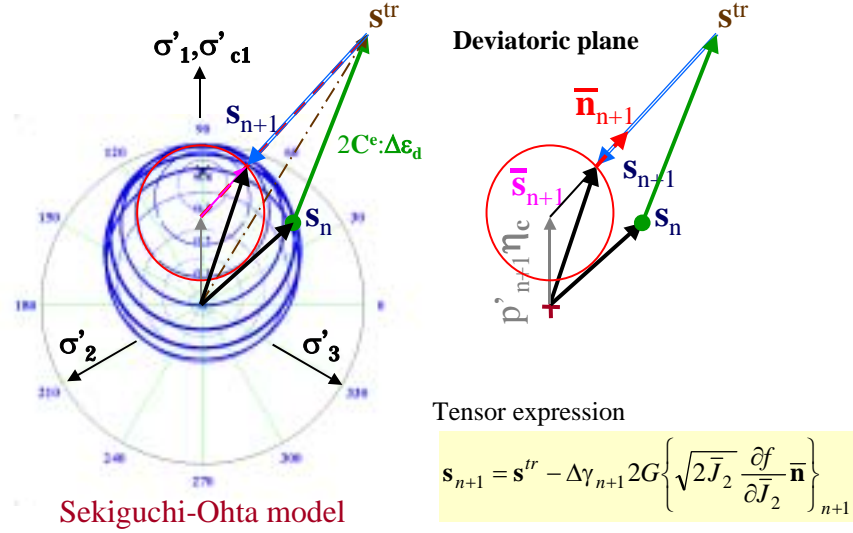
Figure 8.3 Non-coaxial Return Path

$$\text{f}(\boldsymbol{\sigma}', \boldsymbol{\sigma}'_c) \equiv f(I_1, \overline{J}_2, I_{c1}) = MD \ln\left(\frac{I_1}{I_{c1}}\right) + \frac{3\sqrt{3\overline{J}_2}}{I_1} D = 0$$

$\mathbf{1} \equiv \delta_{ij}\mathbf{e}_i \otimes \mathbf{e}_j$	$\mathbf{I} \equiv \frac{1}{2}\left[\delta_{ik}\delta_{jl} + \delta_{il}\delta_{jk}\right] \cdot \mathbf{e}_i \otimes \mathbf{e}_j \otimes \mathbf{e}_k \otimes \mathbf{e}_l$		$\mathbf{A} \equiv \mathbf{I} - \frac{1}{3}(\mathbf{1} \otimes \mathbf{1})$
$I_1 = tr(\boldsymbol{\sigma}') = \mathbf{1} : \boldsymbol{\sigma}' = 3p'$	$I_{c1} = tr(\boldsymbol{\sigma}'_c) = \mathbf{1} : \boldsymbol{\sigma}'_c = 3p'_c$		
$\mathbf{s} = \boldsymbol{\sigma}' - \frac{1}{3}I_1\mathbf{1} = \mathbf{A} : \boldsymbol{\sigma}'$	$\mathbf{s}_c = \boldsymbol{\sigma}'_c - \frac{1}{3}I_{c1}\mathbf{1} = \mathbf{A} : \boldsymbol{\sigma}'_c$		
$\boldsymbol{\eta}_c = \dfrac{\mathbf{s}_c}{p'_c} = \dfrac{\mathbf{s}_o}{p'_o}$	$\eta_o = \dfrac{3(1 - K_o)}{1 + 2K_o}$	$\boldsymbol{\eta}_c = \sqrt{\dfrac{2}{3}}\eta_o diag\left\{-\dfrac{\sqrt{6}}{6}, \dfrac{\sqrt{6}}{3}, -\dfrac{\sqrt{6}}{6}\right\}$	
$\overline{\mathbf{s}} = \mathbf{s} - \frac{1}{3}I_1\boldsymbol{\eta}_c = \left(\mathbf{A} - \frac{1}{3}\boldsymbol{\eta}_c \otimes \mathbf{1}\right) : \boldsymbol{\sigma}'$		$\overline{J}_2 = \frac{1}{2}tr(\overline{\mathbf{s}}^2) = \frac{1}{2}\overline{\mathbf{s}} : \overline{\mathbf{s}}$	

Box 8.1 Sekiguchi-Ohta Plasticity Model

8-2-3 Rate constitutive equations

In general, return-mapping methods are based on a set of equations expressed below,
Additive decomposition of strain rate

$$\dot{\boldsymbol{\varepsilon}}^e = \dot{\boldsymbol{\varepsilon}} - \dot{\boldsymbol{\varepsilon}}^p \tag{8.56}$$

Stress-strain relationship

$$\dot{\boldsymbol{\sigma}}' = \mathbf{c}^e : (\dot{\boldsymbol{\varepsilon}} - \dot{\boldsymbol{\varepsilon}}^p) \tag{8.57}$$

Nonlinear elastic stiffness

$$\mathbf{c}^e = \mathbf{c}^e(\boldsymbol{\sigma}') = K\mathbf{1} \otimes \mathbf{1} + 2G\mathbf{A} \tag{8.58}$$

Flow rule (associative case)

$$\dot{\boldsymbol{\varepsilon}}^p = \gamma \partial_{\boldsymbol{\sigma}'} f \tag{8.59}$$

Evolution law of hardening (isotropic hardening)

$$\dot{p}'_c = \partial^2_{\alpha\alpha}\mathsf{H}\dot{\alpha} = \frac{p'_c}{MD}\dot{\alpha} \qquad \text{where} \qquad \alpha = \mathbf{1} : \boldsymbol{\varepsilon}^p \text{ (See Appendix B-11)} \tag{8.60}$$

Stress hardening

$$\mathbf{\sigma'}_c = \mathbf{\sigma'}_c(p'_c) \qquad \text{where} \quad \mathbf{\sigma'}_c = p'_c \left\{ \mathbf{1} + \sqrt{\frac{2}{3}} \eta_o \mathbf{n}_c \right\} \quad \text{(See Appendix B-2)} \tag{8.61}$$

Yield function

$$f(\mathbf{\sigma'}, \mathbf{\sigma'}_c) \tag{8.62}$$

where bulk and shear moduli are

$$K = K(p') = \frac{p'}{\kappa}(1 + e_o), \quad G = G(p') = \frac{3(1 - 2v')}{2(1 + v')} K(p') \tag{8.63),(8.64}$$

All of these are subject to the Kuhn-Tucker complementarity conditions

$$\gamma \geq 0; f \leq 0; \gamma f = 0 \tag{8.65}$$

and with the initial conditions

$$\left\{ \mathbf{\varepsilon}, \mathbf{\varepsilon}^p, \mathbf{\sigma'}, \mathbf{\sigma'}_c \right\} \Big|_{t=t_n} = \left\{ \mathbf{\varepsilon}_n, \mathbf{\varepsilon}_n^p, \mathbf{\sigma'}_n, \mathbf{\sigma'}_{cn} \right\} \tag{8.66}$$

The summary of rate-independent plasticity is shown in Figure 8.5. Figure 8.6 summarizes hardening potential and related equations.

8-2-4 Return-mapping in strain space

Basically, return-mapping method has been developed in stress space [1,11,13]. The updated stress is split into elastic-trial stress and plastic-corrector stress, which is iteratively determined by correcting the trial stress. Though return mapping cast in stress space is more obvious and simpler than that of strain space in formulation, both methods are equivalent each other. However, in the problem of nonlinear, stress-dependent material stiffness, return mapping in strain space is superior to that of stress space in formulation. (9). In strain space, return-mapping method is formulated by keeping driving strain into trial strain variable. The schematization of the concept is shown in Figure 8.4.

Concerning with Figure 8.4, $\mathbf{\varepsilon}_n^e$ is an elastic strain converged in previous step, $\Delta\mathbf{\varepsilon}^e$ is an elastic strain increment, $\mathbf{\varepsilon}_{n+1}^e$ is an elastic strain increment in the new step. It is straightforward that,

$$\mathbf{\varepsilon}_{n+1}^e = \mathbf{\varepsilon}_n^e + \Delta\mathbf{\varepsilon}^e \tag{8.67}$$
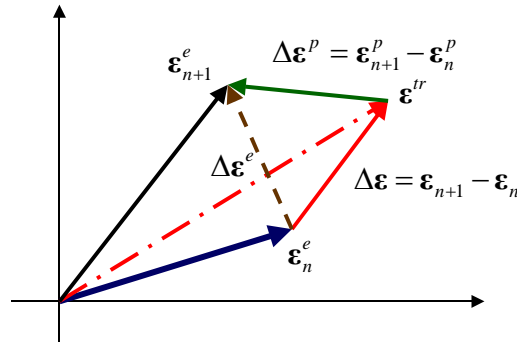
Figure 8.4 Schematization of elastic-trial-plastic-corrector in strain-space

However, the solution in Eq.(8.67) will be searched by the split operation procedure involving two steps. Firstly, the integration of the elastic equations as shown in Eq.(8.68) using elastic trial is taken as the initial condition for the plastic equations. Secondly, the relaxation of the elastically predicted strains onto an updated yield surface using the plastic corrector is taken for plastic equations as shown in Eq.(8.69). The solutions of both steps are iteratively obtained using Newton method.

$$\mathbf{\varepsilon}^{tr} = \mathbf{\varepsilon}_n^e + \Delta\mathbf{\varepsilon} \tag{8.68}$$

$$\mathbf{\varepsilon}_{n+1}^e = \mathbf{\varepsilon}^{tr} - \Delta\mathbf{\varepsilon}^p \tag{8.69}$$

$\Delta\mathbf{\varepsilon}$ is strain increment (driving strain for nonlinear system), $\Delta\mathbf{\varepsilon}_p$ is plastic strain increment, trial strain is the sum of $\mathbf{\varepsilon}_n^e$ and $\Delta\mathbf{\varepsilon}$. Trial strain $\mathbf{\varepsilon}^{tr}$ is given to the system. Plastic strain increment $\Delta\mathbf{\varepsilon}_p$ can be determined iteratively. Finally, elastic strain at the new step $\mathbf{\varepsilon}_{n+1}^e$ can be obtained.

$$\boxed{\begin{array}{l} \textbf{Rate-independent plasticity} \\[4pt] \dot{\boldsymbol{\varepsilon}}^e = \dot{\boldsymbol{\varepsilon}} - \dot{\boldsymbol{\varepsilon}}^p \\[4pt] \dot{\boldsymbol{\sigma}}' = \mathbf{c}^e : \dot{\boldsymbol{\varepsilon}}^e \\[4pt] \mathbf{c}^e = \mathbf{c}^e(\boldsymbol{\sigma}') \\[4pt] \dot{\boldsymbol{\varepsilon}}^p = \gamma \partial_{\boldsymbol{\sigma}'} f(\boldsymbol{\sigma}', \boldsymbol{\sigma}'_c(p'_c)) \\[4pt] \dot{p}'_c = \partial^2_{\alpha\alpha} \mathsf{H}\dot{\alpha} \quad \text{where} \quad \alpha = \mathbf{1}:\boldsymbol{\varepsilon}^p \\[4pt] f = f(\boldsymbol{\sigma}', \boldsymbol{\sigma}'_c(p'_c)) \\[4pt] \gamma \geq 0 \quad | \quad f \leq 0 \quad | \quad \gamma f = 0 \end{array}}$$

Elastic-plastic strain decomposition

Elastic stress-strain relationship

Nonlinear elastic stiffness

Associated flow rule

Isotropic hardening law

Yield function

Kuhn-Tucker complementarity condition

Figure 8.5 Governing equations for rate-independent models

$$\boxed{\begin{array}{l} \mathsf{H}(\alpha) = p'_o\left(\overline{\lambda} - \overline{\kappa}\right)\exp\left(\dfrac{\alpha}{\overline{\lambda} - \overline{\kappa}}\right) \\[10pt] p'_c = \partial_\alpha \mathsf{H}(\alpha) = p'_{cn}\exp\left(\dfrac{\alpha - \alpha_n}{\overline{\lambda} - \overline{\kappa}}\right) \\[10pt] \dfrac{dp'_c}{d\alpha} = \partial^2_{\alpha\alpha}\mathsf{H}(\alpha) = \dfrac{p'_c}{\overline{\lambda} - \overline{\kappa}} \\[10pt] \text{where} \quad \overline{\lambda} - \overline{\kappa} = \dfrac{\lambda - \kappa}{1 + e_o} = MD \end{array}}$$

Hardening potential function

Stress hardening parameter

Evolution law of hardening

Figure 8.6 Usage of hardening potential function applicable to the SO model

8-2-5 Nonlinear system

Backward Euler scheme is used to integrate the rate constitutive equations in previous section. Yield condition can be enforced at the end of the step. State variables at time step n+1 are updated from the converged values at the end of the previous time step n. Based on integration scheme employed by Simo & Taylor (1985) [1], a set of nonlinear equations shown in Figure 8.7 is consistent with their rate form shown in Figure 8.5. The corresponding variables are to be solved in regard to a driving strain increment imposed to the system. Underlined in Figure 8.7, all of variables can be solved by Newton method for a given incremental strain or trial strain. For a particular case of constant elastic stiffness tensor, the equation system will reduced to the mathematical framework originally set by Aravas (1987), U. Pennsylvania

There is an implicit relation between Eq.II and Eq.III. That is, a nonlinear elastic stiffness tensor of Eq.III cannot be evaluated without determining a stress tensor of Eq.II. In opposite, a stress tensor of Eq.II cannot be evaluated without determining a nonlinear elastic stiffness tensor of Eq.III. Borja1 simplified this difficulty using constant elastic moduli which is determined from stresses converged in previous steps (forward Euler scheme). The more sophisticated stress-dependent elastic stiffness tensor applied to an isotropic model can be evaluated implicitly (backward Euler scheme) by a method suggested by Borja et al. (1998) [7], however, relevant expressions are cumbersome and seemingly complicated for an anisotropic model. In this study, a method mixed between two previous methods is employed, namely, semi-backward Euler scheme. Stress-dependent elastic stiffness tensor is explicitly determined from a previous iterative step instead of the previously converged step or implicit expressions explained earlier.

8-2-6 Reduced form of nonlinear system

However, to solve the nonlinear system of 6 six variables by Newton method, an inversed gradient of residuals of the whole system would be required and become cumbersome in analysis. In order to reduce the order of the equation system, some equations will be substituted by other equations, resulting in reduction of number of variables, though a compacted equation system becomes complex.

There are many ways to reduce the nonlinear system by equation substitutions among them. The efficient way is carried out substituted Eq.IV into Eq.I, Eq.II,III,V into VI. Reduction of hardening function was suggested by Borja et al.(1998). As a result, variables are reduced from six to two, i.e., elastic strain increment and consistency parameter.

Current state at time t= t_{n+1}				
Variables	$\boldsymbol{\sigma'}_{n+1}$	$\boldsymbol{\varepsilon}^p_{n+1}$	p'_{cn+1}	$\Delta\gamma_{n+1}$ *indicate unknowns of a system*

I	$\boldsymbol{\varepsilon}^e_{n+1} = \boldsymbol{\varepsilon}_{n+1} - \boldsymbol{\varepsilon}^p_{n+1} = \boldsymbol{\varepsilon}^e_n + \left\{\boldsymbol{\varepsilon}_{n+1} - \boldsymbol{\varepsilon}_n\right\} - \left\{\boldsymbol{\varepsilon}^p_{n+1} - \boldsymbol{\varepsilon}^p_n\right\} = \boldsymbol{\varepsilon}^{tr} - \left\{\boldsymbol{\varepsilon}^p_{n+1} - \boldsymbol{\varepsilon}^p_n\right\}$
II	$\boldsymbol{\sigma'}_{n+1} - \boldsymbol{\sigma'}_n = \mathbf{c}^e_{n+1} : \left\{\boldsymbol{\varepsilon}^e_{n+1} - \boldsymbol{\varepsilon}^e_n\right\}$
III	$\mathbf{c}^e_{n+1} = \mathbf{c}^e(\boldsymbol{\sigma'}_{n+1})$
IV	$\boldsymbol{\varepsilon}^p_{n+1} - \boldsymbol{\varepsilon}^p_n = \Delta\gamma_{n+1} f_{\boldsymbol{\sigma'}n+1}$
V	$p'_{cn+1} = \mathsf{H}_\alpha(\mathbf{1}:\boldsymbol{\varepsilon}^p_{n+1}) = p'_{cn}\exp\left(\dfrac{\varepsilon^p_{v\,n+1} - \varepsilon^p_{v\,n}}{\bar{\lambda} - \bar{\kappa}}\right)$
VI	$f_{n+1} = f(\boldsymbol{\sigma'}_{n+1}, \boldsymbol{\sigma'}_c(p'_{cn+1}))$

$\Delta\gamma_{n+1} \geq 0$	$f_{n+1} \leq 0$	$\Delta\gamma_{n+1}f_{n+1} = 0$

Figure 8.7 Backward Euler Incremental Form
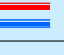
Reduced forms of equation system		
Variables	$\boldsymbol{\varepsilon}^e_{n+1}$	$\Delta\gamma_{n+1}$ *indicate unknowns of a system*

IV→I	$\boldsymbol{\varepsilon}^e_{n+1} = \boldsymbol{\varepsilon}^{tr} - \Delta\gamma_{n+1}\partial_{\boldsymbol{\sigma'}}f_{n+1}$ where $\boldsymbol{\varepsilon}^{tr} = \boldsymbol{\varepsilon}^e_n + \boldsymbol{\varepsilon}_{n+1} - \boldsymbol{\varepsilon}_n$
II&III V→VI	$f_{n+1} = f(\boldsymbol{\sigma'}(\boldsymbol{\varepsilon}^e_{n+1}), \boldsymbol{\sigma'}_c(p'_{cn+1}(\boldsymbol{\varepsilon}^e_{n+1}))) = 0$ for $\Delta\gamma_{n+1} \geq 0$
Back Substitution	$\boldsymbol{\sigma'}_{n+1} = \boldsymbol{\sigma'}_n + \mathbf{c}^e_{n+1}(\boldsymbol{\sigma'}_{n+1}) : \left\{\boldsymbol{\varepsilon}^e_{n+1} - \boldsymbol{\varepsilon}^e_n\right\}$ $p'_{cn+1} = \mathsf{H}_\alpha(\mathbf{1}:\Delta\gamma_{n+1}\partial_{\boldsymbol{\sigma'}}f_{n+1}) = \mathsf{H}_\alpha(\mathbf{1}:\left\{\boldsymbol{\varepsilon}^{tr} - \boldsymbol{\varepsilon}^e_{n+1}\right\})$ $\qquad = p'_{cn}\exp\left(\dfrac{\varepsilon^{tr}_v - \varepsilon^e_{v\,n+1}}{\bar{\lambda} - \bar{\kappa}}\right)$ $\boldsymbol{\varepsilon}^p_{n+1} = \boldsymbol{\varepsilon}^p_n + \Delta\gamma_{n+1}\partial_{\boldsymbol{\sigma'}}f_{n+1}(\boldsymbol{\sigma'}_{n+1}, p'_{cn+1})$

Figure 8.8 Reduced Incremental Form

8-3 Linearization

	Residuals		Expressions	Unknowns		
Nonlinear system	**r**	$\bar{\mathbf{r}}$	$\boldsymbol{\varepsilon}^e_{n+1} - \boldsymbol{\varepsilon}^{tr} + \Delta\gamma_{n+1}f_{\boldsymbol{\sigma'}n+1} = \mathbf{0}$	**x**	$\mathbf{x}_1$	$\boldsymbol{\varepsilon}^e_{n+1}$
		f	$f\left(\boldsymbol{\sigma'}(\boldsymbol{\varepsilon}^e_{n+1}), p'_{cn}\exp\left(\dfrac{\mathbf{1}:\left\{\boldsymbol{\varepsilon}^{tr} - \boldsymbol{\varepsilon}^e_{n+1}\right\}}{\bar{\lambda} - \bar{\kappa}}\right)\right) = 0$		x_2	$\Delta\gamma_{n+1}$

Figure 8.9 A set of residuals of nonlinear system

Nonlinear system of residuals given in Figure 8.9 can be solved using Newton's method. The Newton loop for searching unknown variable **x** is shown in Figure 8.10.

$$\mathbf{r}^{(0)} = \begin{Bmatrix} 0 \\ f \end{Bmatrix} \quad \Rightarrow \quad \delta\mathbf{x}^{(k)} = -\left[\mathbf{\Omega}^{-1}\right]^{(k)} \cdot \mathbf{r}^{(k)} \quad \Rightarrow \quad \mathbf{x}^{(k+1)} = \mathbf{x}^{(k)} + \delta\mathbf{x}^{(k)} \quad \Rightarrow \quad k \leftarrow k+1$$

$$\text{loop}$$

Figure 8.10 Loop of Newton's method

Details of equation manipulation using algorithmic moduli are given in Appendix F. All of procedures can be summarized by Figure 8.11.

Figure 8.11 Introduction of algorithmic moduli in Newton's method

8-4 Consistent tangential moduli in regard to the SO model

The exact linearization of stress tensor by strain tensor implies tangential moduli. Depended on whether forward Euler or backward Euler difference scheme is employed for stress update, tangential moduli can be formulated to continuum or consistent tangential tensor. It is well known that the use of the consistent tangential moduli preserves the asymptotic rate of quadratic convergence of the global iterations.

8-4-1 Continuum vs. consistent tangential moduli

A difference between continuum and consistent tangential moduli is that continuum moduli employ a previous stress as a basis to determine stiffness gradient while a consistent moduli employs a current stress correctly enforced on yield surface as a basis to determine stiffness gradient. As a result, the consistent moduli is consistent with exact linearization of Newton's method, therefore, a quadratic rate of convergence can be achieved in iteration. Figure 8.12 shows an idealized concept of continuum and consistent moduli, which are referred to stress update scheme by forward Euler and backward Euler respectively. However, in the study, semi-backward Euler is employed as a mixed scheme between forward and backward difference. Nonlinear elastic stiffness is forwardly updated by a previously iterative stress update referred by superscript <k-1>. This technique can reduce effort for equation formulation since variation of elastic stiffness tensor would result in the sixth-order tensor if fully implicit (backward Euler) is implemented. As a consequence, the exact linearization cannot preserve, the rate of convergence may not be as attractive as Newton's method can do. However, the methodology is equivalent to quasi-Newton in which a quadratic rate of convergence is, more or less, able to achieve. There is no difference in accuracy of both methods; however, the unconditional stability is not conserved.

$$\mathbf{c}^{ep} = \frac{\partial \boldsymbol{\sigma}}{\partial \boldsymbol{\varepsilon}} = \frac{\partial \boldsymbol{\sigma}}{\partial \boldsymbol{\varepsilon}^e} : \frac{\partial \{\boldsymbol{\varepsilon} - \boldsymbol{\varepsilon}^p\}}{\partial \boldsymbol{\varepsilon}} = \mathbf{c}^e : \left[\mathbf{I} - \frac{\partial \boldsymbol{\varepsilon}^p}{\partial \boldsymbol{\varepsilon}} \right]$$

Forward Euler

$$\boldsymbol{\sigma}_{n+1} = \boldsymbol{\sigma}_n + \mathbf{c}_n^{ep} : \Delta \boldsymbol{\varepsilon}$$

$$\mathbf{c}_n^{ep} = \mathbf{c}_n^e : \left[\mathbf{I} - \left. \frac{\partial \boldsymbol{\varepsilon}^p}{\partial \boldsymbol{\varepsilon}} \right|_n \right]$$

Backward Euler

$$\boldsymbol{\sigma}_{n+1} = \boldsymbol{\sigma}_n + \mathbf{c}_{n+1}^{ep} : \Delta \boldsymbol{\varepsilon}$$

$$\mathbf{c}_{n+1}^{ep} = \mathbf{c}_{n+1}^e : \left[\mathbf{I} - \left. \frac{\partial \boldsymbol{\varepsilon}^p}{\partial \boldsymbol{\varepsilon}} \right|_{n+1} \right]$$

Semi-Backward Euler

$$\boldsymbol{\sigma}_{n+1}^{<k>} = \boldsymbol{\sigma}_n + \mathbf{c}_{n+1}^{ep<k-1>} : \Delta \boldsymbol{\varepsilon}$$

$$\mathbf{c}_{n+1}^{ep<k-1>} = \mathbf{c}_{n+1}^e (\boldsymbol{\sigma}_{n+1}^{<k-1>}) : \left[\mathbf{I} - \left. \frac{\partial \boldsymbol{\varepsilon}^p}{\partial \boldsymbol{\varepsilon}} \right|_{n+1}^{<k>} \right]$$
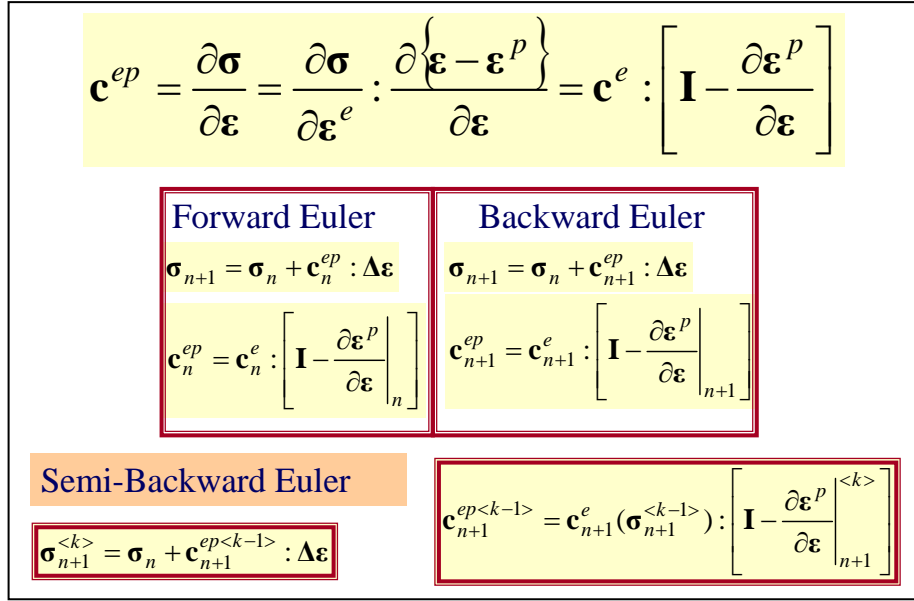
Figure 8.12 Forward, backward and semi-back Euler for stress update scheme

8-4-2 Backward Euler Incremental Form

A rate-independent constitutive equations are integrated by backward Euler scheme to obtain the backward incremental form as shown in Figure 8.13. The updated state of variables can be solve by stress update algorithm described in previous chapter.

Governing equations ➡ Backward Euler by driven strain $\Delta\boldsymbol{\varepsilon}$

Rate-independent

$$\dot{\boldsymbol{\sigma}}' = \mathbf{c}^e : (\dot{\boldsymbol{\varepsilon}} - \dot{\boldsymbol{\varepsilon}}^p)$$

$$\dot{\boldsymbol{\varepsilon}}^p = \gamma \mathbf{r}(\boldsymbol{\sigma}', p'_c)$$

$$\dot{p}'_c = \frac{p'_c}{MD}\left(\mathbf{1} : \dot{\boldsymbol{\varepsilon}}^p\right)$$

$$f = f(\boldsymbol{\sigma}', p'_c)$$

| $\gamma \geq 0$ | $f \leq 0$ | $\gamma f = 0$ |

Incremental form | $\Delta\boldsymbol{\varepsilon} = \boldsymbol{\varepsilon}_{n+1} - \boldsymbol{\varepsilon}_n$ | $\Delta\boldsymbol{\varepsilon}^e = \Delta\boldsymbol{\varepsilon} - \Delta\boldsymbol{\varepsilon}^p$

$$\boldsymbol{\sigma}'^{<k>}_{n+1} - \boldsymbol{\sigma}'_n = \mathbf{c}^e_{n+1}(\boldsymbol{\sigma}'^{<k-1>}_{n+1}) : \{\boldsymbol{\varepsilon}_{n+1} - \boldsymbol{\varepsilon}_n - \Delta\gamma_{n+1}\partial_{\boldsymbol{\sigma}'} f_{n+1}\}$$

$$\boldsymbol{\varepsilon}^p_{n+1} - \boldsymbol{\varepsilon}^p_n = \Delta\gamma_{n+1}\partial_{\boldsymbol{\sigma}'} f_{n+1}$$

$$p'_{cn+1} = p'_{cn}\exp(\frac{\varepsilon^p_{v\,n+1} - \varepsilon^p_{v\,n}}{MD})$$

$$f_{n+1} = f\left(\boldsymbol{\sigma}'_{n+1}, p'_{cn+1}\right)$$

| $\Delta\gamma_{n+1} \geq 0$ | $f_{n+1} \leq 0$ | $\Delta\gamma_{n+1}f_{n+1} = 0$ |

Associative case

$$\mathbf{r} = \frac{\partial f}{\partial \boldsymbol{\sigma}'}$$

indicate unknowns of a system

Solve by stress update algorithm
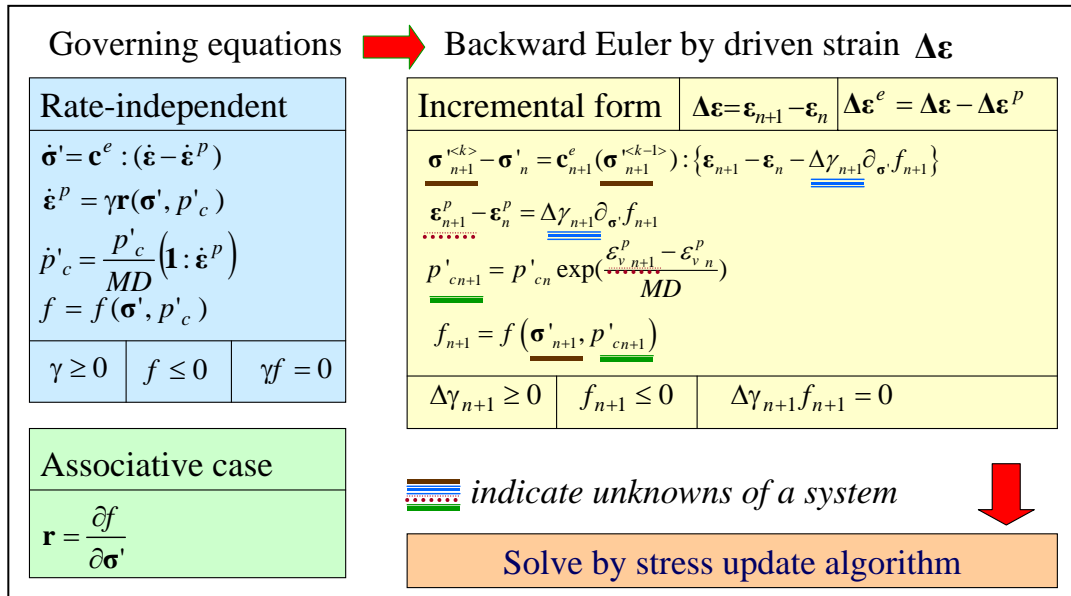
Figure 8.13 Backward incremental constitutive equations for anisotropic plasticity

8-4-3 Scalar variation

Two of scalar differential variables can be solved linearly and expressed in terms of stress tensor. This technique of equation manipulation is adopted from Borja et al. (2001) [9]. Subsequently, these scalar variation is substituted back to the differential equation of stress. The details of manipulation are obviously shown in Figure 8.15. As a result, the implicit differential expression in terms of stress tensor is obtained. By manipulation of stress tensor and separate strain tensor to another side of equation as shown by flow equation in Figure 8.16 . A consistent tangential tensor is obtained.

8-4-4 Consistent tangential operator

Refer to equation manipulation described in Figure 8.16. The consistent tangential tensor in accordance with

anisotropic models is expressed by,

$$\mathbf{c}^{ep} = \left[\mathbf{c}^{e-1} + \Delta\gamma \partial_{\sigma'\sigma'}^2 f - \partial_{\sigma'} f \otimes \Delta\gamma \frac{\partial_{\sigma'\sigma'}^2 f : \mathbf{1}}{\left(\mathbf{1}:\partial_{\sigma'}f\right)} - \frac{MD}{\partial_{p'_c} f p'_c \left(\mathbf{1}:\partial_{\sigma'}f\right)} \partial_{\sigma'} f \otimes \partial_{\sigma'} f \right]^{-1} \tag{8.70}$$

$d\sigma'_{n+1}$	$d\varepsilon^p_{n+1}$	dp'_c	$d\Delta\gamma$
$d\sigma'^{<k>}_{n+1} = \mathbf{c}^{e<k-1>}_{n+1} : \left(d\varepsilon_{n+1} - d\varepsilon^p_{n+1}\right)$			
$d\varepsilon^p_{n+1} = \Delta\gamma d\partial_{\sigma'}f_{n+1} + \partial_{\sigma'}f_{n+1} \otimes d\Delta\gamma_{n+1}$			
$dp'_{c_{n+1}} = \dfrac{p'_{c_{n+1}}}{MD}\left(\mathbf{1}:d\varepsilon^p_{n+1}\right)$			
$df_{n+1} = \partial_{\sigma'}f : d\sigma'_{n+1} + \partial_{p'_c}f : dp'_{c_{n+1}}$			

$d\sigma'_{n+1}$	dp'_c	$d\Delta\gamma$	Omit subscript n+1
$d\sigma' = \mathbf{c}^e : \left\{ d\varepsilon - \left\{ \Delta\gamma \partial_{\sigma'\sigma'}^2 f : d\sigma' + \partial_{\sigma'}f \otimes d\Delta\gamma \right\} \right\}$			
$dp'_c = \dfrac{p'_c}{MD}\left(\mathbf{1} : \left\{ \Delta\gamma \partial_{\sigma'\sigma'}^2 f : d\sigma' + \partial_{\sigma'}f \otimes d\Delta\gamma \right\} \right)$			
$\partial_{\sigma'}f : d\sigma' + \partial_{p'_c}f : dp'_c = 0$			

Chain rule: $d\partial_{\sigma'}f_{n+1} = \partial_{\sigma'\sigma'}^2 f : d\sigma'\big|_{n+1} + \partial_{\sigma'p'_c}^2 f : dp'_c\big|_{n+1} = \partial_{\sigma'\sigma'}^2 f : d\sigma'\big|_{n+1}$

indicate unknowns of a system

$\partial_{\sigma'p'_c}^2 f = \mathbf{0}$

For uncoupling model between stress and hardening parameter i.e., SO but not for MCC model
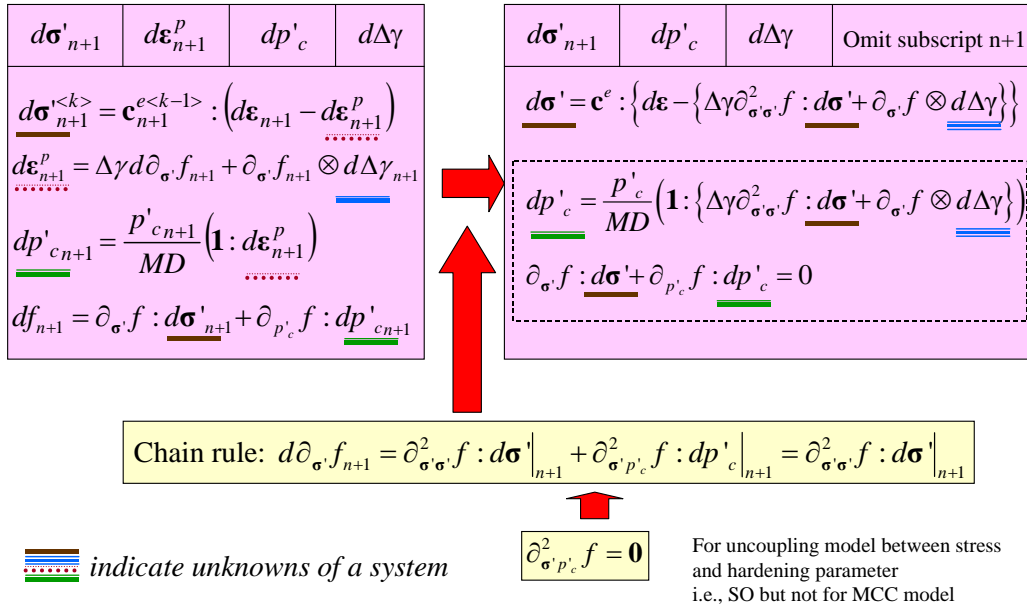
Figure 8.14 Differential form of backward incremental anisotropic constitutive equations

Plastic modulus defined in Appendix B is used to reduce plastic hardening terms found in Eq.(8.70). According to the SO model, plastic modulus H_p is shown in Eq.(8.71). Using an expression in Eq.(8.71) to deduce Eq.(8.70) results in the consistent tangential tensor in regard to the SO model as shown in Eq.(8.72).

$$\frac{MD}{p'_c}dp'_c - \left(\mathbf{1}:\partial_{\sigma'}f\right)d\Delta\gamma = \mathbf{1}:\Delta\gamma\partial_{\sigma'\sigma'}^2 f : d\sigma'$$

$$-\partial_{p'_c}f : dp'_c = \partial_{\sigma'}f : d\sigma'$$

matrix format

$$\begin{bmatrix} \dfrac{MD}{p'_c} & -\left(\mathbf{1}:\partial_{\sigma'}f\right) \\ -\partial_{p'_c}f & 0 \end{bmatrix}\begin{Bmatrix} dp'_c \\ d\Delta\gamma \end{Bmatrix} = \begin{Bmatrix} \Delta\gamma\left\{\mathbf{1}:\partial_{\sigma'\sigma'}^2 f\right\}:d\sigma' \\ \partial_{\sigma'}f : d\sigma' \end{Bmatrix}$$

matrix inverse

$$\begin{Bmatrix} dp'_c \\ d\Delta\gamma \end{Bmatrix} = \begin{bmatrix} \dfrac{MD}{p'_c} & -\left(\mathbf{1}:\partial_{\sigma'}f\right) \\ -\partial_{p'_c}f & 0 \end{bmatrix}^{-1}\begin{Bmatrix} \Delta\gamma\left\{\mathbf{1}:\partial_{\sigma'\sigma'}^2 f\right\}:d\sigma' \\ \partial_{\sigma'}f : d\sigma' \end{Bmatrix}$$

Inverse solution

$$\begin{Bmatrix} dp'_c \\ d\Delta\gamma \end{Bmatrix} = \begin{bmatrix} 0 & \dfrac{-1}{\partial_{p'_c}f} \\ \dfrac{-1}{\left(\mathbf{1}:\partial_{\sigma'}f\right)} & \dfrac{-1}{\partial_{p'_c}f\left(\mathbf{1}:\partial_{\sigma'}f\right)}\dfrac{MD}{p'_c} \end{bmatrix}\begin{Bmatrix} \Delta\gamma\left\{\mathbf{1}:\partial_{\sigma'\sigma'}^2 f\right\}:d\sigma' \\ \partial_{\sigma'}f : d\sigma' \end{Bmatrix}$$

$$d\sigma' = \mathbf{c}^e : \left\{ d\varepsilon - \left\{ \Delta\gamma \partial_{\sigma'\sigma'}^2 f : d\sigma' + \partial_{\sigma'}f \otimes d\Delta\gamma \right\} \right\}$$

$$dp'_c = \frac{-1}{\partial_{p'_c}f}\partial_{\sigma'}f : d\sigma'$$

$$d\Delta\gamma = \frac{-1}{\left(\mathbf{1}:\partial_{\sigma'}f\right)}\left\{ \Delta\gamma\mathbf{1}:\partial_{\sigma'\sigma'}^2 f + \frac{MD}{\partial_{p'_c}f p'_c}\partial_{\sigma'}f \right\}:d\sigma'$$
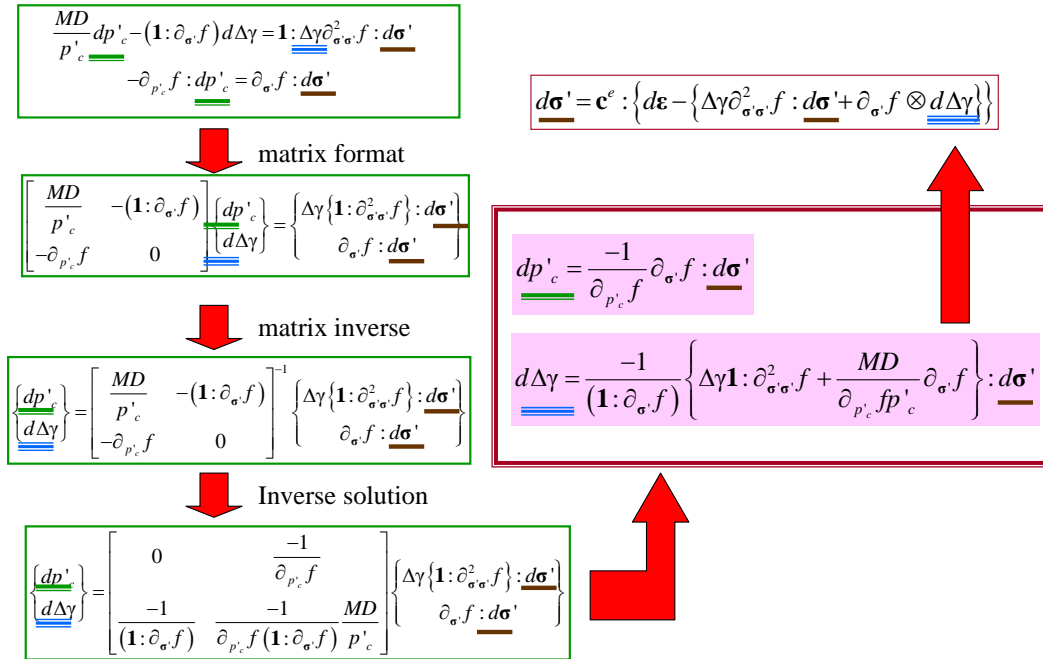
Figure 8.15 Variation of stress hardening and consistency parameters

$$H_p = -\frac{\frac{\partial f}{\partial p'_c} p'_c \left(\mathbf{1} : \partial_{\boldsymbol{\sigma}'} f\right)}{MD} = \mathbf{1} : \partial_{\boldsymbol{\sigma}'} f \tag{8.71}$$

$$\mathbf{c}^{ep} = \left[\mathbf{c}^{e-1} + \frac{1}{\mathbf{1} : \partial_{\boldsymbol{\sigma}'} f} \partial_{\boldsymbol{\sigma}'} f \otimes \partial_{\boldsymbol{\sigma}'} f + \Delta\gamma \left[\mathbf{I} - \frac{1}{\mathbf{1} : \partial_{\boldsymbol{\sigma}'} f} \partial_{\boldsymbol{\sigma}'} f \otimes \mathbf{1} \right] : \partial^2_{\boldsymbol{\sigma}'\boldsymbol{\sigma}'} f \right]^{-1} \tag{8.72}$$
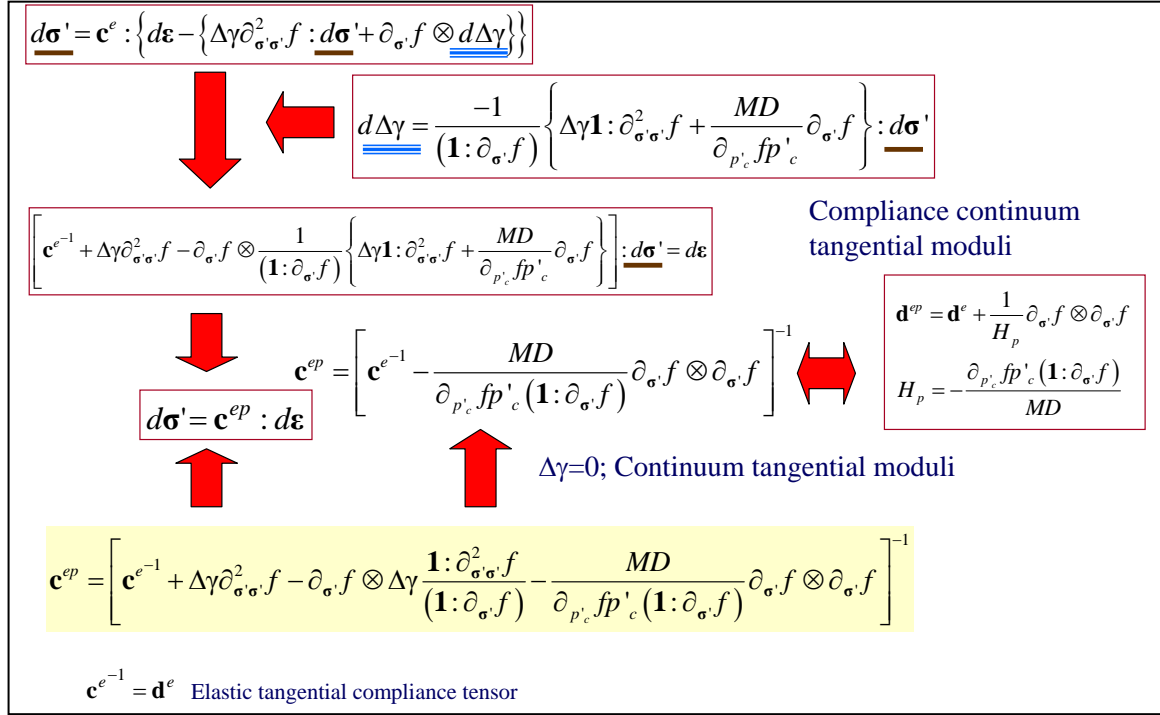
Figure 8.16 Consistent tangential tensor in accordance with the anisotropic models

Substitution of $\Delta\gamma = 0$ into either Eq.(8.70) or (8.72) would result in continuum tangential tensor, which can invert to compliance of continuum tangential tensor as shown in Eq.(8.73). The expression is the same expression shown in Appendix B and hence verify the result.

$$\mathbf{c}^{ep-1} = \mathbf{d}^{ep} = \mathbf{c}^{e-1} + \frac{\partial_{\boldsymbol{\sigma}'} f \otimes \partial_{\boldsymbol{\sigma}'} f}{\mathbf{1} : \partial_{\boldsymbol{\sigma}'} f} \tag{8.73}$$

8-5 References

1 Simo, J.C. & Tayor, R.L.: "Consistent tangent operators for rate-independent elastoplasticity", Comput. Methods Appl. Mech. Engrg., 48, 101-118 (1985).

2 Ortiz, M. & Simo, J.C.: "An analysis of a new class of integration algorithms for elastoplastic constitutive relations", Int. J. Numer. Methods Engrg., 23, 353-366 (1986).

3 Aravas, N.: "On the numerical integration of a class of pressure-dependent plasticity model", Int. J. Numer. Methods Engrg., 20, 1395-1416 (1987).

4 Ortiz, M. & Martin, J.B.:"Symmetry-preserving return mapping algorithms and incrementally extremal paths: A unification of concepts", Int. J. Numer. Anal. Meth. Geomech., 16, 737-756 (1992).

5 Simo, J.C.:"Algorithms for static and dynamic multiplicative plasticity that preserve the classical return mapping schemes of the infinitesimal theory", Comput. Methods Appl. Mech. Engrg., 99, 61-112 (1992).

6 Alawaji, H., Runesson, K. & Sture, S.:"Implicit integration in soil plasticity under mixed control for drained and undrained response", Int. J. Numer. Methods Engrg., 20, 1395-1416 (1987).

7 Borja, R.I. & Tamagnini, C.: "Cam-Clay plasticity, Part III: Extension of the infinitesimal model to include finite strains", Comput. Methods Appl. Mech. Engrg., 155, 73-95, (1998).

8 Luccioni, L.X., Pestana, J.M. & Rodriguez-Marek, A.: "An implicit integration algorithm for the finite element implementation of a nonlinear anisotropic material model including hysteretic nonlinearity", Comput. Methods Appl. Mech. Engrg., 190, 1827-1844 (2000).

9 Borja, R.I., Lin, C.H. & Montáns, F.J.:"Cam-Clay plasticity, part IV: Implicit integration of anisotropic

bounding surface model with nonlinear hyperelasticity and ellipsoidal loading function", Comput. Methods Appl. Mech. Engrg., 190, 3293-3323 (2001).

10 Manzari, M.T. & Prachathananukit, R.:"On integration of a cyclic soil plasticity model", Int. J. Numer. Anal. Meth. Geomech., 25, 525-549 (2001).

11 Borja, R.I. & Seung, R.L.: "Cam-Clay plasticity, part I: implicit integration of elasto-plastic constitutive relations", Comput. Methods Appl. Mech. Engrg., 78, 49-72 (1990).

12 Pipatpongsa, T., Iizuka, A., Kobayashi, I., Ohta, H. & Suzuki, Y.: "Nonlinear analysis for stress-strain-strength of clays using return-mapping algorithms", Journal of Applied Mechanics, JSCE, 4, 295-306 (2001).

13 Borja, R.I., Cam-Clay plasticity, Part II: "Implicit integration of constitutive equation based on a nonlinear elastic stress predictor", Comput. Methods Appl. Mech. Engrg. 88, 225-240 (1991)

CHAPTER 9
Tensorial Inversion Technique

9-1 Introduction

It is a tough computational effort to determine consistent tangential tensor as previously derived in Chapter 8. A determination of implicit tensor inversion would require exceedingly numerous nested loops for each step and iteration to reach a converged solution and hence diminish the attractiveness of return-mapping algorithms. In this chapter, a numerical inversion technique applied to forth-order tensor is introduced to by-pass laborious procedures needed to determine consistent tangential tensor in regard to anisotropic plasticity model. Formularization and verification of an inversion algorithm is demonstrated from elastic tangential tensors, continuum tangential tensors and consistent tangential tensors for both the Sekiguchi-Ohta model and the original Cam-clay model.

9-1-1 Inversion of square matrix

For a square matrix $\mathbf{A}_{(n \times n)}$ having eigen values and eigen vectors are $\lambda_{(n)}$ and $\mathbf{v}^{(n)}$

$$\mathbf{A}\mathbf{v}^{(k)} = \lambda_k \mathbf{v}^{(k)} \tag{9.1}$$

Combination of whole elements of eigen vectors of matrix $\mathbf{A}$ can be shown by,

$$\mathbf{A}\mathbf{Q} = \mathbf{Q}\mathbf{\Lambda} \tag{9.2}$$

$\mathbf{Q}$ is a modal matrix (orthogonal matrix) given by,

$$\mathbf{Q} = \begin{bmatrix} \mathbf{v}^{(1)} & \mathbf{v}^{(2)} & .. & .. & \mathbf{v}^{(n)} \end{bmatrix} = \begin{bmatrix} v_{11} & v_{21} & .. & .. & v_{1n} \\ v_{12} & v_{22} & .. & .. & v_{2n} \\ .. & .. & & & .. \\ .. & .. & & & .. \\ v_{1n} & v_{2n} & .. & .. & v_{nn} \end{bmatrix} \tag{9.3}$$

where $\mathbf{\Lambda}$ is a spectral matrix of A (diagonal matrix) given by,

$$\mathbf{\Lambda} = diag\begin{bmatrix} \lambda_1 & \lambda_2 & .. & .. & \lambda_n \end{bmatrix} = \begin{bmatrix} \lambda_1 & 0 & .. & .. & 0 \\ 0 & \lambda_2 & .. & .. & 0 \\ .. & .. & & & .. \\ .. & .. & & & .. \\ 0 & 0 & .. & .. & \lambda_n \end{bmatrix} \tag{9.4}$$

The spectral representation of matrix $\mathbf{A}$ can be given by,

$$\mathbf{A} = \mathbf{Q} \cdot \mathbf{\Lambda} \cdot \mathbf{Q}^{-1} = \mathbf{Q} \cdot \mathbf{\Lambda} \cdot \mathbf{Q}^T = \sum_{i=1}^{n} \lambda_i \begin{bmatrix} v_i \otimes v_i \end{bmatrix} \tag{9.5}$$

The similarity transformations can be expressed as,

$$f(\mathbf{A}) = \mathbf{Q} \cdot f(\mathbf{\Lambda}) \cdot \mathbf{Q}^{-1} \tag{9.6}$$

if $\mathbf{A}$ is symmetric matrix, then

$$f(\mathbf{A}) = \mathbf{Q} \cdot f(\mathbf{\Lambda}) \cdot \mathbf{Q}^T \tag{9.7}$$

Inversion of matrix $\mathbf{A}$ can be performed using similarity transformations as,

$$\mathbf{A}^{-1} = \mathbf{Q} \cdot \mathbf{\Lambda}^{-1} \cdot \mathbf{Q}^T \tag{9.8}$$

It is obvious that the inversion of $\mathbf{A}$ is still kept in form of modal matrix, that is, the vector basic of inversion of matrix $\mathbf{A}$ is the same vector basic of matrix $\mathbf{A}$.

9-1-2 Inversion of forth-order tensor

The identity forth-order tensor can be written by a sum of isotropic and deviatoric forth-order tensor as,

$$\mathbf{I} = \frac{1}{3}\mathbf{1} \otimes \mathbf{1} + \mathbf{A} \tag{9.9}$$

9-2 Elastic tangential compliance tensor

9-2-1 Linear stiffness moduli

Isotropic elastic tangential tensor is given by two independent material parameters and two tensor bases shown below, (See Appendix E)

$$\mathbf{c}^e = K\mathbf{1} \otimes \mathbf{1} + 2G\mathbf{A} \tag{9.10}$$

The elastic tangential compliance tensor is assumed to base on two reciprocal bases in corresponding to identity forth-order tensor, and two unknown material parameters as,

$$\mathbf{d}^e = a_1\left[\mathbf{I}:\mathbf{1}\otimes\mathbf{1}\right] + a_2\left[\mathbf{I}:\mathbf{A}\right] = a_1\mathbf{1}\otimes\mathbf{1} + a_2\mathbf{A} \tag{9.11}$$

The double product of tensor in Eq.(9.10) and Eq.(9.11) is

$$\begin{aligned}
\mathbf{c}^e : \mathbf{d}^e &= \left[K\mathbf{1}\otimes\mathbf{1} + 2G\mathbf{A}\right]:\left[a_1\mathbf{1}\otimes\mathbf{1} + a_2\mathbf{A}\right] \\
&= \left[K\mathbf{1}\otimes\mathbf{1}\right]:\left[a_1\mathbf{1}\otimes\mathbf{1}\right] + \left[K\mathbf{1}\otimes\mathbf{1}\right]:\left[a_2\mathbf{A}\right] + \left[2G\mathbf{A}\right]:\left[a_1\mathbf{1}\otimes\mathbf{1}\right] + \left[2G\mathbf{A}\right]:\left[a_2\mathbf{A}\right] \\
&= 3Ka_1\mathbf{1}\otimes\mathbf{1} + 0 + 0 + 2Ga_2\mathbf{A}
\end{aligned} \tag{9.12}$$

If Eq.(9.11) is an inversion of Eq.(9.10), then the double product should equal to an identity forth-order tensor defined in Eq.(9.9). Collection of independent coefficients respected to tensor bases are shown below,

$$\begin{aligned}
\mathbf{c}^e : \mathbf{d}^e &= \mathbf{I} \\
3Ka_1\mathbf{1}\otimes\mathbf{1} + 2Ga_2\mathbf{A} &= \frac{1}{3}\mathbf{1}\otimes\mathbf{1} + \mathbf{A} \\
\left(3Ka_1 - \frac{1}{3}\right)\mathbf{1}\otimes\mathbf{1} + \left(2Ga_2 - 1\right)\mathbf{A} &= \mathbf{0}
\end{aligned} \tag{9.13}$$

Since tensor bases are not zero tensor, each scalar coefficient shown in Eq.(9.13) must be zero. As a result, unknown scalar coefficients assumed in Eq.(9.11) can be determined as following,

$$\begin{aligned}
3Ka_1 - \frac{1}{3} &= 0 \\
a_1 &= \frac{1}{9K}
\end{aligned} \tag{9.14}$$

$$\begin{aligned}
2Ga_2 - 1 &= 0 \\
a_2 &= \frac{1}{2G}
\end{aligned} \tag{9.15}$$

Substitution on unknown scalar identified by Eq.(9.14),(9.15) ino Eq.(9.11) obtains an elastic tangential compliance tensor.

$$\mathbf{d}^e = \frac{1}{9K}\mathbf{1}\otimes\mathbf{1} + \frac{1}{2G}\mathbf{A} \tag{9.16}$$

9-2-2 Nonlinear stiffness moduli (secant moduli)

Isotropic elastic tangential tensor of nonlinear secant moduli is given by three independent parameters and three tensor bases shown below, (See Appendix E)

$$\mathbf{c}^e_{n+1} = a_1\mathbf{1}\otimes\mathbf{1} + 2G_s\mathbf{A} + \sqrt{\frac{2}{3}}\Delta q\,\mathbf{m}\otimes\mathbf{1} \tag{9.17}$$

where $\quad a_1 = K_{n+1}, a_2 = 2G_s, a_3 = \sqrt{\dfrac{2}{3}}\Delta q \tag{9.18}$

$$\Delta q = 3\mu'\frac{\partial K_s}{\Delta\boldsymbol{\varepsilon}^e_{n+1}}\Delta\varepsilon^e_s, \quad \mathbf{m} = \frac{\Delta\boldsymbol{\varepsilon}^e_d}{\left\|\Delta\boldsymbol{\varepsilon}^e_d\right\|}, \quad \Delta\varepsilon^e_s = \sqrt{\frac{2}{3}}\left\|\Delta\boldsymbol{\varepsilon}^e_d\right\| \tag{9.19}$$

The tensor bases of elastic tangential compliance tensor is reciprocally assumed to be

$$\mathbf{d}^e_{n+1} = b_1\mathbf{1}\otimes\mathbf{1} + b_2\mathbf{A} + b_3\mathbf{1}\otimes\mathbf{m} + b_4\mathbf{m}\otimes\mathbf{1} + b_5\mathbf{m}\otimes\mathbf{m} \tag{9.20}$$

Double product of $\mathbf{d}^e_{n+1}$ and $\mathbf{c}^e_{n+1}$ results in forth-order tensor whose scalar products respected to each independent tensor bases are shown in Table Table 9.1.

		$\mathbf{1}\otimes\mathbf{1}$	$\mathbf{A}$	$\mathbf{1}\otimes\mathbf{m}$	$\mathbf{m}\otimes\mathbf{1}$	$\mathbf{m}\otimes\mathbf{m}$
$b_1\mathbf{1}\otimes\mathbf{1}:\left[a_1\mathbf{1}\otimes\mathbf{1} + a_2\mathbf{A} + a_3\mathbf{m}\otimes\mathbf{1}\right]$	$=$	$3a_1b_1$				
$b_2\mathbf{A}:\left[a_1\mathbf{1}\otimes\mathbf{1} + a_2\mathbf{A} + a_3\mathbf{m}\otimes\mathbf{1}\right]$	$=$		a_2b_2		a_3b_2	
$b_3\mathbf{1}\otimes\mathbf{m}:\left[a_1\mathbf{1}\otimes\mathbf{1} + a_2\mathbf{A} + a_3\mathbf{m}\otimes\mathbf{1}\right]$	$=$	a_3b_3		a_2b_3		
$b_4\mathbf{m}\otimes\mathbf{1}:\left[a_1\mathbf{1}\otimes\mathbf{1} + a_2\mathbf{A} + a_3\mathbf{m}\otimes\mathbf{1}\right]$	$=$				$3a_1b_4$	
$b_5\mathbf{m}\otimes\mathbf{m}:\left[a_1\mathbf{1}\otimes\mathbf{1} + a_2\mathbf{A} + a_3\mathbf{m}\otimes\mathbf{1}\right]$	$=$				a_3b_5	a_2b_5

Table 9.1 Double product of $\mathbf{d}^e_{n+1}$ and $\mathbf{c}^e_{n+1}$

$$\mathbf{d}^e_{n+1} : \mathbf{c}^e_{n+1} = \begin{bmatrix}\left(3a_1b_1 + a_3b_3\right)\mathbf{1}\otimes\mathbf{1} + a_2b_2\mathbf{A} + a_2b_3\mathbf{1}\otimes\mathbf{m} + \\ \left(a_3b_2 + 3a_1b_4 + a_3b_5\right)\mathbf{m}\otimes\mathbf{1} + a_2b_5\mathbf{m}\otimes\mathbf{m}\end{bmatrix} = \frac{1}{3}\mathbf{1}\otimes\mathbf{1} + \mathbf{A} \tag{9.21}$$

By comparing coefficients of tensor bases of both sides of Eq.(9.21), linear algebra equations can be taken,

$$3b_1a_1 + a_3b_3 \quad = \quad \frac{1}{3}$$

$$a_2b_2 \quad = \quad 1$$

$$a_2b_3 \quad = \quad 0 \tag{9.22}$$

$$a_3b_2 + 3a_1b_4 + a_3b_5 \quad = \quad 0$$

$$a_2b_5 \quad = \quad 0$$

Solutions of a linear system in Eq.(9.22) are shown by,

$$b_1 = \frac{1}{9a_1}, \quad b_2 = \frac{1}{a_2}, \quad b_3 = 0, \quad b_4 = -\frac{a_3}{3a_1a_2}, \quad b_5 = 0 \tag{9.23}$$

Substitute Eq.(9.18) into Eq.(9.23), then

$$b_1 = \frac{1}{9K_{n+1}}, \quad b_2 = \frac{1}{2G_s}, \quad b_3 = 0, \quad b_4 = -\sqrt{\frac{2}{3}}\frac{\Delta q}{6K_{n+1}G_s}, \quad b_5 = 0 \tag{9.24}$$

Substitution of unknown coefficients obtained in Eq.(9.24) to Eq.(9.20) obtains an elastic tangential compliance tensor given by,

$$\mathbf{d}_{n+1}^e = \frac{1}{9K_{n+1}}\mathbf{1}\otimes\mathbf{1} + \frac{1}{2G_s}\mathbf{A} - \sqrt{\frac{2}{3}}\frac{\Delta q}{6K_{n+1}G_s}\mathbf{m}\otimes\mathbf{1} \tag{9.25}$$

Verification of the result is shown below by double product of $\mathbf{c}_{n+1}^e$ and $\mathbf{d}_{n+1}^e$. It is found that double product is valid by yielding the identity tensor.

$$\mathbf{c}_{n+1}^e : \mathbf{d}_{n+1}^e = \left[K_{n+1}\mathbf{1}\otimes\mathbf{1} + 2G_s\mathbf{A} + \sqrt{\frac{2}{3}}\Delta q\mathbf{m}\otimes\mathbf{1} \right] : \left[\frac{1}{9K_{n+1}}\mathbf{1}\otimes\mathbf{1} + \frac{1}{2G_s}\mathbf{A} - \sqrt{\frac{2}{3}}\frac{\Delta q}{6K_{n+1}G_s}\mathbf{m}\otimes\mathbf{1} \right]$$

$$= \frac{1}{3}\mathbf{1}\otimes\mathbf{1} + \mathbf{A} - \sqrt{\frac{2}{3}}\frac{\Delta q}{3K_{n+1}}\mathbf{m}\otimes\mathbf{1} + \sqrt{\frac{2}{3}}\frac{\Delta q}{3K_{n+1}}\mathbf{m}\otimes\mathbf{1} = \mathbf{I} \tag{9.26}$$

9-3 Continuum tangential compliance tensor

The continuum tangential elastoplastic forth-order tensor in regard to the SO model is given by five tensor bases and corresponding five constitutive coefficients. (See Appendix B)

$$\mathbf{c}^{ep} = \left(K - \frac{K^2\beta^2}{H_{ep}} \right)\mathbf{1}\otimes\mathbf{1} + 2G\mathbf{A} - \frac{\sqrt{6}GK\beta}{H_{ep}}\left(\mathbf{1}\otimes\bar{\mathbf{n}} + \bar{\mathbf{n}}\otimes\mathbf{1}\right) - \frac{6G^2}{H_{ep}}\bar{\mathbf{n}}\otimes\bar{\mathbf{n}} \tag{9.27}$$

$$H_{ep} = K\beta^2 + 3G + \frac{I_1}{3D}\beta, \quad \beta = M - 3\frac{\sqrt{3\bar{J}_2}}{I_1} - \sqrt{\frac{3}{2}}\left(\boldsymbol{\eta}_c : \bar{\mathbf{n}}\right) \tag{9.28),(9.29)}$$

Spectral representation of $\mathbf{c}^{ep}$ in Eq.(9.27) can be given by

$$\mathbf{c}^{ep} = a_1\mathbf{1}\otimes\mathbf{1} + a_2\mathbf{A} + a_3\mathbf{1}\otimes\bar{\mathbf{n}} + a_4\bar{\mathbf{n}}\otimes\mathbf{1} + a_5\bar{\mathbf{n}}\otimes\bar{\mathbf{n}} \tag{9.30}$$

Spectral representation of $(\mathbf{c}^{ep})^{-1}$ is presumably given by

$$\mathbf{c}^{ep^{-1}} = b_1\mathbf{1}\otimes\mathbf{1} + b_2\mathbf{A} + b_3\mathbf{1}\otimes\bar{\mathbf{n}} + b_4\bar{\mathbf{n}}\otimes\mathbf{1} + b_5\bar{\mathbf{n}}\otimes\bar{\mathbf{n}} \tag{9.31}$$

Eq.(9.30) and (9.31) share common tensor bases. A double product between them is an identity forth-order tensor shown by,

$$\mathbf{c}^{ep} : \mathbf{c}^{ep^{-1}} = \mathbf{I} = \frac{1}{3}\mathbf{1}\otimes\mathbf{1} + \mathbf{A} \tag{9.32}$$

$\mathbf{c}^{ep} : \mathbf{c}^{ep^{-1}} =$	*Scalar*	B	b_1	b_2	b_3	b_4	b_5
	A	*Tensor*	$\mathbf{1}\otimes\mathbf{1}$	$\mathbf{A}$	$\mathbf{1}\otimes\bar{\mathbf{n}}$	$\bar{\mathbf{n}}\otimes\mathbf{1}$	$\bar{\mathbf{n}}\otimes\bar{\mathbf{n}}$
	a_1	$\mathbf{1}\otimes\mathbf{1}$	$3(\mathbf{1}\otimes\mathbf{1})$	$\mathbf{0}$	$3(\mathbf{1}\otimes\bar{\mathbf{n}})$	$\mathbf{0}$	$\mathbf{0}$
	a_2	$\mathbf{A}$	$\mathbf{0}$	$\mathbf{A}$	$\mathbf{0}$	$\bar{\mathbf{n}}\otimes\mathbf{1}$	$\bar{\mathbf{n}}\otimes\bar{\mathbf{n}}$
	a_3	$\mathbf{1}\otimes\bar{\mathbf{n}}$	$\mathbf{0}$	$\mathbf{1}\otimes\bar{\mathbf{n}}$	$\mathbf{0}$	$\mathbf{1}\otimes\mathbf{1}$	$\mathbf{1}\otimes\bar{\mathbf{n}}$
	a_4	$\bar{\mathbf{n}}\otimes\mathbf{1}$	$3(\bar{\mathbf{n}}\otimes\mathbf{1})$	$\mathbf{0}$	$3(\bar{\mathbf{n}}\otimes\bar{\mathbf{n}})$	$\mathbf{0}$	$\mathbf{0}$
	a_5	$\bar{\mathbf{n}}\otimes\bar{\mathbf{n}}$	$\mathbf{0}$	$\bar{\mathbf{n}}\otimes\bar{\mathbf{n}}$	$\mathbf{0}$	$\bar{\mathbf{n}}\otimes\mathbf{1}$	$\bar{\mathbf{n}}\otimes\bar{\mathbf{n}}$

Table 9.2 Tensorial components of double product betweem $\mathbf{c}^{ep}$ and $(\mathbf{c}^{ep})^{-1}$

index	Tensor	Scalar components	$\mathbf{c}^{ep} : \mathbf{c}^{ep\,-1}$
(1)	$\mathbf{1} \otimes \mathbf{1}$	$3a_1 b_1 + a_3 b_4$	$\frac{1}{3}$
(2)	$\mathbf{A}$	$a_2 b_2$	1
(3)	$\mathbf{1} \otimes \mathbf{\bar{n}}$	$3a_1 b_3 + a_3 b_2 + a_3 b_5$	0
(4)	$\mathbf{\bar{n}} \otimes \mathbf{1}$	$a_2 b_4 + 3a_4 b_1 + a_5 b4$	0
(5)	$\mathbf{\bar{n}} \otimes \mathbf{\bar{n}}$	$a_2 b_5 + 3a_4 b_3 + a_5 b_2 + a_5 b_5$	0

Table 9.3 Scalar components of double product betweem $\mathbf{c}^{ep}$ and $(\mathbf{c}^{ep})^{-1}$

By comparing coefficients of tensor bases of double product with that of identity tensor, a linear equation system with b_1-b_5 as unknown variables can be generated.

$$
\begin{bmatrix}
3a_1 & 0 & 0 & a_3 & 0 \\
0 & a_2 & 0 & 0 & 0 \\
0 & a_3 & 3a_1 & 0 & a_3 \\
3a_4 & 0 & 0 & a_2+a_5 & 0 \\
0 & a_5 & 3a_4 & 0 & a_2+a_5
\end{bmatrix}
\cdot
\begin{Bmatrix}
b_1 \\ b_2 \\ b_3 \\ b_4 \\ b_5
\end{Bmatrix}
=
\begin{Bmatrix}
\frac{1}{3} \\ 1 \\ 0 \\ 0 \\ 0
\end{Bmatrix}
\tag{9.33}
$$

Unknown variables b_1-b_5 (notified by vector $\mathbf{B}$) can be solved linearly by,

$$
\mathbf{B} =
\begin{bmatrix}
3a_1 & 0 & 0 & a_3 & 0 \\
0 & a_2 & 0 & 0 & 0 \\
0 & a_3 & 3a_1 & 0 & a_3 \\
3a_4 & 0 & 0 & a_2+a_5 & 0 \\
0 & a_5 & 3a_4 & 0 & a_2+a_5
\end{bmatrix}^{-1}
\cdot
\begin{Bmatrix}
\frac{1}{3} \\ 1 \\ 0 \\ 0 \\ 0
\end{Bmatrix}
=
\frac{1}{a_1 a_2 - a_3 a_4 + a_1 a_5}
\begin{Bmatrix}
\dfrac{a_2 + a_5}{9} \\[2mm]
\dfrac{a_1 a_2 - a_3 a_4 + a_1 a_5}{a_2} \\[2mm]
-\dfrac{a_3}{3} \\[2mm]
-\dfrac{a_4}{3} \\[2mm]
\dfrac{-\left(a_1 a_5 - a_3 a_4\right)}{a_2}
\end{Bmatrix}
\tag{9.34}
$$

Constitutive coefficients a_1-a_5 (notified by vector $\mathbf{A}$) are substituted into Eq.(9.34), therefore, $\mathbf{B}$ can be determined and hence the constitutive coefficients for $(\mathbf{c}^{ep})^{-1}$.

$$
\mathbf{A} =
\begin{Bmatrix}
a_1 \\ a_2 \\ a_3 \\ a_4 \\ a_5
\end{Bmatrix}
= \frac{1}{H_{ep}}
\begin{Bmatrix}
KH_{ep} - K^2\beta^2 \\
2GH_{ep} \\
-\sqrt{6}GK\beta \\
-\sqrt{6}GK\beta \\
-6G^2
\end{Bmatrix}
, \quad
\mathbf{B} =
\begin{Bmatrix}
b_1 \\ b_2 \\ b_3 \\ b_4 \\ b_5
\end{Bmatrix}
= \frac{D}{I_1}
\begin{Bmatrix}
\dfrac{1}{9}\dfrac{3KD\beta + I_1}{KD} \\[2mm]
\dfrac{I_1}{2GD} \\[2mm]
\sqrt{\dfrac{3}{2}} \\[2mm]
\sqrt{\dfrac{3}{2}} \\[2mm]
\dfrac{9}{2\beta}
\end{Bmatrix}
\tag{9.35),(9.36}
$$

Finally, continuum tangential compliance elastoplastic forth-order tensor in regard to the SO model can be determined. The expression is consistent with a derivation given in Appendix B.

$$
\mathbf{d}^{ep} = \mathbf{c}^{ep\,-1} = \left(\frac{1}{9K} + \frac{D\beta}{3I_1}\right)\mathbf{1}\otimes\mathbf{1} + \frac{1}{2G}\mathbf{A} + \sqrt{\frac{3}{2}}\frac{D}{I_1}\left[\mathbf{1}\otimes\mathbf{\bar{n}} + \mathbf{\bar{n}}\otimes\mathbf{1}\right] + \frac{9D}{2I_1\beta}\mathbf{\bar{n}}\otimes\mathbf{\bar{n}}
\tag{9.37}
$$

9-4 Invariant-based spectral composition of the first derivative of the SO model

In the realm of plasticity theory, the first derivative of the yield function with respect to stress tensor (in Eq.(9.38)) gives the associative plastic flow direction, which is outward normal to the yield surface or plastic potential. According to the SO model, the flow direction is separated into isotropic and deviatoric directions governed by invariant-based second-order tensor bases $\mathbf{1}$ and $\mathbf{\bar{n}}$ (See Appendix B). The flow magnitudes in

corresponding to tensor bases can be derived from the yield function. Herein, the constitutive coefficients r_1 and r_2 derived from the SO model are shown in Figure 9.1.

$$\frac{\partial f}{\partial \boldsymbol{\sigma}'} = r_1 \mathbf{1} + r_2 \bar{\mathbf{n}} \tag{9.38}$$
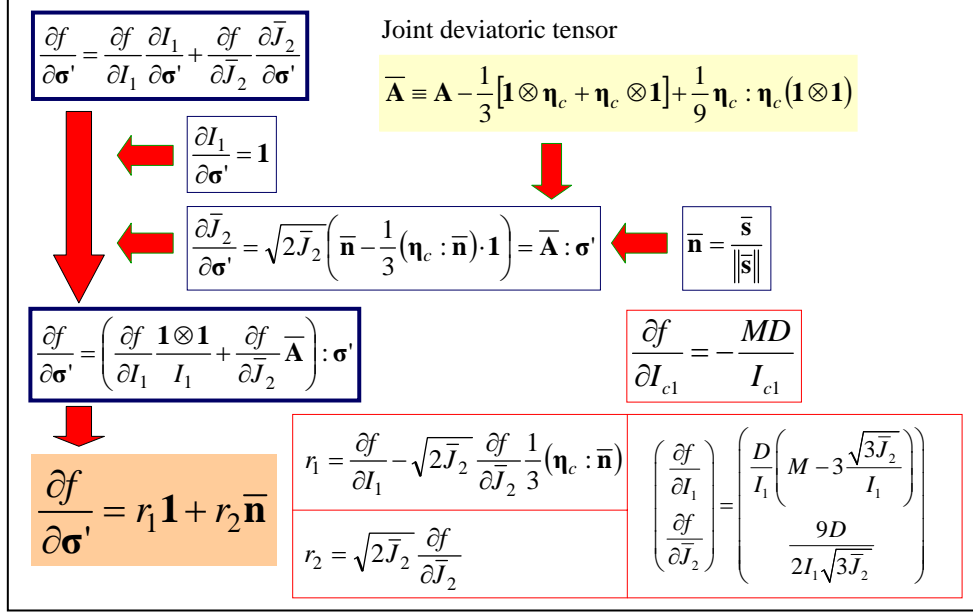
Figure 9.1 The first derivative of the SO model

9-5 Invariant-based spectral composition of the second derivative of the SO model

Directional derivative of the flow direction given in previous section can be expressed by the second derivative of the yield function with respect to stress tensor (in Eq.(9.39)). The resulted forth-order tensor is necessary in formulation of return-mapping algorithms. There are 7 independent tensor bases with corresponding constitutive coefficients shown by H_1-H_7. Since $H_3=H_4$ and $H_6=H_7$, the tensorial expression for the second-derivative of the SO model is found symmetric. The details of each tensorial and scalar composition are shown in Figure 9.2.
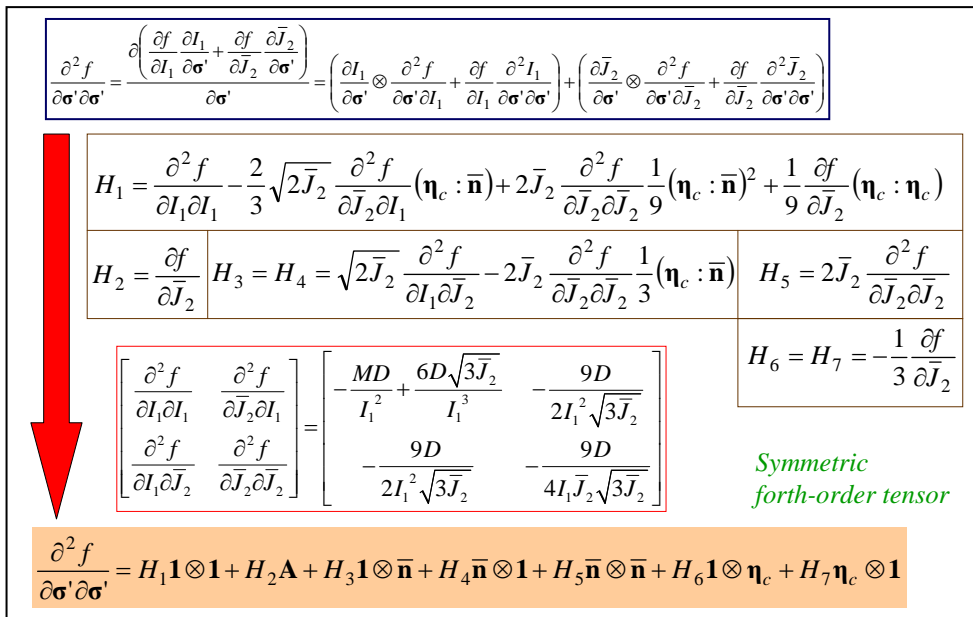
Figure 9.2 The second derivative of the SO model

$$\frac{\partial^2 f}{\partial \boldsymbol{\sigma}' \partial \boldsymbol{\sigma}'} = H_1 \mathbf{1} \otimes \mathbf{1} + H_2 \mathbf{A} + H_3 \mathbf{1} \otimes \overline{\mathbf{n}} + H_4 \overline{\mathbf{n}} \otimes \mathbf{1} + H_5 \overline{\mathbf{n}} \otimes \overline{\mathbf{n}} + H_6 \mathbf{1} \otimes \boldsymbol{\eta}_c + H_7 \boldsymbol{\eta}_c \otimes \mathbf{1} \qquad (9.39)$$

9-6 Algorithmic tensor

In linearization process of a constitutive equation, an algorithmic tensor is defined for convenience in equation manipulation. According to Ortiz, M. & Martin, J.B. (1989) [2] tensor $\boldsymbol{\Xi}$ is defined in terms of Hessian forth-order tensor as,

$$\boldsymbol{\Xi} \equiv \left[\mathbf{d}^e + \Delta\gamma \frac{\partial^2 f}{\partial \boldsymbol{\sigma}' \partial \boldsymbol{\sigma}'} \right]^{-1} \qquad (9.40)$$

Concerned with elasticity tensor of linear stiffness moduli and the second derivative of the SO model, a spectral representation of $\boldsymbol{\Xi}^{-1}$ can be expressed by 10 composition of mapping forth-order tensor bases $\mathbb{S} \times \mathbb{S}$ in stress space $\mathbb{S}$ where $\mathbf{1}, \overline{\mathbf{n}}, \boldsymbol{\eta} \in \mathbb{S}$; $\mathbb{S} = \left\{ \boldsymbol{\xi} : \mathbb{R}^3 \to \mathbb{R}^3 \middle| \boldsymbol{\xi} = \boldsymbol{\xi}^T \right\}$

$$\boldsymbol{\Xi}^{-1} = a_1 \mathbf{1} \otimes \mathbf{1} + a_2 \mathbf{A} + a_3 \mathbf{1} \otimes \overline{\mathbf{n}} + a_4 \overline{\mathbf{n}} \otimes \mathbf{1} + a_5 \overline{\mathbf{n}} \otimes \overline{\mathbf{n}} + a_6 \mathbf{1} \otimes \boldsymbol{\eta}_c + a_7 \boldsymbol{\eta}_c \otimes \mathbf{1}$$
$$+ a_8 \overline{\mathbf{n}} \otimes \boldsymbol{\eta}_c + a_9 \boldsymbol{\eta}_c \otimes \overline{\mathbf{n}} + a_{10} \boldsymbol{\eta}_c \otimes \boldsymbol{\eta}_c \qquad (9.41)$$

where the corresponding constitutive invariant-based coefficient a_1-a_{10} are shown as following, (See Appendix E and F)

$$a_1 = \Delta\gamma H_1 + \frac{1}{9K}, \quad a_2 = \Delta\gamma H_2 + \frac{1}{2G}, \quad a_3 = \Delta\gamma H_3, \quad a_4 = \Delta\gamma H_4, \quad a_5 = \Delta\gamma H_5, a_6 = \Delta\gamma H_6, \quad a_7 = \Delta\gamma H_7,$$
$$a_8 = a_9 = a_{10} = 0 \qquad (9.42)$$

The algorithmic tensor $\boldsymbol{\Xi}$ obtained by an inversion of tensor shown in Eq.(9.41) is supposed to share common tensor bases reciprocally. The constitutive invariant-based unknown variables b1-b10 are identified in accordance with a1-a10. A spectral decomposition of an algorithmic tensor $\boldsymbol{\Xi}$ is written by,

$$\boldsymbol{\Xi} = b_1 \mathbf{1} \otimes \mathbf{1} + b_2 \mathbf{A} + b_3 \mathbf{1} \otimes \overline{\mathbf{n}} + b_4 \overline{\mathbf{n}} \otimes \mathbf{1} + b_5 \overline{\mathbf{n}} \otimes \overline{\mathbf{n}} + b_6 \mathbf{1} \otimes \boldsymbol{\eta}_c + b_7 \boldsymbol{\eta}_c \otimes \mathbf{1}$$
$$+ b_8 \overline{\mathbf{n}} \otimes \boldsymbol{\eta}_c + b_9 \boldsymbol{\eta}_c \otimes \overline{\mathbf{n}} + b_{10} \boldsymbol{\eta}_c \otimes \boldsymbol{\eta}_c \qquad (9.43)$$

A double product of $\boldsymbol{\Xi}^{-1}$ and $\boldsymbol{\Xi}$ is enforced to result in an identity forth-order tensor.

$$\boldsymbol{\Xi}^{-1} : \boldsymbol{\Xi} \equiv \mathbf{I} = \frac{1}{3} \mathbf{1} \otimes \mathbf{1} + \mathbf{A} \qquad (9.44)$$

Tensorial components of double product are shown by in Table 9.4 which the first and second column notify scalar coefficients (identified by **a**) and tensor bases of $\boldsymbol{\Xi}^{-1}$ while the first and second row notify unknown coefficients (identified by **b**) and tensor bases of $\boldsymbol{\Xi}$ respectively. Table 9.5 shows composition of scalar components of double product in corresponding to each tensor bases. Since this double product is specified as the identity forth-order tensor **I**, which is related to two tensor bases $\mathbf{1} \otimes \mathbf{1}$ and **A** as shown in Eq.(9.44). For arbitrary tensor bases or non-zero tensor bases, a set of 10 linear equations matching coefficients of these tensor bases can be formulated. Reminding that $\mathbf{b} = \{b_1$-$b_{10}\}$ are unknown variables, equation system given in Table 9.6 is sufficient to solve for unknown coefficients **b** using inversion of 10x10 matrix.

9-6-1 Reduced form of algorithmic tensor

Table 9.6 shows a linear equation system to solve constitutive unknown coefficients of inversed $\boldsymbol{\Xi}$ providing that a determinant of a linear system is not zero. The solution can be solved both numerically and algebraically however the method can be more effective and simpler if a symmetric condition is considered. In a case that symmetry is preserved in Eq.(9.40), an amount of unknown variables can be reduced by adding conditions,

$$a_3 = a_4, a_6 = a_7, a_8 = a_9 \qquad (9.45)$$

As a consequence, Eq.(9.41),(9.43) can be reduced as shown in Eq.(9.46),(9.47) in which an amount of unknown variables is reduced from 10 to 7.

$$\boldsymbol{\Xi}^{-1} = a_1 \mathbf{1} \otimes \mathbf{1} + a_2 \mathbf{A} + a_3 \left[\mathbf{1} \otimes \overline{\mathbf{n}} + \overline{\mathbf{n}} \otimes \mathbf{1} \right] + a_5 \overline{\mathbf{n}} \otimes \overline{\mathbf{n}} + a_6 \left[\mathbf{1} \otimes \boldsymbol{\eta}_c + \boldsymbol{\eta}_c \otimes \mathbf{1} \right]$$
$$+ a_8 \left[\overline{\mathbf{n}} \otimes \boldsymbol{\eta}_c + \boldsymbol{\eta}_c \otimes \overline{\mathbf{n}} \right] + a_{10} \boldsymbol{\eta}_c \otimes \boldsymbol{\eta}_c \qquad (9.46)$$

$$\boldsymbol{\Xi} = b_1 \mathbf{1} \otimes \mathbf{1} + b_2 \mathbf{A} + b_3 \left[\mathbf{1} \otimes \overline{\mathbf{n}} + \overline{\mathbf{n}} \otimes \mathbf{1} \right] + b_5 \overline{\mathbf{n}} \otimes \overline{\mathbf{n}} + b_6 \left[\mathbf{1} \otimes \boldsymbol{\eta}_c + \boldsymbol{\eta}_c \otimes \mathbf{1} \right]$$
$$+ b_8 \left[\overline{\mathbf{n}} \otimes \boldsymbol{\eta}_c + \boldsymbol{\eta}_c \otimes \overline{\mathbf{n}} \right] + b_{10} \boldsymbol{\eta}_c \otimes \boldsymbol{\eta}_c \qquad (9.47)$$

The implementation of reduced spectral components is shown in Table 9.7. As shown in Table 9.8, coefficient $a_1, a_2, a_3, a_5, a_6, a_8$ and a_{10} can be evaluated. Providing that a determinant noted in (I) is not zero, vector **b** noted in (II) can be determined; therefore, a closed-form of $\boldsymbol{\Xi}$ can be obtained as noted in (III).

Table 9.4 Tensorial components of a double product of Ξ^{-1} and Ξ

$\Xi^{-1}:\Xi=$

scalar $\to$ **b**	tensor	b_1 $1\otimes 1$	b_2 $\mathbf{A}$	b_3 $1\otimes\bar{\mathbf{n}}$	b_4 $\bar{\mathbf{n}}\otimes 1$	b_5 $\bar{\mathbf{n}}\otimes\bar{\mathbf{n}}$	b_6 $1\otimes\boldsymbol{\eta}_c$	b_7 $\boldsymbol{\eta}_c\otimes 1$	b_8 $\bar{\mathbf{n}}\otimes\boldsymbol{\eta}_c$	b_9 $\boldsymbol{\eta}_c\otimes\bar{\mathbf{n}}$	b_{10} $\boldsymbol{\eta}_c\otimes\boldsymbol{\eta}_c$
a_1	$1\otimes 1$	$3(1\otimes 1)$	0	$3(1\otimes\bar{\mathbf{n}})$	0	0	$3(1\otimes\boldsymbol{\eta}_c)$	0	0	0	0
a_2	$\mathbf{A}$	0	$\mathbf{A}$	0	$\bar{\mathbf{n}}\otimes 1$	$\bar{\mathbf{n}}\otimes\bar{\mathbf{n}}$	0	$\boldsymbol{\eta}_c\otimes 1$	$\bar{\mathbf{n}}\otimes\boldsymbol{\eta}_c$	$\boldsymbol{\eta}_c\otimes\bar{\mathbf{n}}$	$\boldsymbol{\eta}_c\otimes\boldsymbol{\eta}_c$
a_3	$1\otimes\bar{\mathbf{n}}$	0	$1\otimes\bar{\mathbf{n}}$	0	$1\otimes 1$	$1\otimes\bar{\mathbf{n}}$	0	$\bar{\mathbf{n}}:\boldsymbol{\eta}_c(1\otimes 1)$	$1\otimes\boldsymbol{\eta}_c$	$\bar{\mathbf{n}}:\boldsymbol{\eta}_c(1\otimes\bar{\mathbf{n}})$	$\bar{\mathbf{n}}:\boldsymbol{\eta}_c(1\otimes\boldsymbol{\eta}_c)$
a_4	$\bar{\mathbf{n}}\otimes 1$	$3(\bar{\mathbf{n}}\otimes 1)$	0	$3(\bar{\mathbf{n}}\otimes\bar{\mathbf{n}})$	0	0	$3(\bar{\mathbf{n}}\otimes\boldsymbol{\eta}_c)$	0	0	0	0
a_5	$\bar{\mathbf{n}}\otimes\bar{\mathbf{n}}$	0	$\bar{\mathbf{n}}\otimes\bar{\mathbf{n}}$	0	$\bar{\mathbf{n}}\otimes 1$	$\bar{\mathbf{n}}\otimes\bar{\mathbf{n}}$	0	$\bar{\mathbf{n}}:\boldsymbol{\eta}_c(\bar{\mathbf{n}}\otimes 1)$	$\bar{\mathbf{n}}\otimes\boldsymbol{\eta}_c$	$\bar{\mathbf{n}}:\boldsymbol{\eta}_c(\bar{\mathbf{n}}\otimes\bar{\mathbf{n}})$	$\bar{\mathbf{n}}:\boldsymbol{\eta}_c(\bar{\mathbf{n}}\otimes\boldsymbol{\eta}_c)$
a_6	$1\otimes\boldsymbol{\eta}_c$	0	$1\otimes\boldsymbol{\eta}_c$	0	$\boldsymbol{\eta}_c:\bar{\mathbf{n}}(1\otimes 1)$	$\boldsymbol{\eta}_c:\bar{\mathbf{n}}(1\otimes\bar{\mathbf{n}})$	0	$\boldsymbol{\eta}_c:\boldsymbol{\eta}_c(1\otimes 1)$	$\bar{\mathbf{n}}:\boldsymbol{\eta}_c(1\otimes\boldsymbol{\eta}_c)$	$\boldsymbol{\eta}_c:\boldsymbol{\eta}_c(1\otimes\bar{\mathbf{n}})$	$\boldsymbol{\eta}_c:\boldsymbol{\eta}_c(1\otimes\boldsymbol{\eta}_c)$
a_7	$\boldsymbol{\eta}_c\otimes 1$	$3(\boldsymbol{\eta}_c\otimes 1)$	0	$3(\boldsymbol{\eta}_c\otimes\bar{\mathbf{n}})$	0	0	$3(\boldsymbol{\eta}_c\otimes\boldsymbol{\eta}_c)$	0	0	0	0

Table 9.5 Scalar components of a double product of Ξ^{-1} and Ξ

Index	Tensor	Scalar components	$\Xi^{-1}:\Xi$
(1)	$1\otimes 1$	$3a_1b_1 + a_3b_4 + \bar{\mathbf{n}}:\boldsymbol{\eta}_c(a_3b_7 + a_6b_4) + \boldsymbol{\eta}_c:\boldsymbol{\eta}_c a_6b_7$	$\frac{1}{3}$
(2)	$\mathbf{A}$	a_2b_2	1
(3)	$1\otimes\bar{\mathbf{n}}$	$3a_1b_3 + a_3b_2 + a_3b_5 + \bar{\mathbf{n}}:\boldsymbol{\eta}_c a_6b_5 + \bar{\mathbf{n}}:\boldsymbol{\eta}_c a_3b_9 + \boldsymbol{\eta}_c:\boldsymbol{\eta}_c a_6b_9$	0
(4)	$\bar{\mathbf{n}}\otimes 1$	$a_2b_4 + 3a_4b_1 + a_5b_4 + \bar{\mathbf{n}}:\boldsymbol{\eta}_c a_5b_7$	0
(5)	$\bar{\mathbf{n}}\otimes\bar{\mathbf{n}}$	$a_2b_5 + 3a_4b_3 + a_5b_2 + a_5b_5 + \bar{\mathbf{n}}:\boldsymbol{\eta}_c a_5b_9$	0
(6)	$1\otimes\boldsymbol{\eta}_c$	$3a_1b_6 + a_6b_2 + a_3b_8 + \bar{\mathbf{n}}:\boldsymbol{\eta}_c a_3b_{10} + \boldsymbol{\eta}_c:\boldsymbol{\eta}_c a_6b_{10} + \bar{\mathbf{n}}:\boldsymbol{\eta}_c a_6b_8$	0
(7)	$\boldsymbol{\eta}_c\otimes 1$	$a_2b_7 + 3a_7b_1$	0
(8)	$\bar{\mathbf{n}}\otimes\boldsymbol{\eta}_c$	$3a_4b_6 + a_2b_8 + a_5b_8 + \bar{\mathbf{n}}:\boldsymbol{\eta}_c a_5b_{10}$	0
(9)	$\boldsymbol{\eta}_c\otimes\bar{\mathbf{n}}$	$3a_7b_3 + a_2b_9$	0
(10)	$\boldsymbol{\eta}_c\otimes\boldsymbol{\eta}_c$	$3a_7b_6 + a_2b_{10}$	0

Linear algebra

$$
\mathbf{b} = \begin{bmatrix}
3a_1 & 0 & 0 & a_3+\mathbf{n}:\boldsymbol{\eta}_c a_6 & 0 & 0 & \mathbf{n}:\boldsymbol{\eta}_c a_3+\boldsymbol{\eta}_c:\boldsymbol{\eta}_c a_6 & 0 & 0 & 0 \\
0 & a_2 & 0 & 0 & 0 & 0 & 0 & 0 & 0 & 0 \\
0 & a_3 & 3a_1 & 0 & a_3+\mathbf{n}:\boldsymbol{\eta}_c a_6 & 0 & 0 & 0 & \mathbf{n}:\boldsymbol{\eta}_c a_3+\boldsymbol{\eta}_c:\boldsymbol{\eta}_c a_6 & 0 \\
3a_4 & 0 & 0 & a_2+a_5 & 0 & 0 & \mathbf{n}:\boldsymbol{\eta}_c a_5 & 0 & 0 & 0 \\
0 & a_5 & 3a_4 & 0 & a_2+a_5 & 0 & 0 & 0 & \mathbf{n}:\boldsymbol{\eta}_c a_5 & 0 \\
0 & a_6 & 0 & 0 & 0 & 3a_1 & 0 & a_3+\mathbf{n}:\boldsymbol{\eta}_c a_6 & 0 & \mathbf{n}:\boldsymbol{\eta}_c a_3+\boldsymbol{\eta}_c:\boldsymbol{\eta}_c a_6 \\
3a_7 & 0 & 0 & 0 & 0 & 0 & a_2 & 0 & 0 & 0 \\
0 & 0 & 0 & 0 & 0 & 3a_4 & 0 & a_2+a_5 & 0 & \mathbf{n}:\boldsymbol{\eta}_c a_5 \\
0 & 0 & 3a_7 & 0 & 0 & 0 & 0 & 0 & a_2 & 0 \\
0 & 0 & 0 & 0 & 0 & 3a_7 & 0 & 0 & 0 & a_2
\end{bmatrix}^{-1}
\begin{Bmatrix}
\frac{1}{3} \\ 1 \\ 0 \\ 0 \\ 0 \\ 0 \\ 0 \\ 0 \\ 0 \\ 0
\end{Bmatrix}
$$

Determinant of non-singular matrix

$$
\det(\mathbf{b}) = -27a_2 \begin{pmatrix}
a_2 a_4 a_3 + a_6 a_2 a_4 \mathbf{n}:\boldsymbol{\eta}_c + a_2 a_3 a_7 \mathbf{n}:\boldsymbol{\eta}_c + a_5 a_7 a_6 \boldsymbol{\eta}_c:\boldsymbol{\eta}_c \\
+a_2 a_7 a_6 \boldsymbol{\eta}_c:\boldsymbol{\eta}_c - a_1 a_2 a_5 - a_1 a_2^2 - a_5 a_6 a_7 \left(\mathbf{n}:\boldsymbol{\eta}_c\right)^2
\end{pmatrix}^3
$$

Table 9.6 Linear equation system for solving coefficients of Ξ which is obtained from the inversion of Ξ^{-1}

9-6-2 Variation of consistency parameter and elastic strain

Variation of consistency parameter $\delta\Delta\gamma$ and elastic strain $\delta\boldsymbol{\varepsilon}^e$ determined on each iteration can be evaluated by Eq.(9.48),(9.49). Multiplication of forth-order tensor in massive computation may expend a considerable attempt, however, it is able to minimize the obstacle by expanding the compositions into the individual multiplications of tensor bases and constitutive invariant-based coefficient.

$$
\delta\Delta\gamma = \frac{f - \left\{\partial_{\boldsymbol{\sigma}'}f + \frac{1}{3K}\mathbf{1}\right\}:\{\Xi:\overline{\mathbf{r}}\}}{\left\{\partial_{\boldsymbol{\sigma}'}f + \frac{1}{3K}\mathbf{1}\right\}:\{\Xi:\partial_{\boldsymbol{\sigma}'}f\}} = \frac{f - \left(\partial_{\boldsymbol{\sigma}'}f:\Xi:\overline{\mathbf{r}} + \frac{3}{9K}\mathbf{1}:\{\Xi:\overline{\mathbf{r}}\}\right)}{\partial_{\boldsymbol{\sigma}'}f:\Xi:\partial_{\boldsymbol{\sigma}'}f + \frac{1}{3K}\mathbf{1}:\{\Xi:\partial_{\boldsymbol{\sigma}'}f\}}
\tag{9.48}
$$

$$
\delta\boldsymbol{\varepsilon}^e = -\left[\mathbf{d}^e:\Xi\right]:\left\{\overline{\mathbf{r}} + \delta\Delta\gamma f_{\boldsymbol{\sigma}'}\right\}
\tag{9.49}
$$

Some common expression $\Xi:\partial_{\boldsymbol{\sigma}'}f = \Xi^T:\partial_{\boldsymbol{\sigma}'}f$, $\Xi:\mathbf{1} = \Xi^T:\mathbf{1}$, $\partial_{\boldsymbol{\sigma}'}f:\Xi:\partial_{\boldsymbol{\sigma}'}f$, $\mathbf{1}:\{\Xi:\partial_{\boldsymbol{\sigma}'}f\}$ can be previously computed in regard to their constitutive invariant-based coefficients by considering Eq.(9.50)-(9.55),

$$
\Xi:\partial_{\boldsymbol{\sigma}'}f = c_1\mathbf{1} + c_2\overline{\mathbf{n}} + c_3\boldsymbol{\eta}_c
\tag{9.50}
$$

where the coefficients c1,c2,c3 are determined as following Table 9.9 and Table 9.10.

$$
\Xi:\mathbf{1} = 3b_1 r_1 \mathbf{1} + 3b_3 r_1 \overline{\mathbf{n}} + 3b_5 r_1 \boldsymbol{\eta}_c , \quad \mathbf{1}:\Xi:\partial_{\boldsymbol{\sigma}'}f = 3c_1
\tag{9.51),(9.52}
$$

$$
\partial_{\boldsymbol{\sigma}'}f:\Xi:\partial_{\boldsymbol{\sigma}'}f =
\begin{array}{|c|c|c|c|c|}
\hline
scalar & \mathbf{c} & c_1 & c_2 & c_3 \\
\hline
\mathbf{r} & tensor & \mathbf{1} & \overline{\mathbf{n}} & \boldsymbol{\eta}_c \\
r_1 & \mathbf{1} & 3 & 0 & 0 \\
r_2 & \overline{\mathbf{n}} & 0 & 1 & \overline{\mathbf{n}}:\boldsymbol{\eta}_c \\
\hline
\end{array}
= 3r_1 c_1 + r_2 c_2 + \left(\overline{\mathbf{n}}:\boldsymbol{\eta}_c\right) r_2 c_3
\tag{9.53}
$$

$$
\Xi^T:\left\{\partial_{\boldsymbol{\sigma}'}f + \frac{1}{3K}\mathbf{1}\right\} = \Xi:\partial_{\boldsymbol{\sigma}'}f + \frac{1}{3K}\Xi:\mathbf{1}
\tag{9.54}
$$

$$
= \left\{c_1\mathbf{1} + c_2\overline{\mathbf{n}} + c_3\boldsymbol{\eta}_c\right\} + \frac{1}{K}\left\{b_1 r_1 \mathbf{1} + b_3 r_1 \overline{\mathbf{n}} + b_5 r_1 \boldsymbol{\eta}_c\right\}
$$

$$
\left\{\partial_{\boldsymbol{\sigma}'}f + \frac{1}{3K}\mathbf{1}\right\}:\{\Xi:\partial_{\boldsymbol{\sigma}'}f\} = 3\left(r_1 + \frac{1}{3K}\right)c_1 + r_2 c_2 + \left(\overline{\mathbf{n}}:\boldsymbol{\eta}_c\right) r_2 c_3
\tag{9.55}
$$

A composition of $\mathbf{d}^e:\Xi$ can be found in Table 9.11-Table 9.12.

Table 9.7 Reduced spectral components of double product between Ξ^{-1} and Ξ

$\Xi^{-1}:\Xi=$

scalar	**b**	b_1	b_2	$b_3=b_4$	←	b_5	$b_6=b_7$	←	$b_8=b_9$	←	b_{10}
a	*tensor*	$1\otimes1$	$\mathbf{A}$	$1\otimes\bar{n}+\bar{n}\otimes1$	←	$\bar{n}\otimes\bar{n}$	$1\otimes\eta_c+\eta_c\otimes1$	←	$\bar{n}\otimes\eta_c+\eta_c\otimes\bar{n}$	←	$\eta_c\otimes\eta_c$
a_1	$1\otimes1$	$3(1\otimes1)$	0	$3(1\otimes\bar{n})$	←	0	$3(1\otimes\eta_c)$	←	0	←	0
a_2	$\mathbf{A}$	0	$\mathbf{A}$	$\bar{n}\otimes1$	←	$\bar{n}\otimes\bar{n}$	$\eta_c\otimes1$	←	$\bar{n}\otimes\eta_c+\eta_c\otimes\bar{n}$	←	$\eta_c\otimes\eta_c$
$a_3=a_4$	$1\otimes\bar{n}+\bar{n}\otimes1$	$3(\bar{n}\otimes1)$	$1\otimes\bar{n}$	$3(\bar{n}\otimes\bar{n})+1\otimes1$	←	$1\otimes\bar{n}$	$3(\bar{n}\otimes\eta_c)+\bar{n}:\eta_c(1\otimes1)$	←	$1\otimes\eta_c+\bar{n}:\eta_c(1\otimes\bar{n})$	←	$\bar{n}:\eta_c(1\otimes\eta_c)$
↑	↑	↑	↑	↑	↑	↑	↑	↑	↑	↑	↑
a_5	$\bar{n}\otimes\bar{n}$	0	$\bar{n}\otimes\bar{n}$	$\bar{n}\otimes1$	←	$\bar{n}\otimes\bar{n}$	$\bar{n}:\eta_c(\bar{n}\otimes1)$	←	$\bar{n}\otimes\eta_c+\bar{n}:\eta_c(\bar{n}\otimes\bar{n})$	←	$\bar{n}:\eta_c(\bar{n}\otimes\eta_c)$
$a_6=a_7$	$1\otimes\eta_c+\eta_c\otimes1$	$3(\eta_c\otimes1)$	$1\otimes\eta_c$	$3(\eta_c\otimes\bar{n})+\eta_c:\bar{n}(1\otimes1)$	←	$\eta_c:\bar{n}(1\otimes\bar{n})$	$3(\eta_c\otimes\eta_c)+\eta_c:\eta_c(1\otimes1)$	←	$\bar{n}:\eta_c(1\otimes\eta_c)+\eta_c:\eta_c(1\otimes\bar{n})$	←	$\eta_c:\eta_c(1\otimes\eta_c)$
↑	↑	↑	↑	↑	↑	↑	↑	↑	↑	↑	↑

Index	Tensor	Scalar components	$\Xi^{-1}:\Xi$
(1)	$1\otimes1$	$3a_1b_1+a_3b_4+\bar{n}:\eta_c(a_3b_7+a_6b_4)+\eta_c:\eta_c a_6b_7$	$\frac{1}{3}$
(2)	$\mathbf{A}$	a_2b_2	1
(3)	$1\otimes\bar{n}+\bar{n}\otimes1$	$3a_1b_3+a_3b_2+a_3b_5+\bar{n}:\eta_c a_6b_5+\bar{n}:\eta_c a_3b_9+\eta_c:\eta_c a_6b_9+a_2b_4+3a_4b_1+a_5b_4+\bar{n}:\eta_c a_5b_7$	0
(4)	↑	↑	↑
(5)	$\bar{n}\otimes\bar{n}$	$a_2b_5+3a_4b_3+a_5b_2+a_5b_5+\bar{n}:\eta_c a_5b_9$	0
(6)	$1\otimes\eta_c+\eta_c\otimes1$	$3a_1b_6+a_6b_2+a_3b_8+\bar{n}:\eta_c a_3b_{10}+\eta_c:\eta_c a_6b_{10}+\bar{n}:\eta_c a_6b_8+a_2b_7+3a_7b_1$	0
(7)	↑	↑	↑
(8)	$\bar{n}\otimes\eta_c+\eta_c\otimes\bar{n}$	$3a_4b_6+a_2b_8+a_5b_8+\bar{n}:\eta_c a_5b_{10}+3a_7b_3+a_2b_9$	0
(9)	↑	↑	↑
(10)	$\eta_c\otimes\eta_c$	$3a_7b_6+a_2b_{10}$	0

Table 9.8 Determination of constitutive invariant-based coefficients of algorithmic forth-order tensor

I	$\text{DB} := \left(-a_2 \cdot a_6^2 \cdot \eta c\eta_c - a_6^2 \cdot \eta c\eta_c \cdot a_5 + a_1 \cdot a_2^2 - 2 \cdot a_2 \cdot a_3 \cdot a_6 \cdot n\_\eta_c - a_2 \cdot a_3^2 + a_1 \cdot a_2 \cdot a_5 + a_6^2 \cdot n\_\eta_c^2 \cdot a_5 \right)$	
II	$\mathbf{b} := \text{DB}^{-1} \cdot \begin{bmatrix} \dfrac{1}{9} \cdot a_2 \cdot \left(a_2 + a_5 \right) \\[2mm] \text{DB} \cdot \dfrac{1}{a_2} \\[2mm] \dfrac{-1}{3} \cdot a_2 \cdot a_3 + \dfrac{1}{3} \cdot a_6 \cdot n\_\eta_c \cdot a_5 \\[2mm] \dfrac{\left(-a_1 \cdot a_2 \cdot a_5 + a_2 \cdot a_3^2 + a_6^2 \cdot \eta c\eta_c \cdot a_5 \right)}{a_2} \\[2mm] \dfrac{-1}{3} \cdot \left(a_2 + a_5 \right) \cdot a_6 \\[2mm] \left(a_2 \cdot a_3 - a_6 \cdot n\_\eta_c \cdot a_5 \right) \cdot \dfrac{a_6}{a_2} \\[2mm] \left(a_2 + a_5 \right) \cdot \dfrac{a_6^2}{a_2} \end{bmatrix}$	$a_1 = \Delta\gamma H_1 + \dfrac{1}{9K}$ $a_2 = \Delta\gamma H_2 + \dfrac{1}{2G}$ $a_3 = \Delta\gamma H_3 = a_4 = \Delta\gamma H_4$ $a_5 = \Delta\gamma H_5$ $a_6 = \Delta\gamma H_6 = a_7 = \Delta\gamma H_7$ $n\_\eta_c = \overline{\mathbf{n}} : \boldsymbol{\eta}_c$ $\eta c\eta_c = \boldsymbol{\eta}_c : \boldsymbol{\eta}_c$
III	$\boldsymbol{\Xi} = b_1 \mathbf{1} \otimes \mathbf{1} + b_2 \mathbf{A} + b_3 \left[\mathbf{1} \otimes \overline{\mathbf{n}} + \overline{\mathbf{n}} \otimes \mathbf{1} \right] + b_4 \overline{\mathbf{n}} \otimes \overline{\mathbf{n}} + b_5 \left[\mathbf{1} \otimes \boldsymbol{\eta}_c + \boldsymbol{\eta}_c \otimes \mathbf{1} \right] + b_6 \left[\overline{\mathbf{n}} \otimes \boldsymbol{\eta}_c + \boldsymbol{\eta}_c \otimes \overline{\mathbf{n}} \right] + b_7 \boldsymbol{\eta}_c \otimes \boldsymbol{\eta}_c$	

$$\mathbf{\Xi}:\partial_{\sigma'}f \;=$$

scalar	$\mathbf{r}$	r_1	r_2
$\mathbf{b}$	*tensor*	$\mathbf{1}$	$\bar{\mathbf{n}}$
b_1	$\mathbf{1}\otimes\mathbf{1}$	$3\cdot\mathbf{1}$	$\mathbf{0}$
b_2	$\mathbf{A}$	$\mathbf{0}$	$\bar{\mathbf{n}}$
b_3	$\mathbf{1}\otimes\bar{\mathbf{n}}+\bar{\mathbf{n}}\otimes\mathbf{1}$	$3\cdot\bar{\mathbf{n}}$	$\mathbf{1}$
b_4	$\bar{\mathbf{n}}\otimes\bar{\mathbf{n}}$	$\mathbf{0}$	$\bar{\mathbf{n}}$
b_5	$\mathbf{1}\otimes\boldsymbol{\eta}_c+\boldsymbol{\eta}_c\otimes\mathbf{1}$	$3\cdot\boldsymbol{\eta}_c$	$\left(\bar{\mathbf{n}}:\boldsymbol{\eta}_c\right)\mathbf{1}$
b_6	$\bar{\mathbf{n}}\otimes\boldsymbol{\eta}_c+\boldsymbol{\eta}_c\otimes\bar{\mathbf{n}}$	$\mathbf{0}$	$\left(\bar{\mathbf{n}}:\boldsymbol{\eta}_c\right)\bar{\mathbf{n}}+\boldsymbol{\eta}_c$
b_7	$\boldsymbol{\eta}_c\otimes\boldsymbol{\eta}_c$	$\mathbf{0}$	$\left(\bar{\mathbf{n}}:\boldsymbol{\eta}_c\right)\boldsymbol{\eta}_c$

Table 9.9 Tensorial components of $\mathbf{\Xi}:\partial_{\sigma'}f$

coefficient	tensor	scalar component
c_1	$\mathbf{1}$	$3b_1r_1+\left(b_3+b_5\left(\bar{\mathbf{n}}:\boldsymbol{\eta}_c\right)\right)r_2$
c_2	$\bar{\mathbf{n}}$	$3b_3r_1+\left(b_2+b_4+b_6\left(\bar{\mathbf{n}}:\boldsymbol{\eta}_c\right)\right)r_2$
c_3	$\boldsymbol{\eta}_c$	$3b_5r_1+\left(b_6+b_7\left(\bar{\mathbf{n}}:\boldsymbol{\eta}_c\right)\right)r_2$

Table 9.10 Scalar components of $\mathbf{\Xi}:\partial_{\sigma'}f$

$$\mathbf{d}^e:\mathbf{\Xi} \;=$$

scalar	$\mathbf{b}$	b_1	b_2	b_3	b_4	b_5	b_6	b_7
	tensor	$\mathbf{1}\otimes\mathbf{1}$	$\mathbf{A}$	$\mathbf{1}\otimes\bar{\mathbf{n}}+\bar{\mathbf{n}}\otimes\mathbf{1}$	$\bar{\mathbf{n}}\otimes\bar{\mathbf{n}}$	$\mathbf{1}\otimes\boldsymbol{\eta}_c+\boldsymbol{\eta}_c\otimes\mathbf{1}$	$\bar{\mathbf{n}}\otimes\boldsymbol{\eta}_c+\boldsymbol{\eta}_c\otimes\bar{\mathbf{n}}$	$\boldsymbol{\eta}_c\otimes\boldsymbol{\eta}_c$
$\left(9K\right)^{-1}$	$\mathbf{1}\otimes\mathbf{1}$	$3\left(\mathbf{1}\otimes\mathbf{1}\right)$	$\mathbf{0}$	$3\left(\mathbf{1}\otimes\bar{\mathbf{n}}\right)$	$\mathbf{0}$	$3\left(\mathbf{1}\otimes\boldsymbol{\eta}_c\right)$	$\mathbf{0}$	$\mathbf{0}$
$\left(2G\right)^{-1}$	$\mathbf{A}$	$\mathbf{0}$	$\mathbf{A}$	$\bar{\mathbf{n}}\otimes\mathbf{1}$	$\bar{\mathbf{n}}\otimes\bar{\mathbf{n}}$	$\boldsymbol{\eta}_c\otimes\mathbf{1}$	$\bar{\mathbf{n}}\otimes\boldsymbol{\eta}_c+\boldsymbol{\eta}_c\otimes\bar{\mathbf{n}}$	$\boldsymbol{\eta}_c\otimes\boldsymbol{\eta}_c$

Table 9.11 Tensorial components of $\mathbf{d}^e:\mathbf{\Xi}$

index	tensor	scalar component
(1)	$\mathbf{1}\otimes\mathbf{1}$	$3\left(9K\right)^{-1}b_1$
(2)	$\mathbf{A}$	$\left(2G\right)^{-1}b_2$
(3)	$\mathbf{1}\otimes\bar{\mathbf{n}}$	$3\left(9K\right)^{-1}b_3$
(4)	$\bar{\mathbf{n}}\otimes\mathbf{1}$	$\left(2G\right)^{-1}b_3$
(5)	$\bar{\mathbf{n}}\otimes\bar{\mathbf{n}}$	$\left(2G\right)^{-1}b_4$
(6)	$\mathbf{1}\otimes\boldsymbol{\eta}_c$	$3\left(9K\right)^{-1}b_5$
(7)	$\boldsymbol{\eta}_c\otimes\mathbf{1}$	$\left(2G\right)^{-1}b_5$
(8)	$\bar{\mathbf{n}}\otimes\boldsymbol{\eta}_c$	$\left(2G\right)^{-1}b_6$
(9)	$\boldsymbol{\eta}_c\otimes\bar{\mathbf{n}}$	$\left(2G\right)^{-1}b_6$
(10)	$\boldsymbol{\eta}_c\otimes\boldsymbol{\eta}_c$	$\left(2G\right)^{-1}b_7$

Table 9.12 Scalar components of $\mathbf{d}^e:\mathbf{\Xi}$

9-7 Consistent tangential tensor

9-7-1 Compliance of consistent tangential tensor in regard to the SO model

The consistent tangential tensor derived in Chapter 8 is expressed implicitly in terms of inversion form of compliance consistent tangential tensor as shown in Eq.(9.56),(9.57).

$$\mathbf{c}^{ep-1} = \mathbf{c}^{e-1} + \frac{1}{H_p} \partial_{\boldsymbol{\sigma}'} f \otimes \partial_{\boldsymbol{\sigma}'} f + \Delta\gamma \partial^2_{\boldsymbol{\sigma}'\boldsymbol{\sigma}'} f - \Delta\gamma \partial_{\boldsymbol{\sigma}'} f \otimes \frac{\partial^2_{\boldsymbol{\sigma}'\boldsymbol{\sigma}'} f : \mathbf{1}}{H_p} \tag{9.56}$$

where $H_p = -\dfrac{\partial f}{\partial I_{c1}} \dfrac{I_{c1}}{MD} \mathbf{1} : \dfrac{\partial f}{\partial \boldsymbol{\sigma}'} = \mathbf{1} : \dfrac{\partial f}{\partial \boldsymbol{\sigma}'}, \quad \dfrac{\partial f}{\partial I_{c1}} = -\dfrac{MD}{I_{c1}}$ (9.57)

In order to express explicitly or in closed-form expression for $\mathbf{c}^{ep}$, the inversion algorithm will be applied in the similar way of previous section. However, symmetry is not preserved in consistent tangential tensor even flow rule is associative [1,2] because hardening law in regard to critical state model is not associative but empirical rule [3]. Iinvariant-based spectral composition of $\mathbf{c}^{ep-1}$ is expressed by 10 constitutive coefficients and tensor bases as,

$$\mathbf{c}^{ep-1} = \sum_{i=1}^{10} u_i [\mathbf{T}_i] \tag{9.58}$$

$\dfrac{\partial f}{\partial \boldsymbol{\sigma}'} = r_1 \mathbf{1} + r_2 \bar{\mathbf{n}}$

$\dfrac{\partial f}{\partial \boldsymbol{\sigma}'} \otimes \dfrac{\partial f}{\partial \boldsymbol{\sigma}'} = r_1^2 \mathbf{1} \otimes \mathbf{1} + r_1 r_2 [\mathbf{1} \otimes \bar{\mathbf{n}} + \bar{\mathbf{n}} \otimes \mathbf{1}] + r_2^2 \bar{\mathbf{n}} \otimes \bar{\mathbf{n}}$

$\dfrac{\partial f}{\partial \boldsymbol{\sigma}'} : \mathbf{1} = 3r_1$

$\dfrac{\partial_{\boldsymbol{\sigma}'} f \otimes \partial_{\boldsymbol{\sigma}'} f}{\mathbf{1} : \partial_{\boldsymbol{\sigma}'} f} = \dfrac{r_1}{3} \mathbf{1} \otimes \mathbf{1} + \dfrac{r_2}{3} \mathbf{1} \otimes \bar{\mathbf{n}} + \dfrac{r_2}{3} \bar{\mathbf{n}} \otimes \mathbf{1} + \dfrac{r_2^2}{3 r_1} \bar{\mathbf{n}} \otimes \bar{\mathbf{n}}$

$\dfrac{\partial^2 f}{\partial \boldsymbol{\sigma}' \partial \boldsymbol{\sigma}'} = H_1 \mathbf{1} \otimes \mathbf{1} + H_2 \mathbf{A} + H_3 \mathbf{1} \otimes \bar{\mathbf{n}} + H_4 \bar{\mathbf{n}} \otimes \mathbf{1} + H_5 \bar{\mathbf{n}} \otimes \bar{\mathbf{n}} + H_6 \mathbf{1} \otimes \boldsymbol{\eta}_c + H_7 \boldsymbol{\eta}_c \otimes \mathbf{1}$

$\mathbf{1} : \dfrac{\partial^2 f}{\partial \boldsymbol{\sigma}' \partial \boldsymbol{\sigma}'} = 3\{H_1 \mathbf{1} + H_3 \bar{\mathbf{n}} + H_6 \boldsymbol{\eta}_c\}$

$\dfrac{\partial_{\boldsymbol{\sigma}'} f \otimes \mathbf{1} : \partial^2_{\boldsymbol{\sigma}'\boldsymbol{\sigma}'} f}{\mathbf{1} : \partial_{\boldsymbol{\sigma}'} f} = H_1 \mathbf{1} \otimes \mathbf{1} + H_3 \mathbf{1} \otimes \bar{\mathbf{n}} + H_6 \mathbf{1} \otimes \boldsymbol{\eta}_c + \dfrac{r_2}{r_1} H_1 \bar{\mathbf{n}} \otimes \mathbf{1} + \dfrac{r_2}{r_1} H_3 \bar{\mathbf{n}} \otimes \bar{\mathbf{n}} + \dfrac{r_2}{r_1} H_6 \bar{\mathbf{n}} \otimes \boldsymbol{\eta}_c$

$\mathbf{c}^{e-1} = \mathbf{d}^e = (9K)^{-1} \mathbf{1} \otimes \mathbf{1} + (2G)^{-1} \mathbf{A}$

$$\mathbf{c}^{ep} = \left[\mathbf{c}^{e-1} + \frac{\partial_{\boldsymbol{\sigma}'} f \otimes \partial_{\boldsymbol{\sigma}'} f}{\mathbf{1} : \partial_{\boldsymbol{\sigma}'} f} + \Delta\gamma \left[\mathbf{I} - \frac{\partial_{\boldsymbol{\sigma}'} f \otimes \mathbf{1}}{\mathbf{1} : \partial_{\boldsymbol{\sigma}'} f} \right] : \partial^2_{\boldsymbol{\sigma}'\boldsymbol{\sigma}'} f \right]^{-1}$$
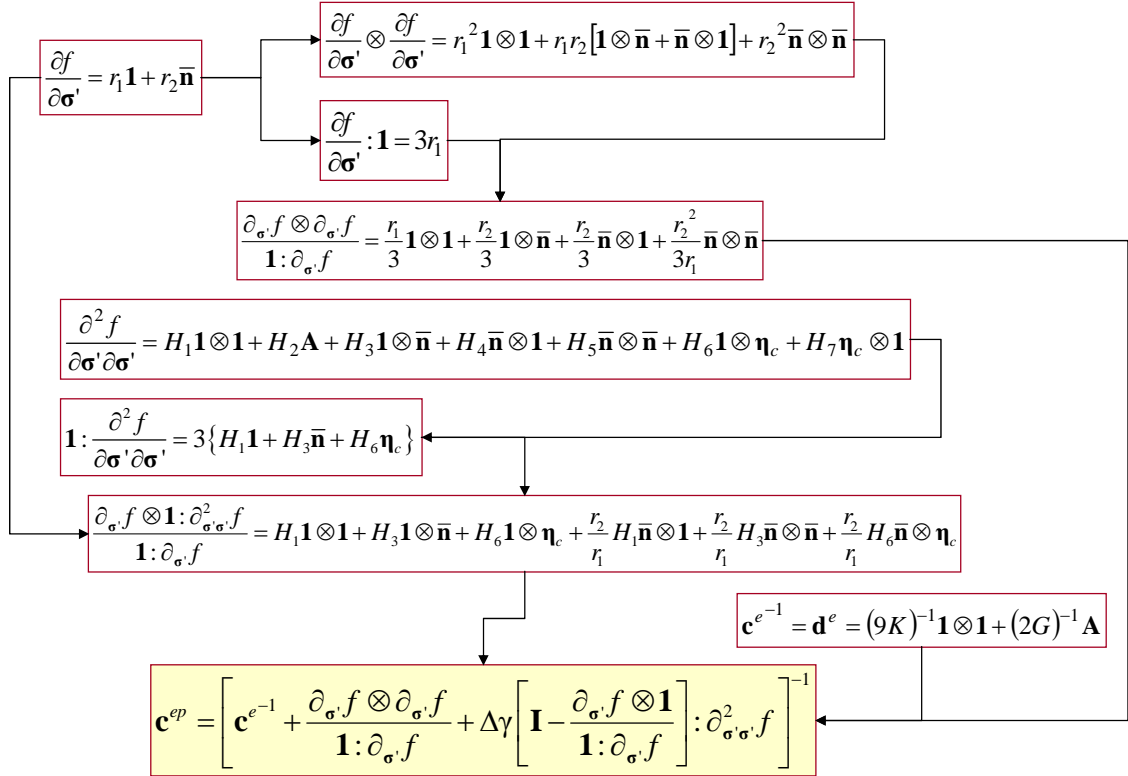
Figure 9.3 Consistent $\mathbf{c}^{ep-1}$ in terms of invariant-based spectral composition

By following a process outlined in Figure 9.3, descriptions of constitutive coefficients u_1-u_{10} and corresponding tensor bases $\mathbf{T}_1$-$\mathbf{T}_{10}$ are shown in Table 9.13. Though the constitutive coefficients u_9 and u_{10} are zero, the tensor bases $\mathbf{T}_9$ and $\mathbf{T}_{10}$ cannot be disregarded because whole tensor bases are required to correctly relate stress-to-strain mapping to strain-to-stress mapping. $\mathbf{T}_2$ marks a deviatoric forth-order tensor $\mathbf{A}$ while forth-order tensor bases $\mathbf{T}_1,\mathbf{T}_3$-$\mathbf{T}_{10}$ are formulated by multiple tensor product of 3 basic symmetric second-order tensor, which are, (See Appendix B)

$$\mathbf{1} = diag[1 \quad 1 \quad 1] \tag{9.59}$$

$$\bar{\mathbf{n}} = \frac{\bar{\mathbf{s}}}{\|\bar{\mathbf{s}}\|} \quad \text{where} \quad \bar{\mathbf{s}} = \mathbf{s} - p'\boldsymbol{\eta}_c = \left[\mathbf{A} - \frac{1}{3} \boldsymbol{\eta}_c \otimes \mathbf{1} \right] : \boldsymbol{\sigma}' \tag{9.60}$$

$$\boldsymbol{\eta}_{c(t=0)} = \boldsymbol{\eta}_o = \sqrt{\frac{2}{3}} \eta_o diag \left[-\frac{\sqrt{6}}{6} \quad \frac{\sqrt{6}}{3} \quad -\frac{\sqrt{6}}{6} \right] \tag{9.61}$$

Double products (double contraction) of these basic tensors with deviatoric forth-order tensor $\mathbf{A}$ result in second-order tensor shown by,

$$\mathbf{A} : \mathbf{1} = \mathbf{0}, \quad \mathbf{A} : \boldsymbol{\eta}_c = \boldsymbol{\eta}_c, \quad \mathbf{A} : \bar{\mathbf{n}} = \bar{\mathbf{n}} \tag{9.62),(9.63),(9.64}$$

Double products among these basic tensors result in scalar values shown by

$$\mathbf{1} : \mathbf{1} = 3, \quad \mathbf{1} : \boldsymbol{\eta}_c = 0, \quad \mathbf{1} : \bar{\mathbf{n}} = 0, \quad \bar{\mathbf{n}} : \bar{\mathbf{n}} = 1 \tag{9.65),(9.66),(9.67),(9.68}$$

Index	T	Scalar	components	u
(1)	$\mathbf{1}\otimes\mathbf{1}$	$\left(9K\right)^{-1}+\dfrac{r_1}{3}$		u_1
(2)	$\mathbf{A}$	$\left(2G\right)^{-1}+\Delta\gamma H_2$		u_2
(3)	$\mathbf{1}\otimes\overline{\mathbf{n}}$	$\dfrac{r_2}{3}$		u_3
(4)	$\overline{\mathbf{n}}\otimes\mathbf{1}$	$\Delta\gamma\left(H_4-\dfrac{r_2}{r_1}H_1\right)+\dfrac{r_2}{3}$		u_4
(5)	$\overline{\mathbf{n}}\otimes\overline{\mathbf{n}}$	$\Delta\gamma\left(H_5-\dfrac{r_2}{r_1}H_3\right)+\dfrac{r_2^2}{3r_1}$		u_5
(6)	$\mathbf{1}\otimes\boldsymbol{\eta}_c$	0		u_6
(7)	$\boldsymbol{\eta}_c\otimes\mathbf{1}$	$\Delta\gamma H_7$		u_7
(8)	$\overline{\mathbf{n}}\otimes\boldsymbol{\eta}_c$	$-\Delta\gamma\dfrac{r_2}{r_1}H_6$		u_8
(9)	$\boldsymbol{\eta}_c\otimes\overline{\mathbf{n}}$	0		u_9
(10)	$\boldsymbol{\eta}_c\otimes\boldsymbol{\eta}_c$	0		u_{10}

Table 9.13 Spectral components of $\mathbf{c}^{ep-1}$

Based on Eq.(9.59)-(9.61), it is concluded that the reciprocal bases $\mathbf{1},\overline{\mathbf{n}},\boldsymbol{\eta}_c \in \mathbb{S}$ are neither unit tensors nor mutually orthogonal tensor. Though orthonormal bases are obvious, reciprocal bases employed in the study is convenient to deal with axis-transformation for anisotropic material response in particular.

$$
\mathbf{u}=\begin{Bmatrix} u_1 \\ u_2 \\ u_3 \\ u_4 \\ u_5 \\ u_6 \\ u_7 \\ u_8 \\ u_9 \\ u_{10} \end{Bmatrix}=\begin{Bmatrix} \dfrac{1}{9K}+\dfrac{D\beta}{9p'} \\[6pt] \dfrac{1}{2G}+\dfrac{3D}{2p'\overline{q}}\Delta\gamma \\[6pt] \dfrac{D}{\sqrt{6}p'} \\[6pt] \dfrac{D}{\sqrt{6}p'}+\dfrac{D}{\sqrt{6}\beta p'}\left(\dfrac{\left(2\beta-3M+\dfrac{\overline{q}}{p'}\right)}{p'}-\dfrac{M\left(\beta-M+\dfrac{3}{2M}(\boldsymbol{\eta}_c:\boldsymbol{\eta}_c)\right)}{\overline{q}}\right)\Delta\gamma \\[6pt] \dfrac{3D}{2\beta p'}-\dfrac{3D}{2\beta p'}\dfrac{\left(M-2\dfrac{\overline{q}}{p'}\right)}{\overline{q}}\Delta\gamma \\[6pt] 0 \\[6pt] -\dfrac{D}{2p'\overline{q}}\Delta\gamma \\[6pt] \dfrac{3\sqrt{6}D}{4\beta p'\overline{q}}\Delta\gamma \\[6pt] 0 \\[6pt] 0 \end{Bmatrix}
\tag{9.69}
$$

where $\beta=M-\dfrac{\overline{q}}{p'}-\sqrt{\dfrac{3}{2}}(\overline{\mathbf{n}}:\boldsymbol{\eta}_c)$, $\overline{q}=\sqrt{3\overline{J}_2}$

According to the SO model with linear elastic moduli (nonlinear elastic moduli by semi-backward Euler), the corresponding constitutive coefficients u_1-u_{10} shown in Eq.(9.69)are evaluated by Eq.(9.56). All of these terms can be numerically evaluated at a current step. Consistency parameter $\Delta\gamma$ is iteratively updated using algorithmic tensor (Refer to Eq.(9.48)). Although nonlinear elastic moduli are in flavor for computation, linear elastic moduli

with backward update (semi-backward Euler) can be used for simple formulation with similar accuracy but slower in convergence. For exact form of nonlinear elastic moduli, the elasticity tensor derived in Appendix E should be employed.

$$\mathbf{u}^{T} = \left\{ \frac{1}{9} \frac{p'+KD\beta}{Kp'} \quad \frac{1}{2G} \quad \frac{D}{\sqrt{6}p'} \quad \frac{D}{\sqrt{6}p'} \quad \frac{3}{2} \frac{D}{p'\beta} \quad 0 \quad 0 \quad 0 \quad 0 \quad 0 \right\}$$ (9.70)

It is observed that a consistent $\mathbf{c}^{ep-1}$ is not symmetric forth-order tensor by the fact that; $u_3 \neq u_4$, $u_6 \neq u_7$ and $u_8 \neq u_9$. A substitution of $\Delta\gamma=0$ into expression of $\mathbf{u}$ for consistent $\mathbf{c}^{ep-1}$ in Eq.(9.69) results in expression of $\mathbf{u}$ for continuum $\mathbf{c}^{ep-1}$ as shown in Eq.(9.70), which is previously shown in Eq.(9.36) (note p'=3I$_1$). The continuum is symmetric forth-order tensor by the fact that; $u_3=u_4$. This method can use to verify a consistent expression with a continuum expression.

9-7-2 Consistent tangential tensor in regard to the SO model

Consistent tangential tensor can be obtained by the inversion of $\mathbf{c}^{ep-1}$. Expanding of Eq.(9.58) is shown by Eq.(9.71),

$$\mathbf{c}^{ep-1} = u_1\left[\mathbf{1}\otimes\mathbf{1}\right] + u_2\left[\mathbf{A}\right] + u_3\left[\mathbf{1}\otimes\overline{\mathbf{n}}\right] + u_4\left[\overline{\mathbf{n}}\otimes\mathbf{1}\right] + u_5\left[\overline{\mathbf{n}}\otimes\overline{\mathbf{n}}\right] + u_6\left[\mathbf{1}\otimes\boldsymbol{\eta}_c\right]$$
$$+ u_7\left[\boldsymbol{\eta}_c\otimes\mathbf{1}\right] + u_8\left[\overline{\mathbf{n}}\otimes\boldsymbol{\eta}_c\right] + u_9\left[\boldsymbol{\eta}_c\otimes\overline{\mathbf{n}}\right] + u_{10}\left[\boldsymbol{\eta}_c\otimes\boldsymbol{\eta}_c\right]$$ (9.71)

The inversion algorithm starts by expressing an inversed form of $\mathbf{c}^{ep-1}$ to be coaxial with itself. The tensor bases do not change but scalar coefficients do change by mapping law in the space. To evaluate these quantities, the identity of double product is imposed by referring to Eq.(9.73).

$$\mathbf{c}^{ep} = v_1\left[\mathbf{1}\otimes\mathbf{1}\right] + v_2\left[\mathbf{A}\right] + v_3\left[\mathbf{1}\otimes\overline{\mathbf{n}}\right] + v_4\left[\overline{\mathbf{n}}\otimes\mathbf{1}\right] + v_5\left[\overline{\mathbf{n}}\otimes\overline{\mathbf{n}}\right] + v_6\left[\mathbf{1}\otimes\boldsymbol{\eta}_c\right]$$
$$+ v_7\left[\boldsymbol{\eta}_c\otimes\mathbf{1}\right] + v_8\left[\overline{\mathbf{n}}\otimes\boldsymbol{\eta}_c\right] + v_9\left[\boldsymbol{\eta}_c\otimes\overline{\mathbf{n}}\right] + v_{10}\left[\boldsymbol{\eta}_c\otimes\boldsymbol{\eta}_c\right]$$ (9.72)

$$\mathbf{c}^{ep-1} : \mathbf{c}^{ep} = \mathbf{I} = \frac{1}{3}\left[\mathbf{1}\otimes\mathbf{1}\right] + \left[\mathbf{A}\right]$$ (9.73)

Double product between $\mathbf{c}^{ep-1}$ in Eq.(9.71) and $\mathbf{c}^{ep}$ in Eq.(9.72) is shown in Table 9.14. The unknown scalar quantities v_1-v_{10} assumed in expression of $\mathbf{c}^{ep}$ in Eq.(9.72) is finally determined by a system of 10 linear equations given by Eq.(9.74) providing that determinant D_v given by Eq.(9.75) is not zero.

$$D_v = -\left(\begin{array}{c} \left(\overline{\mathbf{n}}:\boldsymbol{\eta}_c\right)^2 u_3 u_7 u_8 - \left(\overline{\mathbf{n}}:\boldsymbol{\eta}_c\right)^2 u_5 u_6 u_7 + \overline{\mathbf{n}}:\boldsymbol{\eta}_c u_2 u_3 u_7 - \overline{\mathbf{n}}:\boldsymbol{\eta}_c u_1 u_2 u_8 + \overline{\mathbf{n}}:\boldsymbol{\eta}_c u_2 u_4 u_6 \\ -\boldsymbol{\eta}_c:\boldsymbol{\eta}_c u_3 u_7 u_8 + u_2 u_3 u_4 + \boldsymbol{\eta}_c:\boldsymbol{\eta}_c u_5 u_6 u_7 + \boldsymbol{\eta}_c:\boldsymbol{\eta}_c u_2 u_6 u_7 - u_1 u_2 u_5 - u_2^2 u_1 \end{array} \right)$$ (9.74)

$$\begin{bmatrix} 3u_1 & 0 & 0 & u_3+\mathbf{n}:\boldsymbol{\eta}_c u_6 & 0 & 0 & \mathbf{n}:\boldsymbol{\eta}_c u_3 + \boldsymbol{\eta}_c:\boldsymbol{\eta}_c u_6 & 0 & 0 & 0 \\ 0 & u_2 & 0 & 0 & 0 & 0 & 0 & 0 & 0 & 0 \\ 0 & u_3 & 3u_1 & 0 & u_3+\mathbf{n}:\boldsymbol{\eta}_c u_6 & 0 & 0 & 0 & \mathbf{n}:\boldsymbol{\eta}_c u_3 + \boldsymbol{\eta}_c:\boldsymbol{\eta}_c u_6 & 0 \\ 3u_4 & 0 & 0 & u_2+u_5+\mathbf{n}:\boldsymbol{\eta}_c u_8 & 0 & 0 & \mathbf{n}:\boldsymbol{\eta}_c u_5 + \boldsymbol{\eta}_c:\boldsymbol{\eta}_c u_8 & 0 & 0 & 0 \\ 0 & u_5 & 3u_4 & 0 & u_2+u_5+\mathbf{n}:\boldsymbol{\eta}_c u_8 & 0 & 0 & 0 & \mathbf{n}:\boldsymbol{\eta}_c u_5 + \boldsymbol{\eta}_c:\boldsymbol{\eta}_c u_8 & 0 \\ 0 & u_6 & 0 & 0 & 0 & 3u_1 & 0 & u_3+\mathbf{n}:\boldsymbol{\eta}_c u_6 & 0 & \mathbf{n}:\boldsymbol{\eta}_c u_3 + \boldsymbol{\eta}_c:\boldsymbol{\eta}_c u_6 \\ 3u_7 & 0 & 0 & 0 & 0 & 0 & u_2 & 0 & 0 & 0 \\ 0 & u_8 & 0 & 0 & 0 & 3u_4 & 0 & u_2+u_5+\mathbf{n}:\boldsymbol{\eta}_c u_8 & 0 & \mathbf{n}:\boldsymbol{\eta}_c u_5 + \boldsymbol{\eta}_c:\boldsymbol{\eta}_c u_8 \\ 0 & 0 & 3u_7 & 0 & 0 & 0 & 0 & 0 & u_2 & 0 \\ 0 & 0 & 0 & 0 & 0 & 3u_7 & 0 & 0 & 0 & u_2 \end{bmatrix}$$ (9.75)

Solutions for v_1-v_{10} (denote by vector $\mathbf{v}$) are presented in terms of u_1-u_{10} as shown in Figure 9.4 And hence, a consistent $\mathbf{c}^{ep}$ can be determined. It is found that a consistent $\mathbf{c}^{ep}$ is not symmetric forth-order tensor due to non-symmetry of $\mathbf{c}^{ep-1}$.

According to the mathematical implementation of consistent $\mathbf{c}^{ep-1}$ shown in Eq.(9.56), to obtain a consistent $\mathbf{c}^{ep}$ for the anisotropic plasticity model in 3D standpoint, it is required to invert 6x6 matrix at each Gauss point per iteration, which can reduce the powerfulness of return-mapping algorithms. The proposed inversion algorithm allows a direct evaluation of an exact linearization of material stiffness inexpensively. Furthermore, a quadratic rate of global convergence of Newton's method can be achieved with less computational effort required by conventional anisotropic plasticity model [2].

The proposed inversion algorithm can be considered as the extension of method proposed by Borja, R.I. et al. [1,4,5] for isotropic Critical-state models [6] to be applicable to anisotropic Critical-state models. Moreover, the concept may break similar difficulties that are seemingly appeared in computation for anisotropic or complicated model by return-mapping algorithms [7,8,9,10,11].

Table 9.14 Invariant-based spectral composition of double product of $\mathbf{c}^{ep\text{-}1}$ and $\mathbf{c}^{ep}$

	scalar	$\mathbf{v}$	v_1	v_2	v_3	v_4	v_5	v_6	v_7	v_8	v_9	v_{10}
	$\mathbf{u}$	*tensor*	$\mathbf{1}\otimes\mathbf{1}$	$\mathbf{A}$	$\mathbf{1}\otimes\bar{\mathbf{n}}$	$\bar{\mathbf{n}}\otimes\mathbf{1}$	$\bar{\mathbf{n}}\otimes\bar{\mathbf{n}}$	$\mathbf{1}\otimes\boldsymbol{\eta}_c$	$\boldsymbol{\eta}_c\otimes\mathbf{1}$	$\bar{\mathbf{n}}\otimes\boldsymbol{\eta}_c$	$\boldsymbol{\eta}_c\otimes\bar{\mathbf{n}}$	$\boldsymbol{\eta}_c\otimes\boldsymbol{\eta}_c$
$\mathbf{c}^{ep\text{-}1}:\mathbf{c}^{ep} = $	u_1	$\mathbf{1}\otimes\mathbf{1}$	$3(\mathbf{1}\otimes\mathbf{1})$	0	$3(\mathbf{1}\otimes\bar{\mathbf{n}})$	0	0	$3(\mathbf{1}\otimes\boldsymbol{\eta}_c)$	0	0	0	0
	u_2	$\mathbf{A}$	0	$\mathbf{A}$	0	$\bar{\mathbf{n}}\otimes\mathbf{1}$	$\bar{\mathbf{n}}\otimes\bar{\mathbf{n}}$	0	$\boldsymbol{\eta}_c\otimes\mathbf{1}$	$\bar{\mathbf{n}}\otimes\boldsymbol{\eta}_c$	$\boldsymbol{\eta}_c\otimes\bar{\mathbf{n}}$	$\boldsymbol{\eta}_c\otimes\boldsymbol{\eta}_c$
	u_3	$\mathbf{1}\otimes\bar{\mathbf{n}}$	0	$\mathbf{1}\otimes\bar{\mathbf{n}}$	0	$\mathbf{1}\otimes\mathbf{1}$	$\mathbf{1}\otimes\bar{\mathbf{n}}$	0	$\bar{\mathbf{n}}:\boldsymbol{\eta}_c(\mathbf{1}\otimes\mathbf{1})$	$\mathbf{1}\otimes\boldsymbol{\eta}_c$	$\bar{\mathbf{n}}:\boldsymbol{\eta}_c(\mathbf{1}\otimes\bar{\mathbf{n}})$	$\bar{\mathbf{n}}:\boldsymbol{\eta}_c(\mathbf{1}\otimes\boldsymbol{\eta}_c)$
	u_4	$\bar{\mathbf{n}}\otimes\mathbf{1}$	$3(\bar{\mathbf{n}}\otimes\mathbf{1})$	0	$3(\bar{\mathbf{n}}\otimes\bar{\mathbf{n}})$	0	0	$3(\bar{\mathbf{n}}\otimes\boldsymbol{\eta}_c)$	0	0	0	0
	u_5	$\bar{\mathbf{n}}\otimes\bar{\mathbf{n}}$	0	$\bar{\mathbf{n}}\otimes\bar{\mathbf{n}}$	0	$\bar{\mathbf{n}}\otimes\mathbf{1}$	$\bar{\mathbf{n}}\otimes\bar{\mathbf{n}}$	0	$\bar{\mathbf{n}}:\boldsymbol{\eta}_c(\bar{\mathbf{n}}\otimes\mathbf{1})$	$\bar{\mathbf{n}}\otimes\boldsymbol{\eta}_c$	$\bar{\mathbf{n}}:\boldsymbol{\eta}_c(\bar{\mathbf{n}}\otimes\bar{\mathbf{n}})$	$\bar{\mathbf{n}}:\boldsymbol{\eta}_c(\bar{\mathbf{n}}\otimes\boldsymbol{\eta}_c)$
	u_6	$\mathbf{1}\otimes\boldsymbol{\eta}_c$	0	$\mathbf{1}\otimes\boldsymbol{\eta}_c$	0	$\bar{\mathbf{n}}:\boldsymbol{\eta}_c(\mathbf{1}\otimes\mathbf{1})$	$\bar{\mathbf{n}}:\boldsymbol{\eta}_c(\mathbf{1}\otimes\bar{\mathbf{n}})$	0	$\boldsymbol{\eta}_c:\boldsymbol{\eta}_c(\mathbf{1}\otimes\mathbf{1})$	$\bar{\mathbf{n}}:\boldsymbol{\eta}_c(\mathbf{1}\otimes\boldsymbol{\eta}_c)$	$\boldsymbol{\eta}_c:\boldsymbol{\eta}_c(\mathbf{1}\otimes\bar{\mathbf{n}})$	$\boldsymbol{\eta}_c:\boldsymbol{\eta}_c(\mathbf{1}\otimes\boldsymbol{\eta}_c)$
	u_7	$\boldsymbol{\eta}_c\otimes\mathbf{1}$	$3(\boldsymbol{\eta}_c\otimes\mathbf{1})$	0	$3(\boldsymbol{\eta}_c\otimes\bar{\mathbf{n}})$	0	0	$3(\boldsymbol{\eta}_c\otimes\boldsymbol{\eta}_c)$	0	0	0	0
	u_8	$\bar{\mathbf{n}}\otimes\boldsymbol{\eta}_c$	0	$\bar{\mathbf{n}}\otimes\boldsymbol{\eta}_c$	0	$\bar{\mathbf{n}}:\boldsymbol{\eta}_c(\bar{\mathbf{n}}\otimes\mathbf{1})$	$\bar{\mathbf{n}}:\boldsymbol{\eta}_c(\bar{\mathbf{n}}\otimes\bar{\mathbf{n}})$	0	$\boldsymbol{\eta}_c:\boldsymbol{\eta}_c(\bar{\mathbf{n}}\otimes\mathbf{1})$	$\bar{\mathbf{n}}:\boldsymbol{\eta}_c(\bar{\mathbf{n}}\otimes\boldsymbol{\eta}_c)$	$\boldsymbol{\eta}_c:\boldsymbol{\eta}_c(\bar{\mathbf{n}}\otimes\bar{\mathbf{n}})$	$\boldsymbol{\eta}_c:\boldsymbol{\eta}_c(\bar{\mathbf{n}}\otimes\boldsymbol{\eta}_c)$
	u_9	$\boldsymbol{\eta}_c\otimes\bar{\mathbf{n}}$	0	$\boldsymbol{\eta}_c\otimes\bar{\mathbf{n}}$	0	$\boldsymbol{\eta}_c\otimes\mathbf{1}$	$\boldsymbol{\eta}_c\otimes\bar{\mathbf{n}}$	0	$\bar{\mathbf{n}}:\boldsymbol{\eta}_c(\boldsymbol{\eta}_c\otimes\mathbf{1})$	$\boldsymbol{\eta}_c\otimes\boldsymbol{\eta}_c$	$\bar{\mathbf{n}}:\boldsymbol{\eta}_c(\boldsymbol{\eta}_c\otimes\bar{\mathbf{n}})$	$\bar{\mathbf{n}}:\boldsymbol{\eta}_c(\boldsymbol{\eta}_c\otimes\boldsymbol{\eta}_c)$
	u_{10}	$\boldsymbol{\eta}_c\otimes\boldsymbol{\eta}_c$	0	$\boldsymbol{\eta}_c\otimes\boldsymbol{\eta}_c$	0	$\bar{\mathbf{n}}:\boldsymbol{\eta}_c(\boldsymbol{\eta}_c\otimes\mathbf{1})$	$\bar{\mathbf{n}}:\boldsymbol{\eta}_c(\boldsymbol{\eta}_c\otimes\bar{\mathbf{n}})$	0	$\boldsymbol{\eta}_c:\boldsymbol{\eta}_c(\boldsymbol{\eta}_c\otimes\mathbf{1})$	$\bar{\mathbf{n}}:\boldsymbol{\eta}_c(\boldsymbol{\eta}_c\otimes\boldsymbol{\eta}_c)$	$\boldsymbol{\eta}_c:\boldsymbol{\eta}_c(\boldsymbol{\eta}_c\otimes\bar{\mathbf{n}})$	$\boldsymbol{\eta}_c:\boldsymbol{\eta}_c(\boldsymbol{\eta}_c\otimes\boldsymbol{\eta}_c)$

Index	*Tensor*	*Scalar components*	$\mathbf{I}$
(1)	$\mathbf{1}\otimes\mathbf{1}$	$3u_1v_1 + u_3v_4 + \bar{\mathbf{n}}:\boldsymbol{\eta}_c(u_3v_7 + u_6v_4) + \boldsymbol{\eta}_c:\boldsymbol{\eta}_c u_6v_7$	$\frac{1}{3}$
(2)	$\mathbf{A}$	u_2v_2	1
(3)	$\mathbf{1}\otimes\bar{\mathbf{n}}$	$3u_1v_3 + u_3v_2 + u_3v_5 + \bar{\mathbf{n}}:\boldsymbol{\eta}_c(u_6v_5 + u_3v_9) + \boldsymbol{\eta}_c:\boldsymbol{\eta}_c u_6v_9$	0
(4)	$\bar{\mathbf{n}}\otimes\mathbf{1}$	$u_2v_4 + 3u_4v_1 + u_5v_4 + \bar{\mathbf{n}}:\boldsymbol{\eta}_c(u_5v_7 + u_8v_4) + \boldsymbol{\eta}_c:\boldsymbol{\eta}_c u_8v_7$	0
(5)	$\bar{\mathbf{n}}\otimes\bar{\mathbf{n}}$	$u_2v_5 + 3u_4v_3 + u_5v_2 + u_5v_5 + \bar{\mathbf{n}}:\boldsymbol{\eta}_c(u_5v_9 + u_8v_5) + \boldsymbol{\eta}_c:\boldsymbol{\eta}_c u_8v_9$	0
(6)	$\mathbf{1}\otimes\boldsymbol{\eta}_c$	$3u_1v_6 + u_6v_2 + u_3v_8 + \bar{\mathbf{n}}:\boldsymbol{\eta}_c(u_3v_{10} + u_6v_8) + \boldsymbol{\eta}_c:\boldsymbol{\eta}_c u_6v_{10}$	0
(7)	$\boldsymbol{\eta}_c\otimes\mathbf{1}$	$u_2v_7 + 3u_7v_1 + u_9v_4 + \bar{\mathbf{n}}:\boldsymbol{\eta}_c(u_{10}v_4 + u_9v_7) + \boldsymbol{\eta}_c:\boldsymbol{\eta}_c u_{10}v_7$	0
(8)	$\bar{\mathbf{n}}\otimes\boldsymbol{\eta}_c$	$3u_4v_6 + u_2v_8 + u_5v_8 + \bar{\mathbf{n}}:\boldsymbol{\eta}_c(u_5v_{10} + u_8v_8) + u_8v_2 + \boldsymbol{\eta}_c:\boldsymbol{\eta}_c u_8v_{10}$	0
(9)	$\boldsymbol{\eta}_c\otimes\bar{\mathbf{n}}$	$3u_7v_3 + u_2v_9 + u_9v_2 + u_9v_5 + \bar{\mathbf{n}}:\boldsymbol{\eta}_c(u_{10}v_5 + u_9v_9) + \boldsymbol{\eta}_c:\boldsymbol{\eta}_c u_{10}v_9$	0
(10)	$\boldsymbol{\eta}_c\otimes\boldsymbol{\eta}_c$	$3u_7v_6 + u_2v_{10} + u_{10}v_2 + u_9v_8 + \bar{\mathbf{n}}:\boldsymbol{\eta}_c(u_{10}v_8 + u_9v_{10}) + \boldsymbol{\eta}_c:\boldsymbol{\eta}_c u_{10}v_{10}$	0

$$D_v = -\begin{pmatrix} n\_\eta\,_c{}^2 \cdot u_8 \cdot u_7 \cdot 3 - n\_\eta\,_c{}^2 \cdot u_6 \cdot u_5 \cdot u_7 + n\_\eta\,_c \cdot u_2 \cdot u_7 \cdot 3 - n\_\eta\,_c \cdot u_2 \cdot u_8 \cdot 1 \cdots \\ + n\_\eta\,_c \cdot u_2 \cdot u_4 \cdot 6 - u_3 \cdot \eta c\eta\,_c \cdot u_8 \cdot u_7 + u_3 \cdot u_2 \cdot u_4 + u_7 \cdot u_5 \cdot u_6 \cdot \eta c\eta\,_c + u_7 \cdot u_2 \cdot u_6 \cdot \eta c\eta\,_c - u_2 \cdot u_1 \cdot u_5 - u_2{}^2 \cdot u_1 \end{pmatrix}$$

$$\Delta\gamma = 0$$

$$V = D_v^{-1} \cdot \begin{bmatrix} \frac{1}{9}\cdot(u_2 + u_5 + n\_\eta\,_c \cdot u_8)\cdot u_2 \\ \frac{1}{u_2}\cdot D_v \\ \frac{-1}{3}\cdot u_3 \cdot u_2 + \frac{1}{3}\cdot n\_\eta\,_c \cdot u_6 \cdot u_5 - \frac{1}{3}\cdot n\_\eta\,_c \cdot u_3 \cdot u_8 \\ \frac{-1}{3}\cdot u_2 \cdot u_4 + \frac{1}{3}\cdot n\_\eta\,_c \cdot u_5 \cdot u_7 + \frac{1}{3}\cdot \eta c\eta\,_c \cdot u_8 \cdot u_7 \\ \frac{\left(-u_2 \cdot u_1 \cdot u_5 + u_3 \cdot u_2 \cdot u_4 - u_3 \cdot \eta c\eta\,_c \cdot u_8 \cdot u_7 + u_7 \cdot u_5 \cdot u_6 \cdot \eta c\eta\,_c\right)}{u_2} \\ \frac{-1}{3}\cdot u_2 \cdot u_6 - \frac{1}{3}\cdot u_6 \cdot u_5 + \frac{1}{3}\cdot u_3 \cdot u_8 \\ \frac{-1}{3}\cdot(u_2 + u_5 + n\_\eta\,_c \cdot u_8)\cdot u_7 \\ \frac{\left(-u_2 \cdot u_8 \cdot u_1 + u_2 \cdot u_4 \cdot u_6 - u_6 \cdot u_5 \cdot u_7 \cdot n\_\eta\,_c + u_3 \cdot u_7 \cdot u_8 \cdot n\_\eta\,_c\right)}{u_2} \\ \left(u_3 \cdot u_2 - n\_\eta\,_c \cdot u_6 \cdot u_5 + n\_\eta\,_c \cdot u_3 \cdot u_8\right)\frac{u_7}{u_2} \\ -\left(-u_2 \cdot u_6 - u_6 \cdot u_5 + u_3 \cdot u_8\right)\frac{u_7}{u_2} \end{bmatrix}$$

spectral index	table T tensor	v scalar
(1)	$\mathbf{1}\otimes\mathbf{1}$	v_1
(2)	$\mathbf{A}$	v_2
(3)	$\mathbf{1}\otimes\overline{\mathbf{n}}$	v_3
(4)	$\overline{\mathbf{n}}\otimes\mathbf{1}$	v_4
(5)	$\overline{\mathbf{n}}\otimes\overline{\mathbf{n}}$	v_5
(6)	$\mathbf{1}\otimes\boldsymbol{\eta}$	v_6
(7)	$\boldsymbol{\eta}\otimes\mathbf{1}$	v_7
(8)	$\overline{\mathbf{n}}\otimes\boldsymbol{\eta}$	v_8
(9)	$\boldsymbol{\eta}\otimes\overline{\mathbf{n}}$	v_9
(10)	$\boldsymbol{\eta}\otimes\boldsymbol{\eta}$	v_{10}

$$\begin{bmatrix} (p'\cdot\beta + 3\cdot D\cdot G)\cdot\dfrac{K}{(p'\cdot\beta + 3\cdot D\cdot G + \beta^2\cdot D\cdot K)} \\ 2\cdot G \\ -\sqrt{6}\cdot D\cdot\beta\cdot G\cdot\dfrac{K}{(p'\cdot\beta + 3\cdot D\cdot G + \beta^2\cdot D\cdot K)} \\ -\sqrt{6}\cdot D\cdot\beta\cdot G\cdot\dfrac{K}{(p'\cdot\beta + 3\cdot D\cdot G + \beta^2\cdot D\cdot K)} \\ -6\cdot G^2\cdot\dfrac{D}{(p'\cdot\beta + 3\cdot D\cdot G + \beta^2\cdot D\cdot K)} \\ 0 \\ 0 \\ 0 \\ 0 \\ 0 \end{bmatrix}$$

$$\mathbf{c}^{ep} = \sum_{i=1}^{10} v_i\left[\mathbf{T}_i\right]$$

Figure 9.4 Consistent tangential tensor for the SO model

9-7-3 Consistent tangential tensor in regard to the original Cam-clay model

$$\boxed{\eta_o = 0} \quad \boxed{\boldsymbol{\eta}_c = \mathbf{0}} \quad \boxed{\overline{J}_2 = J_2} \quad \boxed{\overline{\mathbf{n}} = \mathbf{n}}$$

$$r_1 = \frac{\partial f}{\partial I_1}$$

$$r_2 = \sqrt{2\overline{J}_2}\,\frac{\partial f}{\partial \overline{J}_2}$$

$$\begin{pmatrix} \dfrac{\partial f}{\partial I_1} \\ \dfrac{\partial f}{\partial \overline{J}_2} \end{pmatrix} = \begin{pmatrix} \dfrac{D}{I_1}\left(M - 3\dfrac{\sqrt{3\overline{J}_2}}{I_1}\right) \\ \dfrac{9D}{2I_1\sqrt{3\overline{J}_2}} \end{pmatrix}$$

$$\begin{bmatrix} \dfrac{\partial^2 f}{\partial I_1 \partial I_1} & \dfrac{\partial^2 f}{\partial \overline{J}_2 \partial I_1} \\ \dfrac{\partial^2 f}{\partial I_1 \partial \overline{J}_2} & \dfrac{\partial^2 f}{\partial \overline{J}_2 \partial \overline{J}_2} \end{bmatrix} = \begin{bmatrix} -\dfrac{MD}{I_1^2} + \dfrac{6D\sqrt{3\overline{J}_2}}{I_1^3} & -\dfrac{9D}{2I_1^2\sqrt{3\overline{J}_2}} \\ -\dfrac{9D}{2I_1^2\sqrt{3\overline{J}_2}} & -\dfrac{9D}{4I_1\overline{J}_2\sqrt{3\overline{J}_2}} \end{bmatrix}$$

$$H_1 = \frac{\partial^2 f}{\partial I_1 \partial I_1} \quad H_2 = \frac{\partial f}{\partial \overline{J}_2} \quad H_3 = H_4 = \sqrt{2\overline{J}_2}\,\frac{\partial^2 f}{\partial I_1 \partial \overline{J}_2} \quad H_5 = 2\overline{J}_2\,\frac{\partial^2 f}{\partial \overline{J}_2 \partial \overline{J}_2}$$

$$\frac{\partial f}{\partial \boldsymbol{\sigma}'} = r_1\mathbf{1} + r_2\overline{\mathbf{n}}$$

$$\frac{\partial^2 f}{\partial \boldsymbol{\sigma}'\partial \boldsymbol{\sigma}'} = H_1\mathbf{1}\otimes\mathbf{1} + H_2\mathbf{A} + H_3\mathbf{1}\otimes\overline{\mathbf{n}} + H_4\overline{\mathbf{n}}\otimes\mathbf{1} + H_5\overline{\mathbf{n}}\otimes\overline{\mathbf{n}}$$

$$\mathbf{c}^{ep-1} \longrightarrow \mathbf{c}^{ep}$$
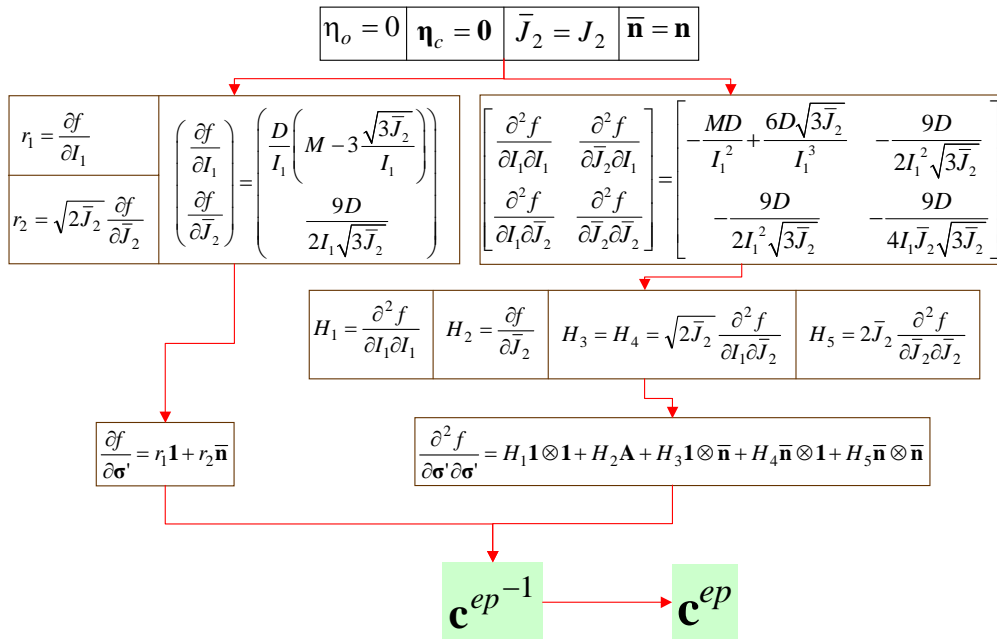
Figure 9.5 Consistent tangential tensor in terms of invariant-based spectral composition

In order to verify the closed form obtained in Eq.(9.72), a closed-form of $\mathbf{c}^{ep}$ applicable to the original Cam-clay (CC) model given by Yatomi, C. & Suzuki, Y. (2001) [6] will be compared. This 0adopted solution was derived by a method introduced by Borja, R.I. & Lee, S.R. (1990) to the modified Cam-clay model. The SO model can be simply reduced to the original CC model by taking η_o to zero. A components of consistent $\mathbf{c}^{ep}$ in regard to the CC model can be derived as outlined in Figure 9.5.

$$u_6 = 0 \quad u_7 = 0 \quad u_8 = 0 \quad \beta = M - \frac{q}{p'}$$

Explicit Coefficients

Index	T	Scalar components	u
(1)	$\mathbf{1} \otimes \mathbf{1}$	$(9K)^{-1} + \dfrac{r_1}{3}$	u_1
(2)	$\mathbf{A}$	$(2G)^{-1} + \Delta\gamma\, H_2$	u_2
(3)	$\mathbf{1} \otimes \overline{\mathbf{n}}$	$\dfrac{r_2}{3}$	u_3
(4)	$\overline{\mathbf{n}} \otimes \mathbf{1}$	$\Delta\gamma\left(H_4 - \dfrac{r_2}{r_1}H_1\right) + \dfrac{r_2}{3}$	u_4
(5)	$\overline{\mathbf{n}} \otimes \overline{\mathbf{n}}$	$\Delta\gamma\left(H_5 - \dfrac{r_2}{r_1}H_3\right) + \dfrac{r_2^2}{3r_1}$	u_5

$$\mathbf{u} = \left\{ \begin{array}{c} \dfrac{1}{9K} + \dfrac{D\beta}{9p'} \\[2mm] \dfrac{1}{2G} + \dfrac{3D\Delta\gamma}{2p'^2(M-\beta)} \\[2mm] \dfrac{D}{\sqrt{6}p'} \\[2mm] -\dfrac{(M-\beta)D}{\sqrt{6}p'^2\beta}\Delta\gamma + \dfrac{D}{\sqrt{6}p'} \\[2mm] \dfrac{3D(M-2\beta)}{2p'^2(M-\beta)\beta}\Delta\gamma + \dfrac{3D}{2p'\beta} \end{array} \right\}$$

$$\mathbf{c}^{ep\,-1} = u_1 \mathbf{1}\otimes\mathbf{1} + u_2\mathbf{A} + u_3\mathbf{1}\otimes\overline{\mathbf{n}} + u_4\overline{\mathbf{n}}\otimes\mathbf{1} + u_5\overline{\mathbf{n}}\otimes\overline{\mathbf{n}}$$

Figure 9.6 Compliance of consistent tangential tensor in regard to the CC model

Explicit Coefficient

$$D_v = u_1 u_2 u_5 - u_2 u_3 u_4 + u_1 u_2^{2}$$

$$D_v = \frac{1}{36}\cdot\left(3\cdot\Delta\gamma\cdot D\cdot G - p'^2\cdot\beta + p'^2\cdot M\right)\cdot\frac{\left(3\cdot\Delta\gamma\cdot K\cdot M\cdot G\cdot D^2 + 3\cdot p'\cdot G\cdot D\cdot\Delta\gamma + 3\cdot D\cdot p'^2\cdot G + D\cdot K\cdot p'^2\cdot\beta^2 + p'^3\cdot\beta\right)}{\left[p'^5\cdot\left[(-\beta+M)\cdot\left[\beta\cdot\left(G^2\cdot K\right)\right]\right]\right]}$$

$$\mathbf{v} = D_v^{-1}\left\{ \begin{array}{c} \dfrac{1}{9}(u_2 + u_5)u_2 \\[2mm] u_1 u_5 - u_3 u_4 + u_1 u_2 \\[2mm] -\dfrac{1}{3}u_2 u_3 \\[2mm] -\dfrac{1}{3}u_2 u_4 \\[2mm] -u_1 u_5 + u_3 u_4 \end{array} \right\}$$

$$\mathbf{v} = \left[\begin{array}{c} K\cdot p'\cdot\dfrac{\left(p'^2\cdot\beta + 3\cdot\Delta\gamma\cdot D\cdot G + 3\cdot D\cdot p'\cdot G\right)}{\left(3\cdot\Delta\gamma\cdot K\cdot M\cdot G\cdot D^2 + 3\cdot p'\cdot G\cdot D\cdot\Delta\gamma + 3\cdot D\cdot p'^2\cdot G + D\cdot K\cdot p'^2\cdot\beta^2 + p'^3\cdot\beta\right)} \\[2mm] 2\cdot(-\beta + M)\cdot G\cdot\dfrac{p'^2}{\left(3\cdot\Delta\gamma\cdot D\cdot G - p'^2\cdot\beta + p'^2\cdot M\right)} \\[2mm] -\sqrt{6}\cdot K\cdot D\cdot\beta\cdot G\cdot\dfrac{p'^2}{\left(3\cdot\Delta\gamma\cdot K\cdot M\cdot G\cdot D^2 + 3\cdot p'\cdot G\cdot D\cdot\Delta\gamma + 3\cdot D\cdot p'^2\cdot G + D\cdot K\cdot p'^2\cdot\beta^2 + p'^3\cdot\beta\right)} \\[2mm] \sqrt{2}\cdot\sqrt{3}\cdot K\cdot(\Delta\gamma\cdot M - \Delta\gamma\cdot\beta - p'\cdot\beta)\cdot D\cdot p'\cdot\dfrac{G}{\left(3\cdot\Delta\gamma\cdot K\cdot M\cdot G\cdot D^2 + 3\cdot p'\cdot G\cdot D\cdot\Delta\gamma + 3\cdot D\cdot p'^2\cdot G + D\cdot K\cdot p'^2\cdot\beta^2 + p'^3\cdot\beta\right)} \\[2mm] -6\cdot\dfrac{\left(-\Delta\gamma\cdot\beta^2\cdot D\cdot K + \Delta\gamma\cdot D\cdot K\cdot M^2 - \Delta\gamma\cdot D\cdot K\cdot M\cdot\beta - 2\cdot\Delta\gamma\cdot p'\cdot\beta + \Delta\gamma\cdot M\cdot p' - p'^2\cdot\beta + p'^2\cdot M\right)\cdot p'^2\cdot D\cdot G^2}{\left[\left(3\cdot\Delta\gamma\cdot D\cdot G - p'^2\cdot\beta + p'^2\cdot M\right)\cdot\left(3\cdot\Delta\gamma\cdot K\cdot M\cdot G\cdot D^2 + 3\cdot p'\cdot G\cdot D\cdot\Delta\gamma + 3\cdot D\cdot p'^2\cdot G + D\cdot K\cdot p'^2\cdot\beta^2 + p'^3\cdot\beta\right)\right]} \end{array} \right]$$

Coefficient of Consistent $\mathbf{C}^{ep}$

Non-symmetric forth-order tensor

$$\mathbf{c}^{ep} = v_1 \mathbf{1}\otimes\mathbf{1} + v_2\mathbf{A} + v_3\mathbf{1}\otimes\overline{\mathbf{n}} + v_4\overline{\mathbf{n}}\otimes\mathbf{1} + v_5\overline{\mathbf{n}}\otimes\overline{\mathbf{n}}$$

Figure 9.7 Consistent tangential tensor in regard to the CC model

A removal of anisotropic response in the SO model reduce a number of individual basis to five instead of ten as shown in Figure 9.6. Ther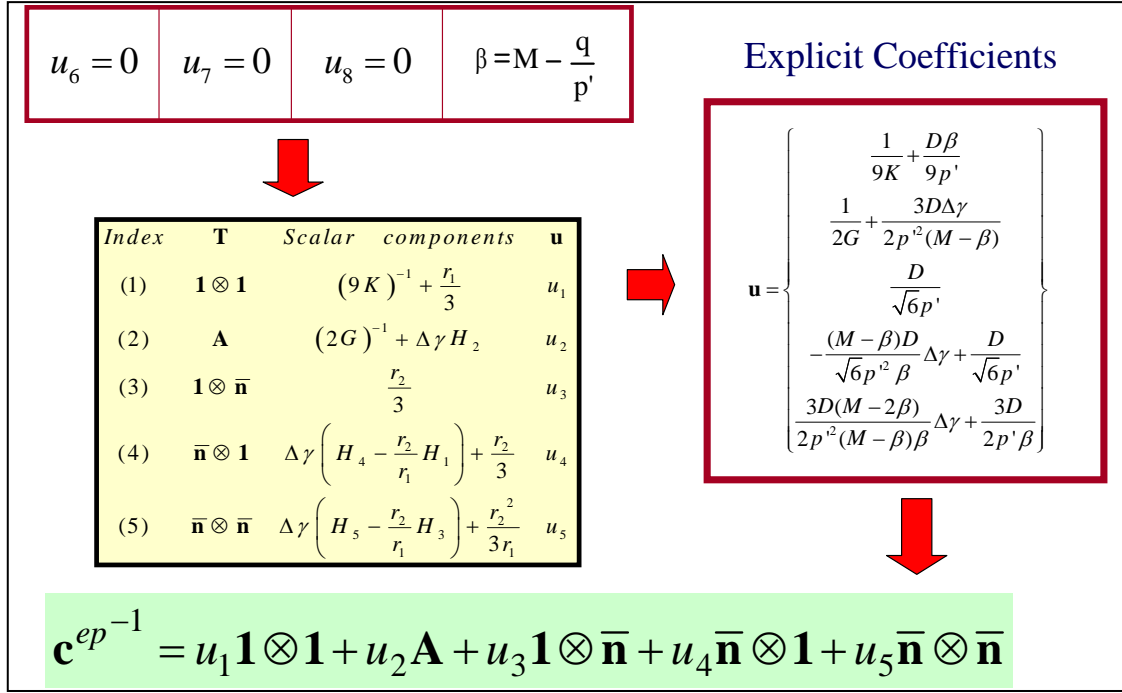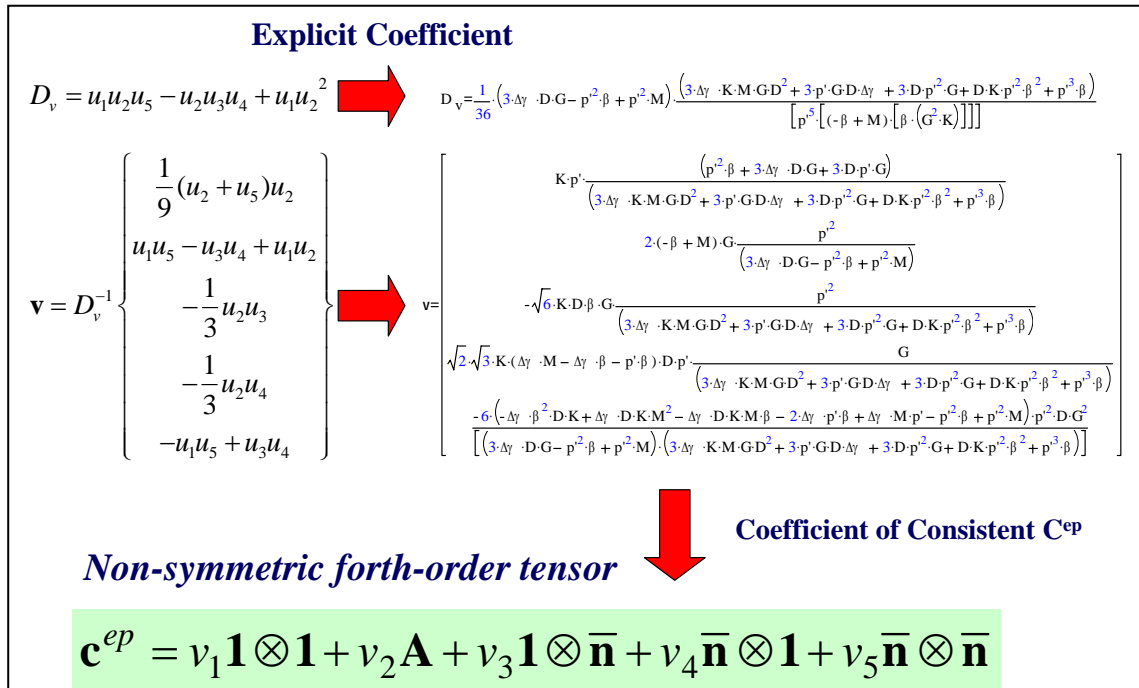efore, anisotropic features are a major source of difficulty when formulating a plastic constitutive model into return-mapping scheme. The constitutive coefficients u_1-u_5 can be evaluated as represented in Figure 9.6. By a similar manner applied in previous section, an inversion of non-symmetric $\mathbf{c}^{ep-1}$ is given in terms of the constitutive coefficients v_1-v_5 as shown in Eq.(9.76). A non-symmetric consistent tangential forth-order tensor in regard to the CC model is thus obtained. The expansion of solution given by Yatomi, C. & Suzuki, Y. (2001) reaches the same result shown in Eq.(9.76). Therefore, the inversion algorithm proposed in the study is proven by a certain degree. The algorithm proposed is simpler and rather straightforward than equation manipulation technique introduced by Borja, R.I. et al. (1990). The procedures to evaluate $\mathbf{c}^{ep}$ by the inversion algorithm are concluded in Figure 9.7. A verification of result in Eq.(9.76) is carried out by substituting $\Delta\gamma=0$ into Eq.(9.76) to degenerate a symmetric continuum tangential tensor as shown in Eq.(9.77), which is satisfied

with a standard form.

$$\mathbf{v} = \frac{1}{3(Dp'+KMD^2)G\Delta\gamma + p'^2(p'\beta+3DG+DK\beta^2)} \left\{ \begin{array}{c} Kp'^2(p'\beta+3GD)+3Kp'DG\Delta\gamma \\ \dfrac{2Gp'^2(M-\beta)\left(p'^2(3GD+p'\beta+\beta^2KD)+3\Delta\gamma GD(p'+KDM)\right)}{p'^2(M-\beta)+3\Delta\gamma DG} \\ -\sqrt{6}p'^2\beta KGD \\ \sqrt{6}GDKp'\left((M-\beta)\Delta\gamma - p'\beta\right) \\ \dfrac{-6G^2p'^2D(p'^2(M-\beta)+\Delta\gamma\left(p'(M-2\beta)+DK(M^2-M\beta-\beta^2)\right))}{(p'^2(M-\beta)+3\Delta\gamma GD)} \end{array} \right\} \tag{9.76}$$

$$\mathbf{v} = \frac{1}{p'\beta+3DG+DK\beta^2} \left\{ \begin{array}{c} K\left(3GD+p'\beta\right) \\ 2G(p'\beta+3DG+DK\beta^2) \\ -\sqrt{6}KDG\beta \\ -\sqrt{6}KDG\beta \\ -6G^2D \end{array} \right\} \tag{9.77}$$

9-8 References

1 Borja, R.I. & Lee, S.R., "Cam-Clay plasticity, Part I: Implicit integration of elasto-plastic constitutive relations", Comput. Methods Appl. Mech. Engrg. 78: pp.49-72, 1990

2 Ortiz, M. & Martin, J.B., "Symmetry-preserving return mapping algorithms and incrementally extremal paths: a unification of concepts", Int. J. Numer. Methods Engrg. 28, pp.1839-1853, 1989

3 Schofield, A. & Wroth, P., Critical State Soil Mechanics, McGRAW-HILL, 1968

4 Borja, R.I., "Cam-Clay plasticity, Part II: Implicit integration of constitutive equation based on a nonlinear elastic stress predictor", Comput. Methods Appl. Mech. Engrg. 88, pp.225-240, 1991

5 Borja, R.I. & Tamagnini, C., "Cam-Clay plasticity, Part III: Extension of the infinitesimal model to include finite strains", Comput. Methods Appl. Mech. Engrg. 155, pp.73-95, 1998

6 Yatomi, C. & Suzuki, Y., "Finite element method analysis of soil/water coupling problems using implicit elasto-plastic calculation algorithm", Journal of Applied Mechanics Vol.4, JSCE, 345-356, 2001

7 Chaboche, J.L & Cailletaud, G., "Integration methods for complex plastic constitutive equations", Comput. Methods Appl. Mech. Engrg. 133, pp.125-155, 1996

8 Luccioni, L.X., Pestana, J.M. & Rodriguez-Marek, A., "An implicit integration algorithm for the finite element implementation of a nonlinear anisotropic material model including hysteretic nonlinearity", Comput. Methods Appl. Mech. Engrg., 190, 1827-1844, 2000

9 Borja, R.I., Chao-Hua, L. & Francisco, J.M., "Cam-Clay plasticity, Part IV: Implicit integration of anisotropic bounding surface model with nonlinear Hyperelasticity and ellipsoidal loading function", Comput. Methods Appl. Mech. Engrg. 190, pp.3293-3323, 2001

10 Manzari, M.T. & Prachathananukit, R., "On integration of a cyclic soil plasticity model", Int. J. Numer. Anal. Methods Geomech. 25, pp.525-549, 2001

11 Rouainia, M. & Wood, D.M., "Implicit numerical integration for a kinematic hardening soil plasticity model", Int. J. Numer. Anal. Methods Geomech. 25, pp.1305-1325, 2001

CHAPTER 10

Implicit Finite Element Method

10.1 Matrix Notation

The brief recall of the basic matrix notation used in finite element modeling applied to continuum mechanics is given. The standard conventions are used to abandon tensor in favor of matrix and vector.

10.1.1 Three dimensions implementation

For 3D formularization, the following notations are employed for stress, strain, plastic strain and stiffness matrix.

$$\boldsymbol{\varepsilon} = \left\{ \begin{array}{c} \varepsilon_{xx} \\ \varepsilon_{yy} \\ \varepsilon_{zz} \\ 2\varepsilon_{xy} \\ 2\varepsilon_{yz} \\ 2\varepsilon_{xz} \end{array} \right\}, \quad \boldsymbol{\varepsilon}^P = \left\{ \begin{array}{c} \varepsilon_{xx}^p \\ \varepsilon_{yy}^p \\ \varepsilon_{zz}^p \\ 2\varepsilon_{xy}^p \\ 2\varepsilon_{yz}^p \\ 2\varepsilon_{xz}^p \end{array} \right\}, \quad \boldsymbol{\sigma} = \left\{ \begin{array}{c} \sigma_{xx} \\ \sigma_{yy} \\ \sigma_{zz} \\ \sigma_{xy} \\ \sigma_{yz} \\ \sigma_{xz} \end{array} \right\}, \quad \mathbf{C} = \begin{bmatrix} C_{1111} & C_{1122} & C_{1133} & C_{1112} & C_{1113} & C_{1123} \\ C_{1122} & C_{2222} & C_{2233} & C_{2212} & C_{2213} & C_{2223} \\ C_{1133} & C_{2233} & C_{3333} & C_{3312} & C_{3313} & C_{3323} \\ C_{1112} & C_{2212} & C_{3312} & C_{1212} & C_{1213} & C_{1223} \\ C_{1113} & C_{2213} & C_{3313} & C_{1213} & C_{1313} & C_{1323} \\ C_{1123} & C_{2223} & C_{3323} & C_{1223} & C_{1323} & C_{2323} \end{bmatrix} \tag{10.1}$$

Correspondingly, the identity forth-order tensor is reduced to (6x6) matrix while identity second-order tensor is reduced to (6x1) vector as shown below respectively,

$$\mathbf{I} = \begin{bmatrix} 1 & 0 & 0 & 0 & 0 & 0 \\ 0 & 1 & 0 & 0 & 0 & 0 \\ 0 & 0 & 1 & 0 & 0 & 0 \\ 0 & 0 & 0 & 1/2 & 0 & 0 \\ 0 & 0 & 0 & 0 & 1/2 & 0 \\ 0 & 0 & 0 & 0 & 0 & 1/2 \end{bmatrix}, \quad \mathbf{1} = \left\{ \begin{array}{c} 1 \\ 1 \\ 1 \\ 0 \\ 0 \\ 0 \end{array} \right\} \tag{10.2}$$

The deviatoric forth-order tensor $\mathbf{A}$ is reduced to,

$$\mathbf{A} = \mathbf{I} - \frac{1}{3}\mathbf{1} \otimes \mathbf{1} = \begin{bmatrix} 2/3 & -1/3 & -1/3 & 0 & 0 & 0 \\ -1/3 & 2/3 & -1/3 & 0 & 0 & 0 \\ -1/3 & -1/3 & 2/3 & 0 & 0 & 0 \\ 0 & 0 & 0 & 1/2 & 0 & 0 \\ 0 & 0 & 0 & 0 & 1/2 & 0 \\ 0 & 0 & 0 & 0 & 0 & 1/2 \end{bmatrix} \tag{10.3}$$

Isotropic elastic tensor (See [1]) can be represented by using Eq.(10.2) and (10.3) as,

$$\mathbf{c}^e = K(\mathbf{1} \otimes \mathbf{1}) + 2G\mathbf{A} = \begin{bmatrix} K+4G/3 & K-2G/3 & K-2G/3 & 0 & 0 & 0 \\ K-2G/3 & K+4G/3 & K-2G/3 & 0 & 0 & 0 \\ K-2G/3 & K-2G/3 & K+4G/3 & 0 & 0 & 0 \\ 0 & 0 & 0 & G & 0 & 0 \\ 0 & 0 & 0 & 0 & G & 0 \\ 0 & 0 & 0 & 0 & 0 & G \end{bmatrix} \tag{10.4}$$

Also, the double dot or double contraction is reduced to dot product in the sense that,

$$\boldsymbol{\sigma} : \boldsymbol{\varepsilon} = \sigma_{ij}\varepsilon_{ij} \Rightarrow \boldsymbol{\sigma} \cdot \boldsymbol{\varepsilon} = \sigma_i \varepsilon_i \quad \text{and} \quad \boldsymbol{\sigma} = \mathbf{C} : \boldsymbol{\varepsilon}^e = C_{ijkl}\varepsilon_{kl}^e \Rightarrow \boldsymbol{\sigma} = \mathbf{C} \cdot \boldsymbol{\varepsilon}^e = C_{ij}\varepsilon_j^e \tag{10.5}$$

However, double product of stress tensor to stress tensor (not to strain tensor) needs to be modified. The following example show how to modified the product,

$$J_2 = \frac{1}{2}\mathbf{s}_{(3x3)} : \mathbf{s}_{(3x3)} \Rightarrow \frac{1}{2}\mathbf{s}_{(6x1)} \cdot \mathbf{I}^{-1}{}_{(6x6)} \cdot \mathbf{s}_{(6x1)} \quad \text{and} \quad \mathbf{c}_{(3x3x3x3)} : \mathbf{c}_{(3x3x3x3)} \Rightarrow \mathbf{c}_{(6x6)} \cdot \mathbf{I}^{-1}{}_{(6x6)} \cdot \mathbf{c}_{(6x6)} \tag{10.6}$$

The double product modification lead to different definition for inversion, for example define Ξ' as an inversion of Ξ, then

$$\Xi_{(3x3x3x3)} : \Xi'_{(3x3x3x3)} = \mathbf{I}_{(3x3x3x3)} \Rightarrow \Xi_{(6x6)} \cdot \mathbf{I}^{-1}{}_{(6x6)} \cdot \Xi'_{(6x6)} = \mathbf{I}_{(6x6)} \tag{10.7}$$

It is found that the inversion of Ξ in reduced format is

$$\Xi'_{(6x6)} = \mathbf{I}_{(6x6)} \cdot \Xi^{-1}{}_{(6x6)} \cdot \mathbf{I}_{(6x6)} \tag{10.8}$$

10.1.2 Two dimensions implementation both for plane strain/axi-symmetric

For 2D formularization, the following notations are employed for stress, strain, plastic strain and stiffness matrix.

$$\boldsymbol{\varepsilon} = \begin{Bmatrix} \varepsilon_{xx} \\ \varepsilon_{yy} \\ 2\varepsilon_{xy} \\ \varepsilon_{zz} \end{Bmatrix}, \quad \boldsymbol{\varepsilon}^p = \begin{Bmatrix} \varepsilon_{xx}^p \\ \varepsilon_{yy}^p \\ 2\varepsilon_{xy}^p \\ \varepsilon_{zz}^p \end{Bmatrix}, \quad \boldsymbol{\sigma} = \begin{Bmatrix} \sigma_{xx} \\ \sigma_{yy} \\ \sigma_{xy} \\ \sigma_{zz} \end{Bmatrix}, \quad \mathbf{C} = \begin{bmatrix} C_{11} & C_{12} & C_{13} & C_{14} \\ C_{21} & C_{22} & C_{23} & C_{24} \\ C_{31} & C_{32} & C_{33} & C_{34} \\ C_{41} & C_{42} & C_{43} & C_{44} \end{bmatrix} \tag{10.9}$$

Correspondingly, the identity forth-order tensor is reduced to (4x4) matrix while identity second-order tensor is reduced to (4x1) vector as shown below respectively,

$$\mathbf{I} = \begin{bmatrix} 1 & 0 & 0 & 0 \\ 0 & 1 & 0 & 0 \\ 0 & 0 & 1/2 & 0 \\ 0 & 0 & 0 & 1 \end{bmatrix}, \quad \mathbf{1} = \begin{Bmatrix} 1 \\ 1 \\ 0 \\ 1 \end{Bmatrix} \tag{10.10}$$

The deviatoric forth-order tensor $\mathbf{A}$ is reduced to,

$$\mathbf{A} = \mathbf{I} - \frac{1}{3}\mathbf{1} \otimes \mathbf{1} = \begin{bmatrix} 2/3 & -1/3 & 0 & -1/3 \\ -1/3 & 2/3 & 0 & -1/3 \\ 0 & 0 & 1/2 & 0 \\ -1/3 & -1/3 & 0 & 2/3 \end{bmatrix} \tag{10.11}$$

Isotropic elastic tensor can be represented by using Eq.(10.2) and (10.3) as,

$$\mathbf{c}^e = K(\mathbf{1} \otimes \mathbf{1}) + 2G\mathbf{A} = \begin{bmatrix} K+4G/3 & K-2G/3 & 0 & K-2G/3 \\ K-2G/3 & K+4G/3 & 0 & K-2G/3 \\ 0 & 0 & G & 0 \\ K-2G/3 & K-2G/3 & 0 & K+4G/3 \end{bmatrix} \tag{10.12}$$

The other modifications are similar to those suggested for 3 dimension implementation.

10.2 Numerical Integration

Numerical integration is used extensively in finite element method (See more details in [5, 2, 3, 4]). Principles of numerical integration will be summarized by the following sections. The concept of iso-parametric finite element will be reviewed. Interpolation functions for geometry transformation will be examined.

10.2.1 Gauss-Legendre quadrature

The Gauss-Legendre quadrature is the most popular method for numerical integration technique. The sampling points (Gauss points) and weights H is based on the Legendre polynomial. In general, integration can be approximated by,

$$\int_{-1}^{+1} f(r)dr = \sum_{k=1}^{n} H_k f(a_k) \tag{10.13}$$

By the same manner, double integrations is approximated by,

$$\int_{-1}^{+1}\int_{-1}^{+1} f(r,s)drds = \sum_{i=1}^{n}\sum_{j=1}^{n} H_i H_j f(a_i, a_j) \tag{10.14}$$

The sampling points and weights for 2 to 5 points integration are given in Table 10.1 (See [5]).

n	a	H
1	0.000000000	2.000000000
2	± 0.577350269	1.000000000
3	0.774596669	0.555555555
	0.000000000	0.888888888
	- 0.774596669	0.555555555
4	± 0.861136312	0.347854845
	± 0.339981043	0.652145155
5	± 0.538469310	0.478628670
	0.000000000	0.568888889
	± 0.906179845	0.236726885

Table 10.1 Abscissae and weight coefficients of the Gauss-Legendre quadrature formula

10.2.2 Shape function

A shape or weight function can be defined based on the Lagrange polynomial interpolation defined as the product of,

$$L_k(x) = \prod_{\substack{m=1 \\ k \neq m}}^{n} \frac{x - x_m}{x_k - x_m} \tag{10.15}$$

Where n is a number of nodes. When $x = x_k$, the product becomes unity. However, when $x = x_m$, the product become zero. For one-dimensional element of two nodes from –1 to 1, node one is -1 and node two is 1. The corresponding shape functions at node number one and number two can be defined by,

$$L_1(\xi) = \frac{\xi - \xi_2}{\xi_1 - \xi_2} = \frac{\xi - 1}{(-1) - (1)} = -\frac{1}{2}\xi + \frac{1}{2} \tag{10.16}$$

$$L_2(\xi) = \frac{\xi - \xi_1}{\xi_2 - \xi_1} = \frac{\xi - (-1)}{(1) - (-1)} = \frac{1}{2}\xi + \frac{1}{2} \tag{10.17}$$

For one-dimensional element of three nodes from –1 to 1, node one is -1, node two is 1 and node three is 0. The corresponding shape functions at node number one to node number three can be defined by,

$$L_1(\xi) = \frac{\xi - \xi_2}{\xi_1 - \xi_2} \frac{\xi - \xi_3}{\xi_1 - \xi_3} = \frac{1}{2}\xi(\xi - 1) \tag{10.18}$$

$$L_2(\xi) = \frac{\xi - \xi_1}{\xi_2 - \xi_1} \frac{\xi - \xi_3}{\xi_2 - \xi_3} = \frac{1}{2}\xi(\xi + 1) \tag{10.19}$$

$$L_3(\xi) = \frac{\xi - \xi_1}{\xi_3 - \xi_1} \frac{\xi - \xi_2}{\xi_3 - \xi_2} = -(\xi + 1)(\xi - 1) \tag{10.20}$$

Shape function corresponding to any node will equal to 1, the biggest weight number, at its own node. The plot of shape functions along with its domain between -1 to 1 can be viewed in Figure 10.1. For two dimensions, the corresponding shape functions is extended by,

$$L_{mn}(x, y) = L_m(x)L_n(y) \tag{10.21}$$

Two-dimensional shape functions are applied in two-dimensional FEM. A particular quadrilateral domain between -1 and 1 on both x and y directions will be considered in the next section.
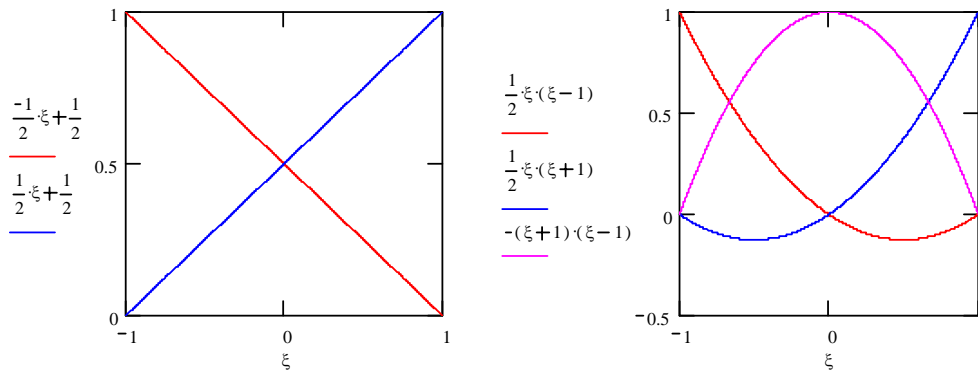
Figure 10.1 Weight distribution of shape function (left: two nodes, right: three nodes)

10.2.3 Iso-parametric quadrilateral element

Even in rather complicated problem, certain properties along the boundaries and interior of the element is conveniently integrated by interpolation function in a normalized space defined by boundaries lying at ±1. A generalized geometry of element is defined by local coordinate system. A mathematical coordinate transformation is required for shape functions and their derivatives in order to evaluate local stiffness matrix using numerical integration. Four-node and nine-node quadrilateral iso-parametric elements are shown in Figure 10.2 and Figure 10.3 respectively.
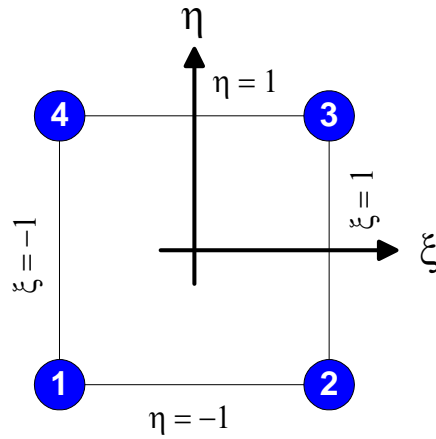
Figure 10.2 4-node displacement-based element with 2x2 Gauss integration
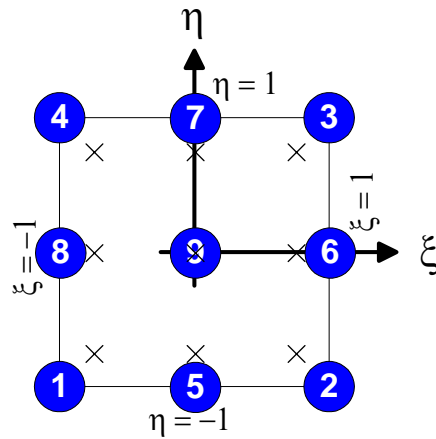
Figure 10.3 9-node displacement-based element with 3x3 Gauss integration

The (2x2) shape functions associated to each node number as ordered in Figure 10.2 are determined in Eq.(10.22). while the (3x3) shape functions associated to each node number as ordered in Figure 10.3 are determined in Eq.(10.23). ξ and η are called iso-parameters. Moreover (ξ, η) is called natural or generalized coordinates.

$$\hat{\mathbf{N}}_{4x1}(\xi,\eta) = \begin{Bmatrix} L_{11}(\xi,\eta) \\ L_{21}(\xi,\eta) \\ L_{22}(\xi,\eta) \\ L_{12}(\xi,\eta) \end{Bmatrix} = \begin{Bmatrix} \dfrac{1}{4}(\xi-1)(\eta-1) \\ -\dfrac{1}{4}(\xi+1)(\eta-1) \\ \dfrac{1}{4}(\xi+1)(\eta+1) \\ -\dfrac{1}{4}(\xi-1)(\eta+1) \end{Bmatrix} \tag{10.22}$$

$$\hat{\mathbf{N}}_{9x1}(\xi,\eta) = \begin{Bmatrix} L_{11}(\xi,\eta) \\ L_{21}(\xi,\eta) \\ L_{22}(\xi,\eta) \\ L_{12}(\xi,\eta) \\ L_{31}(\xi,\eta) \\ L_{23}(\xi,\eta) \\ L_{32}(\xi,\eta) \\ L_{13}(\xi,\eta) \\ L_{33}(\xi,\eta) \end{Bmatrix} = \begin{Bmatrix} \frac{1}{4}\xi\eta(\xi-1)(\eta-1) \\ \frac{1}{4}\xi\eta(\xi+1)(\eta-1) \\ \frac{1}{4}\xi\eta(\xi+1)(\eta+1) \\ \frac{1}{4}\xi\eta(\xi-1)(\eta+1) \\ -\frac{1}{2}(\xi+1)(\xi-1)(\eta-1)\eta \\ -\frac{1}{2}(\xi+1)\xi(\eta+1)(\eta-1) \\ -\frac{1}{2}(\xi+1)(\xi-1)(\eta+1)\eta \\ -\frac{1}{2}(\xi-1)\xi(\eta+1)(\eta-1) \\ (\xi+1)(\xi-1)(\eta+1)(\eta-1) \end{Bmatrix} \tag{10.23}$$

10.2.4 Interpolation function

For prescribed global xy-coordinates of nodal points in a rectangular element model, interpolation functions for global xy-coordinate matching to local $\xi\eta$-coordinate can be expressed by,

$$x(\xi,\eta) = \hat{\mathbf{N}}(\xi,\eta) \cdot \hat{\mathbf{x}}, \quad y(\xi,\eta) = \hat{\mathbf{N}}(\xi,\eta) \cdot \hat{\mathbf{y}} \tag{10.24}$$

where $\hat{\mathbf{x}}$ is the corresponding global x-coordinates as ordered in the similar way with local ξ-coordinates. For example, $\hat{\mathbf{x}}^T = \{x_1 \quad x_2 \quad x_3 \quad x_4\}$ for (2x2)-nodes element are the x-coordinates of nodal 1-4 in Figure 10.2.

By using local-coordinate system, global xy-coordinate system is easy to refer. According to Eq.(10.24), the middle point in element can be referred by local coordinate system of (0,0). Then, global coordinate system is matched by,

$$x(0,0) = \frac{1}{4}(x_1 + x_2 + x_3 + x_4), \quad y(0,0) = \frac{1}{4}(y_1 + y_2 + y_3 + y_4) \tag{10.25}$$

Unit volume of orthogonal infinitesimal element of dx by dy can be related to infinitesimal element dξ by dη using Jacobian of the transformation [6],

$$dv = dxdy = \left| \frac{\partial(x,y)}{\partial(\xi,\eta)} \right| d\xi d\eta \tag{10.26}$$

If x and y are differentiable in a region, the Jacobian of x and y with respect to ξ and η are defied by

$$\mathbf{J}_{(2x2)} = \left[\frac{\partial(x,y)}{\partial(\xi,\eta)} \right]^T = \begin{bmatrix} \frac{\partial x}{\partial \xi} & \frac{\partial x}{\partial \eta} \\ \frac{\partial y}{\partial \xi} & \frac{\partial y}{\partial \eta} \end{bmatrix}^T \tag{10.27}$$

According to Eq.(10.24) and chain rule, Jocobian in Eq.(10.27) is determined,

$$\mathbf{J} = \begin{bmatrix} \frac{\partial \hat{\mathbf{N}}(\xi,\eta)}{\partial \xi} \cdot \hat{\mathbf{x}} & \frac{\partial \hat{\mathbf{N}}(\xi,\eta)}{\partial \xi} \cdot \hat{\mathbf{y}} \\ \frac{\partial \hat{\mathbf{N}}(\xi,\eta)}{\partial \eta} \cdot \hat{\mathbf{x}} & \frac{\partial \hat{\mathbf{N}}(\xi,\eta)}{\partial \eta} \cdot \hat{\mathbf{y}} \end{bmatrix} = \begin{bmatrix} \sum \frac{\partial N_i}{\partial \xi} x_i & \sum \frac{\partial N_i}{\partial \xi} y_i \\ \sum \frac{\partial N_i}{\partial \eta} x_i & \sum \frac{\partial N_i}{\partial \eta} y_i \end{bmatrix} \tag{10.28}$$

Derivative of interpolation function for 4-node element is shown below,

$$\hat{\mathbf{N}}'_{(2x4)}(\xi,\eta) = \begin{bmatrix} \frac{\partial \hat{\mathbf{N}}}{\partial \xi} \\ \frac{\partial \hat{\mathbf{N}}}{\partial \eta} \end{bmatrix} = \begin{bmatrix} \frac{\partial N_1}{\partial \xi} & \frac{\partial N_2}{\partial \xi} & \frac{\partial N_3}{\partial \xi} & \frac{\partial N_4}{\partial \xi} \\ \frac{\partial N_1}{\partial \eta} & \frac{\partial N_2}{\partial \eta} & \frac{\partial N_3}{\partial \eta} & \frac{\partial N_4}{\partial \eta} \end{bmatrix} = \frac{1}{4}\begin{bmatrix} \eta-1 & -\eta+1 & \eta+1 & -\eta-1 \\ \xi-1 & -\xi-1 & \xi+1 & -\xi+1 \end{bmatrix} \tag{10.29}$$

Derivative of interpolation function for 9-node element is shown below,

$$\hat{\mathbf{N}}'_{(2x9)}(\xi,\eta) = \begin{bmatrix} \dfrac{\partial\hat{\mathbf{N}}}{\partial\xi} \\[2mm] \dfrac{\partial\hat{\mathbf{N}}}{\partial\eta} \end{bmatrix} = \begin{bmatrix} \frac{1}{4}(2\xi-1)(\eta-1)\eta & \frac{1}{4}\xi(\xi-1)(2\eta-1) \\[2mm] \frac{1}{4}(2\xi+1)(\eta-1)\eta & \frac{1}{4}\xi(\xi+1)(2\eta-1) \\[2mm] \frac{1}{4}(2\xi+1)(\eta+1)\eta & \frac{1}{4}\xi(\xi+1)(2\eta+1) \\[2mm] \frac{1}{4}(2\xi-1)(\eta+1)\eta & \frac{1}{4}\xi(\xi-1)(2\eta+1) \\[2mm] -\xi(\eta-1)\eta & -\frac{1}{2}(\xi+1)(\xi-1)(2\eta-1) \\[2mm] -\frac{1}{2}(\eta+1)(\eta-1)(2\xi+1) & -\xi(\xi+1)\eta \\[2mm] -\xi(\eta+1)\eta & -\frac{1}{2}(\xi+1)(\xi-1)(2\eta+1) \\[2mm] -\frac{1}{2}(\eta+1)(\eta-1)(2\xi-1) & -\xi(\xi-1)\eta \\[2mm] 2\xi(\eta+1)(\eta-1) & 2(\xi+1)(\xi-1)\eta \end{bmatrix}^T \tag{10.30}$$

Jacobian matrix can be written as a product of two matrices given by,

$$\mathbf{J}_{(2x2)} = \hat{\mathbf{N}}'\cdot\{\hat{\mathbf{x}}\quad\hat{\mathbf{y}}\} \tag{10.31}$$

where $\{\hat{\mathbf{x}}\quad\hat{\mathbf{y}}\}$ is referred to set of global coordinates with respect to type of element. In case of 4-node element,

$$\{\hat{\mathbf{x}}\quad\hat{\mathbf{y}}\} = \begin{Bmatrix} x_1 & y_1 \\ x_2 & y_2 \\ x_3 & y_3 \\ x_4 & y_4 \end{Bmatrix} \tag{10.32}$$

10.3 Element

Properties in element include nodal displacements, stress and strain. The inter-relation between these properties will be presented. Interpolation functions given in previous section are used to determined strain from nodal displacements. The fundamental theory for the development of a local stiffness matrix to relate strain to stress will be examined.

10.3.1 Displacements
The interpolation function is applied to interpolate the displacement field based on nodal displacements.

$$u(\xi,\eta) = \hat{\mathbf{N}}(\xi,\eta)\cdot\hat{\mathbf{u}}, \quad v(\xi,\eta) = \hat{\mathbf{N}}(\xi,\eta)\cdot\hat{\mathbf{v}} \tag{10.33}$$

where u and v refer to displacement field in x and y direction respectively, $\hat{\mathbf{u}}$ and $\hat{\mathbf{v}}$ refer to the nodal displacements x and y direction respectively as ordered in Figure 10.2.

$$\hat{\mathbf{u}} = \{u_1\quad u_2\quad u_3\quad u_4\}^T, \quad \hat{\mathbf{v}} = \{v_1\quad v_2\quad v_3\quad v_4\}^T \tag{10.34}$$

By the result of Eq.(10.33)-(10.34), vector of displacement can be given by,

$$\begin{Bmatrix} u \\ v \end{Bmatrix} = \begin{Bmatrix} N_i u_i \\ N_i v_i \end{Bmatrix} = \mathbf{N}\cdot\mathbf{u}_e \tag{10.35}$$

where $\mathbf{N}$ is interpolation matrix and $\mathbf{u}^e$ is vector of nodal displacements. In case of 4-node element,

$$\mathbf{N}_{(2x8)} = \begin{Bmatrix} N_1 & 0 & N_2 & 0 & N_3 & 0 & N_4 & 0 \\ 0 & N_1 & 0 & N_2 & 0 & N_3 & 0 & N_4 \end{Bmatrix} \tag{10.36}$$

$$\mathbf{u}_{e(8x1)} = \{u_1\quad v_1\quad u_2\quad v_2\quad u_3\quad v_3\quad u_4\quad v_4\}^T \tag{10.37}$$

10.3.2 Strain
In regard to 2-dimensional plane strain quadrilateral element, small strain is defined by,

$$\mathbf{\varepsilon}_{(4\times1)} = \begin{Bmatrix} \varepsilon_{xx} \\ \varepsilon_{yy} \\ \gamma_{xy} \\ \varepsilon_{zz} \end{Bmatrix}_{(4\times1)} = \begin{Bmatrix} \dfrac{\partial u}{\partial x} \\ \dfrac{\partial v}{\partial y} \\ \dfrac{\partial u}{\partial y} + \dfrac{\partial v}{\partial x} \\ 0 \end{Bmatrix}_{(4\times1)} \tag{10.38}$$

According to Eq.(10.38), the partial derivatives of u and v with respect to global coordinate x and y is required. The chain rule is applied in the following form,

$$\begin{Bmatrix} \dfrac{\partial u}{\partial x} \\ \dfrac{\partial u}{\partial y} \end{Bmatrix} = \begin{Bmatrix} \dfrac{\partial \mathbf{\hat{N}}}{\partial x} \\ \dfrac{\partial \mathbf{\hat{N}}}{\partial y} \end{Bmatrix} \cdot \mathbf{\hat{u}} = \begin{Bmatrix} \dfrac{\partial \mathbf{\hat{N}}}{\partial \xi}\dfrac{\partial \xi}{\partial x} + \dfrac{\partial \mathbf{\hat{N}}}{\partial \eta}\dfrac{\partial \eta}{\partial x} \\ \dfrac{\partial \mathbf{\hat{N}}}{\partial \xi}\dfrac{\partial \xi}{\partial y} + \dfrac{\partial \mathbf{\hat{N}}}{\partial \eta}\dfrac{\partial \eta}{\partial y} \end{Bmatrix} \cdot \mathbf{\hat{u}} \tag{10.39}$$

Derivatives of interpolation function with respect to global coordinates in Eq.(10.39) can be related to derivatives of interpolation function with respect to local coordinates by,

$$\begin{Bmatrix} \dfrac{\partial \mathbf{\hat{N}}}{\partial x} \\ \dfrac{\partial \mathbf{\hat{N}}}{\partial y} \end{Bmatrix} = \begin{bmatrix} \dfrac{\partial \xi}{\partial x} & \dfrac{\partial \eta}{\partial x} \\ \dfrac{\partial \xi}{\partial y} & \dfrac{\partial \eta}{\partial y} \end{bmatrix} \cdot \begin{Bmatrix} \dfrac{\partial \mathbf{\hat{N}}}{\partial \xi} \\ \dfrac{\partial \mathbf{\hat{N}}}{\partial \eta} \end{Bmatrix} = \begin{bmatrix} \dfrac{\partial(\xi,\eta)}{\partial(x,y)} \end{bmatrix}^{T} \cdot \mathbf{\hat{N}}' \tag{10.40}$$

Referring to Jacobian assigned in Eq.(10.27), the above equation can be written by,

$$\mathbf{N}' = J^{-1}_{(2x2)} \cdot \mathbf{\hat{N}}' \tag{10.41}$$

where $\mathbf{N}'$ is matrix contained derivatives of interpolation function with respect to global coordinates. In case of 4-node element,

$$\mathbf{N}'_{(2x4)} = \begin{Bmatrix} \dfrac{\partial \mathbf{\hat{N}}}{\partial x} \\ \dfrac{\partial \mathbf{\hat{N}}}{\partial y} \end{Bmatrix} = \begin{Bmatrix} \dfrac{\partial N_1}{\partial x} & \dfrac{\partial N_2}{\partial x} & \dfrac{\partial N_3}{\partial x} & \dfrac{\partial N_4}{\partial x} \\ \dfrac{\partial N_1}{\partial y} & \dfrac{\partial N_2}{\partial y} & \dfrac{\partial N_3}{\partial y} & \dfrac{\partial N_4}{\partial y} \end{Bmatrix} \tag{10.42}$$

Partial derivative shown in Eq.(10.38) can be expressed as operations and displacement variables by,

$$\mathbf{\varepsilon}_{(4\times1)} = \begin{bmatrix} \dfrac{\partial}{\partial x} & 0 \\ 0 & \dfrac{\partial}{\partial y} \\ \dfrac{\partial}{\partial y} & \dfrac{\partial}{\partial x} \\ 0 & 0 \end{bmatrix}_{(4\times2)} \cdot \begin{Bmatrix} u \\ v \end{Bmatrix}_{(2\times1)} = \begin{bmatrix} \dfrac{\partial}{\partial x} & 0 \\ 0 & \dfrac{\partial}{\partial y} \\ \dfrac{\partial}{\partial y} & \dfrac{\partial}{\partial x} \\ 0 & 0 \end{bmatrix}_{(4\times2)} \cdot \begin{Bmatrix} N_1 & 0 & N_2 & 0 & N_3 & 0 & N_4 & 0 \\ 0 & N_1 & 0 & N_2 & 0 & N_3 & 0 & N_4 \end{Bmatrix} \cdot \mathbf{u}_e \tag{10.43}$$

As a result, the kinematic matrix $\mathbf{B}_e$ in Eq.(10.44) defines the kinematic relation between the strain vector $\mathbf{\varepsilon}$ and the nodal displacement $\mathbf{u}_e$. In case of 4-node element represented in Figure 10.4, under plane strain condition, $\mathbf{B}_e$ is defined by Eq.(10.45),

$$\mathbf{\varepsilon} = \mathbf{B}_e \cdot \mathbf{u}_e \tag{10.44}$$

$$\mathbf{B}_e = \begin{bmatrix} \dfrac{\partial N_1}{\partial x} & 0 & \dfrac{\partial N_2}{\partial x} & 0 & \dfrac{\partial N_3}{\partial x} & 0 & \dfrac{\partial N_4}{\partial x} & 0 \\ 0 & \dfrac{\partial N_1}{\partial y} & 0 & \dfrac{\partial N_2}{\partial y} & 0 & \dfrac{\partial N_3}{\partial y} & 0 & \dfrac{\partial N_4}{\partial y} \\ \dfrac{\partial N_1}{\partial y} & \dfrac{\partial N_1}{\partial x} & \dfrac{\partial N_2}{\partial y} & \dfrac{\partial N_2}{\partial x} & \dfrac{\partial N_3}{\partial y} & \dfrac{\partial N_3}{\partial x} & \dfrac{\partial N_4}{\partial y} & \dfrac{\partial N_4}{\partial x} \\ 0 & 0 & 0 & 0 & 0 & 0 & 0 & 0 \end{bmatrix} \tag{10.45}$$

In case of 4-node element under axi-symmetric condition, the similar fashion can be achieved as shown below,

$$
\boldsymbol{\varepsilon} = \begin{Bmatrix} \varepsilon_{rr} \\ \varepsilon_{zz} \\ \varepsilon_{rz} \\ \varepsilon_{\theta\theta} \end{Bmatrix} = \begin{Bmatrix} \dfrac{\partial u}{\partial r} \\ \dfrac{\partial v}{\partial z} \\ \dfrac{\partial u}{\partial z} + \dfrac{\partial v}{\partial r} \\ \dfrac{u}{r} \end{Bmatrix} = \begin{bmatrix} \dfrac{\partial}{\partial r} & 0 \\ 0 & \dfrac{\partial}{\partial z} \\ \dfrac{\partial}{\partial z} & \dfrac{\partial}{\partial r} \\ \dfrac{1}{r} & 0 \end{bmatrix} \cdot \begin{bmatrix} N_1 & 0 & N_2 & 0 & N_3 & 0 & N_4 & 0 \\ 0 & N_1 & 0 & N_2 & 0 & N_3 & 0 & N_4 \end{bmatrix} \cdot \mathbf{u}_e
$$

$$
= \begin{bmatrix} \dfrac{\partial N_1}{\partial r} & 0 & \dfrac{\partial N_2}{\partial r} & 0 & \dfrac{\partial N_3}{\partial r} & 0 & \dfrac{\partial N_4}{\partial r} & 0 \\ 0 & \dfrac{\partial N_1}{\partial z} & 0 & \dfrac{\partial N_2}{\partial z} & 0 & \dfrac{\partial N_3}{\partial z} & 0 & \dfrac{\partial N_4}{\partial z} \\ \dfrac{\partial N_1}{\partial z} & \dfrac{\partial N_1}{\partial r} & \dfrac{\partial N_2}{\partial z} & \dfrac{\partial N_2}{\partial r} & \dfrac{\partial N_3}{\partial z} & \dfrac{\partial N_3}{\partial r} & \dfrac{\partial N_4}{\partial z} & \dfrac{\partial N_4}{\partial r} \\ \dfrac{N_1}{r} & 0 & \dfrac{N_2}{r} & 0 & \dfrac{N_3}{r} & 0 & \dfrac{N_4}{r} & 0 \end{bmatrix} \cdot \mathbf{u}_e = \mathbf{B}_{e(4\times 8)} \cdot \mathbf{u}_{e(8\times 1)}
$$

(10.46)
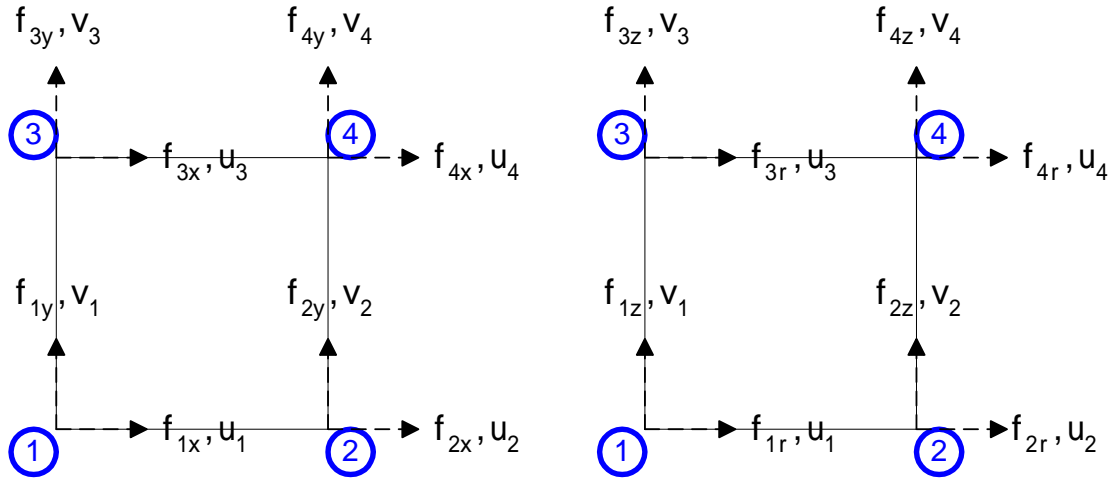
Figure 10.4 Nodal displacements and internal forces for 4-node element under plain strain and axi-symmetric conditions

10.3.3 Stiffness matrix

Actually, the stiffness matrix is defined by integration of stiffness field over element domain,

$$
\mathbf{k}_e = \int_{\Omega^e} \mathbf{B}_e^T \mathbf{c}^{ep} \mathbf{B}_e d\Omega^e
$$

(10.47)

By using Gauss-Legendre quadrature, the domain integration will be reduced to the summation on Gauss points in the element given by

$$
\mathbf{k}_e = \sum_{i=1}^{n}\sum_{j=1}^{n} \mathbf{B}_e^T(\xi_i,\eta_j)\mathbf{c}^{ep}\mathbf{B}_e(\xi_i,\eta_i)H_i H_j d\Omega^e
$$

(10.48)

Herein n is a number of Gauss points in each direction, (ξ_i,η_j) is local coordinates of Gauss points, H_i and H_j are weight functions defined in Table 10.1. Moreover, using Jacobian transformation, global domain can be mapped to local domain by,

$$
d\Omega^e = dxdy = \left| \mathbf{J}(\xi_i,\eta_j) \right| d\xi d\eta
$$

(10.49)

The consistent tangential moduli $\mathbf{c}^{ep}$ is determined by 10 coefficients with 10 tensor basics introduced in Chapter 9. In stress update algorithm, the algorithmic moduli Ξ is also computed directly from 10 coefficients with 10 tensor basics. The direct evaluation dramatically reduces time needed for performing the inversion of those moduli. See summary in Figure 10.5.

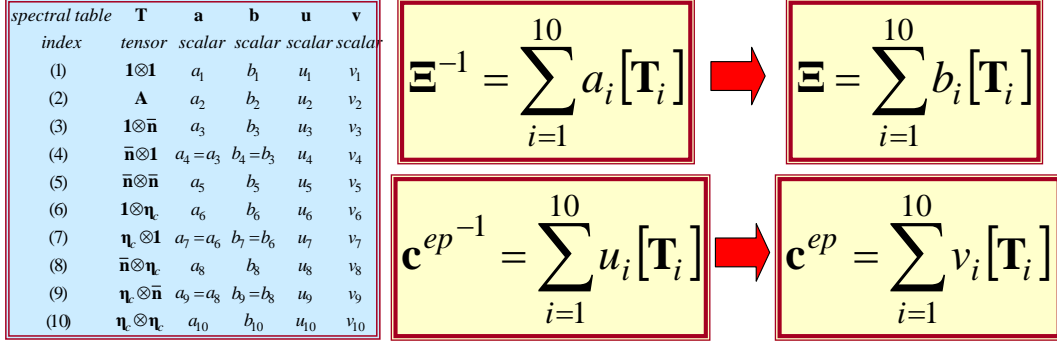| spectral table index	T tensor	a scalar	b scalar	u scalar	v scalar
(1)	$\mathbf{1}\otimes\mathbf{1}$	a_1	b_1	u_1	v_1
(2)	$\mathbf{A}$	a_2	b_2	u_2	v_2
(3)	$\mathbf{1}\otimes\bar{\mathbf{n}}$	a_3	b_3	u_3	v_3
(4)	$\bar{\mathbf{n}}\otimes\mathbf{1}$	$a_4=a_3$	$b_4=b_3$	u_4	v_4
(5)	$\bar{\mathbf{n}}\otimes\bar{\mathbf{n}}$	a_5	b_5	u_5	v_5
(6)	$\mathbf{1}\otimes\boldsymbol{\eta}_c$	a_6	b_6	u_6	v_6
(7)	$\boldsymbol{\eta}_c\otimes\mathbf{1}$	$a_7=a_6$	$b_7=b_6$	u_7	v_7
(8)	$\bar{\mathbf{n}}\otimes\boldsymbol{\eta}_c$	a_8	b_8	u_8	v_8
(9)	$\boldsymbol{\eta}_c\otimes\bar{\mathbf{n}}$	$a_9=a_8$	$b_9=b_8$	u_9	v_9
(10)	$\boldsymbol{\eta}_c\otimes\boldsymbol{\eta}_c$	a_{10}	b_{10}	u_{10}	v_{10}

$$\boldsymbol{\Xi}^{-1}=\sum_{i=1}^{10}a_i\left[\mathbf{T}_i\right] \quad\Rightarrow\quad \boldsymbol{\Xi}=\sum_{i=1}^{10}b_i\left[\mathbf{T}_i\right]$$

$$\mathbf{c}^{ep^{-1}}=\sum_{i=1}^{10}u_i\left[\mathbf{T}_i\right] \quad\Rightarrow\quad \mathbf{c}^{ep}=\sum_{i=1}^{10}v_i\left[\mathbf{T}_i\right]$$

Figure 10.5 Constitutive matrices

10.4 Global Solution Scheme

For most engineering practice, the non-linear response is primarily attributed by material non-linearity while geometric non-linearity is a second importance. In this study, the geometric non-linearity is not the main focus, therefore, infinitesimal deformations and strains are considered. In displacement-based FEM, a solution previously converged at time t=t_n is known and satisfied global equilibrium requirement which can be shown by unbalanced force,

$$\mathbf{F}^{\text{int}}(\boldsymbol{\sigma}'_n)-\mathbf{F}_n^{ext}=\mathbf{0} \tag{10.50}$$

where $\mathbf{d}_n$ is the nodal displacement vector at time t=t_n . $\mathbf{F}_n^{ext}$ is the vector of applied nodal forces and $\mathbf{F}_n^{\text{int}}=\mathbf{F}^{\text{int}}(\boldsymbol{\sigma}'_n)$ is the vector of internal forces obtained from stresses $\boldsymbol{\sigma}'_n$ in element.

A solution in terms of displacement $\mathbf{d}_{n+1}$ at t=t_{n+1} for a new loading $\mathbf{F}_{n+1}^{ext}$ can be solved by Eq.(10.51).

$$\Delta\mathbf{F}(\mathbf{d}_{n+1})=\mathbf{F}^{\text{int}}(\boldsymbol{\sigma}'_{n+1})-\mathbf{F}_{n+1}^{ext}=\mathbf{0} \tag{10.51}$$

where

$$\mathbf{F}_{n+1}^{ext}=\int_{\Gamma_u}\mathbf{N}^T\mathbf{b}_{n+1}d\Gamma_u+\int_{\Gamma_\sigma}\mathbf{N}^T\mathbf{t}_{n+1}d\Gamma_\sigma \tag{10.52}$$

$$\mathbf{F}^{\text{int}}(\boldsymbol{\sigma}'_{n+1})=\mathop{\mathbf{A}}\limits_{e=1}^{ne}\int_{\Omega^e}\mathbf{B}_e^T\boldsymbol{\sigma}'_{n+1}\,d\Omega^e \tag{10.53}$$

where $\mathop{\mathbf{A}}\limits_{e=1}^{ne}$ is assembly operator for all assemblage elements in spatial domain.

According to the Newton method, a solution can be obtained iteratively from a previous iteration (k) as shown in Eq.(10.54) Let $(\bullet)_{n+1}^{(k)}$ be the value of a variable $(\bullet)$ at the kth iteration during the load step in $[t_n,t_{n+1}]$.

$$\mathbf{d}_{n+1}^{(k+1)}=\mathbf{d}_{n+1}^{(k)}-\left\{\left[\frac{\partial\Delta\mathbf{F}(\mathbf{d})}{\partial\mathbf{d}}\right]^{-1}\cdot\Delta\mathbf{F}(\mathbf{d})\right\}\bigg|_{n+1}^{(k)} \tag{10.54}$$

where

$$\frac{\partial\Delta\mathbf{F}(\mathbf{d})}{\partial\mathbf{d}}\bigg|_{n+1}^{(k)}=\frac{\partial(\mathbf{F}^{\text{int}}(\boldsymbol{\sigma}'_{n+1})-\mathbf{F}_{n+1}^{ext})}{\partial\mathbf{d}_{n+1}}\bigg|^{(k)}=\frac{\partial\mathbf{F}^{\text{int}}(\boldsymbol{\sigma}'^{(k)}_{n+1})}{\partial\mathbf{d}_{n+1}^{(k)}} \tag{10.55}$$

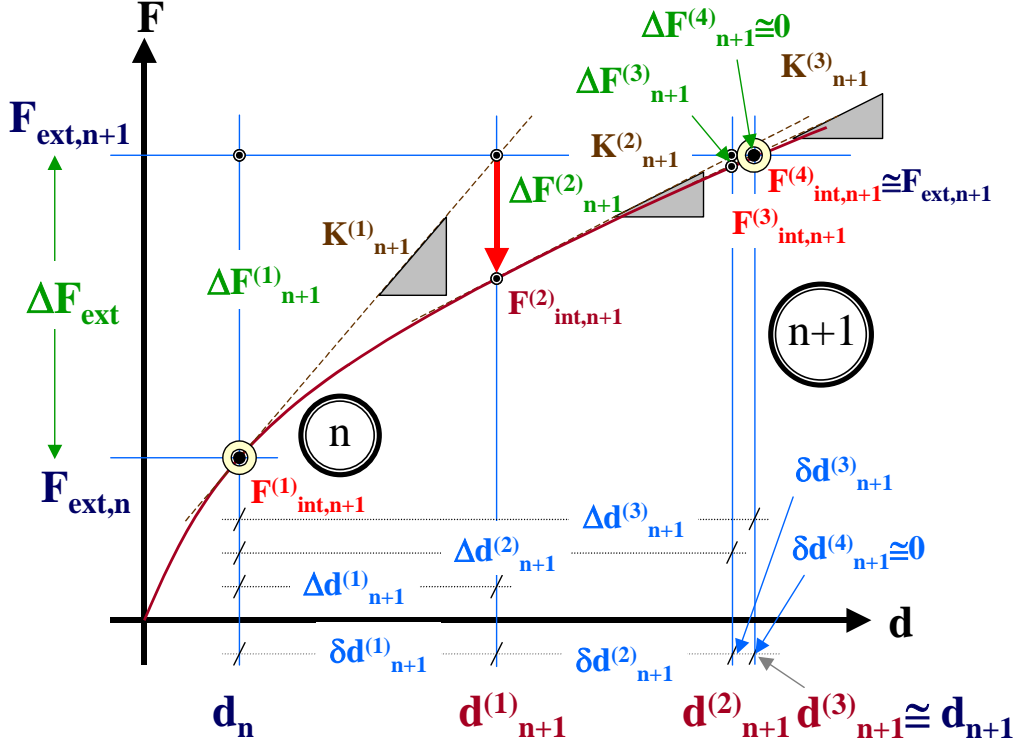The schematization of the global solution is shown in Figure 10.6.

Figure 10.6 Schematization of global solution

10.5 Global Iterative Procedures

The gradient in Eq.(10.55) can be derived by chain rule as followed,

$$\frac{\partial \mathbf{F}^{\text{int}}(\boldsymbol{\sigma}'^{(k)}_{n+1})}{\partial \boldsymbol{\sigma}'^{(k)}_{n+1}} = \mathop{A}_{e=1}^{ne} \int_{\Omega^e} \mathbf{B}_e^T \frac{\partial \boldsymbol{\sigma}'^{(k)}_{n+1}}{\partial \boldsymbol{\varepsilon}^{(k)}_{n+1}} \frac{\partial \boldsymbol{\varepsilon}^{(k)}_{n+1}}{\partial \mathbf{d}^{(k)}_{n+1}} d\Omega^e$$

$$= \mathop{A}_{e=1}^{ne} \int_{\Omega^e} \mathbf{B}_e^T \mathbf{c}^{ep(k)}_{n+1} \mathbf{B}_e d\Omega^e \tag{10.56}$$

$$= \mathop{A}_{e=1}^{ne} \mathbf{k}^{(k)}_{en+1} = \mathbf{K}^{(k)}_{n+1}$$

where $\quad \mathbf{c}^{ep(k)}_{n+1} = \dfrac{\partial \boldsymbol{\sigma}'^{(k)}_{n+1}}{\partial \boldsymbol{\varepsilon}^{(k)}_{n+1}}$ $\tag{10.57}$

Herein, the consistent tangential stiffness tensor Eq.(10.57) is employed in Eq.(10.56). $\mathbf{K}^{(k)}_{n+1}$ is the global tangent stiffness matrix evaluated ate iteration (k).

Refer to Eq.(10.54), the variation of $\mathbf{d}_{n+1}$ of each iteration can be computed by,

$$\delta \mathbf{d}^{(k+1)}_{n+1} = \mathbf{d}^{(k+1)}_{n+1} - \mathbf{d}^{(k)}_{n+1} = \left[\frac{\partial \Delta \mathbf{F}(\mathbf{d}^{(k)}_{n+1})}{\partial \mathbf{d}^{(k)}_{n+1}} \right]^{-1} \cdot \Delta \mathbf{F}(\mathbf{d}^{(k)}_{n+1})$$

$$= -\left[\mathbf{K}^{(k)}_{n+1} \right]^{-1} \cdot \left\{ \mathbf{F}^{\text{int}}(\boldsymbol{\sigma}'^{(k)}_{n+1}) - \mathbf{F}^{ext}_{n+1} \right\} \tag{10.58}$$

The full Newton iteration procedure to solve these equilibriums equations can be summarized in Eqs.(10.59)-(10.60). The new displacement is updated iteratively by Eq.(10.61)

$$\mathbf{K}^{(k)}_{n+1} \cdot \delta \mathbf{d}^{(k+1)}_{n+1} = -\left\{ \mathbf{F}^{\text{int}}(\boldsymbol{\sigma}'^{(k)}_{n+1}) - \mathbf{F}^{ext}_{n+1} \right\} \tag{10.59}$$

$$\Delta \mathbf{d}^{(k+1)}_{n+1} = \Delta \mathbf{d}^{(k)}_{n+1} + \delta \mathbf{d}^{(k+1)}_{n+1} \tag{10.60}$$

$$\mathbf{d}^{(k+1)}_{n+1} = \mathbf{d}_n + \Delta \mathbf{d}^{(k+1)}_{n+1} = \mathbf{d}^{(k)}_{n+1} + \delta \mathbf{d}^{(k+1)}_{n+1} \tag{10.61}$$

with initial conditions given by previously converged values at step $t=t_n$,

$$\mathbf{K}^{(1)}_{n+1} = \mathbf{K}_n ; \boldsymbol{\sigma}'^{(1)}_{n+1} = \boldsymbol{\sigma}'_n ; \mathbf{F}^{\text{int}}(\boldsymbol{\sigma}'^{(1)}_{n+1}) = \mathbf{F}^{\text{int}}_n ; \mathbf{d}^{(1)}_{n+1} = \mathbf{d}_n \tag{10.62}$$

$$\mathbf{F}_{n+1}^{ext} = \int_{\Gamma_u} \mathbf{N}^T \mathbf{b}_{n+1} d\Gamma_u + \int_{\Gamma_\sigma} \mathbf{N}^T \mathbf{t}_{n+1} d\Gamma_\sigma$$

$$\mathbf{F}^{int}(\boldsymbol{\sigma}'^{(k)}_{n+1}) = \mathop{A}_{e=1}^{ne} \int_{\Omega^e} \mathbf{B}_e^T \boldsymbol{\sigma}'^{(k)}_{n+1} d\Omega^e$$

$$\mathbf{k}_{en+1}^{(k)} = \int_{\Omega^e} \mathbf{B}_e^T \mathbf{c}^{ep(k)}_{n+1} \mathbf{B}_e^T d\Omega^e \quad \mathbf{K}_{n+1}^{(k)} = \mathop{A}_{e=1}^{ne} \mathbf{k}_{en+1}^{(k)}$$

$$\left\{ \mathbf{K}_{n+1}^{(k)} \right\} \delta \mathbf{d}_{n+1}^{(k+1)} = -\left[\mathbf{F}^{int}(\boldsymbol{\sigma}'^{(k)}_{n+1}) - \mathbf{F}_{n+1}^{ext} \right]$$

$$\Delta \mathbf{d}_{n+1}^{(k+1)} = \Delta \mathbf{d}_{n+1}^{(k)} + \delta \mathbf{d}_{n+1}^{(k+1)}$$

$$\frac{\left\| \mathbf{F}_{n+1}^{int(k)} - \mathbf{F}_{n+1}^{ext} \right\|}{\left\| \mathbf{F}_{n+1}^{ext} \right\|} < TOL_3 \quad \text{and} \quad \frac{\left| \delta \mathbf{d}_{n+1}^{<k+1>} \cdot \Delta \mathbf{F}_{n+1}^{<k>} \right|}{\left| \delta \mathbf{d}_{n+1}^{<1>} \cdot \Delta \mathbf{F}_{n+1}^{<1>} \right|} < TOL_4$$

Return-mapping algorithm

$$\mathbf{F}^{int}(\boldsymbol{\sigma}'^{(k+1)}_{n+1}) = \mathop{A}_{e=1}^{ne} \int_{\Omega^e} \mathbf{B}_e^T \boldsymbol{\sigma}'^{(k+1)}_{n+1} d\Omega^e$$
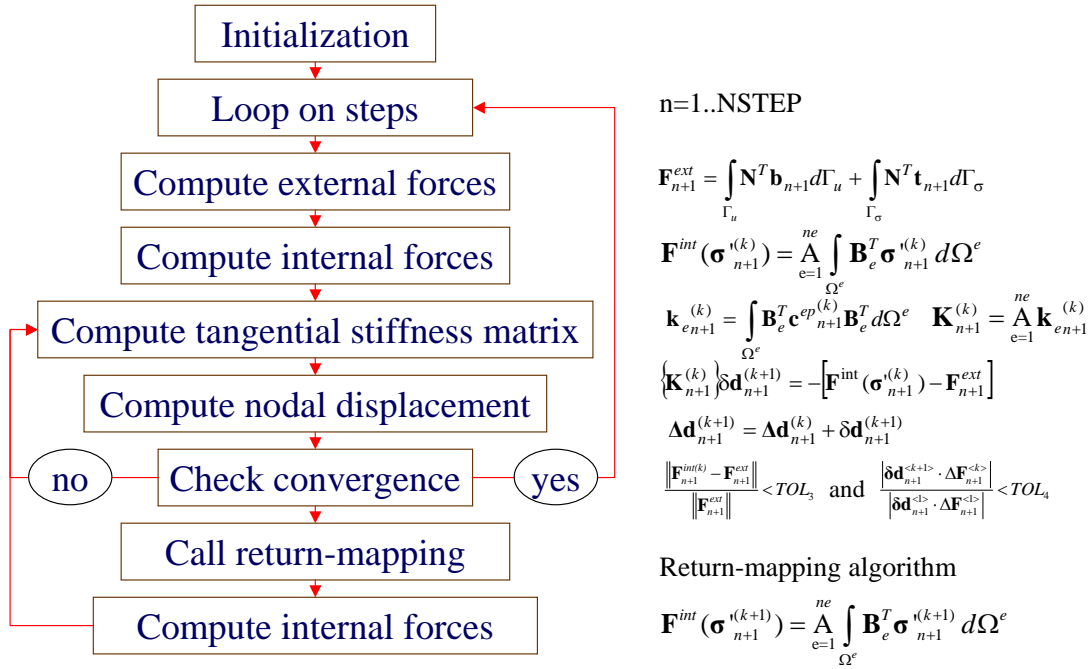
Figure 10.7 Global iterative procedures

A sequence of linear system in Eq.(10.59) solves a non-linear system in Eq.(10.51). The iteration would be preceded until the sufficiently small convergence is reached. Convergence is measured in terms of residual force norm Eq.(10.63) and the discrete energy norm Eq.(10.64), which is computed from the residual force vector and the incremental nodal displacement vector.

$$\frac{\left\| \mathbf{F}_{n+1}^{int(k)} - \mathbf{F}_{n+1}^{ext} \right\|}{\left\| \mathbf{F}_{n+1}^{ext} \right\|} < TOL_{force} \tag{10.63}$$

$$\frac{\left| \delta \mathbf{d}_{n+1}^{(k+1)} \cdot \Delta \mathbf{F}_{n+1}^{(k)} \right|}{\left| \delta \mathbf{d}_{n+1}^{(1)} \cdot \Delta \mathbf{F}_{n+1}^{(1)} \right|} < TOL_{energy} \quad \text{where} \quad \Delta \mathbf{F}_{n+1}^{(k)} = \mathbf{F}^{int}(\boldsymbol{\sigma}'^{(k)}_{n+1}) - \mathbf{F}_{n+1}^{ext} \tag{10.64}$$

Summary of global iterative procedures are shown in Figure 10.7.

10.6 Local Iterative Procedures

At each global iteration, local iteration is invoked to correct or relax a stress by enforcing back to yield surface. On each element, by the standard iso-parametric interpolation function, the incremental nodal displacement calculated in global level is used to calculate incremental strains at each Gauss points using kinematic matrix or strain-displacement matrix as shown in Eq.(10.65).

$$\Delta \boldsymbol{\varepsilon}_{n+1} = \mathbf{B}_e^T \cdot \Delta \mathbf{d}_{n+1}^{(k+1)} \tag{10.65}$$

At each Gauss point in material level, the information on initial state variables (typically, stress, strain, plastic strain and hardening variables) and applied strain increment are passed to the stress update algorithm. Using local iterative procedures presented in Figure 10.8, the constitutive model computes the material response over finite increments of strain. The details of update algorithms are shown in Chapter 6 for state of stress at corner and Chapter 7 for regular yield function in which the return paths generated by the algorithm is viewed as non-coaxial mapping as shown in Figure 10.9.
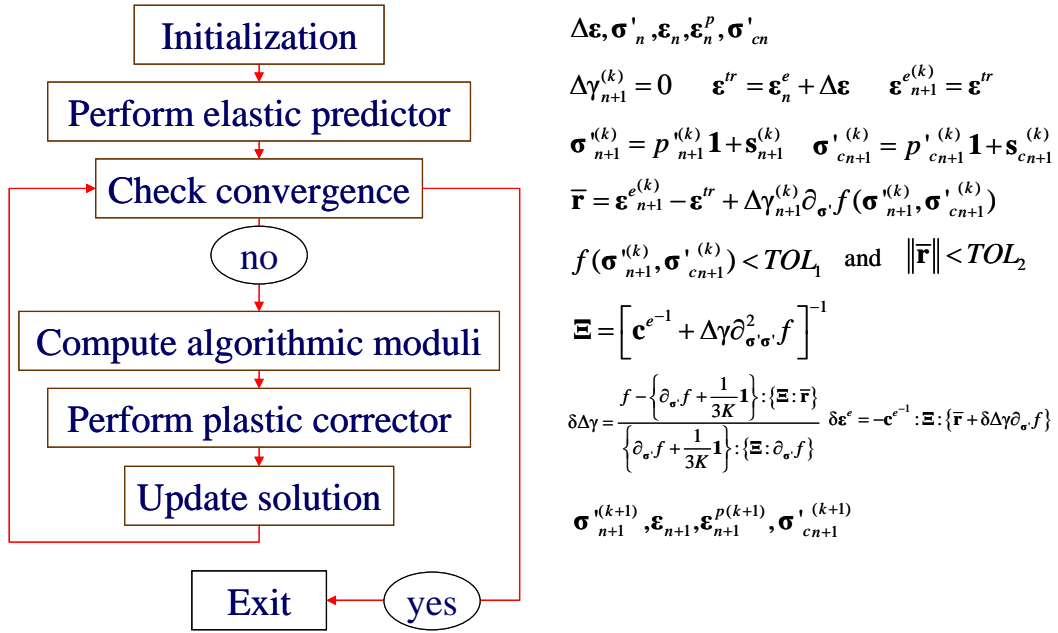
$$\Delta\boldsymbol{\varepsilon},\boldsymbol{\sigma'}_n,\boldsymbol{\varepsilon}_n,\boldsymbol{\varepsilon}_n^p,\boldsymbol{\sigma'}_{cn}$$

$$\Delta\gamma_{n+1}^{(k)}=0 \qquad \boldsymbol{\varepsilon}^{tr}=\boldsymbol{\varepsilon}_n^e+\Delta\boldsymbol{\varepsilon} \qquad \boldsymbol{\varepsilon}_{n+1}^{e(k)}=\boldsymbol{\varepsilon}^{tr}$$

$$\boldsymbol{\sigma}_{n+1}^{'(k)}=p_{n+1}^{'(k)}\mathbf{1}+\mathbf{s}_{n+1}^{(k)} \qquad \boldsymbol{\sigma'}_{cn+1}^{(k)}=p_{cn+1}^{'(k)}\mathbf{1}+\mathbf{s}_{cn+1}^{(k)}$$

$$\bar{\mathbf{r}}=\boldsymbol{\varepsilon}_{n+1}^{e(k)}-\boldsymbol{\varepsilon}^{tr}+\Delta\gamma_{n+1}^{(k)}\partial_{\sigma'}f(\boldsymbol{\sigma}_{n+1}^{'(k)},\boldsymbol{\sigma'}_{cn+1}^{(k)})$$

$$f(\boldsymbol{\sigma}_{n+1}^{'(k)},\boldsymbol{\sigma'}_{cn+1}^{(k)})<TOL_1 \quad \text{and} \quad \|\bar{\mathbf{r}}\|<TOL_2$$

$$\boldsymbol{\Xi}=\left[\mathbf{c}^{e-1}+\Delta\gamma\partial_{\sigma'\sigma'}^2 f\right]^{-1}$$

$$\delta\Delta\gamma=\frac{f-\left\{\partial_\sigma f+\frac{1}{3K}\mathbf{1}\right\}:\{\boldsymbol{\Xi}:\bar{\mathbf{r}}\}}{\left\{\partial_\sigma f+\frac{1}{3K}\mathbf{1}\right\}:\{\boldsymbol{\Xi}:\partial_\sigma f\}} \qquad \delta\boldsymbol{\varepsilon}^e=-\mathbf{c}^{e-1}:\boldsymbol{\Xi}:\{\bar{\mathbf{r}}+\delta\Delta\gamma\partial_\sigma f\}$$

$$\boldsymbol{\sigma}_{n+1}^{'(k+1)},\boldsymbol{\varepsilon}_{n+1},\boldsymbol{\varepsilon}_{n+1}^{p(k+1)},\boldsymbol{\sigma'}_{cn+1}^{(k+1)}$$

Figure 10.8 Local iterative procedures

The whole algorithm can be considered as the interaction of the object modules that are element, node, material, assembly, spatial domain, iteration and linear system as given in Figure 10.10. The algorithm starts from calculating external nodal forces in node module. By the same time, nodal internal forces determined from initial stresses and the corresponding local stiffness matrix are carried out in element module using interpolation functions. In assembly module, the global stiffness matrix is determined together with the assembly of unbalanced nodal forces. Iteration module controls the convergence of solution given by the incremental displacement. The incremental displacement is used to determined strain increment in element module. The prescribed strain increment drives return mapping algorithm to evaluate stress in material module. The updated stress is employed to determined internal forces. The algorithm will be repeated until the converged displacement is reached.
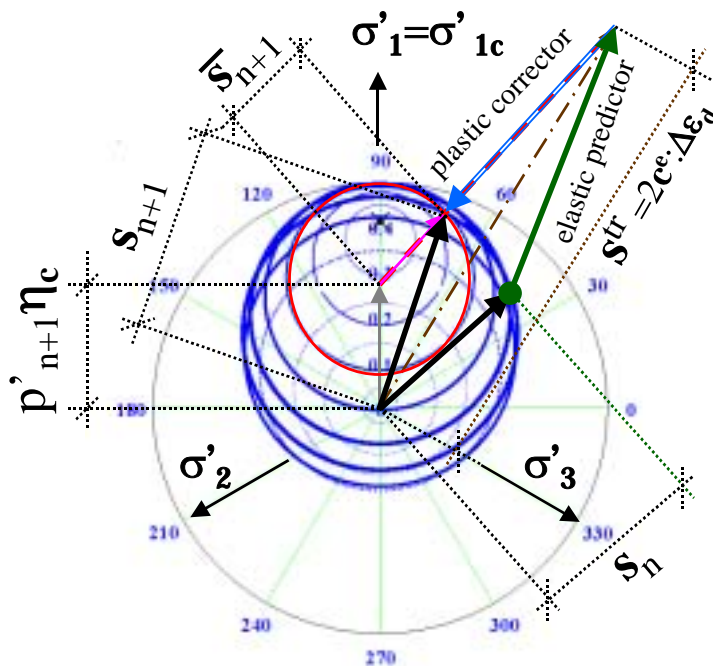

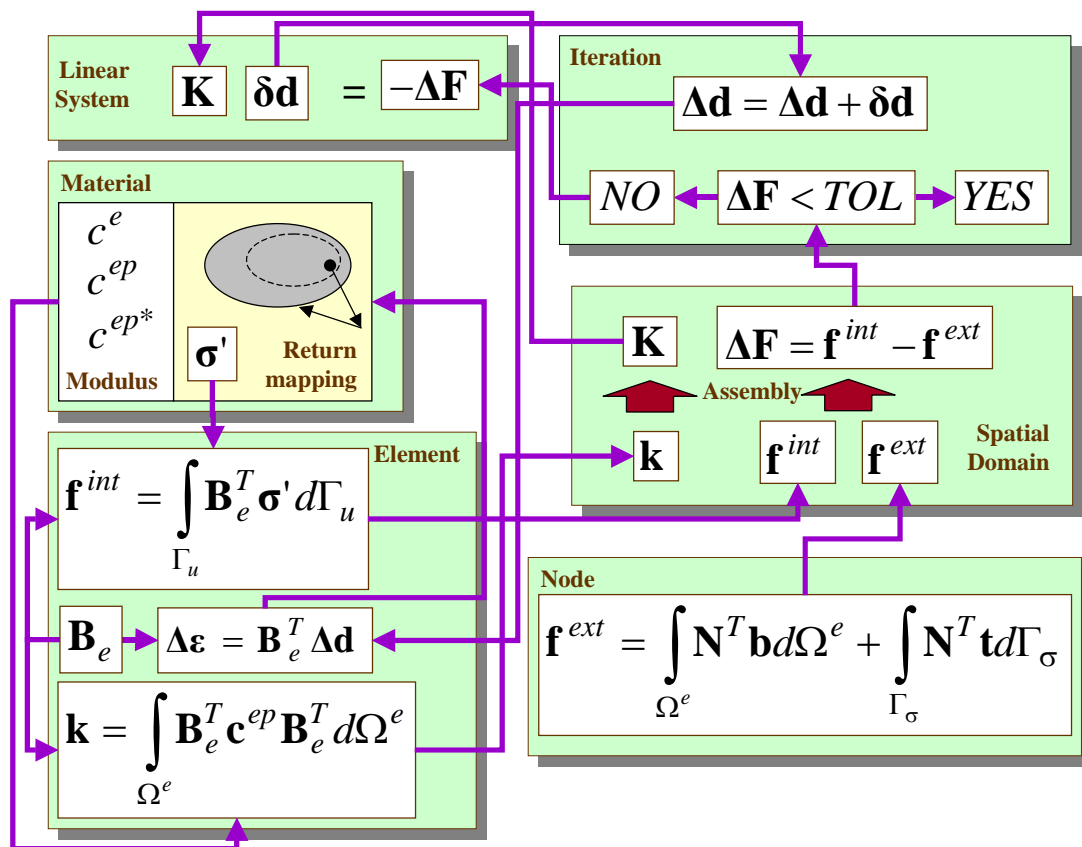Figure 10.9 Non-coaxial return paths is observed on the SO yield surface

Figure 10.10 Object interactions

10.7 References

1 Saada, A.S., "Elasticity: theory and applications", Pergamon Press Ltd., 1974

2 Hughes, Thomas J.R., "The finite element method: linear static and dynamic finite element analysis",
Prentice-Hall, Inc., 1987

3 Bathe, Klaus-Jürgen, "Finite element procedures", Prentice-Hall, Inc., 1996

4 Zienkiewicz, O.C. & Taylor, R.L., "The finite element method - vol. 1: basic formulation and linear problems",
McGraw-Hill, Inc., 1989

5 Buchanan, George R.,"Thoery and problems of finite element analysis", Schaum's outline series,
McGraw-Hill, Inc., 1994

6 Spiegel, M.R., "Theory and Problems of Advanced Calculus", McGraw-Hill, Inc., 1974

CHAPTER 11

Numerical Analysis

11.1 Initial-boundary-value-problem

A numerical simulation is presented to illustrate the performance of the return-mapping algorithms and the practical importance of consistent tangential stiffness tensor in a Newton solution procedure.

11.1.1 Simulation of CD test

The numerical simulation of drained bi-axial (plane strain) compression tests up to half of over-burden pre-consolidation pressure. Soft clay parameters and FEM mesh are shown in Figure 11.1. Iso-parametric rectangular element with 2x2-Gauss points is employed. A tolerance is set to 10^{-5} for both global and local iterations. Maximum iteration number is limited to 50.
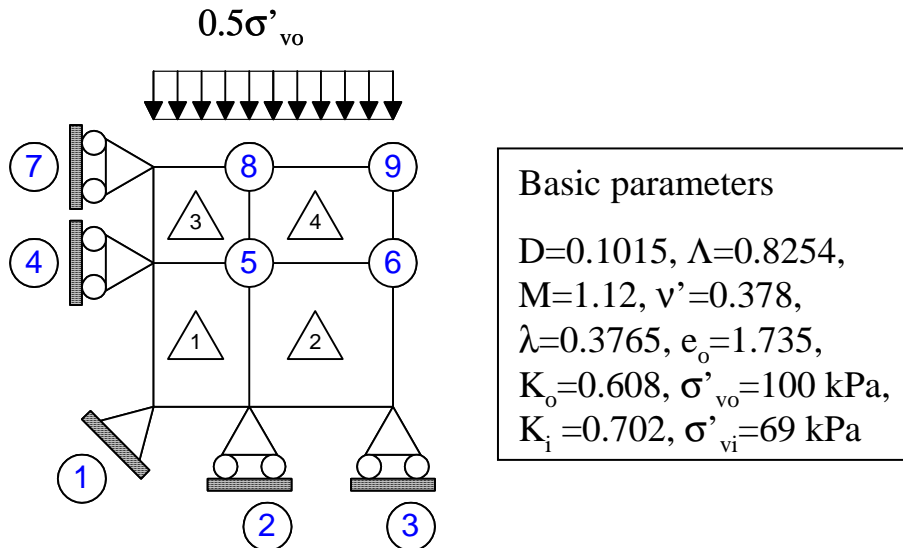
Figure 11.1 FEM mesh and basic parameters

11.1.2 Effect of load increments

Figure 11.2 shows the calculation results with varying load increments of 1, 5, 10, 20 and 50. By 50 increments, the solution does not change significantly and hence the exact solution by the algorithm is achieved. It is found that the resulting solutions can reach a convergence with considerably accuracy even by a relatively large strain.
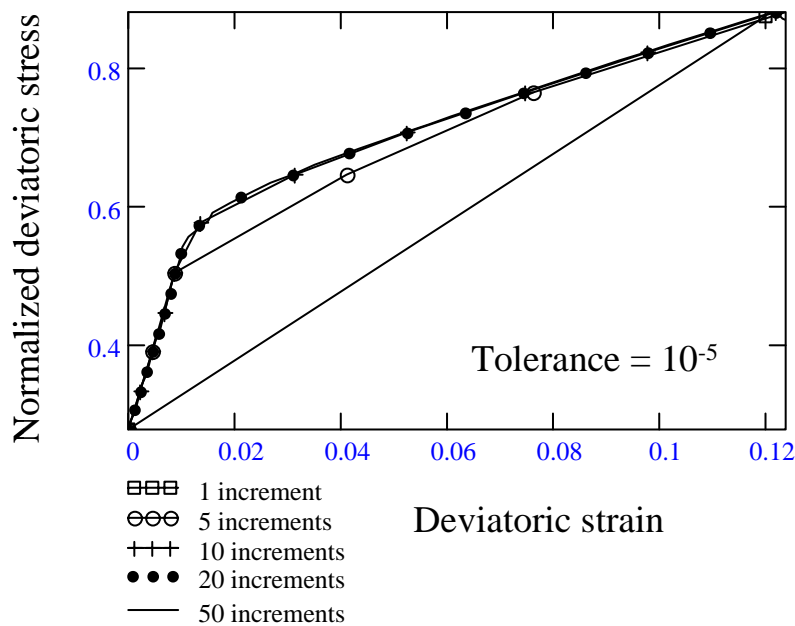
Figure 11.2 Comparison of results based on different load increments
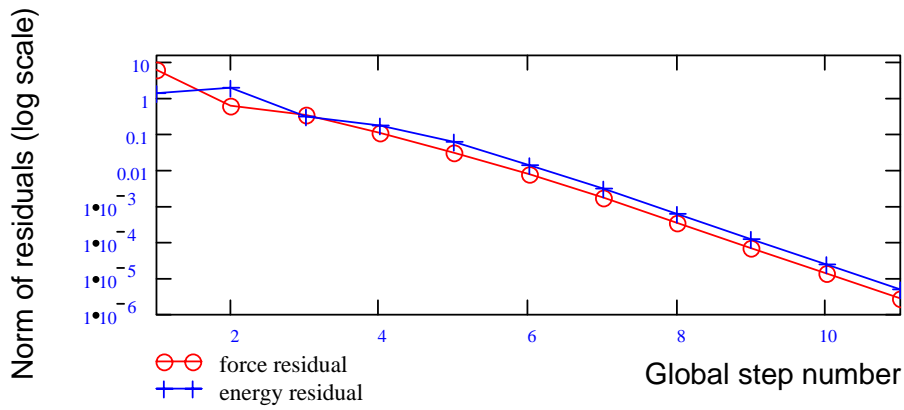
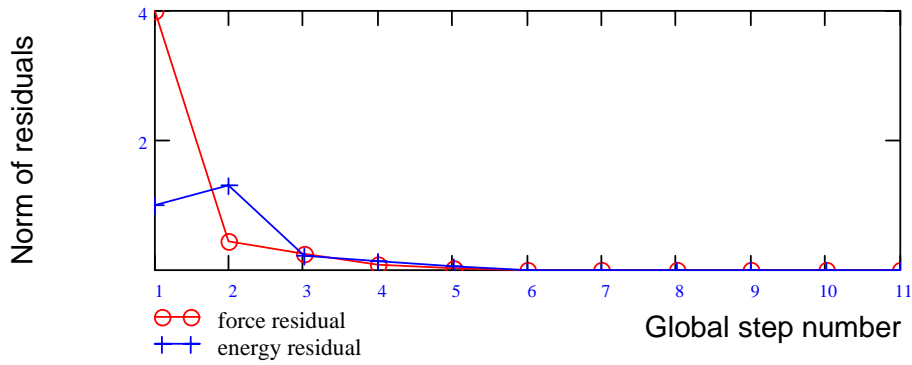### 11.1.3 Rate of global convergence

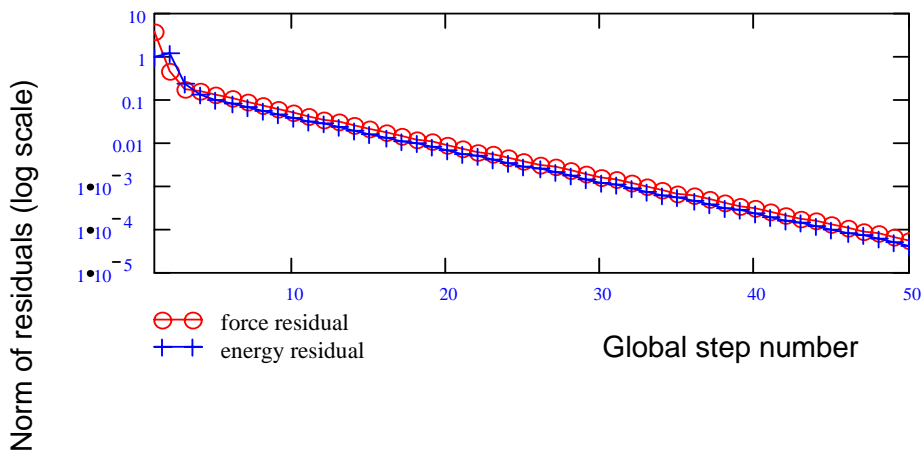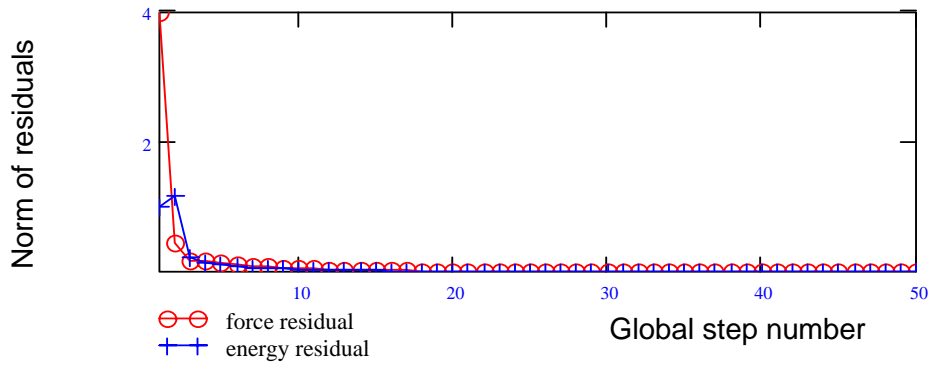Figure 11.3 Results achieved by employing consistent tangential modulus

Figure 11.4 Results achieved by employing continuum tangential moduli

According to calculation results shown in Figure 11.3 and Figure 11.4, it was found the solution which is employed consistent tangential moduli reaches a convergence with quadratic rate while that of continuum tangential moduli showed a sign of losing this performance. A norm of residuals governed by consistent tangential moduli reach 10^{-5} by 10 iterations while that of continuum tangential moduli spent more than 50 iterations to achieve the same accuracy.

11.2 Accuracy assessment

Isoerror maps of stress update algorithms are often used as the key numerical testing. [1, 2, 3] The procedures are developed based on a strain-controlled homogeneous problem to typically assess the overall accuracy of the algorithms. The stress points, which represent regular state of stress on the yield surface, are selected, i.e., uniaxial, biaxial and pure shear. The calculation can be performed in terms of principal values of the strain and stress tensors without loss of generality. At each selected point, a sequence of normalized strain increments is specified to obtain the resulting stress contour map generated by the algorithm relative to the exact solution, the value for which further repeatedly sub-incrementing produces no change in numerical results is taken as the exact solution.

From the results, level of error can be roughly observed. As a rule, good accuracy (within 5 percent) is obtained for moderate strain increments of the order of the characteristic yield strains. [4]

11.2.1 Characteristics strains
The characteristics strains are given by the specific strain at current yield stress. For K_o-consolidated clays, the characteristics strains are given in terms of volumetric and deviatoric strains as shown below,

$$\varepsilon_{vy} = \frac{p'_o}{K(p'_o)} = \frac{p'_o}{p'_o / \overline{\kappa}} = \overline{\kappa} \tag{11.1}$$

$$\varepsilon_{sy} = \frac{q_o}{3G(p'_o)} = \frac{q_o}{3\mu' p'_o / \overline{\kappa}} = \frac{\overline{\kappa}\eta_o}{3\mu'} \tag{11.2}$$

In numerical illustration in this section, the characteristics strains are obtained as,

$$\varepsilon_{vy} = 2.387\% , \quad \varepsilon_{sy} = 1.591\% \tag{11.3}$$

11.2.2 Relative error
Relative error is calculated in compare with the exact solutions marked by $\boldsymbol{\sigma}'^*$ and $\boldsymbol{\sigma}'_c{}^*$

$$ERR = \sqrt{\frac{\{\boldsymbol{\sigma}' - \boldsymbol{\sigma}'^*\}:\{\boldsymbol{\sigma}' - \boldsymbol{\sigma}'^*\} + \{\boldsymbol{\sigma}'_c - \boldsymbol{\sigma}'_c{}^*\}:\{\boldsymbol{\sigma}'_c - \boldsymbol{\sigma}'_c{}^*\}}{\boldsymbol{\sigma}'^* : \boldsymbol{\sigma}'^* + \boldsymbol{\sigma}'_c{}^* : \boldsymbol{\sigma}'_c{}^*}} \times 100\% \tag{11.4}$$

In case of axi-symmetric stress condition, components of Eq.(11.4) can be simplified. The stress error can be represented by,

$$\{\boldsymbol{\sigma}' - \boldsymbol{\sigma}'^*\}:\{\boldsymbol{\sigma}' - \boldsymbol{\sigma}'^*\} = \{(p' - p'^*)\mathbf{1} + \mathbf{s} - \mathbf{s}^*\}:\{(p' - p'^*)\mathbf{1} + \mathbf{s} - \mathbf{s}^*\}$$
$$= 3(p' - p'^*)^2 + \{\mathbf{s} - \mathbf{s}^*\}:\{\mathbf{s} - \mathbf{s}^*\} \tag{11.5}$$
$$= 3(p' - p'^*)^2 + \frac{2}{3}(q - q^*)^2$$

The hardening variable error can be represented by,

$$\{\boldsymbol{\sigma}'_c - \boldsymbol{\sigma}'_c{}^*\}:\{\boldsymbol{\sigma}'_c - \boldsymbol{\sigma}'_c{}^*\} = \{(p'_c - p'_c{}^*)\mathbf{1} + \mathbf{s}_c - \mathbf{s}_c{}^*\}:\{(p'_c - p'_c{}^*)\mathbf{1} + \mathbf{s}_c - \mathbf{s}_c{}^*\}$$
$$= 3(p'_c - p'_c{}^*)^2 + \{\mathbf{s}_c - \mathbf{s}_c{}^*\}:\{\mathbf{s}_c - \mathbf{s}_c{}^*\} \tag{11.6}$$
$$= 3(p'_c - p'_c{}^*)^2 + \frac{2}{3}(q_c - q_c{}^*)^2 = \left(3 + \frac{2}{3}\eta_o{}^2\right)(p'_c - p'_c{}^*)^2$$

The magnitude of error are sum of both stress and hardening variables.

$$\boldsymbol{\sigma}'^* : \boldsymbol{\sigma}'^* + \boldsymbol{\sigma}'_c{}^* : \boldsymbol{\sigma}'_c{}^* = 3p'^{*2} + \frac{2}{3}q^{*2} + \left(3 + \frac{2}{3}\eta_o{}^2\right)p'_c{}^{*2} \tag{11.7}$$

As a result, Eq.(11.4) is reduced to,

$$ERR = \sqrt{\frac{3(p' - p'^*)^2 + \frac{2}{3}(q - q^*)^2 + \left(3 + \frac{2}{3}\eta_o{}^2\right)(p'_c - p'_c{}^*)^2}{3p'^{*2} + \frac{2}{3}q^{*2} + \left(3 + \frac{2}{3}\eta_o{}^2\right)p'_c{}^{*2}}} \times 100\% \tag{11.8}$$

11.2.3 Sub-step and Closest-point-projection methods

The comparison between results obtained by sub-step (SS) and closest-point-projection (CPP) methods are compared. It was found that even a single step, CPP can give a better solution than SS. Figure 11.5-Figure 11.6 showed calculation results by applying different constant strain increments. η_o is stress ratio q/p' at corner. η_i is stress ratio at initial stress. η_t is stress ratio at final stress.
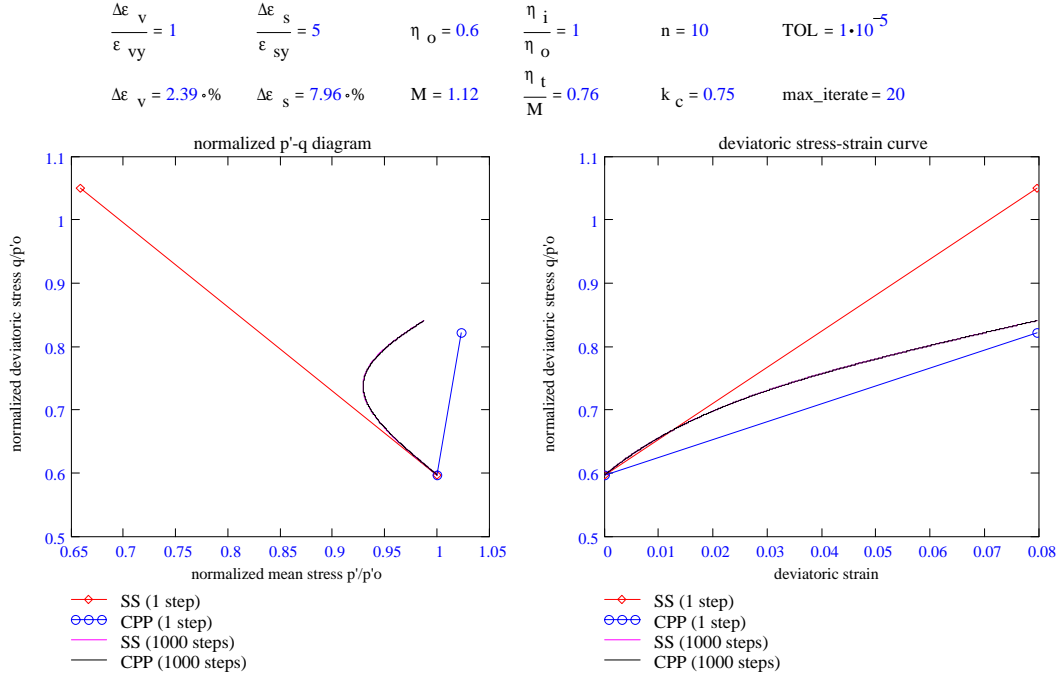

Figure 11.5 Comparisons between results obtained by SS and CPP on upper yield surface
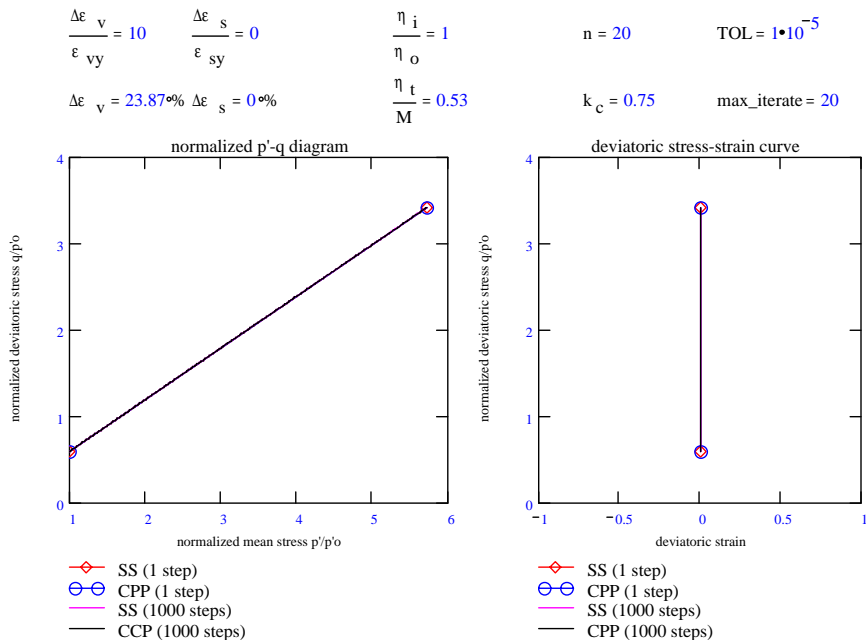
Figure 11.6 Comparisons between resulted obtained by SS and CPP on yield corner

Figure 11.7 and Figure 11.8 show results obtained by CPP and SS with varying strain increment steps. For a finer step both SS and CPP gave the same results as shown in Figure 11.9 (for example 1000 steps). It was found that the solutions by CPP are more stable than that of SS especially for large strain increment.
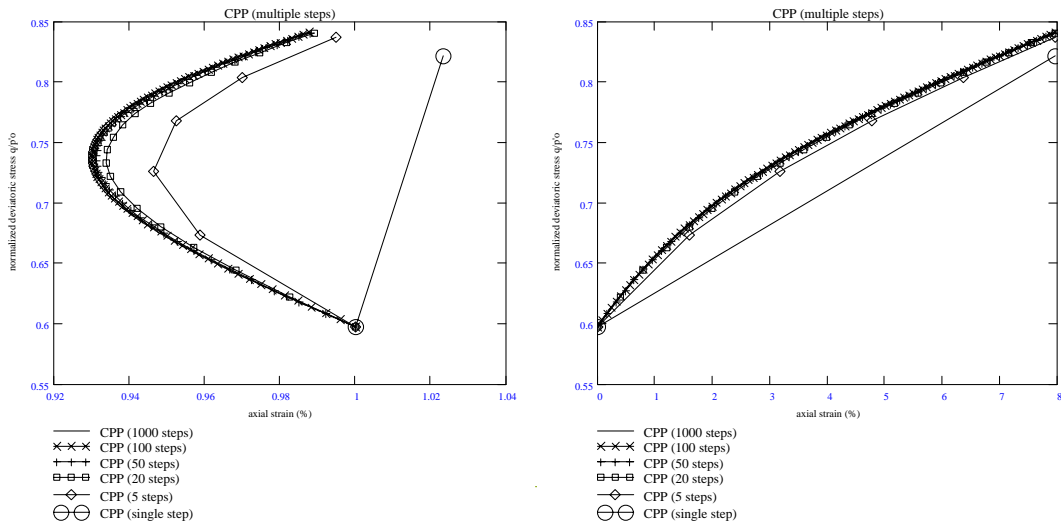

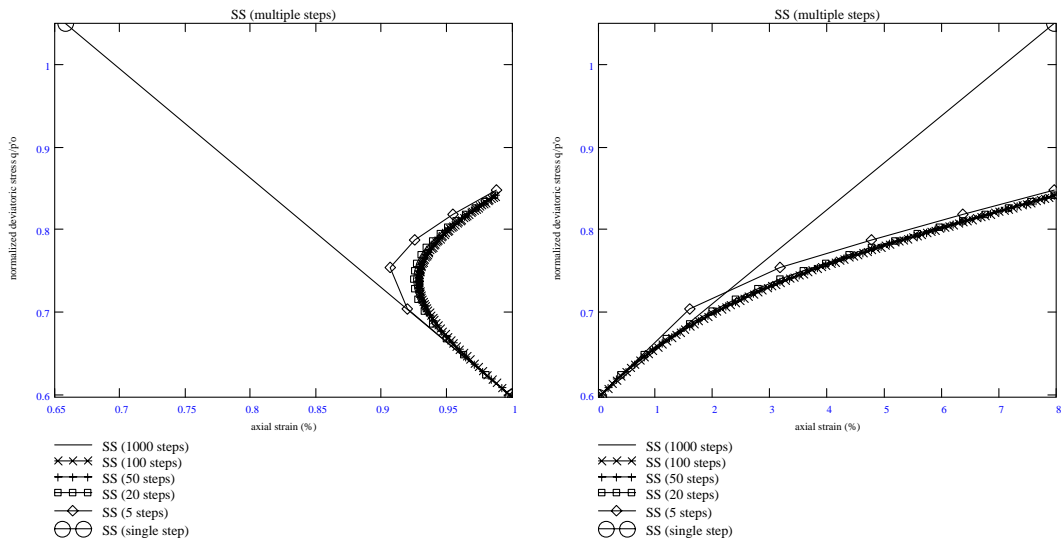Figure 11.7 Results by CPP with 1, 5, 20, 50, 100 and 1000 increment steps

Figure 11.8 Results by SS with 1, 5, 20, 50, 100 and 1000 increment steps
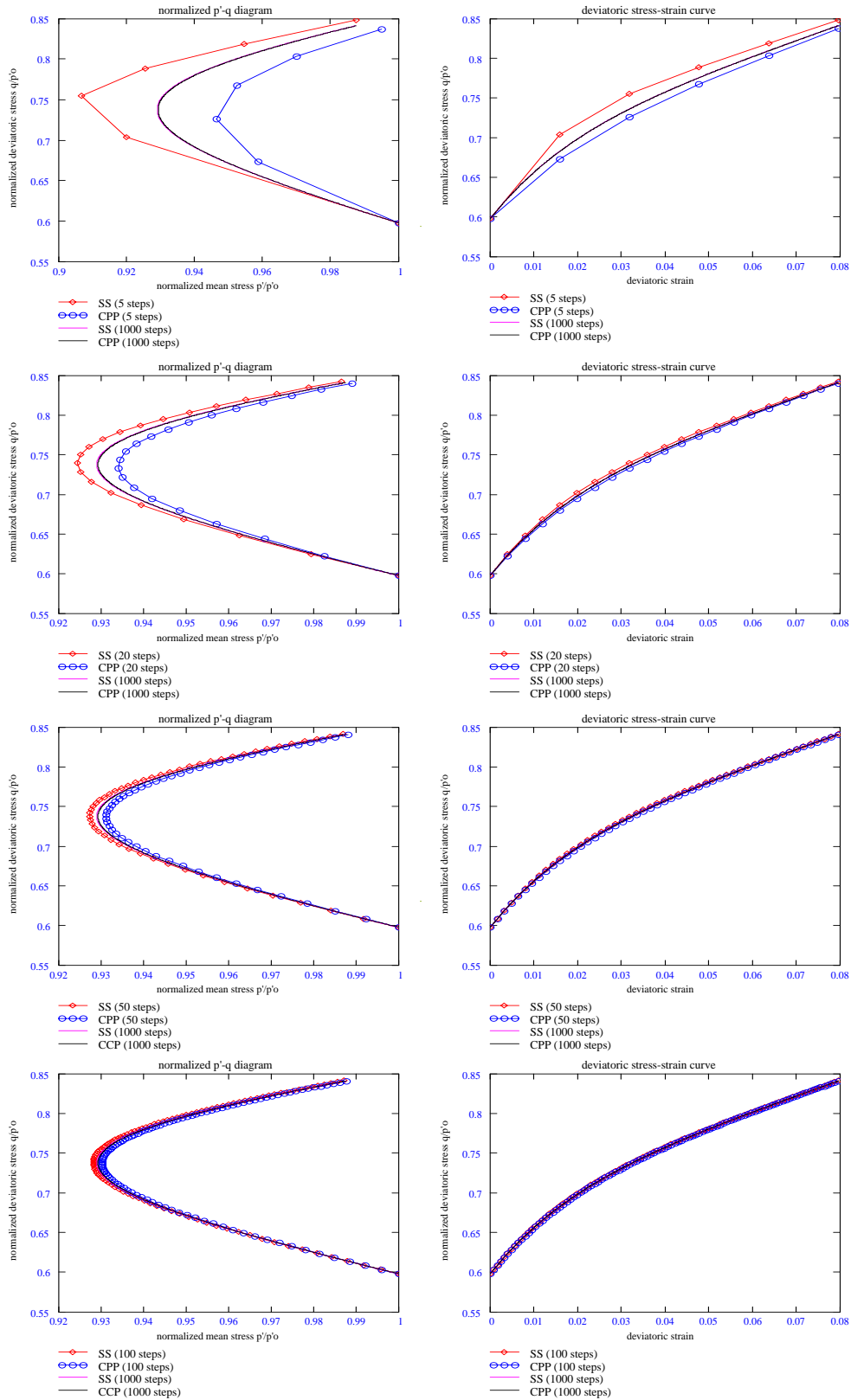
Figure 11.9 Comparisons of results given by SS and CPP with different step increments
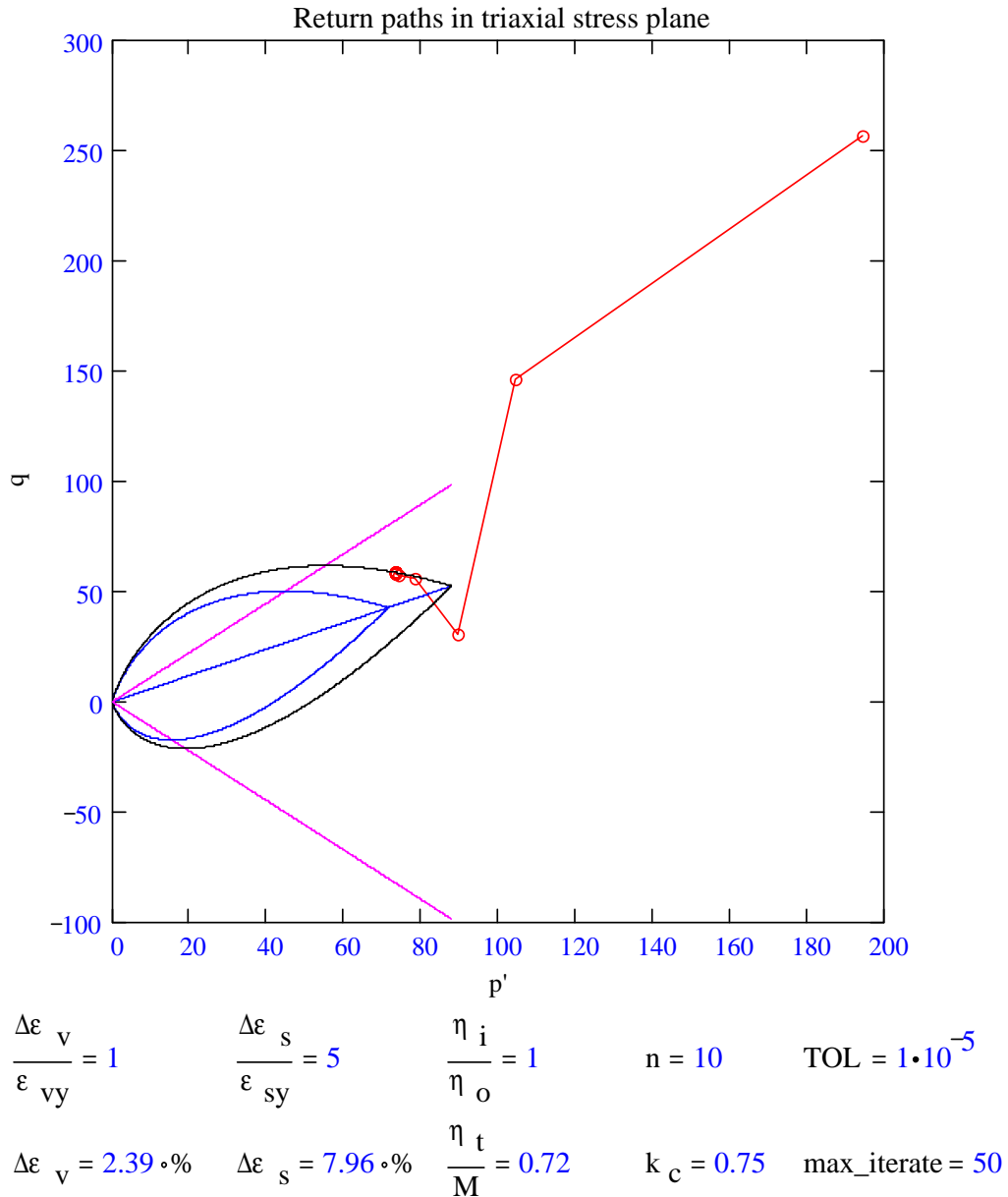
Return paths in triaxial stress plane

$$\frac{\Delta\varepsilon_v}{\varepsilon_{vy}} = 1 \qquad \frac{\Delta\varepsilon_s}{\varepsilon_{sy}} = 5 \qquad \frac{\eta_i}{\eta_o} = 1 \qquad n = 10 \qquad \text{TOL} = 1\cdot10^{-5}$$

$$\Delta\varepsilon_v = 2.39\circ\% \qquad \Delta\varepsilon_s = 7.96\circ\% \qquad \frac{\eta_t}{M} = 0.72 \qquad k_c = 0.75 \qquad \text{max\_iterate} = 50$$

Figure 11.10 Return path of converged stress

Figure 11.10 shows how stress return from trial stress to solution on yield surface by driven strains. Herein, a driven volumetric strain is as much as characteristics volumetric strain and a driven deviatoric strain is as much as 5 times of characteristics deviatoric strain.

11.2.4 Isoerror maps

Under axi-symmetric condition, isoerror maps generated by stress update algorithms are presented by Figure 11.11-Figure 11.22. The initial stresses are assigned at $\eta = \eta_o$ and $\eta = \frac{2}{3}M$. Relative error is calculated by Eq.(11.8). Errors were found no more than 6% in a domain of driven strain $10\varepsilon_{vy}$ by $10\varepsilon_{sy}$. Isoerror maps can figure stability and accuracy of algorithms under a specific domain of imposed strains.
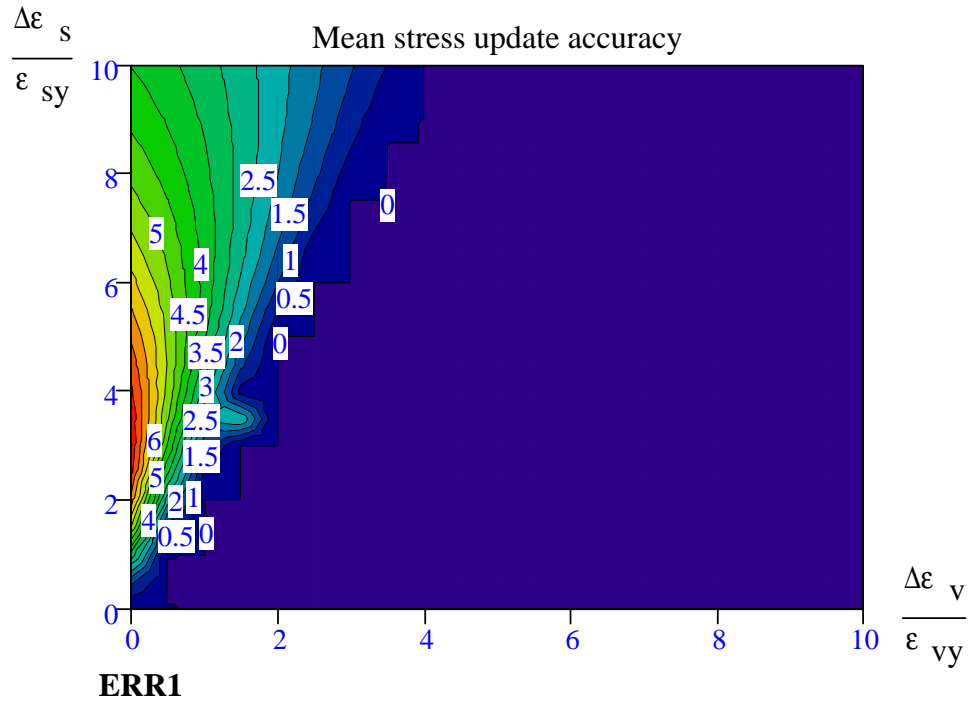
Figure 11.11 Isoerror map of mean stress for initial stress on slope η_o
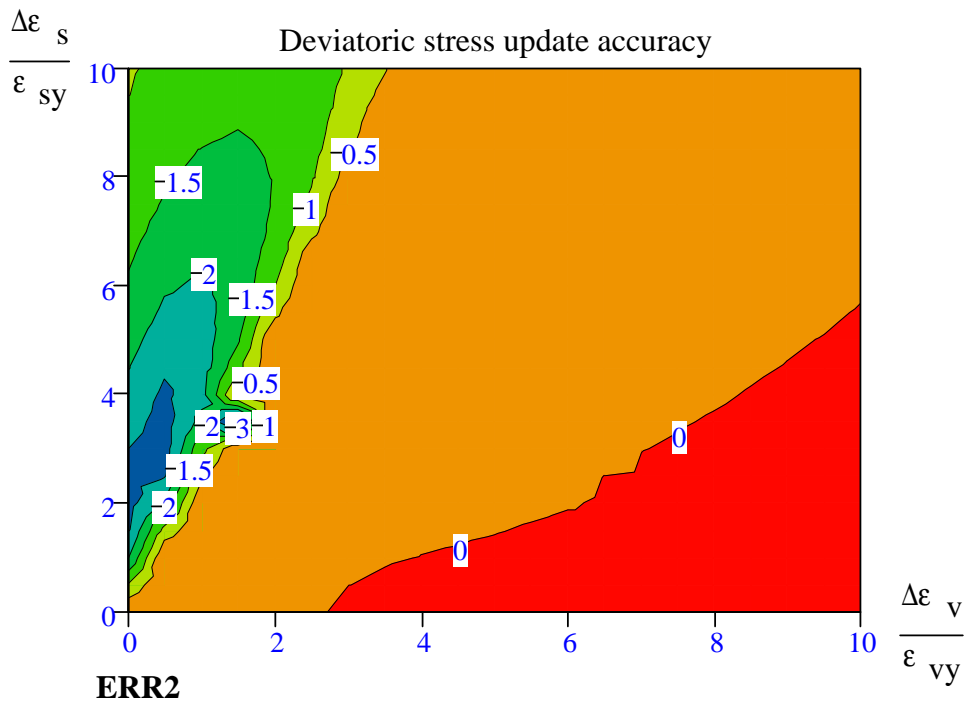
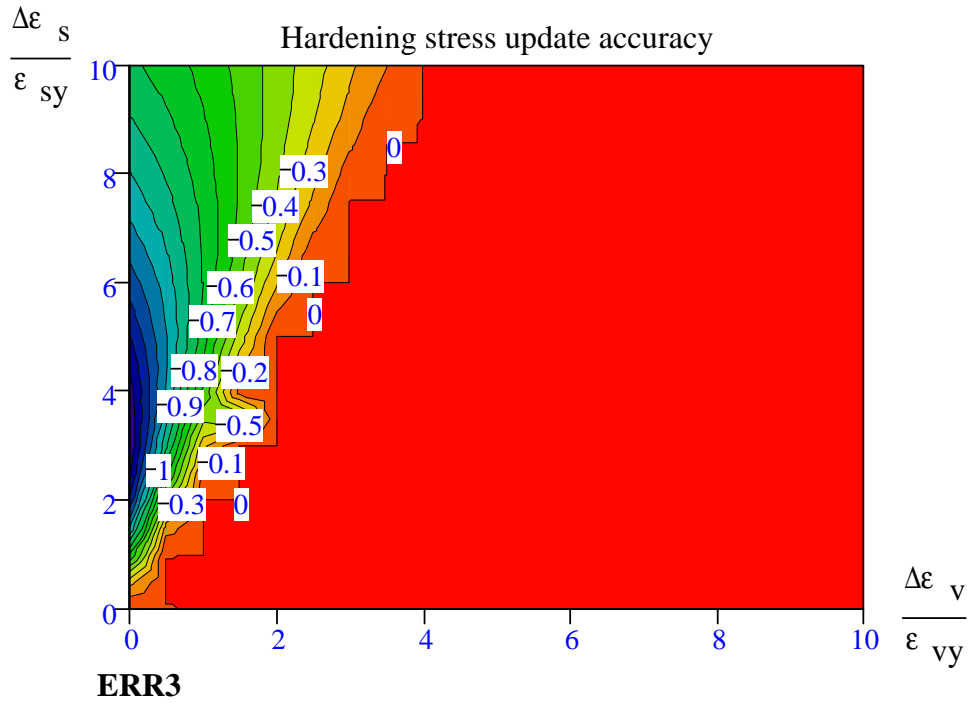Figure 11.12 Isoerror map of deviatoric stress for initial stress on slope η_o

$$\frac{\Delta\varepsilon_s}{\varepsilon_{sy}}$$

Hardening stress update accuracy

$$\frac{\Delta\varepsilon_v}{\varepsilon_{vy}}$$

ERR3

Figure 11.13 Isoerror map of hardening variable for initial stress on slope η_o

$$\frac{\Delta\varepsilon_s}{\varepsilon_{sy}}$$

Overall stress update accuracy

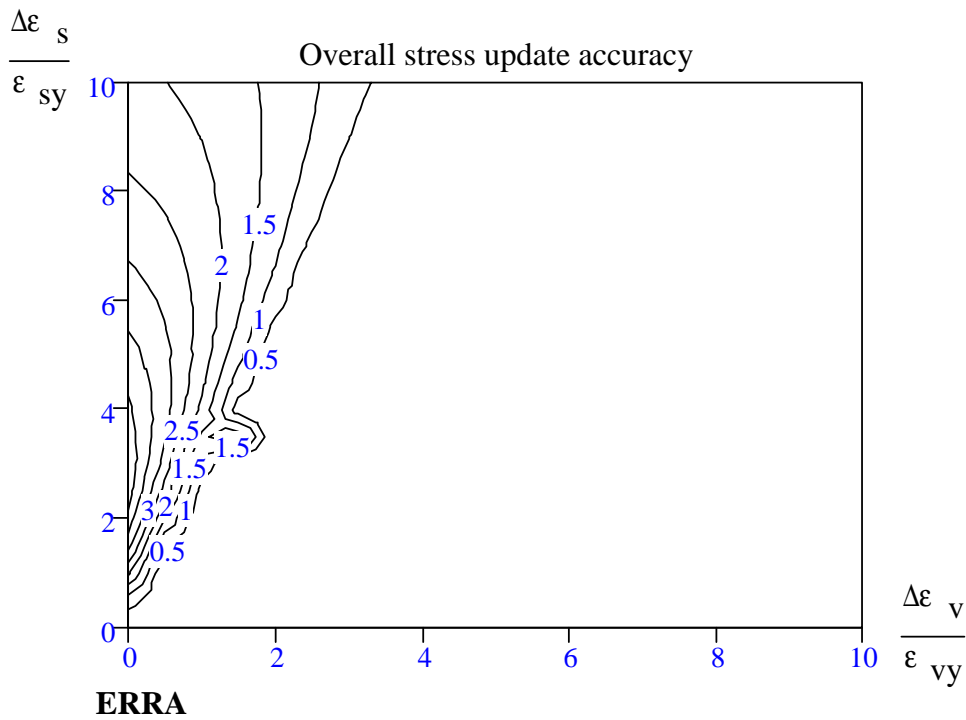$$\frac{\Delta\varepsilon_v}{\varepsilon_{vy}}$$

ERRA

Figure 11.14 Isoerror map of overall update for initial stress on slope η_o
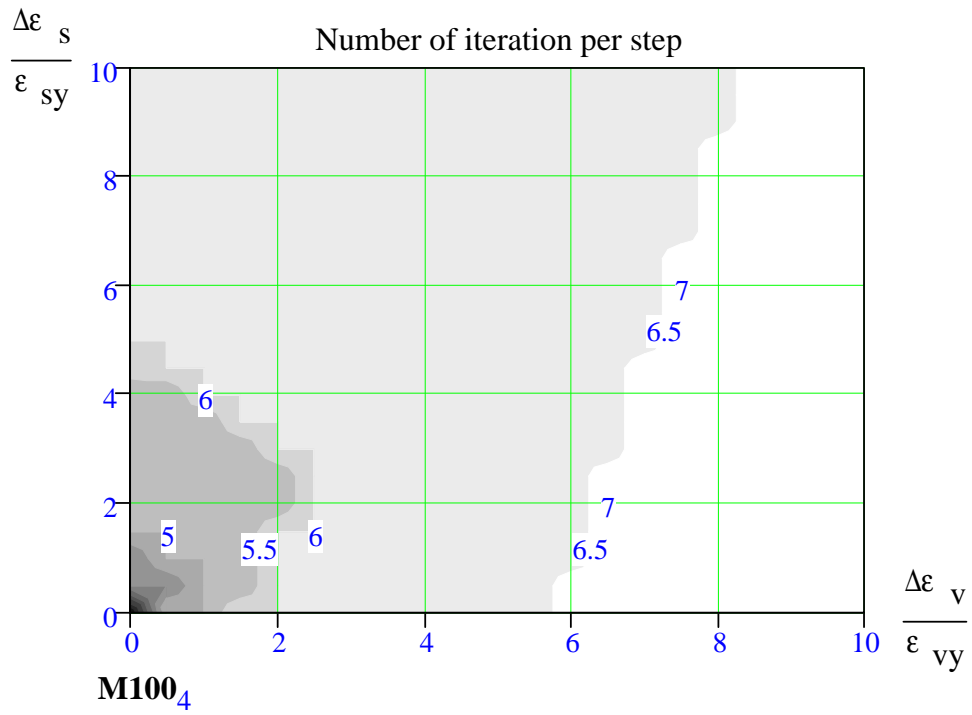
Figure 11.15 Iteration number by 100 steps for initial stress on slope η_o
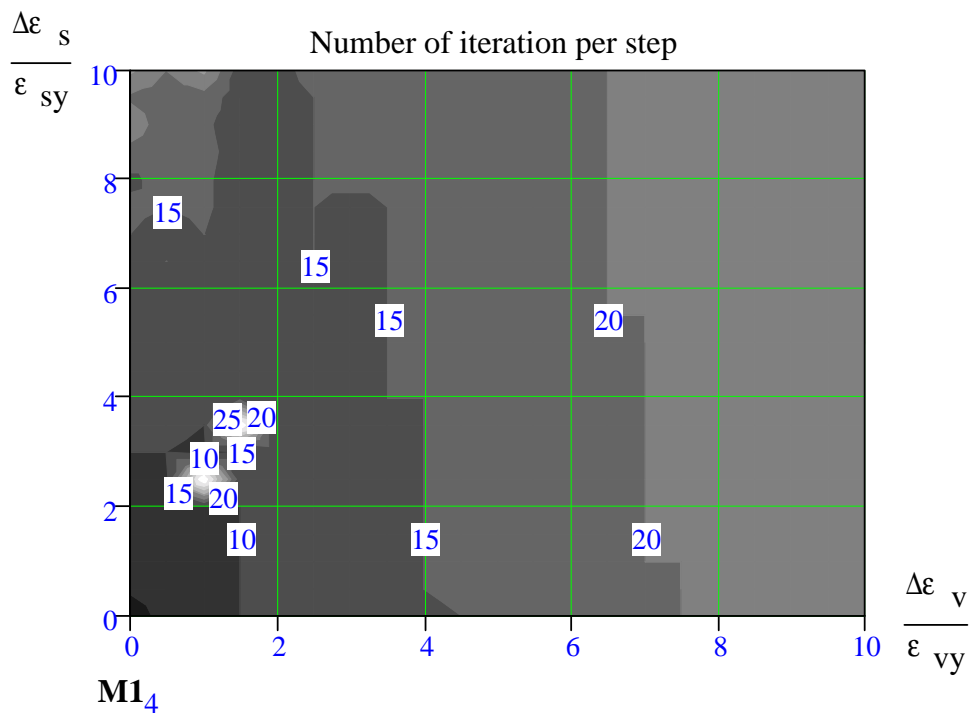

Figure 11.16 Iteration number by single step for initial stress on slope η_o
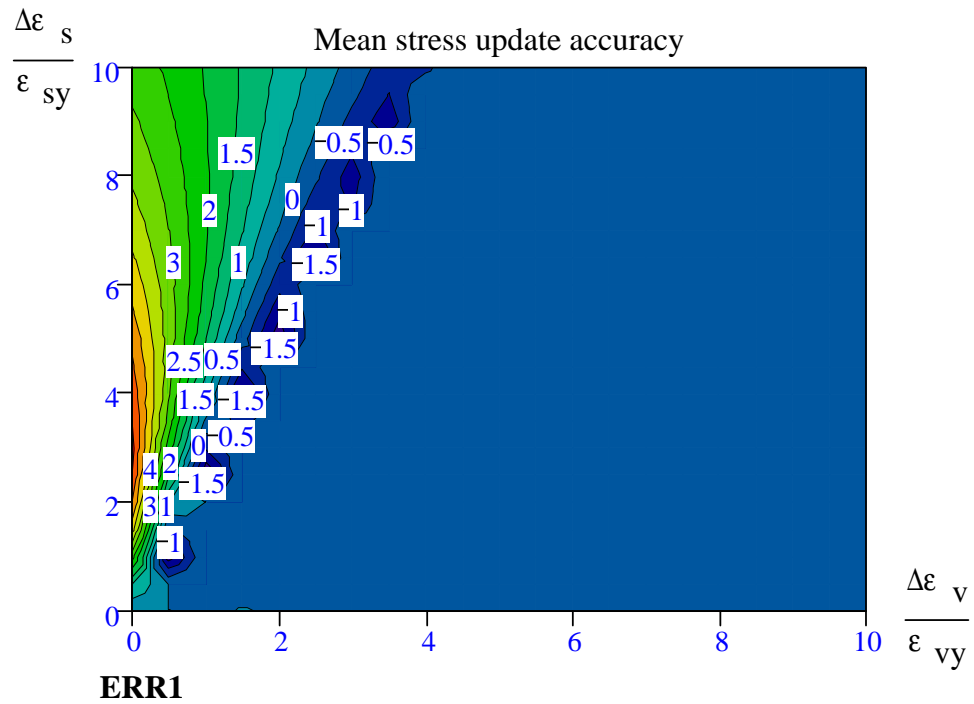
Figure 11.17 Isoerror map of mean stress for initial stress on slope 2M/3
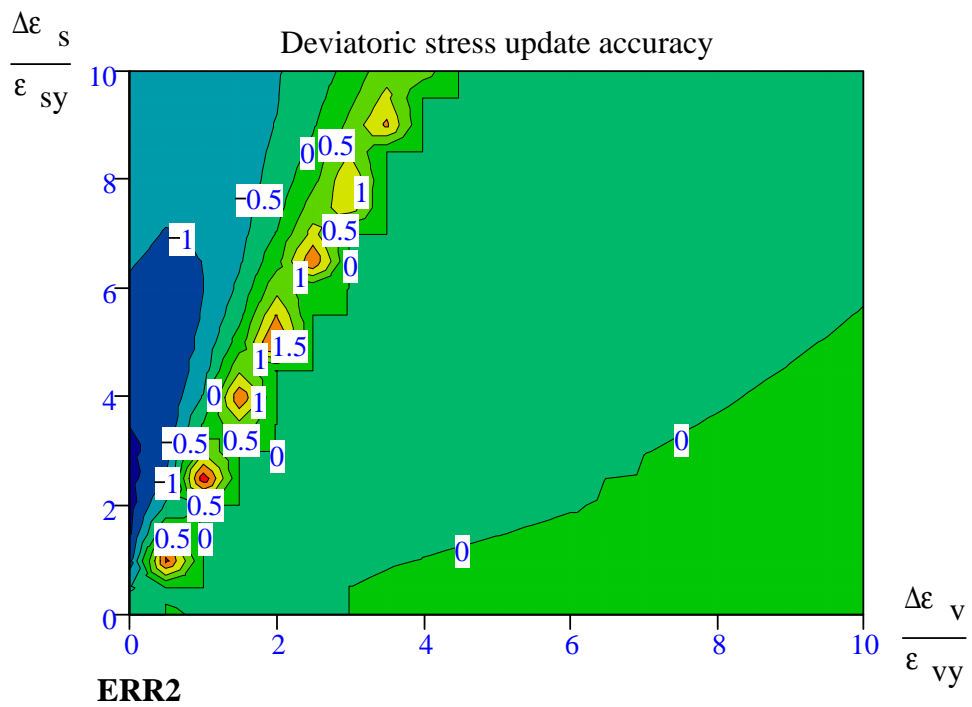
Figure 11.18 Isoerror map of deviatoric stress for initial stress on slope 2M/3

$\dfrac{\Delta\varepsilon_s}{\varepsilon_{sy}}$

Hardening stress update accuracy

ERR3

$\dfrac{\Delta\varepsilon_v}{\varepsilon_{vy}}$
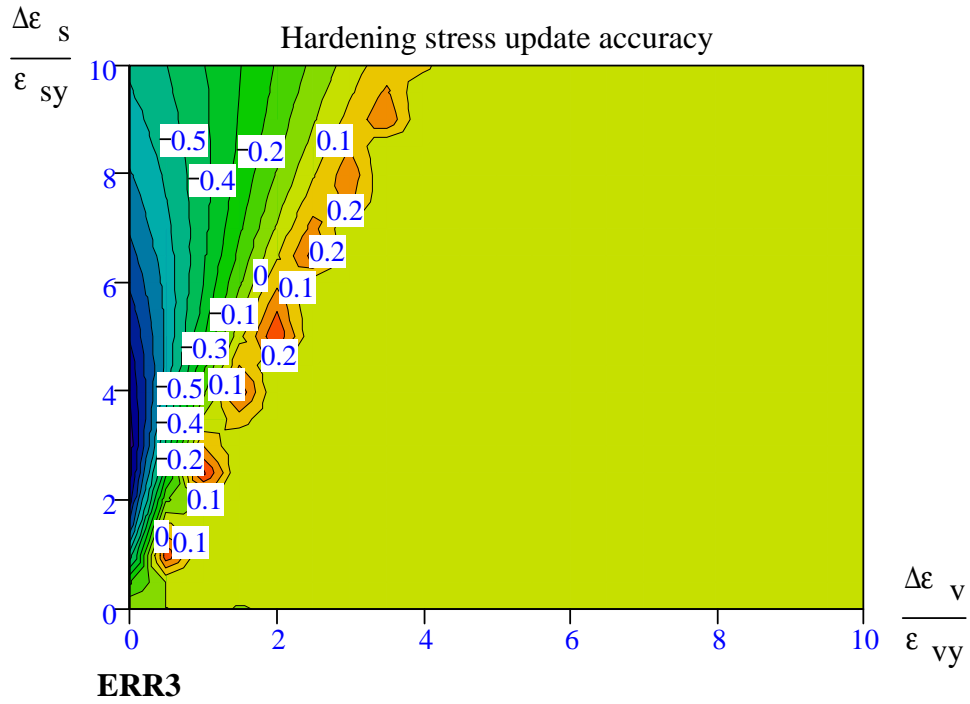
Figure 11.19 Isoerror map of hardening variables for initial stress on slope 2M/3

$\dfrac{\Delta\varepsilon_s}{\varepsilon_{sy}}$

Overall stress update accuracy

ERRA

$\dfrac{\Delta\varepsilon_v}{\varepsilon_{vy}}$

Figure 11.20 Isoerror map of overall update for initial stress on slope 2M/3
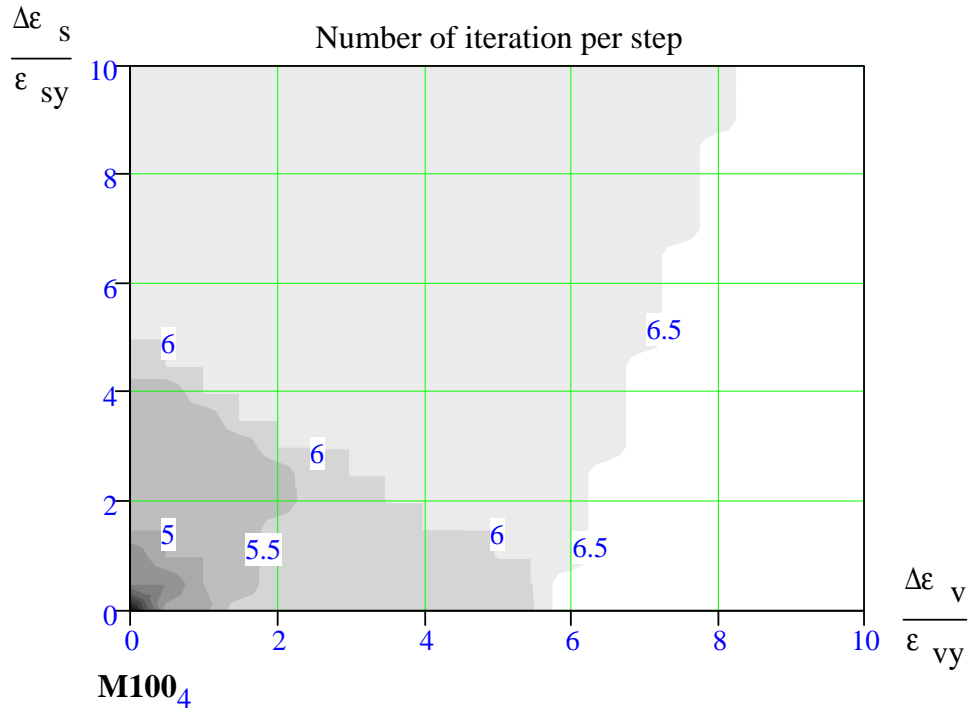
Figure 11.21 Iteration number by 100 steps for initial stress on slope 2M/3

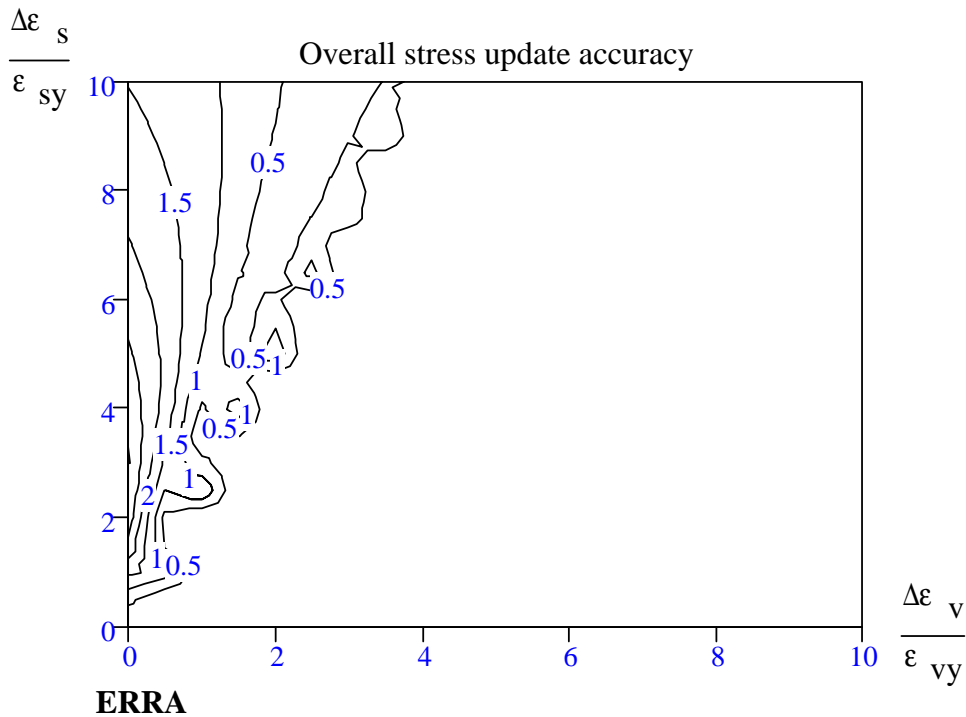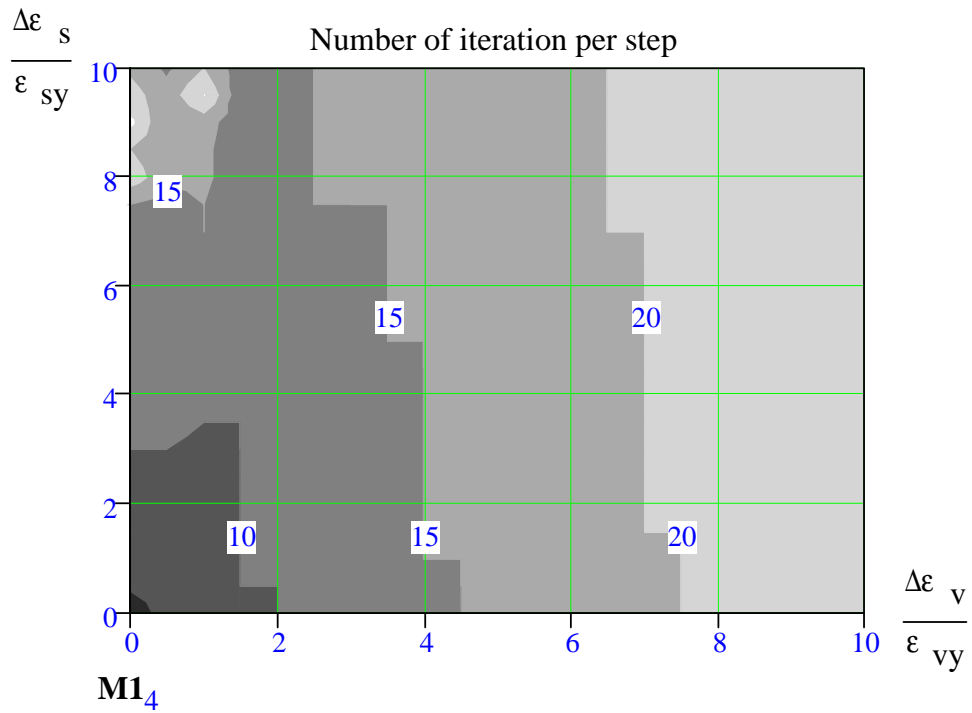Figure 11.22 Iteration number by single step for initial stress on slope 2M/3

11.3 References

1 Ortiz, M. & Popov, E.P., Accuracy and stability of integration algorithms for elastoplastic constitutive relations, Int. J. Num. Meth. Engrg., Vol. 21, No. 9, pp. 1561- 1576, 1985
2 Ortiz, M. & Simo, J.C., An analysis of a new class of integration algorithms for elastoplastic constitutive relations, Int. J. Num. Meth. Engrg., Vol. 23, No. 3, pp. 353- 366, 1986
3 Simo, J.C. and Taylor, R.L., A consistent return mapping algorithm for plane strain elastoplasticity, Int. J. Num. Meth. Engrg., Vol. 22, pp. 649-670, 1986
4 Simo, J.C. & Hughes, T.J.R., Computational inelasticity, SPRINGER, 1997

CHAPTER 12
Summary and Discussion

Details of theoretical development contributed in this thesis are developed in each chapter. In generally, the newly-proposed theories are summarized as following.

12.1 Generalized form of the Sekiguchi-Ohta model

The new form of the Sekiguchi-Ohta model shown in Eq.(12.1) is proposed in terms of the current stress-hardening parameter instead of using a strain-hardening parameter as employed in the original model. The new form is proven to satisfy objectivity by referring to the current state of stress tensor and the current state of hardening stress tensor. The expression is consisted of three stress invariants and two material parameters.

Stress invariants employed are those of the first invariant of stress tensor (I_1), the first invariant of hardening stress tensor (I_{c1}) and the joint second invariant between stress and hardening stress tensors $\bar{J}_2$. It is found that the anisotropic feature of the model is due to the contribution of $\bar{J}_2$. Material parameters are the Critical state parameter (M) and dilatancy parameter (D).

$$f(\boldsymbol{\sigma}', \boldsymbol{\sigma}'_c) = f(I_1, \bar{J}_2, I_{c1}) = MD \ln\left(\frac{I_1}{I_{c1}}\right) + D \frac{3\sqrt{3\bar{J}_2}}{I_1} \tag{12.1}$$

where

$$\mathbf{1} = \delta_{ij}\mathbf{e}_i \otimes \mathbf{e}_j, \quad \mathbf{I} = \frac{1}{2}\left[\delta_{ik}\delta_{jl} + \delta_{il}\delta_{jk}\right]\mathbf{e}_i \otimes \mathbf{e}_j \otimes \mathbf{e}_k \otimes \mathbf{e}_l, \quad \mathbf{A} = \mathbf{I} - \frac{1}{3}(\mathbf{1} \otimes \mathbf{1}) \qquad (12.2), (12.3), (12.4)$$

$$I_1 = 3p' = \boldsymbol{\sigma}':\mathbf{1}, \quad I_{c1} = 3p'_c = \boldsymbol{\sigma}'_c:\mathbf{1}, \quad \mathbf{s}_c = \mathbf{A}:\boldsymbol{\sigma}'_c \qquad (12.5), (12.6), (12.7)$$

$$\boldsymbol{\eta}_c = \frac{\mathbf{s}_c}{p'_c}, \quad \bar{\mathbf{s}} = \left[\mathbf{A} - \frac{1}{3}\boldsymbol{\eta}_c \otimes \mathbf{1}\right]:\boldsymbol{\sigma}', \quad \bar{J}_2 = \frac{1}{2}\bar{\mathbf{s}}:\bar{\mathbf{s}} \qquad (12.8), (12.9), (12.10)$$

12.2 Stiffness matrix considering the corner of the SO model

Eq.(12.11) shows the stiffness matrix for the particular case of K_o-condition or at-rest condition where the current stress is positioned at the current stress hardening, or in other words, the stress in located in the corner of the SO model. The stiffness matrix using an implementation from single yield surface would lead to an erroneous solution.

The particular stiffness matrix is developed on Koiter's associated flow rule. As a result, the model can give a reasonable feature under loading and unloading during K_o-condition. This development settles the strongest argument of the model and interprets the physical meaning of the corner in yield surface.

$$\mathbf{c}^{ep}* = (1-\Lambda)K\mathbf{1} \otimes \mathbf{1} + \sqrt{\frac{2}{3}}(1-\Lambda)\eta_o K\mathbf{n}_c \otimes \mathbf{1} + 2G\left[\mathbf{A} - \mathbf{n}_c \otimes \mathbf{n}_c\right] \tag{12.11}$$

where

$$\bar{\kappa} = \frac{\kappa}{1+e_o}, \quad \bar{\lambda} = \frac{\lambda}{1+e_o}, \quad \Lambda = 1 - \frac{\kappa}{\lambda} \qquad (12.12), (12.13), (12.14)$$

$$K = \frac{p'}{\bar{\kappa}}, \quad G = \mu'K, \quad \mu' = \frac{3(1-2\nu')}{2(1+\nu')} \qquad (12.15), (12.16), (12.17)$$

$$\eta_o = \frac{3(1-K_o)}{1+2K_o}, \quad \mathbf{n}_c = \frac{\mathbf{s}_c}{\|\mathbf{s}_c\|} \qquad (12.18), (12.19)$$

12.3 K_o-value in regard to the SO model

In corresponding to the interpretation of 1-D K_o consolidation phenomenon, Eq.(12.20) reveals the theoretical K_o expression based on the SO model. This simple expression can predict K_o value close to a correlation generally used in soil mechanics. By this result, K_o expression indicated by the SO model can give more reasonable K_o value better than those of specified by other Critical state models. Moreover, Poisson's ratio can be designated to have a relation with friction angle of soil material as shown in Eq.(12.21).

$$K_o = \frac{15 - \sqrt{9 + 16M^2}}{6 + 2\sqrt{9 + 16M^2}} \tag{12.20}$$

$$\nu' = \frac{K_o}{1+K_o} = \frac{9\sqrt{9+16M^2} - 8M^2 - 27}{9\sqrt{9+16M^2} + 8M^2 - 27} \tag{12.21}$$

12.4 Update algorithm in regard to the SO model

For a prescribed strain increment, the algorithm for evaluating stress, stress-hardening parameter, elastic and plastic strains based on Backward-Euler difference scheme are provided by procedural steps listed below. A current loading step is denoted by subscript n+1 while a previous loading step is denoted by subscript n. Because solution of this non-linear system is obtained by Newton method, the loop of calculations is performed iteratively using superscript (k) as iteration number. When the variables at iteration (k+1) and (k) are not been changed much far from an acceptable tolerance, the calculation is terminated. Finally, all variables in Gauss point level are updated.

1. Input $\Delta\boldsymbol{\varepsilon},\boldsymbol{\sigma}'_{n},\boldsymbol{\sigma}'_{cn},\boldsymbol{\varepsilon}_{n},\boldsymbol{\varepsilon}^{e}_{n},\boldsymbol{\varepsilon}^{p}_{n}$

2. Set $k=0$, $\Delta\gamma^{(k)}_{n+1}=0$

$$\boldsymbol{\varepsilon}_{n+1}=\boldsymbol{\varepsilon}_{n}+\Delta\boldsymbol{\varepsilon},\quad \boldsymbol{\varepsilon}^{\mathrm{e}(k)}_{n+1}=\boldsymbol{\varepsilon}^{e}_{n}+\Delta\boldsymbol{\varepsilon}+\delta\boldsymbol{\varepsilon}^{\mathrm{p}(k+1)}_{n+1}$$

$$\delta\boldsymbol{\varepsilon}^{\mathrm{p}(k)}_{n+1}=\mathbf{0},\quad \boldsymbol{\varepsilon}^{\mathrm{p}(k)}_{n+1}=\boldsymbol{\varepsilon}^{p}_{n}+\delta\boldsymbol{\varepsilon}^{\mathrm{p}(k)}_{n+1}$$

3. Predict $\boldsymbol{\sigma}'^{(k)}_{n+1}=\boldsymbol{\sigma}'(\boldsymbol{\varepsilon}^{e(k)}_{n+1})$, $\boldsymbol{\sigma}'^{(k)}_{cn+1}=\boldsymbol{\sigma}'(\boldsymbol{\varepsilon}^{e(k)}_{n+1})$

4. Check $f^{(k)}_{n+1}=f\left(\boldsymbol{\sigma}'(\boldsymbol{\varepsilon}^{e(k)}_{n+1}),\boldsymbol{\sigma}'_{c}(\boldsymbol{\varepsilon}^{e(k)}_{n+1})\right)$

$$\overline{\mathbf{r}}^{(k)}_{n+1}=\boldsymbol{\varepsilon}^{e}_{n+1}-\boldsymbol{\varepsilon}^{e}_{n}-\Delta\boldsymbol{\varepsilon}+\Delta\gamma_{n+1}\partial_{\boldsymbol{\sigma}}f_{n+1}\Big|^{(k)}$$

If $f^{(k)}_{n+1}<TOL_{1}$ and $\left\|\overline{\mathbf{r}}^{(k)}_{n+1}\right\|<TOL_{2}$ then

Set $(\bullet)_{n+1}=(\bullet)^{(k)}_{n+1}$ and Goto 9

5. Compute $\boldsymbol{\Xi}^{(k)}_{n+1}=\left[\tilde{\mathbf{c}}^{e^{-1}}+\Delta\gamma\partial^{2}_{\boldsymbol{\sigma}'\boldsymbol{\sigma}'}f\right]^{-1}\Big|^{(k)}_{n+1}$

6. Correct $\delta\Delta\gamma^{(k)}_{n+1}=\dfrac{f-\left(\partial_{\boldsymbol{\sigma}'}f+\dfrac{1}{3\tilde{K}}\mathbf{1}\right):\left\{\boldsymbol{\Xi}:\overline{\mathbf{r}}\right\}\Big|^{(k)}}{\left\{\partial_{\boldsymbol{\sigma}'}f+\dfrac{1}{3\tilde{K}}\mathbf{1}\right\}:\left\{\boldsymbol{\Xi}:\partial_{\boldsymbol{\sigma}'}f\right\}\Big|_{n+1}}$

$$\delta\boldsymbol{\varepsilon}^{\mathrm{e}(k)}_{n+1}=-\tilde{\mathbf{c}}_{e}^{-1}:\boldsymbol{\Xi}:\left\{\overline{\mathbf{r}}+\partial_{\boldsymbol{\sigma}'}f\delta\Delta\gamma\right\}\Big|^{(k)}_{n+1}$$

7. Update $\begin{Bmatrix}\boldsymbol{\varepsilon}^{e}\\\Delta\gamma\end{Bmatrix}^{(k+1)}_{n+1}=\begin{Bmatrix}\boldsymbol{\varepsilon}^{e}\\\Delta\gamma\end{Bmatrix}^{(k)}_{n+1}+\begin{Bmatrix}\delta\boldsymbol{\varepsilon}^{e}\\\delta\Delta\gamma\end{Bmatrix}^{(k)}_{n+1}$

$$\delta\boldsymbol{\varepsilon}^{\mathrm{p}(k+1)}_{n+1}=\boldsymbol{\varepsilon}^{e}_{n}+\Delta\boldsymbol{\varepsilon}-\boldsymbol{\varepsilon}^{\mathrm{e}(k+1)}_{n+1}$$

$$\boldsymbol{\varepsilon}^{\mathrm{p}(k+1)}_{n+1}=\boldsymbol{\varepsilon}^{p}_{n}+\delta\boldsymbol{\varepsilon}^{\mathrm{p}(k+1)}_{n+1}$$

8. Set $k\leftarrow k+1$ Goto 3

9. Output $\boldsymbol{\sigma}'_{n+1},\boldsymbol{\sigma}'_{cn+1},\boldsymbol{\varepsilon}_{n+1},\boldsymbol{\varepsilon}^{e}_{n+1},\boldsymbol{\varepsilon}^{p}_{n+1},\Delta\gamma_{n+1}$ and Exit

where

$$\Delta\varepsilon^{e}_{v}=\left\{\boldsymbol{\varepsilon}^{e}_{n+1}-\boldsymbol{\varepsilon}^{e}_{n}\right\}:\mathbf{1},\quad p'_{n+1}=p'_{n}\exp\left(\frac{\Delta\varepsilon^{e}_{v}}{\bar{\kappa}}\right),\quad \Delta p'=p'_{n+1}-p'_{n} \qquad (12.22),\ (12.23),\ (12.24)$$

$$\Delta\boldsymbol{\varepsilon}^{e}_{d}=\boldsymbol{\varepsilon}^{e}_{d_{n+1}}-\boldsymbol{\varepsilon}^{e}_{d_{n}}=\mathbf{A}:\left\{\boldsymbol{\varepsilon}^{e}_{n+1}-\boldsymbol{\varepsilon}^{e}_{n}\right\} \qquad (12.25)$$

$$\mathbf{s}_{n+1}=\mathbf{s}_{n}+2\tilde{G}\Delta\boldsymbol{\varepsilon}^{e}_{d} \qquad (12.26)$$

$$\boldsymbol{\sigma}'_{n+1}=p'_{n+1}\mathbf{1}+\mathbf{s}_{n+1} \qquad (12.27)$$

$$\tilde{K}=\frac{\Delta p'}{\Delta\varepsilon^{e}_{v}}\ \text{in which}\ \lim_{\Delta\varepsilon^{e}_{v}\to o}\tilde{K}=\frac{p'_{n}}{\bar{\kappa}} \qquad (12.28),\ (12.29)$$

$$\tilde{G}=\mu'\tilde{K} \qquad (12.30)$$

$$\tilde{\mathbf{c}}^{e}=\tilde{K}\mathbf{1}\otimes\mathbf{1}+2\tilde{G}\mathbf{A} \qquad (12.31)$$

$$\Delta\varepsilon^{p}_{v}=\Delta\varepsilon_{v}-\Delta\varepsilon^{e}_{v} \qquad (12.32)$$

$$p'_{cn+1} = p'_{cn} \exp\left(\frac{\Delta \varepsilon_v^p}{MD}\right) \tag{12.33}$$

$$\boldsymbol{\sigma}'_{cn+1} = p'_{cn+1}\{\mathbf{1} + \boldsymbol{\eta_c}\} \tag{12.34}$$

12.5 Consistent tangential moduli in regard to the SO model

The current stress, hardening variable and consistency parameter determined by update algorithm is used to calculate the consistent tangential moduli as shown in Eq.(12.35).

$$\tilde{\mathbf{c}}^{ep(k)}_{n+1} = \tilde{\mathbf{c}}^{ep}(\boldsymbol{\sigma}^{(k)}_{n+1}, \boldsymbol{\sigma}'^{(k)}_{cn+1}, \Delta\gamma^{(k)}_{n+1}) = \left[\tilde{\mathbf{c}}^{e-1} + \frac{\partial_{\boldsymbol{\sigma}'}f \otimes \partial_{\boldsymbol{\sigma}'}f}{\mathbf{1}:\partial_{\boldsymbol{\sigma}'}f} + \Delta\gamma\left[\mathbf{I} - \frac{\partial_{\boldsymbol{\sigma}'}f \otimes \mathbf{1}}{\mathbf{1}:\partial_{\boldsymbol{\sigma}'}f}\right]:\partial^2_{\boldsymbol{\sigma}'\boldsymbol{\sigma}'}f\right]^{(k)\,-1}_{n+1} \tag{12.35}$$

It is noted that there is no plastic material parameter, i.e., M (critical state parameter), D (dilatancy parameter) in the expression because they are contained in Eq.(12.1). That is, the consistent tangential moduli shown in Eq.(12.35) is matched with the form of yield function shown in Eq.(12.1). In other words, if the yield function is alternatively expressed by $M\ln\left(\dfrac{I_1}{I_{c1}}\right) + \dfrac{3\sqrt{3\bar{J}_2}}{I_1}$ or $\dfrac{MI_1}{3}\ln\left(\dfrac{I_1}{I_{c1}}\right) + \sqrt{3\bar{J}_2}$, then the corresponding consistent tangential moduli would be different with that appeared in Eq.(12.35). The consistent tangential is employed in local stiffness matrix of each element as shown in Eq.(12.36). The global stiffness matrix is the summation of whole local stiffness matrix as shown in Eq.(12.37).

$$\mathbf{k}^{(k)}_{en+1} = \int_{\Omega^e} \mathbf{B}_e^T \tilde{\mathbf{c}}^{ep(k)}_{n+1}\mathbf{B}_e d\Omega^e \tag{12.36}$$

$$\mathbf{K}^{(k)}_{n+1} = \overset{ne}{\underset{e=1}{\mathrm{A}}} \mathbf{k}^{(k)}_{en+1} \tag{12.37}$$

12.6 Exact form of the consistent tangential tensor in regard to the SO model

The consistent tangent moduli shown in Eq.(12.35) is initially expressed in form of compliance consistent format. The tensorial expression in Eq.(12.38) is expressed by 10 components of forth-order tensor. The forth-order tensor bases are given in Eq.(12.50) and their corresponding coefficients are given in Eq. (12.49).

$$\tilde{\mathbf{c}}^{ep-1} = \sum_{i=1}^{10} u_i \mathbf{T}_i \tag{12.38}$$

$$u_1 = \frac{1}{9K} + \frac{D\beta}{9p'} \tag{12.39}$$

$$u_2 = \frac{1}{2G} + \frac{3D}{2p'\bar{q}}\Delta\gamma \tag{12.40}$$

$$u_3 = \frac{D}{\sqrt{6}p'} \tag{12.41}$$

$$u_4 = \frac{D}{\sqrt{6}p'} + \frac{D}{\sqrt{6}\beta p'}\left(\frac{\left(2\beta - 3M + \dfrac{\bar{q}}{p'}\right)}{p'} - \frac{M\left(\beta - M + \dfrac{3}{2M}(\boldsymbol{\eta}_c : \boldsymbol{\eta}_c)\right)}{\bar{q}}\right)\Delta\gamma \tag{12.42}$$

$$u_5 = \frac{3D}{2\beta p'} - \frac{3D}{2\beta p'}\frac{\left(M - 2\dfrac{\bar{q}}{p'}\right)}{\bar{q}}\Delta\gamma \tag{12.43}$$

$$u_6 = 0 \tag{12.44}$$

$$u_7 = -\frac{D}{2p'\bar{q}}\Delta\gamma \tag{12.45}$$

$$u_8 = \frac{3\sqrt{6}D}{4\beta p'\bar{q}}\Delta\gamma \tag{12.46}$$

$$u_9 = 0 \tag{12.47}$$

$$u_{10} = 0 \tag{12.48}$$

$$\mathbf{u} = \{u_1 \quad u_2 \quad u_3 \quad u_4 \quad u_5 \quad u_6 \quad u_7 \quad u_8 \quad u_9 \quad u_{10}\}^T \tag{12.49}$$

$$\mathbf{T} = \{\mathbf{T}_1 \quad \mathbf{T}_2 \quad \mathbf{T}_3 \quad \mathbf{T}_4 \quad \mathbf{T}_5 \quad \mathbf{T}_6 \quad \mathbf{T}_7 \quad \mathbf{T}_8 \quad \mathbf{T}_9 \quad \mathbf{T}_{10}\}$$
$$= \{\mathbf{1} \otimes \mathbf{1} \quad \mathbf{A} \quad \mathbf{1} \otimes \overline{\mathbf{n}} \quad \overline{\mathbf{n}} \otimes \mathbf{1} \quad \overline{\mathbf{n}} \otimes \overline{\mathbf{n}} \quad \mathbf{1} \otimes \boldsymbol{\eta}_c \quad \boldsymbol{\eta}_c \otimes \mathbf{1} \quad \overline{\mathbf{n}} \otimes \boldsymbol{\eta}_c \quad \boldsymbol{\eta}_c \otimes \overline{\mathbf{n}} \quad \boldsymbol{\eta}_c \otimes \boldsymbol{\eta}_c\} \tag{12.50}$$

where

$$\beta = M - \frac{\overline{q}}{p'} - \sqrt{\frac{3}{2}} (\boldsymbol{\eta}_c : \overline{\mathbf{n}}), \quad \overline{q} = \sqrt{3\overline{J}_2}, \quad \overline{\mathbf{n}} = \frac{\overline{\mathbf{s}}}{\|\overline{\mathbf{s}}\|} \tag{12.51), (12.52), (12.53}$$

However, the explicit expression of the consistent tangential tensor can be obtained by Eq.(12.54) with the same forth-order tensor bases but different material coefficients. The material coefficients are calculated by means of inversed linear mapping which are presented in Eq.(12.55)-(12.56). By explicitly determined form of the consistent tangential tensor using this technique, the computation time is dreadfully reduced in compare with using implicit one which is needed to be inversed at run-time level.

$$\tilde{\mathbf{c}}^{ep} = \sum_{i=1}^{10} v_i \mathbf{T}_i \tag{12.54}$$

$$\mathbf{v} = \begin{Bmatrix} v_1 \\ v_2 \\ v_3 \\ v_4 \\ v_5 \\ v_6 \\ v_7 \\ v_8 \\ v_9 \\ v_{10} \end{Bmatrix} = \frac{1}{D_v} \begin{Bmatrix} \frac{1}{9}(u_2 + u_5 + \overline{\mathbf{n}} : \boldsymbol{\eta}_c u_8)u_2 \\[2mm] \frac{1}{u_2} D_v \\[2mm] \frac{1}{3}\left(-u_2 u_3 + \overline{\mathbf{n}} : \boldsymbol{\eta}_c u_5 u_6 - \overline{\mathbf{n}} : \boldsymbol{\eta}_c u_3 u_8\right) \\[2mm] \frac{1}{3}\left(-u_2 u_4 + \overline{\mathbf{n}} : \boldsymbol{\eta}_c u_5 u_7 + \boldsymbol{\eta}_c : \boldsymbol{\eta}_c u_7 u_8\right) \\[2mm] \dfrac{-u_1 u_2 u_5 + u_2 u_3 u_4 + \boldsymbol{\eta}_c : \boldsymbol{\eta}_c u_3 u_7 u_8 + \boldsymbol{\eta}_c : \boldsymbol{\eta}_c u_5 u_6 u_7}{u_2} \\[2mm] \frac{1}{3}\left(-u_2 u_6 - u_5 u_6 + u_3 u_8\right) \\[2mm] -\frac{1}{3}\left(u_2 + u_5 + \overline{\mathbf{n}} : \boldsymbol{\eta}_c u_8\right)u_7 \\[2mm] \dfrac{-u_2 u_8 u_1 + u_2 u_4 u_6 - \overline{\mathbf{n}} : \boldsymbol{\eta}_c u_5 u_6 u_7 + \overline{\mathbf{n}} : \boldsymbol{\eta}_c u_3 u_7 u_8}{u_2} \\[2mm] \left(u_2 u_3 - \overline{\mathbf{n}} : \boldsymbol{\eta}_c u_5 u_6 + \overline{\mathbf{n}} : \boldsymbol{\eta}_c u_3 u_8\right)\dfrac{u_7}{u_2} \\[2mm] -\left(-u_2 u_6 - u_5 u_6 + u_3 u_8\right)\dfrac{u_7}{u_2} \end{Bmatrix} \tag{12.55}$$

$$D_v = -\left(\overline{\mathbf{n}} : \boldsymbol{\eta}_c\right)^2 u_3 u_7 u_8 + \left(\overline{\mathbf{n}} : \boldsymbol{\eta}_c\right)^2 u_5 u_6 u_7 - \overline{\mathbf{n}} : \boldsymbol{\eta}_c u_2 u_3 u_7 + \overline{\mathbf{n}} : \boldsymbol{\eta}_c u_1 u_2 u_8 - \overline{\mathbf{n}} : \boldsymbol{\eta}_c u_2 u_4 u_6$$
$$+ \boldsymbol{\eta}_c : \boldsymbol{\eta}_c u_3 u_7 u_8 - u_2 u_3 u_4 - \boldsymbol{\eta}_c : \boldsymbol{\eta}_c u_5 u_6 u_7 - \boldsymbol{\eta}_c : \boldsymbol{\eta}_c u_2 u_6 u_7 + u_1 u_2 u_5 + u_2^2 u_1 \tag{12.56}$$

Return-mapping method shows a good performance for coarse or large increment steps. The adequate accuracy can be obtained even a single step solution. Though, return-mapping method needs many updated steps, these tasks are carried out in local matrix, not in the global matrix. And global convergence due to Newton method meets quadratic rate due to the consistent tangential tensor. As a result, there is a promising sign of applying the method in large-scale computation like those of 3-dimensional numerical application, finite deformation and soil dynamic where efficient update procedure is necessary to reduce computational time but with high accuracy and stability.

Thus, this dissertation provides the basis for the unfolded areas for applying the Sekiguchi-Ohta model in higher rank of numerical analyses.

APPENDICES

Appendix A: Tensor analysis

A-1 The forth-order deviatoric tensor

The forth-order deviatoric tensor is defined by,

$$\mathbf{A} = \mathbf{I} - \left[\frac{1}{3} (\mathbf{1} \otimes \mathbf{1}) \right] \tag{A.1}$$

where its component is shown by,

$$A_{ijkl} = \frac{1}{2} \left[\delta_{ik} \delta_{jl} + \delta_{il} \delta_{jk} \right] - \frac{1}{3} \delta_{ij} \delta_{kl} \tag{A.2}$$

A symmetric property can be checked by

$$\mathbf{A}^T = \mathbf{I}^T - \left[\frac{1}{3} (\mathbf{1} \otimes \mathbf{1}) \right]^T = \mathbf{I} - \left[\frac{1}{3} (\mathbf{1}^T \otimes \mathbf{1}^T) \right] = \mathbf{I} - \left[\frac{1}{3} (\mathbf{1} \otimes \mathbf{1}) \right] = \mathbf{A} \tag{A.3}$$

A deviatoric projection of a second-order stress tensor is given by

$$\mathbf{A} : \boldsymbol{\sigma} = \left[\mathbf{I} - \frac{1}{3} (\mathbf{1} \otimes \mathbf{1}) \right] : \boldsymbol{\sigma} = \boldsymbol{\sigma} - \frac{1}{3} (\mathbf{1} : \boldsymbol{\sigma}) \mathbf{1} = \mathbf{s} \tag{A.4}$$

A double product with a second-order isotropic tensor

$$\mathbf{A} : \mathbf{1} = \left[\mathbf{I} - \frac{1}{3} (\mathbf{1} \otimes \mathbf{1}) \right] : \mathbf{1} = \mathbf{I} : \mathbf{1} - \frac{1}{3} (\mathbf{1} \otimes \mathbf{1}) : \mathbf{1}$$

$$= \mathbf{1} - \frac{1}{3} (\mathbf{1} : \mathbf{1}) : \mathbf{1} = \mathbf{1} - \frac{1}{3} (3) : \mathbf{1} = \mathbf{1} - \mathbf{1} = \mathbf{0} \tag{A.5}$$

A double product with a forth-order deviatoric tensor

$$\mathbf{A} : \mathbf{A} = \left[\mathbf{I} - \frac{1}{3} (\mathbf{1} \otimes \mathbf{1}) \right] : \left[\mathbf{I} - \frac{1}{3} (\mathbf{1} \otimes \mathbf{1}) \right]$$

$$= \mathbf{I} : \mathbf{I} - \frac{1}{3} \mathbf{I} : (\mathbf{1} \otimes \mathbf{1}) - \frac{1}{3} (\mathbf{1} \otimes \mathbf{1}) : \mathbf{I} + \frac{1}{9} (\mathbf{1} \otimes \mathbf{1}) : (\mathbf{1} \otimes \mathbf{1})$$

$$= \mathbf{I} - \frac{1}{3} (\mathbf{1} \otimes \mathbf{1}) - \frac{1}{3} \mathbf{I}^T : (\mathbf{1} \otimes \mathbf{1}) + \frac{1}{3} (\mathbf{1} \otimes \mathbf{1})$$

$$= \mathbf{I} - \frac{1}{3} (\mathbf{1} \otimes \mathbf{1}) - \frac{1}{3} \mathbf{I} : (\mathbf{1} \otimes \mathbf{1}) + \frac{1}{3} (\mathbf{1} \otimes \mathbf{1})$$

$$= \mathbf{I} - \frac{1}{3} (\mathbf{1} \otimes \mathbf{1}) - \frac{1}{3} (\mathbf{1} \otimes \mathbf{1}) + \frac{1}{3} (\mathbf{1} \otimes \mathbf{1}) = \mathbf{I} - \frac{1}{3} (\mathbf{1} \otimes \mathbf{1}) = \mathbf{A} \tag{A.6}$$

A double product with a second-order stress deviator

$$\mathbf{A} : \mathbf{s} = \mathbf{A} : (\mathbf{A} : \boldsymbol{\sigma}) = (\mathbf{A} : \mathbf{A}) : \boldsymbol{\sigma} = \mathbf{A} : \boldsymbol{\sigma} = \mathbf{s} \tag{A.7}$$

$$\mathbf{A} : \boldsymbol{\eta}_c = \mathbf{A} : \frac{\mathbf{s}_c}{p'_c} = \frac{1}{p'_c} \mathbf{A} : \mathbf{s}_c = \frac{\mathbf{s}_c}{p'_c} = \boldsymbol{\eta}_c \tag{A.8}$$

A double product with a forth-order identity tensor

$$\mathbf{A} : \mathbf{I} = \left[\mathbf{I} - \frac{1}{3} (\mathbf{1} \otimes \mathbf{1}) \right] : \mathbf{I} = \mathbf{I} : \mathbf{I} - \frac{1}{3} \mathbf{I} : (\mathbf{1} \otimes \mathbf{1}) = \mathbf{I} - \frac{1}{3} (\mathbf{1} \otimes \mathbf{1}) = \mathbf{A} \tag{A.9}$$

A-2 The forth-order anisotropically deviatoric tensor

The forth-order anisotropic tensor is defined by,

$$\bar{\mathbf{A}} = \mathbf{A} - \frac{1}{3} [\mathbf{1} \otimes \boldsymbol{\eta}_c + \boldsymbol{\eta}_c \otimes \mathbf{1}] + \frac{1}{9} (\boldsymbol{\eta}_c : \boldsymbol{\eta}_c) \mathbf{1} \otimes \mathbf{1} \tag{A.10}$$

A symmetric property can be checked by

$$\bar{\mathbf{A}}^T = \mathbf{A}^T - \frac{1}{3} [\mathbf{1} \otimes \boldsymbol{\eta}_c + \boldsymbol{\eta}_c \otimes \mathbf{1}]^T + \frac{1}{9} (\boldsymbol{\eta}_c : \boldsymbol{\eta}_c) [\mathbf{1} \otimes \mathbf{1}]^T$$

$$= \mathbf{A} - \frac{1}{3} [\boldsymbol{\eta}_c \otimes \mathbf{1} + \mathbf{1} \otimes \boldsymbol{\eta}_c]^T + \frac{1}{9} (\boldsymbol{\eta}_c : \boldsymbol{\eta}_c) \mathbf{1} \otimes \mathbf{1} = \bar{\mathbf{A}} \tag{A.11}$$

A double product with a second-order isotropic tensor

$$\overline{\mathbf{A}}:\mathbf{1} = \mathbf{A}:\mathbf{1} - \frac{1}{3}[\mathbf{1}\otimes\boldsymbol{\eta}_c + \boldsymbol{\eta}_c\otimes\mathbf{1}]:\mathbf{1} + \frac{1}{9}(\boldsymbol{\eta}_c:\boldsymbol{\eta}_c)[\mathbf{1}\otimes\mathbf{1}]:\mathbf{1}$$

$$= \mathbf{0} - \frac{1}{3}\{3\boldsymbol{\eta}_c\} + \frac{1}{3}(\boldsymbol{\eta}_c:\boldsymbol{\eta}_c)\mathbf{1} = -\boldsymbol{\eta}_c + \frac{1}{3}(\boldsymbol{\eta}_c:\boldsymbol{\eta}_c)\mathbf{1} \tag{A.12}$$

$$= -\left[\mathbf{A} - \frac{1}{3}\mathbf{1}\otimes\boldsymbol{\eta}_c\right]:\boldsymbol{\eta}_c$$

A double product with a second-order anisotropic stress ratio

$$\overline{\mathbf{A}}:\boldsymbol{\eta}_c = \mathbf{A}:\boldsymbol{\eta}_c - \frac{1}{3}[\mathbf{1}\otimes\boldsymbol{\eta}_c + \boldsymbol{\eta}_c\otimes\mathbf{1}]:\boldsymbol{\eta}_c + \frac{1}{9}(\boldsymbol{\eta}_c:\boldsymbol{\eta}_c)[\mathbf{1}\otimes\mathbf{1}]:\boldsymbol{\eta}_c$$

$$= \boldsymbol{\eta}_c - \frac{1}{3}(\boldsymbol{\eta}_c:\boldsymbol{\eta}_c)\mathbf{1} \tag{A.13}$$

$$= \left[\mathbf{A} - \frac{1}{3}\mathbf{1}\otimes\boldsymbol{\eta}_c\right]:\boldsymbol{\eta}_c$$

An anisotropic projection of a second-order stress tensor is given by

$$\overline{\mathbf{A}}:\boldsymbol{\sigma} = \overline{\mathbf{A}}:\left\{p'\{\mathbf{1}+\boldsymbol{\eta}_c\} + \overline{\mathbf{s}}\right\}$$

$$= \left\{\overline{\mathbf{A}}:p'\{\mathbf{1}+\boldsymbol{\eta}_c\} + \overline{\mathbf{A}}:\overline{\mathbf{s}}\right\} \tag{A.14}$$

$$= \overline{\mathbf{A}}:\overline{\mathbf{s}}$$

A-3 Directional derivative of a norm of second-order stress deviator
For a given second-order tensor, a norm associated with a scalar product is

$$\|\mathbf{s}\| = \sqrt{\mathbf{s}:\mathbf{s}} \tag{A.15}$$

A square of Eq.(A.15) is,

$$\|\mathbf{s}\|^2 = \mathbf{s}:\mathbf{s} \tag{A.16}$$

The derivative of Eq.(A.16) with respect to $\mathbf{s}$ is,

$$2\|\mathbf{s}\|\frac{\partial\|\mathbf{s}\|}{\partial\mathbf{s}} = \mathbf{s}:\mathbf{I} + \mathbf{s}:\mathbf{I} = 2\mathbf{s} \tag{A.17}$$

For a non-zero s tensor, Eq.(A.17) gives Eq.(A.18) where $\mathbf{n}$ is a unit normal of deviator $\mathbf{s}$

$$\frac{\partial\|\mathbf{s}\|}{\partial\mathbf{s}} = \frac{\mathbf{s}}{\|\mathbf{s}\|} = \mathbf{n} \tag{A.18}$$

A-4 Derivative of a unit normal field of second-order stress deviator
A unit normal field for a given second-order tensor $\mathbf{s}$ is defined by

$$\mathbf{n} = \frac{\mathbf{s}}{\|\mathbf{s}\|} \tag{A.19}$$

A derivative of $\mathbf{n}$ with respect to $\mathbf{s}$ can be given by

$$\frac{\partial\mathbf{n}}{\partial\mathbf{s}} = \frac{1}{\|\mathbf{s}\|}\frac{\partial\mathbf{s}}{\partial\mathbf{s}} + \mathbf{s}\otimes\frac{\partial\|\mathbf{s}\|^{-1}}{\partial\mathbf{s}} = \frac{1}{\|\mathbf{s}\|}\mathbf{I} - \frac{\mathbf{s}}{\|\mathbf{s}\|^2}\otimes\frac{\partial\|\mathbf{s}\|}{\partial\mathbf{s}} \tag{A.20}$$

Substitute Eq.(A.18) into Eq.(A.20), obtain

$$\frac{\partial\mathbf{n}}{\partial\mathbf{s}} = \frac{1}{\|\mathbf{s}\|}\mathbf{I} - \frac{1}{\|\mathbf{s}\|^2}\mathbf{s}\otimes\mathbf{n} = \frac{1}{\|\mathbf{s}\|}\mathbf{I} - \frac{1}{\|\mathbf{s}\|}\mathbf{n}\otimes\mathbf{n} = \frac{1}{\|\mathbf{s}\|}(\mathbf{I} - \mathbf{n}\otimes\mathbf{n}) \tag{A.21}$$

A-5 Relation between a norm of second-order tensor and the second invariant
The second invariant of stress is expressed by

$$J_2 = \frac{1}{2}\mathbf{s}:\mathbf{s} \tag{A.22}$$

According to Eq.(A.16), Eq.(A.22) can be rewritten as,

$$J_2 = \frac{1}{2}\|\mathbf{s}\|^2 \quad \text{or} \quad \|\mathbf{s}\| = \sqrt{2J_2} \tag{A.23}$$

According to Eqs.(A.19), (A.23), $\mathbf{s}$ can be given by,

$$\mathbf{s} = \|\mathbf{s}\|\mathbf{n} = \sqrt{2J_2}\,\mathbf{n} \tag{A.24}$$

Appendix B: Sekiguchi-Ohta plasticity

B-1 Generalized Sekiguchi-Ohta model

Without losing the generality, the SO yield/potential function can be expressed in convex format based on three invariants by

$$f(I_1, \bar{J}_2, I_{c1}) = MD\ln\left(\frac{I_1}{I_{c1}}\right) + D\frac{3\sqrt{3\bar{J}_2}}{I_1} \tag{B.1}$$

The partial derivatives with respect to these invariants are shown below

$$\frac{\partial f}{\partial I_1} = \frac{D}{I_1}\left(M - 3\frac{\sqrt{3\bar{J}_2}}{I_1}\right) \tag{B.2}$$

$$\frac{\partial f}{\partial \bar{J}_2} = \frac{9D}{2\sqrt{3\bar{J}_2}I_1} \tag{B.3}$$

$$\frac{\partial f}{\partial I_{c1}} = -\frac{MD}{I_{c1}} \tag{B.4}$$

B-2 Cartesian coordinate system in principal stress space

Relation between Cartesian coordinates system in principal stress space is expressed by using transformation tensor Q.

$$\mathbf{x} = \mathbf{Q}\cdot\boldsymbol{\sigma}' \tag{B.5}$$

$$\text{where} \quad \mathbf{Q} = \begin{bmatrix} 0 & \frac{-1}{\sqrt{2}} & \frac{1}{\sqrt{2}} \\ \sqrt{\frac{2}{3}} & \frac{-1}{\sqrt{6}} & \frac{-1}{\sqrt{6}} \\ \frac{1}{\sqrt{3}} & \frac{1}{\sqrt{3}} & \frac{1}{\sqrt{3}} \end{bmatrix}, \quad \boldsymbol{\sigma}' = \begin{pmatrix} \sigma'_1 \\ \sigma'_2 \\ \sigma'_3 \end{pmatrix}, \quad \mathbf{x} = \begin{pmatrix} x_1 \\ x_2 \\ x_3 \end{pmatrix} \tag{B.6}$$

x_3-axis is coincided with hydrostatic pressure axis and the principal mean stress is marked by,

$$x_3 = \sqrt{3}p' \tag{B.7}$$

Substitute Eq.(B.7) into Eq.(B.5) and solve for the arbitrary stress,

$$\boldsymbol{\sigma}' = \mathbf{Q}^T\cdot\mathbf{x} \tag{B.8}$$

The locus of yield surface intersecting with a constant mean stress can be obtained by substituting Eq.(B.8) into the yield function. Consequently, the SO yield functions can be expressed by,

$$f(\boldsymbol{\sigma}', p'_c) = MD\ln\left(\frac{p'}{p'_c}\right) + D\sqrt{\frac{3x_2^2 - 2\sqrt{6}x_2\eta_o p' + 2\eta_o^2 p'^2 + 3x_1^2}{p'^2}} = 0 \tag{B.9}$$

Rearrange Eq.(B.9) to a particular form below

$$x_1^2 + \left(x_2 - \frac{2}{\sqrt{6}}\eta_o p'\right)^2 = \left(\frac{2M}{\sqrt{6}}\ln\left(\frac{p'}{p'_c}\right)p'\right)^2 \tag{B.10}$$

Transform Eq.(B.10) to a polar coordinate system by introducing

$$R = \frac{2M}{\sqrt{6}}\ln\left(\frac{p'}{p'_c}\right)p', \quad x_1 = R\sin\omega, \quad x_2 = R\cos\omega + \frac{2}{\sqrt{6}}\eta_o p' \tag{B.11}, \text{ (B.12), (B.13)}$$

where $\omega \in [0, 2\pi]$, $p' \in (0, p'_c]$

B-3 Evaluation of normalized deviatoric stress at the corner of yield surface

Consolidation stress kept at the corner of the SO yield surface for t=0 can be expressed by

$$\boldsymbol{\sigma}'_c = \sigma'_{vc}\, diag[K_o \quad 1 \quad K_o] \tag{B.14}$$

where σ'_{vc} is a vertical direction component of the consolidation stress history

Mean stress, stress deviator, normalized stress deviator, deviatoric stress and unit normal for consolidation stress $\boldsymbol{\sigma}'_c$ are given below respectively,

$$p'_c = \frac{1}{3}(\mathbf{1}:\boldsymbol{\sigma}'_c) = \frac{1}{3}(1+2K_o)\sigma'_{vc} \tag{B.15}$$

$$\mathbf{s}_c = \boldsymbol{\sigma}'_c - p'_c \mathbf{1} = (1 - K_o)\sigma'_{vc} \, diag\left[-\frac{1}{3} \quad \frac{2}{3} \quad -\frac{1}{3} \right] \tag{B.16}$$

$$\boldsymbol{\eta}_c = \frac{\mathbf{s}_c}{p'_c} = 3\frac{1-K_o}{1+2K_o} \, diag\left[-\frac{1}{3} \quad \frac{2}{3} \quad -\frac{1}{3} \right] \tag{B.17}$$

$$q_c = \sqrt{\frac{3}{2}} \|\mathbf{s}_c\| = (1 - K_o)\sigma'_{vc} \tag{B.18}$$

$$\mathbf{n}_c = \frac{\mathbf{s}_c}{\|\mathbf{s}_c\|} = diag\left[-\frac{\sqrt{6}}{6} \quad \frac{\sqrt{6}}{3} \quad -\frac{\sqrt{6}}{6} \right] \tag{B.19}$$

According to Eq.(B.15)-(B.19), $\boldsymbol{\sigma'}_c$ can be represented by,

$$\boldsymbol{\sigma}'_c = p'_c \mathbf{1} + \mathbf{s}_c = p'_c \{\mathbf{1} + \boldsymbol{\eta}_c\} = p'_c \left\{ \mathbf{1} + \sqrt{\frac{2}{3}}\eta_o \mathbf{n}_c \right\} \tag{B.20}$$

Since there is no consideration of rotational hardening in the study, the subsequent normalized stress ratio is kept constant as η_o. The initial normalized stress ratio η_o mutually has a relation with a coefficient of earth pressure at rest K_o as shown in Eq.(B.22).

$$\frac{q_c}{p'_c} = \frac{q_o}{p'_o} = \eta_o \tag{B.21}$$

$$\eta_o = 3\frac{1-K_o}{1+2K_o} \Leftrightarrow K_o = \frac{3-\eta_o}{2\eta_o + 3} \tag{B.22}$$

Using Eq.(B.17) and (B.22), an anisotropic second-order tensor $\boldsymbol{\eta_c}$ can be written in form of a unit normal defined in Eq.(B.19) and η_o

$$\boldsymbol{\eta}_c = \sqrt{\frac{2}{3}}\frac{q_c}{p'_c}\mathbf{n}_c = \sqrt{\frac{2}{3}}\eta_o \, diag\left[-\frac{\sqrt{6}}{6} \quad \frac{\sqrt{6}}{3} \quad -\frac{\sqrt{6}}{6} \right] \tag{B.23}$$

Some scalar products of $\boldsymbol{\eta_c}$ and its unit normal are shown below.

$$\boldsymbol{\eta}_c : \boldsymbol{\eta}_c = \frac{2}{3}\eta_o^2, \qquad \boldsymbol{\eta}_c : \mathbf{n}_c = \frac{\sqrt{6}}{3}\eta_o \tag{B.24},(B.25)$$

By expression, though Eq.(B.26) equals to Eq.(B.17), it should be regarded in mind that it does not equal in sense of frame indifferent. $\boldsymbol{\eta}_o$ is referred to orientation at t=0 while $\boldsymbol{\eta}_c$ is referred to orientation at current time and marked under material configuration.

$$\boldsymbol{\eta}_o = 3\frac{1-K_o}{1+2K_o} \, diag\left[-\frac{1}{3} \quad \frac{2}{3} \quad -\frac{1}{3} \right] \tag{B.26}$$

B-4 Derivative of an anisotropic tensor

A derivative of $\boldsymbol{\eta}_c$ with respect to $\boldsymbol{\sigma'}_c$ can be given by

$$\frac{\partial \boldsymbol{\eta}_c}{\partial \boldsymbol{\sigma}'_c} = \frac{\partial\left\{ \dfrac{\mathbf{s}_c}{p'_c} \right\}}{\partial \boldsymbol{\sigma}'_c} = \frac{1}{p'_c}\frac{\partial \mathbf{s}_c}{\partial \boldsymbol{\sigma}'_c} + \mathbf{s}_c \otimes \frac{\partial p'^{-1}_c}{\partial \boldsymbol{\sigma}'_c} = \frac{1}{p'_c}\mathbf{A} - \frac{1}{p'^2_c}\mathbf{s}_c \otimes \frac{\partial p'_c}{\partial \boldsymbol{\sigma}'_c}$$

$$= \frac{1}{p'_c}\mathbf{A} - \frac{1}{3p'^2_c}\mathbf{s}_c \otimes \mathbf{1} = \frac{1}{p'_c}\left[\mathbf{A} - \frac{\mathbf{s}_c}{3p'_c} \otimes \mathbf{1} \right] \tag{B.27}$$

$$= \frac{1}{p'_c}\left[\mathbf{A} - \frac{1}{3}\boldsymbol{\eta}_c \otimes \mathbf{1} \right]$$

B-5 Gradient of a joint invariant with respect to stress tensor

$$\overline{\mathbf{s}} = \mathbf{s} - p'\boldsymbol{\eta}_c = \mathbf{A} : \boldsymbol{\sigma}' - \frac{1}{3}(\mathbf{1} : \boldsymbol{\sigma}')\boldsymbol{\eta}_c = \left[\mathbf{A} - \frac{1}{3}\boldsymbol{\eta}_c \otimes \mathbf{1} \right] : \boldsymbol{\sigma}' \tag{B.28}$$

$$\overline{J}_2 = \frac{1}{2}\overline{\mathbf{s}} : \overline{\mathbf{s}} \tag{B.29}$$

By Chain's rule and definition of a joint invariant defined in Eq. (B.28)-(B.29)

$$\frac{\partial \overline{J}_2}{\partial \boldsymbol{\sigma}'} = \frac{\partial \overline{J}_2}{\partial \overline{\mathbf{s}}} : \frac{\partial \overline{\mathbf{s}}}{\partial \boldsymbol{\sigma}'} \tag{B.30}$$

where $\dfrac{\partial \bar{J}_2}{\partial \bar{\mathbf{s}}} = \bar{\mathbf{s}}$, $\dfrac{\partial \bar{\mathbf{s}}}{\partial \boldsymbol{\sigma}'} = \dfrac{\partial}{\partial \boldsymbol{\sigma}'}\left\{ \mathbf{s} - \dfrac{1}{3}(\mathbf{1}:\boldsymbol{\sigma}')\,\boldsymbol{\eta}_c \right\} = \mathbf{A} - \dfrac{1}{3}\boldsymbol{\eta}_c \otimes \mathbf{1}$ 　(B.31),(B.32)

$$\frac{\partial \bar{J}_2}{\partial \boldsymbol{\sigma}'} = \bar{\mathbf{s}} : \left[\mathbf{A} - \frac{1}{3}\boldsymbol{\eta}_c \otimes \mathbf{1} \right] = \left[\mathbf{A} - \frac{1}{3}\boldsymbol{\eta}_c \otimes \mathbf{1} \right]^T : \bar{\mathbf{s}} = \left[\mathbf{A}^T - \frac{1}{3}\mathbf{1} \otimes \boldsymbol{\eta}_c \right] : \bar{\mathbf{s}}$$ 　(B.33)

Substitute Eq.(B.28) into Eq.(B.33)

$$\frac{\partial \bar{J}_2}{\partial \boldsymbol{\sigma}'} = \left[\mathbf{A} - \frac{1}{3}\mathbf{1} \otimes \boldsymbol{\eta}_c \right] : \left[\mathbf{A} - \frac{1}{3}\boldsymbol{\eta}_c \otimes \mathbf{1} \right] : \boldsymbol{\sigma}' = \bar{\mathbf{A}} : \boldsymbol{\sigma}'$$ 　(B.34)

where $\bar{\mathbf{A}} = \mathbf{A} - \dfrac{1}{3}\left[\mathbf{1} \otimes \boldsymbol{\eta}_c + \boldsymbol{\eta}_c \otimes \mathbf{1} \right] + \dfrac{1}{9}(\boldsymbol{\eta}_c : \boldsymbol{\eta}_c)\,\mathbf{1} \otimes \mathbf{1}$ 　(B.35)

A scalar product of $\boldsymbol{\eta}_c$ is shown in Eq.(B.24)

Alternatively, Eq.(B.33) can be expanded by $\sqrt{2J_2}\,\mathbf{n}$

$$\frac{\partial \bar{J}_2}{\partial \boldsymbol{\sigma}'} = \left[\mathbf{A} - \frac{1}{3}\mathbf{1} \otimes \boldsymbol{\eta}_c \right] : \bar{\mathbf{s}} = \left[\mathbf{A} - \frac{1}{3}\mathbf{1} \otimes \boldsymbol{\eta}_c \right] : \sqrt{2\bar{J}_2}\,\bar{\mathbf{n}}$$
$$= \sqrt{2\bar{J}_2}\left[\bar{\mathbf{n}} - \frac{1}{3}(\boldsymbol{\eta}_c : \bar{\mathbf{n}})\,\mathbf{1} \right]$$ 　(B.36)

B-6 Gradient of a joint invariant with respect to hardening stress tensor

Refer to Eq.(B.29) and (B.31)

$$\frac{\partial \bar{J}_2}{\partial \boldsymbol{\sigma}'_c} = \frac{\partial \bar{J}_2}{\partial \bar{\mathbf{s}}} : \frac{\partial \bar{\mathbf{s}}}{\partial \boldsymbol{\sigma}'_c} = \bar{\mathbf{s}} : \frac{\partial \bar{\mathbf{s}}}{\partial \boldsymbol{\sigma}'_c}$$ 　(B.37)

According to Eq.(B.28)

$$\frac{\partial \bar{\mathbf{s}}}{\partial \boldsymbol{\sigma}'_c} = \frac{\partial}{\partial \boldsymbol{\sigma}'_c}\left\{ \mathbf{s} - p'\boldsymbol{\eta}_c \right\} = -p'\frac{\partial \boldsymbol{\eta}_c}{\partial \boldsymbol{\sigma}'_c}$$ 　(B.38)

Substitute Eq.(B.27) into (B.38)

$$\frac{\partial \bar{\mathbf{s}}}{\partial \boldsymbol{\sigma}'_c} = -\frac{p'}{p'_c}\left[\mathbf{A} - \frac{1}{3}\boldsymbol{\eta}_c \otimes \mathbf{1} \right] = -\frac{I_1}{I_{c1}}\left[\mathbf{A} - \frac{1}{3}\boldsymbol{\eta}_c \otimes \mathbf{1} \right]$$ 　(B.39)

Substitute Eq.(B.39) into (B.37)

$$\frac{\partial \bar{J}_2}{\partial \boldsymbol{\sigma}'_c} = -\bar{\mathbf{s}} : \frac{p'}{p'_c}\left[\mathbf{A} - \frac{1}{3}\boldsymbol{\eta}_c \otimes \mathbf{1} \right] = -\frac{I_1\sqrt{2\bar{J}_2}}{I_{c1}}\left[\mathbf{A} - \frac{1}{3}\mathbf{1} \otimes \boldsymbol{\eta}_c \right] : \bar{\mathbf{n}}$$
$$= -\frac{I_1\sqrt{2\bar{J}_2}}{I_{c1}}\left[\bar{\mathbf{n}} - \frac{1}{3}(\boldsymbol{\eta}_c : \bar{\mathbf{n}})\,\mathbf{1} \right]$$ 　(B.40)

In short, $\dfrac{\partial \bar{J}_2}{\partial \boldsymbol{\sigma}'_c} = -\dfrac{p'}{p'_c}\left[\mathbf{A} - \dfrac{1}{3}\boldsymbol{\eta}_c \otimes \mathbf{1} \right]^T : \left[\mathbf{A} - \dfrac{1}{3}\boldsymbol{\eta}_c \otimes \mathbf{1} \right] : \boldsymbol{\sigma}' = -\dfrac{I_1}{I_{c1}}\bar{\mathbf{A}} : \boldsymbol{\sigma}'$ 　(B.41)

It is noted that in regard to isotropic hardening generally applied in the SO model, though $\boldsymbol{\eta}_c$ is kept as constant as its initial value $\boldsymbol{\eta}_o$, the second-order tensor as defined in Eq.(B.17), the derivative shown in Eq.(B.41) does not become zero tensor.

$$\frac{\partial \bar{J}_2}{\partial \boldsymbol{\sigma}'_c} \neq \mathbf{0} \quad \text{but} \quad \frac{\partial \bar{J}_2}{\partial \boldsymbol{\sigma}'_o} = \mathbf{0}$$ 　(B.42)

B-7 First derivatives of the Sekiguchi-Ohta yield function with respect to stress tensor

By chain rule, the derivative can be written in terms of stress invariants

$$\frac{\partial f(I_1, \bar{J}_2, I_{c1})}{\partial \boldsymbol{\sigma}'} = \frac{\partial f}{\partial I_1}\frac{\partial I_1}{\partial \boldsymbol{\sigma}'} + \frac{\partial f}{\partial \bar{J}_2}\frac{\partial \bar{J}_2}{\partial \boldsymbol{\sigma}'} + \frac{\partial f}{\partial I_{c1}}\frac{\partial I_{c1}}{\partial \boldsymbol{\sigma}'}$$ 　(B.43)

where $\dfrac{\partial I_1}{\partial \boldsymbol{\sigma}'} = \dfrac{\partial(\mathbf{1}:\boldsymbol{\sigma}')}{\partial \boldsymbol{\sigma}'} = \mathbf{1} : \dfrac{\partial \boldsymbol{\sigma}'}{\partial \boldsymbol{\sigma}'} = \mathbf{1}$ 　(B.44)

$\dfrac{\partial \bar{J}_2}{\partial \boldsymbol{\sigma}'} = \bar{\mathbf{A}} : \boldsymbol{\sigma}' = \sqrt{2\bar{J}_2}\left[\bar{\mathbf{n}} - \dfrac{1}{3}(\boldsymbol{\eta}_c : \bar{\mathbf{n}})\,\mathbf{1} \right]$ 　(See Appendix B-5) 　(B.45)

$\dfrac{\partial I_{c1}}{\partial \boldsymbol{\sigma}'} = \dfrac{\partial(\mathbf{1}:\boldsymbol{\sigma}'_c)}{\partial \boldsymbol{\sigma}'} = \mathbf{1} : \dfrac{\partial \boldsymbol{\sigma}'_c}{\partial \boldsymbol{\sigma}'} = \mathbf{0}$ 　(B.46)

Substitute Eq.(B.44),(B.45) and (B.46) into Eq.(B.43), obtain

$$\frac{\partial f}{\partial \boldsymbol{\sigma}'} = \frac{\partial f}{\partial I_1}\mathbf{1} + \frac{\partial f}{\partial \bar{J}_2}\bar{\mathbf{A}}:\boldsymbol{\sigma}' = \frac{\partial f}{\partial I_1}\frac{(\mathbf{1}:\boldsymbol{\sigma}')}{I_1}\mathbf{1} + \frac{\partial f}{\partial \bar{J}_2}\bar{\mathbf{A}}:\boldsymbol{\sigma}' = \left(\frac{\partial f}{\partial I_1}\frac{\mathbf{1}\otimes\mathbf{1}}{I_1} + \frac{\partial f}{\partial \bar{J}_2}\bar{\mathbf{A}}\right):\boldsymbol{\sigma}' \tag{B.47}$$

Alternative form of Eq.(B.47) can be given by

$$\frac{\partial f}{\partial \boldsymbol{\sigma}'} = \frac{\partial f}{\partial I_1}\mathbf{1} + \frac{\partial f}{\partial \bar{J}_2}\sqrt{2\bar{J}_2}\left[\bar{\mathbf{n}} - \frac{1}{3}(\boldsymbol{\eta}_c:\bar{\mathbf{n}})\mathbf{1}\right]$$

$$= \left(\frac{\partial f}{\partial I_1} - \sqrt{2\bar{J}_2}\frac{\partial f}{\partial \bar{J}_2}\frac{1}{3}(\boldsymbol{\eta}_c:\bar{\mathbf{n}})\right)\mathbf{1} + \sqrt{2\bar{J}_2}\frac{\partial f}{\partial \bar{J}_2}\bar{\mathbf{n}} \tag{B.48}$$

where $\quad \bar{\mathbf{n}} = \dfrac{\bar{\mathbf{s}}}{\sqrt{\bar{\mathbf{s}}:\bar{\mathbf{s}}}} = \dfrac{\bar{\mathbf{s}}}{\sqrt{2\bar{J}_2}}$, $\quad \dfrac{\partial f}{\partial I_1} = \dfrac{D}{I_1}\left(M - 3\dfrac{\sqrt{3\bar{J}_2}}{I_1}\right)$, $\quad \sqrt{2\bar{J}_2}\dfrac{\partial f}{\partial \bar{J}_2} = \sqrt{\dfrac{3}{2}}\dfrac{3D}{I_1}$ $\tag{B.49}$

In compacted from, Eq.(B.48) can be expressed as,

$$\frac{\partial f}{\partial \boldsymbol{\sigma}'} = r_1\mathbf{1} + r_2\bar{\mathbf{n}} \tag{B.50}$$

$$r_1 = \left(\frac{\partial f}{\partial I_1} - \sqrt{2\bar{J}_2}\frac{\partial f}{\partial \bar{J}_2}\frac{1}{3}(\boldsymbol{\eta}_c:\bar{\mathbf{n}})\right) \tag{B.51}$$

$$r_2 = \sqrt{2\bar{J}_2}\frac{\partial f}{\partial \bar{J}_2} \tag{B.52}$$

B-8 First derivatives of the Sekiguchi-Ohta yield function with respect to hardening stress tensor

By chain rule, the derivative can be written in terms of stress invariants

$$\frac{\partial f(I_1, \bar{J}_2, I_{c1})}{\partial \boldsymbol{\sigma}'_c} = \frac{\partial f}{\partial I_1}\frac{\partial I_1}{\partial \boldsymbol{\sigma}'_c} + \frac{\partial f}{\partial \bar{J}_2}\frac{\partial \bar{J}_2}{\partial \boldsymbol{\sigma}'_c} + \frac{\partial f}{\partial I_{c1}}\frac{\partial I_{c1}}{\partial \boldsymbol{\sigma}'_c} \tag{B.53}$$

where $\quad \dfrac{\partial I_1}{\partial \boldsymbol{\sigma}'_c} = \dfrac{\partial (\mathbf{1}:\boldsymbol{\sigma}')}{\partial \boldsymbol{\sigma}'_c} = \mathbf{0}$ $\tag{B.54}$

$$\frac{\partial \bar{J}_2}{\partial \boldsymbol{\sigma}'_c} = -\bar{\mathbf{s}}:\frac{p'}{p'_c}\left[\mathbf{A} - \frac{1}{3}\boldsymbol{\eta}_c\otimes\mathbf{1}\right] = -\frac{I_1}{I_{c1}}\bar{\mathbf{A}}:\boldsymbol{\sigma}' \quad \text{(See Appendix B-6)} \tag{B.55}$$

$$\frac{\partial I_{c1}}{\partial \boldsymbol{\sigma}'_c} = \frac{\partial (\mathbf{1}:\boldsymbol{\sigma}'_c)}{\partial \boldsymbol{\sigma}'_c} = \mathbf{1} \tag{B.56}$$

Substitute Eq.(B.54),(B.55) and (B.56) into (B.53), obtain

$$\frac{\partial f}{\partial \boldsymbol{\sigma}'_c} = -\frac{\partial f}{\partial \bar{J}_2}\frac{I_1}{I_{c1}}\bar{\mathbf{A}}:\boldsymbol{\sigma}' + \frac{\partial f}{\partial I_{c1}}\mathbf{1} \tag{B.57}$$

In alternative form,

$$\frac{\partial f}{\partial \boldsymbol{\sigma}'_c} = -\frac{\partial f}{\partial \bar{J}_2}\bar{\mathbf{s}}:\frac{p'}{p'_c}\left[\mathbf{A} - \frac{1}{3}\boldsymbol{\eta}_c\otimes\mathbf{1}\right] + \frac{\partial f}{\partial I_{c1}}\mathbf{1}$$

$$= -\frac{\partial f}{\partial \bar{J}_2}\left[\mathbf{A} - \frac{1}{3}\mathbf{1}\otimes\boldsymbol{\eta}_c\right]:\bar{\mathbf{s}}\frac{I_1}{I_{c1}} + \frac{\partial f}{\partial I_{c1}}\mathbf{1}$$

$$= -\frac{\partial f}{\partial \bar{J}_2}\left[\bar{\mathbf{s}} - \frac{1}{3}(\boldsymbol{\eta}_c:\bar{\mathbf{s}})\mathbf{1}\right]\frac{I_1}{I_{c1}} + \frac{\partial f}{\partial I_{c1}}\mathbf{1} \tag{B.58}$$

$$= -\sqrt{2\bar{J}_2}\frac{\partial f}{\partial \bar{J}_2}\left[\bar{\mathbf{n}} - \frac{1}{3}(\boldsymbol{\eta}_c:\bar{\mathbf{n}})\mathbf{1}\right]\frac{I_1}{I_{c1}} + \frac{\partial f}{\partial I_{c1}}\mathbf{1}$$

$$= \left[\frac{\partial f}{\partial I_{c1}} + \frac{I_1}{I_{c1}}\sqrt{2\bar{J}_2}\frac{\partial f}{\partial \bar{J}_2}\frac{1}{3}(\boldsymbol{\eta}_c:\bar{\mathbf{n}})\right]\mathbf{1} - \frac{I_1}{I_{c1}}\sqrt{2\bar{J}_2}\frac{\partial f}{\partial \bar{J}_2}\bar{\mathbf{n}}$$

where $\quad \dfrac{\partial f}{\partial I_{c1}} = -\dfrac{MD}{I_{c1}}$

In compacted form Eq.(B.58) can be reduced as,

$$\frac{\partial f}{\partial \boldsymbol{\sigma}'_c} = s_1\mathbf{1} + s_2\bar{\mathbf{n}}$$

where $s_1 = \dfrac{\partial f}{\partial I_{c1}} + \dfrac{I_1}{3I_{c1}}\sqrt{2\overline{J}_2}\,\dfrac{\partial f}{\partial \overline{J}_2}(\boldsymbol{\eta}_c : \overline{\mathbf{n}})$ (B.59)

$s_2 = -\dfrac{I_1}{I_{c1}}\sqrt{2\overline{J}_2}\,\dfrac{\partial f}{\partial \overline{J}_2}$ (B.60)

B-9 Evolution of hardening parameters

$\varepsilon_v^p = \dfrac{\lambda - \kappa}{1+e_o}\ln\left(\dfrac{p'_c}{p'_o}\right) = MD\ln\left(\dfrac{p'_c}{p'_o}\right)$ (B.61)

Volumetric strain rate can be obtained by taking a time derivative on Eq.(B.61)

$\dot{\varepsilon}_v^p = MD\dfrac{\dot{p}'_c}{p'_c}$ (B.62)

Rate of plastic flow and volumetric plastic strain are obtained by flow rule

$\dot{\boldsymbol{\varepsilon}}^p = \gamma\dfrac{\partial f}{\partial \boldsymbol{\sigma}'}, \quad \dot{\varepsilon}_v^p = \gamma\,tr\left(\dfrac{\partial f}{\partial \boldsymbol{\sigma}'}\right)$ (B.63),(B.64)

According to Eq.(B.62) and (B.64), evolution of p'$_c$ is given by

$\dot{p}'_c = \dfrac{p'_c}{MD}\dot{\varepsilon}_v^p = \gamma\dfrac{p'_c}{MD}tr\left(\dfrac{\partial f}{\partial \boldsymbol{\sigma}'}\right)$ (B.65)

In terms of first invariant of $\boldsymbol{\sigma}'_c$

$\dot{I}_{c1} = \gamma\dfrac{I_{c1}}{MD}tr\left(\dfrac{\partial f}{\partial \boldsymbol{\sigma}'}\right)$ (B.66)

Refer to Eq.(B.14), (B.15), the evolution of $\boldsymbol{\sigma}'_c$ can be expressed by

$\dot{\boldsymbol{\sigma}}'_c = \dot{\sigma}'_{vc}\,diag\begin{bmatrix} K_o & 1 & K_o \end{bmatrix} = \dfrac{\dot{I}_{c1}}{I_{c1}}\boldsymbol{\sigma}'_c = \dfrac{\dot{p}'_c}{p'_c}\boldsymbol{\sigma}'_c$ (B.67)

Substitute Eq.(B.66) into (B.67) and write compactly as

$\dot{\boldsymbol{\sigma}}'_c = \dfrac{\gamma}{MD}tr\left(\dfrac{\partial f}{\partial \boldsymbol{\sigma}'}\right)\boldsymbol{\sigma}'_c = \gamma\mathbf{h}$ (B.68)

where $\mathbf{h} = \dfrac{1}{MD}tr\left(\dfrac{\partial f}{\partial \boldsymbol{\sigma}'}\right)\boldsymbol{\sigma}'_c$ (B.69)

According to Eq.(B.15), it is noted that

$\mathbf{1}:\dot{\boldsymbol{\sigma}}'_c = \gamma\mathbf{1}:\mathbf{h} = 3\dot{p}'_c = \dot{I}_{c1}$ (B.70)

For generalized concept, according to Eq.(B.20), the evolution of hardening stress should consider the rotational hardening noted by $\dot{\boldsymbol{\eta}}_c$ in expression given below,

$\dot{\boldsymbol{\sigma}}'_c = \dot{p}'_c\left\{\mathbf{1}+\boldsymbol{\eta}_c\right\} + p'_c\,\dot{\boldsymbol{\eta}}_c$ (B.71)

Therefore, it should be reminded that the derivations of Eqs.(B.67)-(B.70) in this section are merely particularized for $\dot{\boldsymbol{\eta}}_c = \mathbf{0}$. This fact is one of the assumptions intrinsically sustained in the SO model. Consequently, Eqs.(B.72),(B.73) can be followed by,

$\dot{\boldsymbol{\sigma}}'_c = \dot{p}'_c\left\{\mathbf{1}+\boldsymbol{\eta}_c\right\}$ (B.72)

$\dfrac{\partial \boldsymbol{\sigma}'_c}{\partial p'_c} = \mathbf{1}+\boldsymbol{\eta}_c$ (B.73)

B-10 The derivatives of the Sekiguchi-Ohta yield function with respect to virgin K$_o$-consolidation pressure

Derivate of the SO model with respect to p'$_c$ can be given in according to Eqs.(B.50), (B.73), (B.4) as

$$\begin{aligned}
\frac{\partial f}{\partial p'_c} &= \frac{\partial f}{\partial \boldsymbol{\sigma}'_c} : \frac{\partial \boldsymbol{\sigma}'_c}{\partial p'_c} = \left\{s_1\mathbf{1}+s_2\overline{\mathbf{n}}\right\}:\left\{\mathbf{1}+\boldsymbol{\eta}_c\right\} = 3s_1 + s_2\left(\boldsymbol{\eta}_c : \overline{\mathbf{n}}\right) \\
&= 3\frac{\partial f}{\partial I_{c1}} + \frac{I_1}{I_{c1}}\sqrt{2\overline{J}_2}\,\frac{\partial f}{\partial \overline{J}_2}\left(\boldsymbol{\eta}_c : \overline{\mathbf{n}}\right) - \frac{I_1}{I_{c1}}\sqrt{2\overline{J}_2}\,\frac{\partial f}{\partial \overline{J}_2}\left(\boldsymbol{\eta}_c : \overline{\mathbf{n}}\right) \\
&= 3\frac{\partial f}{\partial I_{c1}} = -\frac{3MD}{I_{c1}} = -\frac{MD}{p'_c}
\end{aligned}$$ (B.74)

By short proof:
$$\frac{\partial f}{\partial p'_c} = \frac{\partial f}{\partial I_c} : \frac{\partial I_c}{\partial p'_c} = -\frac{MD}{I_{c1}}3 = -\frac{MD}{p'_c} \tag{B.75}$$

B-11 Consequence of a consistency relation

Requirement for consistency condition is

$$\dot{f} = \frac{\partial f}{\partial \boldsymbol{\sigma}'} : \dot{\boldsymbol{\sigma}}' + \frac{\partial f}{\partial \boldsymbol{\sigma}'_c} : \dot{\boldsymbol{\sigma}}'_c \equiv 0 \tag{B.76}$$

Substitute incremental stress-strain relation and evolution of hardening parameter Eq.(B.68) into Eq.(B.76),

$$\dot{f} = \frac{\partial f}{\partial \boldsymbol{\sigma}'} : \mathbf{c}^e : \left(\dot{\boldsymbol{\varepsilon}} - \gamma \frac{\partial f}{\partial \boldsymbol{\sigma}'} \right) + \frac{\partial f}{\partial \boldsymbol{\sigma}'_c} : \gamma \mathbf{h} \equiv 0 \tag{B.77}$$

Collect for consistency parameter γ and solve for γ

$$\frac{\partial f}{\partial \boldsymbol{\sigma}'} : \mathbf{c}^e : \dot{\boldsymbol{\varepsilon}} - \gamma \left(\frac{\partial f}{\partial \boldsymbol{\sigma}'} : \mathbf{c}^e : \frac{\partial f}{\partial \boldsymbol{\sigma}'} - \frac{\partial f}{\partial \boldsymbol{\sigma}'_c} : \mathbf{h} \right) = 0$$

$$\gamma = \frac{\dfrac{\partial f}{\partial \boldsymbol{\sigma}'} : \mathbf{c}^e : \dot{\boldsymbol{\varepsilon}}}{\dfrac{\partial f}{\partial \boldsymbol{\sigma}'} : \mathbf{c}^e : \dfrac{\partial f}{\partial \boldsymbol{\sigma}'} - \dfrac{\partial f}{\partial \boldsymbol{\sigma}'_c} : \mathbf{h}} = \frac{\dfrac{\partial f}{\partial \boldsymbol{\sigma}'} : \mathbf{c}^e : \dot{\boldsymbol{\varepsilon}}}{H_e + H_p} \tag{B.78}$$

where $H_e = \dfrac{\partial f}{\partial \boldsymbol{\sigma}'} : \mathbf{c}^e : \dfrac{\partial f}{\partial \boldsymbol{\sigma}'}$, $H_p = -\dfrac{\partial f}{\partial \boldsymbol{\sigma}'_c} : \mathbf{h}$, $\mathbf{c}^e = K\mathbf{1} \otimes \mathbf{1} + 2G\mathbf{A}$

Consider a product (double contraction) between $\mathbf{c}^e$ and Eq.(B.48) below

$$\mathbf{c}^e : \frac{\partial f}{\partial \boldsymbol{\sigma}'} = (K\mathbf{1} \otimes \mathbf{1} + 2G\mathbf{A}) : \left(\left(\frac{\partial f}{\partial I_1} - \sqrt{2\overline{J}_2} \frac{\partial f}{\partial \overline{J}_2} \frac{1}{3}(\boldsymbol{\eta}_c : \overline{\mathbf{n}}) \right) \mathbf{1} + \sqrt{2\overline{J}_2} \frac{\partial f}{\partial \overline{J}_2} \overline{\mathbf{n}} \right)$$

$$= 3K \left(\frac{\partial f}{\partial I_1} - \sqrt{2\overline{J}_2} \frac{\partial f}{\partial \overline{J}_2} \frac{1}{3}(\boldsymbol{\eta}_c : \overline{\mathbf{n}}) \right) \mathbf{1} + 2G\sqrt{2\overline{J}_2} \frac{\partial f}{\partial \overline{J}_2} \overline{\mathbf{n}} \tag{B.79}$$

Pre-multiply (double contraction) with Eq.(B.48), elastic modulus H_e can be given by

$$H_e = \frac{\partial f}{\partial \boldsymbol{\sigma}'} : \mathbf{c}^e : \frac{\partial f}{\partial \boldsymbol{\sigma}'} = 9K \left(\frac{\partial f}{\partial I_1} - \sqrt{2\overline{J}_2} \frac{\partial f}{\partial \overline{J}_2} \frac{1}{3}(\boldsymbol{\eta}_o : \overline{\mathbf{n}}) \right)^2 + 2G \left(\sqrt{2\overline{J}_2} \frac{\partial f}{\partial \overline{J}_2} \right)^2 \tag{B.80}$$

Consider plastic modulus H_p by referring to Eq.(B.58) and (B.68)

$$H_p = -\frac{\partial f}{\partial \boldsymbol{\sigma}'_c} : \mathbf{h} = -\left[-\frac{\partial f}{\partial \overline{J}_2} \overline{\mathbf{s}} : \frac{p'}{p'_c} \left[\mathbf{A} - \frac{1}{3}\boldsymbol{\eta}_c \otimes \mathbf{1} \right] + \frac{\partial f}{\partial I_{c1}} \mathbf{1} \right] : \frac{1}{MD} tr \left(\frac{\partial f}{\partial \boldsymbol{\sigma}'} \right) \boldsymbol{\sigma}'_c$$

$$= \frac{\partial f}{\partial \overline{J}_2} \overline{\mathbf{s}} : \frac{p'}{p'_c} \left[\mathbf{A} - \frac{1}{3}\boldsymbol{\eta}_c \otimes \mathbf{1} \right] : \boldsymbol{\sigma}'_c - \frac{\partial f}{\partial I_{c1}} \frac{1}{MD} tr \left(\frac{\partial f}{\partial \boldsymbol{\sigma}'} \right) \mathbf{1} : \boldsymbol{\sigma}'_c$$

$$= \frac{\partial f}{\partial \overline{J}_2} \overline{\mathbf{s}} : \frac{p'}{p'_c} \left[\mathbf{A} : \boldsymbol{\sigma}'_c - \frac{1}{3}(\mathbf{1} : \boldsymbol{\sigma}'_c)\boldsymbol{\eta}_c \right] - \frac{\partial f}{\partial I_{c1}} \frac{I_{c1}}{MD} tr \left(\frac{\partial f}{\partial \boldsymbol{\sigma}'} \right)$$

$$= \frac{\partial f}{\partial \overline{J}_2} \overline{\mathbf{s}} : \frac{p'}{p'_c} \left[\mathbf{s}_c - p'_c \frac{\mathbf{s}_c}{p'_c} \right] - \frac{\partial f}{\partial I_{c1}} \frac{I_{c1}}{MD} tr \left(\frac{\partial f}{\partial \boldsymbol{\sigma}'} \right)$$

$$= -\frac{\partial f}{\partial I_{c1}} \frac{I_{c1}}{MD} tr \left(\frac{\partial f}{\partial \boldsymbol{\sigma}'} \right) = tr \left(\frac{\partial f}{\partial \boldsymbol{\sigma}'} \right) \tag{B.81}$$

where $\dfrac{\partial f}{\partial I_{c1}} = -\dfrac{MD}{I_{c1}}$ (B.82)

Substitute Eq.(B.82) into (B.81), as a result $H_p = tr \left(\dfrac{\partial f}{\partial \boldsymbol{\sigma}'} \right) = \mathbf{1} : \dfrac{\partial f}{\partial \boldsymbol{\sigma}'}$ (B.83)

B-12 Continuum tangential moduli

Incremental stress-strain relation is given by

$$\dot{\boldsymbol{\sigma}}' = \mathbf{c}^e : \dot{\boldsymbol{\varepsilon}}^e = \mathbf{c}^e : \{\dot{\boldsymbol{\varepsilon}} - \dot{\boldsymbol{\varepsilon}}^p\} = \mathbf{c}^e : \left\{ \dot{\boldsymbol{\varepsilon}} - \gamma \frac{\partial f}{\partial \boldsymbol{\sigma}'} \right\} \tag{B.84}$$

Substitute Eq.(B.78) into (B.84), obtain

$$\dot{\boldsymbol{\sigma}}' = \mathbf{c}^e : \left\{ \dot{\boldsymbol{\varepsilon}} - \left(\frac{\dfrac{\partial f}{\partial \boldsymbol{\sigma}'} : \mathbf{c}^e : \dot{\boldsymbol{\varepsilon}}}{H_e + H_p} \right) \frac{\partial f}{\partial \boldsymbol{\sigma}'} \right\} = \left[\mathbf{c}^e - \frac{\mathbf{c}^e : \dfrac{\partial f}{\partial \boldsymbol{\sigma}'} \otimes \dfrac{\partial f}{\partial \boldsymbol{\sigma}'} : \mathbf{c}^e}{H_e + H_p} \right] : \dot{\boldsymbol{\varepsilon}} \tag{B.85}$$

According to Eq.(B.48), isotropic component can be taken by

$$\frac{\partial f}{\partial \boldsymbol{\sigma}'} : \mathbf{1} = 3\frac{D}{I_1}\left(M - 3\frac{\sqrt{3\bar{J}_2}}{I_1} - \sqrt{\frac{3}{2}}\left(\boldsymbol{\eta}_c : \bar{\mathbf{n}} \right) \right) = 3\frac{D}{I_1}\beta \tag{B.86}$$

Introduce the modular ratio β defined by

$$\beta = M - 3\frac{\sqrt{3\bar{J}_2}}{I_1} - \sqrt{\frac{3}{2}}\left(\boldsymbol{\eta}_c : \bar{\mathbf{n}} \right) \tag{B.87}$$

According to Eq.(B.48), deviatoric component can be taken by

$$\mathbf{A} : \frac{\partial f}{\partial \boldsymbol{\sigma}'} = \sqrt{2\bar{J}_2}\frac{\partial f}{\partial \bar{J}_2}\bar{\mathbf{n}} = \sqrt{\frac{3}{2}}\frac{3D}{I_1}\bar{\mathbf{n}} \tag{B.88}$$

Rewrite Eq.(B.79), (B.80) and (B.83) by using Eq.(B.86), (B.87) and (B.88)

$$\mathbf{c}^e : \frac{\partial f}{\partial \boldsymbol{\sigma}'} = 3\frac{D}{I_1}\left(K\beta\mathbf{1} + 2G\sqrt{\frac{3}{2}}\bar{\mathbf{n}} \right) \tag{B.89}$$

$$H_e = \frac{\partial f}{\partial \boldsymbol{\sigma}'} : \mathbf{c}^e : \frac{\partial f}{\partial \boldsymbol{\sigma}'} = \left(3\frac{D}{I_1} \right)^2\left(K\beta^2 + 3G \right) \tag{B.90}$$

$$H_p = \frac{\partial f}{\partial \boldsymbol{\sigma}'} : \mathbf{1} = 3\frac{D}{I_1}\beta \tag{B.91}$$

Continuum tangential moduli can be determined in accordance with Eq.(B.85) as

$$\mathbf{c}^{ep} = \mathbf{c}^e - \frac{\mathbf{c}^e : \dfrac{\partial f}{\partial \boldsymbol{\sigma}'} \otimes \dfrac{\partial f}{\partial \boldsymbol{\sigma}'} : \mathbf{c}^e}{H_e + H_p} \tag{B.92}$$

where $\quad \dfrac{\partial f}{\partial \boldsymbol{\sigma}'} : \mathbf{c}^e = \left\{ \dfrac{\partial f}{\partial \boldsymbol{\sigma}'} : \mathbf{c}^e \right\}^T = 3\dfrac{D}{I_1}\left(K\beta\mathbf{1} + 2G\sqrt{\dfrac{3}{2}}\bar{\mathbf{n}} \right), \qquad H_e + H_p = \left(3\dfrac{D}{I_1} \right)^2\left(K\beta^2 + 3G \right) + 3\dfrac{D}{I_1}\beta$

$$\mathbf{c}^e : \frac{\partial f}{\partial \boldsymbol{\sigma}'} \otimes \frac{\partial f}{\partial \boldsymbol{\sigma}'} : \mathbf{c}^e = \left(3\frac{D}{I_1} \right)^2\left(K\beta\mathbf{1} + \sqrt{6}G\bar{\mathbf{n}} \right) \otimes \left(K\beta\mathbf{1} + \sqrt{6}G\bar{\mathbf{n}} \right)$$

Expand Eq.(B.92) to (B.93) and reduce to Eq.(B.94)

$$\mathbf{c}^{ep} = K\mathbf{1} \otimes \mathbf{1} + 2G\mathbf{A} - \frac{\left(K\beta\mathbf{1} + \sqrt{6}G\bar{\mathbf{n}} \right) \otimes \left(K\beta\mathbf{1} + \sqrt{6}G\bar{\mathbf{n}} \right)}{K\beta^2 + 3G + \dfrac{I_1}{3D}\beta} \tag{B.93}$$

$$\mathbf{c}^{ep} = v_1\mathbf{1} \otimes \mathbf{1} + v_2\mathbf{A} + v_3\mathbf{1} \otimes \bar{\mathbf{n}} + v_4\bar{\mathbf{n}} \otimes \mathbf{1} + v_5\bar{\mathbf{n}} \otimes \bar{\mathbf{n}} \tag{B.94}$$

where $\quad v_1 = \dfrac{3GK + \dfrac{I_1}{3D}K\beta}{K\beta^2 + 3G + \dfrac{I_1}{3D}\beta} = K\dfrac{3DG + p'\beta}{3GD + KD\beta^2 + + p'\beta}, \qquad v_2 = 2G,$

$$v_3 = v_4 = \frac{-\sqrt{6}GK\beta}{K\beta^2 + 3G + \dfrac{I_1}{3D}\beta} = \frac{-\sqrt{6}KDG\beta}{3GD + KD\beta^2 + p'\beta}, \quad v_5 = \frac{-6G^2}{K\beta^2 + 3G + \dfrac{I_1}{3D}\beta} = \frac{-6G^2D}{3GD + KD\beta^2 + p'\beta}$$

B-13 Compliance of continuum tangential moduli

A strain increment is composed of elastic and plastic parts. In relation to compliance stiffness tensor and flow rule, the expression can be presented by

$$\dot{\boldsymbol{\varepsilon}} = \dot{\boldsymbol{\varepsilon}}^e + \dot{\boldsymbol{\varepsilon}}^p = \mathbf{c}^{e-1} : \dot{\boldsymbol{\sigma}}' + \gamma\frac{\partial f}{\partial \boldsymbol{\sigma}'} \tag{B.95}$$

where $\quad \mathbf{c}^{e-1} = \dfrac{1}{9K}\mathbf{1} \otimes \mathbf{1} + \dfrac{1}{2G}\mathbf{A}$ \hfill (B.96)

Substituted by Eq.(B.83), consistency condition in Eq.(B.76) can be shown by

$$\dot{f} = \frac{\partial f}{\partial \boldsymbol{\sigma}'} : \dot{\boldsymbol{\sigma}}' + \frac{\partial f}{\partial \boldsymbol{\sigma}'_c} : \gamma \mathbf{h} = \frac{\partial f}{\partial \boldsymbol{\sigma}'} : \dot{\boldsymbol{\sigma}}' - \gamma H_p \equiv 0 \tag{B.97}$$

From Eq.(B.97), solve for γ

$$\gamma = \frac{1}{H_p} \frac{\partial f}{\partial \boldsymbol{\sigma}'} : \dot{\boldsymbol{\sigma}}' \tag{B.98}$$

Substitute Eq.(B.98) into Eq.(B.95), obtain

$$\dot{\boldsymbol{\varepsilon}} = \mathbf{c}^{e^{-1}} : \dot{\boldsymbol{\sigma}}' + \left(\frac{1}{H_p} \frac{\partial f}{\partial \boldsymbol{\sigma}'} : \dot{\boldsymbol{\sigma}} \right) \frac{\partial f}{\partial \boldsymbol{\sigma}'} = \left[\mathbf{c}^{e^{-1}} + \frac{1}{H_p} \frac{\partial f}{\partial \boldsymbol{\sigma}'} \otimes \frac{\partial f}{\partial \boldsymbol{\sigma}'} \right] : \dot{\boldsymbol{\sigma}} \tag{B.99}$$

According to Eq.(B.48) and (B.87), tensor product below can be reduced by

$$\frac{\partial f}{\partial \boldsymbol{\sigma}'} \otimes \frac{\partial f}{\partial \boldsymbol{\sigma}'} = \left\{ \frac{D}{I_1} \beta \mathbf{1} + \sqrt{\frac{3}{2}} \frac{3D}{I_1} \bar{\mathbf{n}} \right\} \otimes \left\{ \frac{D}{I_1} \beta \mathbf{1} + \sqrt{\frac{3}{2}} \frac{3D}{I_1} \bar{\mathbf{n}} \right\}$$

$$= \left(\frac{D}{I_1} \beta \right)^2 \mathbf{1} \otimes \mathbf{1} + 3\sqrt{\frac{3}{2}} \left(\frac{D}{I_1} \right)^2 \beta [\mathbf{1} \otimes \bar{\mathbf{n}} + \bar{\mathbf{n}} \otimes \mathbf{1}] + \frac{3}{2} \left(\frac{3D}{I_1} \right)^2 \bar{\mathbf{n}} \otimes \bar{\mathbf{n}}$$

As a consequence, the compliance of continuum tangential moduli are given by

$$\mathbf{c}^{ep^{-1}} = \mathbf{c}^{e^{-1}} + \frac{1}{H_p} \frac{\partial f}{\partial \boldsymbol{\sigma}'} \otimes \frac{\partial f}{\partial \boldsymbol{\sigma}'} = \mathbf{c}^{e^{-1}} + \left(\frac{D}{I_1} \right) \left[\frac{\beta}{3} \mathbf{1} \otimes \mathbf{1} + \sqrt{\frac{3}{2}} [\mathbf{1} \otimes \bar{\mathbf{n}} + \bar{\mathbf{n}} \otimes \mathbf{1}] + \frac{9}{2\beta} \bar{\mathbf{n}} \otimes \bar{\mathbf{n}} \right] \tag{B.100}$$

A compacted formulation can be expressed by

$$\mathbf{c}^{ep^{-1}} = u_1 \mathbf{1} \otimes \mathbf{1} + u_2 \mathbf{A} + u_3 \mathbf{1} \otimes \bar{\mathbf{n}} + u_4 \bar{\mathbf{n}} \otimes \mathbf{1} + u_5 \bar{\mathbf{n}} \otimes \bar{\mathbf{n}} \tag{B.101}$$

where $\quad u_1 = \frac{1}{9K} + \frac{D}{I_1} \frac{\beta}{3} = \frac{p' + DK\beta}{9Kp'}$, $\quad u_2 = \frac{1}{2G}$, $\quad u_3 = u_4 = \frac{\sqrt{6}}{6} \frac{D}{p'}$, $\quad u_5 = \frac{3D}{2p'\beta}$

B-14 Isotropic hardening potential

Potential energy defined in regard to isotropic consolidation response is

$$\mathsf{H}(\alpha) = p'_o \left(\bar{\lambda} - \bar{\kappa} \right) \exp(\frac{\alpha}{\bar{\lambda} - \bar{\kappa}}) \tag{B.102}$$

where $\quad \alpha = \varepsilon_v^p$

Stress hardening parameter corresponding to strain hardening parameter α is defined by isotropic hardening law given below,

$$p'_c = \partial_\alpha \mathsf{H}(\alpha) = p'_o \exp(\frac{\alpha}{\bar{\lambda} - \bar{\kappa}}) \tag{B.103}$$

According to an incremental analysis, the step-wised p'_c is practically employed using subscript n to indicate time step, that is,

$$p'_{cn} = \partial_\alpha \mathsf{H}(\alpha_n) = p'_o \exp(\frac{\alpha_n}{\bar{\lambda} - \bar{\kappa}}) \tag{B.104}$$

The alternative isotropic hardening law based on step-wised computation can be obtained by dividing Eq.(B.103) by (B.104),

$$p'_c = p'_{cn} \exp(\frac{\alpha - \alpha_n}{\bar{\lambda} - \bar{\kappa}}) \tag{B.105}$$

Define nonlinear plastic modulus as

$$H(p'_c) = \frac{dp'_c}{d\alpha} = \partial_{\alpha\alpha}^2 \mathsf{H}(\alpha) = \frac{p'_c}{\bar{\lambda} - \bar{\kappa}} \tag{B.106}$$

Rate of change for p'_c is expressed by

$$\dot{p}'_c = H(p'_c)\dot{\alpha} = \frac{p'_c}{\bar{\lambda} - \bar{\kappa}} \dot{\alpha} \tag{B.107}$$

It is noted that

$$\bar{\lambda} - \bar{\kappa} = \frac{\lambda - \kappa}{1 + e_o} = MD \tag{B.108}$$

Appendix C: Ohta-Hata plasticity

C-1 Forms of Ohta-Hata yield function

The Ohta-Hata model is a particular form of the Sekiguchi-Ohta model for the triaxial stress condition. The mathematical point of discontinuity is found due to a turning sign given by an absolute function existed in the expression. Consequently, it is a common discontinuous point for both models. The expression for Ohta-Hata yield function is presented below,

$$f(\boldsymbol{\sigma}',\alpha) \equiv MD\ln\left(\frac{p'}{p_o'}\right) + D\left|\frac{q}{p'} - \eta_o\right| - \alpha = 0 \tag{C.1}$$

where

$$p' = \frac{1}{3}\mathbf{1}:\boldsymbol{\sigma}' = \frac{1}{3}tr(\boldsymbol{\sigma}') = \frac{1}{3}I_1 \tag{C.2}$$

$$q = \sqrt{\frac{3}{2}\mathbf{s}:\mathbf{s}} = \sqrt{\frac{3}{2}tr(\mathbf{s}^2)} = \sqrt{3J_2} \tag{C.3}$$

$$\eta_o = \eta_c = \frac{q_c}{p'_c} = \frac{3\sqrt{3J_{c2}}}{I_{c1}}, \qquad \alpha = \int\dot{\varepsilon}_v^p\,dt \tag{C.4},(C.5)$$

In terms of stress invariants

$$f(I_1, J_2, I_{c1}) \equiv MD\ln\left(\frac{I_1}{I_{c1}}\right) + D\left|\frac{3\sqrt{3J_2}}{I_1} - \frac{3\sqrt{3J_{c2}}}{I_{c1}}\right| = 0 \tag{C.6}$$

The discontinuity caused by absolute sign breaks Eq.(C.6) separately into two continuous functions intersecting at the singular corner. One of function regulates the yield locus on a compression side while another one regulates the yield locus on an extension side. Both yield loci are named simply as upper and lower yield loci given by,

$$f_U(I_1, J_2, I_{c1}) \equiv MD\ln\left(\frac{I_1}{I_{c1}}\right) + D\left(\frac{3\sqrt{3J_2}}{I_1} - \frac{3\sqrt{3J_{c2}}}{I_{c1}}\right) = 0 \tag{C.7}$$

$$f_L(I_1, J_2, I_{c1}) \equiv MD\ln\left(\frac{I_1}{I_{c1}}\right) - D\left(\frac{3\sqrt{3J_2}}{I_1} - \frac{3\sqrt{3J_{c2}}}{I_{c1}}\right) = 0 \tag{C.8}$$

C-2 First derivatives of the upper and lower yield loci with respect to stress tensor

For a smooth surface, the derivative with respect to stress tensor is

$$\frac{\partial f}{\partial\boldsymbol{\sigma}'} = \frac{\partial f}{\partial I_1}\frac{\partial I_1}{\partial\boldsymbol{\sigma}'} + \frac{\partial f}{\partial J_2}\frac{\partial J_2}{\partial\boldsymbol{\sigma}'} = \frac{\partial f}{\partial I_1}\frac{\partial I_1}{\partial\boldsymbol{\sigma}'} + \frac{\partial f}{\partial J_2}\frac{\partial J_2}{\partial\mathbf{s}}:\frac{\partial\mathbf{s}}{\partial\boldsymbol{\sigma}'} \tag{C.9}$$

where

$$\frac{\partial I_1}{\partial\boldsymbol{\sigma}'} = \mathbf{1}, \quad \frac{\partial J_2}{\partial\mathbf{s}} = \mathbf{s}, \quad \frac{\partial\mathbf{s}}{\partial\boldsymbol{\sigma}'} = \mathbf{A}, \quad \frac{\partial J_2}{\partial\boldsymbol{\sigma}'} = \frac{\partial J_2}{\partial\mathbf{s}}:\frac{\partial\mathbf{s}}{\partial\boldsymbol{\sigma}'} = \boldsymbol{\sigma}:\mathbf{A} = \mathbf{A}^T:\boldsymbol{\sigma} = \mathbf{s}$$

As a result, Eq.(C.9) is reduced to

$$\frac{\partial f}{\partial\boldsymbol{\sigma}'} = \frac{\partial f}{\partial I_1}\mathbf{1} + \frac{\partial f}{\partial J_2}\mathbf{s} = \frac{\partial f}{\partial I_1}\mathbf{1} + \sqrt{2J_2}\frac{\partial f}{\partial J_2}\mathbf{n} \tag{C.10}$$

where

$$\mathbf{n} = \frac{\mathbf{s}}{\sqrt{\mathbf{s}:\mathbf{s}}} = \frac{\mathbf{s}}{\sqrt{2J_2}} \tag{C.11}$$

The derivatives of upper and lower yield loci with respect to stress are expressed in terms of stress invariants by (See Appendix C-1)

$$\frac{\partial f_U}{\partial\boldsymbol{\sigma}'} = \frac{\partial f_U}{\partial I_1}\mathbf{1} + \frac{\partial f_U}{\partial J_2}\mathbf{s} = \frac{\partial f_U}{\partial I_1}\mathbf{1} + \sqrt{2J_2}\frac{\partial f_U}{\partial J_2}\mathbf{n} \tag{C.12}$$

$$\frac{\partial f_L}{\partial\boldsymbol{\sigma}'} = \frac{\partial f_L}{\partial I_1}\mathbf{1} + \frac{\partial f_L}{\partial J_2}\mathbf{s} = \frac{\partial f_L}{\partial I_1}\mathbf{1} + \sqrt{2J_2}\frac{\partial f_L}{\partial J_2}\mathbf{n} \tag{C.13}$$

where

$$\frac{\partial f_U}{\partial I_1} = \frac{D}{I_1}\left(M - 3\frac{\sqrt{3J_2}}{I_1}\right), \qquad \sqrt{2J_2}\frac{\partial f_U}{\partial J_2} = \sqrt{\frac{3}{2}}\frac{3D}{I_1} \tag{C.14},(C.15)$$

$$\frac{\partial f_L}{\partial I_1} = \frac{D}{I_1}\left(M + 3\frac{\sqrt{3J_2}}{I_1}\right), \qquad \sqrt{2J_2}\frac{\partial f_L}{\partial J_2} = -\sqrt{\frac{3}{2}}\frac{3D}{I_1} \tag{C.16},(C.17)$$

C-3 Consequence of a consistency relation at the corner

Consistency parameters are determined from consistency conditions subjected on both upper and lower yield loci to ensure both loci are active and activated under loading condition. Equate time derivatives of both upper and lower yield loci to zero and evaluate consistency parameters γ_U and γ_L.

$$\dot{f}_U = \frac{\partial f_U}{\partial \boldsymbol{\sigma}'} : \dot{\boldsymbol{\sigma}}' + \frac{\partial f_U}{\partial p'_c} \dot{p}'_c = 0 \tag{C.18}$$

$$\dot{f}_L = \frac{\partial f_L}{\partial \boldsymbol{\sigma}'} : \dot{\boldsymbol{\sigma}}' + \frac{\partial f_L}{\partial p'_c} \dot{p}'_c = 0 \tag{C.19}$$

The evolution law of isotropic stress hardening parameter is

$$\dot{p}'_c = \frac{p'_c}{MD} \dot{\varepsilon}_v^p \qquad \text{(See also Appendix B-7)} \tag{C.20}$$

The derivatives of upper and lower yield loci respective to p'$_c$ are shown by

$$\frac{\partial f_U}{\partial p'_c} = \frac{\partial f_L}{\partial p'_c} = -\frac{MD}{p'_c} \tag{C.21}$$

Substitute Eq.(C.20)-(C.21) into Eq.(C.18)-(C.19) and using incremental stress-strain relation, obtain the following equations,

$$\dot{f}_U = \frac{\partial f_U}{\partial \boldsymbol{\sigma}'} : \mathbf{c}^e : \left(\dot{\boldsymbol{\varepsilon}} - \dot{\boldsymbol{\varepsilon}}^p \right) - \dot{\boldsymbol{\varepsilon}}^p : \mathbf{1} = 0 \tag{C.22}$$

$$\dot{f}_L = \frac{\partial f_L}{\partial \boldsymbol{\sigma}'} : \mathbf{c}^e : \left(\dot{\boldsymbol{\varepsilon}} - \dot{\boldsymbol{\varepsilon}}^p \right) - \dot{\boldsymbol{\varepsilon}}^p : \mathbf{1} = 0 \tag{C.23}$$

$$\text{where} \qquad \mathbf{c}^e = K \mathbf{1} \otimes \mathbf{1} + 2G\mathbf{A} \tag{C.24}$$

$$K = K(p') = \frac{\Lambda}{MD(1-\Lambda)} p', \quad G = G(p') = \mu' K(p') \tag{C.25),(C.26}$$

$$\Lambda = 1 - \frac{\kappa}{\lambda}, \quad \mu' = \frac{3}{2}\left(\frac{1-2\nu'}{1+\nu'}\right) \tag{C.27),(C.28}$$

Koiter's associated flow rule (See also Chapter 3)

$$\dot{\boldsymbol{\varepsilon}}^p = \gamma_U \frac{\partial f_U}{\partial \boldsymbol{\sigma}'} + \gamma_L \frac{\partial f_L}{\partial \boldsymbol{\sigma}'} \tag{C.29}$$

Rewrite Eq.(C.22) and (C.23) by substituting Koiter's associated flow rule Eq.(C.29)

$$\frac{\partial f_U}{\partial \boldsymbol{\sigma}'} : \mathbf{c}^e : \left(\dot{\boldsymbol{\varepsilon}} - \left(\gamma_U \frac{\partial f_U}{\partial \boldsymbol{\sigma}'} + \gamma_L \frac{\partial f_L}{\partial \boldsymbol{\sigma}'} \right) \right) - \left(\gamma_U \frac{\partial f_U}{\partial \boldsymbol{\sigma}'} + \gamma_L \frac{\partial f_L}{\partial \boldsymbol{\sigma}'} \right) : \mathbf{1} = 0$$

$$\frac{\partial f_L}{\partial \boldsymbol{\sigma}'} : \mathbf{c}^e : \left(\dot{\boldsymbol{\varepsilon}} - \left(\gamma_U \frac{\partial f_U}{\partial \boldsymbol{\sigma}'} + \gamma_L \frac{\partial f_L}{\partial \boldsymbol{\sigma}'} \right) \right) - \left(\gamma_U \frac{\partial f_U}{\partial \boldsymbol{\sigma}'} + \gamma_L \frac{\partial f_L}{\partial \boldsymbol{\sigma}'} \right) : \mathbf{1} = 0$$

And rearrange to the followings,

$$\gamma_U \left(\frac{\partial f_U}{\partial \boldsymbol{\sigma}'} : \mathbf{c}^e : \frac{\partial f_U}{\partial \boldsymbol{\sigma}'} + \frac{\partial f_U}{\partial \boldsymbol{\sigma}'} : \mathbf{1} \right) + \gamma_L \left(\frac{\partial f_U}{\partial \boldsymbol{\sigma}'} : \mathbf{c}^e : \frac{\partial f_L}{\partial \boldsymbol{\sigma}'} + \frac{\partial f_L}{\partial \boldsymbol{\sigma}'} : \mathbf{1} \right) = \frac{\partial f_U}{\partial \boldsymbol{\sigma}'} : \mathbf{c}^e : \dot{\boldsymbol{\varepsilon}}$$

$$\gamma_U \left(\frac{\partial f_L}{\partial \boldsymbol{\sigma}'} : \mathbf{c}^e : \frac{\partial f_U}{\partial \boldsymbol{\sigma}'} + \frac{\partial f_U}{\partial \boldsymbol{\sigma}'} : \mathbf{1} \right) + \gamma_L \left(\frac{\partial f_L}{\partial \boldsymbol{\sigma}'} : \mathbf{c}^e : \frac{\partial f_L}{\partial \boldsymbol{\sigma}'} + \frac{\partial f_L}{\partial \boldsymbol{\sigma}'} : \mathbf{1} \right) = \frac{\partial f_L}{\partial \boldsymbol{\sigma}'} : \mathbf{c}^e : \dot{\boldsymbol{\varepsilon}}$$

Rearrange above equations by collecting consistency parameters and rewrite simply by Eq. (C.30) and (C.31)

$$\gamma_U \left(H_{UU}^e + H_U^p \right) + \gamma_L \left(H_{UL}^e + H_L^p \right) = L_U \tag{C.30}$$

$$\gamma_U \left(H_{LU}^e + H_U^p \right) + \gamma_L \left(H_{LL}^e + H_L^p \right) = L_L \tag{C.31}$$

$$\text{where} \quad L_U = \frac{\partial f_U}{\partial \boldsymbol{\sigma}'} : \mathbf{c}^e : \dot{\boldsymbol{\varepsilon}}, \quad L_L = \frac{\partial f_L}{\partial \boldsymbol{\sigma}'} : \mathbf{c}^e : \dot{\boldsymbol{\varepsilon}} \tag{C.32),(C.33}$$

$$H_{UU}^e = \frac{\partial f_U}{\partial \boldsymbol{\sigma}'} : \mathbf{c}^e : \frac{\partial f_U}{\partial \boldsymbol{\sigma}'}, \quad H_{UL}^e = \frac{\partial f_U}{\partial \boldsymbol{\sigma}'} : \mathbf{c}^e : \frac{\partial f_L}{\partial \boldsymbol{\sigma}'}, \tag{C.34),(C.35}$$

$$H_{LU}^e = \frac{\partial f_L}{\partial \boldsymbol{\sigma}'} : \mathbf{c}^e : \frac{\partial f_U}{\partial \boldsymbol{\sigma}'}, \quad H_{LL}^e = \frac{\partial f_L}{\partial \boldsymbol{\sigma}'} : \mathbf{c}^e : \frac{\partial f_L}{\partial \boldsymbol{\sigma}'}, \tag{C.36),(C.37}$$

$$H_U^p = tr\left(\frac{\partial f_U}{\partial \boldsymbol{\sigma}'} \right), \quad H_L^p = tr\left(\frac{\partial f_L}{\partial \boldsymbol{\sigma}'} \right) \tag{C.38),(C.39}$$

Formulate Eq.(C.30) and (C.31) to linear algebraic system and solved for consistency parameters

$$\begin{pmatrix} \gamma_U \\ \gamma_L \end{pmatrix} = \mathbf{X}^{-1} \cdot \begin{pmatrix} L_U \\ L_L \end{pmatrix} \tag{C.40}$$

where $\mathbf{X} = \begin{bmatrix} H_{UU}^e + H_U^p & H_{UL}^e + H_L^p \\ H_{LU}^e + H_U^p & H_{LL}^e + H_L^p \end{bmatrix}$ is a non-singular [4x4] matrix $\tag{C.41}$

$\mathbf{X}$ is defined as a matrix of coupled-hardening plasticity of the upper and lower yield function.

C-4 Matrix of coupled-hardening plasticity

Double product between forth-order elasticity tensor and gradient of upper and lower yield functions are as following,

$$\mathbf{c}^e : \frac{\partial f_U}{\partial \boldsymbol{\sigma}'} = (K\mathbf{1} \otimes \mathbf{1} + 2G\mathbf{A}) : \left(\frac{\partial f_U}{\partial I_1}\mathbf{1} + \sqrt{2J_2}\frac{\partial f_U}{\partial J_2}\mathbf{n} \right) = 3K\frac{\partial f_U}{\partial I_1}\mathbf{1} + 2G\sqrt{2J_2}\frac{\partial f_U}{\partial J_2}\mathbf{n} \tag{C.42}$$

$$\mathbf{c}^e : \frac{\partial f_L}{\partial \boldsymbol{\sigma}'} = (K\mathbf{1} \otimes \mathbf{1} + 2G\mathbf{A}) : \left(\frac{\partial f_L}{\partial I_1}\mathbf{1} + \sqrt{2J_2}\frac{\partial f_L}{\partial J_2}\mathbf{n} \right) = 3K\frac{\partial f_L}{\partial I_1}\mathbf{1} + 2G\sqrt{2J_2}\frac{\partial f_L}{\partial J_2}\mathbf{n} \tag{C.43}$$

As a result, Eq.(C.34)-(C.37) can be written as,

$$H_{UU}^e = \left(\frac{\partial f_U}{\partial I_1}\mathbf{1} + \sqrt{2J_2}\frac{\partial f_U}{\partial J_2}\mathbf{n} \right) : \left(3K\frac{\partial f_U}{\partial I_1}\mathbf{1} + 2G\sqrt{2J_2}\frac{\partial f_U}{\partial J_2}\mathbf{n} \right)$$

$$= 9K\left(\frac{\partial f_U}{\partial I_1} \right)^2 + 2G\left(\sqrt{2J_2}\frac{\partial f_U}{\partial J_2} \right)^2 \tag{C.44}$$

By the same manner,

$$H_{UL}^e = 9K\frac{\partial f_U}{\partial I_1}\frac{\partial f_L}{\partial I_1} + 2G\left(2J_2 \frac{\partial f_U}{\partial J_2}\frac{\partial f_L}{\partial J_2} \right) \tag{C.45}$$

$$H_{LU}^e = 9K\frac{\partial f_L}{\partial I_1}\frac{\partial f_U}{\partial I_1} + 2G\left(2J_2 \frac{\partial f_L}{\partial J_2}\frac{\partial f_U}{\partial J_2} \right) \tag{C.46}$$

$$H_{LL}^e = 9K\frac{\partial f_L}{\partial I_1}\frac{\partial f_L}{\partial I_1} + 2G\left(2J_2 \frac{\partial f_L}{\partial J_2}\frac{\partial f_L}{\partial J_2} \right) \tag{C.47}$$

Eq.(C.38)-(C.39) can be further reduced as,

$$H_U^p = \frac{\partial f_U}{\partial \boldsymbol{\sigma}'} : \mathbf{1} = 3\frac{\partial f_U}{\partial I_1}, \quad H_L^P = \frac{\partial f_L}{\partial \boldsymbol{\sigma}'} : \mathbf{1} = 3\frac{\partial f_L}{\partial I_1} \tag{C.48),(C.49}$$

According to Eq.(C.14)-(C.17), Eq.(C.44)-(C.49) are defined as,

$$H_{UU}^e = \left(\frac{3D}{I_1} \right)^2 \left(K\beta_U^2 + 3G \right), \quad H_{UL}^e = \left(3\frac{D}{I_1} \right)^2 \left(K\beta_U\beta_L - 3G \right) \tag{C.50),(C.51}$$

$$H_{LU}^e = \left(3\frac{D}{I_1} \right)^2 \left(K\beta_L\beta_U - 3G \right), \quad H_{LL}^e = \left(\frac{3D}{I_1} \right)^2 \left(K\beta_L^2 + 3G \right) \tag{C.52),(C.53}$$

$$H_U^p = 3\frac{D}{I_1}\beta_U, \quad H_L^P = 3\frac{D}{I_1}\beta_L \tag{C.54),(C.55}$$

where $\beta_U = M - 3\frac{\sqrt{3J_2}}{I_1}, \quad \beta_L = M + 3\frac{\sqrt{3J_2}}{I_1}$ $\tag{C.56),(C.57}$

Substitution of Eq.(C.50)-(C.55) into Eq.(C.41) results in,

$$\mathbf{X} = \left(3\frac{D}{I_1} \right)^2 \begin{bmatrix} K\beta_U^2 + 3G + \frac{I_1}{3D}\beta_U & K\beta_U\beta_L - 3G + \frac{I_1}{3D}\beta_L \\ K\beta_L\beta_U - 3G + \frac{I_1}{3D}\beta_U & K\beta_L^2 + 3G + \frac{I_1}{3D}\beta_L \end{bmatrix} \tag{C.58}$$

Verify a non-singular $\mathbf{X}$ matrix by evaluating a determinant of $\mathbf{X}$, given by,

$$\det(\mathbf{X}) = \left(3\frac{D}{I_1} \right)^4 \left(x_{UU}x_{LL} - x_{LU}x_{UL} \right) \tag{C.59}$$

where

$$x_{UU} x_{LL} = \left(K\beta_U^2 + 3G + \frac{I_1}{3D}\beta_U \right)\left(K\beta_L^2 + 3G + \frac{I_1}{3D}\beta_L \right) \tag{C.60}$$

$$x_{LU} x_{UL} = \left(K\beta_L\beta_U - 3G + \frac{I_1}{3D}\beta_U \right)\left(K\beta_U\beta_L - 3G + \frac{I_1}{3D}\beta_L \right) \tag{C.61}$$

Expansion of Eq.(C.60) and (C.61) in Eq.(C.59) result in,

$$\det(\mathbf{X}) = \left(3\frac{D}{I_1} \right)^4 (\beta_U + \beta_L)G\left(3K(\beta_U + \beta_L) + \frac{2I_1}{D} \right) \tag{C.62}$$

Substitute Eq.(C.56),(C.57) into (C.62), obtain non-zero $\det(\mathbf{X})$ as shown in Eq.(C.63), therefore, $\mathbf{X}$ is a positive definite and the inverse of $\mathbf{X}$ is existed as given in Eq.(C.64).

$$\det(\mathbf{X}) = \left(3\frac{D}{I_1} \right)^4 4GM\left(3KM + \frac{I_1}{D} \right) \tag{C.63}$$

$$\mathbf{X}^{-1} = \frac{\left(3\frac{D}{I_1} \right)^2}{\det(\mathbf{X})}\begin{bmatrix} K\beta_L^2 + 3G + \frac{I_1}{3D}\beta_L & -\left(K\beta_U\beta_L - 3G + \frac{I_1}{3D}\beta_L \right) \\ -\left(K\beta_L\beta_U - 3G + \frac{I_1}{3D}\beta_U \right) & K\beta_U^2 + 3G + \frac{I_1}{3D}\beta_U \end{bmatrix} \tag{C.64}$$

C-5 Incremental stress-strain relation at the corner

Incremental stress-strain relation using Koiter's associated flow rule is given by,

$$\dot{\boldsymbol{\sigma}}' = \mathbf{c}^e : \left\{ \dot{\boldsymbol{\varepsilon}} - \dot{\boldsymbol{\varepsilon}}^p \right\} \tag{C.65}$$

where

$$\dot{\boldsymbol{\varepsilon}}^p = \gamma_U \frac{\partial f_U}{\partial \boldsymbol{\sigma}'} + \gamma_L \frac{\partial f_L}{\partial \boldsymbol{\sigma}'} = \begin{pmatrix} \gamma_U \\ \gamma_L \end{pmatrix} \cdot \begin{pmatrix} \frac{\partial f_U}{\partial \boldsymbol{\sigma}'} \\ \frac{\partial f_L}{\partial \boldsymbol{\sigma}'} \end{pmatrix} \tag{C.66}$$

Consider a double product of elasticity tensor and plastic flow,

$$\mathbf{c}^e : \dot{\boldsymbol{\varepsilon}}^p = \mathbf{c}^e : \left\{ \gamma_U \frac{\partial f_U}{\partial \boldsymbol{\sigma}'} + \gamma_L \frac{\partial f_L}{\partial \boldsymbol{\sigma}'} \right\} = \begin{pmatrix} \gamma_U \\ \gamma_L \end{pmatrix} \cdot \begin{pmatrix} \mathbf{c}^e : \frac{\partial f_U}{\partial \boldsymbol{\sigma}'} \\ \mathbf{c}^e : \frac{\partial f_L}{\partial \boldsymbol{\sigma}'} \end{pmatrix} \tag{C.67}$$

Substituting for consistency parameters from Eq.(C.40) gives Eq.(C.67) as,

$$\mathbf{c}^e : \dot{\boldsymbol{\varepsilon}}^p = \mathbf{X}^{-1} \cdot \begin{pmatrix} \frac{\partial f_U}{\partial \boldsymbol{\sigma}'} : \mathbf{c}^e : \dot{\boldsymbol{\varepsilon}} \\ \frac{\partial f_L}{\partial \boldsymbol{\sigma}'} : \mathbf{c}^e : \dot{\boldsymbol{\varepsilon}} \end{pmatrix} \cdot \begin{pmatrix} \mathbf{c}^e : \frac{\partial f_U}{\partial \boldsymbol{\sigma}'} \\ \mathbf{c}^e : \frac{\partial f_L}{\partial \boldsymbol{\sigma}'} \end{pmatrix} = \boldsymbol{\chi} \cdot \begin{pmatrix} \frac{\partial f_U}{\partial \boldsymbol{\sigma}'} : \mathbf{c}^e : \dot{\boldsymbol{\varepsilon}} \\ \frac{\partial f_L}{\partial \boldsymbol{\sigma}'} : \mathbf{c}^e : \dot{\boldsymbol{\varepsilon}} \end{pmatrix} \cdot \begin{pmatrix} \mathbf{c}^e : \frac{\partial f_U}{\partial \boldsymbol{\sigma}'} \\ \mathbf{c}^e : \frac{\partial f_L}{\partial \boldsymbol{\sigma}'} \end{pmatrix} \tag{C.68}$$

where $\quad \boldsymbol{\chi} = \mathbf{X}^{-1} \tag{C.69}$

Defining components of $\boldsymbol{\chi}$ in a way that $\chi_{UU} = \chi_{1,1}; \chi_{UL} = \chi_{1,2}; \chi_{LU} = \chi_{2,1}; \chi_{LL} = \chi_{2,2}$, then Eq.(C.68) can be expanded as,

$$\mathbf{c}^e : \dot{\boldsymbol{\varepsilon}}^p = \begin{pmatrix} \chi_{UU} \frac{\partial f_U}{\partial \boldsymbol{\sigma}'} : \mathbf{c}^e : \dot{\boldsymbol{\varepsilon}} + \chi_{UL} \frac{\partial f_L}{\partial \boldsymbol{\sigma}'} : \mathbf{c}^e : \dot{\boldsymbol{\varepsilon}} \\ \chi_{LU} \frac{\partial f_U}{\partial \boldsymbol{\sigma}'} : \mathbf{c}^e : \dot{\boldsymbol{\varepsilon}} + \chi_{LL} \frac{\partial f_L}{\partial \boldsymbol{\sigma}'} : \mathbf{c}^e : \dot{\boldsymbol{\varepsilon}} \end{pmatrix} \cdot \begin{pmatrix} \mathbf{c}^e : \frac{\partial f_U}{\partial \boldsymbol{\sigma}'} \\ \mathbf{c}^e : \frac{\partial f_L}{\partial \boldsymbol{\sigma}'} \end{pmatrix} \tag{C.70}$$

$$= \left(\chi_{UU}\mathbf{c}^e : \frac{\partial f_U}{\partial \boldsymbol{\sigma}} \otimes \frac{\partial f_U}{\partial \boldsymbol{\sigma}} : \mathbf{c}^e + \chi_{UL}\mathbf{c}^e : \frac{\partial f_U}{\partial \boldsymbol{\sigma}} \otimes \frac{\partial f_L}{\partial \boldsymbol{\sigma}} : \mathbf{c}^e + \chi_{LU}\mathbf{c}^e : \frac{\partial f_L}{\partial \boldsymbol{\sigma}} \otimes \frac{\partial f_U}{\partial \boldsymbol{\sigma}} : \mathbf{c}^e + \chi_{LL}\mathbf{c}^e : \frac{\partial f_L}{\partial \boldsymbol{\sigma}} \otimes \frac{\partial f_L}{\partial \boldsymbol{\sigma}} : \mathbf{c}^e \right) : \dot{\boldsymbol{\varepsilon}}$$

Defining a particular second-order tensor basis below can reduce the above equation as expressed in Eq.(C.72)

$$\begin{pmatrix} \mathbf{g}_U \\ \mathbf{g}_L \end{pmatrix} = \begin{Bmatrix} \mathbf{c}^e : \frac{\partial f_U}{\partial \boldsymbol{\sigma}'} \\ \mathbf{c}^e : \frac{\partial f_L}{\partial \boldsymbol{\sigma}'} \end{Bmatrix} = \begin{Bmatrix} \frac{\partial f_U}{\partial \boldsymbol{\sigma}'} : \mathbf{c}^{eT} \\ \frac{\partial f_L}{\partial \boldsymbol{\sigma}'} : \mathbf{c}^{eT} \end{Bmatrix} = \begin{Bmatrix} \frac{\partial f_U}{\partial \boldsymbol{\sigma}'} : \mathbf{c}^e \\ \frac{\partial f_L}{\partial \boldsymbol{\sigma}'} : \mathbf{c}^e \end{Bmatrix} \tag{C.71}$$

where $\mathbf{g}_U, \mathbf{g}_L \in \mathsf{S}; \quad \mathsf{S} = \left\{ \boldsymbol{\xi} : \mathsf{R}^3 \rightarrow \mathsf{R}^3 \,\middle|\, \boldsymbol{\xi} = \boldsymbol{\xi}^T \right\}$

$$\mathbf{c}^e : \dot{\boldsymbol{\varepsilon}}^p = \left(\chi_{UU} \mathbf{g}_U \otimes \mathbf{g}_U + \chi_{UL} \mathbf{g}_U \otimes \mathbf{g}_L + \chi_{LU} \mathbf{g}_L \otimes \mathbf{g}_U + \chi_{LL} \mathbf{g}_L \otimes \mathbf{g}_L \right) : \dot{\boldsymbol{\varepsilon}} \tag{C.72}$$

Therefore, an incremental stress-strain relation defined in Eq.(C.65) can be reduced as,

$$\dot{\boldsymbol{\sigma}}' = \left(\mathbf{c}^e - \sum_{\alpha,\beta \in \{U,L\}} \chi_{\alpha,\beta} \left(\mathbf{g}_\alpha \otimes \mathbf{g}_\beta \right) \right) : \dot{\boldsymbol{\varepsilon}} \tag{C.73}$$

C-6 Vector basis associated to plastic flow at the corner

The vector basis $\mathbf{g}_U$ and its conjugate $\mathbf{g}_L$ defined in Eq.(C.71) can be employed to define the direction of plastic flow at the corner. Accordingly, the covariant components of $\dot{\boldsymbol{\varepsilon}}$ in respect to the bases $\{\, \mathbf{g}_U \quad \mathbf{g}_L \,\}$ are shown by,

$$\begin{pmatrix} L_U \\ L_L \end{pmatrix} = \begin{Bmatrix} \mathbf{g}_U : \dot{\boldsymbol{\varepsilon}} \\ \mathbf{g}_L : \dot{\boldsymbol{\varepsilon}} \end{Bmatrix} \tag{C.74}$$

where $\begin{Bmatrix} \mathbf{g}_U \\ \mathbf{g}_L \end{Bmatrix}$ is bases for stress space S associated to the corner

The loading vector components L_U, L_L defined in Eq.(C.32) and (C.33) are, therefore, corresponding to those of Eq.(C.74). The consistency parameters γ_U, γ_L can be interpreted as the covariant components of $\dot{\boldsymbol{\varepsilon}}$, relative to the bases associated to $\{\, \mathbf{g}_U \quad \mathbf{g}_L \,\}$ as shown in Eq.(C.75), which is compatible with Eq.(C.40).
Post-multiply Eq.(C.40) by $\dot{\boldsymbol{\varepsilon}}$, obtain

$$\begin{pmatrix} \gamma_U \\ \gamma_L \end{pmatrix} = \boldsymbol{\chi} \cdot \begin{Bmatrix} \mathbf{g}_U : \dot{\boldsymbol{\varepsilon}} \\ \mathbf{g}_L : \dot{\boldsymbol{\varepsilon}} \end{Bmatrix} \tag{C.75}$$

C-7 Continuum tangential stiffness tensor at the hardening vertex

The tangent elastoplastic moduli for a stress state at the corner are defined in corresponding to Eq.(C.73) as

$$\mathbf{c}^{ep}* = \mathbf{c}^e - \sum_{\alpha,\beta \in \{U,L\}} \chi_{\alpha,\beta} \left(\mathbf{g}_\alpha \otimes \mathbf{g}_\beta \right) \tag{C.76}$$

where $\mathbf{c}^e = K\mathbf{1} \otimes \mathbf{1} + 2G\mathbf{A}$

Herein, a superscript "*" in $\mathbf{c}^{ep}*$ is used to distinguishes from $\mathbf{c}^{ep}$ which is employed on a smooth yield surface.
Expanding second-order basis defined in Eq.(C.71) gives,

$$\mathbf{g}_U = \mathbf{c}^e : \frac{\partial f_U}{\partial \boldsymbol{\sigma}'} = \frac{\partial f_U}{\partial \boldsymbol{\sigma}'} : \mathbf{c}^e = \frac{3D}{I_1} \left(K\beta_U \mathbf{1} + 2G\sqrt{\frac{3}{2}} \mathbf{n} \right) \tag{C.77}$$

$$\mathbf{g}_L = \mathbf{c}^e : \frac{\partial f_L}{\partial \boldsymbol{\sigma}'} = \frac{\partial f_L}{\partial \boldsymbol{\sigma}'} : \mathbf{c}^e = \frac{3D}{I_1} \left(K\beta_L \mathbf{1} - 2G\sqrt{\frac{3}{2}} \mathbf{n} \right) \tag{C.78}$$

The following tensor products form bases for $\mathsf{S} \times \mathsf{S}$

$$\mathbf{g}_U \otimes \mathbf{g}_U = \left(\frac{3D}{I_1} \right)^2 \left(K\beta_U \mathbf{1} + \sqrt{6}G\mathbf{n} \right) \otimes \left(K\beta_U \mathbf{1} + \sqrt{6}G\mathbf{n} \right) \tag{C.79}$$

$$\mathbf{g}_U \otimes \mathbf{g}_L = \left(\frac{3D}{I_1} \right)^2 \left(K\beta_U \mathbf{1} + \sqrt{6}G\mathbf{n} \right) \otimes \left(K\beta_L \mathbf{1} - \sqrt{6}G\mathbf{n} \right) \tag{C.80}$$

$$\mathbf{g}_L \otimes \mathbf{g}_U = \left(\frac{3D}{I_1} \right)^2 \left(K\beta_L \mathbf{1} - \sqrt{6}G\mathbf{n} \right) \otimes \left(K\beta_U \mathbf{1} + \sqrt{6}G\mathbf{n} \right) \tag{C.81}$$

$$\mathbf{g}_L \otimes \mathbf{g}_L = \left(\frac{3D}{I_1} \right)^2 \left(K\beta_L \mathbf{1} - \sqrt{6}G\mathbf{n} \right) \otimes \left(K\beta_L \mathbf{1} - \sqrt{6}G\mathbf{n} \right) \tag{C.82}$$

Expansion of the summation part in Eq.(C.76) yield,

$$\sum_{\alpha,\beta \in \{U,L\}} \chi_{\alpha,\beta} \mathbf{g}_\alpha \otimes \mathbf{g}_\beta = \chi_{U,U} \mathbf{g}_U \otimes \mathbf{g}_U + \chi_{U,L} \mathbf{g}_U \otimes \mathbf{g}_L + \chi_{L,U} \mathbf{g}_L \otimes \mathbf{g}_U + \chi_{L,L} \mathbf{g}_L \otimes \mathbf{g}_L$$

where

$$\chi_{U,U} \cdot \left(g_U \otimes \ g_U \right) = \begin{bmatrix} \dfrac{1}{3} \cdot K^2 \cdot \beta_U^2 \cdot \dfrac{\left(3 \cdot K \cdot \beta_L^2 \cdot D + 9 \cdot G \cdot D + I_1 \cdot \beta_L \right)}{\left[G \cdot \left[\left(\beta_L + \beta_U \right) \cdot \left(3 \cdot K \cdot D \cdot \beta_U + 3 \cdot K \cdot \beta_L \cdot D + 2 \cdot I_1 \right) \right] \right]} \\[4mm] \dfrac{1}{3} \cdot K \cdot \beta_U \cdot \sqrt{6} \cdot \dfrac{\left(3 \cdot K \cdot \beta_L^2 \cdot D + 9 \cdot G \cdot D + I_1 \cdot \beta_L \right)}{\left[\left(\beta_L + \beta_U \right) \cdot \left(3 \cdot K \cdot D \cdot \beta_U + 3 \cdot K \cdot \beta_L \cdot D + 2 \cdot I_1 \right) \right]} \\[4mm] \dfrac{1}{3} \cdot K \cdot \beta_U \cdot \sqrt{6} \cdot \dfrac{\left(3 \cdot K \cdot \beta_L^2 \cdot D + 9 \cdot G \cdot D + I_1 \cdot \beta_L \right)}{\left[\left(\beta_L + \beta_U \right) \cdot \left(3 \cdot K \cdot D \cdot \beta_U + 3 \cdot K \cdot \beta_L \cdot D + 2 \cdot I_1 \right) \right]} \\[4mm] 2 \cdot G \cdot \dfrac{\left(3 \cdot K \cdot \beta_L^2 \cdot D + 9 \cdot G \cdot D + I_1 \cdot \beta_L \right)}{\left[\left(\beta_L + \beta_U \right) \cdot \left(3 \cdot K \cdot D \cdot \beta_U + 3 \cdot K \cdot \beta_L \cdot D + 2 \cdot I_1 \right) \right]} \end{bmatrix} \cdot \begin{bmatrix} (\mathbf{1} \otimes \mathbf{1}) \\ (\mathbf{1} \otimes \mathbf{n}) \\ (\mathbf{n} \otimes \mathbf{1}) \\ (\mathbf{n} \otimes \mathbf{n}) \end{bmatrix}$$

$$\chi_{U,L} \cdot \left(g_U \otimes \ g_L \right) = \begin{bmatrix} \dfrac{-1}{3} \cdot K^2 \cdot \beta_U \cdot \beta_L \cdot \dfrac{\left(3 \cdot K \cdot \beta_U \cdot \beta_L \cdot D - 9 \cdot G \cdot D + I_1 \cdot \beta_L \right)}{\left[G \cdot \left[\left(\beta_L + \beta_U \right) \cdot \left(3 \cdot K \cdot D \cdot \beta_U + 3 \cdot K \cdot \beta_L \cdot D + 2 \cdot I_1 \right) \right] \right]} \\[4mm] \dfrac{1}{3} \cdot K \cdot \beta_U \cdot \sqrt{6} \cdot \dfrac{\left(3 \cdot K \cdot \beta_U \cdot \beta_L \cdot D - 9 \cdot G \cdot D + I_1 \cdot \beta_L \right)}{\left[\left(\beta_L + \beta_U \right) \cdot \left(3 \cdot K \cdot D \cdot \beta_U + 3 \cdot K \cdot \beta_L \cdot D + 2 \cdot I_1 \right) \right]} \\[4mm] \dfrac{-1}{3} \cdot \sqrt{6} \cdot K \cdot \beta_L \cdot \dfrac{\left(3 \cdot K \cdot \beta_U \cdot \beta_L \cdot D - 9 \cdot G \cdot D + I_1 \cdot \beta_L \right)}{\left[\left(\beta_L + \beta_U \right) \cdot \left(3 \cdot K \cdot D \cdot \beta_U + 3 \cdot K \cdot \beta_L \cdot D + 2 \cdot I_1 \right) \right]} \\[4mm] 2 \cdot G \cdot \dfrac{\left(3 \cdot K \cdot \beta_U \cdot \beta_L \cdot D - 9 \cdot G \cdot D + I_1 \cdot \beta_L \right)}{\left[\left(\beta_L + \beta_U \right) \cdot \left(3 \cdot K \cdot D \cdot \beta_U + 3 \cdot K \cdot \beta_L \cdot D + 2 \cdot I_1 \right) \right]} \end{bmatrix} \cdot \begin{bmatrix} (\mathbf{1} \otimes \mathbf{1}) \\ (\mathbf{1} \otimes \mathbf{n}) \\ (\mathbf{n} \otimes \mathbf{1}) \\ (\mathbf{n} \otimes \mathbf{n}) \end{bmatrix}$$

$$\chi_{L,U} \cdot \left(g_L \otimes \ g_U \right) = \begin{bmatrix} \dfrac{-1}{3} \cdot K^2 \cdot \beta_U \cdot \beta_L \cdot \dfrac{\left(3 \cdot K \cdot \beta_U \cdot \beta_L \cdot D - 9 \cdot G \cdot D + I_1 \cdot \beta_U \right)}{\left[G \cdot \left[\left(\beta_L + \beta_U \right) \cdot \left(3 \cdot K \cdot D \cdot \beta_U + 3 \cdot K \cdot \beta_L \cdot D + 2 \cdot I_1 \right) \right] \right]} \\[4mm] \dfrac{-1}{3} \cdot \sqrt{6} \cdot K \cdot \beta_L \cdot \dfrac{\left(3 \cdot K \cdot \beta_U \cdot \beta_L \cdot D - 9 \cdot G \cdot D + I_1 \cdot \beta_U \right)}{\left[\left(\beta_L + \beta_U \right) \cdot \left(3 \cdot K \cdot D \cdot \beta_U + 3 \cdot K \cdot \beta_L \cdot D + 2 \cdot I_1 \right) \right]} \\[4mm] \dfrac{1}{3} \cdot K \cdot \beta_U \cdot \sqrt{6} \cdot \dfrac{\left(3 \cdot K \cdot \beta_U \cdot \beta_L \cdot D - 9 \cdot G \cdot D + I_1 \cdot \beta_U \right)}{\left[\left(\beta_L + \beta_U \right) \cdot \left(3 \cdot K \cdot D \cdot \beta_U + 3 \cdot K \cdot \beta_L \cdot D + 2 \cdot I_1 \right) \right]} \\[4mm] 2 \cdot G \cdot \dfrac{\left(3 \cdot K \cdot \beta_U \cdot \beta_L \cdot D - 9 \cdot G \cdot D + I_1 \cdot \beta_U \right)}{\left[\left(\beta_L + \beta_U \right) \cdot \left(3 \cdot K \cdot D \cdot \beta_U + 3 \cdot K \cdot \beta_L \cdot D + 2 \cdot I_1 \right) \right]} \end{bmatrix} \cdot \begin{bmatrix} (\mathbf{1} \otimes \mathbf{1}) \\ (\mathbf{1} \otimes \mathbf{n}) \\ (\mathbf{n} \otimes \mathbf{1}) \\ (\mathbf{n} \otimes \mathbf{n}) \end{bmatrix}$$

$$\chi_{L,L} \cdot \left(g_L \otimes \ g_L \right) = \begin{bmatrix} \dfrac{1}{3} \cdot K^2 \cdot \beta_L^2 \cdot \dfrac{\left(3 \cdot K \cdot \beta_U^2 \cdot D + 9 \cdot G \cdot D + I_1 \cdot \beta_U \right)}{\left[G \cdot \left[\left(\beta_L + \beta_U \right) \cdot \left(3 \cdot K \cdot D \cdot \beta_U + 3 \cdot K \cdot \beta_L \cdot D + 2 \cdot I_1 \right) \right] \right]} \\[4mm] \dfrac{-1}{3} \cdot \sqrt{6} \cdot K \cdot \beta_L \cdot \dfrac{\left(3 \cdot K \cdot \beta_U^2 \cdot D + 9 \cdot G \cdot D + I_1 \cdot \beta_U \right)}{\left[\left(\beta_L + \beta_U \right) \cdot \left(3 \cdot K \cdot D \cdot \beta_U + 3 \cdot K \cdot \beta_L \cdot D + 2 \cdot I_1 \right) \right]} \\[4mm] \dfrac{-1}{3} \cdot \sqrt{6} \cdot K \cdot \beta_L \cdot \dfrac{\left(3 \cdot K \cdot \beta_U^2 \cdot D + 9 \cdot G \cdot D + I_1 \cdot \beta_U \right)}{\left[\left(\beta_L + \beta_U \right) \cdot \left(3 \cdot K \cdot D \cdot \beta_U + 3 \cdot K \cdot \beta_L \cdot D + 2 \cdot I_1 \right) \right]} \\[4mm] 2 \cdot G \cdot \dfrac{\left(3 \cdot K \cdot \beta_U^2 \cdot D + 9 \cdot G \cdot D + I_1 \cdot \beta_U \right)}{\left[\left(\beta_L + \beta_U \right) \cdot \left(3 \cdot K \cdot D \cdot \beta_U + 3 \cdot K \cdot \beta_L \cdot D + 2 \cdot I_1 \right) \right]} \end{bmatrix} \cdot \begin{bmatrix} (\mathbf{1} \otimes \mathbf{1}) \\ (\mathbf{1} \otimes \mathbf{n}) \\ (\mathbf{n} \otimes \mathbf{1}) \\ (\mathbf{n} \otimes \mathbf{n}) \end{bmatrix}$$

$$\sum_{\alpha,\beta \in \{U,L\}} \chi_{\alpha,\beta} \left(\mathbf{g}_\alpha \otimes \mathbf{g}_\beta \right) = \frac{3 \left(\beta_U + \beta_L \right) K^2 D \mathbf{1} \otimes \mathbf{1} + \dfrac{\sqrt{6}}{3} \left(\beta_U - \beta_L \right) K I_1 \mathbf{n} \otimes \mathbf{1}}{3 \left(\beta_U + \beta_L \right) K D + 2 I_1} + 2 G \mathbf{n} \otimes \mathbf{n} \tag{C.83}$$

Expression of coupled plastic modulus in above equation, substituted for β_U and β_L by Eq.(C.56),(C.57), in the bases defined in Eq.(C.79)-(C.82), emerges a non-symmetric forth-order tensor as,

$$\sum_{\alpha,\beta\in\{U,L\}} \chi_{\alpha,\beta}\left(\mathbf{g}_\alpha\otimes\mathbf{g}_\beta\right)=\frac{3K^2MD}{3KDM+I_1}\mathbf{1}\otimes\mathbf{1}-\sqrt{6}\frac{K\sqrt{3J_2}}{3KDM+I_1}\mathbf{n}\otimes\mathbf{1}+2G\mathbf{n}\otimes\mathbf{n} \tag{C.84}$$

For a particular stress state at the corner by a hardening stress on both yield loci, that is, state of stress is placed at the corner coincided with the singular hardening vertex in stress space, using Eq.B.18, a unit normal $\mathbf{n}$ reveals as,

$$\mathbf{n}\big|_{\sigma'=\sigma'_c}=\mathbf{n}_c=\sqrt{\frac{3}{2}}\frac{\boldsymbol{\eta}_c}{\eta_o}=diag\left[-\frac{\sqrt{6}}{6}\quad\frac{\sqrt{6}}{3}\quad-\frac{\sqrt{6}}{6}\right] \tag{C.85}$$

$$\text{where}\qquad \eta_o=3\frac{\sqrt{3J_{c2}}}{I_{c1}}=3\frac{\sqrt{3J_2}}{I_1}=3\frac{1-K_o}{1+2K_o}\qquad\text{(See also Appendix B-2)} \tag{C.86}$$

Consequently, the tangent elastoplastic moduli at the corner defined in Eq.(C.76) can be explicitly reduced to,

$$\mathbf{c}^{ep}*=\left(K-\frac{3K^2MD}{3KDM+I_1}\right)\mathbf{1}\otimes\mathbf{1}+\sqrt{\frac{2}{3}}\frac{\eta_o KI_1}{(3KDM+I_1)}\mathbf{n}_c\otimes\mathbf{1}+2G\left[\mathbf{A}-\mathbf{n}_c\otimes\mathbf{n}_c\right] \tag{C.87}$$

Substitution into Eq.(C.87) for I_1 by p' from Eq.(C.2), for p' by K from Eq.(C.25), for D by Eq.(C.88) and for λ by Eq.(C.89), a compacted form of $\mathbf{c}^{ep}$ at the corner is given by Eq.(C.90) as,

$$D=\frac{\lambda-\kappa}{M(1+e_o)}\,,\qquad \lambda=\frac{\kappa}{1-\Lambda} \tag{C.88),(C.89}$$

$$\mathbf{c}^{ep}*=(1-\Lambda)K\mathbf{1}\otimes\mathbf{1}+\sqrt{\frac{2}{3}}(1-\Lambda)\eta_o K\mathbf{n}_c\otimes\mathbf{1}+2G\left[\mathbf{A}-\mathbf{n}_c\otimes\mathbf{n}_c\right] \tag{C.90}$$

It is found that the continuum tangential stiffness tensor at the corner of Hata-Ohta and Sekiguchi-Ohta models are asymmetric forth-order tensor.

C-8 Consistency parameters in regard to the hardening vertex

Based on conditions of stress state at the corner employed in Appendix C-7, Eq.(C.56) and (C.57) can be specified as,

$$\beta_U=M-\eta_o,\quad \beta_L=M+\eta_o \tag{C.91),(C.92}$$

In addition to Eq.(C.91),(C.92), X and its inversion defined in Eq.(C.58) and (C.64) can be specified by giving p'=p'c as,

$$\mathbf{X}=\left(\frac{D}{p'_c}\right)^2\begin{bmatrix}K\left(M-\eta_o\right)^2+3G+\dfrac{p'_c}{D}\left(M-\eta_o\right) & K\left(M-\eta_o\right)\left(M+\eta_o\right)-3G+\dfrac{p'_c}{D}\left(M+\eta_o\right)\\[2ex] K\left(M+\eta_o\right)\left(M-\eta_o\right)-3G+\dfrac{p'_c}{D}\left(M-\eta_o\right) & K\left(M+\eta_o\right)^2+3G+\dfrac{p'_c}{D}\left(M+\eta_o\right)\end{bmatrix} \tag{C.93}$$

$$\boldsymbol{\chi}=\mathbf{X}^{-1}=\frac{\left(\dfrac{D}{p'_c}\right)^2}{12D^3GM\left(\dfrac{KDM+p'_c}{p'^4_c}\right)}\begin{bmatrix}K\left(M+\eta_o\right)^2+3G+\dfrac{p'_c}{D}\left(M+\eta_o\right) & -\left(K\left(M^2-\eta_o^2\right)-3G+\dfrac{p'_c}{D}\left(M+\eta_o\right)\right)\\[2ex] -\left(K\left(M^2-\eta_o^2\right)-3G+\dfrac{p'_c}{D}\left(M-\eta_o\right)\right) & K\left(M-\eta_o\right)^2+3G+\dfrac{p'_c}{D}\left(M-\eta_o\right)\end{bmatrix} \tag{C.94}$$

According to $\boldsymbol{\chi}$ specified above in accompanied by Eq. (C.74), (C.77), (C.78) substituted by Eq.(C.91), (C.92), the consistency parameters defined in Eq.(C.40) can be evaluated as,

$$\gamma_U=\left[\frac{1}{6}\frac{Kp'_c\left(3MGD-\eta_o^2p'_c-M\eta_o p'_c\right)}{GDM(KDM+p'_c)}\mathbf{1}+\frac{\left(M+\eta_o\right)p'_c}{\sqrt{6}DM}\mathbf{n}_c\right]:\dot{\boldsymbol{\varepsilon}} \tag{C.95}$$

$$\gamma_L=\left[\frac{1}{6}\frac{Kp'_c\left(3MGD-\eta_o^2p'_c+M\eta_o p'_c\right)}{GDM(KDM+p'_c)}\mathbf{1}-\frac{\left(M-\eta_o\right)p'_c}{\sqrt{6}DM}\mathbf{n}_c\right]:\dot{\boldsymbol{\varepsilon}} \tag{C.96}$$

$\mathbf{n}_c$ is the unit normal pointed from hydrostatic axis to the corner. Magnitude of consistency parameter is depended on driving variable $\dot{\boldsymbol{\varepsilon}}$, combination of value γ_U and γ_L can judge loading/unloading condition. In addition, it can interpret whether the subsequent stress is still placed on the corner or out of the corner during loading.

C-9 Plastic flow at the hardening vertex

Concerning with Eq.(C.66), plastic flow at the hardening vertex or corner is defined by assigning $\sigma'=\sigma'_c$,

$$\dot{\boldsymbol{\varepsilon}}^p = \left\{ \gamma_U \frac{\partial f_U}{\partial \boldsymbol{\sigma}'} + \gamma_L \frac{\partial f_L}{\partial \boldsymbol{\sigma}'} \right\}\bigg|_{\boldsymbol{\sigma}'=\boldsymbol{\sigma}'_c} \tag{C.97}$$

where γ_u and γ_l are defined in Eq.(C.95),(C.96)

In according to Eq.(C.12)-(C.17), the gradients of yield surface in stress space on $\boldsymbol{\sigma}' = \boldsymbol{\sigma}'_c$ are expressed by,

$$\frac{\partial f_U}{\partial \boldsymbol{\sigma}'}\bigg|_{\boldsymbol{\sigma}'=\boldsymbol{\sigma}'_c} = \frac{D}{3 p'_c}(M - \eta_o)\mathbf{1} + \sqrt{\frac{3}{2}}\frac{D}{p'_c}\mathbf{n}_c \tag{C.98}$$

$$\frac{\partial f_L}{\partial \boldsymbol{\sigma}'}\bigg|_{\boldsymbol{\sigma}'=\boldsymbol{\sigma}'_c} = \frac{D}{3 p'_c}(M + \eta_o)\mathbf{1} - \sqrt{\frac{3}{2}}\frac{D}{p'_c}\mathbf{n}_c \tag{C.99}$$

As a result, the plastic flow at the hardening vertex is determined by substituting Eq.(C.98),(C.99) into Eq.(C.97).

$$\dot{\boldsymbol{\varepsilon}}^p = \left[\frac{KMD}{3(KMD + p'_c)}\mathbf{1}\otimes\mathbf{1} - \frac{Kp'_c\,\eta_o}{\sqrt{6}G(KMD + p'_c)}\mathbf{n}_c\otimes\mathbf{1} + \mathbf{n}_c\otimes\mathbf{n}_c \right]:\dot{\boldsymbol{\varepsilon}} \tag{C.100}$$

Eq.(C.100) can be further reduced by substitution of K from Eq.(C.25), G from Eq.(C.26), D from Eq.(C.88) and λ from Eq.(C.89), $\mathbf{n}_c$ from Eq.(C.85). Consequently,

$$\dot{\boldsymbol{\varepsilon}}^p = \left[\frac{\Lambda}{3}\mathbf{1}\otimes\mathbf{1} - \frac{1-\Lambda}{\sqrt{6}\mu'}\eta_o\mathbf{n}_c\otimes\mathbf{1} + \mathbf{n}_c\otimes\mathbf{n}_c \right]:\dot{\boldsymbol{\varepsilon}} \tag{C.101}$$

C-10 Plastic flow under K_o consolidation

Effective stress under K_o-condition for a given overburden pressure σ'_a is given by

$$\boldsymbol{\sigma}' = \begin{bmatrix} \sigma'_{xx} & \sigma'_{xy} & \sigma'_{xz} \\ \sigma'_{yx} & \sigma'_{yy} & \sigma'_{yz} \\ \sigma'_{zx} & \sigma'_{zy} & \sigma'_{zz} \end{bmatrix} = \begin{bmatrix} K_o\sigma'_a & 0 & 0 \\ 0 & \sigma'_a & 0 \\ 0 & 0 & K_o\sigma'_a \end{bmatrix} \tag{C.102}$$

The corresponding effective mean stress and deviatoric stress are given by

$$p' = \frac{1}{3}tr(\boldsymbol{\sigma}') = \frac{1 + 2K_o}{3}\sigma'_a \tag{C.103}$$

During K_o-consolidation, an imposed strain rate is given by solely axial rate of strain as,

$$\dot{\boldsymbol{\varepsilon}} = \begin{bmatrix} \dot{\varepsilon}_{xx} & \dot{\varepsilon}_{xy} & \dot{\varepsilon}_{xz} \\ \dot{\varepsilon}_{yx} & \dot{\varepsilon}_{yy} & \dot{\varepsilon}_{yz} \\ \dot{\varepsilon}_{zx} & \dot{\varepsilon}_{zy} & \dot{\varepsilon}_{zz} \end{bmatrix} = \begin{bmatrix} 0 & 0 & 0 \\ 0 & \dot{\varepsilon}_a & 0 \\ 0 & 0 & 0 \end{bmatrix} \tag{C.104}$$

As a consequence, volumetric strain rate, deviatoric strain rate and a unit normal corresponding to an imposed strain rate given in Eq.(C.104) are as following,

$$\dot{\varepsilon}_v = \dot{\boldsymbol{\varepsilon}}:\mathbf{1} = \dot{\varepsilon}_a, \qquad \dot{\varepsilon}_s = \sqrt{\frac{2}{3}\dot{\boldsymbol{\varepsilon}}_d:\dot{\boldsymbol{\varepsilon}}_d} = \sqrt{\frac{2}{3}\dot{\boldsymbol{\varepsilon}}:\mathbf{A}:\dot{\boldsymbol{\varepsilon}}} = \frac{2}{3}\dot{\varepsilon}_a \tag{C.105),(C.106}$$

$$\mathbf{n} = \frac{\mathbf{A}:\dot{\boldsymbol{\varepsilon}}}{\sqrt{\dot{\boldsymbol{\varepsilon}}:\mathbf{A}:\dot{\boldsymbol{\varepsilon}}}} = diag\left[-\frac{\sqrt{6}}{6} \quad \frac{\sqrt{6}}{3} \quad -\frac{\sqrt{6}}{6} \right] \tag{C.107}$$

It is found that the unit normal $\mathbf{n}$ for the imposed strain rate under uni-axial compression is coaxial with $\mathbf{n}_c$ specified for the unit normal of stress at the hardening vertex. Accordingly, Eq.(C.104)-(C.107) can be written simply by,

$$\dot{\boldsymbol{\varepsilon}} = \frac{1}{3}\dot{\varepsilon}_v\mathbf{1} + \sqrt{\frac{3}{2}}\dot{\varepsilon}_s\mathbf{n} = \frac{1}{3}\dot{\varepsilon}_v\mathbf{1} + \sqrt{\frac{3}{2}}\dot{\varepsilon}_s\mathbf{n}_c = \left\{ \frac{1}{3}\mathbf{1} + \sqrt{\frac{2}{3}}\mathbf{n}_c \right\}\dot{\varepsilon}_a \tag{C.108}$$

Plastic flow at the hardening vertex can be determined by substitution of Eq. (C.108) into Eq. (C.101), obtain

$$\dot{\boldsymbol{\varepsilon}}^p = \left[\frac{\Lambda}{3}\mathbf{1}\otimes\mathbf{1} - \frac{1-\Lambda}{\sqrt{6}\mu'}\eta_o\mathbf{n}_c\otimes\mathbf{1} + \mathbf{n}_c\otimes\mathbf{n}_c \right]:\left\{ \frac{1}{3}\mathbf{1} + \sqrt{\frac{2}{3}}\mathbf{n}_c \right\}\dot{\varepsilon}_a$$

$$= \left\{ \frac{\Lambda}{3}\mathbf{1} + \left(\frac{2\mu' - (1-\Lambda)\eta_o}{\sqrt{6}\mu'} \right)\mathbf{n}_c \right\}\dot{\varepsilon}_a$$

$$= \frac{1}{3\mu'} \dot{\varepsilon}_a \begin{bmatrix} \frac{1}{2}(\eta_o - 2\mu')(1-\Lambda) & 0 & 0 \\ 0 & \mu'(2+\Lambda) - \eta_o(1-\Lambda) & 0 \\ 0 & 0 & \frac{1}{2}(\eta_o - 2\mu')(1-\Lambda) \end{bmatrix} \tag{C.109}$$

in which $\quad \dot{\varepsilon}_a^p = \dfrac{\mu'(2+\Lambda) - \eta_o(1-\Lambda)}{3\mu'} \dot{\varepsilon}_a$ (C.110)

Based on result of Eq.(C.109), volumetric and deviatoric rate of plastic strain are

$$\dot{\varepsilon}_v^p = \mathbf{1} : \dot{\boldsymbol{\varepsilon}}^p = \Lambda \dot{\varepsilon}_a \tag{C.111}$$

$$\dot{\varepsilon}_s^p = \sqrt{\frac{2}{3}\dot{\boldsymbol{\varepsilon}}^p : \mathbf{A} : \dot{\boldsymbol{\varepsilon}}^p} = \frac{2\mu' - \eta_o(1-\Lambda)}{3\mu'} \dot{\varepsilon}_a \tag{C.112}$$

C-11 Incremental stress under K_o loading condition

Incremental stress during loading condition can be determined by a stress-strain relation using tangential stiffness tensor given in Eq.(C.90) as,

$$\dot{\boldsymbol{\sigma}}' = \mathbf{c}^{ep} * : \dot{\boldsymbol{\varepsilon}} = (1-\Lambda)K\dot{\varepsilon}_a \left\{ \mathbf{1} + \sqrt{\frac{2}{3}}\eta_o \mathbf{n}_c \right\} = (1-\Lambda)K\dot{\varepsilon}_a \left\{ \mathbf{1} + \boldsymbol{\eta}_c \right\}$$

$$= \frac{3(1-\Lambda)K}{1+2K_o} \dot{\varepsilon}_a \begin{bmatrix} K_o & 0 & 0 \\ 0 & 1 & 0 \\ 0 & 0 & K_o \end{bmatrix} \tag{C.113}$$

where $\quad \mathbf{1} + \boldsymbol{\eta}_c = \dfrac{3}{1+2K_o} diag\begin{bmatrix} K_o & 1 & K_o \end{bmatrix}$

Eq.(C.113) can be verified by the ratio of incremental horizontal stress to incremental vertical stress as,

$$K_o = \frac{\dot{\boldsymbol{\sigma}}_{11}}{\dot{\boldsymbol{\sigma}}_{22}} = \frac{\dot{\boldsymbol{\sigma}}_{33}}{\dot{\boldsymbol{\sigma}}_{22}} \tag{C.114}$$

in which $\quad \dot{\boldsymbol{\sigma}}_{22} = \dot{\sigma}'_a = \dfrac{3(1-\Lambda)K}{1+2K_o}\dot{\varepsilon}_a$ (C.115)

The corresponding incremental effective mean stress and deviatoric stress are shown by Eq.(C.116) and (C.117), in which K, Λ are substituted by Eq.(C.25) and Eq.(C.27).

$$\dot{p}' = \frac{1}{3}tr(\dot{\boldsymbol{\sigma}}') = (1-\Lambda)K\dot{\varepsilon}_a = \frac{p'(1+e_o)}{\lambda}\dot{\varepsilon}_a \tag{C.116}$$

$$q' = \sqrt{\frac{3}{2}\dot{\boldsymbol{\sigma}}' : \mathbf{A} : \dot{\boldsymbol{\sigma}}'} = \frac{p'\eta_o(1+e_o)}{\lambda}\dot{\varepsilon}_a \tag{C.117}$$

Moreover, Eq.(C.115) implies the e-ln(σ'_v) relation is hold by substituting for K, Λ and p' by Eq.(C.25), Eq.(C.27) and Eq.(C.103) respectively, achieve

$$\dot{\varepsilon}_a = \frac{\lambda}{1+e_o}\frac{\dot{\sigma}'_a}{\sigma'_a} \tag{C.118}$$

C-12 Incremental stress under K_o unloading condition

During unloading, there is no plastic flow, thus, elastic behavior is recovered. It is trivial to employ elastic tangential stiffness tensor in incremental stress-strain relation as,

$$\dot{\boldsymbol{\sigma}}' = \mathbf{c}^e : \dot{\boldsymbol{\varepsilon}} = [K\mathbf{1}\otimes\mathbf{1} + 2G\mathbf{A}] : \left\{ \frac{1}{3}\mathbf{1} + \sqrt{\frac{2}{3}}\mathbf{n}_c \right\}\dot{\varepsilon}_a$$

$$= \left\{ K\mathbf{1} + 2G\sqrt{\frac{2}{3}}\mathbf{n}_c \right\}\dot{\varepsilon}_a$$

$$= \frac{1}{3}\dot{\varepsilon}_a \begin{bmatrix} 3K-2G & 0 & 0 \\ 0 & 3K+4G & 0 \\ 0 & 0 & 3K-2G \end{bmatrix} \tag{C.119}$$

K_o unloading can be expressed by the ratio of incremental lateral stress to incremental vertical stress using a

relation defined in Eq.(C.121). The relation between K_o unloading and effective Poisson's ratio can be established as,

$$K_o = \frac{\dot{\sigma}'_{11}}{\dot{\sigma}'_{22}} = \frac{3K - 2G}{3K + 4G} = \frac{v'}{1 - v'} \tag{C.120}$$

$$\mu' = \frac{G}{K} = \frac{3(1 - 2v')}{2(1 + v')} \qquad \text{(see also Eq.(C.26),(C.28))} \tag{C.121}$$

Substitutions of K and G from relations given in Eq.(C.25)-(C.28) into Eq.(C.119) while employing K_o as shown in Eq.(C.120) and p' in Eq.(C.103) give nonlinear elastic stress-strain relation during unloading as,

$$\dot{\sigma}' = \frac{(1 + e_o)\sigma'_a}{\kappa} \dot{\varepsilon}_a \begin{bmatrix} \dfrac{v'}{1 - v'} & 0 & 0 \\ 0 & 1 & 0 \\ 0 & 0 & \dfrac{v'}{1 - v'} \end{bmatrix} \tag{C.122}$$

in which $\dot{\sigma}_{22} = \dot{\sigma}'_a = \dfrac{(1 + e_o)\sigma'_a}{\kappa} \dot{\varepsilon}_a$ (C.123)

The incremental elastic stress-strain relation during K_o unloading in vertical direction can be verified by Eq.(C.123) in a way that,

$$\dot{\varepsilon}_a^e = \frac{\kappa}{1 + e_o} \frac{\dot{\sigma}'_a}{\sigma'_a} \tag{C.124}$$

C-13 Coefficient of volume compressibility under K_o loading condition

The definition of coefficient of volume compressibility is defined by

$$m_v \equiv \frac{\dot{\varepsilon}_v}{\dot{p}'} \tag{C.125}$$

As a result, m_v defined in Eq.(C.125) can be verified by Eq(C.126) in which p' in Eq.(C.116) is substituted by a relation in Eq.(C.103).

$$m_v = \frac{\dot{\varepsilon}_a}{\dot{p}'} = \frac{\lambda}{(1 + e_o)p'} = \frac{3\lambda}{(1 + e_o)(1 + 2K_o)\sigma'_a} \tag{C.126}$$

C-14 K_o value during loading condition

By considering Eq.(C.118) and (C.124), vertical plastic strain increment can be determined by

$$\dot{\varepsilon}_a^p = \dot{\varepsilon}_a - \dot{\varepsilon}_a^e = \frac{\lambda - \kappa}{1 + e_o} \frac{\dot{\sigma}'_a}{\sigma'_a} = \Lambda \frac{\lambda}{(1 + e_o)} \frac{\dot{\sigma}'_a}{\sigma'_a} = \Lambda \dot{\varepsilon}_a \tag{C.127}$$

Equating Eq.(C.127) to Eq.(C.110) and solve for η_o as given by,

$$\eta_o = 2\mu' \tag{C.128}$$

Substitutions of η_o from Eq.(C.86) and μ' from Eq.(C.121) reach the conclusion that,

$$K_o = \frac{v'}{1 - v'} \tag{C.129}$$

It is found that K_o values obtained from both elastic and elastoplastic models share the common value. Hence, the unified relation between K_o and effective Poisson's ratio can be guaranteed. It is emphasized that without the application of Koiter's associated flow rule, the proof cannot carry out.

$$K_{o(elastic)} = K_{o(elastoplastic)} = \frac{v'}{1 - v'} \tag{C.130}$$

Substitution of results obtained in Eq.(C.130) into Eq.(C.109) and (C.112) settles the following deduction in Eq.(C.131),(C.132), that is, lateral strain increment is zero under elastic, plastic and elastoplastic response during K_o condition. This conclusion is consistent with the fact that K_o consolidation is a sort of 1-D deformation.

$$\dot{\varepsilon}^p = \Lambda \dot{\varepsilon}_a \left\{ \frac{1}{3} \mathbf{1} + \sqrt{\frac{3}{2}} \mathbf{n}_c \right\} = diag[0 \quad \Lambda \dot{\varepsilon}_a \quad 0] \tag{C.131}$$

$$\frac{\dot{\varepsilon}_s^p}{\dot{\varepsilon}_v^p} = \frac{\dot{\varepsilon}_s^e}{\dot{\varepsilon}_v^e} = \frac{\dot{\varepsilon}_s}{\dot{\varepsilon}_v} = \frac{2}{3} \tag{C.132}$$

Appendix D: K_o value

D-1 Rate of strain under uni-axial test condition

Under tri-axial test condition, rate of strain is given by,

$$\dot{\mathbf{\varepsilon}} = \begin{bmatrix} \dot{\varepsilon}_r & 0 & 0 \\ 0 & \dot{\varepsilon}_a & 0 \\ 0 & 0 & \dot{\varepsilon}_r \end{bmatrix} \tag{D.1}$$

Axial and lateral rate of strain can be reformed to volumetric and deviatoric parts as,

$$\begin{Bmatrix} \dot{\varepsilon}_v \\ \dot{\varepsilon}_s \end{Bmatrix} = \begin{bmatrix} 1 & 2 \\ \dfrac{2}{3} & -\dfrac{2}{3} \end{bmatrix} \begin{Bmatrix} \dot{\varepsilon}_a \\ \dot{\varepsilon}_r \end{Bmatrix} \tag{D.2}$$

For particular case of uni-axial test condition, rate of strain is given by,

$$\dot{\mathbf{\varepsilon}} = \begin{bmatrix} 0 & 0 & 0 \\ 0 & \dot{\varepsilon}_a & 0 \\ 0 & 0 & 0 \end{bmatrix} \tag{D.3}$$

Accordingly, volumetric and deviatoric rate of strain are

$$\dot{\varepsilon}_v = \dot{\varepsilon}_a , \quad \dot{\varepsilon}_s = \frac{2}{3}\dot{\varepsilon}_a \tag{D.4), (D.5}$$

It is noted that strain rate ratio of deviatoric to volumetric part is 2/3 for this particular case,

$$\frac{\dot{\varepsilon}_s}{\dot{\varepsilon}_v} = \frac{2}{3} \tag{D.6}$$

D-2 Rate of stress under uni-axial test condition

Stress tensor and stress rate tensor can be expressed by isotropic and deviatoric parts as,

$$\mathbf{\sigma}' = p'\mathbf{1} + \mathbf{s} = p'\mathbf{1} + \sqrt{\frac{2}{3}}q\mathbf{n} , \quad \dot{\mathbf{\sigma}}' = \dot{p}'\mathbf{1} + \dot{\mathbf{s}} = \dot{p}'\mathbf{1} + \sqrt{\frac{2}{3}}\dot{q}\mathbf{n} \tag{D.7), (D.8}$$

Under uni-axial condition, state of stress is taken in formed of isotropic and deviatoric stress where σ'_a is referred to an axial stress,

$$p' = \left(\frac{1+2K_o}{3}\right)\sigma'_a , \quad q = (1-K_o)\sigma'_a \tag{D.9), (D.10}$$

As a result, the ratio of deviatoric to isotropic stress is obtained by

$$\eta_o = \frac{q}{p'} = 3\frac{1-K_o}{1+2K_o} \tag{D.11}$$

According to Eq.(D.11), K_o and η_o value can relate each other by,

$$K_o = \frac{3-\eta_o}{3+2\eta_o} \tag{D.12}$$

In summary, the stress ratio and ratio of rate of stress are constant under K_o condition, that is,

$$\frac{q}{p'} = \frac{\dot{q}}{\dot{p}'} = \eta_o \tag{D.13}$$

D-3 The original Cam-clay model

The original Cam-clay model's yield function is expressed by,

$$f = MD\ln\left(\frac{p'}{p'_c}\right) + D\frac{q}{p'} \tag{D.14}$$

Dilatancy parameter is related to compression indices by,

$$D = \frac{\lambda-\kappa}{(1+e)M} \quad \text{where} \quad \Lambda = 1-\frac{\kappa}{\lambda} \quad \text{or} \quad \frac{\lambda-\kappa}{\kappa} = \frac{\Lambda}{1-\Lambda} \tag{D.15}$$

Evolution law for hardening parameter is expressed by,

$$\dot{p}'_c = \frac{p'_c}{MD}\dot{\varepsilon}_v^p \tag{D.16}$$

As a result, the partial derivatives of hardening variable are obtained as following,

$$\frac{\partial p'_c}{\partial \varepsilon_v^p} = \frac{p'_c}{MD}, \quad \frac{\partial p'_c}{\partial \varepsilon_s^p} = 0 \qquad\qquad\text{(D.17), (D.18)}$$

Derivatives of yield function with respect to stress tensor can be generally presented in terms of isotropic and deviatoric parts as,

$$\frac{\partial f}{\partial \boldsymbol{\sigma}'} = \frac{\partial f}{\partial p'}\frac{\partial p'}{\partial \boldsymbol{\sigma}'} + \frac{\partial f}{\partial q}\frac{\partial q}{\partial \boldsymbol{\sigma}'} = \frac{1}{3}\frac{\partial f}{\partial p'}\mathbf{1} + \sqrt{\frac{3}{2}}\frac{\partial f}{\partial q}\mathbf{n} \qquad\qquad\text{(D.19)}$$

where deviatoric stress tensor , unit deviatoric stress tensor and deviatoric stress are given by,

$$\mathbf{s} = \sqrt{\frac{2}{3}}q\mathbf{n}, \quad \mathbf{n} = \frac{\mathbf{s}}{\|\mathbf{s}\|}, \quad q = \sqrt{\frac{3}{2}}\|\mathbf{s}\| = \sqrt{\frac{3}{2}\mathbf{s}:\mathbf{s}} \qquad\qquad\text{(D.20), (D.21), (D.22)}$$

Derivatives of yield function with respect to isotropic pressure, deviatoric stress and hardening parameter are,

$$\frac{\partial f}{\partial p'} = \frac{D}{p'}\left(M - \frac{q}{p'}\right), \quad \frac{\partial f}{\partial q} = \frac{D}{p'}, \quad \frac{\partial f}{\partial p'_c} = -\frac{MD}{p'_c} \qquad\qquad\text{(D.23), (D.24), (D.25)}$$

D-4 Plastic rate of strain
By flow rule, the emerged rate of plastic strain is determined by,

$$\dot{\boldsymbol{\varepsilon}}^p = \gamma\frac{\partial f}{\partial \boldsymbol{\sigma}'} = \dot{\varepsilon}_v^p\mathbf{1} + \dot{\boldsymbol{\varepsilon}}_d^p \qquad\qquad\text{(D.26)}$$

Plastic rate of strain is conveniently expressed in terms of isotropic and deviatoric parts as,

$$\dot{\varepsilon}_v^p = \dot{\boldsymbol{\varepsilon}}^p : \mathbf{1} = \gamma\frac{\partial f}{\partial p'}, \quad \dot{\varepsilon}_s^p = \sqrt{\frac{2}{3}\dot{\boldsymbol{\varepsilon}}_d^p : \dot{\boldsymbol{\varepsilon}}_d^p} = \gamma\frac{\partial f}{\partial q} \qquad\qquad\text{(D.27), (D.28)}$$

where $\dot{\boldsymbol{\varepsilon}}_d^p = \mathbf{A} : \dot{\boldsymbol{\varepsilon}}^p = \gamma\sqrt{\frac{3}{2}}\frac{\partial f}{\partial q}\mathbf{n}$

By consistency condition, the below scalar equation can be obtained,

$$\dot{f} = \frac{\partial f}{\partial \boldsymbol{\sigma}'}:\dot{\boldsymbol{\sigma}}' + \frac{\partial f}{\partial p'_c}\dot{p}'_c = \left(\frac{1}{3}\frac{\partial f}{\partial p'}\mathbf{1} + \sqrt{\frac{3}{2}}\frac{\partial f}{\partial q}\mathbf{n}\right):\dot{\boldsymbol{\sigma}}' + \frac{\partial f}{\partial p'_c}\dot{p}'_c = \frac{\partial f}{\partial p'}\dot{p}' + \frac{\partial f}{\partial q}\dot{q} + \frac{\partial f}{\partial p'_c}\dot{p}'_c \qquad\text{(D.29)}$$

where $\dot{p}'_c = \frac{\partial p'_c}{\partial \varepsilon_v^p}\dot{\varepsilon}_v^p + \frac{\partial p'_c}{\partial \varepsilon_s^p}\dot{\varepsilon}_s^p$

According to (D.29), consistency parameter is able to be solved,

$$\frac{\partial f}{\partial p'}\dot{p}' + \frac{\partial f}{\partial q}\dot{q} + \frac{\partial f}{\partial p'_c}\dot{p}'_c = 0$$

$$\frac{\partial f}{\partial p'}\dot{p}' + \frac{\partial f}{\partial q}\dot{q} + \frac{\partial f}{\partial p'_c}\left(\frac{\partial p'_c}{\partial \varepsilon_v^p}\dot{\varepsilon}_v^p + \frac{\partial p'_c}{\partial \varepsilon_s^p}\dot{\varepsilon}_s^p\right) = 0$$

$$\frac{\partial f}{\partial p'}\dot{p}' + \frac{\partial f}{\partial q}\dot{q} + \gamma\frac{\partial f}{\partial p'_c}\left(\frac{\partial p'_c}{\partial \varepsilon_v^p}\frac{\partial f}{\partial p'} + \frac{\partial p'_c}{\partial \varepsilon_s^p}\frac{\partial f}{\partial q}\right) = 0 \qquad\qquad\text{(D.30)}$$

$$\gamma = -\frac{\dfrac{\partial f}{\partial p'}\dot{p}' + \dfrac{\partial f}{\partial q}\dot{q}}{\dfrac{\partial f}{\partial p'_c}\left(\dfrac{\partial p'_c}{\partial \varepsilon_v^p}\dfrac{\partial f}{\partial p'} + \dfrac{\partial p'_c}{\partial \varepsilon_s^p}\dfrac{\partial f}{\partial q}\right)}$$

According to Eq.(D.27), (D.28) and (D.30), rate of plastic strain are then obtained,

$$\begin{Bmatrix}\dot{\varepsilon}_v^p \\ \dot{\varepsilon}_s^p\end{Bmatrix} = \frac{-1}{\dfrac{\partial f}{\partial p'_c}\left(\dfrac{\partial p'_c}{\partial \varepsilon_v^p}\dfrac{\partial f}{\partial p'} + \dfrac{\partial p'_c}{\partial \varepsilon_s^p}\dfrac{\partial f}{\partial q}\right)}\begin{bmatrix}\dfrac{\partial f}{\partial p'}\dfrac{\partial f}{\partial p'} & \dfrac{\partial f}{\partial q}\dfrac{\partial f}{\partial p'} \\ \dfrac{\partial f}{\partial p'}\dfrac{\partial f}{\partial q} & \dfrac{\partial f}{\partial q}\dfrac{\partial f}{\partial q}\end{bmatrix}\begin{Bmatrix}\dot{p}' \\ \dot{q}\end{Bmatrix} \qquad\text{(D.31)}$$

D-5 K_o value in regard to the original Cam-clay model
Elastic parts of volumetric and deviatoric rate of strain are calculated by the stress-strain relationship,

$$\begin{Bmatrix} \dot{\varepsilon}_v^e \\ \dot{\varepsilon}_s^e \end{Bmatrix} = \begin{bmatrix} \dfrac{1}{K} & 0 \\ 0 & \dfrac{1}{3G} \end{bmatrix} \begin{Bmatrix} \dot{p}' \\ \dot{q} \end{Bmatrix} \tag{D.32}$$

Elastic bulk and shear moduli are reinstated as shown below,

$$K = \frac{p'}{\kappa}(1+e), \quad G = \mu' K \quad \text{where} \quad \mu' = \frac{G}{K} = \frac{3(1-2\nu')}{2(1+\nu')} \tag{D.33), (D.34}$$

Using the original Cam-clay plasticity, Eq.(D.30) can be substituted to,

$$\gamma = -\frac{\dfrac{D}{p'}\left(M - \dfrac{q}{p'}\right)\dot{p}' + \dfrac{D}{p'}\dot{q}}{-\dfrac{MD}{p'_c}\dfrac{p'_c}{MD}\dfrac{D}{p'}\left(M - \dfrac{q}{p'}\right)} = \frac{\left(M - \dfrac{q}{p'}\right)\dot{p}' + \dot{q}}{M - \dfrac{q}{p'}} = \frac{(M-\eta)\dot{p}' + \dot{q}}{M - \eta} \tag{D.35}$$

Referring to Eq.(D.31), the plastic strain rate governed by the original Cam-clay is given by,

$$\begin{Bmatrix} \dot{\varepsilon}_v^p \\ \dot{\varepsilon}_s^p \end{Bmatrix} = \frac{D}{p'} \begin{bmatrix} M-\eta & 1 \\ 1 & \dfrac{1}{M-\eta} \end{bmatrix} \begin{Bmatrix} \dot{p}' \\ \dot{q} \end{Bmatrix} \tag{D.36}$$

Accoring to Eq.(D.15) and (D.33), common term employed in Eq.(D.36) is reduced to,

$$\frac{D}{p'} = \frac{\Lambda}{1-\Lambda}\frac{\kappa}{(1+e)Mp'} = \frac{\Lambda}{1-\Lambda}\frac{1}{KM} \tag{D.37}$$

Summation of elastic and plastic parts leads to total rate of strain,

$$\begin{Bmatrix} \dot{\varepsilon}_v \\ \dot{\varepsilon}_s \end{Bmatrix}_{\eta=\eta_o} = \begin{Bmatrix} \dot{\varepsilon}_v^e + \dot{\varepsilon}_v^p \\ \dot{\varepsilon}_s^e + \dot{\varepsilon}_s^p \end{Bmatrix} = \begin{bmatrix} \dfrac{1}{K} + \dfrac{D}{p'}(M-\eta_o) & \dfrac{D}{p'} \\ \dfrac{D}{p'} & \dfrac{1}{3G} + \dfrac{D}{p'}\dfrac{1}{M-\eta_o} \end{bmatrix} \begin{Bmatrix} \dot{p}' \\ \eta_o \dot{p}' \end{Bmatrix} \tag{D.38}$$

Under K_o condition, volumetric and deviatoric parts of total strain rate are characterized by substituting Eq.(D.13) into Eq.(D.38),

$$\dot{\varepsilon}_v = \left(\frac{1}{K} + \frac{D}{p'}(M-\eta_o) + \frac{D}{p'}\eta_o\right)\dot{p}' = \frac{1}{K}\left(1 + \frac{\Lambda}{1-\Lambda}\right)\dot{p}' = \frac{1}{(1-\Lambda)K}\dot{p}' \tag{D.39}$$

$$\dot{\varepsilon}_s = \left(\frac{\eta_o}{3\mu' K} + \frac{D}{p'} + \frac{D}{p'(M-\eta_o)}\eta_o\right)\dot{p}' = \left(\frac{\eta_o}{3\mu'} + \frac{\Lambda}{(1-\Lambda)(M-\eta_o)}\right)\frac{\dot{p}'}{K} \tag{D.40}$$

Substitution of Eq.(D.39)-(D.40) into Eq.(D.6) results in,

$$\frac{(1-\Lambda)\eta_o}{3\mu'} + \frac{\Lambda}{M-\eta_o} = \frac{2}{3} \tag{D.41}$$

where elastic component can be seen by $\dfrac{(1-\Lambda)\eta_o}{3\mu'}$ while plastic component is seen by $\dfrac{\Lambda}{M-\eta_o}$.

By solving Eq.(D.41), η_o is obtained in complicated expression as,

$$\eta_o = \frac{1}{(2\cdot(1-\Lambda))}\cdot\left(M - \Lambda\cdot M + 2\cdot\mu' + \sqrt{M^2 - 2\cdot\Lambda\cdot M^2 - 4\cdot\mu'\cdot M + \Lambda^2\cdot M^2 + 4\cdot\Lambda\cdot M\cdot\mu' + 4\cdot\mu'^2 + 12\cdot\Lambda\cdot\mu' - 12\cdot\Lambda^2\cdot\mu'}\right)$$

In regard to Eq.(D.12), the corresponding K_o expression can be given by,

$$K_o = \frac{-1}{2}\cdot\frac{\left(-6\cdot\Lambda + 6 + \Lambda\cdot M - M - 2\cdot\mu' + \sqrt{\Lambda^2\cdot M^2 - 2\cdot\Lambda\cdot M^2 + 4\cdot\Lambda\cdot M\cdot\mu' + M^2 - 4\cdot\mu'\cdot M + 4\cdot\mu'^2 - 12\cdot\Lambda^2\cdot\mu' + 12\cdot\Lambda\cdot\mu'}\right)}{\left(3\cdot\Lambda - 3 + \Lambda\cdot M - M - 2\cdot\mu' + \sqrt{\Lambda^2\cdot M^2 - 2\cdot\Lambda\cdot M^2 + 4\cdot\Lambda\cdot M\cdot\mu' + M^2 - 4\cdot\mu'\cdot M + 4\cdot\mu'^2 - 12\cdot\Lambda^2\cdot\mu' + 12\cdot\Lambda\cdot\mu'}\right)}$$

Under particular consideration, the expression show in Eq.(D.41) can be reduced by,

Case (1): Purely plastic contribution

Substitute $\Lambda = 1$ into Eq.(D.41) then $\eta_o = M - \dfrac{3}{2}$; $K_o = \dfrac{9-2M}{4M}$ (D.42)

Case (2): Purely elastic contribution

Substitute $\Lambda = 0$ into Eq.(D.43) then $\eta_o = 2\mu'$; $K_o = \dfrac{\nu'}{1-\nu'}$ (D.43)

Case (3): Ignorance of elastic shear

Substitute $\mu' \to \infty$ into Eq.(D.41) then $\eta_o = M - \frac{3}{2}\Lambda$; $K_o = \frac{6 - 2M + 3\Lambda}{6 + 4M - 6\Lambda}$ (D.44)

Case (4): Corresponding Poisson's ratio to K_o value

Substitute $\mu' = \frac{\eta_o}{2}$ into Eq.(D.41) then $\eta_o = M - \frac{3}{2}$; $K_o = \frac{9 - 2M}{4M}$ (D.45)

D-6 K_o value in regard to the modified Cam-clay model

The modified Cam-clay model's yield function is given by,

$$f = q^2 - M^2 p'(p_c' - p') = 0$$ (D.46)

Evolution law for hardening parameter is similar to those of the original Cam-clay model's. Derivatives of yield function with respect to isotropic pressure, deviatoric stress and hardening parameter are,

$$\frac{\partial f}{\partial p'} = M^2(2p' - p_c') = p'(M^2 - \eta^2), \quad \frac{\partial f}{\partial q} = 2q, \quad \frac{\partial f}{\partial p_c'} = -M^2 p'$$ (D.47), (D.48), (D.49)

Using the original Cam-clay plasticity, Eq.(D.30) can be substituted to,

$$\gamma = -\frac{\frac{\partial f}{\partial p'}\dot{p}' + \frac{\partial f}{\partial q}\dot{q}}{\frac{\partial f}{\partial p_c'}\frac{\partial p_c'}{\partial \varepsilon_v^p}\frac{\partial f}{\partial p'}} = -\frac{p'(M^2 - \eta^2)\dot{p}' + 2q\dot{q}}{-M^2 p'\frac{p_c'}{MD}p'(M^2 - \eta^2)}$$

$$= \frac{\dot{p}' + \frac{2\eta\dot{q}}{M^2 - \eta^2}}{p'^2 \frac{M^2 - \eta^2}{MD}}$$ (D.50)

Referring to Eq.(D.31), the plastic strain rate governed by the original Cam-clay is given by,

$$\begin{Bmatrix} \dot{\varepsilon}_v^p \\ \dot{\varepsilon}_s^p \end{Bmatrix} = \frac{MD}{p'}\begin{bmatrix} 1 & \frac{2\eta}{M^2 - \eta^2} \\ \frac{2\eta}{M^2 - \eta^2} & \frac{4\eta^2}{(M^2 - \eta^2)^2} \end{bmatrix}\begin{Bmatrix} \dot{p}' \\ \dot{q} \end{Bmatrix}$$ (D.51)

Under K_o condition, volumetric and deviatoric parts of plastic strain rate are characterized by substituting Eq.(D.13) into Eq.(D.51),

$$\dot{\varepsilon}_v^p = \frac{MD}{p'}\left(1 + \frac{2\eta_o}{M^2 - \eta_o^2}\right)\dot{p}'$$ (D.52)

$$\dot{\varepsilon}_s^p = \frac{2\eta_o MD}{(M^2 - \eta_o^2)p'}\left(1 + \frac{2\eta_o^2}{M^2 - \eta_o^2}\right)\dot{p}'$$ (D.53)

The ratio of rate of plastic deviatoric to plastic volumetric strain can be found by,

$$\frac{\dot{\varepsilon}_s^p}{\dot{\varepsilon}_v^p} = \frac{2\eta_o}{M^2 - \eta_o^2}$$ (D.54)

The elastic volumetric and deviatoric strain increments under K_o-condition can be given by,

$$\begin{Bmatrix} \dot{\varepsilon}_v^e \\ \dot{\varepsilon}_s^e \end{Bmatrix}_{\eta = \eta_o} = \begin{bmatrix} \frac{\kappa}{1+e}\frac{1}{p'} & 0 \\ 0 & \frac{\kappa}{1+e}\frac{1}{3\mu'p'} \end{bmatrix}\begin{Bmatrix} \dot{p}' \\ \eta_o\dot{p}' \end{Bmatrix}$$ (D.55)

The ratio of rate of elastic deviatoric to plastic volumetric strain can be found by,

$$\left.\frac{\dot{\varepsilon}_s^e}{\dot{\varepsilon}_v^e}\right|_{\eta = \eta_o} = \frac{\eta_o}{3\mu'}$$ (D.56)

The ratio of volumetric rate of plastic strain to elastic strain in 1-D deformation can be obtained by using compression indices,

$$\frac{\dot{\varepsilon}_v^p}{\dot{\varepsilon}_v^e} = \frac{\kappa}{\lambda - \kappa} = \frac{\Lambda}{1 - \Lambda}$$ (D.57)

By definition of irreversibility ratio in 1-D deformation, the following relation is obtained,

$$\frac{\dot{\varepsilon}_v^p}{\dot{\varepsilon}_v} = \Lambda \tag{D.58}$$

According to elastic-plastic strain decomposition, rate of deviatoric strain is given by

$$\dot{\varepsilon}_s^e + \dot{\varepsilon}_s^p = \dot{\varepsilon}_s \tag{D.59}$$

Normalize Eq. (D.59) by rate of volumetric strain results in,

$$\frac{\dot{\varepsilon}_s^e}{\dot{\varepsilon}_v} + \frac{\dot{\varepsilon}_s^p}{\dot{\varepsilon}_v} = \frac{\dot{\varepsilon}_s^e}{\dot{\varepsilon}_v^e \left(1 + \frac{\dot{\varepsilon}_v^p}{\dot{\varepsilon}_v^e}\right)} + \frac{\dot{\varepsilon}_s^p}{\dot{\varepsilon}_v} \frac{\dot{\varepsilon}_v^p}{\dot{\varepsilon}_v^p} = \frac{\dot{\varepsilon}_s}{\dot{\varepsilon}_v} \tag{D.60}$$

Substitution of Eq.(D.6), (D.56), (D.57) and (D.58) into Eq. (D.60) yields,

$$\frac{(1-\Lambda)\eta_o}{3\mu'} + \frac{2\eta_o\Lambda}{M^2 - \eta_o^2} = \frac{2}{3} \tag{D.61}$$

where elastic component can be seen by $\dfrac{(1-\Lambda)\eta_o}{3\mu'}$ while plastic component is seen by $\dfrac{2\Lambda\eta_o}{M^2 - \eta_o^2}$.

Solution of Eq.(D.61) is extremely complicated, as a result, this expression can be reduced by considering particular cases,

Case (1): Purely plastic contribution

Substitute $\Lambda = 1$ into Eq.(D.61) then $\eta_o = \dfrac{\sqrt{9+4M^2}-3}{2}$; $K_o = \dfrac{9-\sqrt{9+4M^2}}{2\sqrt{9+4M^2}}$ \hfill (D.62)

Case (2): Purely elastic contribution

Substitute $\Lambda = 0$ into Eq. (D.61) then $\eta_o = 2\mu'$; $K_o = \dfrac{\nu'}{1-\nu'}$ \hfill (D.63)

Case (3): Ignorance of elastic shear

Substitute $\mu' \to \infty$ into Eq. (D.61) then $\eta_o = \dfrac{\sqrt{9\Lambda^2 + 4M^2} - 3\Lambda}{2}$;

$$K_o = \frac{6 + 3\Lambda - \sqrt{9\Lambda^2 + 4M^2}}{6 - 6\Lambda + 2\sqrt{9\Lambda^2 + 4M^2}} \tag{D.64}$$

Case (4): Corresponding Poisson's ratio to K_o value

Substitute $\mu' = \dfrac{\eta_o}{2}$ into Eq.(D.61) then $\eta_o = \dfrac{\sqrt{9+4M^2}-3}{2}$; $K_o = \dfrac{9-\sqrt{9+4M^2}}{2\sqrt{9+4M^2}}$ \hfill (D.65)

D-7 The singularity found in the SO model at K_o-line

The singularity in the SO model is found at the point where the direction of plastic flow which is coincided with the gradient of yield surface is undetermined. Referring to Appendix B, the gradient normal to the SO yield surface is determined by

$$\frac{\partial f}{\partial \boldsymbol{\sigma}'} = \frac{3D}{I_1}\left\{\beta\mathbf{1} + \sqrt{\frac{3}{2}}\bar{\mathbf{n}}\right\} \tag{D.66}$$

where $\beta = M - 3\dfrac{\sqrt{3\bar{J}_2}}{I_1} - \sqrt{\dfrac{3}{2}}(\boldsymbol{\eta}_c : \bar{\mathbf{n}})$, $\bar{\mathbf{n}} = \dfrac{\bar{\mathbf{s}}}{\sqrt{2\bar{J}_2}}$

For a particular point $\boldsymbol{\sigma}' = \boldsymbol{\sigma}'_c$, the relative stress deviator is

$$\bar{\mathbf{s}}\big|_{\boldsymbol{\sigma}'=\boldsymbol{\sigma}'_c} = \mathbf{s} - p'\boldsymbol{\eta}_c\big|_{\boldsymbol{\sigma}'=\boldsymbol{\sigma}'_c} = \mathbf{s}_c - p'_c\,\boldsymbol{\eta}_c = \mathbf{0} \tag{D.67}$$

$$\bar{J}_2\big|_{\boldsymbol{\sigma}'=\boldsymbol{\sigma}'_c} = \frac{1}{2}\bar{\mathbf{s}} : \bar{\mathbf{s}}\bigg|_{\boldsymbol{\sigma}'=\boldsymbol{\sigma}'_c} = 0 \tag{D.68}$$

As a result, $\bar{\mathbf{n}}$ and β in Eq.(D.66) are undetermined at the point $\boldsymbol{\sigma}' = \boldsymbol{\sigma}'_c$ and the gradient of the SO yield surface is not continuous at the corner.

D-8 K_o value in regard to the Sekiguchi-Ohta model

The formulation of incremental stress-strain relation of two stress invariants p' and q during K_o-consolidation can be given by,

$$\begin{Bmatrix} \dot{p}\,' \\ \dot{q} \end{Bmatrix} = \begin{bmatrix} K & 0 \\ 0 & 3G \end{bmatrix} \cdot \begin{Bmatrix} \dot{\varepsilon}_v - \dot{\varepsilon}_v^p \\ \dot{\varepsilon}_s - \dot{\varepsilon}_s^p \end{Bmatrix} \tag{D.69}$$

According to Chapter 4, for a state of stress adjacent to the corner, manipulation for η_o can be compacted by polynomial form,

$$\begin{bmatrix} 2\mu\,'M^4 - 18\mu\,'^3\Lambda^2 \\ 9\mu\,'\Lambda^2 + 2M^4\Lambda - M^4 - 6\mu\,'\Lambda M^2 \\ 2\mu\,'\Lambda^2 M^2 - 12\mu\,'^2\Lambda^2 - 2\mu\,'M^2 \\ M^2 - 2\Lambda M^2 - \Lambda^2 M^2 + 6\mu\,'\Lambda^2 \\ -2\mu\,'\Lambda^2 \\ \Lambda^2 \end{bmatrix} \cdot \begin{bmatrix} 1 \\ \eta_o \\ \eta_o^2 \\ \eta_o^3 \\ \eta_o^4 \\ \eta_o^5 \end{bmatrix} = 0 \tag{D.70}$$

By the assumption that mobilized K_o state gradually approaches to immobilized K_o state for the eventually stabilized state, the relation between Poisson's ratio and K_o value in Eq.(D.71) derived previously under immobilized K_o state would be commonly hold by Eq.(D.70). The equivalent form of Eq.(D.71) can be given by Eq.(D.72) as the relation between η_o and ratio of G/K. Substitution of Eq.(D.72) into Eq.(D.70) reduced the fifth-degree polynomial expression to third-degree as shown in Eq.(D.73)

$$\nu\,' = \frac{K_o}{1+K_o}, \quad \mu\,' = \frac{\eta_o}{2} \tag{D.71}, (D.72)$$

$$\Lambda\eta_o M^2 (2M^2 - 3\eta_o - 2\eta_o^2) = 0 \tag{D.73}$$

Third degree of polynomial expression would give three roots of solution. Correspondingly, the solutions for η_o are displayed in Eq.(D.74)

$$\eta_o = \begin{Bmatrix} 0 \\ \dfrac{-3}{4} - \dfrac{1}{4}\sqrt{9+16M^2} \\ \dfrac{-3}{4} + \dfrac{1}{4}\sqrt{9+16M^2} \end{Bmatrix} \tag{D.74}$$

Using the direction relation between η_o and K_o, K_o values in corresponding to expressions in Eq.(D.74) can be obtained by Eq.(D.75). It is denoted that the conjugate multiplication of denominator can change a form of expression as illustrated in Eq.(D.76).

$$K_o = \begin{Bmatrix} 1 \\ \dfrac{15+\sqrt{9+16M^2}}{6-2\sqrt{9+16M^2}} \\ \dfrac{15-\sqrt{9+16M^2}}{6+2\sqrt{9+16M^2}} \end{Bmatrix} = \begin{Bmatrix} 1 \\ \dfrac{-\left(9\sqrt{9+16M^2}+8M^2+27\right)}{16M^2} \\ \dfrac{9\sqrt{9+16M^2}-8M^2-27}{16M^2} \end{Bmatrix} \tag{D.75}$$

where

$$\frac{15-\sqrt{9+16M^2}}{6+2\sqrt{9+16M^2}} = \frac{15-\sqrt{9+16M^2}}{2\left(3+\sqrt{9+16M^2}\right)} \cdot \frac{3-\sqrt{9+16M^2}}{3-\sqrt{9+16M^2}}$$

$$= \frac{15-\sqrt{9+16M^2}}{2\left(3^2-\left(9+16M^2\right)\right)} \cdot \left(3-\sqrt{9+16M^2}\right) \tag{D.76}$$

$$= \frac{-27+9\sqrt{9+16M^2}-8M^2}{16M^2}$$

In regard to the solutions obtained in Eq.(D.75), $K_o=1$ gives the possible maximum value available for fully elastic material where Poisson's ratio equals to 0.5, signifying a material likes liquid or slurry. This solution is considered as impossible root. Another solution gives a minus K_o value. As a result, there is only root left and considered as the possible solution for K_o value. In order to explore the predicted range of K_o values obtained by Eq.(D.75), plots of predicted K_o expressions are shown in Fig D-1. It is obvious that Eq.(D.77) is the solely reasonable root of the solution.

$$K_o = \frac{15 - \sqrt{9 + 16M^2}}{6 + 2\sqrt{9 + 16M^2}} = \frac{9\sqrt{9 + 16M^2} - 8M^2 - 27}{16M^2} \tag{D.77}$$

The predicted value of K_o in Eq.(D.77) indicates the relation between K_o value and internal friction angle ϕ'. Moreover, Poisson's ratio is also able to related to ϕ' via M by using Eqs.(D.71), (D.77) as shown below,

$$\nu' = \frac{9\sqrt{9 + 16M^2} - 8M^2 - 27}{9\sqrt{9 + 16M^2} + 8M^2 - 27} \tag{D.78}$$

Values of K_o and ν' for an extremely low friction angle like those of slurry can be achieved by taking a limit of Eq.(D.77) and (D.78) when M converge to zero as,

$$\lim_{M \to 0} \frac{15 - \sqrt{9 + 16M^2}}{6 + 2\sqrt{9 + 16M^2}} = 1, \qquad \lim_{M \to 0} \frac{9\sqrt{9 + 16M^2} - 8M^2 - 27}{9\sqrt{9 + 16M^2} + 8M^2 - 27} = \frac{1}{2} \tag{D.79, D.80}$$

The above results show a reasonable values, e.g., when $\phi'=0$, M=0, then $K_o=1$ and $\nu'=0.5$.
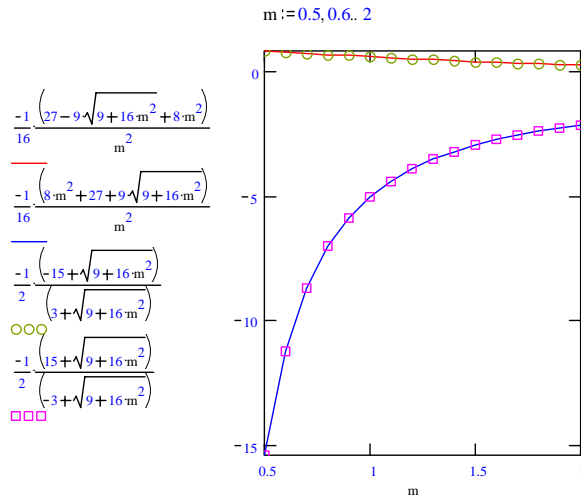
Figure D-1: A monitored range of theoretical K_o values varied by practical range of Critical state parameter

D-9 K_o expressions in regard to various Critical state models

K_o expressions evaluated by original Cam-clay, modified Cam-clay and Sekiguchi-Ohta models under particular case (4) as shown in Eq.(D.45), (D.65) and (D.77) respectively are plotted in Figure D-2. It is found that expression given by Sekiguchi-Ohta model rather matches with Jaky's correlation than others.
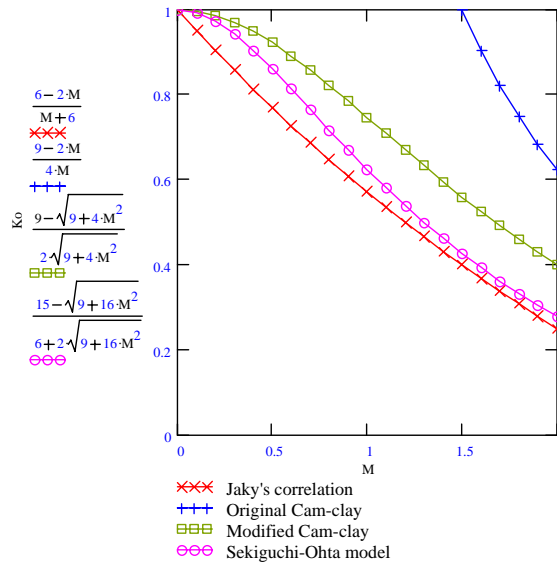
Figure D-2: K_o expressions given by various Critical state models

Appendix E: Soil elasticity

E-1 Stress and strain components

An effective stress can be written in form of mean stress and stress deviator as,

$$\boldsymbol{\sigma}' = p'\mathbf{1} + \mathbf{s} \tag{E.1}$$

Mean stress and stress deviator can be obtained by,

$$p' = \frac{1}{3}\mathbf{1}:\boldsymbol{\sigma}', \quad \mathbf{s} = \mathbf{A}:\boldsymbol{\sigma}' \tag{E.2},(E.3)$$

Correspondingly, an elastic strain can be written in form of volumetric strain and strain deviator as,

$$\boldsymbol{\varepsilon}^e = \frac{1}{3}\varepsilon_v^e\mathbf{1} + \boldsymbol{\varepsilon}_d^e \tag{E.4}$$

Volumetric strain and strain deviator can be obtained by,

$$\boldsymbol{\varepsilon}_v^e = \mathbf{1}:\boldsymbol{\varepsilon}^e, \quad \boldsymbol{\varepsilon}_d^e = \mathbf{A}:\boldsymbol{\varepsilon}^e \tag{E.5},(E.6)$$

Deviatoric stress and strain are defined by,

$$q = \sqrt{\frac{3}{2}}\|\mathbf{s}\|, \quad \varepsilon_s^e = \sqrt{\frac{2}{3}}\|\boldsymbol{\varepsilon}_d^e\| \tag{E.7},(E.8)$$

Unit normal of stress deviator and strain deviator are defined by,

$$\mathbf{n} = \frac{\mathbf{s}}{\|\mathbf{s}\|}, \quad \mathbf{m} = \frac{\boldsymbol{\varepsilon}_d^e}{\|\boldsymbol{\varepsilon}_d^e\|} \tag{E.9),~(E.10)$$

Using Eq.(E.9) and (E.7), Eq.(E.1) can be written as,

$$\boldsymbol{\sigma}' = p'\mathbf{1} + \sqrt{\frac{2}{3}}q\mathbf{n} \tag{E.11}$$

E-2 Linear stiffness moduli

For an isotropic material obeyed Hooke's law, linear stiffness moduli can given in terms of bulk and shear moduli. Relations between mean stress and volumetric strain, stress deviator and strain deviator are given by Eq.(E.12).

$$p' = K\varepsilon_v^e, \quad \mathbf{s} = 2G\boldsymbol{\varepsilon}_d^e \tag{E.12),(E.13)$$

Substituting of $\mathbf{s}$ and $\boldsymbol{\varepsilon}^e_{\mathbf{d}}$ in Eq.(E.13) by $\mathbf{s}$ from Eq.(E.9) and $\boldsymbol{\varepsilon}^e_{\mathbf{d}}$ from Eq.(E.10), obtain

$$\|\mathbf{s}\|\mathbf{n} = 2G\|\boldsymbol{\varepsilon}_d^e\|\mathbf{m} \tag{E.14}$$

From above equation, it is found that $\mathbf{m}=\mathbf{n}$, that is, linear elastic stress-strain relation is coaxial. Using Eq.(E.7),(E.8), a scalar of Eq.(E.14) can be expressed as,

$$q = 3G\varepsilon_s^e \tag{E.15}$$

The corresponding elastic tangential tensor can be derived by taking a derivative of stress in Eq.(E.1) by elastic strain. According to chain rule and Eq.(E.12),(E.13), the forth-order tensor of elastic tangential operator can be obtained in terms of bulk and shear components.

$$\mathbf{c}^e = \frac{\partial\boldsymbol{\sigma}'}{\partial\boldsymbol{\varepsilon}^e} = \mathbf{1}\otimes\frac{\partial p'}{\partial\boldsymbol{\varepsilon}^e} + \frac{\partial\mathbf{s}}{\partial\boldsymbol{\varepsilon}^e} \quad \text{where} \quad \frac{\partial\mathbf{s}}{\partial\boldsymbol{\varepsilon}^e} = 2G\frac{\partial\boldsymbol{\varepsilon}_d^e}{\partial\boldsymbol{\varepsilon}^e}$$

$$= \mathbf{1}\otimes\frac{\partial p'}{\partial\varepsilon_v^e}\frac{\partial\varepsilon_v^e}{\partial\boldsymbol{\varepsilon}^e} + 2G\frac{\partial\boldsymbol{\varepsilon}_d^e}{\partial\boldsymbol{\varepsilon}^e} \quad \text{where} \quad \frac{\partial p'}{\partial\varepsilon_v^e} = K, \quad \frac{\partial\varepsilon_v^e}{\partial\boldsymbol{\varepsilon}^e} = \mathbf{1}, \quad \frac{\partial\boldsymbol{\varepsilon}_d^e}{\partial\boldsymbol{\varepsilon}^e} = \mathbf{A}$$

$$= K\mathbf{1}\otimes\mathbf{1} + 2G\mathbf{A} \tag{E.16}$$

If one derive an elastic tangential tensor by taking a derivative of stress in Eq.(E.11) by elastic strain using chain rule and Eq.(E.12)-(E.15), the same result is. (See directional derivative in Appendix A)

$$\mathbf{c}^e = \frac{\partial\boldsymbol{\sigma}'}{\partial\boldsymbol{\varepsilon}^e} = \mathbf{1}\otimes\frac{\partial p'}{\partial\boldsymbol{\varepsilon}^e} + \sqrt{\frac{2}{3}}\mathbf{n}\otimes\frac{\partial q}{\partial\boldsymbol{\varepsilon}^e} + \sqrt{\frac{2}{3}}q\frac{\partial\mathbf{n}}{\partial\mathbf{s}}:\frac{\partial\mathbf{s}}{\partial\boldsymbol{\varepsilon}^e}$$

$$= \mathbf{1}\otimes\frac{\partial p'}{\partial\varepsilon_v^e}\frac{\partial\varepsilon_v^e}{\partial\boldsymbol{\varepsilon}^e} + \sqrt{\frac{2}{3}}\mathbf{n}\otimes\frac{\partial q}{\partial\varepsilon_s^e}\frac{\partial\varepsilon_s^e}{\partial\boldsymbol{\varepsilon}_d^e}:\frac{\partial\boldsymbol{\varepsilon}_d^e}{\partial\boldsymbol{\varepsilon}^e} + \sqrt{\frac{2}{3}}q\frac{1}{\|\mathbf{s}\|}[\mathbf{I}-\mathbf{n}\otimes\mathbf{n}]:2G\mathbf{A}$$

$$= K\mathbf{1}\otimes\mathbf{1} + \sqrt{\frac{2}{3}}\mathbf{n}\otimes3G\sqrt{\frac{2}{3}}\mathbf{n}:\mathbf{A} + 2G[\mathbf{A}-\mathbf{n}\otimes\mathbf{n}]$$

$$= K\mathbf{1}\otimes\mathbf{1} + 2G\mathbf{n}\otimes\mathbf{n} + 2G[\mathbf{A}-\mathbf{n}\otimes\mathbf{n}]$$

$$= K\mathbf{1}\otimes\mathbf{1} + 2G\mathbf{A}$$

In practice, K and G are determined from initial preconsolidated pressure and keep G/K constant.

E-3 Nonlinear stiffness moduli (secant moduli)

According to e-log(p') relation obtained from triaxial tests, rate of change between mean stress volumetric strain can be related by,

$$\dot{p}' = K(p')\dot{\varepsilon}_v^e \qquad \text{where} \quad K(p') = \frac{p'}{\bar{\kappa}}, \quad \bar{\kappa} = \frac{\kappa}{1+e_o} \qquad (E.17),(E.18),(E.19)$$

By keeping G/K constant, shear modulus can be related to bulk modulus and rate of stress deviator can be expressed as,

$$\dot{\mathbf{s}} = 2G(p')\dot{\boldsymbol{\varepsilon}}_d^e \qquad \text{where} \quad G(p') = \mu' K(p'), \quad \mu' = \frac{3(1-2v')}{2(1+v')} \qquad (E.20),(E.21),(E.22)$$

Application of forward-Euler difference to Eq.(E.17),(E.20) gives an incremental form of stress-strain relation by taking subscript n as a previous step and n+1 as a new step.

$$p'_{n+1} - p'_n = K(p'_n)(\varepsilon_{v\,n+1}^e - \varepsilon_{v\,n}^e) = K_n \Delta\varepsilon_v^e \qquad (E.23)$$

$$\mathbf{s}_{n+1} - \mathbf{s}_n = 2G(p'_n)\left\{\boldsymbol{\varepsilon}_{d\,n+1}^e - \boldsymbol{\varepsilon}_{d\,n}^e\right\} = 2G_n \Delta\boldsymbol{\varepsilon}_d^e \qquad (E.24)$$

By the same manner, application of backward-Euler difference to Eq.(E.17),(E.20) gives an incremental form of stress-strain relation as,

$$p'_{n+1} - p'_n = K(p'_{n+1})\left(\varepsilon_{v\,n+1}^e - \varepsilon_{v\,n}^e\right) = K_{n+1} \Delta\varepsilon_v^e \qquad (E.25)$$

$$\mathbf{s}_{n+1} - \mathbf{s}_n = 2G(p'_{n+1})\left\{\boldsymbol{\varepsilon}_{d\,n+1}^e - \boldsymbol{\varepsilon}_{d\,n}^e\right\} = 2G_{n+1} \Delta\boldsymbol{\varepsilon}_d^e \qquad (E.26)$$

The elastic response given by Eq.(E.23),(E.24) is under-estimated while those in Eq. (E.25),(E.26) is over-estimated. However, the more reasonable results can be obtained by a direct integration of Eq.(E.17) where a differential form can be written by,

$$\frac{\dot{p}'}{p'} = \frac{1}{\bar{\kappa}}\dot{\varepsilon}_v^e$$

Taking a definite integral from time step n to n+1 results in a closed-form solution for incremental stress-strain relation given by equations below,

$$\int_{p'_n}^{p'_{n+1}} \frac{1}{p'} dp' = \frac{1}{\bar{\kappa}} \int_{\varepsilon_{v\,n}^e}^{\varepsilon_{v\,n+1}^e} d\varepsilon_v^e$$

$$\ln\left(\frac{p'_{n+1}}{p'_n}\right) = \frac{1}{\bar{\kappa}}\left(\varepsilon_{v\,n+1}^e - \varepsilon_{v\,n}^e\right)$$

$$\varepsilon_{v\,n+1}^e - \varepsilon_{v\,n}^e = \bar{\kappa}\ln\left(\frac{p'_{n+1}}{p'_n}\right) \qquad (E.27)$$

The updated mean stress can be evaluated directly by,

$$p'_{n+1} = p'_n \exp\left(\frac{\varepsilon_{v\,n+1}^e - \varepsilon_{v\,n}^e}{\bar{\kappa}}\right) \qquad (E.28)$$

As a result, secant moduli between time step n and n+1 can be evaluated using Eq.(E.27) by,

$$K_s = K_s(p'_{n+1}, p'_n) = \frac{p'_{n+1} - p'_n}{\varepsilon_{v\,n+1}^e - \varepsilon_{v\,n}^e} = \frac{p'_{n+1} - p'_n}{\bar{\kappa}\ln\left(\frac{p'_{n+1}}{p'_n}\right)} \qquad (E.29)$$

$$G_s = G_s(p'_{n+1}, p'_n) = \mu' K_s(p'_{n+1}, p'_n) \qquad (E.30)$$

Secant moduli are step-dependent. The initial response where singularity takes place can be evaluated by taking limit of Eq.(E.29)

$$K_s(p'_n, p'_n) = \lim_{p'_{n+1} \to p'_n} K_s(p'_{n+1}, p'_n) = \frac{p'_n}{\bar{\kappa}} \qquad (E.31)$$

An incremental stress-strain relation can be given in terms of secant moduli by,

$$p'_{n+1} - p'_n = K_s(p'_{n+1}, p'_n)\left(\varepsilon_{v\,n+1}^e - \varepsilon_{v\,n}^e\right) \qquad (E.32)$$

$$\mathbf{s}_{n+1} - \mathbf{s}_n = 2G_s(p'_{n+1}, p'_n)\left\{\boldsymbol{\varepsilon}_{d\,n+1}^e - \boldsymbol{\varepsilon}_{d\,n}^e\right\} \qquad (E.33)$$

Updated stress can be expressed by

$$p'_{n+1} = p'_n + K_s \Delta\varepsilon_v^e = p'_n \exp\left(\frac{\Delta\varepsilon_v^e}{\bar{\kappa}}\right) \qquad \text{where} \quad \Delta\varepsilon_v^e = \varepsilon_{v\,n+1}^e - \varepsilon_{v\,n}^e \,, \quad \frac{\partial\Delta\varepsilon_v^e}{\partial\boldsymbol{\varepsilon}_{n+1}^e} = \mathbf{1} \tag{E.34}$$

$$\mathbf{s}_{n+1} = \mathbf{s}_n + 2G_s \Delta\boldsymbol{\varepsilon}_d^e \qquad \text{where} \quad \Delta\boldsymbol{\varepsilon}_d^e = \boldsymbol{\varepsilon}_{d\,n+1}^e - \boldsymbol{\varepsilon}_{d\,n}^e \,, \quad \frac{\partial\Delta\boldsymbol{\varepsilon}_d^e}{\partial\boldsymbol{\varepsilon}_{n+1}^e} = \mathbf{A} \tag{E.35}$$

Elastic tangential tensor for updated state is determined by

$$\mathbf{c}_{n+1}^e = \frac{\partial\boldsymbol{\sigma}_{n+1}}{\partial\boldsymbol{\varepsilon}_{n+1}^e} = \mathbf{1}\otimes\frac{\partial p'_{n+1}}{\partial\boldsymbol{\varepsilon}_{n+1}^e} + \frac{\partial\mathbf{s}_{n+1}}{\partial\boldsymbol{\varepsilon}_{n+1}^e} \tag{E.36}$$

According to Eq.(E.34) and (E.35), the derivative of p'$_{n+1}$ and s$_{n+1}$ in regard to elastic strain tensor are given by,

$$\frac{\partial p'_{n+1}}{\partial\boldsymbol{\varepsilon}_{n+1}^e} = \frac{p'_n}{\bar{\kappa}} \exp\left(\frac{\Delta\varepsilon_v^e}{\bar{\kappa}}\right) \frac{\partial\Delta\varepsilon_v^e}{\partial\boldsymbol{\varepsilon}_{n+1}^e} = \frac{p'_{n+1}}{\bar{\kappa}}\mathbf{1} = K_{n+1}\mathbf{1} \tag{E.37}$$

$$\text{where} \quad K_{n+1} = \frac{p'_{n+1}}{\bar{\kappa}} \tag{E.38}$$

$$\frac{\partial\mathbf{s}_{n+1}}{\partial\boldsymbol{\varepsilon}_{n+1}^e} = 2\Delta\boldsymbol{\varepsilon}_d^e \otimes \frac{\partial G_s}{\partial\boldsymbol{\varepsilon}_{n+1}^e} + 2G_s\frac{\partial\Delta\boldsymbol{\varepsilon}_d^e}{\partial\boldsymbol{\varepsilon}_{n+1}^e} = 2\mu'\Delta\boldsymbol{\varepsilon}_d^e \otimes\frac{\partial K_s}{\partial\boldsymbol{\varepsilon}_{n+1}^e} + 2G_s\mathbf{A} \tag{E.39}$$

where the variation of K$_s$ in Eq.(E.29) with respect to ε_{n+1}^e is obtained as,

$$\frac{\partial K_s}{\partial\boldsymbol{\varepsilon}_{n+1}^e} = \frac{\partial K_s}{\partial p'_{n+1}}\frac{\partial p'_{n+1}}{\partial\boldsymbol{\varepsilon}_{n+1}^e} = \left(\frac{1}{\bar{\kappa}\ln\left(\dfrac{p'_{n+1}}{p'_n}\right)} - \frac{p'_{n+1}-p'_n}{\bar{\kappa}\ln\left(\dfrac{p'_{n+1}}{p'_n}\right)^2 p'_{n+1}}\right)K_{n+1}\mathbf{1}$$

$$= \frac{K_s}{\dfrac{p'_{n+1}}{\bar{\kappa}}}\left(\frac{\dfrac{p'_{n+1}}{\bar{\kappa}}-K_s}{p'_{n+1}-p'_n}\right)K_{n+1}\mathbf{1} = K_s\left(\frac{K_{n+1}-K_s}{p'_{n+1}-p'_n}\right)\mathbf{1} \tag{E.40}$$

$$\lim_{p'_{n+1}\to p'_n}\frac{\partial K_s}{\partial\boldsymbol{\varepsilon}_{n+1}^e} = \frac{p'_n}{2\bar{\kappa}^2} \qquad \text{(in particular)} \tag{E.41}$$

Eq.(E.40) can be further reduced by substituting K$_s$ from Eq.(E.29). Eq.(E.42) reaches the same expression given by Borja, R.I. (1991)

$$\frac{\partial K_s}{\partial\boldsymbol{\varepsilon}_{n+1}^e} = \frac{p'_{n+1}-p'_n}{\Delta\varepsilon_v^e}\left(\frac{K_{n+1}-K_s}{p'_{n+1}-p'_n}\right)\mathbf{1}$$

$$= \frac{K_{n+1}-K_s}{\Delta\varepsilon_v^e}\mathbf{1} \tag{E.42}$$

Substitution of Eq.(E.37),(E.39) into Eq.(E.36) obtains the elastic tangential tensor as,

$$\mathbf{c}_{n+1}^e = K_{n+1}\mathbf{1}\otimes\mathbf{1} + 2G_s\mathbf{A} + 2\mu'\frac{\partial K_s}{\partial\boldsymbol{\varepsilon}_{n+1}^e}\Delta\boldsymbol{\varepsilon}_d^e\otimes\mathbf{1} \tag{E.43}$$

Derivation shown below deduces Eq.(E.43) to the same expression given by Borja, R.I. (1991) as,

$$\mathbf{c}_{n+1}^e = K_s\mathbf{1}\otimes\mathbf{1} + 2G_s\mathbf{A} + 2\mu'\frac{\partial K_s}{\partial\boldsymbol{\varepsilon}_{n+1}^e}\Delta\boldsymbol{\varepsilon}_d^e\otimes\mathbf{1} + \frac{\Delta\varepsilon_v^e}{\Delta\varepsilon_v^e}\left(K_{n+1}-K_s\right)\mathbf{1}\otimes\mathbf{1}$$

$$= K_s\mathbf{1}\otimes\mathbf{1} + 2G_s\mathbf{A} + 2\mu'\frac{\partial K_s}{\partial\boldsymbol{\varepsilon}_{n+1}^e}\Delta\boldsymbol{\varepsilon}_d^e\otimes\mathbf{1} + \frac{\partial K_s}{\partial\boldsymbol{\varepsilon}_{n+1}^e}\Delta\varepsilon_v^e\mathbf{1}\otimes\mathbf{1}$$

$$= K_s\mathbf{1}\otimes\mathbf{1} + 2G_s\mathbf{A} + \frac{\partial K_s}{\partial\boldsymbol{\varepsilon}_{n+1}^e}\left[\Delta\varepsilon_v^e\mathbf{1}\otimes\mathbf{1} + 2\mu'\Delta\boldsymbol{\varepsilon}_d^e\otimes\mathbf{1}\right] \tag{E.44}$$

$$= K_s\left[\mathbf{1}\otimes\mathbf{1} + 2\mu'\mathbf{A}\right] + \frac{\partial K_s}{\partial\boldsymbol{\varepsilon}_{n+1}^e}\left[\mathbf{1}\otimes\mathbf{1} + 2\mu'\mathbf{A}\right]:\Delta\boldsymbol{\varepsilon}^e\otimes\mathbf{1}$$

$$= K_s\hat{\mathbf{c}}^e + \frac{\partial K_s}{\partial\boldsymbol{\varepsilon}_{n+1}^e}\hat{\mathbf{c}}^e:\Delta\boldsymbol{\varepsilon}^e\otimes\mathbf{1}$$

$$\text{where} \quad \hat{\mathbf{c}}^e = \mathbf{1}\otimes\mathbf{1} + 2\mu'\mathbf{A} \tag{E.45}$$

It is noted that for an initial state (t$_n$), an elastic tangential tensor is given using forward-Euler difference as,

$$\mathbf{c}_n^e = K_n\mathbf{1}\otimes\mathbf{1} + 2G_n\mathbf{A} \tag{E.46}$$

In this study, the semi-backward Euler is implemented; therefore, the high order of backward incremental terms

is omitted in the derivative. Eq. (E.43) is simplified by ignoring deviatoric elastic strain increment part $2\mu'\dfrac{\partial K_s}{\partial \boldsymbol{\varepsilon}^e_{n+1}}\Delta\boldsymbol{\varepsilon}^e_d \otimes \mathbf{1}$ to reduce the number of tensor basis, the following expression is employed instead.

$$\mathbf{c}^e_{sn+1} = K_{n+1}\mathbf{1}\otimes\mathbf{1} + 2G_s\mathbf{A} \tag{E.47}$$

The semi-backward Euler form of Eq.(E.47) can be interpreted in the sense that, the tensor basis is based on the state at t=t$_n$ but the scalar identity is based on the state at t=t$_{n+1}$.

Appendix F: Linearization

F-1 Second derivatives of the Sekiguchi-Ohta yield function with respect to invariants
Apply chain rule to the first derivatives derived in Appendix B-5 as shown below,

$$\frac{\partial^2 f}{\partial I_1 \partial I_1} = \frac{\partial}{\partial I_1}\left(\frac{\partial f}{\partial I_1}\right) = \frac{\partial}{\partial I_1}\left(\frac{MD}{I_1} - 3\frac{\sqrt{3\bar{J}_2}\,D}{I_1^2}\right) = -\frac{MD}{I_1^2} + \frac{6D\sqrt{3\bar{J}_2}}{I_1^3} \tag{F.1}$$

$$\frac{\partial^2 f}{\partial \bar{J}_2 \partial I_1} = \frac{\partial}{\partial \bar{J}_2}\left(\frac{\partial f}{\partial I_1}\right) = \frac{\partial}{\partial \bar{J}_2}\left(\frac{MD}{I_1} - 3\frac{\sqrt{3\bar{J}_2}\,D}{I_1^2}\right) = -\frac{9D}{2I_1^2\sqrt{3\bar{J}_2}} \tag{F.2}$$

$$\frac{\partial^2 f}{\partial I_1 \partial \bar{J}_2} = \frac{\partial}{\partial I_1}\left(\frac{\partial f}{\partial \bar{J}_2}\right) = \frac{\partial}{\partial I_1}\left(\frac{9D}{2I_1\sqrt{3\bar{J}_2}}\right) = -\frac{9D}{2I_1^2\sqrt{3\bar{J}_2}} \tag{F.3}$$

$$\frac{\partial^2 f}{\partial \bar{J}_2 \partial \bar{J}_2} = \frac{\partial}{\partial \bar{J}_2}\left(\frac{\partial f}{\partial \bar{J}_2}\right) = \frac{\partial}{\partial \bar{J}_2}\left(\frac{9D}{2I_1\sqrt{3\bar{J}_2}}\right) = -\frac{9D}{4I_1\bar{J}_2\sqrt{3\bar{J}_2}} \tag{F.4}$$

Note that in regard to a smooth function; $\dfrac{\partial^2 f}{\partial I_1 \partial \bar{J}_2} = \dfrac{\partial^2 f}{\partial \bar{J}_2 \partial I_1} = -\dfrac{1}{I_1}\dfrac{\partial f}{\partial \bar{J}_2}$ (F.5)

F-2 Second derivatives of the Sekiguchi-Ohta yield function with respect to stress tensor
Referring to Appendix B-5 accompanied by chain rule, the second-order derivative is

$$\frac{\partial^2 f}{\partial \boldsymbol{\sigma}'\partial \boldsymbol{\sigma}'} = \frac{\partial\left(\dfrac{\partial f}{\partial I_1}\dfrac{\partial I_1}{\partial \boldsymbol{\sigma}'} + \dfrac{\partial f}{\partial \bar{J}_2}\dfrac{\partial \bar{J}_2}{\partial \boldsymbol{\sigma}'}\right)}{\partial \boldsymbol{\sigma}'} = \left[\frac{\partial I_1}{\partial \boldsymbol{\sigma}'}\otimes\frac{\partial^2 f}{\partial \boldsymbol{\sigma}'\partial I_1}\right] + \left[\frac{\partial f}{\partial I_1}\frac{\partial^2 I_1}{\partial \boldsymbol{\sigma}'\partial \boldsymbol{\sigma}'}\right] + \left[\frac{\partial \bar{J}_2}{\partial \boldsymbol{\sigma}'}\otimes\frac{\partial^2 f}{\partial \boldsymbol{\sigma}'\partial \bar{J}_2}\right] + \left[\frac{\partial f}{\partial \bar{J}_2}\frac{\partial^2 \bar{J}_2}{\partial \boldsymbol{\sigma}'\partial \boldsymbol{\sigma}'}\right] \tag{F.6}$$

where the second-order derivatives of invariants are

$$\frac{\partial^2 I_1}{\partial \boldsymbol{\sigma}'\partial \boldsymbol{\sigma}'} = \frac{\partial}{\partial \boldsymbol{\sigma}'}\left(\frac{\partial I_1}{\partial \boldsymbol{\sigma}'}\right) = \frac{\partial}{\partial \boldsymbol{\sigma}'}(\mathbf{1}) = \mathbf{0} \tag{F.7}$$

$$\frac{\partial^2 \bar{J}_2}{\partial \boldsymbol{\sigma}'\partial \boldsymbol{\sigma}'} = \frac{\partial}{\partial \boldsymbol{\sigma}'}\left(\frac{\partial \bar{J}_2}{\partial \boldsymbol{\sigma}'}\right) = \frac{\partial}{\partial \boldsymbol{\sigma}'}\left(\bar{\mathbf{A}}:\boldsymbol{\sigma}'\right) = \bar{\mathbf{A}}:\mathbf{I} = \bar{\mathbf{A}} \tag{F.8}$$

By the same manner employed in Appdenix B-5, the first terms shown in Eq.(F.6) expand to,

$$\frac{\partial I_1}{\partial \boldsymbol{\sigma}'}\otimes\frac{\partial^2 f}{\partial \boldsymbol{\sigma}'\partial I_1} = \frac{\partial I_1}{\partial \boldsymbol{\sigma}'}\otimes\left(\frac{\partial^2 f}{\partial I_1 \partial I_1}\frac{\partial I_1}{\partial \boldsymbol{\sigma}'} + \frac{\partial^2 f}{\partial \bar{J}_2 \partial I_1}\frac{\partial \bar{J}_2}{\partial \boldsymbol{\sigma}'}\right)$$

$$= \mathbf{1}\otimes\left(\frac{\partial^2 f}{\partial I_1 \partial I_1}\mathbf{1} + \frac{\partial^2 f}{\partial \bar{J}_2 \partial I_1}\sqrt{2\bar{J}_2}\left(\bar{\mathbf{n}} - \frac{1}{3}(\boldsymbol{\eta}_c:\bar{\mathbf{n}})\mathbf{1}\right)\right)$$

$$= \left(\frac{\partial^2 f}{\partial I_1 \partial I_1}\mathbf{1}\otimes\mathbf{1} + \frac{\partial^2 f}{\partial \bar{J}_2 \partial I_1}\sqrt{2\bar{J}_2}\left(\mathbf{1}\otimes\bar{\mathbf{n}} - \frac{1}{3}(\boldsymbol{\eta}_c:\bar{\mathbf{n}})\mathbf{1}\otimes\mathbf{1}\right)\right)$$

$$= \left(\frac{\partial^2 f}{\partial I_1 \partial I_1} - \frac{1}{3}(\boldsymbol{\eta}_c:\bar{\mathbf{n}})\sqrt{2\bar{J}_2}\frac{\partial^2 f}{\partial \bar{J}_2 \partial I_1}\right)\mathbf{1}\otimes\mathbf{1} + \frac{\partial^2 f}{\partial \bar{J}_2 \partial I_1}\sqrt{2\bar{J}_2}\mathbf{1}\otimes\bar{\mathbf{n}} \tag{F.9}$$

The second terms shown in Eq.(F.6) reduce to zero,

$$\frac{\partial f}{\partial I_1}\frac{\partial^2 I_1}{\partial \boldsymbol{\sigma}'\partial \boldsymbol{\sigma}'} = \mathbf{0} \tag{F.10}$$

The third terms shown in Eq.(F.6) expand to,

$$\frac{\partial \bar{J}_2}{\partial \boldsymbol{\sigma}'}\otimes\frac{\partial^2 f}{\partial \boldsymbol{\sigma}'\partial \bar{J}_2} = \frac{\partial \bar{J}_2}{\partial \boldsymbol{\sigma}'}\otimes\left(\frac{\partial^2 f}{\partial I_1 \partial \bar{J}_2}\frac{\partial I_1}{\partial \boldsymbol{\sigma}'} + \frac{\partial^2 f}{\partial \bar{J}_2 \partial \bar{J}_2}\frac{\partial \bar{J}_2}{\partial \boldsymbol{\sigma}'}\right)$$

$$= \sqrt{2\bar{J}_2}\left(\bar{\mathbf{n}} - \frac{1}{3}(\boldsymbol{\eta}_c:\bar{\mathbf{n}})\mathbf{1}\right)\otimes\left(\frac{\partial^2 f}{\partial I_1 \partial \bar{J}_2}\mathbf{1} + \frac{\partial^2 f}{\partial \bar{J}_2 \partial \bar{J}_2}\sqrt{2\bar{J}_2}\left(\bar{\mathbf{n}} - \frac{1}{3}(\boldsymbol{\eta}_c:\bar{\mathbf{n}})\mathbf{1}\right)\right)$$

$$= \sqrt{2\overline{J}_2}\,\frac{\partial^2 f}{\partial I_1 \partial \overline{J}_2}\left(\overline{\mathbf{n}}\otimes\mathbf{1}-\frac{1}{3}(\boldsymbol{\eta}_c:\overline{\mathbf{n}})\mathbf{1}\otimes\mathbf{1}\right)$$

$$+2\overline{J}_2\,\frac{\partial^2 f}{\partial \overline{J}_2 \partial \overline{J}_2}\left(\overline{\mathbf{n}}\otimes\overline{\mathbf{n}}-\frac{1}{3}(\boldsymbol{\eta}_c:\overline{\mathbf{n}})\overline{\mathbf{n}}\otimes\mathbf{1}-\frac{1}{3}(\boldsymbol{\eta}_c:\overline{\mathbf{n}})\mathbf{1}\otimes\overline{\mathbf{n}}+\frac{1}{9}(\boldsymbol{\eta}_c:\overline{\mathbf{n}})^2\,\mathbf{1}\otimes\mathbf{1}\right)$$

$$=\left(2\overline{J}_2\,\frac{\partial^2 f}{\partial \overline{J}_2 \partial \overline{J}_2}\frac{1}{9}(\boldsymbol{\eta}_c:\overline{\mathbf{n}})^2-\sqrt{2\overline{J}_2}\,\frac{\partial^2 f}{\partial I_1 \partial \overline{J}_2}\frac{1}{3}(\boldsymbol{\eta}_c:\overline{\mathbf{n}})\right)\mathbf{1}\otimes\mathbf{1}$$

$$+\left(\sqrt{2\overline{J}_2}\,\frac{\partial^2 f}{\partial I_1 \partial \overline{J}_2}-2\overline{J}_2\,\frac{\partial^2 f}{\partial \overline{J}_2 \partial \overline{J}_2}\frac{1}{3}(\boldsymbol{\eta}_c:\overline{\mathbf{n}})\right)\overline{\mathbf{n}}\otimes\mathbf{1} \qquad\text{(F.11)}$$

$$+\left(-2\overline{J}_2\,\frac{\partial^2 f}{\partial \overline{J}_2 \partial \overline{J}_2}\frac{1}{3}(\boldsymbol{\eta}_c:\overline{\mathbf{n}})\right)\mathbf{1}\otimes\overline{\mathbf{n}}+\left(2\overline{J}_2\,\frac{\partial^2 f}{\partial \overline{J}_2 \partial \overline{J}_2}\right)\overline{\mathbf{n}}\otimes\overline{\mathbf{n}}$$

The forth terms shown in Eq.(F.6) reduce to,

$$\frac{\partial f}{\partial \overline{J}_2}\frac{\partial^2 \overline{J}_2}{\partial \boldsymbol{\sigma}' \partial \boldsymbol{\sigma}'}=\frac{\partial f}{\partial \overline{J}_2}\overline{\mathbf{A}} \qquad\text{(F.12)}$$

Summation of Eq.(F.9)-(F.12) results in the expansion of Eq.(F.6) as shown by a symmetric forth-order tensor below,

$$\frac{\partial^2 f}{\partial \boldsymbol{\sigma}' \partial \boldsymbol{\sigma}'}=\left(\frac{\partial^2 f}{\partial I_1 \partial I_1}-\frac{2}{3}(\boldsymbol{\eta}_c:\overline{\mathbf{n}})\sqrt{2\overline{J}_2}\,\frac{\partial^2 f}{\partial \overline{J}_2 \partial I_1}+2\overline{J}_2\,\frac{\partial^2 f}{\partial \overline{J}_2 \partial \overline{J}_2}\frac{1}{9}(\boldsymbol{\eta}_c:\overline{\mathbf{n}})^2+\frac{1}{9}(\boldsymbol{\eta}_c:\boldsymbol{\eta}_c)\frac{\partial f}{\partial \overline{J}_2}\right)\mathbf{1}\otimes\mathbf{1}$$

$$+\left(\sqrt{2\overline{J}_2}\,\frac{\partial^2 f}{\partial \overline{J}_2 \partial I_1}-2\overline{J}_2\,\frac{1}{3}(\boldsymbol{\eta}_c:\overline{\mathbf{n}})\frac{\partial^2 f}{\partial \overline{J}_2 \partial \overline{J}_2}\right)[\mathbf{1}\otimes\overline{\mathbf{n}}+\overline{\mathbf{n}}\otimes\mathbf{1}]+2\overline{J}_2\,\frac{\partial^2 f}{\partial \overline{J}_2 \partial \overline{J}_2}\overline{\mathbf{n}}\otimes\overline{\mathbf{n}} \qquad\text{(F.13)}$$

$$+\frac{\partial f}{\partial \overline{J}_2}\left[\mathbf{A}-\frac{1}{3}[\mathbf{1}\otimes\boldsymbol{\eta}_c+\boldsymbol{\eta}_c\otimes\mathbf{1}]\right]$$

The result of above expansion can be represented by a summation of products between invariant-based scalars and the corresponding forth-order tensor basis as shown,

$$\frac{\partial^2 f}{\partial \boldsymbol{\sigma}' \partial \boldsymbol{\sigma}'}=H_1\mathbf{1}\otimes\mathbf{1}+H_2\mathbf{A}+H_3\mathbf{1}\otimes\overline{\mathbf{n}}+H_4\overline{\mathbf{n}}\otimes\mathbf{1}+H_5\overline{\mathbf{n}}\otimes\overline{\mathbf{n}}+H_6\mathbf{1}\otimes\boldsymbol{\eta}_c+H_7\boldsymbol{\eta}_c\otimes\mathbf{1} \qquad\text{(F.14)}$$

where

$$H_1=\frac{\partial^2 f}{\partial I_1 \partial I_1}-\frac{2}{3}\sqrt{2\overline{J}_2}\,\frac{\partial^2 f}{\partial \overline{J}_2 \partial I_1}(\boldsymbol{\eta}_c:\overline{\mathbf{n}})+2\overline{J}_2\,\frac{\partial^2 f}{\partial \overline{J}_2 \partial \overline{J}_2}\frac{1}{9}(\boldsymbol{\eta}_c:\overline{\mathbf{n}})^2+\frac{1}{9}\frac{\partial f}{\partial \overline{J}_2}(\boldsymbol{\eta}_c:\boldsymbol{\eta}_c) \qquad\text{(F.15)}$$

$$H_2=\frac{\partial f}{\partial \overline{J}_2},\quad H_3=H_4=\sqrt{2\overline{J}_2}\,\frac{\partial^2 f}{\partial \overline{J}_2 \partial I_1}-2\overline{J}_2\,\frac{1}{3}(\boldsymbol{\eta}_c:\overline{\mathbf{n}})\frac{\partial^2 f}{\partial \overline{J}_2 \partial \overline{J}_2} \qquad\text{(F.16), (F.17)}$$

$$H_5=2\overline{J}_2\,\frac{\partial^2 f}{\partial \overline{J}_2 \partial \overline{J}_2},\quad H_6=H_7=-\frac{1}{3}\frac{\partial f}{\partial \overline{J}_2} \qquad\text{(F.18), (F.19)}$$

F-3 Derivative of the forth-order anisotropically deviatoric tensor

According to a definition of $\overline{\mathbf{A}}$ (See Appendix A) and by chain's rule,

$$\frac{\partial \overline{\mathbf{A}}}{\partial \boldsymbol{\sigma}'_c}=\frac{\partial\left[\mathbf{A}-\frac{1}{3}[\mathbf{1}\otimes\boldsymbol{\eta}_c+\boldsymbol{\eta}_c\otimes\mathbf{1}]+\frac{1}{9}(\boldsymbol{\eta}_c:\boldsymbol{\eta}_c)[\mathbf{1}\otimes\mathbf{1}]\right]}{\partial \boldsymbol{\sigma}'_c}$$

$$=\frac{\partial \mathbf{A}}{\partial \boldsymbol{\sigma}'_c}-\frac{1}{3}\frac{\partial[\mathbf{1}\otimes\boldsymbol{\eta}_c+\boldsymbol{\eta}_c\otimes\mathbf{1}]}{\partial \boldsymbol{\sigma}'_c}+\frac{1}{9}\frac{\partial(\boldsymbol{\eta}_c:\boldsymbol{\eta}_c)\mathbf{1}\otimes\mathbf{1}}{\partial \boldsymbol{\sigma}'_c}$$

$$=-\frac{1}{3}\left[\mathbf{1}\otimes\frac{\partial\boldsymbol{\eta}_c}{\partial \boldsymbol{\sigma}'_c}+\frac{\partial\boldsymbol{\eta}_c}{\partial \boldsymbol{\sigma}'_c}\otimes\mathbf{1}\right]+\frac{1}{9}\mathbf{1}\otimes\left[\mathbf{1}\otimes\frac{\partial(\boldsymbol{\eta}_c:\boldsymbol{\eta}_c)}{\partial \boldsymbol{\sigma}'_c}+\frac{\partial(\boldsymbol{\eta}_c:\boldsymbol{\eta}_c)}{\partial \boldsymbol{\sigma}'_c}\otimes\mathbf{1}\right] \qquad\text{(F.20)}$$

$$=-\frac{1}{3}\left[\mathbf{1}\otimes\frac{\partial\boldsymbol{\eta}_c}{\partial \boldsymbol{\sigma}'_c}+\frac{\partial\boldsymbol{\eta}_c}{\partial \boldsymbol{\sigma}'_c}\otimes\mathbf{1}\right]+\frac{1}{9}\mathbf{1}\otimes\left[\mathbf{1}\otimes\left[\frac{\partial\boldsymbol{\eta}_c}{\partial \boldsymbol{\sigma}'_c}\right]^T:\boldsymbol{\eta}_c+\left[\frac{\partial\boldsymbol{\eta}_c}{\partial \boldsymbol{\sigma}'_c}\right]^T:\boldsymbol{\eta}_c\otimes\mathbf{1}\right]$$

$$=-\frac{1}{3}\left[\mathbf{1}\otimes\frac{\partial\boldsymbol{\eta}_c}{\partial \boldsymbol{\sigma}'_c}+\frac{\partial\boldsymbol{\eta}_c}{\partial \boldsymbol{\sigma}'_c}\otimes\mathbf{1}-\frac{1}{3}\mathbf{1}\otimes\mathbf{1}\otimes\left[\frac{\partial\boldsymbol{\eta}_c}{\partial \boldsymbol{\sigma}'_c}\right]^T:\boldsymbol{\eta}_c-\frac{1}{3}\mathbf{1}\otimes\left[\frac{\partial\boldsymbol{\eta}_c}{\partial \boldsymbol{\sigma}'_c}\right]^T:\boldsymbol{\eta}_c\otimes\mathbf{1}\right]$$

where (See Appendix B)

$$\mathbf{1} \otimes \frac{\partial \boldsymbol{\eta}_c}{\partial \boldsymbol{\sigma}'_c} = \frac{1}{p'_c}\left[\mathbf{1} \otimes \mathbf{A} - \frac{1}{3}\mathbf{1} \otimes \boldsymbol{\eta}_c \otimes \mathbf{1}\right], \quad \frac{\partial \boldsymbol{\eta}_c}{\partial \boldsymbol{\sigma}'_c} \otimes \mathbf{1} = \frac{1}{p'_c}\left[\mathbf{A} \otimes \mathbf{1} - \frac{1}{3}\boldsymbol{\eta}_c \otimes \mathbf{1} \otimes \mathbf{1}\right]$$

$$\left[\frac{\partial \boldsymbol{\eta}_c}{\partial \boldsymbol{\sigma}'_c}\right]^T : \boldsymbol{\eta}_c = \frac{1}{p'_c}\left[\mathbf{A} - \frac{1}{3}\mathbf{1} \otimes \boldsymbol{\eta}_c\right] : \boldsymbol{\eta}_c = \frac{1}{p'_c}\left[\boldsymbol{\eta}_c - \frac{1}{3}(\boldsymbol{\eta}_c : \boldsymbol{\eta}_c)\mathbf{1}\right]$$

As a result, Eq.(F.20) can be expressed by

$$
\begin{aligned}
\frac{\partial \bar{\mathbf{A}}}{\partial \boldsymbol{\sigma}'_c} &= -\frac{1}{3}\frac{1}{p'_c}\left[\begin{array}{l} \mathbf{1} \otimes \mathbf{A} - \frac{1}{3}\mathbf{1} \otimes \boldsymbol{\eta}_c \otimes \mathbf{1} + \mathbf{A} \otimes \mathbf{1} - \frac{1}{3}\boldsymbol{\eta}_c \otimes \mathbf{1} \otimes \mathbf{1} \\[2mm] -\frac{1}{3}\mathbf{1} \otimes \mathbf{1} \otimes \boldsymbol{\eta}_c - \frac{1}{3}\mathbf{1} \otimes \boldsymbol{\eta}_c \otimes \mathbf{1} + \frac{2}{9}(\boldsymbol{\eta}_c : \boldsymbol{\eta}_c)\mathbf{1} \otimes \mathbf{1} \otimes \mathbf{1} \end{array}\right] \\[3mm]
&= -\frac{1}{3}\frac{1}{p'_c}\left[\begin{array}{l} \left[\mathbf{A} - \frac{1}{3}\mathbf{1} \otimes \boldsymbol{\eta}_c - \frac{1}{3}\boldsymbol{\eta}_c \otimes \mathbf{1} + \frac{1}{9}(\boldsymbol{\eta}_c : \boldsymbol{\eta}_c)\mathbf{1} \otimes \mathbf{1}\right] \otimes \mathbf{1} \\[2mm] +\mathbf{1} \otimes \left[\mathbf{A} - \frac{1}{3}\mathbf{1} \otimes \boldsymbol{\eta}_c - \frac{1}{3}\boldsymbol{\eta}_c \otimes \mathbf{1} + \frac{1}{9}(\boldsymbol{\eta}_c : \boldsymbol{\eta}_c)\mathbf{1} \otimes \mathbf{1}\right] \end{array}\right] \\[3mm]
&= -\frac{1}{3}\frac{1}{p'_c}\left[\bar{\mathbf{A}} \otimes \mathbf{1} + \mathbf{1} \otimes \bar{\mathbf{A}}\right]
\end{aligned}
\tag{F.21}
$$

Eq.(F.21) illustrates a symmetric sixth-order tensor.

F-4 Second derivatives of the Sekiguchi-Ohta yield function with respect to stress tensor and stress hardening tensor

Referring to Appendix B-5 accompanied by chain rule, the second-order derivative is

$$
\begin{aligned}
\frac{\partial^2 f}{\partial \boldsymbol{\sigma}'_c \partial \boldsymbol{\sigma}'} &= \frac{\partial \left(\dfrac{\partial f}{\partial I_1}\dfrac{\partial I_1}{\partial \boldsymbol{\sigma}'} + \dfrac{\partial f}{\partial \bar{J}_2}\dfrac{\partial \bar{J}_2}{\partial \boldsymbol{\sigma}'}\right)}{\partial \boldsymbol{\sigma}'_c} \\[3mm]
&= \left[\frac{\partial I_1}{\partial \boldsymbol{\sigma}'} \otimes \frac{\partial^2 f}{\partial \boldsymbol{\sigma}'_c \partial I_1}\right] + \left[\frac{\partial f}{\partial I_1}\frac{\partial^2 I_1}{\partial \boldsymbol{\sigma}'_c \partial \boldsymbol{\sigma}'}\right] + \left[\frac{\partial \bar{J}_2}{\partial \boldsymbol{\sigma}'} \otimes \frac{\partial^2 f}{\partial \boldsymbol{\sigma}'_c \partial \bar{J}_2}\right] + \left[\frac{\partial f}{\partial \bar{J}_2}\frac{\partial^2 \bar{J}_2}{\partial \boldsymbol{\sigma}'_c \partial \boldsymbol{\sigma}'}\right]
\end{aligned}
\tag{F.22}
$$

where the second-order derivatives of invariants are

$$\frac{\partial^2 I_1}{\partial \boldsymbol{\sigma}'_c \partial \boldsymbol{\sigma}'} = \frac{\partial}{\partial \boldsymbol{\sigma}'_c}\left(\frac{\partial I_1}{\partial \boldsymbol{\sigma}'}\right) = \mathbf{0} \tag{F.23}$$

$$\frac{\partial^2 \bar{J}_2}{\partial \boldsymbol{\sigma}'_c \partial \boldsymbol{\sigma}'} = \frac{\partial}{\partial \boldsymbol{\sigma}'_c}\left(\frac{\partial \bar{J}_2}{\partial \boldsymbol{\sigma}'}\right) = \frac{\partial}{\partial \boldsymbol{\sigma}'_c}\left(\bar{\mathbf{A}} : \boldsymbol{\sigma}'\right) = \frac{\partial \bar{\mathbf{A}}}{\partial \boldsymbol{\sigma}'_c} : \boldsymbol{\sigma}' \tag{F.24}$$

Substitution of Eq.(F.21) into Eq.(F.24) gives,

$$
\begin{aligned}
\frac{\partial^2 \bar{J}_2}{\partial \boldsymbol{\sigma}'_c \partial \boldsymbol{\sigma}'} &= \frac{\partial \bar{\mathbf{A}}}{\partial \boldsymbol{\sigma}'_c} : \boldsymbol{\sigma}' = -\frac{1}{3}\frac{1}{p'_c}\left[\bar{\mathbf{A}} \otimes \mathbf{1} + \mathbf{1} \otimes \bar{\mathbf{A}}\right] : \boldsymbol{\sigma}' \\[3mm]
&= -\frac{1}{3}\frac{1}{p'_c}\left[\bar{\mathbf{A}}(\mathbf{1} : \boldsymbol{\sigma}') + \mathbf{1} \otimes \bar{\mathbf{A}} : \boldsymbol{\sigma}'\right] \\[3mm]
&= -\frac{1}{I_{c1}}\left[I_1\bar{\mathbf{A}} + \mathbf{1} \otimes \{\bar{\mathbf{A}} : \boldsymbol{\sigma}'\}\right]
\end{aligned}
\tag{F.25}
$$

The order of derivatives can be exchanged each other for continuous function, therefore,

$$
\begin{aligned}
\frac{\partial^2 \bar{J}_2}{\partial \boldsymbol{\sigma}' \partial \boldsymbol{\sigma}'_c} &= \frac{\partial}{\partial \boldsymbol{\sigma}'}\left(\frac{\partial \bar{J}_2}{\partial \boldsymbol{\sigma}'_c}\right) = \frac{\partial}{\partial \boldsymbol{\sigma}'}\left(-\frac{I_1}{I_{c1}}\bar{\mathbf{A}} : \boldsymbol{\sigma}'\right) \\[3mm]
&= -\frac{1}{I_{c1}}\left(\bar{\mathbf{A}} : \boldsymbol{\sigma}' \otimes \frac{\partial I_1}{\partial \boldsymbol{\sigma}'} + I_1\bar{\mathbf{A}}\frac{\partial \boldsymbol{\sigma}'}{\partial \boldsymbol{\sigma}'}\right) = -\frac{1}{I_{c1}}\left(\{\bar{\mathbf{A}} : \boldsymbol{\sigma}'\} \otimes \mathbf{1} + \bar{\mathbf{A}}(\mathbf{1} : \boldsymbol{\sigma}')\right) \\[3mm]
&= \left[\frac{\partial^2 \bar{J}_2}{\partial \boldsymbol{\sigma}'_c \partial \boldsymbol{\sigma}'}\right]^T
\end{aligned}
\tag{F.26}
$$

Consider the following terms in Eq.(F.22) using Eqs.(F.26), (F.5) and Appendix B

$$\frac{\partial f}{\partial \bar{J}_2}\frac{\partial^2 \bar{J}_2}{\partial \boldsymbol{\sigma'}_c \partial \boldsymbol{\sigma'}} = \frac{I_1}{I_{c1}}\frac{\partial^2 f}{\partial I_1 \partial \bar{J}_2}\left[I_1\bar{\mathbf{A}} + \mathbf{1}\otimes\left\{\bar{\mathbf{A}}:\boldsymbol{\sigma'}\right\}\right]$$

$$= \frac{I_1}{I_{c1}}\frac{\partial^2 f}{\partial I_1 \partial \bar{J}_2}\left[I_1\bar{\mathbf{A}} + \mathbf{1}\otimes\sqrt{2\bar{J}_2}\left[\bar{\mathbf{n}} - \frac{1}{3}(\boldsymbol{\eta}_c:\bar{\mathbf{n}})\mathbf{1}\right]\right] \qquad \text{(F.27)}$$

$$= \frac{I_1}{I_{c1}}\frac{\partial^2 f}{\partial I_1 \partial \bar{J}_2}\left[I_1\bar{\mathbf{A}} + \sqrt{2\bar{J}_2}\mathbf{1}\otimes\bar{\mathbf{n}} - \frac{1}{3}(\boldsymbol{\eta}_c:\bar{\mathbf{n}})\sqrt{2\bar{J}_2}\mathbf{1}\otimes\mathbf{1}\right]$$

The derivatives of invariants with respect to stress hardening tensor are shown below (See Appendix B)

$$\frac{\partial I_1}{\partial \boldsymbol{\sigma'}_c} = \mathbf{0}, \quad \frac{\partial \bar{J}_2}{\partial \boldsymbol{\sigma'}_c} = -\frac{I_1}{I_{c1}}\bar{\mathbf{A}}:\boldsymbol{\sigma'} = -\frac{I_1\sqrt{2\bar{J}_2}}{I_{c1}}\left[\bar{\mathbf{n}} - \frac{1}{3}(\boldsymbol{\eta}_c:\bar{\mathbf{n}})\mathbf{1}\right] \qquad \text{(F.28), (F.29)}$$

Consider the following terms in Eq.(F.22) using Eqs.(F.28), (F.29), (F.2)

$$\frac{\partial I_1}{\partial \boldsymbol{\sigma'}}\otimes\frac{\partial^2 f}{\partial \boldsymbol{\sigma'}_c \partial I_1} = \frac{\partial I_1}{\partial \boldsymbol{\sigma'}}\otimes\left[\frac{\partial^2 f}{\partial I_1 \partial I_1}\frac{\partial I_1}{\partial \boldsymbol{\sigma'}_c} + \frac{\partial^2 f}{\partial \bar{J}_2 \partial I_1}\frac{\partial \bar{J}_2}{\partial \boldsymbol{\sigma'}_c}\right]$$

$$= -\mathbf{1}\otimes\frac{\partial^2 f}{\partial \bar{J}_2 \partial I_1}\frac{I_1}{I_{c1}}\bar{\mathbf{A}}:\boldsymbol{\sigma'}$$

$$= -\frac{\partial^2 f}{\partial \bar{J}_2 \partial I_1}\frac{I_1\sqrt{2\bar{J}_2}}{I_{c1}}\mathbf{1}\otimes\left[\bar{\mathbf{n}} - \frac{1}{3}(\boldsymbol{\eta}_c:\bar{\mathbf{n}})\mathbf{1}\right] \qquad \text{(F.30)}$$

$$= -\frac{\partial^2 f}{\partial \bar{J}_2 \partial I_1}\frac{I_1\sqrt{2\bar{J}_2}}{I_{c1}}\left[\mathbf{1}\otimes\bar{\mathbf{n}} - \frac{1}{3}(\boldsymbol{\eta}_c:\bar{\mathbf{n}})\mathbf{1}\otimes\mathbf{1}\right]$$

According to Appendix B, the derivatives of joint invariant can be expressed by,

$$\frac{\partial \bar{J}_2}{\partial \boldsymbol{\sigma'}} = \bar{\mathbf{A}}:\boldsymbol{\sigma'} = \sqrt{2\bar{J}_2}\left[\bar{\mathbf{n}} - \frac{1}{3}(\boldsymbol{\eta}_c:\bar{\mathbf{n}})\mathbf{1}\right], \quad \frac{\partial \bar{J}_2}{\partial \boldsymbol{\sigma'}_c} = -\frac{I_1}{I_{c1}}\bar{\mathbf{A}}:\boldsymbol{\sigma'} = -\frac{I_1\sqrt{2\bar{J}_2}}{I_{c1}}\left[\bar{\mathbf{n}} - \frac{1}{3}(\boldsymbol{\eta}_c:\bar{\mathbf{n}})\mathbf{1}\right] \qquad \text{(F.31) ,(F.32)}$$

Consider the following terms in Eq.(F.22) using Eqs.(F.28), (F.4), (F.31) and (F.32)

$$\frac{\partial \bar{J}_2}{\partial \boldsymbol{\sigma'}}\otimes\frac{\partial^2 f}{\partial \boldsymbol{\sigma'}_c \partial \bar{J}_2} = \frac{\partial \bar{J}_2}{\partial \boldsymbol{\sigma'}}\otimes\left[\frac{\partial^2 f}{\partial I_1 \partial \bar{J}_2}\frac{\partial I_1}{\partial \boldsymbol{\sigma'}_c} + \frac{\partial^2 f}{\partial \bar{J}_2 \partial \bar{J}_2}\frac{\partial \bar{J}_2}{\partial \boldsymbol{\sigma'}_c}\right]$$

$$= \frac{\partial^2 f}{\partial \bar{J}_2 \partial \bar{J}_2}\frac{\partial \bar{J}_2}{\partial \boldsymbol{\sigma'}}\otimes\frac{\partial \bar{J}_2}{\partial \boldsymbol{\sigma'}_c}$$

$$= -\frac{\partial^2 f}{\partial \bar{J}_2 \partial \bar{J}_2}\bar{\mathbf{A}}:\boldsymbol{\sigma'}\otimes\frac{I_1}{I_{c1}}\bar{\mathbf{A}}:\boldsymbol{\sigma'} \qquad \text{(F.33)}$$

$$= -\frac{\partial^2 f}{\partial \bar{J}_2 \partial \bar{J}_2}\frac{2\bar{J}_2 I_1}{I_{c1}}\left[\bar{\mathbf{n}} - \frac{1}{3}(\boldsymbol{\eta}_c:\bar{\mathbf{n}})\mathbf{1}\right]\otimes\left[\bar{\mathbf{n}} - \frac{1}{3}(\boldsymbol{\eta}_c:\bar{\mathbf{n}})\mathbf{1}\right]$$

$$= -\frac{\partial^2 f}{\partial \bar{J}_2 \partial \bar{J}_2}\frac{2\bar{J}_2 I_1}{I_{c1}}\left[\frac{1}{9}(\boldsymbol{\eta}_c:\bar{\mathbf{n}})^2\mathbf{1}\otimes\mathbf{1} - \frac{1}{3}(\boldsymbol{\eta}_c:\bar{\mathbf{n}})\bar{\mathbf{n}}\otimes\mathbf{1} - \frac{1}{3}(\boldsymbol{\eta}_c:\bar{\mathbf{n}})\mathbf{1}\otimes\bar{\mathbf{n}} + \bar{\mathbf{n}}\otimes\bar{\mathbf{n}}\right]$$

Referring to Eqs. (F.23), (F.27), (F.30) and (F.33), the second partial derivative is found symmetric as shown below,

$$\frac{\partial^2 f}{\partial \boldsymbol{\sigma'}_c \partial \boldsymbol{\sigma'}} = \begin{bmatrix} \left(\dfrac{I_1^2}{9I_{c1}}\dfrac{\partial^2 f}{\partial I_1 \partial \bar{J}_2}(\boldsymbol{\eta}_c:\boldsymbol{\eta}_c) - \dfrac{2\bar{J}_2 I_1}{9I_{c1}}\dfrac{\partial^2 f}{\partial \bar{J}_2 \partial \bar{J}_2}(\boldsymbol{\eta}_c:\bar{\mathbf{n}})^2\right)\mathbf{1}\otimes\mathbf{1} \\[2ex] + \left(\dfrac{2\bar{J}_2 I_1}{3I_{c1}}\dfrac{\partial^2 f}{\partial \bar{J}_2 \partial \bar{J}_2}(\boldsymbol{\eta}_c:\bar{\mathbf{n}})\right)\mathbf{1}\otimes\bar{\mathbf{n}} \\[2ex] + \left(\dfrac{2\bar{J}_2 I_1}{3I_{c1}}\dfrac{\partial^2 f}{\partial \bar{J}_2 \partial \bar{J}_2}(\boldsymbol{\eta}_c:\bar{\mathbf{n}})\right)\bar{\mathbf{n}}\otimes\mathbf{1} \\[2ex] - \dfrac{2\bar{J}_2 I_1}{I_{c1}}\dfrac{\partial^2 f}{\partial \bar{J}_2 \partial \bar{J}_2}\bar{\mathbf{n}}\otimes\bar{\mathbf{n}} \\[2ex] + \dfrac{I_1^2}{I_{c1}}\dfrac{\partial^2 f}{\partial I_1 \partial \bar{J}_2}\mathbf{A} - \dfrac{I_1^2}{3I_{c1}}\dfrac{\partial^2 f}{\partial I_1 \partial \bar{J}_2}\left[\mathbf{1}\otimes\boldsymbol{\eta}_c + \boldsymbol{\eta}_c\otimes\mathbf{1}\right] \end{bmatrix} \qquad \text{(F.34)}$$

The result of above expansion can be represented by a summation of products between invariant-based scalars

and the corresponding forth-order tensor basis as shown,

$$\frac{\partial^2 f}{\partial \boldsymbol{\sigma'}_c \partial \boldsymbol{\sigma'}} = M_1 \mathbf{1} \otimes \mathbf{1} + M_2 \mathbf{A} + M_3 \mathbf{1} \otimes \bar{\mathbf{n}} + M_4 \bar{\mathbf{n}} \otimes \mathbf{1} + M_5 \bar{\mathbf{n}} \otimes \bar{\mathbf{n}} + M_6 \mathbf{1} \otimes \boldsymbol{\eta}_c + M_7 \boldsymbol{\eta}_c \otimes \mathbf{1} \tag{F.35}$$

where

$$M_1 = \frac{I_1^2}{9 I_{c1}} \frac{\partial^2 f}{\partial I_1 \partial \bar{J}_2} (\boldsymbol{\eta}_c : \boldsymbol{\eta}_c) - \frac{2 \bar{J}_2 I_1}{9 I_{c1}} \frac{\partial^2 f}{\partial \bar{J}_2 \partial \bar{J}_2} (\boldsymbol{\eta}_c : \bar{\mathbf{n}})^2 \tag{F.36}$$

$$M_2 = \frac{I_1^2}{I_{c1}} \frac{\partial^2 f}{\partial I_1 \partial \bar{J}_2} \tag{F.37}$$

$$M_3 = M_4 = \frac{2 \bar{J}_2 I_1}{3 I_{c1}} \frac{\partial^2 f}{\partial \bar{J}_2 \partial \bar{J}_2} (\boldsymbol{\eta}_c : \bar{\mathbf{n}}) \tag{F.38}, \tag{F.39}$$

$$M_5 = -\frac{2 \bar{J}_2 I_1}{I_{c1}} \frac{\partial^2 f}{\partial \bar{J}_2 \partial \bar{J}_2} \tag{F.40}$$

$$M_6 = M_7 = -\frac{I_1^2}{3 I_{c1}} \frac{\partial^2 f}{\partial I_1 \partial \bar{J}_2} \tag{F.41}, \tag{F.42}$$

F-5 Second derivatives of the Sekiguchi-Ohta yield function with respect to stress hardening tensor and stress tensor

By the same manner with previous section, by chain rule, the second-order derivative is,

$$\frac{\partial^2 f}{\partial \boldsymbol{\sigma'} \partial \boldsymbol{\sigma'}_c} = \frac{\partial \left(\frac{\partial f}{\partial I_{c1}} \frac{\partial I_{c1}}{\partial \boldsymbol{\sigma'}_c} + \frac{\partial f}{\partial \bar{J}_2} \frac{\partial \bar{J}_2}{\partial \boldsymbol{\sigma'}_c} \right)}{\partial \boldsymbol{\sigma'}} \tag{F.43}$$

$$= \left[\frac{\partial I_{c1}}{\partial \boldsymbol{\sigma'}_c} \otimes \frac{\partial^2 f}{\partial \boldsymbol{\sigma'} \partial I_{c1}} \right] + \left[\frac{\partial f}{\partial I_{c1}} \frac{\partial^2 I_{c1}}{\partial \boldsymbol{\sigma'} \partial \boldsymbol{\sigma'}_c} \right] + \left[\frac{\partial \bar{J}_2}{\partial \boldsymbol{\sigma'}_c} \otimes \frac{\partial^2 f}{\partial \boldsymbol{\sigma'} \partial \bar{J}_2} \right] + \left[\frac{\partial f}{\partial \bar{J}_2} \frac{\partial^2 \bar{J}_2}{\partial \boldsymbol{\sigma'} \partial \boldsymbol{\sigma'}_c} \right]$$

where the second-order derivatives of invariants are

$$\frac{\partial^2 I_{c1}}{\partial \boldsymbol{\sigma'} \partial \boldsymbol{\sigma'}_c} = \frac{\partial}{\partial \boldsymbol{\sigma'}} \left(\frac{\partial I_{c1}}{\partial \boldsymbol{\sigma'}_c} \right) = \mathbf{0} \tag{F.44}$$

$$\frac{\partial^2 f}{\partial \boldsymbol{\sigma'} \partial I_{c1}} = \frac{\partial \left(\frac{\partial f}{\partial I_{c1}} \right)}{\partial \boldsymbol{\sigma'}} = \frac{\partial \left(-\frac{MD}{I_{c1}} \right)}{\partial \boldsymbol{\sigma'}} = \mathbf{0} \tag{F.45}$$

Consider the following terms in Eq.(F.43) using Eqs.(F.31) and (F.32),

$$\frac{\partial \bar{J}_2}{\partial \boldsymbol{\sigma'}_c} \otimes \frac{\partial^2 f}{\partial \boldsymbol{\sigma'} \partial \bar{J}_2} = -\frac{I_1}{I_{c1}} \bar{\mathbf{A}} : \boldsymbol{\sigma'} \otimes \left(\frac{\partial^2 f}{\partial I_1 \partial \bar{J}_2} \frac{\partial I_1}{\partial \boldsymbol{\sigma'}} + \frac{\partial^2 f}{\partial \bar{J}_2 \partial \bar{J}_2} \frac{\partial \bar{J}_2}{\partial \boldsymbol{\sigma'}} \right)$$

$$= -\frac{I_1 \sqrt{2 \bar{J}_2}}{I_{c1}} \left[\bar{\mathbf{n}} - \frac{1}{3} (\boldsymbol{\eta}_c : \bar{\mathbf{n}}) \mathbf{1} \right] \otimes \left(\frac{\partial^2 f}{\partial I_1 \partial \bar{J}_2} \mathbf{1} + \frac{\partial^2 f}{\partial \bar{J}_2 \partial \bar{J}_2} \sqrt{2 \bar{J}_2} \left(\bar{\mathbf{n}} - \frac{1}{3} (\boldsymbol{\eta}_c : \bar{\mathbf{n}}) \mathbf{1} \right) \right)$$

$$= \begin{bmatrix} \left(-(\boldsymbol{\eta}_c : \bar{\mathbf{n}})^2 \frac{2 \bar{J}_2 I_1}{9 I_{c1}} \frac{\partial^2 f}{\partial \bar{J}_2 \partial \bar{J}_2} + (\boldsymbol{\eta}_c : \bar{\mathbf{n}}) \frac{I_1 \sqrt{2 \bar{J}_2}}{3 I_{c1}} \frac{\partial^2 f}{\partial I_1 \partial \bar{J}_2} \right) \mathbf{1} \otimes \mathbf{1} \\ + (\boldsymbol{\eta}_c : \bar{\mathbf{n}}) \frac{2 \bar{J}_2 I_1}{3 I_{c1}} \frac{\partial^2 f}{\partial \bar{J}_2 \partial \bar{J}_2} \mathbf{1} \otimes \bar{\mathbf{n}} \\ \left(-\frac{I_1 \sqrt{2 \bar{J}_2}}{I_{c1}} \frac{\partial^2 f}{\partial I_1 \partial \bar{J}_2} + \frac{2 \bar{J}_2 I_1}{3 I_{c1}} (\boldsymbol{\eta}_c : \bar{\mathbf{n}}) \frac{\partial^2 f}{\partial \bar{J}_2 \partial \bar{J}_2} \right) \bar{\mathbf{n}} \otimes \mathbf{1} \\ -\frac{I_1 2 \bar{J}_2}{I_{c1}} \frac{\partial^2 f}{\partial \bar{J}_2 \partial \bar{J}_2} \bar{\mathbf{n}} \otimes \bar{\mathbf{n}} \end{bmatrix} \tag{F.46}$$

Consider the following terms in Eq.(F.43) using Eqs.(F.26),

$$\frac{\partial f}{\partial \overline{J}_2}\frac{\partial^2 \overline{J}_2}{\partial \boldsymbol{\sigma}'\partial \boldsymbol{\sigma}'_c} = \left(-I_1\frac{\partial^2 f}{\partial \overline{J}_2 \partial I_1}\right)\left[-\frac{1}{I_{c1}}\left(\left\{\overline{\mathbf{A}}:\boldsymbol{\sigma}'\right\}\otimes\mathbf{1}+\overline{\mathbf{A}}(\mathbf{1}:\boldsymbol{\sigma}')\right)\right]$$

$$= \frac{I_1}{I_{c1}}\frac{\partial^2 f}{\partial \overline{J}_2 \partial I_1}\left(\sqrt{2\overline{J}_2}\left[\overline{\mathbf{n}}-\frac{1}{3}(\boldsymbol{\eta}_c:\overline{\mathbf{n}})\mathbf{1}\right]\otimes\mathbf{1}+I_1\overline{\mathbf{A}}\right)$$

$$= \begin{pmatrix} \left(\dfrac{I_1^2}{9I_{c1}}\dfrac{\partial^2 f}{\partial \overline{J}_2 \partial I_1}(\boldsymbol{\eta}_c:\boldsymbol{\eta}_c)-\dfrac{I_1\sqrt{2\overline{J}_2}}{3I_{c1}}\dfrac{\partial^2 f}{\partial \overline{J}_2 \partial I_1}(\boldsymbol{\eta}_c:\overline{\mathbf{n}})\right)\mathbf{1}\otimes\mathbf{1} \\[3mm] +\dfrac{I_1\sqrt{2\overline{J}_2}}{I_{c1}}\dfrac{\partial^2 f}{\partial \overline{J}_2 \partial I_1}\overline{\mathbf{n}}\otimes\mathbf{1} \\[3mm] +\dfrac{I_1^2}{I_{c1}}\dfrac{\partial^2 f}{\partial \overline{J}_2 \partial I_1}\mathbf{A}-\dfrac{I_1^2}{3I_{c1}}\dfrac{\partial^2 f}{\partial \overline{J}_2 \partial I_1}\left[\mathbf{1}\otimes\boldsymbol{\eta}_c+\boldsymbol{\eta}_c\otimes\mathbf{1}\right] \end{pmatrix} \qquad (\text{F.47})$$

Referring to Eqs.(F.46) and (F.47), Eq.(F.43) can be reduced to,

$$\frac{\partial^2 f}{\partial \boldsymbol{\sigma}'\partial \boldsymbol{\sigma}'_c} = \begin{bmatrix} \left(\dfrac{I_1^2}{9I_{c1}}\dfrac{\partial^2 f}{\partial \overline{J}_2 \partial I_1}(\boldsymbol{\eta}_c:\boldsymbol{\eta}_c)-\dfrac{2\overline{J}_2 I_1}{9I_{c1}}\dfrac{\partial^2 f}{\partial \overline{J}_2 \partial \overline{J}_2}(\boldsymbol{\eta}_c:\overline{\mathbf{n}})^2\right)\mathbf{1}\otimes\mathbf{1} \\[3mm] +\dfrac{2\overline{J}_2 I_1}{3I_{c1}}\dfrac{\partial^2 f}{\partial \overline{J}_2 \partial \overline{J}_2}(\boldsymbol{\eta}_c:\overline{\mathbf{n}})\mathbf{1}\otimes\overline{\mathbf{n}} \\[3mm] +\dfrac{2\overline{J}_2 I_1}{3I_{c1}}\dfrac{\partial^2 f}{\partial \overline{J}_2 \partial \overline{J}_2}(\boldsymbol{\eta}_c:\overline{\mathbf{n}})\overline{\mathbf{n}}\otimes\mathbf{1} \\[3mm] -\dfrac{2\overline{J}_2 I_1}{I_{c1}}\dfrac{\partial^2 f}{\partial \overline{J}_2 \partial \overline{J}_2}\overline{\mathbf{n}}\otimes\overline{\mathbf{n}} \\[3mm] +\dfrac{I_1^2}{I_{c1}}\dfrac{\partial^2 f}{\partial \overline{J}_2 \partial I_1}\mathbf{A}-\dfrac{I_1^2}{3I_{c1}}\dfrac{\partial^2 f}{\partial \overline{J}_2 \partial I_1}\left[\mathbf{1}\otimes\boldsymbol{\eta}_c+\boldsymbol{\eta}_c\otimes\mathbf{1}\right] \end{bmatrix} \qquad (\text{F.48})$$

The solution found in Eq.(F.48) is similar to that of Eq.(F.34) even the order of differentiation is opposite. This property should be hold for continuous function. However, it is not guaranteed at the point of singularity.

F-6 The derivatives of gradient of the SO yield function with respect to virgin K_o-consolidation pressure

The derivative of gradient of the SO yield function with respect to p'_c in corresponding to Appendix B and Eq.(F.35) can be given by,

$$\frac{\partial(\partial_{\boldsymbol{\sigma}'}f)}{\partial p'_c} = \frac{\partial^2 f}{\partial p'_c \partial \boldsymbol{\sigma}'} = \frac{\partial^2 f}{\partial \boldsymbol{\sigma}'_c \partial \boldsymbol{\sigma}'}:\frac{\partial \boldsymbol{\sigma}'_c}{\partial p'_c}$$

$$= \left\{M_1\mathbf{1}\otimes\mathbf{1}+M_2\mathbf{A}+M_3\mathbf{1}\otimes\overline{\mathbf{n}}+M_4\overline{\mathbf{n}}\otimes\mathbf{1}+M_5\overline{\mathbf{n}}\otimes\overline{\mathbf{n}}+M_6\mathbf{1}\otimes\boldsymbol{\eta}_c+M_7\boldsymbol{\eta}_c\otimes\mathbf{1}\right\}:\left\{\mathbf{1}+\boldsymbol{\eta_c}\right\} \qquad (\text{F.49})$$

$$= \left(3M_1+M_3\left(\overline{\mathbf{n}}:\boldsymbol{\eta_c}\right)+M_6\left(\boldsymbol{\eta_c}:\boldsymbol{\eta_c}\right)\right)\mathbf{1}+\left(3M_7+M_2\right)\boldsymbol{\eta}_c+\left(M_5\left(\overline{\mathbf{n}}:\boldsymbol{\eta_c}\right)+3M_4\right)\overline{\mathbf{n}}$$

$$= \mathbf{0}$$

where

$$3M_1+M_3\left(\overline{\mathbf{n}}:\boldsymbol{\eta_c}\right)+M_6\left(\boldsymbol{\eta}_c:\boldsymbol{\eta_c}\right) = \begin{pmatrix} \dfrac{I_1^2}{3I_{c1}}\dfrac{\partial^2 f}{\partial I_1 \partial \overline{J}_2}(\boldsymbol{\eta}_c:\boldsymbol{\eta}_c)-\dfrac{2\overline{J}_2 I_1}{3I_{c1}}\dfrac{\partial^2 f}{\partial \overline{J}_2 \partial \overline{J}_2}(\boldsymbol{\eta}_c:\overline{\mathbf{n}})^2 \\[3mm] +\dfrac{2\overline{J}_2 I_1}{3I_{c1}}\dfrac{\partial^2 f}{\partial \overline{J}_2 \partial \overline{J}_2}(\boldsymbol{\eta}_c:\overline{\mathbf{n}})^2-\dfrac{I_1^2}{3I_{c1}}\dfrac{\partial^2 f}{\partial I_1 \partial \overline{J}_2}(\boldsymbol{\eta}_c:\boldsymbol{\eta_c}) \end{pmatrix} = 0$$

$$3M_4+M_5(\overline{\mathbf{n}}:\boldsymbol{\eta_c}) = \frac{2\overline{J}_2 I_1}{I_{c1}}\frac{\partial^2 f}{\partial \overline{J}_2 \partial \overline{J}_2}(\boldsymbol{\eta}_c:\overline{\mathbf{n}})-\frac{2\overline{J}_2 I_1}{I_{c1}}\frac{\partial^2 f}{\partial \overline{J}_2 \partial \overline{J}_2}(\overline{\mathbf{n}}:\boldsymbol{\eta_c}) = 0$$

$$3M_7+M_2 = -\frac{I_1^2}{I_{c1}}\frac{\partial^2 f}{\partial I_1 \partial \overline{J}_2}+\frac{I_1^2}{I_{c1}}\frac{\partial^2 f}{\partial I_1 \partial \overline{J}_2} = 0$$

According to Appendix B, the short proof can be obtained by,

$$\frac{\partial(\partial_{\boldsymbol{\sigma}'}f)}{\partial p'_c} = -\frac{\sqrt{2\overline{J}_2}}{3}\frac{\partial f}{\partial \overline{J}_2}\left(\overline{\mathbf{n}}:\frac{\partial \boldsymbol{\eta}_c}{\partial p'_c}\right)\mathbf{1} = \mathbf{0} \qquad (\text{F.50})$$

where

$$\frac{\partial f}{\partial \boldsymbol{\sigma}'} = \left(\frac{\partial f}{\partial I_1} - \sqrt{2\overline{J}_2}\, \frac{\partial f}{\partial \overline{J}_2}\, \frac{1}{3}(\boldsymbol{\eta}_c : \overline{\mathbf{n}}) \right)\mathbf{1} + \sqrt{2\overline{J}_2}\, \frac{\partial f}{\partial \overline{J}_2}\, \overline{\mathbf{n}} \tag{F.51}$$

$$\frac{\partial \boldsymbol{\eta}_c}{\partial p'_c} = \frac{\partial \boldsymbol{\eta}_c}{\partial \boldsymbol{\sigma}'_c} : \frac{\partial \boldsymbol{\sigma}'_c}{\partial p'_c} = \frac{1}{p'_c}\left[\mathbf{A} - \frac{1}{3}\boldsymbol{\eta}_c \otimes \mathbf{1} \right] : \{\mathbf{1} + \boldsymbol{\eta}_c\}$$

$$\qquad\qquad \text{(providing that } \dot{\boldsymbol{\eta}}_c = \mathbf{0}) \tag{F.52}$$

$$= \frac{1}{p'_c}\{\boldsymbol{\eta}_c - \boldsymbol{\eta}_c\} = \mathbf{0}$$

F-7 Rate constitutive equations

The rate constitutive equations for inviscid version of Sekiguchi-Ohta plasticity are listed below,

$$\dot{\boldsymbol{\varepsilon}}^e = \dot{\boldsymbol{\varepsilon}} - \dot{\boldsymbol{\varepsilon}}^p \tag{F.53}$$

$$\dot{\boldsymbol{\sigma}}' = \mathbf{c}^e : \dot{\boldsymbol{\varepsilon}}^e \tag{F.54}$$

$$\mathbf{c}^e = \mathbf{c}^e(\boldsymbol{\sigma}') = K(\boldsymbol{\sigma}')\mathbf{1} \otimes \mathbf{1} + 2G(\boldsymbol{\sigma}')\mathbf{A} \tag{F.55}$$

$$\dot{\boldsymbol{\varepsilon}}^p = \gamma \partial_{\boldsymbol{\sigma}'} f(\boldsymbol{\sigma}', \boldsymbol{\sigma}'_c) \tag{F.56}$$

$$\dot{p}'_c = \partial^2_{\alpha\alpha}\mathsf{H}\dot{\alpha} = \frac{p'_c}{\overline{\lambda} - \overline{\kappa}}\dot{\alpha} \qquad \text{where} \qquad \alpha = \mathbf{1} : \boldsymbol{\varepsilon}^p \tag{F.57}$$

$$\boldsymbol{\sigma}'_c = \boldsymbol{\sigma}'_c(p'_c) = p'_c\{\mathbf{1} + \boldsymbol{\eta}_\mathbf{c}\} \tag{F.58}$$

$$\dot{f} = \dot{f}(\boldsymbol{\sigma}', \boldsymbol{\sigma}'_c) = 0 \tag{F.59}$$

$$\gamma \geq 0 \,; f \leq 0 \,; \gamma f = 0 \tag{F.60}$$

F-8 Backwardly incremental constitutive equations

Using $\Delta\boldsymbol{\varepsilon} = \dot{\boldsymbol{\varepsilon}}\Delta t$ and $\Delta\gamma = \gamma\Delta t$ as driving variables between state at t_n to $t_{n+1} = t_n + \Delta t$, rate-independent constitutive Eqs.(F.53)-(F.60) can be integrated backwardly by the followings, (subscription defines a time step)

$$\boldsymbol{\varepsilon}^e_{n+1} - \boldsymbol{\varepsilon}^e_n = \{\boldsymbol{\varepsilon}_{n+1} - \boldsymbol{\varepsilon}^p_{n+1}\} - \{\boldsymbol{\varepsilon}_n - \boldsymbol{\varepsilon}^p_n\} = \{\boldsymbol{\varepsilon}_{n+1} - \boldsymbol{\varepsilon}_n\} - \{\boldsymbol{\varepsilon}^p_{n+1} - \boldsymbol{\varepsilon}^p_n\} = \Delta\boldsymbol{\varepsilon} - \{\boldsymbol{\varepsilon}^p_{n+1} - \boldsymbol{\varepsilon}^p_n\} \tag{F.61}$$

$$\boldsymbol{\sigma}'_{n+1} - \boldsymbol{\sigma}'_n = \mathbf{c}^e_{sn+1} : \{\boldsymbol{\varepsilon}^e_{n+1} - \boldsymbol{\varepsilon}^e_n\} \tag{F.62}$$

$$\mathbf{c}^e_{sn+1} = \mathbf{c}^e_s(\boldsymbol{\sigma}'_{n+1}, \boldsymbol{\sigma}'_n) \tag{F.63}$$

$$\boldsymbol{\varepsilon}^p_{n+1} - \boldsymbol{\varepsilon}^p_n = \Delta\gamma_{n+1}\partial_{\boldsymbol{\sigma}'} f_{n+1} \tag{F.64}$$

$$p'_{cn+1} = p'_{cn}\exp\left(\frac{\varepsilon^p_{v\,n+1} - \varepsilon^p_{v\,n}}{\overline{\lambda} - \overline{\kappa}}\right) \tag{F.65}$$

$$\boldsymbol{\sigma}'_{cn+1} = p'_{cn+1}\{\mathbf{1} + \boldsymbol{\eta}_\mathbf{c}\} = p'_{cn}\exp\left(\frac{\varepsilon^p_{v\,n+1} - \varepsilon^p_{v\,n}}{\overline{\lambda} - \overline{\kappa}}\right)\{\mathbf{1} + \boldsymbol{\eta}_\mathbf{c}\} \tag{F.66}$$

$$f_{n+1} = f(\boldsymbol{\sigma}'_{n+1}, \boldsymbol{\sigma}'_{cn+1}) \tag{F.67}$$

$$\Delta\gamma \geq 0 \,; f_{n+1} \leq 0 \,; \Delta\gamma f_{n+1} = 0 \tag{F.68}$$

Eq.(F.61) can be written in the notion of relaxation from trial state serving as a guessed value for the non-linear system, expressed by

$$\boldsymbol{\varepsilon}^e_{n+1} = \{\Delta\boldsymbol{\varepsilon} + \boldsymbol{\varepsilon}^e_n\} - \{\boldsymbol{\varepsilon}^p_{n+1} - \boldsymbol{\varepsilon}^p_n\} = \boldsymbol{\varepsilon}^{tr} - \{\boldsymbol{\varepsilon}^p_{n+1} - \boldsymbol{\varepsilon}^p_n\} \tag{F.69}$$

$$\text{where} \quad \boldsymbol{\varepsilon}^{tr} = \Delta\boldsymbol{\varepsilon} + \boldsymbol{\varepsilon}^e_n \tag{F.70}$$

F-9 Reduced form of backwardly incremental constitutive equations

Substitutions of Eq.(F.64) into Eqs.(F.69), (F.66) give

$$\boldsymbol{\varepsilon}^e_{n+1} = \boldsymbol{\varepsilon}^{tr} - \Delta\gamma_{n+1}\partial_{\boldsymbol{\sigma}'} f_{n+1} \tag{F.71}$$

$$\boldsymbol{\sigma}'_{cn+1} = p'_{cn}\exp\left(\frac{\mathbf{1} : \{\boldsymbol{\varepsilon}^p_{n+1} - \boldsymbol{\varepsilon}^p_n\}}{\overline{\lambda} - \overline{\kappa}}\right)\{\mathbf{1} + \boldsymbol{\eta}_\mathbf{c}\} = p'_{cn}\exp\left(\frac{\mathbf{1} : \Delta\gamma_{n+1}\partial_{\boldsymbol{\sigma}'} f_{n+1}}{\overline{\lambda} - \overline{\kappa}}\right)\{\mathbf{1} + \boldsymbol{\eta}_\mathbf{c}\} \tag{F.72}$$

Substitutions of Eqs.(F.63) into Eq. (F.62) give implicit form of $\boldsymbol{\sigma}'_{n+1}$ by arranging

$$\boldsymbol{\sigma}'_{n+1} = \boldsymbol{\sigma}'_n + \mathbf{c}^e_s(\boldsymbol{\sigma}'_{n+1}, \boldsymbol{\sigma}'_n) : \{\boldsymbol{\varepsilon}^e_{n+1} - \boldsymbol{\varepsilon}^e_n\} \tag{F.73}$$

Substitions of Eq.(F.71) into Eq.(F.72), and then with Eq.(F.66), obtain Eq.(F.74). Next step is substitutions of Eqs.(F.73), (F.74) into Eq.(F.67), obtaining updated yield function Eq.(F.75) as a function of $\boldsymbol{\varepsilon}^e_{n+1}$.

$$\boldsymbol{\sigma}'_{cn+1}(\boldsymbol{\varepsilon}^e_{n+1}) = p'_{cn} \exp\left(\frac{\mathbf{1}:\left\{\boldsymbol{\varepsilon}^{tr} - \boldsymbol{\varepsilon}^e_{n+1}\right\}}{\bar{\lambda} - \bar{\kappa}}\right)\left\{\mathbf{1} + \boldsymbol{\eta_c}\right\} \tag{F.74}$$

$$f_{n+1}(\boldsymbol{\varepsilon}^e_{n+1}) = f(\boldsymbol{\sigma}'_{n+1}(\boldsymbol{\varepsilon}^e_{n+1}), \boldsymbol{\sigma}'_{cn+1}(\boldsymbol{\varepsilon}^e_{n+1})) = 0 \tag{F.75}$$

As a result, the primitive nonlinear system noted by Eq.(F.61) to Eq.(F.67) is reduced to two nonlinear system of Eq.(F.71) and Eq.(F.75) where Eq.(F.71) contains Eqs.(F.61),(F.64) and Eq.(F.75) contain Eqs. (F.61), (F.62), (F.63), (F.66) and (F.67).

F-10 Consistent elastic moduli

$$\frac{\partial \boldsymbol{\sigma}'_{n+1}}{\partial \boldsymbol{\varepsilon}^e_{n+1}} = \left\{\boldsymbol{\varepsilon}^e_{n+1} - \boldsymbol{\varepsilon}^e_n\right\} : \frac{\partial \mathbf{c}^e_{sn+1}}{\partial \boldsymbol{\sigma}'_{n+1}} : \frac{\partial \boldsymbol{\sigma}'_{n+1}}{\partial \boldsymbol{\varepsilon}^e_{n+1}} + \mathbf{c}^e_{sn+1}$$

$$\left[\mathbf{I} - \left[\frac{\partial \mathbf{c}^e_{sn+1}}{\partial \boldsymbol{\sigma}'_{n+1}}\right]^T : \left\{\boldsymbol{\varepsilon}^e_{n+1} - \boldsymbol{\varepsilon}^e_n\right\}\right] : \frac{\partial \boldsymbol{\sigma}'_{n+1}}{\partial \boldsymbol{\varepsilon}^e_{n+1}} = \mathbf{c}^e_{sn+1} \tag{F.76}$$

$$\mathbf{c}^e_{n+1} = \frac{\partial \boldsymbol{\sigma}'_{n+1}}{\partial \boldsymbol{\varepsilon}^e_{n+1}} = \left[\mathbf{I} - \left[\frac{\partial \mathbf{c}^e_{sn+1}}{\partial \boldsymbol{\sigma}'_{n+1}}\right]^T : \left\{\boldsymbol{\varepsilon}^e_{n+1} - \boldsymbol{\varepsilon}^e_n\right\}\right]^{-1} : \mathbf{c}^e_{sn+1}$$

In this study, to reduce to complexity of tangential elastic tensor, the incremental strain tensor inside stiffness tensor is omitted. The simplified tangential elastic tensor shown below is employed instead in this study.

$$\mathbf{c}^e_{n+1} = \frac{\partial \boldsymbol{\sigma}'_{n+1}}{\partial \boldsymbol{\varepsilon}^e_{n+1}} \approx K_{n+1}\mathbf{1} \otimes \mathbf{1} + 2G_s \mathbf{A} \tag{F.77}$$

The number of tensor basic would become 16 if the incremental strain deviator were included in consideration. The simplification has the consistent tangential moduli lost the fully backward scheme; therefore, it should be called semi-consistent tangential moduli in this study.

F-11 Partial derivative of yield function with respect to elastic strain tensor
According to Eqs.(F.73), (F.74) and (F.75), the partial derivative is given by

$$\frac{\partial f}{\partial \boldsymbol{\varepsilon}^e} = \partial_{\boldsymbol{\sigma}'} f : \frac{\partial \boldsymbol{\sigma}'}{\partial \boldsymbol{\varepsilon}^e} + \partial_{\boldsymbol{\sigma}'_c} f : \frac{\partial \boldsymbol{\sigma}'_c}{\partial \boldsymbol{\varepsilon}^e} \tag{F.78}$$

According to Eq.(F.74), the derivative of stress hardening tensor with respect to elastic strain is,

$$\frac{\partial \boldsymbol{\sigma}'_{cn+1}}{\partial \boldsymbol{\varepsilon}^e_{n+1}} = \frac{\partial \boldsymbol{\sigma}'_{cn+1}}{\partial p'_{cn+1}} \otimes \frac{\partial p'_{cn+1}}{\partial \boldsymbol{\varepsilon}^e_{n+1}} = \left\{\mathbf{1} + \boldsymbol{\eta_c}\right\} \otimes \frac{-p'_{cn}}{\bar{\lambda} - \bar{\kappa}} e \exp\left(\frac{\mathbf{1}:\left\{\boldsymbol{\varepsilon}^{tr} - \boldsymbol{\varepsilon}^e_{n+1}\right\}}{\bar{\lambda} - \bar{\kappa}}\right)\mathbf{1}$$

$$= \left\{\mathbf{1} + \boldsymbol{\eta_c}\right\} \otimes \frac{-p'_c}{\bar{\lambda} - \bar{\kappa}}\mathbf{1} = \frac{-I_{c1}}{3\left(\bar{\lambda} - \bar{\kappa}\right)}\left[\mathbf{1} \otimes \mathbf{1} + \boldsymbol{\eta_c} \otimes \mathbf{1}\right] \tag{F.79}$$

According to Eq.(F.79) and Appendix B, a right term in Eq.(F.78) can be expanded to,

$$\partial_{\boldsymbol{\sigma}'_c} f : \frac{\partial \boldsymbol{\sigma}'_c}{\partial \boldsymbol{\varepsilon}^e} = \left\{\left[\frac{\partial \boldsymbol{\sigma}'_c}{\partial \boldsymbol{\varepsilon}^e}\right]^T : \partial_{\boldsymbol{\sigma}'_c} f\right\}_{n+1} = \frac{-I_{c1}}{3\left(\bar{\lambda} - \bar{\kappa}\right)}\left\{\mathbf{1} \otimes \mathbf{1} + \mathbf{1} \otimes \boldsymbol{\eta_c}\right\} : \left(s_1 \mathbf{1} + s_2 \bar{\mathbf{n}}\right)$$

$$= \frac{-I_{c1}}{3\left(\bar{\lambda} - \bar{\kappa}\right)}\left(3s_1 + s_2\left(\boldsymbol{\eta_c} : \bar{\mathbf{n}}\right)\right)\mathbf{1} = \frac{-I_{c1}}{\bar{\lambda} - \bar{\kappa}}\frac{\partial f}{\partial I_{c1}}\mathbf{1} = \frac{MD}{\bar{\lambda} - \bar{\kappa}}\mathbf{1} \tag{F.80}$$

where $MD = \dfrac{\lambda - \kappa}{1 + e_o} = \bar{\lambda} - \bar{\kappa}$ (F.81)

Substitution of relation in Eq.(F.81) into Eq.(F.80) obtains,

$$\partial_{\boldsymbol{\sigma}'_c} f : \frac{\partial \boldsymbol{\sigma}'_c}{\partial \boldsymbol{\varepsilon}^e} = \mathbf{1} \tag{F.82}$$

As a result of Eq.(F.82), Eq.(F.78) is reduced to,

$$\frac{\partial f}{\partial \boldsymbol{\varepsilon}^e} = \partial_{\boldsymbol{\sigma}'} f : \mathbf{c}^e + \mathbf{1} \tag{F.83}$$

F-12 Partial derivative of yield function gradient with respect to elastic strain tensor
According to Eqs.(F.73), (F.74) and (F.75), the partial derivative is given by

$$\frac{\partial\{\partial_{\sigma'}f\}}{\partial\varepsilon^e} = \partial^2_{\sigma'\sigma'}f : \frac{\partial\sigma'}{\partial\varepsilon^e} + \partial^2_{\sigma'\sigma'_c}f : \frac{\partial\sigma'_c}{\partial\varepsilon^e} \tag{F.84}$$

According to Eqs.(F.79), (F.35), a right term in Eq.(F.84) can be expanded to the following terms,

$$\partial^2_{\sigma'\sigma'_c}f : \frac{\partial\sigma'_c}{\partial\varepsilon^e} = \begin{bmatrix} (3M_1 + M_3(\bar{\mathbf{n}}:\boldsymbol{\eta_c}) + M_6(\boldsymbol{\eta_c}:\boldsymbol{\eta_c}))\mathbf{1}\otimes\mathbf{1} \\ + (3M_4 + M_5(\bar{\mathbf{n}}:\boldsymbol{\eta_c}))\bar{\mathbf{n}}\otimes\mathbf{1} + (3M_7 + M_2)\boldsymbol{\eta_c}\otimes\mathbf{1} \end{bmatrix} \tag{F.85}$$

Referring to Eqs.(F.36)-(F.42), these scalar values in Eq.(F.85) can be evaluated in the same manner with Appendix F-6 as,

$$3M_1 + M_3(\bar{\mathbf{n}}:\boldsymbol{\eta_c}) + M_6(\boldsymbol{\eta_c}:\boldsymbol{\eta_c}) = 0, \quad 3M_4 + M_5(\bar{\mathbf{n}}:\boldsymbol{\eta_c}) = 0, \quad 3M_7 + M_2 = 0 \tag{F.86}$$

Substitution of Eq.(F.86) into Eq.(F.84) obtains,

$$\partial^2_{\sigma'\sigma'_c}f : \frac{\partial\sigma'_c}{\partial\varepsilon^e} = \mathbf{0} \tag{F.87}$$

As a result of Eq.(F.87), Eq.(F.84) is reduced to,

$$\frac{\partial\{\partial_{\sigma'}f\}}{\partial\varepsilon^e} = \partial^2_{\sigma'\sigma'}f : \mathbf{c}^e \tag{F.88}$$

F-13 Algorithmic moduli

A component of unknown variables, unknown variation and residuals are shown below,

$$\mathbf{x} = \begin{Bmatrix} \boldsymbol{\varepsilon}^e_{n+1} \\ \Delta\gamma_{n+1} \end{Bmatrix}, \quad \delta\mathbf{x} = \begin{Bmatrix} \delta\boldsymbol{\varepsilon}^e_{n+1} \\ \delta\Delta\gamma_{n+1} \end{Bmatrix} \tag{F.89},(F.90)$$

$$\mathbf{r} = \begin{Bmatrix} \bar{\mathbf{r}}_{n+1} \\ f_{n+1} \end{Bmatrix} = \begin{Bmatrix} \boldsymbol{\varepsilon}^e_{n+1} - \boldsymbol{\varepsilon}^{tr} + \Delta\gamma_{n+1}\partial_{\sigma'}f_{n+1} \\ f\left(\boldsymbol{\sigma}'(\boldsymbol{\varepsilon}^e_{n+1}), \boldsymbol{\sigma}'_c(\boldsymbol{\varepsilon}^e_{n+1})\right) \end{Bmatrix} \tag{F.91}$$

According to Newton's method, the unknown variation can be evaluated by

$$\delta\mathbf{x} = -\boldsymbol{\Omega}^{-1}\cdot\mathbf{r} \tag{F.92}$$

where the Jacobian matrix is,

$$\boldsymbol{\Omega} = \begin{bmatrix} \dfrac{\partial\bar{\mathbf{r}}}{\partial\mathbf{x}_1} & \dfrac{\partial\bar{\mathbf{r}}}{\partial x_2} \\ \dfrac{\partial f}{\partial\mathbf{x}_1} & \dfrac{\partial f}{\partial x_2} \end{bmatrix} \tag{F.93}$$

Each component of Jacobian matrix $\boldsymbol{\Omega}$ is given below

$$\frac{\partial\bar{\mathbf{r}}}{\partial\mathbf{x}_1} = \mathbf{I} + \Delta\gamma\left[\partial^2_{\sigma'\sigma'}f : \mathbf{c}^e + \partial^2_{\sigma'\sigma'_c}f : \frac{\partial\sigma'_c}{\partial\varepsilon^e}\right]_{n+1} \tag{F.94}$$

$$\frac{\partial\bar{\mathbf{r}}}{\partial x_2} = \partial_{\sigma'}f_{n+1} \tag{F.95}$$

$$\frac{\partial f}{\partial\mathbf{x}_1} = \left\{\partial_{\sigma'}f : \mathbf{c}^e + \partial_{\sigma'_c}f : \frac{\partial\sigma'_c}{\partial\varepsilon^e}\right\}_{n+1} \tag{F.96}$$

$$\frac{\partial f}{\partial x_2} = 0 \tag{F.97}$$

According to the SO model in Appendix B, derivatives referred in Eqs.(F.94)-(F.96) can be taken from Appendices F-11-F-12. As a consequence, Eq.(F.94),(F.96) are reduced to Eqs.(F.98),(F.99)

$$\frac{\partial\bar{\mathbf{r}}}{\partial\mathbf{x}_1} = \mathbf{I} + \left[\Delta\gamma\partial^2_{\sigma'\sigma'}f : \mathbf{c}^e\right]_{n+1} \tag{F.98}$$

$$\frac{\partial f}{\partial\mathbf{x}_1} = \left\{\partial_{\sigma'}f : \mathbf{c}^e\right\}_{n+1} + \mathbf{1} \tag{F.99}$$

To obtain the exact form of variation of unknown variable $\delta\mathbf{x}$, the exact Hessian matrix defined by is introduced for a convenience in equation manipulation as,

$$\boldsymbol{\Xi} = \left[\mathbf{c}^{e-1} + \Delta\gamma\partial^2_{\sigma'\sigma'}f\right]^{-1}_{n+1} \tag{F.100}$$

Omit a subscription n+1, Eq.(F.98) can be further reduced using $\boldsymbol{\Xi}$ defined in Eq.(F.100),

$$\frac{\partial \overline{\mathbf{r}}}{\partial \mathbf{x}_1} = \mathbf{c}^{e-1} : \mathbf{c}^e + \Delta \gamma \partial_{\sigma'\sigma'}^2 f : \mathbf{c}^e = \left[\mathbf{c}^{e-1} + \Delta \gamma \partial_{\sigma'\sigma'}^2 f \right] : \mathbf{c}^e = \mathbf{\Xi}^{-1} : \mathbf{c}^e \tag{F.101}$$

It is an implicit procedure that involves solving a local 6x6 system of equations in inverting matrix $\mathbf{\Xi}$ (second-order tensor) in Eq.(F.100). The more efficient method will be introduced in the next chapter to deal with numerical inversion.

An exact form of unknown variation $\delta \mathbf{x}$ is derived by manipulating equation of residuals shown in Eq.(F.91). Using all of the prescribed determination deduces Eq.(F.92) to Eq.(F.102),(F.103).

$$\mathbf{\Xi}^{-1} : \mathbf{c}^e : \delta \boldsymbol{\varepsilon}^e + \partial_{\sigma'} f \delta \Delta \gamma = -\overline{\mathbf{r}} \tag{F.102}$$

$$\left\{ \partial_{\sigma'} f : \mathbf{c}^e + \mathbf{1} \right\} : \delta \boldsymbol{\varepsilon}^e = -f \tag{F.103}$$

Performing double product of $\left[\mathbf{\Xi}^{-1} : \mathbf{c}^e \right]^{-1}$ to Eq.(F.102) results in,

$$\delta \boldsymbol{\varepsilon}^e + \mathbf{c}^{e-1} : \mathbf{\Xi} : \partial_{\sigma'} f \delta \Delta \gamma = -\mathbf{c}^{e-1} : \mathbf{\Xi} : \overline{\mathbf{r}} \tag{F.104}$$

Next, perform double product of $\left\{ \partial_{\sigma'} f : \mathbf{c}^e + \mathbf{1} \right\}$ to Eq.(F.104), obtain a scalar product,

$$\left\{ \partial_{\sigma'} f : \mathbf{c}^e + \mathbf{1} \right\} : \delta \boldsymbol{\varepsilon}^e + \left\{ \partial_{\sigma'} f : \mathbf{c}^e + \mathbf{1} \right\} : \left\{ \mathbf{c}^{e-1} : \mathbf{\Xi} : \partial_{\sigma'} f \right\} \delta \Delta \gamma$$
$$= -\left\{ \partial_{\sigma'} f : \mathbf{c}^e + \mathbf{1} \right\} : \left\{ \mathbf{c}^{e-1} : \mathbf{\Xi} : \overline{\mathbf{r}} \right\} \tag{F.105}$$

Refer to Eq.(F.103), a term of $\left\{ \partial_{\sigma'} f : \mathbf{c}^e + \mathbf{1} \right\} : \delta \boldsymbol{\varepsilon}^e$ in Eq.(F.105) can be replaced by $-f$, therefore,

$$-f + \left\{ \partial_{\sigma'} f : \mathbf{c}^e + \mathbf{1} \right\} : \left\{ \mathbf{c}^{e-1} : \mathbf{\Xi} : \partial_{\sigma'} f \right\} \delta \Delta \gamma = -\left\{ \partial_{\sigma'} f : \mathbf{c}^e + \mathbf{1} \right\} : \left\{ \mathbf{c}^{e-1} : \mathbf{\Xi} : \overline{\mathbf{r}} \right\} \tag{F.106}$$

From the above equation, $\delta \Delta \gamma$ is then enable to solve,

$$\delta \Delta \gamma = \frac{f - \left\{ \partial_{\sigma'} f : \mathbf{c}^e + \mathbf{1} \right\} : \left\{ \mathbf{c}^{e-1} : \mathbf{\Xi} : \overline{\mathbf{r}} \right\}}{\left\{ \partial_{\sigma'} f : \mathbf{c}^e + \mathbf{1} \right\} : \left\{ \mathbf{c}^{e-1} : \mathbf{\Xi} : \partial_{\sigma'} f \right\}} \tag{F.107}$$

$\delta \Delta \gamma$ can be further reduced by tensorial expansion,

$$\delta \Delta \gamma = \frac{f - \left(\partial_{\sigma'} f : \mathbf{c}^e : \left\{ \mathbf{c}^{e-1} : \mathbf{\Xi} : \overline{\mathbf{r}} \right\} + \mathbf{1} : \left\{ \mathbf{c}^{e-1} : \mathbf{\Xi} : \overline{\mathbf{r}} \right\} \right)}{\partial_{\sigma'} f : \mathbf{c}^e : \left\{ \mathbf{c}^{e-1} : \mathbf{\Xi} : \partial_{\sigma'} f \right\} + \mathbf{1} : \left\{ \mathbf{c}^{e-1} : \mathbf{\Xi} : \partial_{\sigma'} f \right\}}$$

$$= \frac{f - \left(\partial_{\sigma'} f : \mathbf{\Xi} : \overline{\mathbf{r}} + \left\{ \mathbf{c}^{e-1} : \mathbf{1} \right\} : \left\{ \mathbf{\Xi} : \overline{\mathbf{r}} \right\} \right)}{\partial_{\sigma'} f : \mathbf{\Xi} : \partial_{\sigma'} f + \left\{ \mathbf{c}^{e-1} : \mathbf{1} \right\} : \left\{ \mathbf{\Xi} : \partial_{\sigma'} f \right\}}$$

$$= \frac{f - \left(\partial_{\sigma'} f : \mathbf{\Xi} : \overline{\mathbf{r}} + \dfrac{3}{9K} \mathbf{1} : \left\{ \mathbf{\Xi} : \overline{\mathbf{r}} \right\} \right)}{\partial_{\sigma'} f : \mathbf{\Xi} : \partial_{\sigma'} f + \dfrac{1}{3K} \mathbf{1} : \left\{ \mathbf{\Xi} : \partial_{\sigma'} f \right\}}$$

$$= \frac{f - \left(\partial_{\sigma'} f + \dfrac{1}{3K} \mathbf{1} \right) : \left\{ \mathbf{\Xi} : \overline{\mathbf{r}} \right\}}{\left\{ \partial_{\sigma'} f + \dfrac{1}{3K} \mathbf{1} \right\} : \left\{ \mathbf{\Xi} : \partial_{\sigma'} f \right\}} \tag{F.108}$$

Finally $\delta \boldsymbol{\varepsilon}^e$ can be solved by manipulating Eq.(F.102). Using $\delta \Delta \gamma$ in Eq.(F.108), variation of elastic strain is found,

$$\delta \boldsymbol{\varepsilon}^e = -\mathbf{c}^{e-1} : \mathbf{\Xi} : \left\{ \overline{\mathbf{r}} + \partial_{\sigma'} f \delta \Delta \gamma \right\} \tag{F.109}$$

F-14 Backwardly differential form

Differentiation of a system given in Eqs.(F.61)-(F.67) is more complex than solving for unknown variables in the system. The target of the differentiation is to solve for consistent tangential moduli. As a result, expression for stress tensor would not be replaced by other expressions that have been carried out to solve the system. Performing a derivative of Eqs.(F.61)-(F.67) obtain,

$$d \boldsymbol{\varepsilon}_{n+1}^e = d \boldsymbol{\varepsilon}_{n+1} - d \boldsymbol{\varepsilon}_{n+1}^p \tag{F.110}$$

$$d \boldsymbol{\sigma}'_{n+1} = d \mathbf{c}_{sn+1}^e : \left\{ \boldsymbol{\varepsilon}_{n+1}^e - \boldsymbol{\varepsilon}_n^e \right\} + \mathbf{c}_{sn+1}^e : d \boldsymbol{\varepsilon}_{n+1}^e \tag{F.111}$$

$$d\mathbf{c}^e_{sn+1} = \partial_{\boldsymbol{\sigma}'}\mathbf{c}^e_s(\boldsymbol{\sigma}'_{n+1},\boldsymbol{\sigma}'_n):d\boldsymbol{\sigma}'_{n+1} \tag{F.112}$$

$$d\boldsymbol{\varepsilon}^p_{n+1} = \Delta\gamma_{n+1}d\partial_{\boldsymbol{\sigma}'}f_{n+1} + \partial_{\boldsymbol{\sigma}'}f_{n+1}\otimes d\Delta\gamma_{n+1} \tag{F.113}$$

$$d\boldsymbol{\sigma}'_{cn+1} = \left\{\mathbf{1}+\boldsymbol{\eta_c}\right\}\frac{p'_{cn+1}}{\bar{\lambda}-\bar{\kappa}}\mathbf{1}:d\boldsymbol{\varepsilon}^p_{n+1} \tag{F.114}$$

$$df_{n+1} = \partial_{\boldsymbol{\sigma}'}f:d\boldsymbol{\sigma}'_{n+1} + \partial_{\boldsymbol{\sigma}'_c}f:d\boldsymbol{\sigma}'_{cn+1} \tag{F.115}$$

Eq.(F.111) contains a derivative of elastic secant tensor, which is expanded to sixth-order tensor as noted in Eq.(F.112). To approach a solution numerically rather than algebraically, Stress tensors appeared in left and right side in Eq.(F.73) are treated at different iteration <k> as shown below,

$$\boldsymbol{\sigma}'^{<k>}_{n+1} - \boldsymbol{\sigma}'_n = \mathbf{c}^e_{n+1}(\boldsymbol{\sigma}'^{<k-1>}_{n+1},\boldsymbol{\sigma}'_n):\left\{\boldsymbol{\varepsilon}^e_{n+1}-\boldsymbol{\varepsilon}^e_n\right\} \tag{F.116}$$

As a consequence, the derivative of elastic secant tensor can be ignored in the sense that noted in Eq.(F.117). Hence, Eq.(F.112) is taken as zero as shown in Eq.(F.118). The simplified form of Eq. (F.111) is shown by Eq.(F.119)

$$\frac{\partial\mathbf{c}^e_{n+1}(\boldsymbol{\sigma}'^{<k-1>}_{n+1},\boldsymbol{\sigma}'_n)}{\partial\boldsymbol{\sigma}'^{<k>}_{n+1}} = \mathbf{0} \tag{F.117}$$

$$d\mathbf{c}^e_{sn+1} \approx \frac{\partial\mathbf{c}^e_{n+1}(\boldsymbol{\sigma}'^{<k-1>}_{n+1},\boldsymbol{\sigma}'_n)}{\partial\boldsymbol{\sigma}'^{<k>}_{n+1}} = \mathbf{0} \tag{F.118}$$

$$d\boldsymbol{\sigma}'_{n+1} = \mathbf{c}^e_{sn+1}:d\boldsymbol{\varepsilon}^e_{n+1} \tag{F.119}$$

Substitution of Eq.(F.110) into (F.119) obtain,

$$d\boldsymbol{\sigma}'_{n+1} = \mathbf{c}^e_{sn+1}:\left\{d\boldsymbol{\varepsilon}_{n+1}-d\boldsymbol{\varepsilon}^p_{n+1}\right\} \tag{F.120}$$

Consider a term of $d\partial_{\boldsymbol{\sigma}'}f_{n+1}$ in Eq.(F.113),

$$\begin{aligned}d\partial_{\boldsymbol{\sigma}'}f_{n+1} &= \partial^2_{\boldsymbol{\sigma}'\boldsymbol{\sigma}'}f:d\boldsymbol{\sigma}'_{n+1} + \partial^2_{\boldsymbol{\sigma}'\boldsymbol{\sigma}'_c}f:d\boldsymbol{\sigma}'_{cn+1}\\ &= \partial^2_{\boldsymbol{\sigma}'\boldsymbol{\sigma}'}f:d\boldsymbol{\sigma}'_{n+1} + \partial^2_{\boldsymbol{\sigma}'\boldsymbol{\sigma}'_c}f:\frac{\partial\boldsymbol{\sigma}'_c}{\partial p'_c}dp'_{cn+1}\end{aligned} \tag{F.121}$$

According to Eq.(F.49), $\partial^2_{\boldsymbol{\sigma}'\boldsymbol{\sigma}'_c}f:\dfrac{\partial\boldsymbol{\sigma}'_c}{\partial p'_c}$ in Eq.(F.121) is equal to zero, then

$$d\partial_{\boldsymbol{\sigma}'}f_{n+1} = \partial^2_{\boldsymbol{\sigma}'\boldsymbol{\sigma}'}f:d\boldsymbol{\sigma}'_{n+1} \tag{F.122}$$

Substitution of Eq.(F.122) into (F.113) obtains,

$$d\boldsymbol{\varepsilon}^p_{n+1} = \Delta\gamma_{n+1}\partial^2_{\boldsymbol{\sigma}'\boldsymbol{\sigma}'}f:d\boldsymbol{\sigma}'_{n+1} + \partial_{\boldsymbol{\sigma}'}f_{n+1}\otimes d\Delta\gamma_{n+1} \tag{F.123}$$

Substitution of Eq.(F.114) into (F.115) obtain,

$$df_{n+1} = \partial_{\boldsymbol{\sigma}'}f:d\boldsymbol{\sigma}'_{n+1} + \partial_{\boldsymbol{\sigma}'_c}f:\left\{\mathbf{1}+\boldsymbol{\eta_c}\right\}\frac{p'_{cn+1}}{\bar{\lambda}-\bar{\kappa}}\left(\mathbf{1}:d\boldsymbol{\varepsilon}^p_{n+1}\right) \tag{F.124}$$

According to Appendix B and Eq.(F.81), the term $\partial_{\boldsymbol{\sigma}'_c}f:\left\{\mathbf{1}+\boldsymbol{\eta}_c\right\}$ in Eq.(F.124) can be reduced by,

$$\partial_{\boldsymbol{\sigma}'_c}f:\left\{\mathbf{1}+\boldsymbol{\eta}_c\right\} = \partial_{\boldsymbol{\sigma}'_c}f:\frac{\partial\boldsymbol{\sigma}'_c}{\partial p'_c} = \frac{\partial f}{\partial p'_c} = -\frac{MD}{p'_c} = -\frac{\bar{\lambda}-\bar{\kappa}}{p'_c} \tag{F.125}$$

As a result, Eq.(F.124) is reduced in association to Eqs.(F.125), (F.123)

$$\begin{aligned}df_{n+1} &= \partial_{\boldsymbol{\sigma}'}f:d\boldsymbol{\sigma}'_{n+1} - \mathbf{1}:d\boldsymbol{\varepsilon}^p_{n+1}\\ &= \partial_{\boldsymbol{\sigma}'}f:d\boldsymbol{\sigma}'_{n+1} - \mathbf{1}:\left\{\Delta\gamma_{n+1}\partial^2_{\boldsymbol{\sigma}'\boldsymbol{\sigma}'}f:d\boldsymbol{\sigma}'_{n+1}+\partial_{\boldsymbol{\sigma}'}f_{n+1}\otimes d\Delta\gamma_{n+1}\right\}\\ &= \partial_{\boldsymbol{\sigma}'}f:d\boldsymbol{\sigma}'_{n+1} - \left\{\Delta\gamma_{n+1}\left(\partial^2_{\boldsymbol{\sigma}'\boldsymbol{\sigma}'}f:\mathbf{1}\right):d\boldsymbol{\sigma}'_{n+1}+\left(\mathbf{1}:\partial_{\boldsymbol{\sigma}'}f_{n+1}\right)d\Delta\gamma_{n+1}\right\}\\ &= \left\{\partial_{\boldsymbol{\sigma}'}f-\Delta\gamma_{n+1}\left(\partial^2_{\boldsymbol{\sigma}'\boldsymbol{\sigma}'}f:\mathbf{1}\right)\right\}:d\boldsymbol{\sigma}'_{n+1} - \left(\mathbf{1}:\partial_{\boldsymbol{\sigma}'}f_{n+1}\right)d\Delta\gamma_{n+1}\end{aligned} \tag{F.126}$$

According to the consistency requirement, $df_{n+1}=0$, therefore, Eq.(F.126) can be used to solve for $d\Delta\gamma_{n+1}$

$$d\Delta\gamma_{n+1} = \frac{1}{\mathbf{1}:\partial_{\boldsymbol{\sigma}'}f_{n+1}}\left\{\partial_{\boldsymbol{\sigma}'}f-\Delta\gamma_{n+1}\left\{\partial^2_{\boldsymbol{\sigma}'\boldsymbol{\sigma}'}f:\mathbf{1}\right\}\right\}:d\boldsymbol{\sigma}'_{n+1} \tag{F.127}$$

Substitution of Eq.(F.127) into (F.123) obtains,

$$d\boldsymbol{\varepsilon}_{n+1}^{p} = \Delta\gamma_{n+1}\partial_{\boldsymbol{\sigma}'\boldsymbol{\sigma}'}^{2}f : d\boldsymbol{\sigma}'_{n+1} + \partial_{\boldsymbol{\sigma}'}f \otimes \frac{1}{\mathbf{1}:\partial_{\boldsymbol{\sigma}'}f_{n+1}}\left\{\partial_{\boldsymbol{\sigma}'}f - \Delta\gamma_{n+1}\left\{\partial_{\boldsymbol{\sigma}'\boldsymbol{\sigma}}^{2}f:\mathbf{1}\right\}\right\} : d\boldsymbol{\sigma}'_{n+1}$$

$$= \left[\frac{\partial_{\boldsymbol{\sigma}'}f \otimes \partial_{\boldsymbol{\sigma}'}f}{\mathbf{1}:\partial_{\boldsymbol{\sigma}'}f_{n+1}} + \Delta\gamma_{n+1}\left[\partial_{\boldsymbol{\sigma}'\boldsymbol{\sigma}'}^{2}f - \frac{\partial_{\boldsymbol{\sigma}'}f \otimes \left\{\partial_{\boldsymbol{\sigma}'\boldsymbol{\sigma}}^{2}f:\mathbf{1}\right\}}{\mathbf{1}:\partial_{\boldsymbol{\sigma}'}f_{n+1}}\right]\right] : d\boldsymbol{\sigma}'_{n+1} \quad\quad\text{(F.128)}$$

$$= \left[\frac{\partial_{\boldsymbol{\sigma}'}f \otimes \partial_{\boldsymbol{\sigma}'}f}{H_{p}} + \Delta\gamma_{n+1}\left[\mathbf{I} - \frac{\partial_{\boldsymbol{\sigma}'}f \otimes \mathbf{1}}{H_{p}}\right]:\partial_{\boldsymbol{\sigma}'\boldsymbol{\sigma}'}^{2}f\right] : d\boldsymbol{\sigma}'_{n+1}$$

Substitution of Eq.(F.128) into (F.120) obtains,

$$d\boldsymbol{\sigma}'_{n+1} = \mathbf{c}_{sn+1}^{e} : \left\{d\boldsymbol{\varepsilon}_{n+1} - \left[\frac{\partial_{\boldsymbol{\sigma}'}f \otimes \partial_{\boldsymbol{\sigma}'}f}{H_{p}} + \Delta\gamma_{n+1}\left[\mathbf{I} - \frac{\partial_{\boldsymbol{\sigma}'}f \otimes \mathbf{1}}{H_{p}}\right]:\partial_{\boldsymbol{\sigma}'\boldsymbol{\sigma}'}^{2}f\right] : d\boldsymbol{\sigma}'_{n+1}\right\} \quad\quad\text{(F.129)}$$

Manipulation of common terms of $d\boldsymbol{\sigma}'_{n+1}$ to L.H.S., obtains $d\boldsymbol{\varepsilon}_{n+1}$ as

$$\left\{\mathbf{I} + \mathbf{c}_{sn+1}^{e} : \left[\frac{\partial_{\boldsymbol{\sigma}'}f \otimes \partial_{\boldsymbol{\sigma}'}f}{H_{p}} + \Delta\gamma_{n+1}\left[\mathbf{I} - \frac{\partial_{\boldsymbol{\sigma}'}f \otimes \mathbf{1}}{H_{p}}\right]:\partial_{\boldsymbol{\sigma}'\boldsymbol{\sigma}'}^{2}f\right]\right\} : d\boldsymbol{\sigma}'_{n+1} = \mathbf{c}_{sn+1}^{e} : d\boldsymbol{\varepsilon}_{n+1}$$

$$d\boldsymbol{\varepsilon}_{n+1} = \left(\mathbf{c}_{sn+1}^{e}\right)^{-1} : \left\{\mathbf{I} + \mathbf{c}_{sn+1}^{e} : \left[\frac{\partial_{\boldsymbol{\sigma}'}f \otimes \partial_{\boldsymbol{\sigma}'}f}{H_{p}} + \Delta\gamma_{n+1}\left[\mathbf{I} - \frac{\partial_{\boldsymbol{\sigma}'}f \otimes \mathbf{1}}{H_{p}}\right]:\partial_{\boldsymbol{\sigma}'\boldsymbol{\sigma}'}^{2}f\right]\right\} : d\boldsymbol{\sigma}'_{n+1}$$

$$= \left\{\left(\mathbf{c}_{sn+1}^{e}\right)^{-1} + \frac{\partial_{\boldsymbol{\sigma}'}f \otimes \partial_{\boldsymbol{\sigma}'}f}{H_{p}} + \Delta\gamma_{n+1}\left[\mathbf{I} - \frac{\partial_{\boldsymbol{\sigma}'}f \otimes \mathbf{1}}{H_{p}}\right]:\partial_{\boldsymbol{\sigma}'\boldsymbol{\sigma}'}^{2}f\right\} : d\boldsymbol{\sigma}'_{n+1} \quad\quad\text{(F.130)}$$

$$= \mathbf{c}_{n+1}^{ep}{}^{-1} : d\boldsymbol{\sigma}'_{n+1}$$

Inversion of Eq.(F.130) results in,

$$d\boldsymbol{\sigma}'_{n+1} = \mathbf{c}_{n+1}^{ep} : d\boldsymbol{\varepsilon}_{n+1} \quad\quad\text{(F.131)}$$

According to Eq.(F.130), the consistent tangential stiffness forth-order tensor is expressed by

$$\mathbf{c}_{n+1}^{ep} = \left[\mathbf{c}_{sn+1}^{e}{}^{-1} + \frac{1}{H_{p}}\partial_{\boldsymbol{\sigma}'}f \otimes \partial_{\boldsymbol{\sigma}'}f + \Delta\gamma\left[\mathbf{I} - \frac{1}{H_{p}}\partial_{\boldsymbol{\sigma}'}f \otimes \mathbf{1}\right]:\partial_{\boldsymbol{\sigma}'\boldsymbol{\sigma}'}^{2}f\right]^{-1} \quad\quad\text{(F.132)}$$

F-15 Simplification of consistent tangential moduli
According to the inversion of differential form given below,

$$\left[\mathbf{S} + \Delta\mathbf{S}\right]^{-1} \approx \mathbf{S}^{-1} - \mathbf{S}^{-1} : \Delta\mathbf{S} : \mathbf{S}^{-1} \quad\quad\text{(F.133)}$$

By the result of property shown in (F.133), the Eq.(F.132) can be simplified as following,

$$\mathbf{c}_{n+1}^{ep} \approx \mathbf{c}_{sn+1}^{e} - \mathbf{c}_{sn+1}^{e} : \left[\frac{1}{H_{p}}\partial_{\boldsymbol{\sigma}'}f \otimes \partial_{\boldsymbol{\sigma}'}f + \Delta\gamma\left[\mathbf{I} - \frac{1}{H_{p}}\partial_{\boldsymbol{\sigma}'}f \otimes \mathbf{1}\right]:\partial_{\boldsymbol{\sigma}'\boldsymbol{\sigma}'}^{2}f\right] : \mathbf{c}_{sn+1}^{e} \quad\quad\text{(F.134)}$$

F-16 Exact inversion of consistent tangential moduli
According to the inversion of non-singular tensor given below,

$$\left[\mathbf{T} - \mathbf{C} \otimes \mathbf{D}\right]^{-1} = \mathbf{T}^{-1} + \frac{\mathbf{T}^{-1} : \mathbf{C} \otimes \mathbf{D} : \mathbf{T}^{-1}}{1 - \mathbf{D} : \mathbf{T}^{-1} : \mathbf{C}} \quad\quad\text{(F.135)}$$

By the result of property shown in (F.135), the Eq.(F.132) can be simplified as following,

$$\mathbf{T} = \mathbf{c}_{sn+1}^{e}{}^{-1} + \Delta\gamma\left[\mathbf{I} - \frac{1}{H_{p}}\partial_{\boldsymbol{\sigma}'}f \otimes \mathbf{1}\right]:\partial_{\boldsymbol{\sigma}'\boldsymbol{\sigma}'}^{2}f$$

$$\mathbf{c}_{n+1}^{ep} = \mathbf{T}^{-1} - \frac{\mathbf{T}^{-1} : \dfrac{\partial_{\boldsymbol{\sigma}'}f \otimes \partial_{\boldsymbol{\sigma}'}f}{H_{p}} : \mathbf{T}^{-1}}{1 + \dfrac{\partial_{\boldsymbol{\sigma}'}f : \mathbf{T}^{-1} : \partial_{\boldsymbol{\sigma}'}f}{H_{p}}} \quad\quad\text{(F.136)}$$

Appendix G: Form-invariance principle

G-1 Basic invariants

The basic invariants can be written as follows,

$$tr(\boldsymbol{\sigma}') = \boldsymbol{\sigma}'_{ii} \tag{G.1}$$

$$tr(\boldsymbol{\sigma}'^2) = \boldsymbol{\sigma}'_{ij}\,\boldsymbol{\sigma}'_{ji} \tag{G.2}$$

$$tr(\boldsymbol{\sigma}'_c) = \boldsymbol{\sigma}'_{cii} \tag{G.3}$$

$$tr(\boldsymbol{\sigma}'^2_c) = \boldsymbol{\sigma}'_{cij}\,\boldsymbol{\sigma}'_{cji} \tag{G.4}$$

$$tr(\boldsymbol{\sigma}'\boldsymbol{\sigma}'_c) = \boldsymbol{\sigma}'_{ij}\,\boldsymbol{\sigma}'_{cji} \tag{G.5}$$

For two-invariant anisotropic model, 5 of above basic invariants including joint invariant must be retained as arguments in the constitutive law.

G-2 Isotropic invariants

$$I_1 = tr(\boldsymbol{\sigma}') = \boldsymbol{\sigma}'_{ij}\,\boldsymbol{\delta}_{ji} = \boldsymbol{\sigma}'_{ii} \tag{G.6}$$

$$\mathbf{s}_{ij} = \boldsymbol{\sigma}'_{ij} - \frac{1}{3}I_1\boldsymbol{\delta}_{ij} \tag{G.7}$$

$$
\begin{aligned}
J_2 &= \frac{1}{2}tr(\mathbf{s}^2) = \frac{1}{2}\mathbf{s}_{ij}\mathbf{s}_{ji} \\
&= \frac{1}{2}\left\{\boldsymbol{\sigma}'_{ij} - \frac{1}{3}I_1\boldsymbol{\delta}_{ij}\right\}\left\{\boldsymbol{\sigma}'_{ji} - \frac{1}{3}I_1\boldsymbol{\delta}_{ji}\right\} \\
&= \frac{1}{2}\left\{\boldsymbol{\sigma}'_{ij}\,\boldsymbol{\sigma}'_{ji} - \frac{1}{3}I_1\boldsymbol{\sigma}'_{ij}\,\boldsymbol{\delta}_{ji} - \frac{1}{3}I_1\boldsymbol{\delta}_{ij}\boldsymbol{\sigma}'_{ji} + \frac{1}{9}I_1^2\boldsymbol{\delta}_{ij}\boldsymbol{\delta}_{ji}\right\} \\
&= \frac{1}{2}\left\{\boldsymbol{\sigma}'_{ij}\,\boldsymbol{\sigma}'_{ji} - \frac{1}{3}I_1\boldsymbol{\sigma}'_{ij}\,\boldsymbol{\delta}_{ji} - \frac{1}{3}I_1\boldsymbol{\delta}_{ij}\boldsymbol{\sigma}'_{ji} + \frac{1}{9}I_1^2\boldsymbol{\delta}_{ij}\boldsymbol{\delta}_{ji}\right\} \\
&= \frac{1}{2}\left\{tr(\boldsymbol{\sigma}'^2) - \frac{1}{3}I_1^2\right\} \\
&= \frac{1}{2}\left\{tr(\boldsymbol{\sigma}'^2) - \frac{1}{3}tr(\boldsymbol{\sigma}')^2\right\}
\end{aligned}
\tag{G.8}
$$

$$\boldsymbol{\eta}_{ij} = \frac{\mathbf{s}_{ij}}{p'_c} = \frac{3\mathbf{s}_{ij}}{I_{c1}} \tag{G.9}$$

$$I_{c1} = tr(\boldsymbol{\sigma}'_c) = \boldsymbol{\sigma}'_{cij}\,\boldsymbol{\delta}_{ji} = \boldsymbol{\sigma}'_{cii} \tag{G.10}$$

$$\mathbf{s}_{cij} = \boldsymbol{\sigma}'_{cij} - \frac{1}{3}I_{c1}\boldsymbol{\delta}_{ij} \tag{G.11}$$

$$J_{c2} = \frac{1}{2}tr(\mathbf{s}_c^2) = \frac{1}{2}\mathbf{s}_{cij}\mathbf{s}_{cji} = \frac{1}{2}\left\{tr(\boldsymbol{\sigma}'^2_c) - \frac{1}{3}tr(\boldsymbol{\sigma}'_c)^2\right\} \tag{G.12}$$

$$\boldsymbol{\eta}_{cij} = \frac{\mathbf{s}_{cij}}{p'_c} = \frac{3\mathbf{s}_{cij}}{I_{c1}} \tag{G.13}$$

There are no joint invariant appeared in isotropic invariant expressions for both stress and stress hardening variable.

G-3 Anisotropic invariants

The anisotropic invariants are defined as follows,

$$\overline{\mathbf{s}}_{ij} = \mathbf{s}_{ij} - \frac{1}{3}I_1\boldsymbol{\eta}_{cij} \tag{G.14}$$

$$\bar{J}_2 = \frac{1}{2} tr(\bar{\mathbf{s}}^2) = \frac{1}{2}\bar{\mathbf{s}}_{ij}\bar{\mathbf{s}}_{ji}$$

$$= \frac{1}{2}\left\{\mathbf{s}_{ij} - \frac{1}{3}I_1\boldsymbol{\eta}_{\mathbf{c}ij}\right\}\left\{\mathbf{s}_{ji} - \frac{1}{3}I_1\boldsymbol{\eta}_{\mathbf{c}ji}\right\}$$

$$= \frac{1}{2}\left\{\mathbf{s}_{ij}\mathbf{s}_{ji} - \frac{1}{3}I_1\mathbf{s}_{ij}\boldsymbol{\eta}_{\mathbf{c}ji} - \frac{1}{3}I_1\boldsymbol{\eta}_{\mathbf{c}ij}\mathbf{s}_{ji} + \frac{1}{9}I_1^2\boldsymbol{\eta}_{\mathbf{c}ij}\boldsymbol{\eta}_{\mathbf{c}ji}\right\}$$

$$= \frac{1}{2}\left\{2J_2 - \frac{I_1}{I_{c1}}\mathbf{s}_{ij}\mathbf{s}_{cji} - \frac{I_1}{I_{c1}}\mathbf{s}_{cij}\mathbf{s}_{ji} + \frac{I_1^2}{I_{c1}^2}\mathbf{s}_{cij}\mathbf{s}_{cji}\right\}$$

$$= J_2 - \frac{I_1}{I_{c1}}\mathbf{s}_{ij}\mathbf{s}_{cji} + \left(\frac{I_1}{I_{c1}}\right)^2 J_{c2}$$

$$= J_2 - \frac{I_1}{I_{c1}}\left\{tr(\boldsymbol{\sigma}'\boldsymbol{\sigma}'_c) - \frac{1}{3}tr(\boldsymbol{\sigma}')tr(\boldsymbol{\sigma}'_c)\right\} + \left(\frac{I_1}{I_{c1}}\right)^2 J_{c2}$$

$$= J_2 - \frac{I_1}{I_{c1}}\left\{tr(\boldsymbol{\sigma}'\boldsymbol{\sigma}'_c) - \frac{1}{3}I_1 I_{c1}\right\} + \left(\frac{I_1}{I_{c1}}\right)^2 J_{c2}$$

$$= J_2 - \left\{\frac{I_1}{I_{c1}}tr(\boldsymbol{\sigma}'\boldsymbol{\sigma}'_c) - \frac{1}{3}I_1^2\right\} + \left(\frac{I_1}{I_{c1}}\right)^2 J_{c2}$$

$$= \frac{1}{2}\left\{tr(\boldsymbol{\sigma}'^2) - \frac{1}{3}I_1^2\right\} - \left\{\frac{I_1}{I_{c1}}tr(\boldsymbol{\sigma}'\boldsymbol{\sigma}'_c) - \frac{1}{3}I_1^2\right\} + \left(\frac{I_1}{I_{c1}}\right)^2 \frac{1}{2}\left\{tr(\boldsymbol{\sigma}'^2_c) - \frac{1}{3}I_{c1}^2\right\}$$

$$= \frac{1}{2}\left\{tr(\boldsymbol{\sigma}'^2) - \frac{1}{3}I_1^2\right\} - \left\{\frac{I_1}{I_{c1}}tr(\boldsymbol{\sigma}'\boldsymbol{\sigma}'_c) - \frac{1}{3}I_1^2\right\} + \frac{1}{2}\left\{\left(\frac{I_1}{I_{c1}}\right)^2 tr(\boldsymbol{\sigma}'^2_c) - \frac{1}{3}I_1^2\right\}$$

$$= \frac{1}{2}tr(\boldsymbol{\sigma}'^2) - \frac{I_1}{I_{c1}}tr(\boldsymbol{\sigma}'\boldsymbol{\sigma}'_c) + \frac{1}{2}\left(\frac{I_1}{I_{c1}}\right)^2 tr(\boldsymbol{\sigma}'^2_c) \tag{G.15}$$

$$= \frac{1}{2}\left\{tr(\boldsymbol{\sigma}'^2) - 2\frac{tr(\boldsymbol{\sigma}')}{tr(\boldsymbol{\sigma}'_c)}tr(\boldsymbol{\sigma}'\boldsymbol{\sigma}'_c) + \left(\frac{tr(\boldsymbol{\sigma}')}{tr(\boldsymbol{\sigma}'_c)}\right)^2 tr(\boldsymbol{\sigma}'^2_c)\right\}$$

There is a joint invariant $tr(\boldsymbol{\sigma}'\boldsymbol{\sigma}'_c)$ appeared in anisotropic invariant expression. It is found that anisotropic invariant $\bar{J}_2$ is expressed by all of basic invariants defined in Appendix G-1.

G-4 Principle of objectivity

$$I_1^* = tr(\boldsymbol{\sigma}'^*) = tr(\mathbf{Q}\cdot\boldsymbol{\sigma}'\cdot\mathbf{Q}^T) = tr(\mathbf{Q}^T\cdot\mathbf{Q}\cdot\boldsymbol{\sigma}') = tr(\mathbf{1}\cdot\boldsymbol{\sigma}') = I_1 \tag{G.16}$$

$$\mathbf{s}^* = \boldsymbol{\sigma}'^* - \frac{1}{3}I_1^*\mathbf{1}$$

$$= \boldsymbol{\sigma}'^* - \frac{1}{3}I_1^*\mathbf{Q}\cdot\mathbf{Q}^T$$

$$= \mathbf{Q}\cdot\boldsymbol{\sigma}'\cdot\mathbf{Q}^T - \frac{1}{3}\mathbf{Q}\cdot I_1\cdot\mathbf{Q}^T \tag{G.17}$$

$$= \mathbf{Q}\cdot\left\{\boldsymbol{\sigma}' - \frac{1}{3}I_1\right\}\cdot\mathbf{Q}^T$$

$$= \mathbf{Q}\cdot\mathbf{s}\cdot\mathbf{Q}^T$$

$$\begin{aligned}
J_2{}^* &= \frac{1}{2}tr(\mathbf{s}^* \cdot \mathbf{s}^*) = \frac{1}{2}tr(\mathbf{s}^* \cdot \mathbf{s}^*) \\
&= \frac{1}{2}tr(\mathbf{Q}\cdot\mathbf{s}\cdot\mathbf{Q}^T \cdot \mathbf{Q}\cdot\mathbf{s}\cdot\mathbf{Q}^T) \\
&= \frac{1}{2}tr(\mathbf{Q}^T \cdot \mathbf{Q}\cdot\mathbf{s}\cdot\mathbf{s}) \\
&= \frac{1}{2}tr(\mathbf{s}\cdot\mathbf{s}) = J_2
\end{aligned}$$
(G.18)

By the same manner, stress hardening variable is able to expressed

$$I_{c1}{}^* = I_{c1}, \quad \mathbf{s}_c{}^* = \mathbf{Q}\cdot\mathbf{s}_c \cdot\mathbf{Q}^T, \quad J_{c2}{}^* = J_{c2}$$
(G.19), (G.20), (G.21)

$$\begin{aligned}
\boldsymbol{\eta}_c{}^* &= \frac{\mathbf{s}_c{}^*}{p'_c{}^*} = \frac{3\mathbf{s}_c{}^*}{I_{c1}{}^*} \\
&= \frac{3\mathbf{Q}\cdot\mathbf{s}_c \cdot\mathbf{Q}^T}{I_{c1}} \\
&= \mathbf{Q}\cdot\boldsymbol{\eta}_c \cdot\mathbf{Q}^T
\end{aligned}$$
(G.22)

According to Eqs.(G.14),(G.16),(G.17), $\bar{\mathbf{s}}$ is transformed by,

$$\begin{aligned}
\bar{\mathbf{s}}^* &= \mathbf{s}^* - \frac{1}{3}I_1{}^* \boldsymbol{\eta}_c{}^* \\
&= \left\{\mathbf{Q}\cdot\mathbf{s}\cdot\mathbf{Q}^T\right\} - \frac{1}{3}(I_1)\left\{\mathbf{Q}\cdot\boldsymbol{\eta}_c \cdot\mathbf{Q}^T\right\} \\
&= \mathbf{Q}\cdot(\mathbf{s} - \frac{1}{3}I_1\boldsymbol{\eta}_c)\cdot\mathbf{Q}^T \\
&= \mathbf{Q}\cdot\bar{\mathbf{s}}\cdot\mathbf{Q}^T
\end{aligned}$$
(G.23)

Then $\bar{J}_2$ is transformed by,

$$\begin{aligned}
\bar{J}_2{}^* &= \frac{1}{2}tr(\bar{\mathbf{s}}^* \cdot \bar{\mathbf{s}}^*) \\
&= \frac{1}{2}tr\left(\left\{\mathbf{Q}\cdot\bar{\mathbf{s}}\cdot\mathbf{Q}^T\right\}\cdot\left\{\mathbf{Q}\cdot\bar{\mathbf{s}}\cdot\mathbf{Q}^T\right\}\right) \\
&= \frac{1}{2}tr\left(\mathbf{Q}\cdot\bar{\mathbf{s}}\cdot\left\{\mathbf{Q}^T \cdot\mathbf{Q}\right\}\cdot\bar{\mathbf{s}}\cdot\mathbf{Q}^T\right) \\
&= \frac{1}{2}tr\left(\mathbf{Q}\cdot\bar{\mathbf{s}}\cdot\bar{\mathbf{s}}\cdot\mathbf{Q}^T\right) \\
&= \frac{1}{2}tr(\left\{\mathbf{Q}^T \cdot\mathbf{Q}\right\}\cdot\bar{\mathbf{s}}\cdot\bar{\mathbf{s}}) \\
&= \frac{1}{2}tr(\bar{\mathbf{s}}\cdot\bar{\mathbf{s}}) = \bar{J}_2
\end{aligned}$$
(G.24)

In the SO model, generalized stress ratio η^* is replaced by generalized relative stress ratio $\bar{\eta}$. $\bar{\eta}$ can be proven to satisfy the principle of objectivity according to the results in Eqs.(G.16), (G.24) by,

$$\bar{\eta}^* = \frac{3\sqrt{3\bar{J}_2{}^*}}{I_1{}^*} = \frac{3\sqrt{3\bar{J}_2}}{I_1} = \bar{\eta}$$
(G.25)

All of invariants including anisotropic invariant are satisfied the principle of objectivity.